

DELHI COLLEGE OF ENGINEERING



LIBRARY

Class No. _____

Book No. _____

Accession No. _____

Kashmere Gate, Delhi



LIBRARY

DUE DATE

For each day's delay after the due date a fine of 10 P. per vol. shall be charged for the first week, and 50 P. per Vol. per day for subsequent days. Text Book Re. 1.00.

Borrower's No.	Date Due	Borrower's No.	Due Date

Design of Electrical Apparatus

Design of Electrical Apparatus

THIRD EDITION

By

JOHN H. KUHLMANN

*Professor of Electrical Design
University of Minnesota*

*Member American Institute of Electrical Engineers
The American Society for Engineering Education*

*Assisted in the preparation of the third edition
by Assistant Professor N. F. Tsang
Department of Electrical Engineering
University of Minnesota*

NEW YORK · JOHN WILEY & SONS, INC.
LONDON · CHAPMAN & HALL, LIMITED

COPYRIGHT, 1930, 1940, 1950

BY

JOHN H. KILMANN

All Rights Reserved

*This book or any part thereof must not
be reproduced in any form without the
written permission of the publisher*

THIRD EDITION

Fourth Printing, August, 1959

PRINTED IN THE UNITED STATES OF AMERICA

Preface to the Third Edition

The general plan and method of presentation which found favor with many users of the previous editions have not been altered. The design constants and design limits have been revised in line with the latest design practices. The characteristic curves of electrical sheet steels are plotted on semi-logarithmic paper, and the characteristics of cold reduced electrical sheet steels, used in rolled core transformer construction, have been added. The copper tables have been enlarged to include the new wire insulating materials.

In the direct-current design section the sample design calculations have been revised in accordance with the revised output constants. New values of insulation thickness and clearance for the armature slots have been adopted. A discussion of multiplex windings, used on large-capacity machines, has been added.

The method of calculating the field current for a specified load and power factor for synchronous machines has been changed to agree with the procedure adopted by the American Standards Association. The equivalent circuit of a synchronous motor with single- and double-squirrel-cage starting winding is included, and a method of predetermining starting torque, pull-in torque, and starting kva. is given with sample calculations for single- and double-cage starting winding.

The section on induction-motor design has been largely rewritten. New methods for determining motor dimensions are given, and design constant curves are plotted on semi-logarithmic paper. A method of determining the effect of saturation in the leakage flux paths and of calculating the deep bar effect of squirrel-cage rotors has been added. With these additions it is possible to predetermine the starting torque and current with satisfactory accuracy. The circle diagram has been omitted, and all performance values are calculated from the equivalent circuit. A method for the design of small transformers used in control circuits and for power supply in electronic devices has been included with a sample design.

The author wishes to acknowledge the valuable suggestions received from Mr. Robert Fillmore of the University of Minnesota, from Mr. I. C. Benson of Electric Machinery Manufacturing Co., from Mr. W. Field of Engineering Research Associates, and from Mr. O. Underwood of Minneapolis Honeywell Regulator Co. The author is indebted to Mr. Chun-Hsuan Sun for his help in the revision of the sample design problems.

JOHN H. KUHLMANN

MINNEAPOLIS, MINN.
February 20, 1950

Preface to the Second Edition

IN the second edition the general plan of the book has not been altered, but new material has been added and changes have been made in some of the sample problems. In Section I covering direct-current machine design, the sample motor design has been altered to conform more closely to present-day practice.

In Section II, synchronous machine design, a brief discussion has been added on the method of calculating displacement angle, synchronizing power, and other characteristics by the two-reaction method. For this purpose, a method of calculating the synchronous reactances in the direct and quadrature axis has been included.

Induction motor characteristics are more rapidly and conveniently calculated by analytical methods. An analytical method has been added to the section on polyphase motor design. The fractional-horsepower single-phase motor is used in very large numbers for many applications. A method of designing these motors is included with sample designs of two types. The author designed a $\frac{1}{2}$ -horsepower, capacitor-start, single-phase induction motor and supervised the making of dies, assembling fixtures, and tools for the Department of Mechanical Engineering at the University of Minnesota. The complete design of this motor, as well as the test results of the first motor built, have been added. The calculations for a $\frac{1}{4}$ -horsepower, resistance split-phase induction motor are also included; these calculations were made by Mr. R. M. Saunders as his design problem for the course in electrical machine design.

The author wishes to acknowledge with thanks the suggestions and technical information received from Mr. C. G. Veinott, Westinghouse Electric and Manufacturing Company, and Mr. W. R. Appleman, Marathon Electric and Manufacturing Corporation.

JOHN H. KUHLMANN

MINNEAPOLIS, MINN.

February 26, 1940

Preface to the First Edition

THE object of this book is to present a practical method of design in a clear and simple form with explanations of the theory, procedure, and limits of design. The following work is the result of a number of years of practical experience as a designer of electrical apparatus and of nine years of experience as a teacher of the subject. The procedure and methods employed are those used by the professional designer.

The method of treatment adopted for each type of apparatus discussed is, first, to explain the construction of the apparatus to be designed; second, to explain the formulas and procedure; third, to give the design limits established by practice; and fourth, to illustrate with complete sample calculations. The complete design calculations are given for two direct-current machines, two synchronous machines, two induction motors, and four transformers.

Those using the book in the classroom will find it convenient to assign each student the problem, for the particular apparatus to be studied, on a blank design sheet such as used in this book. This sheet should be filled in by the student and submitted to the instructor at the end of the period allotted for the problem. The design sheets used in the text are similar to those used by the commercial designer, and contain the predetermined characteristics and all the data necessary to construct the apparatus.

In the preparation of this work the author found it convenient to treat, first, the direct-current machine; second, the synchronous machine; third, the induction motor; and fourth, the transformer. It is not necessary to follow this order of study in a course in electrical design, because the book has been so prepared that each section is complete in itself.

The author wishes to acknowledge his indebtedness to his brother, F. H. Kuhlmann, for reading the manuscript, and to Professor W. T. Ryan for the privilege to use all material contained in his book, *Design of Electrical Machinery*. He also wishes to express his thanks to the Electric Machinery Manufacturing Company, to the Westinghouse Electric and Manufacturing Company, and to the General Electric Company for technical data and illustrations so generously supplied.

JOHN H. KUHLMANN

Minneapolis, Minnesota,
Nov. 26, 1929

Contents

SECTION I DIRECT CURRENT MACHINES

CHAPTER		PAGE
I	CONSTRUCTION	1
II	VOLTAGE FORMULA AND OUTPUT EQUATION	14
III	ARMATURE WINDINGS AND INSULATION	31
IV	THE MAGNETIC CIRCUIT	64
V	ARMATURE REACTION AND FIELD WINDING DESIGN	81
VI	COMMUTATION AND COMMUTATING POLE DESIGN	99
VII	LOSSES, EFFICIENCY, AND TEMPERATURE RISE	120
VIII	SAMPLE DESIGN	136

SECTION II SYNCHRONOUS MACHINES

IX	CONSTRUCTION	162
X	VOLTAGE FORMULA AND OUTPUT EQUATION	174
XI	ARMATURE WINDING AND INSULATION	188
XII	MAGNETIC CIRCUIT	215
XIII	ARMATURE REACTIONS IN SYNCHRONOUS MACHINES	226
XIV	LOSSES, EFFICIENCY, AND TEMPERATURE RISE	251
XV	SAMPLE DESIGN OF SYNCHRONOUS MOTOR	265

SECTION III—INDUCTION MOTORS

XVI	CONSTRUCTION	289
XVII	THE STATOR	296
XVIII	THE ROTOR	316
XIX	MOTOR CHARACTERISTICS	327
XX	FRACTIONAL-HORSEPOWER SINGLE-PHASE MOTOR DESIGN	356

SECTION IV TRANSFORMERS

XXI	CONSTRUCTION	398
XXII	CORE AND WINDINGS	408
XXXIII	OPERATING CHARACTERISTICS	428
XXIV	SAMPLE TRANSFORMER DESIGNS	435
	APPENDIX	477
	LIST OF SYMBOLS	490
	INDEX	501

*Note: The Appendix, pages 477-500, will
be found in the pocket on the back cover.*

I—DIRECT-CURRENT MACHINES

CHAPTER I

CONSTRUCTION

DIRECT-CURRENT generators and motors may be divided into three general classes: (1) The non-commutating-pole machine, (2) the commutating-pole machine, (3) the compensated machine.

(1) The non-commutating-pole machine is practically obsolete, being used only for generators and motors for low voltages and small capacities.

(2) The commutating-pole machine is built with small poles between the main poles, which are called commutating poles and are magnetized by a winding in series with the armature. The brushes are so placed that the coils, during commutation, come under the influence of the flux from the commutating poles, which flux is of such value and direction that cutting it produces in the coils a voltage which neutralizes the voltage of self-induction. In a generator, the flux from the commutating pole must be in the same direction as the flux from the main pole preceding it, and in a motor it must be in the same direction as the flux from the main pole following it.

(3) The compensated machine may be looked upon as a modified commutating-pole machine. The commutating-pole machine has the exciting winding concentrated on the commutating pole, whereas the compensated machine has part of the exciting winding distributed in the main pole faces. By such construction, the leakage flux of the commutating pole is reduced, which increases the commutation capacity of the machine. The compensated machine has two distinct advantages over the commutating-pole machine. It has a greater commutating capacity and, since the armature cross magnetization under the main pole is neutralized, the maximum voltage between adjacent commutator segments is reduced. By taking advantage of these two points, it is possible to increase the speed of generators and to build motors for more difficult cycles of operation.

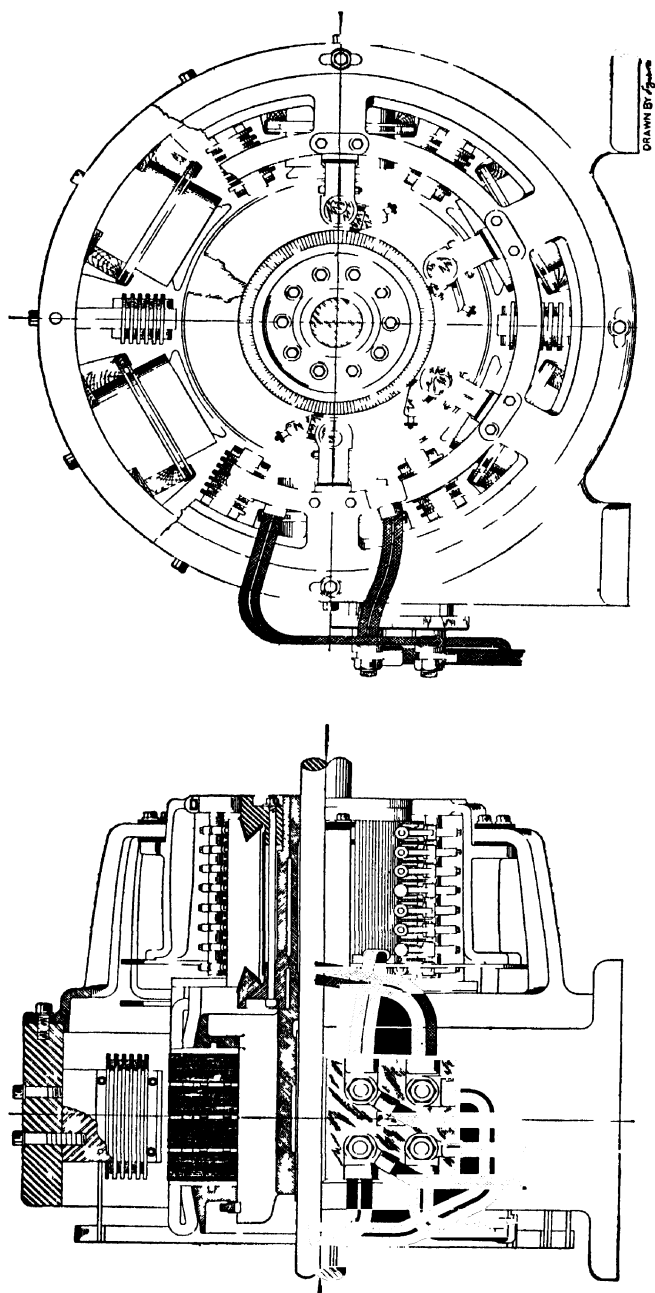


FIG 1 —Assembly drawing of direct-current generator, 300 kw, 900 r p m, 250 volts

The type of construction generally used for direct-current generators and motors is shown in Fig. 1.

Spider.—The spider of a direct-current generator or motor is the frame upon which the armature laminations are assembled. By designing the spider with large axial ventilating ducts, good ventilation of the inside of the armature is obtained and the weight of the armature is kept small. The spider for large machines is either a steel casting or is fabricated from rolled steel.¹ Figure 2 shows a cast steel spider of a large-diameter, slow-speed machine. For machines with small armature diameter, the type of construction shown in Fig. 3 is used, that is, the spider is part of the armature lamination.

Armature.—The armature of direct-current generators and motors is built up of electric sheet-steel laminations varying in thickness from 0.0141 to 0.025 in. The laminations are punched to correct size by means of dies, carefully annealed and insulated. For arma-

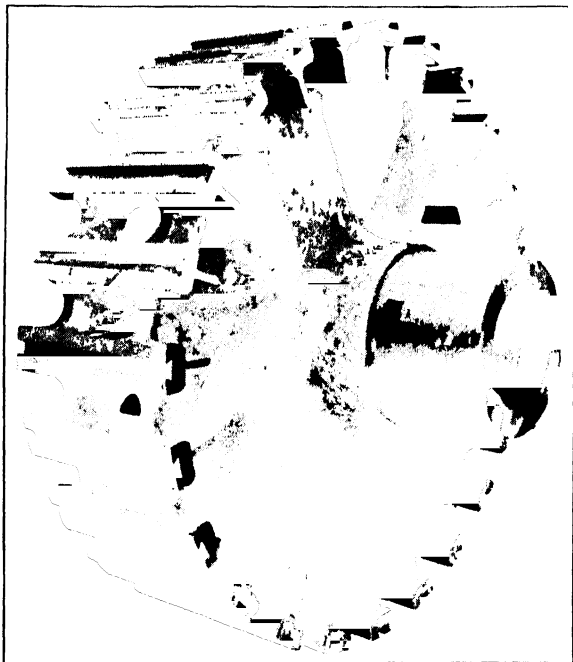


FIG. 2.—Armature spider for 1700-h.p., 90 to 205-r.p.m., 600-volt motor.

ture diameters smaller than approximately 30 in., the armature laminations are punched in one piece, whereas for larger armature diameters the circle is divided into several segments. One segment for a large-diameter, slow-speed machine is shown in Fig. 4.

The usual method of insulating the armature punchings is that of applying a thin coat of core plate varnish to each side of the punching. The insulating varnish is generally applied by passing the punchings between two rolls coated with the insulating varnish. The varnish on

¹ "Standard Lane of Direct-Current Machines Fabricated by Arc Welding," Electric Journal, Vol. 25, p. 575, Dec., 1928.

the punchings is either air dried or artificially dried. When the artificial drying process is used, the punchings are first passed over an open flame, to burn out the volatile matter in the varnish, and then through

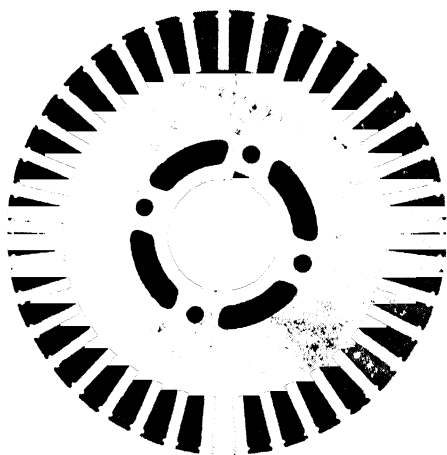


FIG. 3.—Armature punching with spider.

an oven, to bake the varnish. Paper is sometimes used to insulate the armature laminations from one another. The paper is applied to the sheet steel before it is punched out.

The insulated armature punchings are assembled on the spider between two end-plates. These are cast of the same material as the spider. The end-plate on the commutator end of the armature is often cast in one piece with the spider. The one on the opposite end, however, is always a

separate casting, and is used to press the laminations tightly together to prevent vibrations. The end-plates extend to the bottom of the armature slots and, therefore, do not support the armature



FIG. 4 —One segment for large-diameter armature with welded duct spacers.

teeth (see Fig. 1). For all except very small motors and generators, which have round or very shallow slots, the armature teeth must be supported by a tooth support.

The tooth support generally consists of a piece of rolled steel, spot-welded to the end lamination. The position of the tooth support and the shape of the section of the rolled steel piece are shown in Fig. 4.

The length of the armature iron is divided into sections, as shown in Fig. 1, by radial ventilating ducts; these are usually from $\frac{1}{4}$ to $\frac{3}{4}$ in. wide. The narrow duct is used on the small-diameter, high-speed machine, and the wide duct on the large-diameter, slow-speed machine. Except for very small machines, such as fractional horsepower motors, there is always a ventilating duct at each end of the armature laminations. When the length of the armature exceeds approximately 4 in., the armature also is divided into sections by radial ventilating ducts. Enough ducts should be used so that the length of each section will not be more than 3 in.

The ventilating duct spacer must extend from the top of each tooth to the inside of the armature lamination so that neither the teeth nor the inside edge of the armature lamination will flare and close the duct when the punchings are pressed together. Loose armature laminations will vibrate and produce a buzzing noise, because of the flux reversals in the armature core. The construction of the ventilating duct spacer is similar to that of the tooth support shown in Fig. 4.

On motors and generators with totally enclosed frame, such as street railway motors, the radial ventilating ducts are often omitted. For this type of construction, the cooling air is forced through the machine, parallel to the shaft, by a fan mounted on the shaft at the end of the armature opposite to the commutator.

The armature coils are placed into the slots with the required amount of insulation between armature iron and coils, and the slots are sealed with wedges. The type of wedge generally used is of horn fiber impregnated with paraffin. The position and thickness of the wedge are shown in Fig. 5 *a* and *b*. Bands of phosphor bronze or steel wire are used to hold the armature coil end-connections in position. The slots are not always sealed by wedges; they are sometimes left open and the coils held in place by phosphor bronze or steel band wires as Fig. 6 shows.

Commutator.—The commutator is built up of hard-drawn, copper segments, insulated from one another by mica. The thickness of the mica insulation varies from 0.02 to 0.06 in. and depends upon the diam-

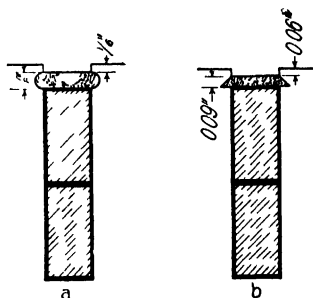


FIG. 5.

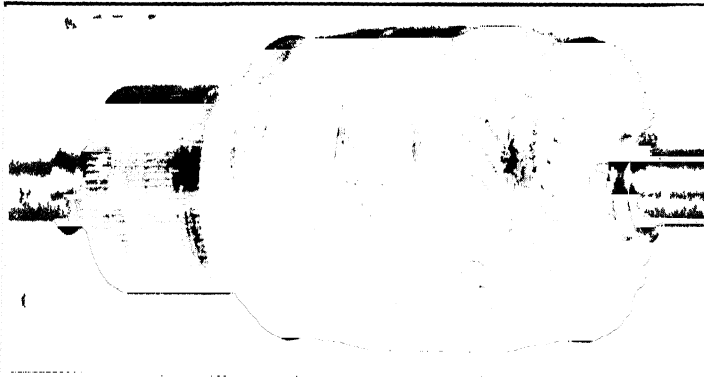


Fig. 6.—Complete armature for 7½-h p, 1750-r p m, 230-volt, 4-pole, shunt-wound motor

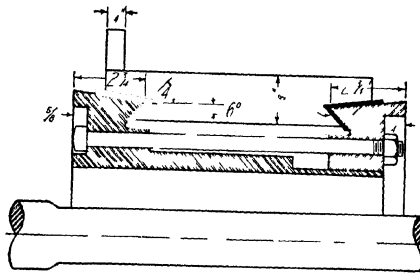


FIG. 7—Two V-ring commutator construction

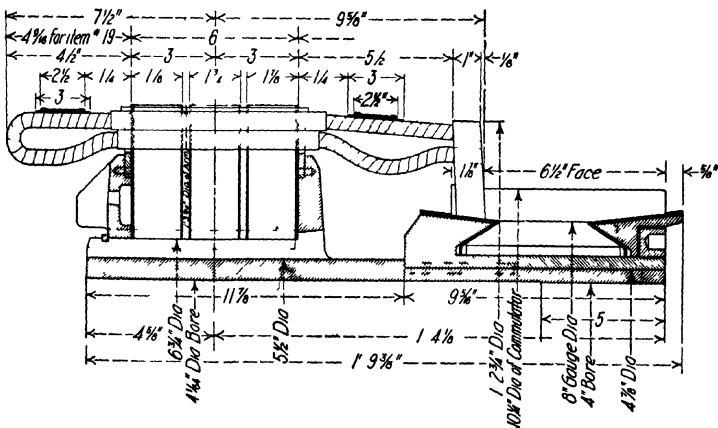


Fig. 8 -Armature and commutator assembly, 50-h p, 850-r p m, 230-volt, shunt-wound motor

eter of the commutator and the voltage between adjacent segments. The mica ² used for commutator insulation must be one of the soft

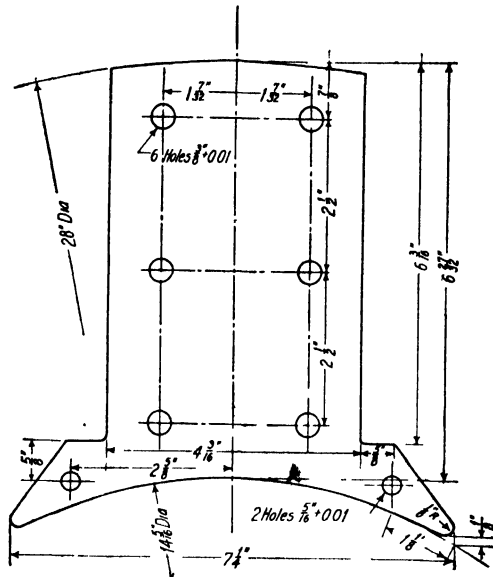


FIG. 9.—Detail drawing of pole punching, 50-kw., 1200-r.p.m. generator.

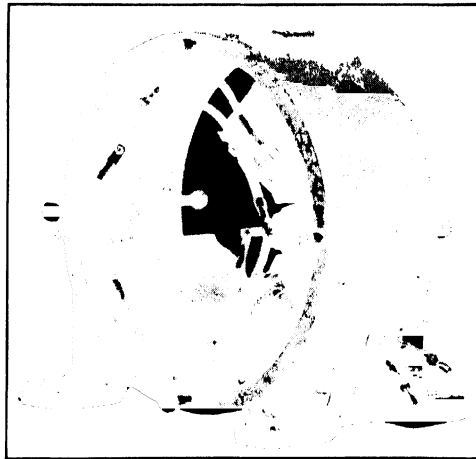


FIG. 10.—Field yoke with partially assembled field poles, 7½-h.p., 1750-r.p.m., 4-pole motor.

²See "The Manufacture of Built-Up Mica," Electric Journal, Vol. 21, p. 10, Jan., 1924; "Types of Commutator Construction," Electric Journal, Vol. 23, Nov., 1926, p. 565.

varieties so that the copper and mica will wear down at the same rate.

The mica and copper segments are clamped between V-shaped clamping rings and insulated from them by micanite, usually about $\frac{1}{8}$ in. thick. The assembled commutator is pressed on the shaft of

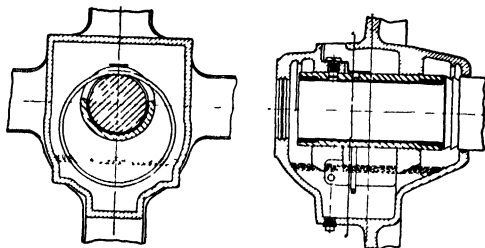


FIG. 11.—Cross-section of sleeve bearing and bearing housing.

the machine or on an extension of the armature spider. When the diameter of the commutator will permit, axial ducts are provided on the inside of the commutator for cooling purposes.

The two V-ring construction generally used is shown in Fig. 7.

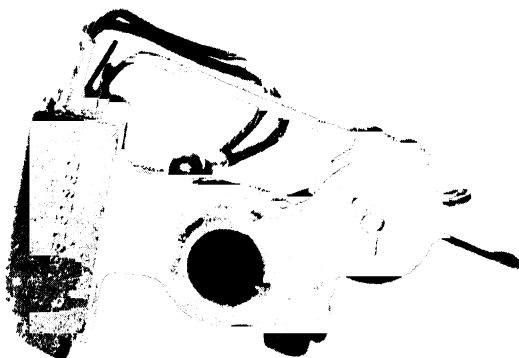


FIG. 12.—Brush holder with brush.

This method of construction can be used for high-speed commutators for peripheral speeds from 4000 to 6000 ft. per min. for lengths up to about 24 in. For longer commutators, the three V-ring construction or the shrink-ring construction is used. The armature and commutator assembly for a 50-hp. general purpose motor is shown in Fig. 8.

Field Poles.—The main poles of most modern machines are built up of sheet steel laminations, usually from 0.025 to 0.05 in. thick. The laminations are riveted together with no insulation between them. Figure 9 shows the usual shape of the laminations, with pole body and pole shoe punched in one piece. The shape of the pole body for the laminated pole construction is rectangular or square, whereas for cast steel poles with laminated pole shoes the pole body is often of circular shape, to obtain minimum length of mean-turn for the field coil.

The objection to the cast steel pole construction lies in the fact that



FIG. 13.—Brush yoke

it is difficult to obtain castings of uniform material and free from defects. With open armature slots, the type generally used for direct-current motors and generators, cast steel pole shoes can not be used, because of the excessive eddy current losses in the pole face due to the air gap flux pulsations produced by the armature slots.

The field winding may be wound directly on the pole, with the necessary insulation between winding and pole, or may be wound on a form completely insulated and placed on the pole. The form-wound field coil is generally preferred because of the ease with which repairs can be made.

The commutating pole is often made of cast steel, for large high-speed machines, and for machines subjected to large load fluctuations,

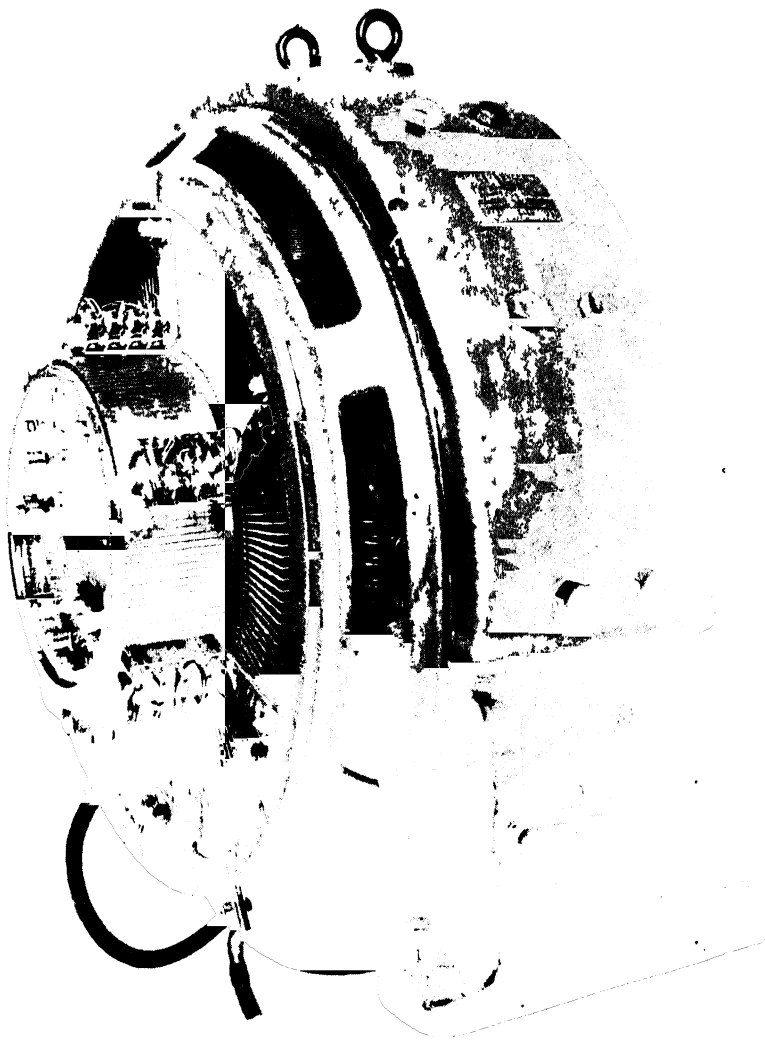


FIG 14 —Engine-type generator.

the laminated pole is used. The commutating-pole winding is generally form-wound, insulated, and placed on the pole. The field frame, with assembled and connected field windings, is shown in Fig. 10.

Field Yoke.—The yoke is the frame to which the field poles are bolted (see Fig. 10). The section of the yoke must have the required

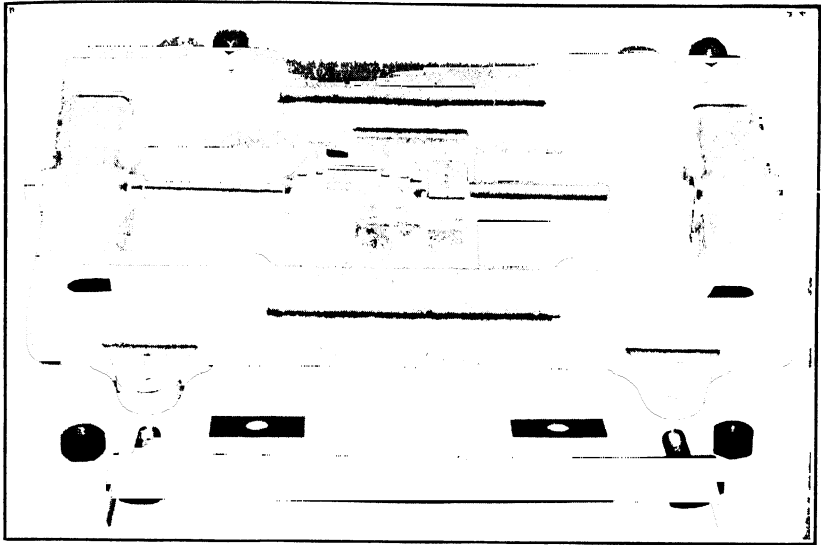


FIG 15 —Belt tightener base.

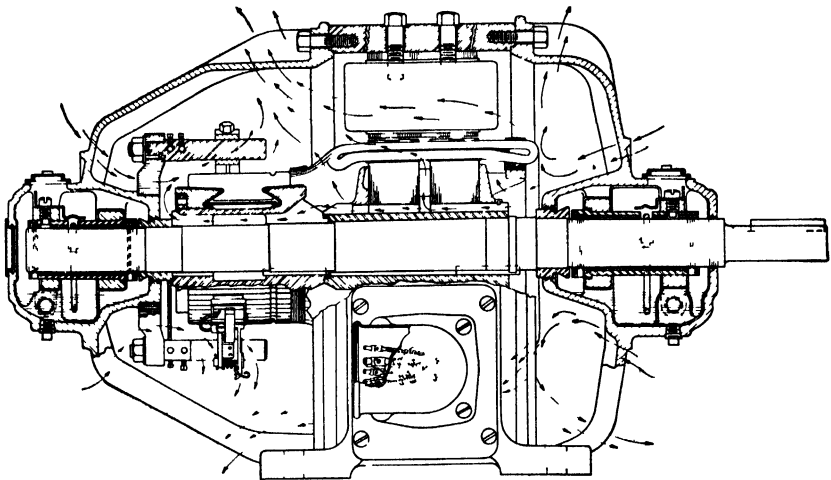


FIG 16 —Assembly drawing of bracket type motor.

area for the flux and must also have the required mechanical strength to support the machine. Because of the difficulty of obtaining steel

castings free from internal strains, cracks, blow-holes, and the like, the yokes of large direct-current generators are being built up of $\frac{1}{4}$ -in. steel plates. On smaller diameter machines, rolled steel is being used. The feet are riveted or welded to the frame.

Bearings.—The bearings of most modern direct-current machines are of the ring oiling type. The bronze bearing is generally preferred

for small machines; for large motors and for the larger generators babbitt bearings are used. The position of the bearing in the bearing housing and the method of mounting are shown in Fig. 11.

Ball bearings and roller bearings are being used frequently for direct-current motors. Figure 18 shows the assembly drawing of a ball-bearing motor.

Brush Holder and Brush Yoke.—

Many different types of brush holders³ have been used for direct-current generators and motors. The type generally used on modern machines is shown in Fig. 12. The brush holders are mounted on studs or arms which are generally brass rods, from $\frac{1}{2}$ to 1 in. in diameter. The brush studs are pressed into openings properly spaced in the bearing bracket, Fig. 18, or are mounted on a brush yoke, which is supported by the bearing bracket, Fig. 16. One type of brush yoke with brush arms, brush holders, and brushes is shown in Fig. 13.

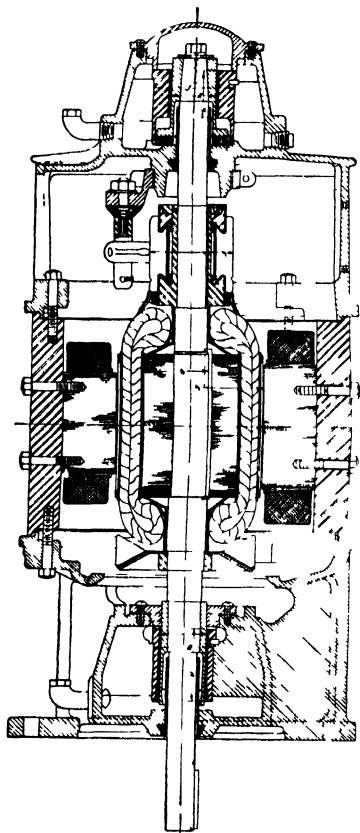


FIG. 17.—Cross-section of vertical motor

On engine type machines, for which the electrical manufacturer does not supply either the shaft or the bearings, the brush arms are supported by a brush yoke, as shown in Fig. 14. For pedestal type machines the type of brush yoke shown in Fig. 13, or the type shown in Fig. 14, may be used.

³ See "The Development of The Direct-Current Generator in America," by B. G. Lamme, *Electric Journal*, Vol. 12, p. 164.

Base.—All belted type motors and generators are mounted on a belt-tightener base or on rails. The base or rails are bolted down, and the machine can be moved on the base by means of a ratchet device. A type of belt-tightener base often used is shown in Fig. 15.

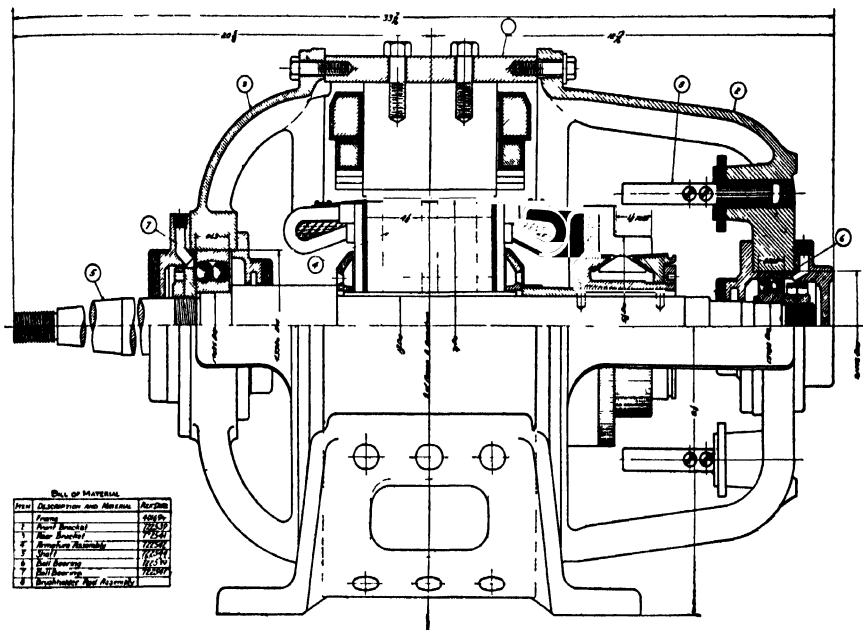


FIG. 18⁴ Assembly drawing of ball-bearing motor.

Motor and Generator Assembly.—Figure 16 is an assembly drawing of a bracket type motor, and Fig. 17 is a cross-section of a vertical type motor. An assembly drawing of a ball bearing, bracket type motor is shown in Fig. 18.

⁴ From Electric Journal, Oct., 1924, p. 484.

CHAPTER II

VOLTAGE FORMULA AND OUTPUT EQUATION

Voltage Formula.—The formula for the induced voltage in a direct-current armature is usually written in the following form,

$$E = \frac{\phi p N n}{a \times 60 \times 10^8} \text{ volts,} \quad (1)$$

where E is the voltage induced in the armature winding between adjacent brushes. When the induced voltage E is known, the flux per pole,

$$\phi = \frac{E a \times 60 \times 10^8}{N n p} \text{ lines.} \quad (2)$$

For the design of electrical machinery, it is often convenient to use a hypothetical total flux for the machine, instead of the flux per pole. To determine this hypothetical total flux, the flux density in the air gap is assumed to have maximum value over the entire pole pitch, that is, the shape of the field form is assumed to be rectangular, as shown in Fig. 19. The ratio of the area under the true field form to the area of the hypothetical rectangular field form is called the field form distribution factor f_d . The hypothetical total flux,

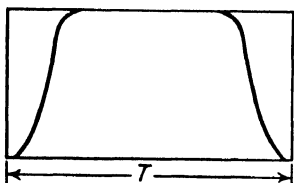


FIG. 19.

$$\phi_t = \frac{\phi p}{f_d}. \quad (3)$$

Substituting for ϕ , in formula 3, the value given by formula 2,

$$\phi_t = \frac{E a p \times 60 \times 10^8}{N n p f_d} = \frac{E a \times 60 \times 10^8}{N n f_d} \text{ lines.} \quad (4)$$

Output Equation.—The capacity of a given armature diameter and length is dependent, to a large extent, upon ventilation. The best design, from an engineering standpoint, gives a maximum output at a minimum cost. A point of primary importance in accomplishing this

is to ventilate the various parts, to dissipate the maximum watts loss with the least amount of heating. Ventilation, however, can be so good as to make it impracticable to work the machine to its limit, from a heating standpoint, on account of its efficiency reaching a value below the practicable point. Rarely, if ever, assuming reasonably good ventilation, is it practicable to rate direct-current machines on a continuous temperature basis, since invariably commutation or efficiency, or both, will be the limiting factor, rather than temperature.

The armature output of a direct-current generator, expressed in kilowatts, is as follows:

$$\text{Kw}_a = EI_a \times 10^{-3}. \quad (5)$$

From formula 4,

$$E = \frac{\phi_t N n f_a}{a \times 60 \times 10^8} \text{ volts.}$$

Substituting this expression for E into equation 5 above, the output of the armature in kilowatts will be,

$$\text{Kw}_a = \frac{\phi_t N n f_a I_a}{a \times 60 \times 10^{11}}. \quad (6)$$

The total flux is equal to the product of gap area times the maximum air gap density,

$$\phi_t = \pi D l B_g \text{ lines.} \quad (7)$$

If Q equals the ampere conductors per inch of armature periphery, then,

$$Q = \frac{N I_a}{a \pi D} \quad (8)$$

and

$$\frac{N I_a}{a} = \pi D Q.$$

Substituting the expression for ϕ_t from formula 7, and the expression for $\frac{N I_a}{a}$ from formula 8, into the output equation 6,

$$\text{Kw}_a = \frac{n f_a \pi D Q \pi D B_g l}{60 \times 10^{11}} = \frac{n D^2 l f_a Q B_g \pi^2}{60 \times 10^{11}}.$$

This equation may be rearranged into the following form:

$$\frac{D^2 l n}{\text{Kw}_a} = \frac{60 \times 10^{11}}{f_a Q B_g \pi^2} = \frac{60.8 \times 10^{10}}{f_a Q B_g}. \quad (9)$$

The value of B_g , the maximum air gap density, is limited by the permissible value of B_{t2} , the maximum tooth density. The maximum tooth density exists at the root of the tooth and is calculated by the following formula:

$$B_{t2} = \frac{\phi_t}{w_{t2}k_1lS} \text{ lines per sq. in.}$$

Substituting for the total flux, the value given in equation 7, the maximum tooth density,

$$B_{t2} = \frac{B_a \pi D}{w_{t2}k_1lS} \text{ lines per sq. in.}$$

This equation shows that the tooth density is directly proportional to the air gap density, for a given number and size of slots. The m.m.f.

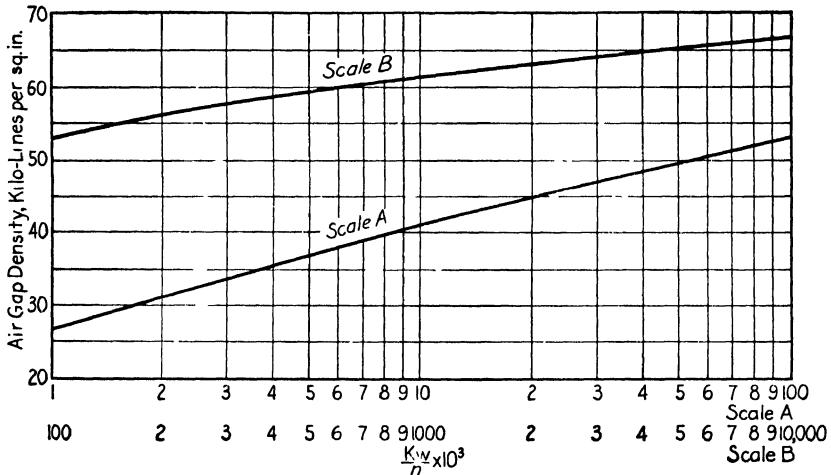


FIG. 20.—Air gap densities for direct-current generators and motors.

required to send the flux through the teeth will be large for high tooth densities, which, in turn, will require a large amount of field copper. The iron losses in the teeth will also be large for high tooth densities. The maximum tooth density, the density at the root of the tooth, should generally not exceed 150,000 lines per square inch. The air gap density must then be lower for machines with small diameters than for machines with large diameters, because of the greater tooth taper for the small diameter machines.

Air gap densities that may be used for preliminary design may be taken from the curve, Fig. 20.

The value of Q in formula 9, the ampere conductors per inch of armature circumference, is limited by commutation, efficiency, cost of construction, and armature heating. The ampere conductors per inch,

for a given rating, may be increased by increasing the number of conductors or by decreasing the armature diameter. By increasing the number of conductors, the reactance voltage will be increased, as will be shown later. If the diameter of the armature is decreased, the length of the armature must be increased in order to have enough iron to carry the flux, and the slots will have to be made deeper in order to accommodate the larger number of ampere conductors per inch of armature circumference. Both of these changes increase the reactance voltage, as may be seen from the reactance voltage formula. Commutation is therefore the limiting factor in the choice of the ampere conductors per inch of armature circumference for machines without commutating poles, whereas for machines with commutating poles, efficiency, cost of construction, and armature heating are the limiting factors. For non-commutating pole machines, Q is usually from 300 to 600. Average values of Q for commutating-pole machines are given in Fig. 21.

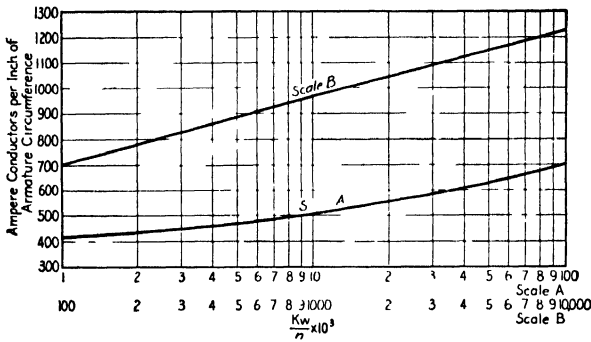


FIG 21 — Ampere conductors per inch of armature circumference for commutating-pole, direct-current generators and motors.

The air gap flux distribution factor, f_d , depends upon the shape of the field form. The method of obtaining the field form and the field form distribution factor is shown on page 23. The value of the field form distribution factor is, for the shape of pole shoe generally used, approximately equal to the ratio of the pole arc to the pole pitch. The usual values are 0.60 to 0.75.

By substituting average values for f_d , B_p , and Q into equation 9, the right-hand member may be combined into a constant,

$$\frac{D^2 l n}{Kw_a} = C \quad (10)$$

or,

$$D^2 l = \frac{Kw_a C}{\pi} \quad (11)$$

where C is called the output constant. This constant is not the same for all machines; neither will it be the same for all machines of the same kilowatt rating and speed. It depends upon the value of B_g , Q , and f_a . Average values of the output constant for commutating-pole machines for 50° C. rating may be taken from the curves, Fig. 22.

Formula 11 has been developed for a generator. Kw_a in this formula is the armature kilowatt output, which is equal to $E I_a$, where E is the armature induced voltage and I_a is the armature current. For a generator, this exceeds the output rating by the I^2R losses in the armature,

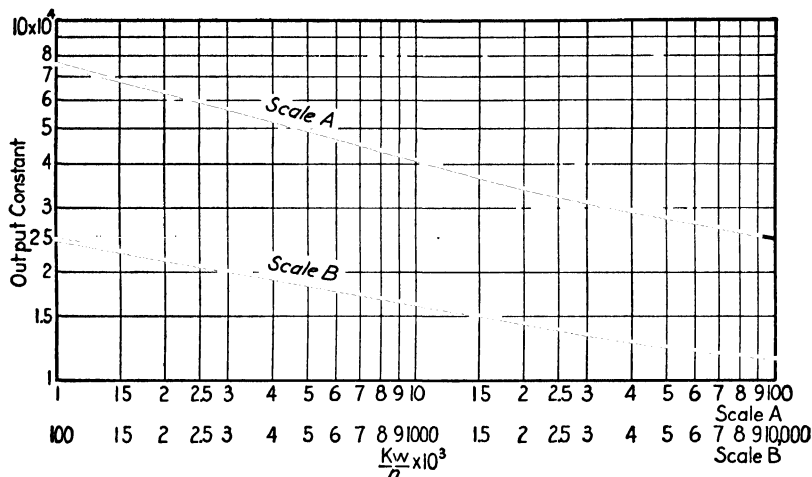


FIG. 22.—Output constants for commutating-pole, direct-current generators and motors.

the brushes, and the various series field windings; the core and mechanical losses are supplied by the prime mover. For a motor, Kw_a exceeds the output rating by the core and mechanical losses, the I^2R losses are supplied by the line. In determining the air gap density, ampere conductors per inch, and output constant, the kilowatt output may be used for either a generator or a motor.

For some motor applications, the torque the motor can produce rather than the horsepower output is the more important. The automobile starting motor is an example of such an application. It is often desirable to be able to determine the diameter and length required to produce a given stalled torque. The induced voltage in a motor armature

$$E = E_T - I_a R_c \text{ volts.}$$

Multiplying both sides of this equation by I_a gives

$$E I_a = E_T I_a - I_a^2 R_c \text{ watts.}$$

$E_T I_a$ is the power delivered to the armature, and $E I_a$ is the power developed. Subtracting core loss and friction and windage losses from the developed power gives the power available at the shaft. The developed power,

$$E I_a = \frac{T_D \times n \times 746}{5250} \text{ watts.}$$

The developed torque,

$$T_D = \frac{E I_a 5250}{n 746} = \frac{7.04 \times E I_a}{n} \text{ lb. ft.}$$

The induced voltage (see equation 4),

$$E = \frac{\phi_t N n f_d}{a \times 60 \times 10^8} \text{ volts.}$$

If this is substituted into the developed torque equation,

$$T_D = \frac{7.04 \phi_t \times f_d \times N I_a}{a \times 60 \times 10^8} \text{ lb. ft.}$$

The total flux, $\phi_t = \pi D l B_g$ and $N I_a = Q a \pi D$. Substituting into the developed torque equation,

$$T_D = \frac{7.04 \pi^2 D^2 l B_g f_d Q}{60 \times 10^8} = D^2 l B_g Q f_d 1.16 \times 10^{-8} \text{ lb. ft.}$$

From this equation the diameter and length can be determined. The values for B_g and Q can be taken from the curves, Figs. 20 and 21, for normal continuous duty machines. For intermittent duty motors, such as the automobile starting motor, the values for B_g and Q may be considerably increased.

Armature Peripheral Speed.—The diameter and length of the armature should be so chosen, whenever possible, that the peripheral speed of the armature will not exceed 6000 ft. per min., as high peripheral speeds lead to expensive constructions and commutation difficulties. For generators for direct connection to steam turbines, the peripheral velocity of the armature may be 15,000 to 20,000 ft. per min. Such generators require special construction and very careful design of the commutating field. Except for turbo-generators, the peripheral velocity of direct-current generators and motors is generally from 1200 to 6000 ft. per min.

The speeds for the smaller size generators are generally chosen to correspond to the standard 60-cycle induction motor speeds. The generators can then be directly connected to standard induction motors

for motor-generator sets. For the large sizes, the speeds are generally made to correspond to the standard 60-cycle synchronous motor speeds. The speeds for slow-speed engine-type generators are generally determined from the engine speeds.

Armature Diameter and Length.—When the output constant is known, the product D^2l is readily found. Either the diameter or the length may be assumed and the other dimension calculated. For high-speed machines, the diameter is limited by the peripheral velocity.

The length of the armature must be kept within certain limits, because it is difficult to ventilate a long armature properly. If long armatures are necessary, as for turbo-generators, special means for ventilation must be provided. For small two-pole machines, the armature length is often made equal to the armature diameter.

If a value for the ratio, armature diameter to pole pitch, is assumed, then the values of D and l can be found from the product D^2l . For motors and generators with peripheral velocity below 6000 ft. per min., the ratio l/τ is generally from 0.50 to 1.0. For turbo-generators, for which long armatures are unavoidable, the ratio l/τ is sometimes larger than 1.0, whereas for slow-speed engine-type generators, for which large diameters are desirable, this ratio may be less than 0.50.

The pole pitch

$$\tau = \frac{\pi D}{p} \quad (12)$$

and

$$\begin{aligned} \frac{l}{\tau} &= (0.50 \text{ to } 1.0), \\ l &= \tau(0.50 \text{ to } 1.0) \\ &= \frac{\pi D}{p} (0.50 \text{ to } 1.0). \end{aligned} \quad (13)$$

Substituting this value for l into the output equation 11,

$$D^2 \frac{\pi D}{p} (0.50 \text{ to } 1.0) = \frac{K_w a C}{n},$$

or

$$D = \sqrt[3]{\frac{K_w a p C}{n\pi(0.5 \text{ to } 1.0)}} = \sqrt[3]{\frac{K_w a C p}{n(1.5 \text{ to } 3.14)}}. \quad (14)$$

The value of l can be found by formula 11.

When designing a line of direct-current generators and motors, the armature diameters should be so chosen that as many ratings as possible

can be obtained with the same armature diameter. There is no fixed rule by which the minimum and maximum length of the armature for each diameter can be determined. These limits will depend upon the operating characteristics desired and upon the cost of construction. The cost of construction will be different for different manufacturers and therefore also the limits of armature length for a given diameter. When in doubt as to the proper value of the armature diameter and length, the only satisfactory method is to make preliminary calculations for two or more machines for different diameter and length and choose the one that will give good operating characteristics for a reasonable cost of construction.

Number of Poles.—In general, the number of poles should be so chosen that good operating characteristics are obtained with minimum weight of active material and minimum cost of construction.

The frequency of the currents in the armature conductors and of the flux reversals in the armature core is directly proportional to the number of poles and speed. The frequency

$$f = \frac{pn}{2 \times 60} \text{ cycles per sec.} \quad (15)$$

The losses in the armature core and teeth will increase with the frequency for a given flux density. To avoid excessive iron losses with high frequencies, the flux density in the armature core and teeth must be kept low, which will require increased armature iron weight. The usual frequencies for direct-current motors and generators are from 15 to 45 cycles per second.

The pole pitch varies directly with the armature diameter and inversely with the number of poles. For a large pole pitch, the length of the armature coil end-connections will be large, and therefore also the losses and the weight of the armature copper. The ampere-turns per pole on the armature vary with the pole pitch, and, since the ratio of the field ampere-turns to the armature ampere-turns should be equal to from 0.8 to 1.25 (see p. 79, Chapter V), it follows that the ampere-turns on the field will also increase with the pole pitch. A large number of ampere-turns on the field require a heavy shunt field winding, which is difficult to ventilate and leads to high shunt field losses. Excepting for very large-capacity, slow-speed machines, it is usually desirable to use a number of poles that will give a pole pitch less than 15 in.

For large-capacity, low-voltage machines, the number of poles may be determined by the amount of current that can be collected by each brush arm. With a brush thickness of $\frac{3}{4}$ in. and with a current density

of 50 to 60 amperes per square inch of brush contact, a current of about 1000 to 1200 amperes per brush arm can be used.

To guide the beginner in selecting a number of poles, the following tables are given:

TABLE I
MEDIUM AND HIGH SPEED

Kw Output	Speed in r.p.m.	No. of Poles
Up to 2	Over 1300	2
2 to 100	Up to 1300	4
50 to 300	Up to 1000	4 or 6
200 to 600	Up to 600	6 to 10
600 to 1000	Up to 500	8 to 12

TABLE II
SLOW SPEED ENGINE TYPE

Kw Output	Speed in r.p.m.	No. of Poles
35 to 150	225 to 300	6
200 to 250	135 to 225	8
250 to 500	100 to 150	10

See also tables given by W. T. Ryan¹ in "Design of Electrical Machinery."

When in doubt as to the number of poles to use for a motor or generator of given kilowatt capacity and speed, it will be necessary to calculate the weight of material, losses, and cost of construction, to determine the number of poles that will give best operating characteristics for the lowest cost.

Design of the Pole Shoe.—The air gap flux distribution curve must have such shape that the best possible commutation will result. To obtain good commutation, the flux density in the air gap must decrease gradually from maximum value under the center of the pole to zero on the center line between two poles, and the flux densities near the neutral point must be low. A field form that drops off rapidly from maximum value to zero not only leads to commutation difficulties but may also give rise to magnetic noises in machines with slotted armatures.

¹ "Design of Electrical Machinery," by W. T. Ryan, Vol. I, pp. 3, 4, and 5, John Wiley & Sons, Inc., New York.

The shape of the field form depends upon the shape of the pole shoe and the per cent pole embrace. The ratio of the pole arc on the armature surface to the pole pitch on the armature surface, expressed in per cent, is called the per cent pole embrace. A large per cent pole embrace is desirable, because it is possible to have a low air gap density with a large flux per pole. On the other hand, the leakage flux, the flux that passes between poles and does not cross the air gap, will be large for a large per cent pole embrace.

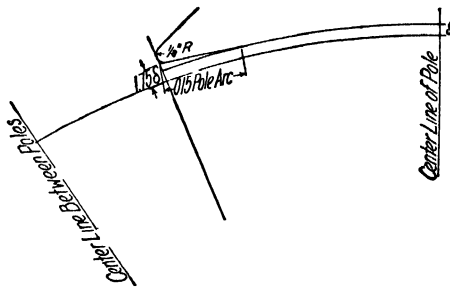


FIG. 23.

For direct-current machines, 60 to 75 per cent pole embrace is generally satisfactory. For commutating-pole motors and generators, the ratio of the pole arc to the pole pitch should generally not exceed 70 per cent. The lower values are necessary to avoid excessive leakage flux for main and commutating-pole. The number of slots embraced by the pole may sometimes determine the pole arc (see page 45).

For commutating-pole machines, 66 per cent pole embrace is generally satisfactory. A good air gap flux distribution curve is obtained with the shape of pole shoe shown in Fig. 23.

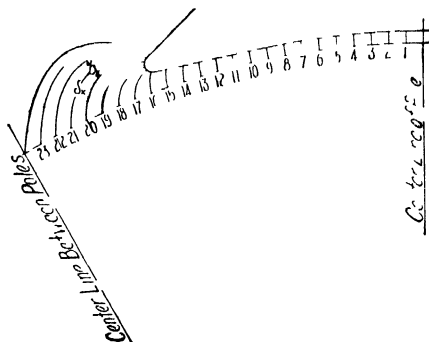


FIG. 24.

Construction of No-Load Field Form.—The useful flux per pole, in passing from the pole shoe into the armature, spreads out over the entire pole pitch. The flux will distribute itself in the air gap in such a way that the total reluctance will be a minimum. The flux path in the air gap under the pole may be assumed to be di-

vided into tubes of force, as shown in Fig. 24, each tube being of unit length in the direction parallel to the shaft.

If b_x is the mean width of such a tube of force, and δ_x the mean length, then the permeance of the tube is proportional to $\frac{b_x}{\delta_x}$, and the flux density, B_x , for a small portion of the armature surface of width a_x , and of unit

length, is proportional to $\frac{b_x}{a_x \delta_x}$. If B_g is the maximum air gap density at the center of the pole, where the air gap has a length δ , then B_g is proportional to $\frac{1}{\delta}$, because a_x is equal to b_x at the center of the pole. Since the same m.m.f. acts on the tube of force at the center of the pole and at the pole tip, the air gap densities are to each other as their respective permeances; that is,

$$B_x : B_g :: \frac{b_x}{a_x \delta_x} : \frac{1}{\delta},$$

or

$$B_x = \frac{b_x \delta}{a_x \delta_x} B_g. \quad (16)$$

To construct the air gap flux distribution curve, it will then be necessary to plot ² the magnetic flux distribution in the air gap. Since

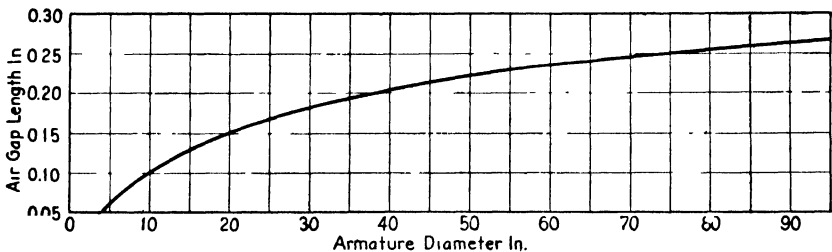


FIG. 25.—Approximate air gap lengths for direct-current generators and motors.

the pole is symmetrical about the center line, it is necessary to lay out only one-half of the pole and one-half of the pole pitch on the armature surface. For this construction the length of the air gap must be known; it may be estimated with the help of the curve Fig. 25.

In plotting magnetic fields, it is generally assumed that the iron of the pole shoe and armature has infinite permeability as compared to air. The flux lines will then leave the pole face and enter the armature at right angles.

The flux and equipotential lines must intersect at right angles and are so drawn that each tube of force is divided into a number of equal squares. From equation 16 it is apparent that the flux density at any point on the armature surface will be proportional to the ratio of

² Archiv für Elektrotechnik, Vol. 11, 1922, p. 85; Electric Journal, Vol. 23, July, 1926, p. 355; General Electric Review, Vol. 29, Nov., 1926, p. 797; A.I.E.E. Journal, Vol. 46, p. 430, and discussion, p. 614.

the length of a side of a square at the center of the pole, to the length of a side of a square at the point on the armature surface under consideration. This is true if the same number of equipotential lines is used at the center of the pole as at the pole tip. For a larger number of squares at the pole tip, the ratio of the sides of the squares must be multiplied by the ratio of the number of squares. The flux plot for a 300-kw., 900-r.p.m. direct-current generator is shown in Fig. 26.

The air gap flux distribution curve is easily obtained from the flux plot by dividing one-half of the pole pitch on the armature surface into

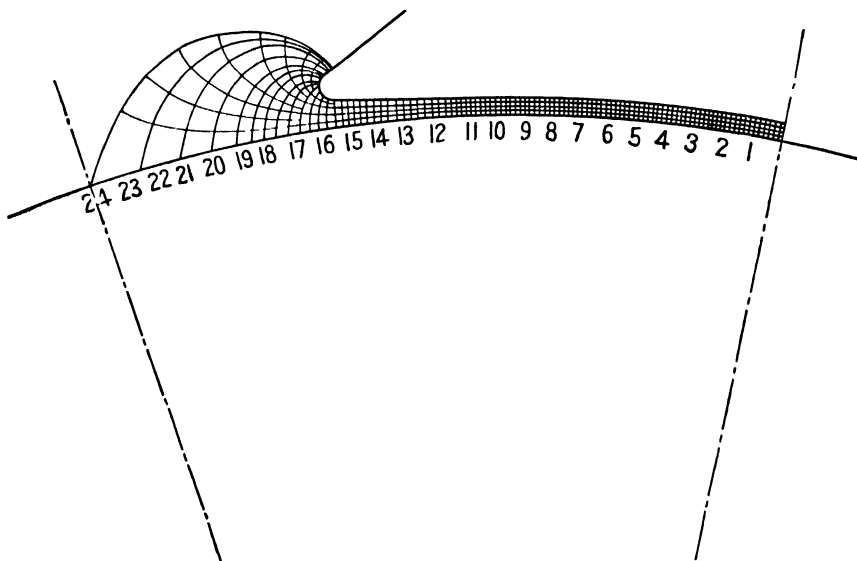


FIG. 26.—Flux plot for 300-kw. generator.

a convenient number of equal parts. The length of the squares is scaled from the drawing for each of the points on the armature surface, and the flux density is calculated as explained above. The density at the center of the pole is taken as 100, or 100 per cent.

By plotting the points on the armature surface as abscissas and corresponding values of flux density as ordinates, the curve, showing the flux distribution on the armature surface, is obtained. Figure 27 shows the flux distribution curve for the flux plot shown in Fig. 26. As Fig. 27 shows, the flux distribution curve does not pass through zero on the center line between poles. By superimposing a portion of the field form of the adjacent pole, which is of opposite polarity, and subtracting the corresponding ordinates, the true field form is obtained.

In Fig. 27, CF is equal to CD but is of opposite polarity. By subtracting the ordinates of CF from CB , the true flux distribution curve, BE , is obtained. The accuracy employed in making the flux plot will determine the accuracy of the flux distribution curve.

The author has used for some time in the design of electrical machinery a very much simplified method³ to obtain the field form. It consists of dividing one-half of the pole pitch on the armature surface into

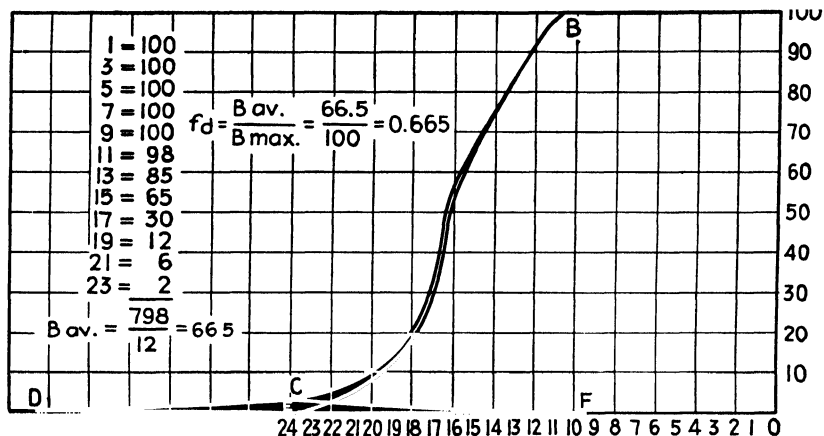


FIG. 27.—Flux distribution curve for flux plot shown in Fig. 26.

a convenient number of parts, and drawing the center line of a tube of force for each point in such a way that it will leave the pole face and enter the armature surface at right angles.

If the length of the air gap at the center of the pole is taken as the unit for measuring the length of the remaining flux lines, and if the average width of the tube of force is assumed to be equal to the maximum width, then formula 16 becomes

$$B_x = B_u \frac{1}{\delta_x} \quad (16a)$$

with δ_x measured in terms of δ , the length of the air gap at the center of the pole. The value of the flux density for each of the points on the armature surface can easily be calculated by formula 16a, and the field form curve plotted. The true field form is obtained in the same way as explained for Fig. 27. The method of drawing the flux lines is shown in Fig. 24 and is for the same pole shown in Fig. 26. The flux distribution curve is shown in Fig. 28.

³ See also Electric Journal, Vol. 24, May, 1927, p. 215.

This method is, obviously, only approximate and gives the density at a point about midway between the armature surface and pole shoe. For the purpose of determining the air gap flux distribution factor, this method is generally sufficiently accurate, because a small error in the determination of the flux distribution curve in the interpolar space will have only a small effect upon the flux distribution constant.

The flux distribution curves shown in Figs. 27 and 28 have been constructed on the assumption that the armature core and pole tips are

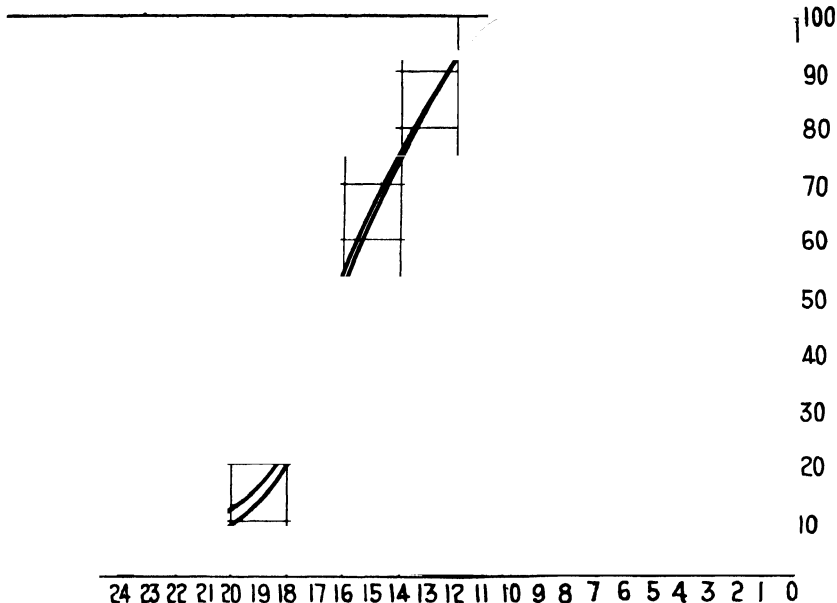


FIG. 28.—Flux distribution curve for flux plot shown in Fig. 24.

not saturated, and that the armature surface is a smooth surface with no slots. The effect of open armature slots is to produce notches in the top of the field form, as shown in Fig. 29, which is the field form of a small direct-current generator taken with an oscillograph. These notches travel along the wave during rotation so that the field forms of Figs. 27 and 28 show the average wave form.

Air Gap Flux Distribution Factor.—The definition of the air gap flux distribution factor has been given above as the ratio of the area under the flux distribution curve to the area of a rectangle having the same base and maximum ordinate. The area under the flux distribution curve can be found by the use of a planimeter; this area divided by the area of a rectangle having the same base and maximum ordinate gives the air gap flux distribution factor.

The flux distribution curve and rectangle have the same base line. The air gap flux distribution factor can, therefore, also be defined as the ratio of the average to the maximum ordinate. The average ordinate can be found by dividing the base line into a number of equal sections, the sum of the mean ordinates of each section divided by the number of ordinates being the average ordinate. Figure 27 shows the air gap flux distribution curve and the calculations for the average ordinate and flux distribution constant for the flux plot shown in Fig. 26.

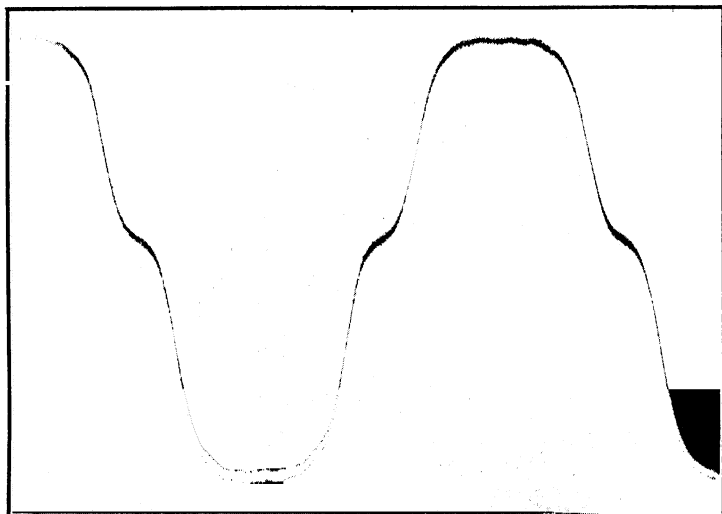


FIG. 29.—Air gap flux distribution curve of 5-kw., 1200-r.p.m., direct-current generator.

Sample Design.—A 300-kw., 900-r.p.m., 230-volt, compound-wound, direct-current generator is to be designed. The generator is to be part of a synchronous motor-generator set, to have commutating poles, and be overcompounded to give a full-load voltage equal to 250 volts. The efficiency of the generator should not be less than 92.0 per cent at full-load and normal voltage, and is to be calculated from the losses in accordance with the A.I.E.E. Standards. The temperature rise of no part of the generator should exceed 50° C. when operating at full load continuously.

$$\frac{Kw}{n} \times 10^3 = \frac{300}{900} \times 10^3 = 333.$$

The output constant from the curve Fig. 22 is 1.97×10^4 .

Table I, page 22, shows that the best design can generally be obtained with 6 poles for a machine of this size and speed.

By formula 14, page 20,

$$D = \sqrt[3]{\frac{K_w C_p}{n(1.5 \text{ to } 3.14)}} = \sqrt[3]{\frac{300 \times 1.97 \times 10^4 \times 6}{900(1.5 \text{ to } 3.14)}}$$

$$= 29.8 \text{ to } 23.1 \text{ in.}$$

The corresponding values for l , the length of the armature, are calculated by formula 11,

$$l = \frac{K_w C}{nD^2} = \frac{300 \times 1.97 \times 10^4}{900 \times 29.8^2 \text{ to } 23.1^2}$$

$$= 7.39 \text{ to } 12.30 \text{ in.}$$

The peripheral speed for 30-in. armature diameter is:

$$v = \frac{\pi D n}{12} = \frac{3.14 \times 29.8 \times 900}{12}$$

$$= 7020 \text{ ft. per min.}$$

and for 23.1-in. armature diameter it is 5450 ft. per min.

In order to avoid expensive constructions, it is generally desirable to use peripheral speeds of 6000 ft. per min. or less. Therefore, an armature diameter of 25 in. is chosen for this design. The peripheral speed will then be

$$v = \frac{\pi D n}{12} = \frac{3.14 \times 25 \times 900}{12}$$

$$= 5890 \text{ ft. per min.}$$

The length of the armature

$$l = \frac{K_w C}{nD^2} = \frac{300 \times 1.97 \times 10^4}{900 \times 25^2}$$

$$= 10.5 \text{ in.}$$

The frequency of the flux reversals in the armature core

$$f = \frac{pn}{2 \times 60} = \frac{6 \times 900}{2 \times 60}$$

$$= 45 \text{ cycles per sec.}$$

The pole pitch on the armature circumference

$$\tau = \frac{\pi D}{p} = \frac{\pi \times 25}{6} = 13.10 \text{ in.}$$

Choosing 66 per cent pole embrace, the pole arc on the armature circumference

$$B = \tau \times 0.66 = 13.10 \times 0.66 = 8.64; \text{ use } 8\frac{5}{8} \text{ in.}$$

The length of the air gap is taken equal to 0.17 in. (see curve Fig. 25). The shape of the pole shoe is made the same as shown in Fig. 23. The flux plot is shown in Fig. 26 and the flux distribution curve in Fig. 27. The air gap flux distribution factor is 0.665.

Consideration of flux distortion (see p. 76) increases the air gap length to 0.20 in. As this differs but little from the original value, the same flux distribution is assumed.

CHAPTER III

ARMATURE WINDINGS AND INSULATION

THE following armature windings are used for modern direct-current generators and motors:

1. Lap Windings.

- (a) Simplex Lap Windings, for which $a = p$
- (b) Multiplex Lap Windings,¹ for which $a = \mu p$

2. Wave Windings.

- (a) Simplex Wave Windings, for which $a = 2$
- (b) Multiplex Wave Windings,¹ for which $a = 2\mu$

3. Frogleg Windings.

Simplex Lap Windings.—A simplex lap winding for a 4-pole machine with 24 armature slots and 2 coil sides per slot is shown in Fig. 30. The position of the coils in the slots and the connection of the coils to the commutator are apparent when tracing the coils of the armature winding. Starting with commutator segment 1, Fig. 30, and passing by front end-connection to coil side 1, in the top of slot 1, along coil side 1 to the back of the armature, along back coil end-connection to coil side 14 in the bottom of slot 7, along coil side 14 to front of armature and along front end-connection to commutator segment 2, one armature coil is traced. Continuing now from commutator segment 2 to coil side 3, across the back of the armature to coil side 16 and then along coil side 16 to commutator segment 3, two armature coils are traced. In this way, after returning to commutator segment 1, along the front end-connection of coil side 48, the entire winding will have been traced.

¹ Multiplex windings are not much used in ordinary machines, and only a brief discussion is presented. The reader wishing further information on these windings is referred to "Armature Winding and Motor Repair," by D. H. Braymer, pp. 1-25, McGraw-Hill Book Co., New York; "Principles of Direct Current Machines," by Alexander Langsdorf, 3rd ed., pp. 116-147, McGraw-Hill Book Co., New York; "Die Gleichstrommaschine," by Dr. Arnold and LaCour, pp. 28-90, Julius Springer, Berlin.

From Fig. 30 it is apparent that the coil sides are arranged in two layers and that the two coil sides connected together by the end-connection on the back of the armature are in different layers, one in the top of a slot and the other in the bottom of a slot. It is also apparent that the slots in which the two sides of each coil lie are a pole pitch apart and that the terminals of each coil connect to adjacent commutator bars.

The interval between the two coil sides connected by the end-

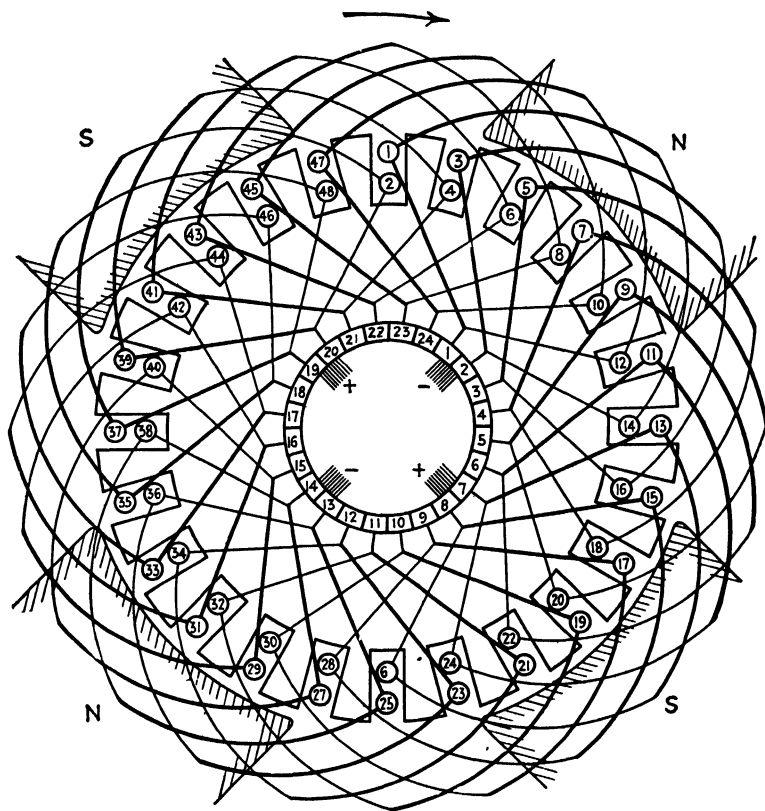


FIG. 30.—Progressive simplex lap winding, $S = 24$, $K = 24$, $p = 4$.

connection on the back of the armature is called the back pitch, Y_1 , and is expressed in terms of the number of coil sides spanned, whereas the interval between the two coil sides connected on the front of the armature is called the front pitch, Y_2 , and is also expressed in terms of the number of coil sides spanned. In tracing the armature winding, we progress in one direction at the back and in the opposite direction at the front of the armature. One pitch, usually the back pitch, is,

therefore, considered positive and the other negative. The algebraic sum of the back and front pitch is called the resultant pitch, and is always equal to 2, for simplex lap windings. The back pitch and front pitch must always be an odd integer.

The interval between the commutator segments to which the terminals of one coil are connected is called the commutator pitch, Y_c , and is expressed in terms of number of commutator segments. Figure 30 shows that the commutator pitch is always equal to one, for a simplex lap winding. The back pitch, front pitch, and commutator pitch are shown in Fig. 31, which is a developed diagram of the winding shown in Fig. 30.

The armature coils may be connected to the commutator segments

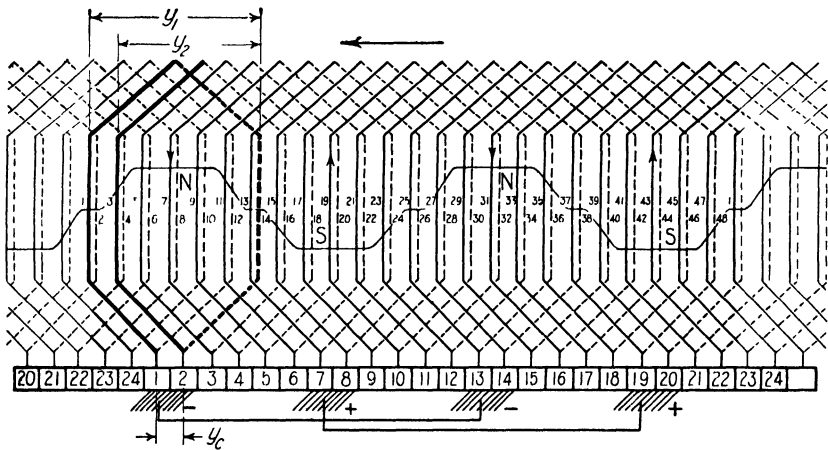


FIG. 31.—Developed progressive simplex lap winding diagram, $S = 24$, $K = 24$, $p = 4$.

as shown in Fig. 32. If we trace the winding starting with commutator segment 1 and passing along front end-connection to coil side 1, along coil side 1 to back of armature, along back end-connection to coil side 14, along coil side 14 to front of armature, we come by front end-connection to commutator segment 24 and not to commutator segment 2, as for the winding shown in Fig. 30. From commutator segment 24 we pass to commutator segment 23, etc. For the winding shown in Fig. 32, we progress around the armature in counterclockwise direction when tracing the winding, whereas for the winding shown in Fig. 30 we progress in the clockwise direction. The winding in Fig. 32 is called a retrogressive winding and that in Fig. 30 a progressive winding. For the progressive winding the back pitch is larger than the front pitch,

whereas for the retrogressive winding the front is larger than the back. The resultant pitch and the commutator pitch are positive for the progressive winding and negative for the retrogressive winding.

It is obvious from Figs. 31 and 32 that the polarity of the progressive winding is opposite to the polarity of the retrogressive winding. A motor with retrogressive armature winding will therefore run in opposite direction to a motor with progressive armature winding. The space required for connecting the armature coils to the commutator and the length of the mean-turn of the armature coil will be slightly larger for the retrogressive winding than for the progressive winding. Since the retrogressive winding offers no advantages over the progressive winding, lap windings should always be made progressive.

The back pitch expressed in terms of the number of slots embraced

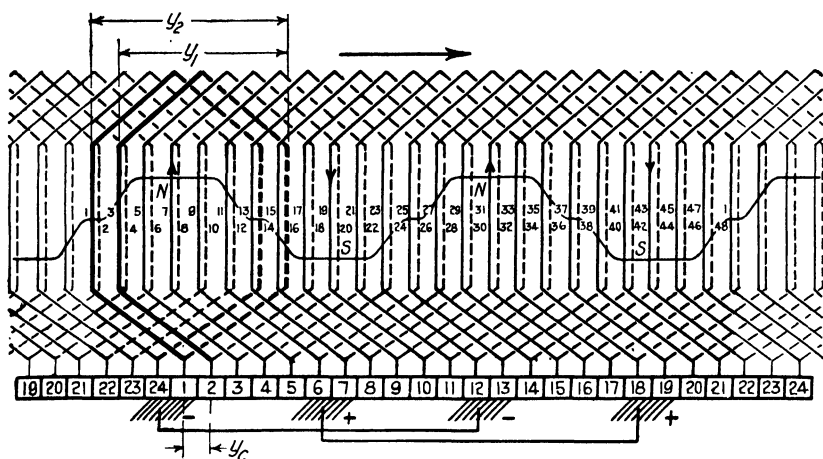


FIG. 32.—Developed retrogressive simplex lap winding diagram.

by the armature coil is called the coil pitch, Y_s ; it is always approximately equal to the number of slots per pole.

The formulas for the simplex lap winding can now be written as follows:

The coil pitch,

$$Y_s = \frac{S}{p} \quad (17)$$

the back pitch and front pitch,

$$Y_1 = C_s Y_s + 1 \quad (18)$$

and

$$Y_2 = Y_1 - 2Y_c \quad (19)$$

and the commutator pitch,

$$Y_c = \pm 1. \quad (20)$$

For the winding shown in Fig. 30,

$$\begin{aligned} Y_s &= \frac{S}{p} = \frac{24}{4} = 6 \\ Y_1 &= C_s Y_s + 1 = 2 \times 6 + 1 = 13 \\ 2Y_c &= Y_1 - Y_2 = 13 - Y_2 \\ Y_2 &= 13 - 2 = 11 \end{aligned}$$

and for the winding shown in Fig. 32,

$$Y_s = 6, \quad Y_1 = 13, \quad Y_2 = 13 + 2 = 15.$$

The windings thus far shown have two coil sides per slot, and the number of slots per pole is an integer. Figure 33 shows a progressive simplex lap winding for a 4-pole machine with 26 slots and 4 coil sides per slot,

$$\begin{aligned} Y_s &= \frac{S}{p} = \frac{26}{4} = 6\frac{1}{2}; \text{ use } 6 \\ Y_1 &= C_s Y_s + 1 = 4 \times 6 + 1 = 25 \\ 2Y_c &= Y_1 - Y_2 = 25 - Y_2 \\ Y_2 &= 25 - 2 = 23. \end{aligned}$$

From this diagram it is obvious that the coil sides short-circuited by the brushes do not all lie in the same position in all the slots. The reason for this is the fact that the winding is chorded, that is, the coil throw is less than full pitch. Chording the armature winding has the effect of decreasing the mean-turn of the armature coil and the weight of the armature copper, but, because of its effect upon commutation, a chording of one slot pitch can ordinarily not be exceeded. For commutating-pole machines, the armature coils should in general not be chorded more than one-half slot pitch, because a wide commutating pole is required for chorded windings, in order that the coils in the commutating zone will be under the effect of the commutating pole.

Simplex Wave Windings.—A simplex wave winding for a 4-pole machine with 25 armature slots and 2 coil sides per slot is shown in Fig. 34. The development of the simplex wave winding is apparent when tracing through the armature winding. Starting with commutator segment 1, in Fig. 34, and passing along front end-connection

to coil side 1, along coil side 1 to the back of the armature, along back end-connection to coil side 14, along coil side 14 to the front of the armature, and along front end-connection to commutator segment 13, one armature coil is traced. Continuing in this way, until $p/2$ coils have been traced, the armature will have been passed around once

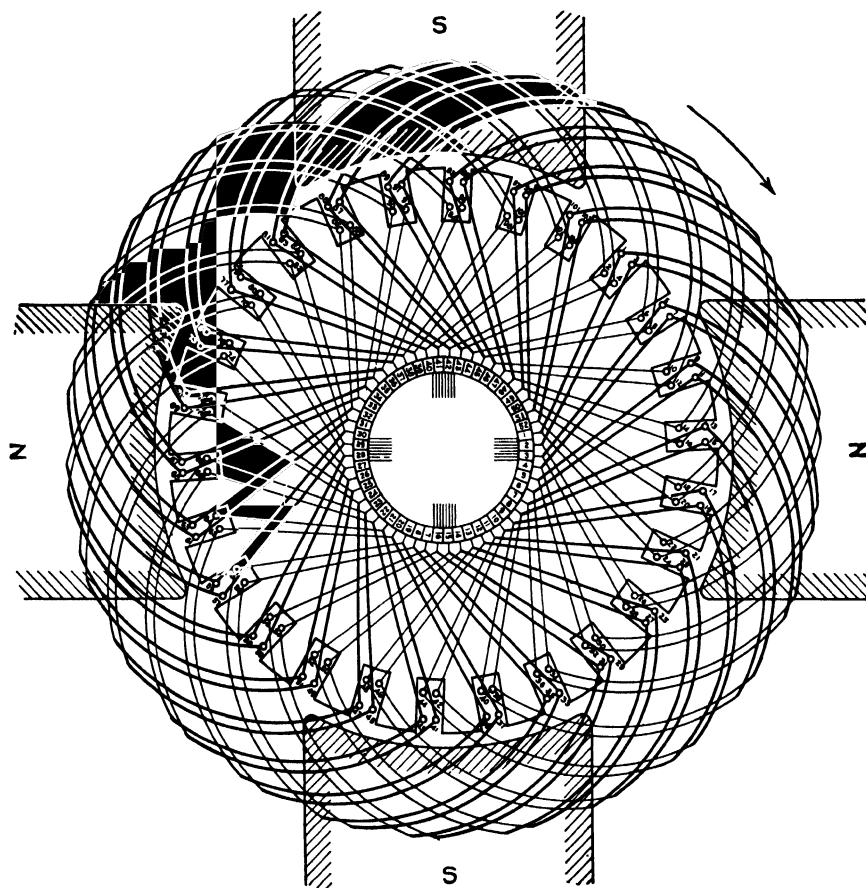


FIG. 33.—Progressive simplex lap winding, $S = 26$, $K = 52$, $p = 4$.

when commutator segment 25, adjacent to segment 1, is encountered. If the armature is passed around in this way as many times as there are commutator segments between the terminals of a coil, the winding will close on commutator segment 1.

Just as for the lap winding, the coil sides of the wave winding are arranged in two layers, with the sides of each coil lying in different

layers and a pole pitch, or nearly so, apart. The terminals of each coil of the wave winding connect to commutator segments, which lie $\frac{2K}{p}$ segments apart.

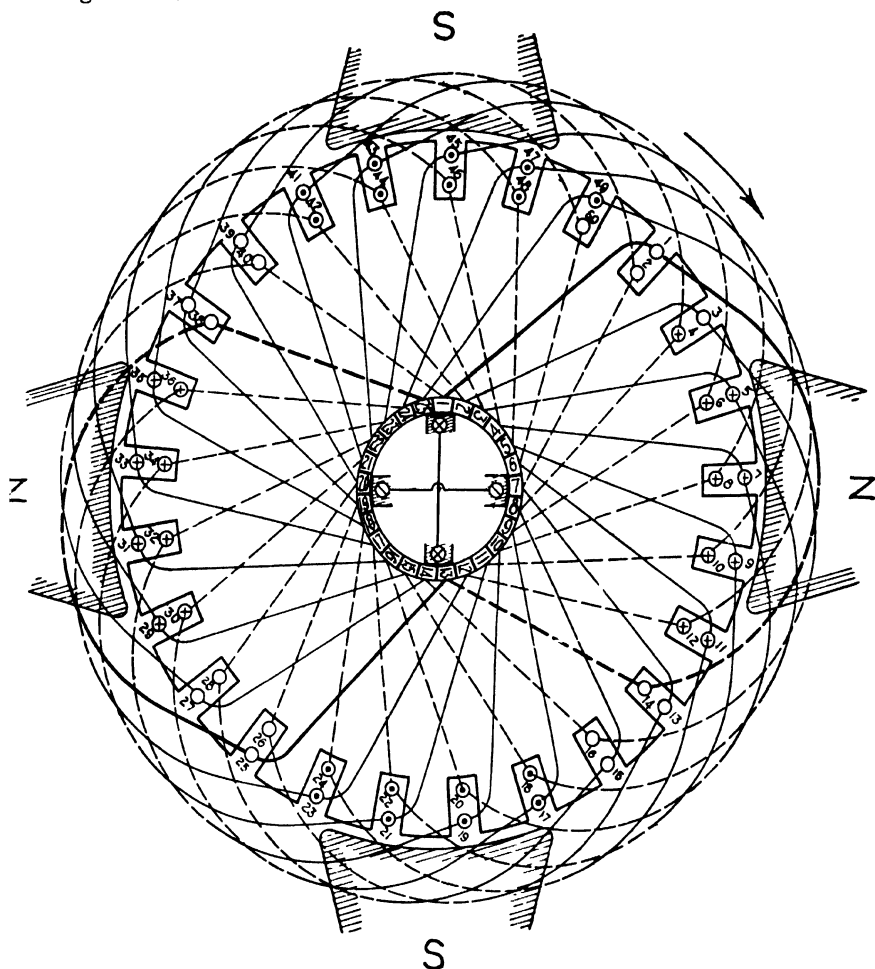


FIG. 34.—Retrogressive simplex wave winding, $S = 25$, $K = 25$, $p = 4$.

The front pitch, back pitch, resultant pitch, and commutator pitch are shown in Fig. 35, which is a developed winding diagram for the winding shown in Fig. 34. It is apparent from this diagram that the back pitch and front pitch are both measured in the same direction and that the resultant pitch is the sum of the back and front pitch.

When tracing a winding, if, after passing around the armature once, connection is made to a commutator segment to the right of the first

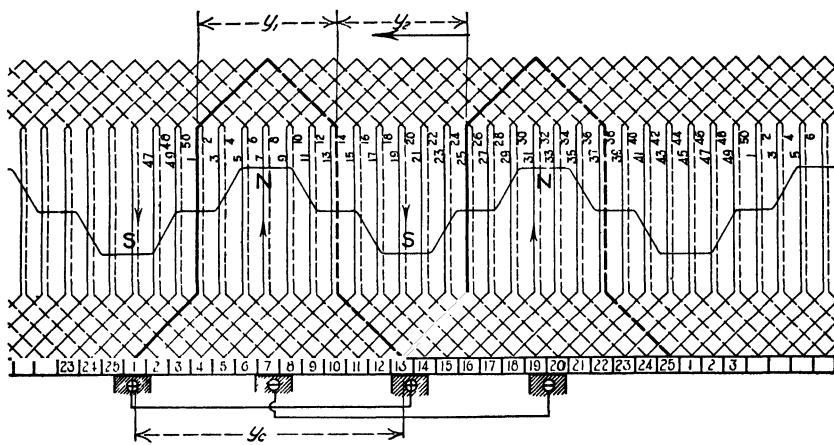


FIG. 35.—Developed retrogressive simplex wave winding diagram,
 $S = 25$, $K = 25$, $p = 4$.

segment, as shown in Fig. 36, the winding is called a progressive winding, and if connection is made to a commutator segment to the left of the first segment, as shown in Fig. 34, it is called a retrogressive

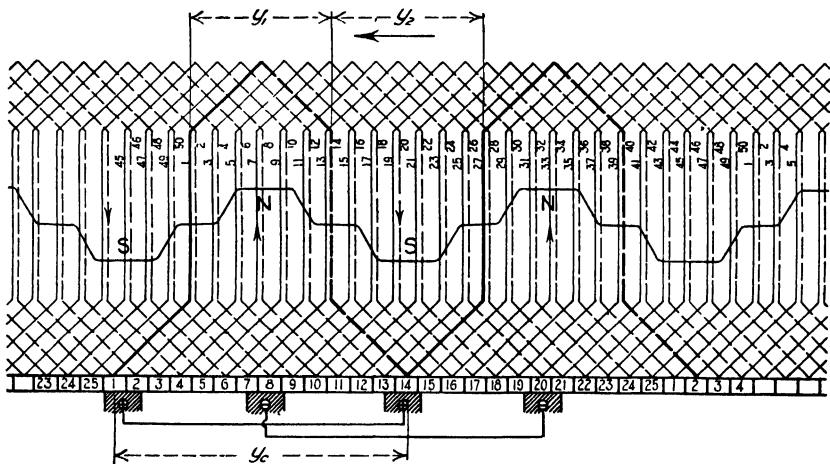


FIG. 36.—Developed progressive simplex wave winding diagram,
 $S = 25$, $K = 25$, $p = 4$.

winding. For wave windings, the retrogressive winding is used whenever possible.

From Figs. 34 and 36 it is apparent that $K \pm 1$ commutator segments are passed over, when passing around the armature once in tracing the winding, and that connection is made to the commutator $p/2$ times, with connection points a commutator pitch, Y_c , apart. Therefore,

$$\frac{p}{2} Y_c = K \pm 1$$

and

$$Y_c = 2 \frac{K \pm 1}{p}. \quad (21)$$

When the positive sign is used, the winding will be progressive and when the negative sign is used, it will be retrogressive. The coil pitch,

$$Y_s \leq \frac{S}{p}$$

and the back pitch and front pitch,

$$Y_1 = C_s Y_s + 1$$

$$Y_2 = 2Y_c - Y_1.$$

For the winding shown in Fig. 34:

$$Y_s \leq \frac{S}{p} = \frac{25}{4} = 6\frac{1}{4} = 6, \quad Y_1 = C_s Y_s + 1 = 2 \times 6 + 1 = 13$$

$$Y_c = \frac{K \pm 1}{p} 2 = \frac{25 - 1}{4} 2 = 12, \quad Y_2 = 2Y_c - Y_1 = 2 \times 12 - 13 = 11$$

and for the winding shown in Fig. 36:

$$Y_s = 6, \quad Y_1 = 13, \quad Y_c = 13, \quad Y_2 = 13.$$

From the developed diagram, Fig. 35, it is obvious that half of all the armature coils are connected in series, so that the number of parallel paths for a simplex wave winding is always 2, regardless of the number of poles. Figure 35 also shows that all brushes of like sign are connected by the coils lying in the neutral zone. It is then not necessary to connect brushes of like sign, and all brushes, with the exception of one positive and one negative, may be omitted. In general, wave-wound machines have as many brush arms as there are poles. In some cases, for example, in street railway motors, it is difficult to obtain access to one or more brush sets. For such cases, sets of brushes are often omitted.

The number of coil sides per slot need not be 2, as shown in Figs. 34 and 35. It can be more than 2, but must be a multiple of 2. The number of coil sides per slot that may be used for any number of poles is much more limited for a wave winding than for a lap winding. If all slots are to have the same number of coil sides and if for K , in formula 21, $\frac{C_s}{2}S$ is used, then

$$Y_c = \frac{\frac{C_s}{2}S \pm 1}{p} 2. \quad (22)$$

If, for example, $C_s = 6$, there is no number of slots, S , for a 6-pole machine that will make the commutator pitch, Y_c , an integer. The accompanying table ² gives the number of coil sides per slot for various numbers of poles, for which a wave winding is possible with all coils connected to the commutator, that is, no dead coils.

TABLE III

No. of Poles	Coil Sides per Slot				
p	C_s				
4	2	—	6	—	
6	2	4	—	8	
8	2	—	6	—	
10	2	4	6	8	
12	2	—	—	—	
14	2	4	6	8	
16	2	—	6	—	

If it is desired to use a certain number of slots for a given number of poles and coil sides per slot, it may not always be possible to have the commutator pitch equal to an integer, with the full number of commutator segments and coils. For example, if it is desired to use 50

² "Die Gleichstrommaschine," Vol. 1, 3rd ed., p. 52, Julius Springer, Berlin.

slots on a 4-pole machine with 6 coil sides per slot, then the commutator pitch,

$$Y_c = \frac{150 \pm 1}{4} 2 = 74\frac{1}{2} \text{ or } 75\frac{1}{2}.$$

But the commutator pitch must be an integer. If one commutator bar is omitted and one coil in the armature winding is not connected, then the commutator pitch,

$$Y_c = \frac{149 \pm 1}{4} 2 = 74 \text{ or } 75.$$

The coil that is not connected is called a "dead coil." It is placed on the armature to keep the armature mechanically balanced but is not connected to the commutator. The number of armature slots will usually be an odd number, as formula 22 shows, and wave windings, therefore, will generally be chorded windings and not pitch windings. What has been stated about chording of lap windings applies also to wave windings.

Equalizer Connections.—From the developed winding diagram shown in Fig. 31 it is obvious that, for the lap winding, all the coils of one armature path lie under adjacent poles. If the flux in the air gap under the poles is not the same for all the poles, the voltage induced in the various armature paths will not be the same. In consequence of this difference in voltage of the armature paths, equalizing currents will flow through the brushes. These equalizing currents may overload the brushes³ and may cause local armature heating and sparking at the brushes. If there is any unbalance in the magnetic circuits, current will flow in the equalizing circuits tending to neutralize the magnetic unbalance. The action of the equalizer connections is frequently not correctly interpreted.³

The inequality of the flux under the poles may be caused by unequal air gap lengths under the poles, by a difference in the shape of the pole shoe, or by non-uniformity of the material of the field poles and yoke, caused by "blow-holes" and the like in cast steel poles and yoke.

If commutator bars which occupy the same position under poles of like polarity are connected, the armature current will be equalized before commutation. These connections between points of the same

³ "History of the Development of the D.C.-Generator in America," *Electric Journal*, Vol. 12, p. 117. See also "Theory of the Action of Equalizer Connections in Lap Windings," by A. D. Moore, *Electric Journal*, Dec., 1926.

potential are called equalizer connections. The interval between equipotential points, expressed in number of commutator bars, is called the equalizer pitch,

$$Y_e = 2 \frac{K}{a}. \quad (23)$$

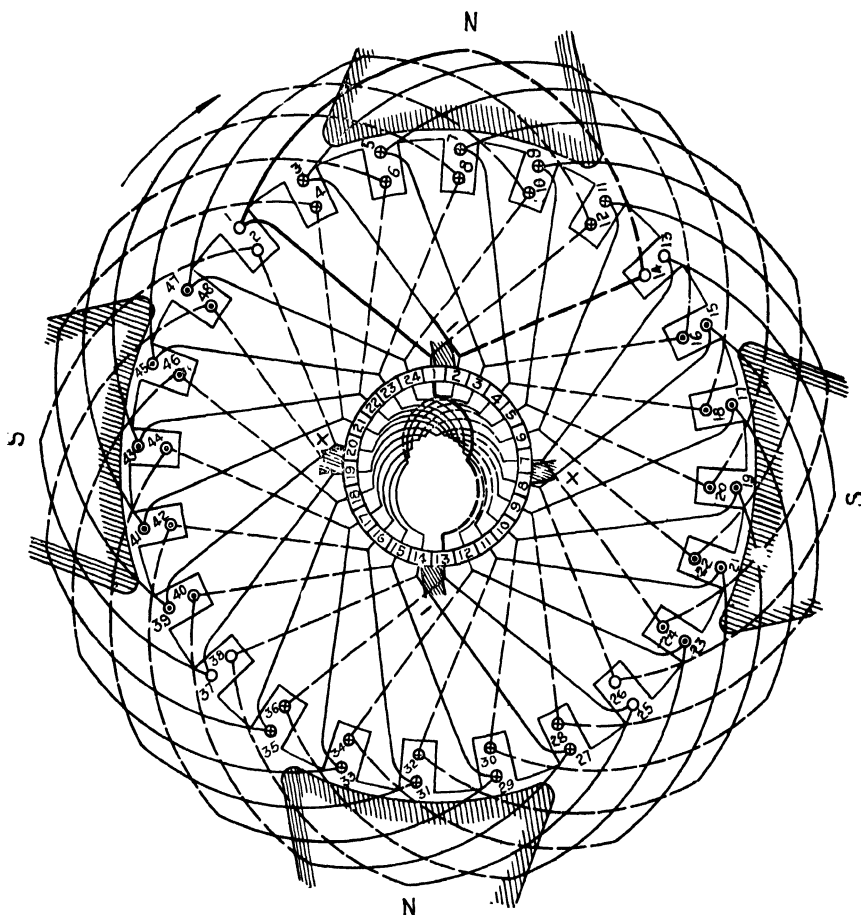


FIG. 37.—Simplex lap winding with equalizer connections.

The best possible equalization is obtained when all points of equal potential are connected by equalizer connections. The number of equalizer connections shown in Fig. 37 is used only for very high-speed and large-capacity machines. An equalizer connection for every 3 or

4 commutator bars has been found to be satisfactory for normal machines.

The section area of the conductor used for equalizer connections depends upon the value of the equalizer current. This current cannot be predetermined. Practice has shown that, with the number of equalizer connections given above, a section area of the equalizer conductor equal to from 0.50 to 1.0 times the section area of the armature conductor is usually satisfactory.

For wave windings, unequal flux under the various poles has no effect upon the voltage induced in each armature path, because all the coils of each path are approximately uniformly distributed under all the poles.

Multiplex Windings.— In a lap winding, if commutator bar 1 is connected to bar 3 through armature coil 1 and bar 3 to bar 5 through coil 2, etc., the winding is known as a duplex lap winding. The number of series conductors between any 2 adjacent brushes will be one-half as many as for the simplex lap winding. There are 2 parallel circuits slightly displaced from each other between adjacent brushes, and the number of parallel paths is doubled, or $a = 2p$. With an even number of commutator bars, it is obvious, by tracing the winding, that a closed loop is formed after one-half of the armature coils have been traced. There will then result 2 independent closed loops. This type of winding is often referred to as doubly re-entrant. With an odd number of commutator bars the loop will not close when tracing one-half of the armature coils. After tracing the remaining half of the armature coils, the winding will close. Such a winding is called singly re-entrant.

By skipping 2 commutator bars, that is, connecting commutator bar 1 to 4 through coil 1, a triplex winding is obtained. Such a winding may have 3 or 1 closed loops, depending upon whether K , the number of commutator bars, is divisible by 3 or not. For this type of winding $a = 3p$.

For a wave winding, if $(p/2)Y_c = K \pm 2$, then when passing around the armature once in tracing the winding, connection will be made not to the commutator bar adjacent to the one started with but to one 2 bar pitches from the starting point. This winding will have 2 independent closed loops or 1 loop, depending upon whether Y_c is even or odd. An examination of this winding shows that one-fourth of the conductors between adjacent brushes are in series and that the winding has 2 times as many parallel paths as the simplex wave winding, or $a = 4$.

For a triplex wave winding $(p/2)Y_c = K \pm 3$. This winding may have 3 independent closed loops or 1 closed loop, depending upon whether

Y_e is divisible by 3 or not. This winding will have 6 parallel paths, or $a = 6$.

Multiplex windings must have equalizer connections not only for the circuits under different poles but also for the different closed loops. In order that the equalizing points do not belong to the same loop, Y_e should be odd for duplex windings and should not be a multiple of 3 for triplex windings. In duplex wave windings equalizers can be connected only at diametrically opposite points ($Y_e = K/2$) and only for even pole pairs (p a multiple of 4). The general conditions which must be satisfied by duplex and triplex windings can be summarized as follows:

$$\text{Duplex lap, } S = \frac{p}{2}(2n+1), \quad m = \frac{K}{S} = 2n+1, \quad Y_e = \frac{2K}{p}.$$

$$\text{Triplex lap, } S = \frac{p}{2}(3n \pm 1), \quad m = 3n \pm 1, \quad Y_e = \frac{2K}{p}.$$

$$\text{Duplex wave, } S = 2n, \quad p = 4n, \quad K = p(Y_e \pm 1), \quad m = 2n+1, \quad Y_e = K/2.$$

$$\text{Triplex wave, } S = 3n, \quad p = 6n, \quad K = \frac{p}{2}Y_e \pm 3, \quad m = 3n \pm 1, \quad Y_e = K/3.$$

In the above, n is any positive integer including 0. $S = 3n$ indicates only that S must be a multiple of 3.

The number and section area of the equalizers required for multiplex lap windings are about the same as for simplex lap windings. For multiplex wave windings a much smaller number of equalizer connections is usually required because each group of series conductors passes successively under each pole.

Examples of multiplex windings.

Triplex wave with one loop

$$p = 18, \quad S = 240, \quad m = 4, \quad K = 960, \quad Y_e = 107, \quad Y_e = 320.$$

Duplex lap with two loops

$$p = 12, \quad S = 210, \quad m = 3, \quad K = 630, \quad Y_e = 105.$$

Duplex lap with two loops

$$p = 12, \quad S = 216, \quad m = 3, \quad K = 648, \quad Y_e = 108.$$

This winding has no interloop equalization because $Y_e = 108$ is an even number and, therefore, is not satisfactory.

Triplex lap with one loop

$$p = 14, \quad S = 245, \quad m = 2, \quad K = 490, \quad Y_e = 70.$$

Frogleg Winding.—The frogleg winding consists of a lap winding and a wave winding placed on the same armature. The wave winding is connected to the commutator at the equipotential points of the lap winding. In this way, the wave winding acts as an equalizer for the lap winding at the same time that it is carrying useful current. This type of winding is described by W. H. Powell and G. M. Albrecht.⁴

Number of Armature Slots.—The total number of conductors, N , can be determined by formula 4,

$$N = \frac{Ea \times 60 \times 10^8}{\phi n f_a}.$$

The conductors per slot must be an integer, and for 2-layer windings they must be an even number. A small number of slots require a large

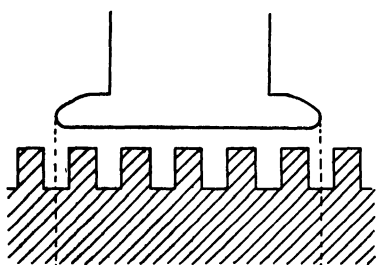


FIG. 38a.

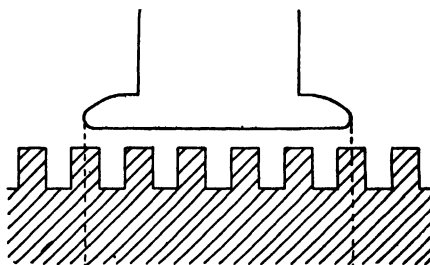


FIG. 38b.

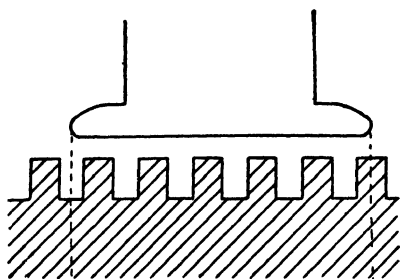
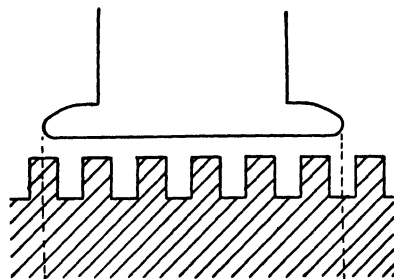
slot, because the number of conductors per slot will then be large. A saving in insulating material is generally possible by the use of a small number of slots, but, because of the effect of a small number of open slots⁵ upon the flux in the air gap, this saving can generally not be realized.

In Fig. 38a, the pole shoe covers 5 armature teeth and the flux from the pole passes through 5 teeth into the armature. In Fig. 38b, the armature is moved $\frac{1}{2}$ tooth pitch to the right, and the flux from the pole passes through 6 teeth into the armature. When the number of slots per pole is a whole number, the number of slots embraced by each pole will be the same for all positions of the armature. For the position of the armature shown in Fig. 38a, the reluctance of the air gap is greater and the flux under the pole is smaller than for the position shown in Fig. 38b. When the armature rotates, the flux in the air gap will necessarily pulsate. Pulsations of the flux in the air gap produce iron losses in the pole shoes and give rise to magnetic noises.

⁴ Iron and Steel Engineer, Vol. 2, Sept. and Nov., 1925.

⁵ "Die Gleichstrommaschine," Vol. 1, 3rd ed., p. 139, Julius Springer, Berlin.

In Fig. 39*a* and *b*, the pole shoe covers $5\frac{1}{2}$ slots. The total reluctance of the flux path and the flux under the pole remain approximately the same for all positions of the armature. From Fig. 39*a* and *b* it may be seen that the reluctance and the flux under the tips of the pole

FIG. 39*a*.FIG. 39*b*.

are not the same for all positions of the armature, and that, when the armature rotates, the flux under the pole oscillates between the pole tips. The oscillating flux in the air gap produces ripples in the voltage induced in the conductors moving under the poles. The pulsations and oscillations of the flux in the air gap will be small when the pole shoes are well beveled, when the air gap is large, and when the slots are narrow in proportion to the width of the teeth.

When the number of slots per pole is equal to a whole number plus $\frac{1}{2}$ (see Fig. 40), the reluctance of the flux path per pair of

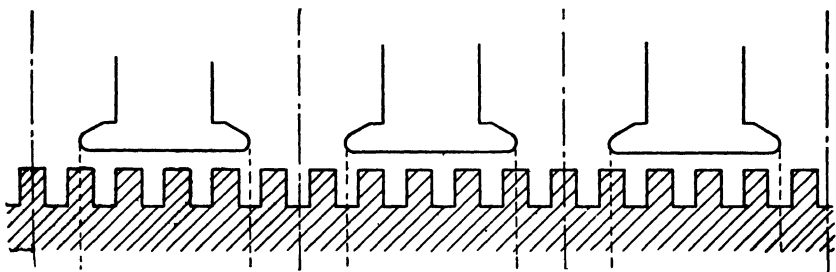


FIG. 40.

poles will be practically constant for all positions of the armature, and there will be no pulsations or oscillations of the flux in the air gap.

To avoid pulsations and oscillations of the flux in the air gap, the number of slots per pole should be equal to a whole number plus $\frac{1}{2}$. When this is not possible or advisable for other reasons, the number of slots per pole arc should be an integer.

Pulsations and oscillations of the flux under the commutating

pole must be avoided, as they may cause sparking. A large air gap under the commutating pole and a small tooth pitch help to reduce the effect of the armature slots upon the flux under the commutating pole. In general, the number of slots between the tips of two adjacent poles should be at least 3, or

$$(1 - \psi) \frac{S}{p} \geq 3.$$

Assuming 66 per cent for ψ , the number of slots per pole,

$$\frac{S}{p} \geq \frac{30}{(1 - 0.66)} \geq 8.82.$$

For machines with small armature diameter, for which the slots per pole will be smaller than as given above, partly closed armature slots will generally be required.

Armature Coil Construction and Insulation.—Armature coils for direct-current machines are wound with insulated wire or with bare



FIG. 41.—Mold for forming armature coils.

rectangular strap copper. The shape of the cross-section of the wire is round, square, or rectangular. The copper tables in the Appendix give the bare and insulated dimensions, the resistance and weight of standard round and square wire, and of some sizes of insulated rectangular wire. The dimensions, resistance, and weight of a number of

sizes of strap copper are also included. Round wire is used mostly in the smaller sizes for small-capacity machines and for high-voltage machines. Square and rectangular wires are used whenever possible,

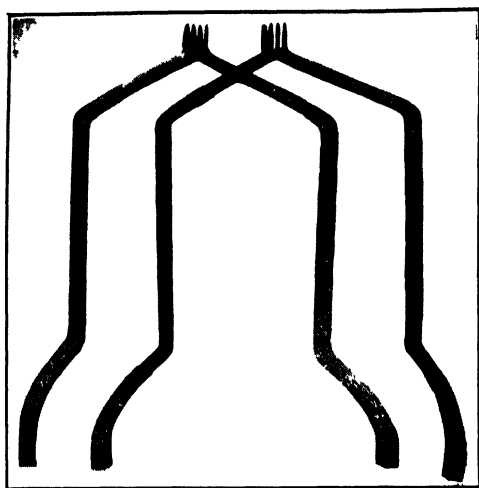


FIG. 42.—One-turn strap copper armature coils for wave winding.

because they give a better space factor and a mechanically stronger coil. Strap copper is used when conductors of large cross-section are required and especially for coils having only one turn.

Bare strap copper coils are formed on a mold, such as shown in Fig. 41. After the coils are formed, they are insulated, to protect them

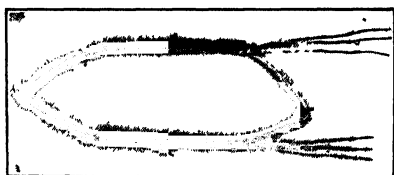


FIG. 43.—Armature coil before being pulled out.

from the neighboring coils in the slot. A completely insulated full coil, comprising four coils, is shown in Fig. 42. The term "coil" refers to the element connecting two commutator bars, the term "full coil," as used hereafter, refers to two or more coils insulated together and placed into the slot as

one coil. The number of coils is equal to the number of commutator bars, and the number of full coils is equal to the number of slots.

Wire-wound coils are not always wound on a form, such as used for strap copper coils, but are often wound into the form shown in Fig. 43 and then pulled into the desired shape by a coil-pulling machine. With this method of winding wire-wound coils, all the coils comprising a full coil are wound at the same time.

Strap-wound armature coils are generally arranged in the slot as shown in Fig. 44, whereas wire-wound coils are arranged as shown in

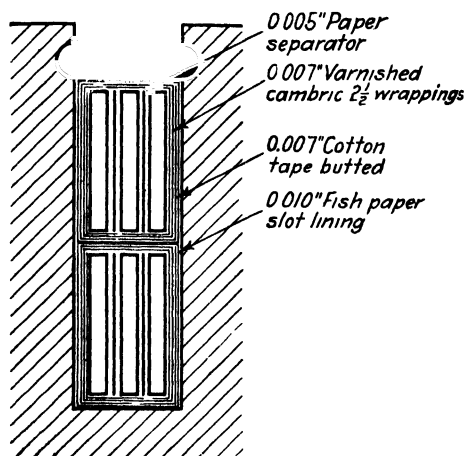


FIG. 44

Figs. 45 and 46. The line through the conductors indicates the conductors in parallel. The voltage between coil sides, side by side in a slot, is equal to the voltage between adjacent commutator bars, because

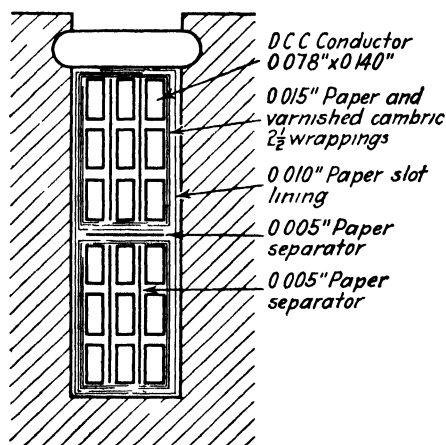


FIG. 45

coils, side by side, are connected to adjacent commutator bars. For coils with more than one turn, the voltage per turn is equal to the coil voltage divided by the number of turns per coil. The voltage per coil, for lap windings, is equal to the degree of multiplicity times the voltage

between adjacent commutator bars, and for wave windings it is this value divided by $\frac{p}{2}$. The voltage per turn for either type of winding is

$$e_t = \frac{a \phi_{sm}}{p l_a} \quad (24)$$

To avoid flashing, the maximum voltage between adjacent commutator bars should be less than 30 volts (see page 54).

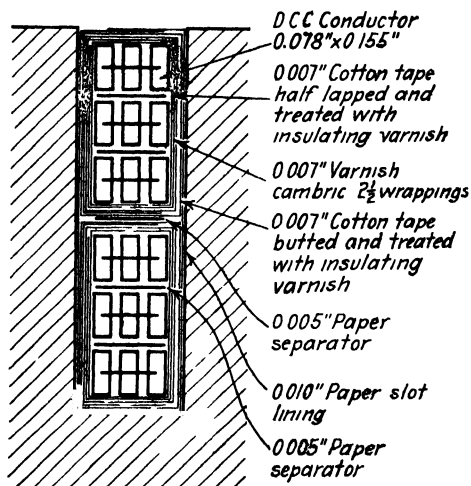


FIG. 46.

The voltage between the coil sides in the top of the slot and those in the bottom is approximately equal to the terminal voltage, because the coil pitch is generally equal to the pole pitch.

The insulation between the winding and core is subjected to mechanical stresses and must, therefore, be heavier than is required for electrical reasons. The standardization rules of the A.I.E.E. require that the insulation between armature core and windings shall withstand, for 1 minute, a 60-cycle effective e.m.f., applied between core and winding, equal to 2 times the terminal voltage of the winding plus 1000 volts. The test voltage is to be applied to the winding after the temperature test, when the windings are at normal operating temperature.

Armature coils wound with bare strap copper are generally insulated with cotton tape. The entire coil is taped half-lapped, with linen-finished cotton tape, generally 0.005 to 0.007 in. thick. The coils are then thoroughly dried in an oven, dipped in flexible baking varnish, and baked at a temperature of 100° C. for 8 or 10 hours or until dry.

For wire-wound coils, double-cotton-covered wire is generally used. For small machines, with a large number of turns of small wire per coil, single-cotton-covered enamel wire is used. After the coils are wound and pulled into the proper shape, they are dried and finished in the manner described in the preceding paragraph. The varnish treatment not only serves as a good insulator but also cements the individual conductors of the coil together and eliminates air pockets. Double-cotton-covered wire may be used for a voltage per turn as high as 25 volts. When the voltage per turn exceeds 25 volts, triple-cotton covering or some other method of insulation must be used.

A large number of insulating materials and a variety of methods⁶ are used for insulating the armature coils from the core. For open slots, which is the type of slot generally used for all except very small machines, and for formed coils, all the insulation may be placed on the coil or all in the slot, or part on the coil and part in the slot as slot lining. The first method is the one most used. For very small machines with partly closed slots, all the insulation between armature coils and core must be placed in the slot as slot lining.

The grade and thickness of insulation necessary on the slot portions of the coil depend upon the voltage of the winding, the size of the coil, and the mechanical stresses it will have to stand when the machine is in operation.

Figure 44 shows a method of insulating the slot portions of armature coils for 250-volt windings with strap-copper coils. The middle conductor of each layer is insulated with cotton tape, half-lapped and treated with insulating varnish. The three coils of each layer are completely insulated before they are placed into the slot. The straight part of the coil is wrapped with empire cloth in such a way that there are three thicknesses on one side and two on the other. The coil end-connections are taped with empire cloth tape, half-lapped. The entire coil is then taped with cotton tape, with the turns of the tape butted on the slot portion of the coil and half-lapped on the end-connections. The coils are then thoroughly dried in an oven, dipped in flexible baking varnish, and baked at a temperature of 100° C. for 8 or 10 hours or until dry.

The slot lining, which is generally fish paper or red-rope paper, from 0.007 to 0.010 in. thick, is used simply to afford mechanical protection to the coils when they are pushed into the slots. The slot lining extends over the top edges of the slot while the armature is being wound. It is cut off flush with the armature surface when the coils

⁶ "Insulation and Design of Electrical Windings," Longmans, Green & Co., London.

are in place and folded over the top of the coil, to protect it when the wedge is put into place. Figure 45 shows a method of insulating the slot portion of wire-wound armature coils for 250-volt windings. After the coils are wound and pulled into the proper shape, they are dipped in insulating varnish and baked. The method of insulating the coil is the same as that shown in Fig. 44, with the exception that a wrapper of paper and varnished cambric instead of empire cloth is used on the straight part of the coil.

Figure 46 shows a method of insulating the slot portion of wire-wound armature coils for 500-volt windings. The varnish-treated coils are taped all over with cotton tape, half-lapped. The taped coils are

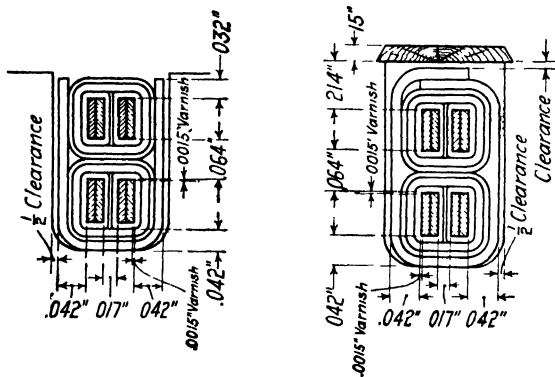


FIG. 47.

again dried, dipped in varnish, and baked. The straight part of the coil is wrapped with empire cloth, or paper and mica, with three thicknesses on one side and two on the other. The coil is then taped all over with cotton tape, with the turns of tape butted on the slot portions and half-lapped on the end-connections. After the coils are treated with insulating varnish and baked, they are placed into the slots in the same way as described for the 250-volt strap-copper coils shown in Fig. 44.

The slot shown in Fig. 46 is not sealed by a wedge, but the coils are held in the slots by band wires. There is no rule by which it is possible to determine when band wires should be used to hold the coils in the slots or when wedges should be used. In general, band wires are used for small-diameter machines, when it is necessary to keep the slot depth as small as possible.

Figure 47 shows a method of insulating direct-current armature coils for open slots, with and without wedge, for voltages including 600 volts.

TABLE IV
INSULATION AND CLEARANCE ALLOWANCE FOR DIRECT-CURRENT
ARMATURE WINDINGS

Voltage	<i>s</i>	<i>2b</i>	Slot Depth			Slot Width		
			Armature Diameter			Armature Diameter		
			10	20	40	10	20	40
0- 300	0.10	1.50	0.27	0.28	0.33	0.060	0.065	0.080
300- 600	0.12	1.75	0.29	0.31	0.37	0.075	0.085	0.095
600-1500	0.14	2.00	0.32	0.34	0.40	0.090	0.095	0.110

In Table IV the depth allowances are for open-type slots closed with wedges. The allowance for the wedge is 0.15 in. For open-type slots with depression for band wires, reduce depth allowance by 0.11 in. For partly closed slots the insulation allowances are taken into account as explained on page 310.

Choice of Armature Winding.—The space occupied by conductor insulation and slot insulation is usually considerable. The proportion of the total slot space occupied by insulation rises rapidly for conductor sections below about 0.01 sq. in. It is, therefore, desirable to choose that winding which will give as large a conductor current as possible. This means that the wave winding is usually preferred for small and medium capacity machines and for high-voltage and slow-speed machines.

Multiplex wave windings are used for large machines with a large number of poles, whereas multiplex lap windings are used only on very large machines, for very high speed. Owing to the limitations imposed by the equalizer connections, multiplex windings are used only when necessary.

For 4-pole machines, it is desirable to choose the armature winding so that the same armature core may be used for two voltages. If, for example, the terminal voltage of a 50-kw. machine is 250 volts when the armature is simplex wave wound, then the same kilowatt-output at one-half the voltage is obtained when the armature is simplex lap wound, with the same number and size of conductors per slot.

The armature winding must also be selected with regard to the maximum voltage between commutator bars, to prevent flashing.⁷ Large-capacity machines will rarely flash when the maximum voltage between commutator bars is 28 volts. For moderate-capacity machines, there is generally no flashing with 35 volts maximum between adjacent

⁷ "Physical Limitations in D.C. Machines," by B. G. Lamme, Trans. A.I.E.E., Vol. 34, p. 1752.

commutator bars, and for very small machines this limit may rise to 60 volts. In general, the maximum voltage between adjacent commutator bars should not exceed 30 volts.

The average voltage between adjacent commutator bars,

$$e_{sa} = \frac{Ep}{K} \text{ volts.} \quad (25)$$

The maximum voltage between adjacent commutator bars for no load or for full load, for machines with compensating windings,

$$e_{sm} = \frac{Ep}{Kf_d} \text{ volts.} \quad (26)$$

For non-compensated machines, the field flux is distorted by the action of the armature flux, and the maximum flux density in the air gap at full load is as much as 30 per cent larger than the maximum flux density in the air gap at no load. The maximum voltage between adjacent commutator bars for non-compensated machines,

$$e_{sm} = \frac{Ep}{Kf_d} 1.3 \text{ volts.} \quad (27)$$

If 0.66 is assumed as an average value for the field form distribution factor, then the average voltage between commutator bars for compensated machines should not exceed 30×0.66 or approximately 20 volts, and for non-compensated machines $\frac{30 \times 0.66}{1.3}$ or approximately 15 volts.

The average voltage between adjacent commutator bars can be calculated for any type of winding in the following manner. The average voltage induced in an armature conductor,

$$e_i = \frac{\phi_i n f_d}{60 \times 10^8} \text{ volts} \quad (28)$$

The average voltage between adjacent commutator bars is then equal to $e_i t_a n_k$, where t_a is the number of turns per armature coil and n_k is the number of conductors in series between adjacent commutator bars for a winding with one turn per coil. For simplex wave winding $n_k = p$, and for simplex lap winding $n_k = 2$. For multiplex wave winding $n_k = p/\mu$, and for multiplex lap winding $n_k = 2/\mu$.

Armature Conductor Section.—The section area of the armature conductor,

$$s_a = \frac{i_a}{A} \text{ sq. in.} \quad (29)$$

The current per path in the armature winding for machines with shunt field windings is

$$i_a = \frac{I \pm i_f}{a} = \frac{I_a}{a} \text{ amperes,} \quad (30)$$

where the negative sign is for motors. The shunt field current must first be estimated. This can be done by means of the curve, Fig. 48, which gives the shunt field current in percentage of the full-load terminal current of the machine.

The current density, A , in the armature copper is limited by the permissible temperature rise of the armature winding and by the effi-

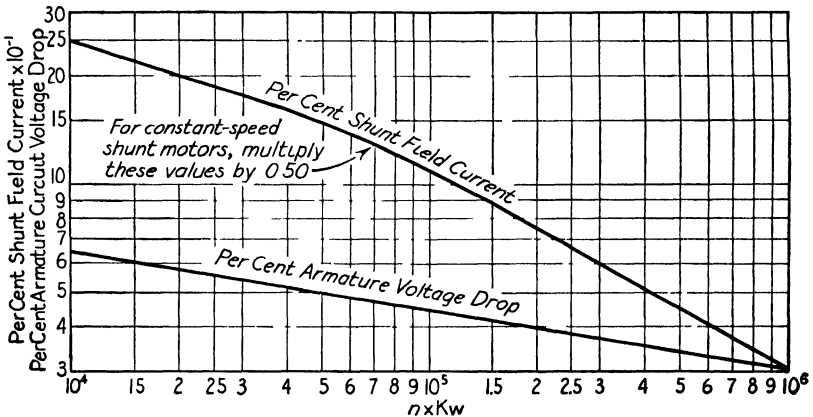


FIG. 48.—Approximate shunt field current and armature circuit voltage drop in per cent of rated current and terminal voltage.

ciency of the machine. The current density to use for the armature conductors can not be accurately predetermined, because of the many variable factors which affect the ventilation of the armature.

Assuming reasonably good ventilation, efficiency rather than temperature rise may be the limiting factor in the choice of A . For a given efficiency, the value of the armature I^2R loss may be assumed and the corresponding value of A calculated. The armature current density should generally be chosen as high as the temperature and efficiency guaranties will permit. This not only leads to a saving in armature copper but also permits the use of shallow armature slots, which aids commutation.

For open-type machines without forced ventilation of the type of construction shown in Chapter I, and with continuous duty rating, the armature conductor current density can be determined with the help of

the curves Fig. 49. For fan-cooled machines slightly higher values may be used, and for totally enclosed machines the values from the curves must be reduced considerably.

Size of Armature Slots.—The dimensions of the armature slots must be so chosen that they will accommodate the armature conductors with the necessary insulation, without producing excessive flux densities in the armature teeth. Wide-open slots produce pulsations of the flux

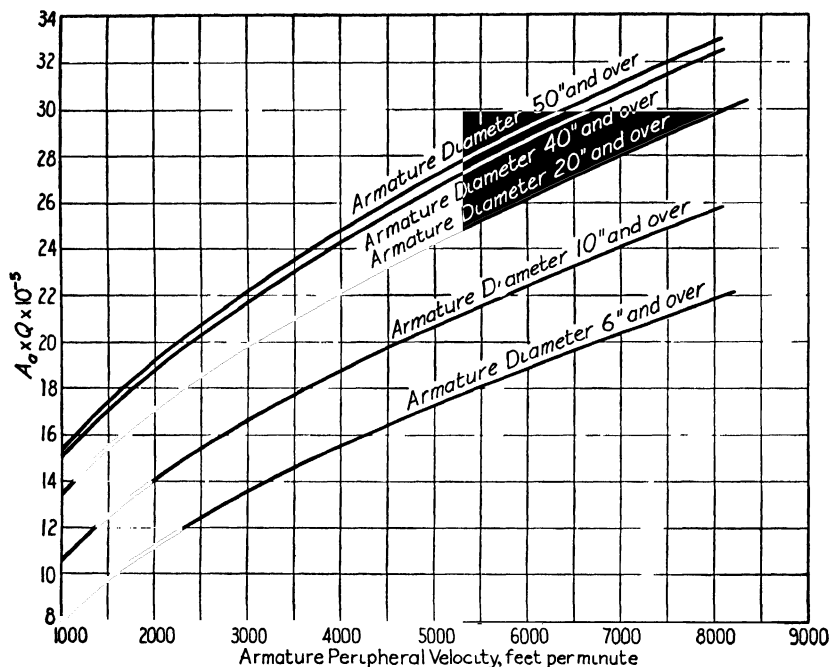


FIG. 49.—Curves to determine armature current density.

in the air gap and increase the reluctance of the flux path in the air gap. The dimensions of the armature slots must therefore also be so chosen that the effect of the slots upon the flux in the air gap will be a minimum. For non-commutating-pole machines, the depth of the slot should generally not exceed 4 times the slot width, because deep slots increase the reactance voltage. For machines with commutating poles, deeper slots may be used, because the commutating pole produces a commutating field to compensate for the reactance voltage. The tooth pitch on the armature circumference,

$$t_1 = \frac{\pi D}{S} \text{ in.} \quad (31)$$

The tooth pitch may serve as a guide when choosing the number of armature slots. For a small tooth pitch the width of the armature tooth will be small, which may lead to difficulties in construction, for the reason that it will be difficult to support the armature teeth at the ventilating ducts and core ends without obstructing the ventilation. The usual range of tooth pitch for direct-current machines is from 0.70 to 1.3 in. For commutating-pole machines it is desirable to reduce the flux pulsation under the commutating pole as much as possible. This is best accomplished by means of a small tooth pitch with narrow slots. This is more fully discussed in a later article, Design of the Commutating Pole. For commutating-pole machines the tooth pitch on the armature surface is usually from 0.70 to 1.0 in. For very small machines with partly closed slots much smaller tooth pitches than those given above are the rule.

The width of the slot should generally be equal to or less than the width of the tooth on the armature circumference. The maximum tooth density, the density at the root of the tooth, should not exceed 155,000 lines per sq. in. For non-commutating poles, high tooth densities are used to minimize the effects of armature reaction, but high tooth densities, especially with high frequencies, produce high iron losses which affect the efficiency and temperature of the machine. High densities in the armature teeth also require a large number of ampere-turns on the shunt field winding, which increases the amount of shunt field copper required. When commutating poles are used, high tooth densities are not necessary, because the commutating pole prevents shifting of the neutral point and furnishes the commutating field.

For the method of insulating the armature coil shown in Fig. 44, the total thickness of the insulation in the width of the slot over the insulated conductors is as follows:

Varnished cambric	$5 \times 0.007 = 0.035$ in.
Paper separator	$2 \times 0.005 = 0.010$
Cotton tape	$2 \times 0.007 = 0.014$
Fish paper slot lining.....	$2 \times 0.010 = 0.020$
	<hr/>
	0.079 in.

and in the depth of the slot:

Varnished cambric.....	$10 \times 0.007 = 0.070$ in.
Cotton tape	$4 \times 0.007 = 0.028$
Fish paper slot lining	$3 \times 0.010 = 0.030$
	<hr/>
	0.128 in.

From the copper tables the dimensions of the armature conductor can be found corresponding to the section area s_a , calculated by formula

29. The method of calculating the width and depth of the slot is shown by the sample designs, page 62.

The dimensions of the armature conductor can be determined approximately by assuming a width of the armature slot equal to 0.4 to 0.45 times the tooth pitch on the armature circumference. Subtracting from this value the space required for insulation plus clearance, the remainder is the space available for the insulated conductors. This space, divided by the number of conductors in the width of the slot, gives the approximate thickness of the insulated conductor. The width of the conductor can be found from the copper table for the thickness and cross-section area required.

Mean-Turn, Resistance, and Weight of Armature Winding.—The shape of the armature coil end-connection for double-layer lap and wave

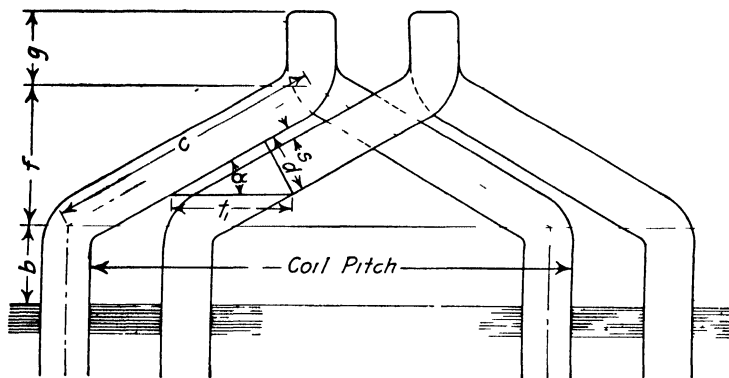


FIG. 50.—Armature coil end-connection.

windings is shown in Fig. 50. The length of the mean-turn can be divided into two parts: the active part, embedded in the armature iron; and the end-connection, the part outside the armature iron. If d in Fig. 50 is the thickness of the coil end-connection plus the clearance between coils, then

$$\sin \alpha = \frac{d}{t_1}, \quad (32)$$

where α is the angle that the straight part of the coil end-connection makes with the edge of the armature coil, and t_1 is the tooth pitch at the armature surface. The clearance, s , between armature coil end-connections depends upon the voltage of the winding and upon the ventilation required; practical values are given in Table IV.

The coil pitch is calculated on a diameter through the mean of the

slot depth and

$$= \frac{\pi(D - d_s)}{p} \text{ in.} \quad (33)$$

The embedded part of the armature coil is allowed to extend beyond the edge of the armature iron a distance b , Fig. 50. Practical values for b are given in Table IV. The loop at the ends of the coils has a mean length approximately equal to the slot depth.

The complete expression for one-half the length of the mean-turn of an armature coil for full pitch windings,

$$L_a = \frac{\pi(D - d_s)}{p \cos \alpha} + 2b + d_s + l \text{ in.} \quad (34)$$

The horizontal extension of the armature coil beyond the armature iron is equal to the sum of $b + f + g$, Fig. 50. Values for b are given in Table IV.

$$f = C \sin \alpha \text{ in.}, \quad (35)$$

and g is approximately equal to the slot depth.

The horizontal extension of the armature coil then is

$$\begin{aligned} &= C \sin \alpha + b + d_s = \frac{1}{2} \frac{\pi(D - d_s)}{p \cos \alpha} \sin \alpha + b + d_s \\ &= \frac{\pi(D - d_s)}{2p} \tan \alpha + b + d_s. \end{aligned}$$

The resistance of the armature winding is

$$R_a = \frac{L_a N r}{a^2 s_a \times 10^6} \text{ ohms,} \quad (36)$$

where $r \times 10^{-6}$ is the resistance of copper per inch of 1 sq. in. cross-section. For 25°C . $r = 0.692$, and $r = 0.826$ for 75°C . If the armature conductor is built up of two or more wires in parallel, as is often done for large machines, the value used for s_a must be the section area of the group of parallel wires.

The resistance of the armature winding at any other temperature, T_2 , can be calculated by formula 37 when its resistance at temperature T_1 is known:

$$R_2 = \frac{234.5 + T_2}{234.5 + T_1} R_1 \text{ ohms.} \quad (37)$$

The bare weight of the armature copper,

$$G_a = L_a N s_a \times 0.321 \text{ lb.} \quad (38)$$

If the armature conductor is built up of two or more parallel wires, s_a must be the section area of the group of parallel wires.

Sample Design: *Design of the Armature Winding.*—From the curve, Fig. 20, Chapter II, the air gap density should be approximately 58 kilo-lines per sq. in. The total flux,

$$\begin{aligned}\phi_t &= \pi D l B_g = \pi \times 25 \times 10.5 \times 58 \\ &= 47,800 \text{ kilo-lines.}\end{aligned}$$

The total number of conductors required is calculated by formula 4. From Fig. 48 for $n \times Kw = 900 \times 300 = 27 \times 10^4$, the approximate voltage drop in the armature, brush contacts, and series and interpole field windings is about 3.8 per cent. The armature induced voltage is then 260 volts.

The average induced voltage per conductor is

$$e_c = \frac{\phi_t n f_d}{60 \times 10^8} = \frac{47,800 \times 10^3 \times 900 \times 0.665}{60 \times 10^8} = 4.76 \text{ volts.}$$

For a simplex lap winding the average voltage between adjacent commutator bars is $2e_c$, or $2 \times 4.76 = 9.52$ volts. This is satisfactory, and the total number of conductors

$$N = \frac{Ea}{e_c} = \frac{260 \times 6}{4.76} = 327.$$

The minimum number of armature slots should be 9 per pole, or 54. For the usual range of slot pitch, 0.70 to 1.30 in., the number of armature slots

$$S = \frac{\pi D}{t_1} = \frac{\pi \times 25}{0.70 \text{ to } 1.3} = 112 \text{ to } 60.$$

Since the number of conductors per slot must be an even integer, 81 slots are selected with 4 conductors per slot.

$$N = 4 \times 81 = 324$$

and

$$\phi_t = \frac{260 \times 6 \times 60 \times 10^8}{324 \times 900 \times 0.665} = 48,300 \text{ kilo-lines.}$$

One turn per coil will be used for this winding, because with two turns per coil only 81 commutator bars would be required, which would lead to a high voltage between adjacent bars. For 2, 4, 6, and in some cases 8 conductors per slot, the number of turns per coil is 1. For larger numbers of conductors per slot, more than 1 turn per coil is generally required.

The sides of the coils are placed in slots 1 and 14, and the back pitch

$$Y_1 = C_s Y_s + 1 = 4 \times 13 + 1 = 53,$$

and the front pitch

$$Y_2 = Y_1 - 2Y_c = 53 - 2 = 51,$$

$$Y_c = 1.$$

The number of commutator bars must always be equal to the number of coils in the armature winding. With 4 conductors per slot and 1 turn per coil, the number of commutator bars will be equal to 162. The average voltage between commutator segments

$$e_{sa} = \frac{Ep}{K} = \frac{260 \times 6}{162} = 9.63 \text{ volts},$$

and the maximum voltage between bars

$$\begin{aligned} e_{sm} &= \frac{Ep}{Kf_d} \times 1.30 = \frac{260 \times 6}{162 \times 0.665} \times 1.30 \\ &= 18.8 \text{ volts.} \end{aligned}$$

The maximum voltage per turn will be equal to the maximum voltage between adjacent commutator bars (formula 24, page 50).

The terminal current at full load

$$\begin{aligned} I &= \frac{Kw \times 10^3}{E_T} = \frac{300 \times 10^3}{250} \\ &= 1200 \text{ amperes.} \end{aligned}$$

From Fig. 48 the shunt field current is approximately 0.63 per cent of the terminal current, or 7.6 amperes.

$$I_a = I + i_f = 1200 + 8 = 1208 \text{ amperes.}$$

The ampere conductors per inch of armature circumference

$$Q = \frac{I_a N}{\pi D a} = \frac{1208 \times 324}{\pi \times 25 \times 6} = 830.$$

For $v = 5890$ ft. per min. and $D = 25$ in., $QA_a = 26.3 \times 10^5$ from Fig. 49, and

$$A_a = \frac{26.3 \times 10^5}{830} = 3170 \text{ amperes per sq. in.}$$

The section area of the armature conductor,

$$S_a = \frac{I_a}{A_a a} = \frac{1208}{3170 \times 6} = 0.0634 \text{ sq. in.}$$

From Table IV the allowance for insulation and clearance is 0.28 in. for the depth and 0.065 in. for the width of the slot. The tooth pitch at the armature circumference,

$$t_1 = \frac{\pi \times D}{S} = \frac{\pi \times 25}{81} = 0.97 \text{ in.}$$

For a slot width equal to $0.4t_1$, $W_s = 0.388$ in. If the conductors are arranged in the slot two wide and two deep, the conductor thickness = $0.5(0.388 - 0.065) = 0.162$ in. From the copper table a conductor 0.109×0.625 in. bare, 0.0656 sq. in. section area, is selected. The dimensions of the slot are then

$$w_s = 2(0.109 + 0.014) + 0.065 = 0.311; \text{ use } 0.31 \text{ in.}$$

$$d_s = 2(0.625 + 0.014) + 0.280 = 1.558; \text{ use } 1.56 \text{ in.}$$

At this point it is well to check the flux density at the root of the teeth as explained in Chapter IV. The armature length is divided into sections by 3 radial ventilating ducts each $\frac{3}{8}$ in. wide. The total section area of the teeth at the root

$$\begin{aligned} S_{t2} &= (10.5 - 3 \times \frac{3}{8})0.92[\pi(25 - 2 \times 1.56) - 81 \times 0.31] \\ &= 377 \text{ sq. in.} \end{aligned}$$

The tooth density at the root of the teeth

$$B_{t2} = \frac{\phi_t}{S_{t2}} = \frac{48,300 \times 10^3}{377} = 128.0 \text{ kilo-lines per sq. in.}$$

The length of the one-half mean-turn of the armature coil is calculated as given on page 59,

$$\sin \alpha = \frac{d}{t_1} = \frac{0.31 + 0.10}{0.97} = 0.422$$

$$\alpha = 25^\circ \text{ and } \cos \alpha = 0.906, \tan \alpha = 0.466$$

$$\begin{aligned} L_a &= \frac{\pi(D - d_s)}{p \cos \alpha} + 2b + d_s + l \\ &= \frac{\pi(25 - 1.56)}{6 \times 0.906} + 1.5 + 1.56 + 10.5 \\ &= 27.10 \text{ in.} \end{aligned}$$

$$\begin{aligned} l_i &= \frac{\pi(D - d_s)}{2p} \tan \alpha + b + d_s \\ &= \frac{\pi(25 - 1.56)}{2 \times 6} 0.466 + 0.75 + 1.56 = 5.17 \text{ in.} \end{aligned}$$

The resistance of the armature winding is calculated for 75° C. because the A.I.E.E. standardization rules specify that the copper losses for all loads should be calculated for a temperature of 75° C.

$$R_a = \frac{L_a N r}{a^2 s_a \times 10^6} = \frac{27.1 \times 324 \times 0.826}{6^2 \times 0.0656 \times 10^6}$$

$$= 0.00307 \text{ ohm.}$$

The voltage drop in the armature winding,

$$I_a R_a = 1208 \times 0.00307 = 3.71 \text{ volts,}$$

or 1.48 per cent of the full-load terminal voltage.

The weight of the armature copper

$$G_a = L_a N s_a \times 0.321 = 27.1 \times 324 \times 0.0656 \times 0.321$$

$$= 185 \text{ lb.}$$

Fifty-four equalizer connections are recommended for this winding, 1 for every 3 commutator bars (see page 41).

CHAPTER IV

THE MAGNETIC CIRCUIT

THE flux per pole that crosses the air gap and enters the armature is calculated by formula 2,

$$\phi = \frac{Ea \times 60 \times 10^8}{pNn}.$$

A definite magnetomotive force is required on each pole, to send this flux through the magnetic circuit. The fundamental law giving the relation between flux and magnetomotive force is expressed as follows:

$$\phi = \frac{0.4 \times \pi \text{ AT } \mu s}{l}.$$

The ampere-turns required to send the flux ϕ through a magnetic circuit of length l and section area s are,

$$\text{AT} = \frac{l\phi}{0.4 \times \pi \mu s}.$$

The flux, ϕ , divided by the section area of the magnetic circuit is equal to the flux density, B , and the ampere-turns,

$$\text{AT} = \frac{lB}{0.4 \times \pi \mu}. \quad (39)$$

In formula 39, l is expressed in centimeters and B in lines per square centimeter. When l is expressed in inches and B in lines per square inch,

$$\text{AT} = \frac{lB}{3.2 \times \mu}. \quad (40)$$

For air, the permeability, μ , is equal to 1; for iron and steel, it is greater than 1 and is not constant but depends upon the flux density. The magnetic characteristics of magnetic materials can be determined only by test. The tests consist of determining the magnetizing force required for different flux densities. For the designer, it is more con-

venient if the magnetizing force, H , is expressed as ampere-turns per inch of flux path instead of in c.g.s. electromagnetic units. If at equals the ampere-turns per inch of flux path, then

$$at = H \times 2.03, \quad (41)$$

where H is the magnetizing force expressed in c.g.s. electromagnetic units. Standard saturation curves for cast iron, cast steel, and open hearth sheet steel, such as used for electrical apparatus, are shown in the Appendix. For a magnetic circuit through iron or steel, the ampere-turns,

$$AT = at \times l, \quad (42)$$

where at equals the ampere-turns per inch length of flux path, as found from the standard saturation curves, and l is the length.

The magnetic circuit for a multi-pole machine is illustrated in Fig. 51, which shows that the magnetic circuit per pair of poles comprises the yoke or field ring, the pole, the air gap, the armature teeth, and the armature iron below the teeth. The material is not the same for the different parts of the magnetic circuit; neither is the density the same. The ampere-turns per pole must therefore be calculated separately for each part of the magnetic circuit. The symbols used to calculate the ampere-turns per pole are as follows:

Material	Magnetic Section	Density	Ampere-turns per Inch	Length of Flux Path	Ampere-turns per Pole
Air gap.....	s_g	B_g	δk	AT_g
Teeth.....	s_t	B_t	at_t	l_t	AT_t
Armature yoke.....	s_{ya}	B_{ya}	at_{ya}	l_{ya}	AT_{ya}
Pole body.....	s_p	B_p	at_p	l_p	AT_p
Field yoke.....	s_{yf}	B_{yf}	at_{yf}	l_{yf}	AT_{yf}

The total ampere-turns per pole for no load and normal voltage,

$$ATP = AT_g + AT_t + AT_{ya} + AT_p + AT_{yf}. \quad (43)$$

Ampere-Turns for the Air Gap.—The maximum flux density in the air gap,

$$B_g = \frac{\phi_t}{s_g}. \quad (44)$$

The flux in the air gap distributes itself over the axial length of the armature, as shown in Fig. 52. The reluctance of the ventilating ducts is equivalent to a reduction of the armature length l , and the fringing at the ends of the core is equivalent to an increase in l . For the purpose of the designer, it is generally sufficiently accurate to assume that these two effects neutralize each other. When the axial length of the pole shoe, l_1 , is equal to the axial length of the armature, the length of

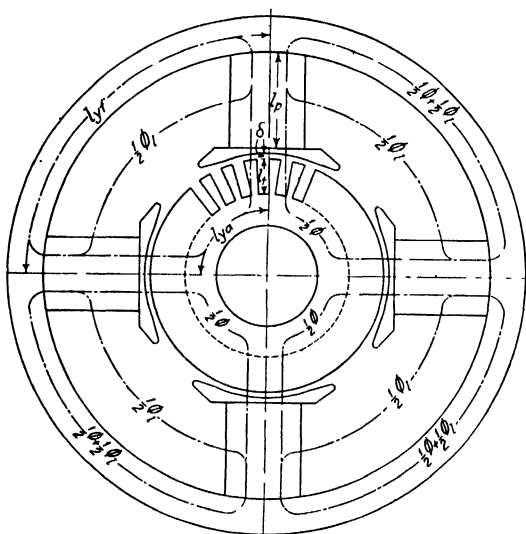


FIG. 51.—Magnetic circuit of four-pole machine without commutating poles.

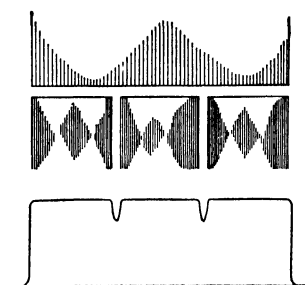


FIG. 52.

the air gap section, l_g , can generally be taken equal to the armature length, and when the axial length of the pole shoe is less than the axial length of the armature,

$$l_g = \frac{1}{2}(l_1 + l).$$

The section area of the air gap,

$$s_g = \pi D l_g. \quad (45)$$

The ampere-turns per pole for the air gap for a smooth armature without slots,

$$\text{AT}_g = \frac{B \delta}{3.2}.$$

For slotted armatures, the reluctance of the air gap is increased, because of the low permeance of the slot space and the high densities in the teeth.

This effect is taken into account by multiplying the ampere-turns for the air gap for a smooth armature by a factor,¹

$$k = \frac{t_1}{w_{t1} + y \delta}, \quad (46)$$

where y is taken from the curve Fig. 53.

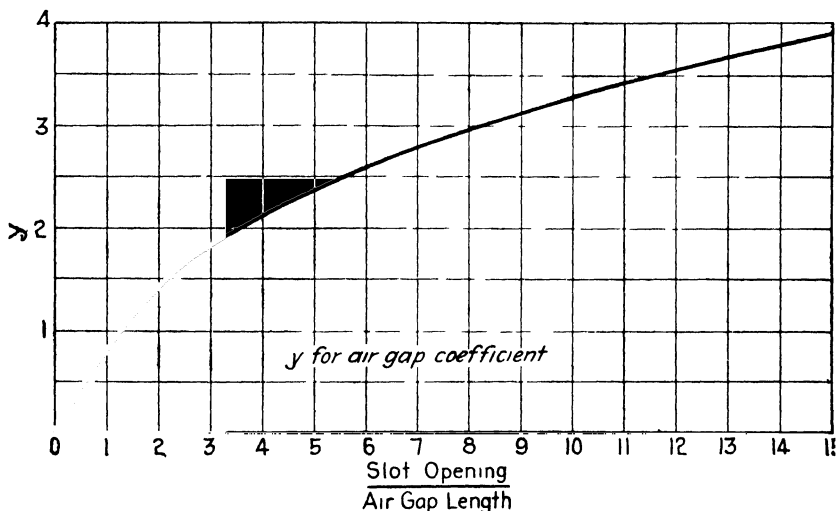


FIG. 53.

The ampere-turns per pole for slotted armatures,

$$AT_a = \frac{B_p \delta k}{3 \cdot 2}. \quad (47)$$

The length of the air gap, δ , may be estimated as explained on page 84, Chapter V.

Ampere-Turns for the Armature Teeth.—When the armature slots have parallel walls, the flux density in the armature teeth is lower at the top of the tooth than at the root of the tooth. The flux density at the top of the tooth,

$$B_{t1} = \frac{\phi_t}{s_{t1}}. \quad (48)$$

¹ "Die Gleichstrommaschine," by Arnold and La Cour, Vol. 1, p. 134, 3rd ed., Julius Springer, Berlin; Electrical World, Vol. 38, p. 884, 1901, and A.I.E.E. Journal, Vol. 46, 1927, p. 431.

The tooth pitch on the armature surface is given by formula 31,

$$t_1 = \frac{\pi D}{S}$$

and the width of the tooth at the armature surface,

$$w_{t1} = t_1 - w_s. \quad (49)$$

The length of the armature is generally divided into sections by radial ventilating ducts, as explained on page 5, Chapter I. A sufficient number of ducts should generally be used, so that the length of each section of iron between two ventilating ducts does not exceed 3 in.

The section area of the armature teeth at the armature surface,

$$s_{t1} = w_{t1}(l - n_d w_d) S k_1, \quad (50)$$

where k_1 is the lamination factor and is generally equal to 0.88 to 0.93.

The section area of the teeth at the bottom of the slot,

$$s_{t2} = w_{t2}(l - n_d w_d) S k_1, \quad (51)$$

and the flux density at the root of the teeth,

$$B_{t2} = \frac{\phi_t}{s_{t2}}. \quad (52)$$

To avoid excessive iron losses in the teeth and to limit the magnetomotive force required to send the flux through the teeth, the density at the root of the teeth should generally not exceed 155,000 lines per sq. in.

In calculating the ampere-turns for the armature teeth, the fact that the flux density increases and the permeance of the iron in the teeth decreases in passing from the top to the bottom of the tooth must be taken into account. Various methods have been proposed to determine the ampere-turns required to send the flux through the armature teeth. The method which uses for the average ampere-turns per inch, the ampere-turns corresponding to a tooth density $\frac{1}{3}$ slot depth from the minimum tooth width has been found to be very satisfactory. The width of the armature tooth at a point $\frac{1}{3}$ slot depth from the minimum tooth width,

$$w_{t3} = \frac{\pi(D - 1 \frac{33d_s}{S})}{S} - w_s. \quad (53)$$

In the design of the armature of some direct-current machines very high flux densities in the teeth often can not be avoided. A portion of the magnetic flux will then pass through the slot and the radial ventilating ducts. The total iron section of the teeth at a point $\frac{1}{3}$ slot depth

from the root of the tooth is $l_n Sw_{i3}$, and the total air and iron section is lSt_3 . If B_{i3} is the real tooth flux density at this section and at the corresponding ampere-turns per inch, then the flux passing through one tooth pitch is

$$B_{i3} l_n w_{i3} + 3.2at(lt_3 - l_n w_{i3}) = B_{i3}' l_n w_{i3}.$$

Dividing both sides of the equation by $l_n w_{i3}$ gives

$$B_{i3}' = B_{i3} + 3.2at \left(\frac{lt_3}{l_n w_{i3}} - 1 \right) = B_{i3} + k_i at,$$

where B_{i3}' is the apparent flux density equal to $\frac{\phi_t}{l_n Sw_{i3}}$ and

$$k_i = 3.2 \left(\frac{lt_3}{l_n w_{i3}} - 1 \right).$$

By assuming values for B_{i3} , the real tooth flux density, the apparent tooth flux density can be calculated and plotted against the ampere-turns per inch. The ampere-turns per pole for the teeth

$$AT_t = at_l l_t, \quad (54)$$

where l_t is the length of the flux path in the teeth and is equal to the slot depth.

Ampere-Turns for the Armature Yoke.—It is apparent from Fig. 51 that each section of the armature iron below the slots carries one-half of the flux per pole. The flux per pole

$$\phi = \frac{\phi_t f_d}{p}$$

and the flux density in the armature yoke

$$B_{ya} = \frac{\phi}{s_{ya}}. \quad (55)$$

If d_{ya} is 2 times the radial depth of the armature iron below the slots, then

$$s_{ya} = (l - n_d w_d) d_{ya} k_1, \quad (56)$$

where $d_{ya} = (D - 2d_s) - D_i$. The flux density in the armature yoke is first assumed and

$$d_{ya} = \frac{\phi}{(l - n_d w_d) k_1 B_{ya}}. \quad (57)$$

The ampere-turns per inch for the value of B_{ya} are found from the standard saturation curve for the material used for the armature

laminations. The ampere-turns per pole required to send the flux through the armature iron below the slots

$$AT_{ya} = at_{ya}l_{ya}. \quad (58)$$

The length of the flux path, l_{ya} , may be taken equal to one-half the pole pitch on the mean circumference of the armature yoke:

$$l_{ya} = \frac{[D - (2d_s + \frac{1}{2}d_{ya})]\pi}{2p}. \quad (59)$$

When commutating poles are used, the flux in the armature iron below the slots is increased in one part and decreased in the other, because of the presence of the commutating-pole flux. The effect of the commutating-pole flux upon the ampere-turns per pole for the armature yoke may be calculated as explained by Dr. Arnold.²

The saturation curve for the commutating-pole magnetic circuit should be a straight line, so that the commutating-pole flux will increase directly with the armature current. To accomplish this, the flux densities in the armature yoke must be chosen well below the "knee" of the saturation curve. For normal designs, the flux densities in the armature core will be so low that the correction for the main pole ampere-turns for the armature yoke, because of the presence of the commutating-pole flux, will not be necessary.

For commutating-pole direct-current motors and generators, the flux density in the armature yoke is therefore generally chosen equal to from 35,000 to 75,000 lines per sq. in.

Ampere-Turns for the Pole.—The flux in the poles is not constant for all sections, but varies, being greatest near the yoke and decreasing toward the pole shoe. Figure 51 shows that the magnetic flux per pole is made up of two parts, one ϕ , which crosses the air gap and enters the armature; and the other, ϕ_l , which does not cross the air gap but passes between poles and is called the leakage flux. The ratio of $\phi + \phi_l$ to ϕ is called the leakage factor,

$$\lambda = \frac{\phi + \phi_l}{\phi} = 1 + \frac{\phi_l}{\phi}. \quad (60)$$

To calculate the flux density in the pole, it may be assumed, without appreciable error, that the flux in the pole is uniform and equal to $\phi\lambda$.

² "Die Gleichstrommaschine," Vol. 1, p. 432, Julius Springer, Berlin; see also "Design of Auxiliary Poles," by A. Brunt, *Electrical Review and Western Electrician*, p. 513, Sept. 9, 1911.

The flux density in the pole

$$B_p = \frac{\phi \lambda}{s_p} \quad (61)$$

The section area of the pole

$$s_p = l_1 w_p \quad (62)$$

The flux density, B_p , should generally not exceed 100,000 lines per sq. in. for laminated poles and 80,000 lines per sq. in. for cast steel poles. From the saturation curve for the kind of material used for the pole, the ampere-turns per inch length of flux path corresponding to the pole density are found, and

$$AT_p = at_p l_p \quad (63)$$

The length of the flux path for the field pole depends upon the space required for the field winding. It can be determined, approximately, by the following method. The shunt field current may be estimated with the help of the curve Fig. 49. The current densities usually satisfactory for shunt field windings are given in Table V. The section area of the field winding conductor is, then,

$$S_f = \frac{I_f}{A_f} \text{ sq. in.}$$

The space factor f_s of the conductor is the ratio of the net copper section area to the insulated conductor diameter squared. The ampere-turns per pole required to send the flux through the air gap, armature teeth, and yoke are calculated as shown above. The ampere-turns per pole required to send the flux through the field pole and field yoke at full load may be taken equal to 30τ . The field winding ampere-turns per pole are then

$$ATP_f = \frac{V_f}{V_0} (AT_g + AT_t + AT_{ya}) + 30\tau,$$

where V_f is the full-load terminal voltage and V_0 is the no-load terminal voltage. The ampere-turns that can be wound per inch height of field winding are given in Table V. The height of the winding space required,

$$h_f = \frac{ATP_f}{at} \text{ in.}$$

The allowance for insulation and clearance of the field winding is usually from 0.10 to 0.15 τ . The radial length of pole which is also the length of the flux path in the pole is, then,

$$l_p = h_f + (0.10 \text{ to } 0.15)\tau \text{ in.}$$

Ampere-Turns for the Field Yoke.—The flux carried by each section of the yoke is equal to $\frac{1}{2}\phi\lambda$, as Fig. 51 shows. The density in the yoke,

$$B_{yf} = \frac{\phi\lambda}{s_{yf}}. \quad (64)$$

TABLE V

v	A_f	Ampere-Turns per Inch, at		
		$f_s = 0.40$	0.60	0.8
1000	1085	590	670	755
2000	1215	615	727	825
3000	1330	640	768	877
4000	1425	655	795	920
5000	1505	672	825	960
6000	1570	685	845	995
7000	1622	700	865	1030
8000	1670	715	885	1063

The section area of the yoke

$$s_{yf} = l_2 d_{yf}. \quad (65)$$

For machines with bearings supported by end-brackets, the yoke should generally extend over the field winding, as shown in Figs. 16 and 18. For machines with pedestal-type bearings, the field windings often extend beyond the yoke, as shown in Fig. 1. The thickness of the yoke, d_{yf} , must be large enough to give the frame the required mechanical strength, and to give a yoke section such that the ampere-turns required to send the flux through the yoke will not be too large. The flux density, rather than the mechanical strength, is generally the determining factor in the choice of the thickness of the field yoke. The thickness of the yoke

$$d_{yf} = \frac{\phi\lambda}{l_2 B_{yf}}. \quad (66)$$

The yoke must carry the flux of the commutating pole as well as the flux of the main poles. The effect of the presence of the commutating-pole flux in the field yoke may be calculated in the same way as for the armature iron below the slots. For normal designs, the flux density in the yoke is generally so low that this correction is not necessary. For a cast steel yoke, B_{yf} should not exceed 65,000 lines per sq. in., and for a rolled steel yoke, B_{yf} should not exceed 80,000 lines per sq. in.

The Field Leakage Factor.—The leakage flux may be divided into four parts, as shown in Fig. 54. The leakage flux for each of the four paths is as follows:

- ϕ_{11} the leakage between inner pole shoe surfaces,
- ϕ_{12} the leakage between the pole shoe end surfaces,
- ϕ_{13} the leakage between inner pole body surfaces,
- ϕ_{14} the leakage between pole body end surfaces.

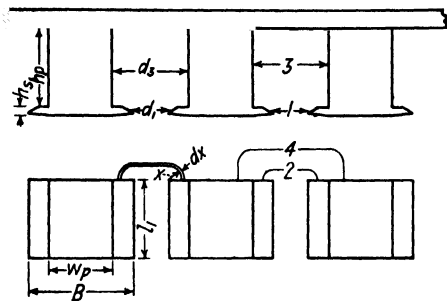


FIG. 54.—Field leakage flux paths.

The leakage flux per pole,

$$\phi_l = \phi_{11} + \phi_{12} + \phi_{13} + \phi_{14}.$$

When the magnetomotive force acting on each of the leakage paths and the reluctance of each path are known, the leakage flux can be calculated as follows:

$$\text{Flux} = \frac{\text{m.m.f.}}{\text{Reluctance}}.$$

The m.m.f. acting across paths 1 and 2 = $2(AT_o + AT_i + AT_{va}) = 2X$. Since the greatest part of the leakage flux passes through air, the reluctance of the part in the iron may be neglected. Assuming that the sides of adjacent poles are parallel, the leakage may be calculated as follows:³

The leakage flux per pole for path 1,

$$\begin{aligned}\phi_{11} &= 2 \times 3.2 \times 2 X \frac{l_1 h_s}{d_1} \\ &= 13X \frac{l_1 h_s}{d_1}.\end{aligned}$$

³ "Electrical Machine Design," by Gray, p. 51, McGraw-Hill Book Co., New York.

The leakage flux per pole for path 2,

$$\begin{aligned}\phi_{l2} &= 4 \times 3.2 \times 2X \int_0^{B/2} \frac{h_s dx}{d_1 + \pi x} \\ &= 25.6X \frac{h_s}{\pi} \log_e \left(\frac{d_1 + \frac{\pi B}{2}}{d_1} \right) \\ &= 19X h_s \log_{10} \left(1 + \frac{\pi B}{2d_1} \right)\end{aligned}$$

The m.m.f. across paths 3 and 4 is zero at the yoke and equal to $2X$ at the pole shoe, and the average value is equal to X . The leakage flux per pole for path 3

$$\begin{aligned}\phi_{l3} &= 2 \times 3.2 \times X \frac{l_1 h_p}{d_3} \\ &= 6.5X \frac{l_1 h_p}{d_3}.\end{aligned}$$

The leakage flux per pole for path 4

$$\begin{aligned}\phi_{l4} &= 4 \times 3.2X \int_0^{B/2} \frac{h_p dx}{d_3 + \pi x} \\ &= 4 \times 3.2X \frac{h_p}{\pi} \log_e \left(\frac{d_3 + \frac{\pi w_p}{2}}{d_3} \right) \\ &= 9.5X h_p \log_{10} \left(1 + \frac{\pi w_p}{2d_3} \right) \\ \lambda &= \frac{\phi + \phi_l}{\phi} = 1 + \frac{\phi_l}{\phi}.\end{aligned}$$

The leakage factor obtained by these formulas is usually too low for 2-, 4-, and 6-pole machines, because no attempt is made to calculate the flux that passes from the pole body side and end surfaces directly to the yoke. For 2-, 4-, and 6-pole machines, the leakage factor is generally assumed. For preliminary calculations, the following values may be used:

4- and 6-pole machines	= 1.20
Multipolar machines 20 to 50 in. in diameter	= 1.20
Multipolar machines larger than 50 in. in diameter	= 1.18

The armature ampere-turns per pole

$$\text{ATP}_a = \frac{I_a N}{2pa}$$

To give stable operation under changing load conditions the ampere-turns per pole for the field winding should be approximately 80 per cent of the armature ampere-turns per pole. By changing the length of the air gap the ampere-turns for the field winding can be adjusted to meet this requirement.

The Open-Circuit Saturation Curve.—The open-circuit saturation curve gives the relation between the terminal voltage at no-load and the corresponding ampere-turns per pole. The method of calculating the ampere-turns for a given voltage has been given above. For the air gap, the permeability is constant for all values of induction. The air gap ampere-turns will therefore vary directly with the voltage. For the remainder of the magnetic circuit, the flux densities must be calculated by direct proportion for the various voltages. The corresponding ampere-turns per inch are taken from the standard saturation curve and multiplied by the length of the respective flux paths to obtain the ampere-turns per pole.

Sample Design: Magnetic Circuit.—The armature laminations are punched from 29 gauge open-hearth electric sheet steel. The length of the armature is divided into sections by 3 radial ventilating ducts each $\frac{3}{8}$ in. wide. The net length of the armature

$$l_n = (10.5 - 3 \times 0.375)0.92 = 8.62 \text{ in.}$$

The flux density at the root of the tooth was checked in the previous chapter and found to be satisfactory. The ampere-turns per pole required to send the flux through the teeth is calculated as explained on page 69.

$$lSt_3 = 10.5\pi(25 - \frac{4}{3} \times 1.56) = 756$$

$$l_nSw_{t3} = 8.62[\pi(25 - \frac{4}{3} \times 1.56) - 81 \times 0.31] = 404$$

$$k_t = 3.2 \left(\frac{756}{404} - 1 \right) = 2.78$$

$$B_{t3}' = B_{t3} + 2.78at.$$

The curve, Fig. 55, shows the values of ampere-turns per inch for various values of B_{t3} . For the full-load induced voltage, 260 volts,

$$B_{t3}' = \frac{\phi_t}{l_n w_{t3} S} = \frac{48,300}{404} = 120 \text{ kilo-lines per sq. in.}$$

From the curve Fig. 55, at $a_t = 346$ and the ampere-turns per pole for the teeth

$$AT_t = 346 \times 1.56 = 540.$$

For other values of induced voltage

E	230	260	285	310
B_{ts}'	106.5	120	131	142.5
a_t	112	346	640	1020
AT_t	175	540	998	1590

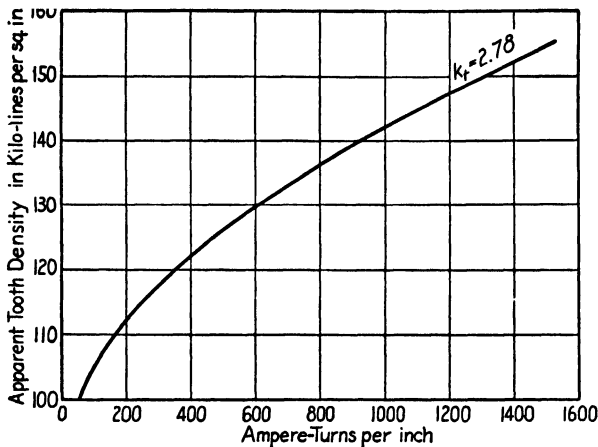


FIG. 55.

The armature ampere-turns per pole

$$ATP_a = \frac{NI_a}{2ap} = \frac{324 \times 1208}{2 \times 6 \times 6} = 5440.$$

For this design the ampere-turns per pole for gap and teeth are to be approximately 0.85 of the armature ampere-turns per pole.

$$AT_g + AT_t = 0.85 \times 5440 = 4620.$$

The ampere-turns per pole for the air gap for full-load induced voltage are, then,

$$AT_g = 4620 - 540 = \frac{B_g \delta k}{3.2}.$$

The length of the air gap required can now be calculated by assuming a value for the air gap coefficient k . The air gap density for $E = 260$,

$$B_g = \frac{48,300}{\pi \times 25 \times 10.5} = 58.5 \text{ kilo-lines per sq. in.}$$

Assuming that $k = 1.1$,

$$\delta = \frac{3.2 \times 4080}{1.1 \times 58.5 \times 10^3} = 0.203 \text{ in.}; \text{ use } 0.20 \text{ in.}$$

For this gap length

$$k = \frac{0.97}{0.66 + 1.25 \times 0.20} = 1.067$$

and

$$\text{AT}_g = \frac{58.5 \times 10^3 \times 0.20 \times 1.067}{3.2} = 3900.$$

For other induced voltages:

E	230	260	285	310
B_g	51.7	58.5	64.1	69.7
AT_g	3450	3900	4280	4650

The flux per pole

$$\begin{aligned} \phi &= \frac{\phi_i f_d}{p} = \frac{48,300 \times 0.665}{6} \\ &= 5350 \text{ kilo-lines.} \end{aligned}$$

For a commutating-pole machine and a frequency of 45 cycles per sec., the armature yoke density should be approximately 75 kilo-lines per sq. in. The depth of the armature yoke

$$\begin{aligned} d_{ya} &= \frac{\phi}{(l - n_d w_d) k_1 B_{ya}} = \frac{5350}{(10.5 - 3 \times \frac{3}{8}) 0.92 \times 75} \\ &= 8.27 \text{ in.} \end{aligned}$$

The inside diameter of the armature

$$\begin{aligned} D_i &= D - 2d_s - d_{ya} = 25 - 2 \times 1.56 - 8.27 \\ &= 13.6 \text{ in.}; \text{ use } 13.5 \text{ in.} \end{aligned}$$

$$d_{ya} = 25 - 3.12 - 13.5 = 8.38 \text{ in.}$$

$$B_{ya} = \frac{5350}{8.62 \times 8.38} = 74.0 \text{ kilo-lines per sq. in.}$$

The armature yoke density is therefore 74 kilo-lines per sq. in., and the ampere-turns per inch from the standard saturation curve for open-hearth steel, $\text{at}_{ya} = 9$.

The length of the flux path in the armature yoke

$$\begin{aligned} l_{ya} &= \frac{[D - (2d_s + \frac{1}{2}d_{ya})]\pi}{2p} = \frac{[25 - (2 \times 1.56 + \frac{1}{2} \times 8.38)]\pi}{2 \times 6} \\ &= 4.6 \text{ in.} \end{aligned}$$

The ampere-turns per pole for the armature yoke

$$AT_{ya} = at_{ya}l_{ya} = 9 \times 4.6 = 42.$$

The ampere-turns per pole for the armature yoke for various voltages are:

E	230	260	285	310
B_{ya}	65.5	74.0	81.1	88.2
at_{ya}	7.0	9.0	13.0	18.0
AT_{ya}	32	42	60	83

The field poles for this generator will be built up of sheet steel laminations, punched from open-hearth sheets approximately 0.023 in. thick. A flux density of 95 kilo-lines per sq. in. is selected for the pole body. For machines with half as many commutating poles as main poles, slightly lower pole densities should be used because the commutating-pole flux returns through the main poles. The leakage flux is assumed to be 20 per cent of the useful flux per pole, and the axial length of the pole is made equal to the armature length, that is,

$$l_1 = 10.5 \text{ in.}$$

The section area of the pole body

$$s_p = \frac{\phi \lambda}{B_p} = \frac{5350 \times 1.20}{95} = 67.6 \text{ sq. in.}$$

The width of the pole body

$$w_p = \frac{s_p}{l_1} = \frac{67.6}{10.5} = 6.44; \text{ use } 6.5 \text{ in.,}$$

and $B_p = 94.1$ kilo-lines per sq. in.

The radial height of the field pole is estimated as explained on page 72. The approximate field current as found from Fig. 48 is 7.6 amperes. The current density for the field winding conductor is taken from Table V. The section area of the conductor for the field winding is then

$$s_f = \frac{7.6}{1560} = 0.00487 \text{ sq. in.}$$

A number 13 square double-cotton-covered copper wire is selected from the copper table. The space factor for the wire

$$f_s = \frac{0.00465}{0.083^2} = 0.675.$$

The ampere-turns that can be wound per inch of radial pole height are 890, from Table V. The sum of the ampere-turns per pole required for

the gap, teeth, and armature yoke for 230 volts is 3646. The estimated ampere-turns per pole for full load

$$\text{ATP}_f = \frac{250}{230} 3646 + 30\tau = 4362.$$

The radial height of the field pole

$$l_p = \frac{4362}{890} + 0.12\tau = 6.47 \text{ in.}$$

The inside diameter of the field yoke $D_{yi} = D + 2\delta + 2l_p = 25 + 2 \times 0.20 + 2 \times 6.47 = 38.34$; use 38.5 in. Then $l_p = 6.55$ in. The ampere-turns per pole for the field pole for various induced voltages are:

E	230	260	285	310
B_p	83.2	94.1	103	112
at_p	29	46.0	78	160
AT_p	190	301	510	1050

The field yoke will be cast steel, and the density 65 kilo-lines per sq. in. The section area

$$s_{yf} = \frac{\phi\lambda}{B_{yf}} = \frac{5350 \times 1.20}{65} = 98.7 \text{ sq. in.}$$

This is the section area of the field yoke on both sides of the diameter.

The generator is to be part of a motor-generator set, and the bearings are to be mounted in pedestals bolted to the base. The extension of the yoke beyond the edge of the pole will be 2.5 in., and the axial length of the field yoke will be 15.5 in.

Two times the depth or thickness of the rectangular yoke section

$$d_{yf} = \frac{s_{yf}}{l_2} = \frac{98.7}{15.5} = 6.37; \text{ use } 6.5 \text{ in.}$$

The flux density in the field yoke

$$B_{yf} = \frac{\phi\lambda}{s_{yf}} = \frac{5350 \times 1.20}{6.5 \times 15.5} = 63.7 \text{ kilo-lines.}$$

The outside diameter

$$D_{yo} = D_{yi} + d_{yf} = 38.5 + 6.5 = 45 \text{ in.}$$

The length of the flux path is taken on the mean diameter

$$l_{yf} = \frac{(D_{yi} + \frac{1}{2}d_{yf})\pi}{2p} = \frac{(38.5 + \frac{1}{2} \times 6.5)\pi}{2 \times 6} = 10.9 \text{ in.}$$

The ampere-turns per inch of flux path taken from the standard saturation curve for cast steel are $at_{yf} = 19$, and the ampere-turns per pole for the field yoke

$$AT_{yf} = at_{yf}l_{yf} = 19 \times 10.9 = 207$$

The ampere-turns per pole for the field yoke for various induced voltages are:

E	230	260	285	310
B_{yf}	56.4	63.7	69.9	76.0
at_{yf}	15	19	22	27
AT_{yf}	164	207	240	294

The total ampere-turns per pole for the magnetic circuit for various induced voltages are summed up below.

E	230	260	285	310
AT_t	175	540	998	1590
AT_g	3450	3900	4280	4650
AT_{ga}	32	42	60	83
AT_p	190	301	510	1050
AT_{yf}	164	207	240	294
ATP	4011	4990	6088	7667

The open-circuit saturation curve plotted from these values is shown in Fig. 57.

CHAPTER V

ARMATURE REACTION AND FIELD WINDING DESIGN

Armature Demagnetizing Ampere-Turns.—Figure 56 shows a four-pole generator with the brushes shifted from the no-load neutral, a distance $b_s/2$ inches of armature circumference. The armature demagnetizing ampere-turns per pole,

$$ATP_d = \frac{1}{2}b_s Q. \quad (67)$$

The ampere conductors per inch of armature circumference,

$$Q = \frac{I_a N}{a\pi D}$$

and

$$\frac{1}{2}b_s = \frac{2\beta\pi D}{360p},$$

where the angle β is expressed in electrical degrees. Making the substitutions, the demagnetizing ampere-turns per pole,

$$\begin{aligned} ATP_d &= \frac{2\beta\pi D I_a N}{360pa\pi D} \\ &= \frac{2\beta}{180} \frac{I_a N}{2pa}. \end{aligned}$$

The armature ampere-turns per pole,

$$ATP_a = \frac{I_a N}{2ap} \quad (68)$$

and the armature demagnetizing ampere-turns per pole,

$$ATP_d = \frac{2\beta}{180} ATP_a \quad (69)$$

To obtain satisfactory commutation in machines without commutating poles, the brushes are shifted from the no-load neutral, so that the coil sides short-circuited by the brushes will lie in a field strength, at no-load,

equal to from 6500 to 13,000 lines per sq. in. The angle corresponding to this brush displacement is generally approximately 18 electrical degrees.

When the machine has commutating poles, the commutating pole produces the commutating field, and the brushes remain in the no-load neutral position for all loads. For commutating-pole machines the angle of brush displacement is zero and therefore also the armature demagnetizing ampere-turns.

Armature Cross-Magnetizing Ampere-Turns.

—All of the armature conductors lying outside of the double angle of brush displacement, 2β , Fig. 56, set up the armature cross-magnetizing field. The flux produced by the conductors that do not lie under the pole shoe has its path so largely in air that it may be neglected. The armature ampere-turns per pole that produce the cross-magnetizing field,

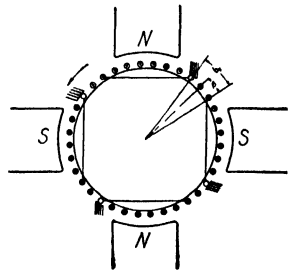


FIG. 56.—Demagnetizing and cross-magnetizing ampere-turns of a four-pole generator.

$$\begin{aligned} ATP_c &= \frac{1}{2} \tau f_a \frac{I_a N}{a \pi D} = \frac{1}{2} f_a \frac{\pi D}{p} \frac{I_a N}{a \pi D} \\ &= f_a ATP_a. \end{aligned} \quad (70)$$

When the magnetic circuit becomes saturated, the reluctance of the path of the main pole flux is increased, because of the distortion of the air gap flux by the armature cross-magnetizing ampere-turns. In consequence, the ampere-turns of the field winding must be increased if the useful flux in the armature is to remain constant.

The method of determining the ampere-turns per pole required to compensate for the demagnetizing effect of the armature cross-magnetizing ampere-turns is given by Dr. Arnold and La Cour.¹ Figure 57 shows the open-circuit saturation curve for a generator. OE is the full-load induced voltage (terminal voltage plus the voltage drop in the armature, series and commutating field windings and brush contacts) and OF is the corresponding number of ampere-turns per pole.

The m.m.f. across the leading pole tip of a generator is decreased by the armature cross-magnetizing ampere-turns per pole,

$$ATP_c = f_a ATP_a, \quad (71)$$

and, as a result, the flux density in the air gap and the voltage induced

¹“Die Gleichstrommaschine,” Vol. 1, 3rd ed., p. 182, Julius Springer, Berlin.

in the conductors under this pole tip are also decreased. The m.m.f. across the trailing pole tip of a generator is increased by the armature cross-magnetizing ampere-turns per pole; as a result, the flux density in the air gap and the voltage induced in the conductors under this pole tip are also increased. The armature cross-magnetizing field will have no effect upon the terminal voltage of the machine when the increase in voltage at the trailing pole tip is equal to the decrease in voltage at the leading pole tip or when the area of the triangle cdG is equal to the area of the triangle abG , Fig. 57. When the area of triangle cdG is equal to the area of triangle abG , the line bG will be shorter than line cG , because the open-circuit saturation curve drops off more rapidly above the line bc than below it. With a pair of dividers set equal to $bc = 2f_a ATP_a$, the line bc may be laid off, so that the area of the triangle abG is equal to the area of the triangle dcG . The bisector of the line bc , $F'G'$, gives the voltage that must be induced in the armature winding at full-load when the brushes are in the no-load neutral, to obtain constant terminal voltage, and OF' is the corresponding number of ampere-turns per pole. The number of ampere-turns that must be added to the main field ampere-turns, to compensate for the demagnetizing effect of the armature cross-magnetizing ampere-turns,

$$= OF' - OF, \text{ Fig. 57.} \quad (72)$$

The areas of the triangles, Fig. 57, can easily be found with a planimeter.

The path of the armature cross-magnetizing field comprises the armature core, the teeth and air gap under the pole tips, and the pole shoe. The saturation curve for this magnetic circuit can be found by calculating the ampere-turns required to send the flux through the teeth and air gap, the ampere-turns required to send the flux through the armature core and pole being so small that they may be neglected. This saturation curve, of the armature cross-magnetizing field, should be used to determine the demagnetizing effect of the armature cross-

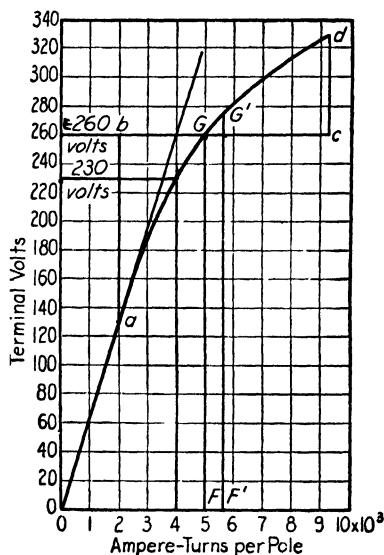


FIG. 57.

magnetizing field. When the open-circuit saturation curve is used, as in Fig. 57, the results will be slightly large. The error is quite small, however, and for practical purposes it is more convenient to use the open-circuit saturation curve.

The extent that the no-load field form is distorted by the armature field varies widely for different designs. The distortion will, obviously, be greater when the armature ampere-turns per pole are high in proportion to the shunt field ampere-turns per pole. The distorting effect of the armature field may be reduced by increasing the reluctance of the armature cross-magnetizing field. This can be done by using well-beveled pole shoes with large air gaps under the pole tips, by using high flux densities in the armature teeth, or by building up the pole as shown in Fig. 58. With properly designed compensating windings in the pole faces, the armature cross-magnetizing field may be completely neutralized. Under these conditions the air gap flux distribution curve for the machine will have the same shape for full-load as for no-load.

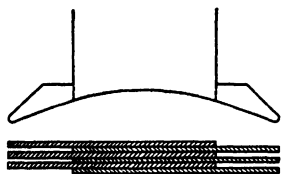


Fig. 58.

In order that the leading pole tip for a generator, the trailing pole tip for a motor, shall not become completely demagnetized, the ampere-turns per pole for air gap and armature teeth for full-load generated voltage should be approximately equal to or greater than f_d ATP_a. The ratio of the ampere-turns per pole for air gap and armature teeth to the armature ampere-turns per pole is usually as follows:

$$\frac{AT_g + AT_t}{ATP_a} = \begin{array}{l} 0.75 \text{ to } 0.95 \text{ interpole machine} \\ 0.50 \text{ to } 0.70 \text{ compensated machine} \end{array} \quad (73)$$

For the method of calculating the length of air gap required to satisfy these ratios see the sample designs.

Shunt and Series Field Ampere-Turns.—Figure 59 shows the open-circuit saturation curve of a generator. OA are the ampere-turns per pole corresponding to the no-load terminal voltage, OE_1 , and OB are the ampere-turns per pole corresponding to the full-load generated voltage, OE . To these ampere-turns must be added the ampere-turns per pole required to compensate for the demagnetizing effect of the armature cross-magnetizing field and the armature demagnetizing ampere-turns per pole when the brushes are shifted from the no-load neutral. The total ampere-turns per pole on the field winding are then equal to OD (Fig. 59).

For a flat-compounded generator, the voltage across the shunt field

winding is practically constant from no-load to full-load, and the shunt field ampere-turns per pole are the ampere-turns corresponding to no-load terminal voltage, OA , Fig. 59. The series field ampere-turns per pole are then equal to the total ampere-turns per pole minus the shunt field ampere-turns per pole = $OD - OA$, Fig. 59.

For an over-compounded generator, the voltage across the shunt field winding is higher at full-load than at no-load. Referring to Fig. 59, the shunt field ampere-turns per pole for an over-compounded generator are (assuming the long shunt connection)

$$ATP_f = \frac{\text{F.L. terminal voltage}}{\text{N.L. terminal voltage}} OA. \quad (74)$$

The series field ampere-turns per pole are equal to the difference between the total ampere-turns per pole and the shunt field ampere-turns per pole. Since the effect of the armature cross-magnetizing field cannot be accurately predetermined, it is usual to increase the series field ampere-turns per pole, determined as given above, approximately 20 per cent. The desired degree of compounding can then be obtained by the use of a series field shunt.

For a shunt-wound motor the generated voltage in the armature winding, E , is equal to the terminal voltage minus the voltage drop in the armature winding, commutating field winding, and brush contacts. The shunt field ampere-turns per pole are equal to the ampere-turns corresponding to full-load generated voltage.

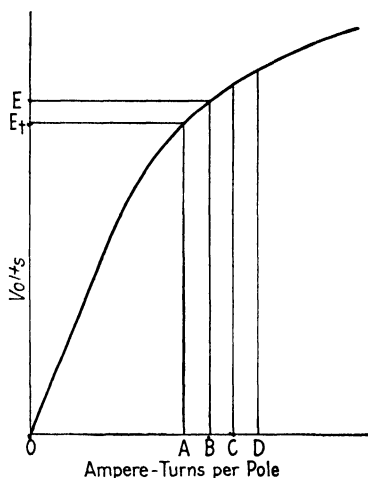


FIG. 59.—Total field ampere-turns per pole.

Design of Field Winding: Shunt Field Winding.—For the shunt field windings, single-cotton-covered, double-cotton-covered, enameled, and single-cotton-covered enameled wires are used. Asbestos-covered wire is used when high operating temperatures are required. The section area of the wire used is either round, square, or rectangular. Cotton-covered wires are sometimes treated with an insulating compound, by passing the wire through an insulating bath during winding. More often, the coils are wound with the dry cotton-covered conductor. The completely wound coils are then dried and dipped into a bath of

insulating varnish or treated with an asphaltum compound by the vacuum process.² Impregnating the coils with asphaltum compound by the vacuum process is more expensive than the varnish treatment, but

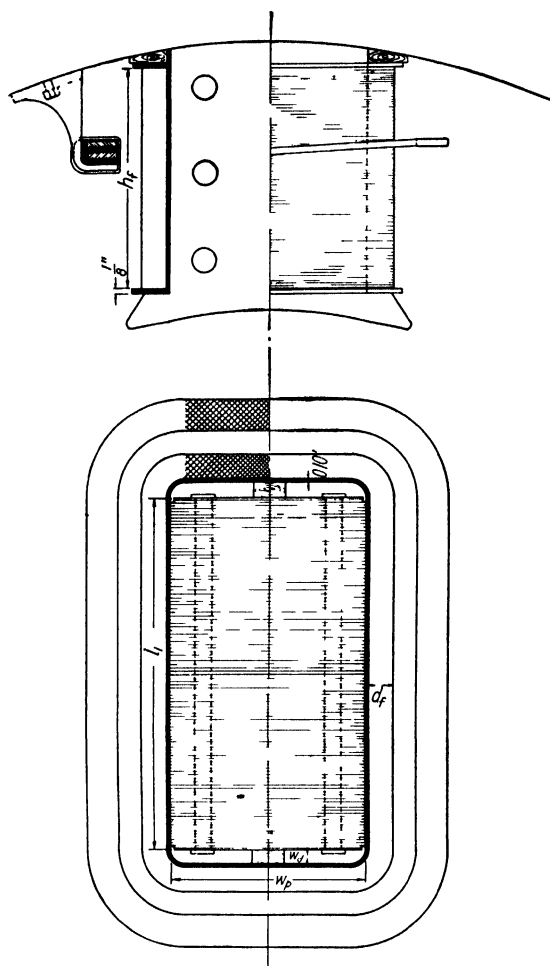


FIG. 60.—Main pole and windings, 300-kw , 250-volt, 900-r.p.m generator.

the asphaltum compound fills the spaces between wires better than insulating varnish and gives better heat dissipation. The coils are usually wound on a form and completely insulated before being placed on the pole.

²See "Insulation and Design of Electrical Windings," by A P M Fleming and R. Johnson, p 68, Longmans, Green & Co , London, also Electrical Journal, Vol. 22, Feb , 1925, p. 95.

A method often used for insulating the shunt field winding from the pole for voltages up to and including 600 volts is shown in Fig. 60. The insulation between the pole body and shunt field coil is usually built up of pressboard or fuller board and is held in place by a wrapper of unbleached muslin. Figure 60 shows a ventilating duct at each end of the pole. This ventilating duct is not provided on all machines, because for some types of construction this duct will be practically closed at the yoke end of the pole. Ventilating ducts between the inside of the shunt field winding and the ends of the pole are most effective when the yoke length is small. These ventilating ducts are usually from $\frac{1}{4}$ in. to $\frac{3}{4}$ in. When heavy shunt field windings are required for large generators, a ventilated coil, as shown in Fig. 61, may be used.

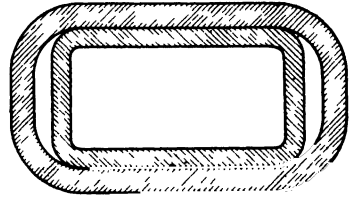


FIG. 61.—Ventilated field coil.

The length of the mean-turn of the shunt field coil can be calculated as follows (see Fig. 60):

$$L_f = 2l_1 + 2(w_p - 2w_d) + \pi[d_f + 2(w_d + \frac{3}{32})] \text{ in.} \quad (75)$$

The resistance of the shunt field winding,

$$R_f = \frac{L_f t_f p r}{s_f 10^6} \text{ ohms,} \quad (76)$$

and

$$i_f = \frac{E_t}{R_f} \text{ amperes.} \quad (77)$$

The ampere-turns per pole on the shunt field winding,

$$i_f t_f = \frac{E_t s_f \times 10^6}{L_f p r}. \quad (78)$$

This equation shows that the number of ampere-turns per pole on the shunt field winding are independent of the number of turns per pole, but vary directly with the cross-section of the conductor.

For generators, the shunt field winding is generally designed for a voltage from 20 to 30 per cent less than the terminal voltage of the machine. Voltage regulation can then be obtained by means of a field rheostat. The section area of the shunt field conductor,

$$s_f = \frac{ATP_f L_f p \times 0.826}{E_t (0.70 \text{ to } 0.80) \times 10^6} \text{ sq. in.} \quad (79)$$

The size of wire having this section area is found from the copper table. When the calculated conductor section lies half way between two standard conductors, half of the shunt field winding may be wound with the next larger conductor and the other half with the next smaller conductor. When two sizes of wire are used,

$$s_f = \frac{s_{f1}l_{f1} + s_{f2}l_{f2}}{l_{f1} + l_{f2}} \text{ sq. in.} \quad (80)$$

The current in the shunt field winding,

$$i_f = s_f A_f \text{ amperes.} \quad (81)$$

The current density for the shunt field winding is given in Table V. The number of turns per pole

$$t_f = \frac{ATP_f}{i_f}. \quad (82)$$

Since the number of turns per pole on the field winding determines the heating, it is well to calculate at this point in the design the expected

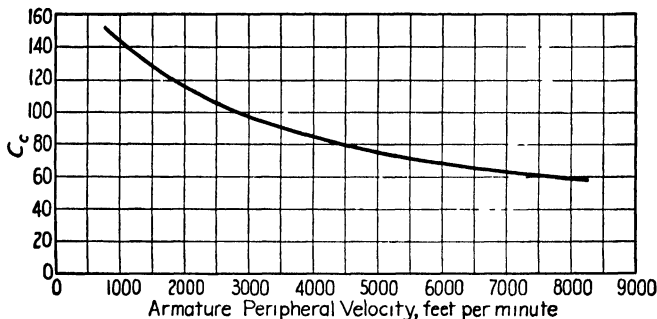


FIG. 62.—Cooling coefficient for shunt field winding.

temperature rise. The cooling surface for a field coil without ventilating ducts is taken equal to the perimeter of the coil section times the mean-turn. The total cooling surface for p coils

$$S_f = 2(d_f + h_f)l_f p \text{ sq. in.,}$$

and the surface per watt loss

$$\frac{S_f}{W_f} = \frac{S_f}{i_f^2 R_f}.$$

The temperature rise

$$T_f = \frac{C_{ef}}{S_f/W_f} \text{ degrees C.}$$

$C_{cf} = C_c + 70(1 - f_s)d_f$ for field coils without ventilating ducts. Here C_c is a cooling coefficient which varies with the armature velocity; usual values for direct-current machines are given in Fig. 62. For field coils with ventilating ducts on each end as shown in Fig. 61 one-half of the duct surface is added to the cooling surface per coil, and

$$C_{cf} = C_c + 55(1 - f_s)d_f.$$

When the ventilating duct passes around the entire coil,

$$C_{cf} = C_c + 35(1 - f_s)d_f.$$

Here, d_f is the thickness of the two coils.

The bare weight of the shunt field copper

$$G_f = L_f t_f p s_f \times 0.321 \text{ lb.} \quad (83)$$

The insulated weight depends upon the kind of insulation on the wire. The copper tables give the insulated weights for wires with standard insulation.

Series Field Winding.—The series field winding is generally wound with rectangular, double-cotton-covered wire when the conductor

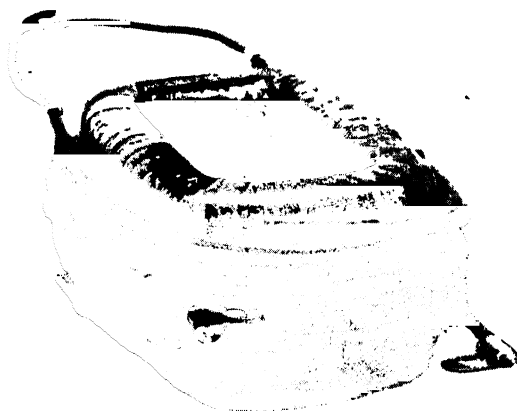


FIG. 63.—Complete field coil with wire-wound series coil outside of shunt coil.

sections is 0.102 sq. in. or less. For larger conductor sections, bare strap copper is generally used, with the turns insulated from one another by paper about 0.010 in. thick or by air spaces. The series field winding is often placed on the outside of the shunt field winding. When bare strap is used, it is wound on edge, and the separate turns are insulated from one another by air spaces. A shunt field coil with square wire series field coil wound on the outside is shown in Fig. 63.

The series field current, I_s , is equal to the terminal current plus the shunt field current when the long shunt connection is used and is equal to the terminal current when the short shunt connection is used. The number of turns per pole on the series field winding

$$t_s = \frac{ATP_s}{I_s}. \quad (84)$$

The section area of the series field conductor

$$s_s = \frac{I_s}{A_s} \text{ sq. in.} \quad (85)$$

The current density in the series field copper cannot always be chosen as high as the temperature rise will permit, because the efficiency is in many cases the limiting factor. For compound-wound generators,

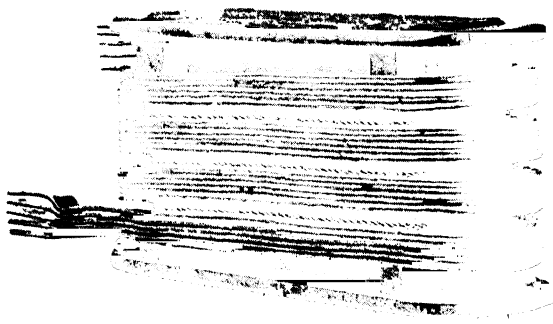


FIG. 64.—Bare ribbon copper commutating field coil.

A_s can be slightly higher than the values for A_f given in Table V, and for series motors for intermittent duty about 30 per cent higher values may be used.

The mean-turn of the series field coil can be determined from a sketch of the coil by a method similar to the one used for the shunt field coil. The resistance of the series field winding

$$R_s = \frac{L_s t_s p r}{s_s \times 10^6} \text{ ohms.} \quad (86)$$

The bare weight of the series field copper

$$G_s = L_s t_s p s_s \times 0.321 \text{ lb.} \quad (87)$$

Commutating Field Winding.—The commutating field winding is connected in series with the armature, and the total armature current

flows through the commutating field winding. As for the series field winding, rectangular double-cotton-covered wire is generally used when the conductor section is equal to 0.102 sq. in. or less. For larger conductor sections, bare strap copper wound on edge is generally used. The turns are then insulated from one another by paper about 0.010 in. thick, by cotton tape on the conductors, or by air spaces. The insulation between the winding and the pole body is generally about $\frac{1}{16}$ in. thick and is built up of fuller board or similar insulating material. A commutating field coil of bare ribbon copper is shown in Fig. 64.

The number of turns per pole for the commutating field winding

$$t_i = \frac{ATP_i}{I_a} \quad (88)$$

The section area of the conductor

$$s_i = \frac{I_a}{A_i} \text{ sq. in.} \quad (89)$$

The current density in the commutating field copper may be approximately equal to $1.4 J$ for strap wound coils and to $0.85 A J$ for wire wound coils.

The length of the mean-turn of the commutating field coil can easily be found from a sketch of the coil. The resistance of the commutating field winding

$$R_i = \frac{L_i t_i p r}{s_i \times 10^6} \text{ ohms.} \quad (90)$$

The bare weight of the commutating field copper

$$G_i = L_i t_i p s_i \times 0.321 \text{ lb.} \quad (91)$$

Design of the Shunt Field Rheostat.—For full-load and normal voltage,

$$R_f + R_{rl} = \frac{E_t}{i_f} \text{ ohms,}$$

where R_{rl} is the shunt field rheostat resistance for full-load and normal terminal voltage. For no-load and normal terminal voltage

$$R_f + R_{ro} = \frac{E_t}{i_{fo}} \text{ ohms}$$

$$R_{ro} = \frac{E_t}{i_{fo}} - R_f \text{ ohms.}$$

To allow for variations in speed and to permit a reduction in voltage below normal

$$R_r = 1.25 \text{ to } 2.0 \left(\frac{E_t}{E} - R_f \right) \text{ ohms.} \quad (92)$$

The resistance steps for the rheostat can be determined by the following graphical method:³ Curve *A*, Fig. 65, is the open-circuit saturation curve for a generator, with terminal voltage plotted in percentage of normal voltage as ordinates and shunt field current as

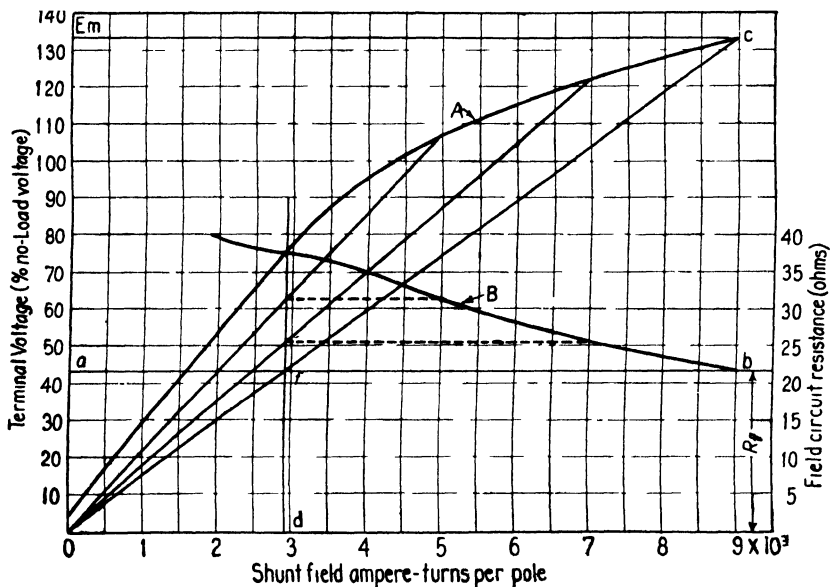


FIG. 65.—Construction of field circuit resistance curve.

abscissas. OE_m is the maximum voltage that can be obtained when the rheostat is all cut out and the generator is self-excited. Oa is the shunt field resistance to a suitable scale, and ab is the shunt field resistance line. The diagonal, Oc , intersects the shunt field resistance line at f , and df is the resistance in the shunt field circuit when the terminal voltage is E_m . The total resistance necessary in the shunt field circuit for other voltages can be found by drawing diagonal lines from a number of points on the open-circuit saturation curve to the origin. The intersections of these lines with df extended give the total resistance necessary in the shunt field circuit for the corresponding voltages. By

³ "Graphische Berechnung von Widerstandsregulatoren," by F. Hunke, *Elektrotechnische Zeitschrift*, Vol. 21, 1900, p. 801, and "Exciter Field Rheostats," by J. F. Formanek, *General Electric Review*, Vol. 28, Feb., 1925, p. 125.

plotting these values of field circuit resistance, as shown in Fig. 65, the field resistance curve, *B*, is obtained. If the field resistance is subtracted from the values of field circuit resistance shown by Curve *B*, Fig. 65, the field rheostat resistance curve is obtained, as shown in Fig. 66. Field rheostats should be so designed that the same variation in voltage is obtained for all the buttons on the rheostat, regardless of the voltage at which the machine is operating. On the assumption of equal voltage increments between buttons, the voltage scale, Fig. 66,

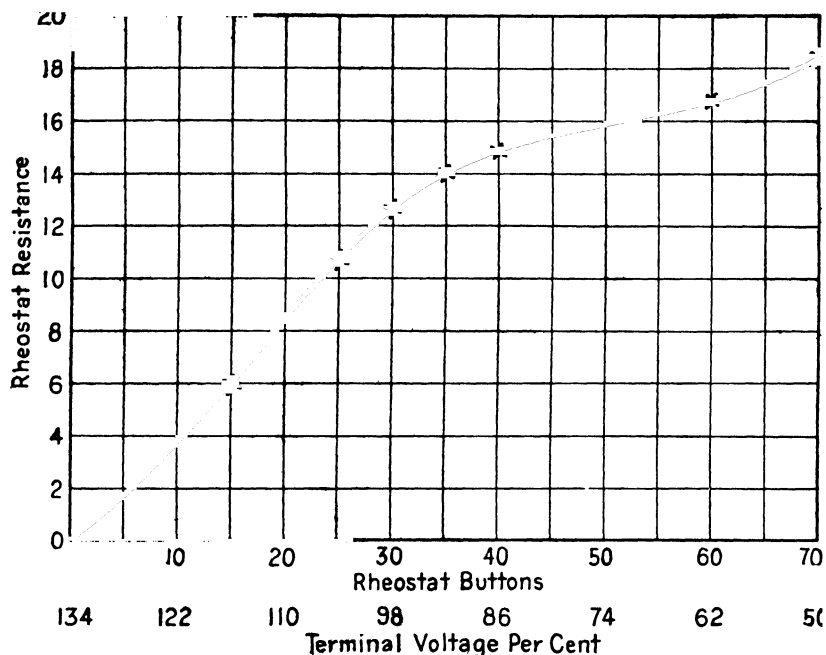


FIG. 66.—Rheostat resistance curve.

may be replaced by a scale showing rheostat buttons. Obviously, it would be impractical to make the resistance different between all buttons of the rheostat, as shown by the curve, Fig. 66. Rheostats are generally built up of resistance units, and if a large number of these can be made alike, the construction of the rheostat will be greatly simplified. The resistance between the buttons of the rheostat can be found by subtracting the resistance for any one button from the resistance of the previous one. This would be a tedious process and would involve considerable time. For practical purposes, it is more convenient to divide the rheostat resistance curve into a number of sections, as indicated by \times , Fig. 66. Straight lines drawn between these points

give a broken curve which nearly coincides with the original. Each of these sections then represents a group of rheostat buttons, for which the resistance is the same. The resistance of each group can easily be found as follows (see Fig. 66): The section of the rheostat resistance curve, for example, between 15 and 25 buttons comprises 10 buttons, and the resistance variation is from 6 to 10.7 ohms, or 4.7 ohms. Divid-

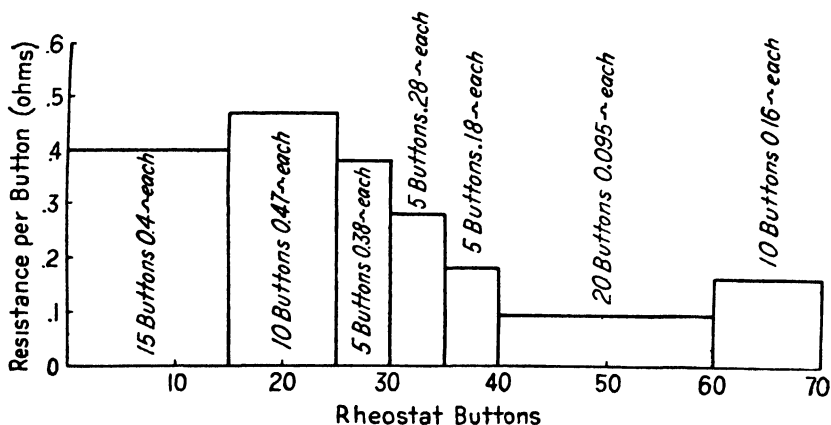


FIG. 67. —Equivalent rheostat resistance curve.

ing this value by the number of buttons for the section, 10, gives the resistance per button equal to 0.47 ohm. Figure 67 shows the resistance between buttons for the various sections of the rheostat.

Sample Design: *Design of Shunt and Series Field Windings.*—The sample generator is to be designed with commutating poles. The brushes will therefore remain in the no-load neutral position and the armature demagnetizing ampere-turns will be equal to zero.

The demagnetizing effect of the armature cross-magnetizing ampere-turns is determined graphically as explained on page 83. The armature cross-magnetizing ampere-turns per pole = $f_a ATP_a = 0.665 \times 5440 = 3620$. The graphic construction for the sample problem is shown in Fig. 57, and the demagnetizing effect of the armature cross-magnetizing field = $OF' - OF = 5620 - 4990 = 630$ ampere-turns.

At no-load, the voltage across the shunt field winding will be 230 volts, and the corresponding ampere-turns per pole are equal to 4020 (see Fig. 57). At full-load, the voltage across the shunt field winding is 250 volts. The shunt field ampere-turns per pole

$$ATP_f = \frac{250}{230} \times 4020 = 4370 \text{ ampere-turns.}$$

The shunt field winding will be designed as shown in Fig. 60, with the series field winding on the outside of the shunt field winding. The depth of the shunt field coil must first be estimated; for this design, 0.75 in. will be used. The length of the mean-turn can easily be calculated from the sketch shown in Fig. 60, which is for the sample design.

$$\begin{aligned} L_f &= 2l_1 + 2(w_p - 2w_d) + \pi[d_f + 2(w_d + \frac{3}{8})] \text{ in.} \\ &= 2 \times 10.5 + 2(6.5 - 2 \times 0.50) + \pi[0.75 + 2(0.50 + 0.10)] \\ &= 38.10 \text{ in.} \end{aligned}$$

The section area of the shunt field conductor

$$\begin{aligned} s_f &= \frac{ATP_f L_f pr}{E_t(0.70 \text{ to } 0.80)10^6} = \frac{4370 \times 38.10 \times 6 \times 0.826}{250 \times 0.75 \times 10^6} \\ &= 0.0044 \text{ sq. in.} \end{aligned}$$

A No. 13 square wire has a section area of 0.00465 sq. in. and a double-cotton-covered diameter of 0.083 in. This wire will be suitable for the shunt field winding. A satisfactory current density for the shunt field conductor is 1560 amperes per sq. in. from Table V. The shunt field winding current is then

$$i_f = A_f \times S_f = 1560 \times 0.00465 = 7.26 \text{ amperes.}$$

For this current the number of shunt field turns per pole

$$t_f = \frac{ATP_f}{i_f} = \frac{4370}{7.26} = 602.$$

From a sketch such as shown in Fig. 60 the height of winding space $h_f = 5.23$ in. The number of turns per layer

$$= \frac{5.23}{0.083} = 63.1; \text{ use } 62.$$

The space for one turn must be allowed in passing from one layer to the next; 62 turns per layer will therefore be used. The number of layers

$$= \frac{602}{62} = 9.72; \text{ use } 10.$$

The number of shunt field turns per pole

$$t_f = 10 \times 62 = 620;$$

the shunt field current

$$i_f = \frac{4370}{620} = 7.06 \text{ amperes;}$$

and the current density

$$A_f = \frac{7.06}{0.00465} = 1518 \text{ amperes per sq. in.}$$

The depth of the field coil, $d_f = 0.083 \times 10 = 0.83$ in. The corrected mean-turn

$$L_f = 38.1 + \pi(0.83 - 0.75) = 38.4 \text{ in.}$$

The resistance at 75° C

$$\begin{aligned} R_f &= \frac{L_f l_f p r}{s_f \times 10^6} = \frac{38.4 \times 620 \times 6 \times 0.826}{0.00465 \times 10^6} \\ &= 25.4 \text{ ohms,} \end{aligned}$$

and the copper loss

$$W_f = i_f^2 R_f = 7.06^2 \times 25.4 = 1265 \text{ watts.}$$

The cooling surface

$$\begin{aligned} S_f &= 2(d_f + h_f) L_f p = 2(0.83 + 5.23) 38.4 \times 6 \\ &= 2800 \text{ sq. in.,} \end{aligned}$$

and the cooling surface per watt loss

$$\frac{S_f}{W_f} = \frac{2800}{1265} = 2.21.$$

It is desirable at this point to check the field winding temperature rise. The cooling coefficient is calculated as explained on page 88.

$$\begin{aligned} C_{ef} &= C_e + 70(1 - f_s) d_f = 69.2 + 70(1 - 0.675) 0.83 \\ &= 88.1 \end{aligned}$$

$$T_f = \frac{C_{ef}}{S_f/W_f} = \frac{88.1}{2.21} = 39.8^\circ \text{ C.}$$

The weight of the shunt field copper

$$\begin{aligned} G_f &= L_f l_f p s_f \times 0.321 \\ &= 38.4 \times 620 \times 6 \times 0.00465 \times 0.321 \\ &= 213 \text{ lb.} \end{aligned}$$

From Fig. 57, the total ampere-turns required on the field winding to generate 250 volts at the terminals of the machine at full-load are found to be 5620 ampere-turns. The shunt field ampere-turns were calculated above and are equal to 4370. The ampere-turns per pole required for the series field will be $5620 - 4370 = 1250$ ampere-turns. For the long shunt connection, the current in the series field winding will be equal to the armature current, I_a . The number of turns per pole for the series field

$$t_s = \frac{1250}{1207} = 1.03; \text{ use } 1.5 \text{ turns.}$$

The ampere-turns per pole on the series field will then be

$$\text{ATP}_s = 1207 \times 1.5 = 1810 \text{ ampere-turns.}$$

It is generally desirable to use a larger number of ampere-turns than the calculations show, to allow for variations in the material of the magnetic circuit, inaccuracies in the determination of armature reaction, etc.

The series field winding will be placed on the outside of the shunt field winding. For a current density of 1800 amperes per sq. in., the section area of the series field conductor

$$s_s = \frac{I_s}{A_s} = \frac{1207}{1800} = 0.672 \text{ sq. in.}$$

A bare, strap copper conductor, wound on edge, will be most suitable for this winding. Three strap conductors, 0.219×1.00 in., in parallel, will be used, each having a section area of 0.216 sq. in. The current density is then

$$A_s = \frac{1207}{3 \times 0.216} = 1860 \text{ amperes per sq. in.}$$

From the sketch, Fig. 60, the mean-turn of the series field winding can easily be calculated in the manner described for the shunt field winding.

$$\begin{aligned} L_s &= 2 \times 10.5 + 2(6.5 - 2 \times 0.5) \\ &\quad + \pi[2(0.5 + 0.10 + 0.83 + 0.5) + 1] + 2 = 49.2, \end{aligned}$$

where 2 in. per turn is added to the mean-turn of the coil to allow for the connections between poles.

The resistance of the series field winding at 75° C.

$$R_s = \frac{L_s t_p r}{s_s \times 10^6} = \frac{49.2 \times 1.5 \times 6 \times 0.826}{0.648 \times 10^6}$$

$$= 0.000564 \text{ ohm.}$$

The voltage drop in the series field winding

$$I_s R_s = 1207 \times 0.000564 = 0.682 \text{ volt,}$$

or 0.273 per cent of the full-load terminal voltage.

It will not be necessary to calculate the cooling surface per watt for this type of series field winding, because experience has shown that for current densities up to about 2000 amperes per sq. in. satisfactory operating temperatures are generally obtained.

The weight of the series field copper

$$G_s = L_s t_p s_s \times 0.321$$

$$= 49.2 \times 1.5 \times 6 \times 0.648 \times 0.321 = 92 \text{ lb.}$$

The shunt field rheostat resistance is calculated by formula 92,

$$R_r = 2.0 \left(\frac{E_t}{I_{fo}} - R_f \right) = 2.0 \left(\frac{230}{6.47} - 25.4 \right)$$

$$= 20.4 \text{ ohms.}$$

The graphic construction, to determine the value of the resistance for the various buttons on the rheostat, is shown in Figs. 65, 66, and 67.

CHAPTER VI

COMMUTATION AND COMMUTATING POLE DESIGN

WHEN the commutator segments to which the armature coils are connected pass under the brushes, the armature coils are successively transferred from one armature path, in which the current has one direction, to an adjoining armature path, in which the current is of opposite direction. During this period the coils are short-circuited by the brush, and the current must be reduced from its original value to zero and then built up again to an equal value in opposite direction.

The time variation of the current in a short-circuited coil may be represented diagrammatically as shown in Fig. 68. In this diagram, ordinates represent values of current and abscissas represent time. Before the coil under consideration enters the commutation period AB , the current in it is equal to $-i_a$, and after the completion of commutation it must be equal to $+i_a$. The curve showing the time variation of the current in the short-circuited coil is called the short-circuit current curve.

Curve 1, Fig. 68, shows the current in the short-circuited coil changing at a uniform rate from $-i_a$ to $+i_a$. This type of commutation is known as straight-line commutation. Straight-line commutation is desirable, because it gives rise to uniform current density at the brush contact surface, and the brush contact loss is a minimum.

Curve 2, Fig. 68, shows that the current has been reversed too rapidly and reaches a value greater than $+i_a$ before commutation is completed. For this case, the current may reach its final value without sparking, but it may involve local current densities at the brush contact surface of sufficient magnitude to produce glowing of the brush, which would lead to high commutator temperatures, rapid deterioration of the brushes, and excessive brush contact losses. This condition is known as over-commutation.

Curve 3, Fig. 68, shows a case of the current not being reversed with sufficient rapidity. The current builds up to a value greater than its initial value. This condition may involve excessive local current densities at the brush contact surface, which would lead to high com-

mutator temperature, excessive loss, and rapid deterioration of the brush. This condition is known as under-commutation.

In the above, no account has been taken of the effect of the mechanical conditions of the commutator and brushes. In order to secure successful commutation, it is necessary to have the best possible contact between brushes and commutator. A most important requirement in securing such contact is that the mica between commutator bars shall not protrude. Where the current passes from the commutator to the brush, the commutator copper is eaten away but the mica remains. If good brush contact is to be maintained, the mica between bars must be worn down mechanically at the same rate that the copper is eaten away. If the copper is eaten away more rapidly than the mica is worn down, the mica will eventually stand above the copper, and the brushes will cease to make good contact, which condition will increase the burning action. To prevent the mica from protruding above the commutator bars, it is now generally under-cut, so that it is a little below the surface of the commutator.

In addition to eliminating sparking, under-cutting the mica allows the use of softer brushes. If the mica is left flush with the commutator, a brush must be used of sufficient hardness to wear down the mica as fast as the copper is eaten away. Such brushes, however, have no self-lubricating qualities and are noisy, especially on high-speed commutators. Lack of lubrication will cause the brushes to chatter and vibrate, leading to bad contact between the brushes and commutator and causing sparking. Graphite brushes or carbon brushes with considerable graphite in them are extremely good for collecting current, but because of their softness they give poor results in wearing down the mica. Because of their graphite constituents, these brushes are largely self-lubricating and thus ride on the commutator more smoothly and much more quietly than ordinary carbon brushes.

To prevent the commutator from wearing down in grooves and forming ridges between the brushes of each brush arm, it has generally been the practice to displace all the positive brushes in one direction and all the negative brushes in the other direction. But since the eating away of the copper occurs only under the brushes of one polarity, it has been found better to stagger the brushes in pairs, so that the eating away of the copper is equalized over the entire commutator.

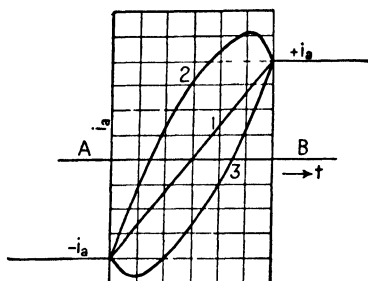


FIG. 68.—Short-circuit current curves.

Sparking at the brushes may also be caused by too high a voltage between adjacent commutator bars. The thickness of the mica between adjacent commutator bars is generally about $\frac{1}{32}$ in. From this it might be presumed that a high voltage between bars is permissible. It has been found, however, that the maximum volts between adjacent commutator bars should generally not exceed approximately 30 volts¹ for large machines. For very small machines, this value may be considerably larger.

Width of Commutating Zone.—The width of the commutating zone or portion of the armature circumference where one or more armature coils are short-circuited is of importance in calculating the reactance voltage and in determining the width of the commutating pole shoe.

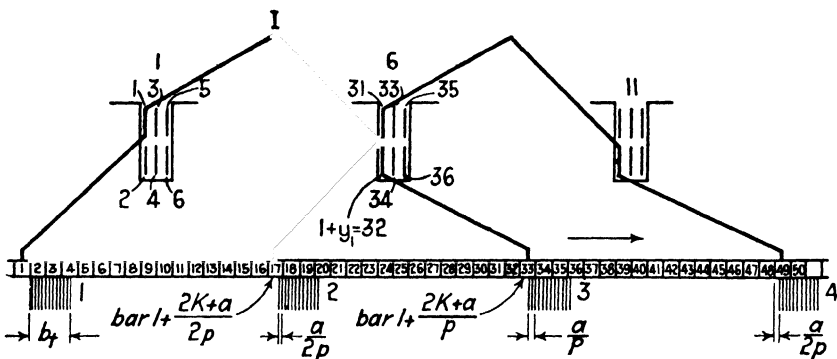


FIG. 69.—Two coils of simplex wave winding; $S=21$, $K=63$, $Y_1=31$, $Y_c=32$.

Figure 69 shows two coils of a simplex wave winding. For the position of the brushes shown, coil 1 is at the moment of beginning commutation. The width of the commutating zone of this coil is determined by the position of brushes 1 and 3 relative to the commutator bars to which the ends of this coil are connected. The distance the armature must move from the time commutator bar 1 comes in contact with brush 1 to the time when it leaves the brush again is

$$(b + 1)\beta_r \text{ in.}, \quad (93)$$

where b is the thickness of the brush or its width along the commutator circumference, expressed in commutator bars, and β_r is the commutator bar pitch reduced to the armature diameter. Equation 93 would give the width of the commutating zone of coil 1, if its commutation

¹"Physical Limitations in D-C Commutating Machines," by B. G. Lammé, A.I.E.E., Vol. 34, p. 1752.

were influenced by brush 1 only. Brush 3 has the effect of reducing the commutating zone of coil 1 an amount equal to the difference between

$\frac{2K \pm a}{p}$ and $2\frac{K}{p}$. The width of the commutating zone for one coil in

inches of armature circumference is then

$$A = \left[b + 1 \pm \left(\frac{2K}{p} - \frac{2K \pm a}{p} \right) \right] \beta_r = \left(b + 1 - \frac{a}{p} \right) \beta_r \text{ in.} \quad (94)$$

After the commutator has moved a distance equal to the width of one commutator bar, the next coil begins commutation, and the width of the commutating zone for the upper or lower part of a slot is

$$\left(b + 1 - \frac{a}{p} + m - 1 \right) \beta_r = \left(b + m - \frac{a}{p} \right) \beta_r \text{ in.} \quad (95)$$

For a full pitch winding, the upper and lower parts of the slot commutate at the same time, and formula 95 gives the width of the commutating zone for such a winding. When chorded windings are used, the conductors in the top part of the slot do not begin commutation at the same time as those in the lower part of the slot. This condition has the effect of increasing the width of the commutating zone. If φ is the difference in phase of commutation between a conductor in the top of a slot and a corresponding conductor in the bottom of a slot, expressed in number of commutator bars, then the width of the commutating zone for either full pitch or chorded windings is

$$w_c = \left(b + m + \varphi - \frac{a}{p} \right) \beta_r. \quad (96)$$

The difference in phase of commutation for the top and bottom of a slot is calculated as follows:²

$$\varphi = \frac{K}{p} - \frac{1}{2}(Y_1 - 1). \quad (97)$$

When $\frac{1}{2}(Y_1 - 1)$ in formula 97 is greater than K/p , or when over-chorded windings are used, the value of φ will be negative. The effect of the phase difference in commutation upon the width of the commutating zone is, however, the same, regardless of the sign of φ . The absolute value of φ with the positive sign must, therefore, always be used in the formula for w_c .

Formula 96 has been derived for the simplex wave winding. It

² "Die Gleichstrommaschine," by Dr. Arnold and La Cour, Vol. 1, 3rd ed., p. 248, Julius Springer, Berlin.

applies equally well, however, to simplex lap windings and multiplex lap and wave windings.

For a wide commutating zone, the coils under commutation will come under the influence of the flux from the main pole tips and the commutating pole will be wide, which condition leads to a heavy leakage flux. Experience has shown that the width of the commutating zone should not exceed 60 per cent of the neutral zone, where the neutral zone is the portion of the armature circumference between two adjacent pole tips = $(1 - \psi)\tau$.

Reactance Voltage.—The coil undergoing commutation has induced in it an e.m.f. of self-induction due to the reversal of the current in the coil, the self-induced e.m.f. always acting to oppose the change in current. If the short-circuited coil is in inductive relation to one or more coils in the same slot undergoing commutation at the same time, there is also induced in it an e.m.f. of mutual induction. This voltage of self and mutual induction induced in a short-circuited armature coil is called the reactance voltage and is the basic cause of sparking.

The reactance voltage may be expressed by the fundamental equation:

$$e_r = (L + M)\frac{di}{dt}, \quad (98)$$

where L is the coefficient of self-induction, M is the coefficient of mutual induction, and di/dt is the rate of change of current in the short-circuited coil.

It is convenient to calculate the coefficient of self and mutual induction at the same time. For this purpose L' is used as the coefficient of self and mutual induction. L' is calculated from the reluctances of the flux paths and the magnetomotive forces acting upon the flux interlinked with the short-circuited coil. It is calculated for the case for which the top and bottom of a slot, containing only two coil sides, commute at the same time, and is later corrected to take into account the actual conditions. To simplify calculations, the flux interlinked with the short-circuited coil is divided into four parts:

- (1) The flux that crosses the slot (Fig. 70).
- (2) The flux that passes through the air gap from the top of one tooth to the top of the next over the armature length $l - l_i$ (Fig. 70).
- (3) The flux that passes through the commutating pole shoe and the commutating pole air gap twice (Fig. 71).
- (4) The flux that surrounds the coil end-connections.

The coefficient of self and mutual induction for each of the four

flux paths is given by A. Brunt³ for commutating-pole machines as follows:

$$L'_1 = 4.25l \frac{d_s}{w_s} t_a^2$$

$$L'_2 = 9.35t_a^2(l - l_i) \log_{10} \frac{2t_1 - w_s}{w_s}$$

$$L'_3 = 2.03l_i t_a^2 \frac{w_i - w_s}{\delta_i}$$

$$L'_4 = 8.12l_s t_a^2.$$

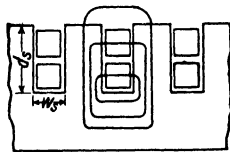


FIG. 70.—Slot and tooth tip leakage paths.

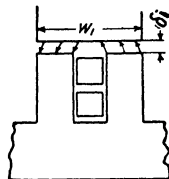


FIG. 71.—Tooth tip leakage path under commutating pole.

For the entire slot,

$$\begin{aligned} L' &= (L'_1 + L'_2 + L'_3 + L'_4) 10^{-8} \text{ henrys} \\ &= \frac{t_a^2}{10^8} \left[4.25l \frac{d_s}{w_s} + 9.35(l - l_i) \log_{10} \frac{2t_1 - w_s}{w_s} \right. \\ &\quad \left. + 2.03l_i \frac{w_i - w_s}{\delta_i} + 8.12l_s \right] \text{ henrys.} \end{aligned} \quad (99)$$

The rate of change of current in the short-circuited coil is assumed to be constant for the entire short-circuit period, that is, commutation is assumed to be linear. For one coil only, neglecting the effect of the other coils in the slot, the average rate of change of current,

$$\frac{di}{dt} = \frac{2i_a}{t} = \frac{2i_a}{A} = \frac{2i_a K n_s}{A},$$

where A is the width of the short-circuited zone of one coil expressed in commutator bars $= b + 1 - \frac{a}{p}$ (see formula 94). When there are

³“Design of Auxiliary Poles,” by A. Brunt, *Electrical Review and Western Electrician*, Vol. 59, 1911, p. 510.

more than two coil sides per slot, the number of commutator bars that must pass under the brush to complete commutation for the coil sides in the top or the bottom of the slot are $A + m - 1$ and the average value of di/dt for the coil sides in the top or the bottom of the slot,

$$\frac{di}{dt} = \frac{m}{A + m - 1} K n_s 2 i_a. \quad (100)$$

Equation 99 is the equation for the coefficient of self and mutual induction when there are two coil sides per slot and when the two coil sides of a slot commutate at the same time. When only one part of a slot is to be considered, then the value of L' must be divided by 2. When the coil sides in the top and bottom of a slot do not commutate at the same time, the mutual influence of the coil sides in the top and bottom of the slot is taken into account by multiplying $\frac{1}{2}L'$ by the factor

$$2 - \frac{\varphi}{A + m - 1}$$

When the coil sides per slot commutate at the same time, φ is equal to zero, and the value of this factor is equal to 2. When the two parts of the slot do not influence each other, φ is equal to $A + m - 1$, and the value of this factor is equal to 1.

Taking into account the mutual influence of the two parts of the slot, the equation for the coefficient of self and mutual induction becomes

$$L' = \frac{t_a^2}{2 \times 10^8} \left[\left(2 - \frac{\varphi}{A + m - 1} \right) \left\{ 4.25 l_s \frac{d_s}{w_s} + 9.35(l - l_i) \log_{10} \frac{2l_1 - w_s}{w_s} + 2.03 l_i \frac{w_i - w_s}{\delta_i} \right\} + 8.12 l_s \right] = \frac{t_a^2}{2 \times 10^8} M.$$

Substituting the expression for L' and for di/dt into the fundamental equation for the reactance voltage,

$$e_r = \frac{K n_s i_a t_a^2}{10^8} \frac{m}{A + m - 1} M.$$

$K t_a i_a$ = the total number of ampere-turns on the armature = $ATP_a p$, therefore,

$$e_r = \frac{ATP_a p t_a n_s}{10^8} \frac{m}{A + m - 1} M. \quad (101)$$

Formula 101 gives the reactance voltage per coil for machines

having as many commutating poles as main poles. When half as many commutating poles as main poles are used, the formula must be changed to the following form:

$$e_r = \frac{ATP_a p t_a n_s}{10^8} \frac{m}{A + m - 1} \left[\left(2 - \frac{\varphi}{A + m - 1} \right) \left\{ 4.25l \frac{d_s}{w_s} + 4.66(2l - l_s) \log_{10} \frac{2t_1 - w_s}{w_s} + 1 \right\} + 8.12l_s \right]. \quad (102)$$

For the derivation of these formulas, the simplex wave winding was assumed. They apply, however, equally well to simplex lap windings and to multiplex lap and wave windings. For interpole machines the reactance voltage per coil should in general not exceed 6 volts.

Design of the Commutating Pole.—The commutating pole is placed between two main poles, so that the coils undergoing commutation will cut the flux in the commutating pole air gap. They are generally made of cast steel or punched from sheet steel with no special pole shoe; that is, the length and width of the pole body are equal to the length and width of the pole shoe. For small and medium sized machines for moderate voltages with Q less than about 650 ampere-conductors per inch of armature circumference half the commutating poles are often omitted primarily for economical reasons.⁴

In order that the short-circuited coils shall come under the influence of the commutating pole, the width of the commutating-pole shoe must be equal to the width of the commutating zone: an allowance of from 1.5 to 2 times the air gap under the commutating pole may be made for the fringing of the flux at the tips of the commutating pole. The width of the commutating pole

$$w_i = w_c - (1.5 \text{ to } 2)\delta_i. \quad (103)$$

The commutating-pole width must also be so chosen that the leakage flux will not be excessive. To avoid excessive leakage, the width of the commutating pole should generally be not greater than one-half the space between adjacent pole tips or

$$w_i \leq \frac{1 - \psi}{2} \tau. \quad (104)$$

The width of the commutating pole must further be chosen with regard to the armature tooth pitch. With narrow commutating poles,

⁴ "The Number of Commutating Poles Used in Direct-Current Machines," by J. A. Elzi, *Electric Journal*, Vol. 22, March, 1925, p. 129.

the pulsations of the commutating-pole flux caused by the armature slots will be large. The pulsations of the commutating-pole flux can be reduced by using a large number of slots, that is, by reducing the tooth pitch. A large air gap under the commutating pole will also help to reduce the flux pulsations. It is, however, not desirable to make the air gap very large, for the main pole flux will then penetrate the commutating-pole air gap. Narrow commutating poles require that the brushes be accurately located in the geometrical neutral position, to avoid the compounding effect of the commutating-pole flux. In general, the commutating-pole width should be larger than 1.5 times the tooth pitch, and if possible, should be a multiple of the tooth pitch (see Chapter III, page 46) or,

$$w_i \geq 1.5t_1. \quad (105)$$

The length of the commutating pole is generally chosen from the standpoint of economy, for the shorter the commutating pole, the shorter will be the mean-turn of the commutating-pole winding and the smaller the copper weight, losses, and leakage flux. The length must, of course, be so chosen that the flux density in the commutating pole will be below the saturation point of the material. The choice of length depends also upon the service for which the machine is intended. For machines designed for large, fluctuating loads or for variable speed motors, for which good commutation is often difficult to obtain, the commutating pole is generally made as long as the main pole. For normal motors and generators with as many commutating poles as main poles, the length

$$l_i = (0.60 \text{ to } 0.80)l_1. \quad (106)$$

For motors and generators with half as many commutating poles as main poles, the commutating-pole length is generally equal to the main-pole length.

The commutating-pole air gap must not be so small as to produce large pulsations of the commutating-pole flux, caused by the armature slot. It must not be made too large so that the main-pole flux will not affect the commutating-pole field. In general

$$\delta_i = (1 \text{ to } 2)\delta. \quad (107)$$

For machines for which good commutation is difficult to obtain, the larger air gap will generally be found more satisfactory.

To obtain straight-line commutation, the voltage induced in the short-circuited coil by the commutating-pole flux must, for every instant of the short-circuit period, be equal and opposite to the reactance

voltage. The reactance voltage is not always a constant value for the entire short-circuit period. If straight-line commutation is assumed, the change of the current volume for either the upper or lower part of the slot can be shown as in Fig. 72a. The following data apply:

$$\beta = 0.163, K = 111, b = 2.3, a = 2, p = 4,$$

$$A = b + 1 - a/p = 2.3 + 1 - \frac{2}{4} = 2.8,$$

$$m = 3, Y_1 = 55, \varphi = 0.75,$$

$$A + m - 1 = 2.8 + 3 - 1 = 4.8.$$

The current volume of either the top or bottom part of the slot changes from $+3i_a$ to $-3i_a$. From the beginning of commutation, for the slot under consideration, to the point a , only coil 1 is in short-circuit; from a to b , coils 1 and 3 are in short-circuit; from b to c , coils 1, 3, and 5 are in short-circuit; from c to d , coils 3 and 5 and from d to e coil 5 are short-circuited. The number of commutator bars that must pass under the brush, to commute the coils in the top or bottom of the slot, is equal to $A + m - 1 = 4.8$, as shown in Fig. 72a.

The reactance voltage in any of the three coils in the top of the slot, not taking into account the influence of the coils in the bottom of the slot, is shown in Fig. 72b, the coils being in short-circuit during the periods indicated by 1, 3, and 5.

Obviously, the coils in the bottom of the slot will have the same reactance voltage as those in the top of the slot, when the influence of the two parts of the slot on each other is not taken into account. When both top and bottom of the slot are considered together, the coils in the bottom of the slot begin commutation φ commutator bars before or after those in the top of the slot. Figure 72c shows the reactance voltage for each of the three coils in the bottom of the slot, commutation beginning $\varphi = 0.75$ commutator bar after the beginning of commutation for the top of the slot. By adding the corresponding ordinates of Fig. 72b, representing the top of the slot, and Fig. 72c,

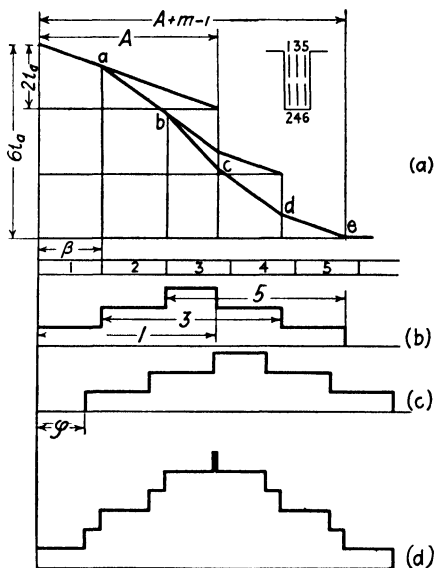


FIG. 72.

representing the bottom of the slot, the resultant reactance voltage for all the coils of the slot is obtained as shown in Fig. 72*d*. The ordinates of Fig. 72*d* represent to a certain scale the reactance voltage of the various coils of the slot.

In order to induce in the short-circuited coil a voltage equal and opposite to the reactance voltage, the flux density at each point in the commutating-pole air gap must be proportional to the reactance voltage at that point. To obtain perfect compensation of the reactance voltage, the commutating-pole shoe should have the shape of the reactance voltage curve, Fig. 72*d*, that is, the length of the commutating-pole air gap at each point of the commutating zone should be inversely proportional to the reactance voltage at that point. Obviously, the commutating-pole shoe will not be built with the shape shown by the curve,

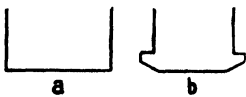


FIG. 73.—Shapes of commutating pole shoe.

Fig. 72*d*, but will have the shape shown in Fig. 73*a* and *b*. Perfect compensation of the reactance voltage is, therefore, not always possible.

It is obvious, from what has been stated above, that the curve showing the variation of the reactance voltage for the commutation period of one slot will be of rectangular shape when there are only two coil sides per slot and when they commute at the same time, that is, when $\varphi = 0$. For such a case, the air gap under the commutating pole will be of the same length for all parts of the pole shoe, and the flux density for all points in the commutating-pole air gap can be made proportional to the reactance voltage. For machines for which commutation difficulties are apt to arise, it is therefore desirable to arrange the armature winding with only two coil sides per slot, with a full pitch winding (see Chapter III). Although beveled commutating-pole shoes are of great help in obtaining the best possible commutation, they should be used only in cases where difficult commutation conditions exist, because they make the machine sensitive to correct brush position. Very good results are generally obtained by using a commutating-pole shoe with a straight face.

Commutating-Pole Ampere-Turns.—Formulas 101 and 102 give the average value of the reactance voltage per coil. To induce a voltage in the short-circuited coils equal and opposite to the average value of the reactance voltage, the average value of the flux density in the commutating-pole air gap, when as many commutating poles as main poles are used, must be

$$B_{av} = \frac{e_r \times 60 \times 10^8}{2t_{av}l_v \times 12} = \frac{Q}{4l_v} \frac{m}{A + m - 1} M \text{ lines per sq. in.} \quad (108)$$

When half of the commutating poles are omitted, the commutating-pole flux affects one side of the coil only, and

$$B_{\theta_1} = \frac{c_r \times 60 \times 10^8}{t_a l_v \times 12} = \frac{Q}{2l_1 A + m - 1} M \text{ lines per sq. in.} \quad (109)$$

The commutating-pole flux,

$$\phi_1 = B_{\theta_1} l_1 w, \text{ lines.} \quad (110)$$

The flux paths of a two-pole generator, with as many commutating

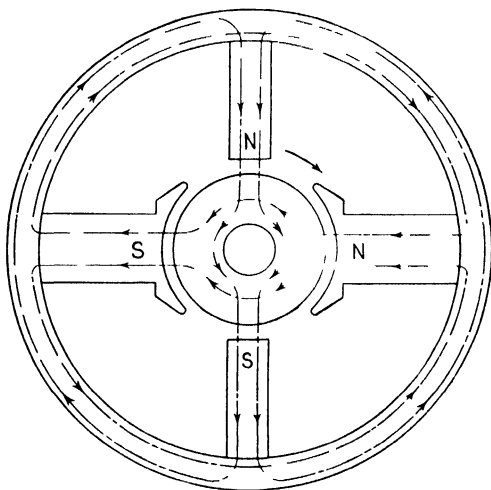


FIG. 74.—Flux paths in a two-pole d.-c. generator.

poles as main poles, are shown in Fig. 74. The ampere-turns for the commutating-pole air gap

$$AT_{\theta_1} = \frac{B_{\theta_1} \delta_1 k}{3 \cdot 2}. \quad (111)$$

The ampere-turns for the remainder of the commutating-pole magnetic circuit can be calculated in the manner described for the main-pole magnetic circuit, Chapter IV.

To the ampere-turns required to send the commutating-pole flux through the magnetic circuit must be added the armature ampere-turns

acting in the interpolar space. The total ampere-turns per commutating pole are then,

$$ATP_i = ATP_a + AT_{gi} + AT_{ti} + AT_{pi} + AT_{yi} + AT_{yf}. \quad (112)$$

When half of the commutating poles are omitted, the commutating-pole flux returns through the main pole and main-pole air gap on each side of the commutating pole. The ampere-turns required to send the commutating-pole flux through the commutating-pole air gap, armature teeth under the commutating pole, armature yoke, and the field yoke are calculated in the same way as given above for machines with as many commutating poles as main poles. To these must be added the ampere-turns required to send the flux through the main pole, main-pole air gap, and the teeth under the main poles. (See footnote, page 70.) The sum of the ampere-turns for the various parts of the magnetic circuit plus the armature ampere-turns per pole gives the total number of ampere-turns required on each commutating pole.

In order to obtain proper compensation of the reactance voltage at all loads, the flux density in the commutating-pole air gap must vary directly with the load current, because the reactance voltage varies directly with the load current. This can only be obtained when the iron parts of the commutating-pole magnetic circuit are unsaturated. For normal machines the ampere-turns for the iron parts of the magnetic circuit are generally equal to from 0.50 to 1.0 times the air gap ampere-turns for the commutating pole. Then,

$$ATP_i = ATP_a + (0.313\delta, B_g, k)(1.5 \text{ to } 2.0). \quad (113)$$

Design of Commutator and Brushes.—The number of commutator bars is always known as soon as the armature winding is determined, because it is equal to the number of armature coils. The commutator diameter is generally from 60 to 80 per cent of the armature diameter. It must be chosen with regard to the peripheral speed and the thickness of the commutator bar.

The commutator peripheral speed is generally about 3000 ft. per min. Peripheral speeds of 6000 ft. per min. are used but should be avoided whenever possible. The higher commutator peripheral speeds generally lead to commutation difficulties.

The minimum thickness of the commutator bar, the thickness at the inside of the commutator, should not be less than 0.06 in., and the maximum thickness, the thickness at the commutator surface, should not be less than 0.1 in. If the thickness of the mica is $\frac{1}{32}$ in., then the

minimum segment pitch is approximately 0.13 in. If a value for β is assumed, the commutator diameter

$$D_c = \frac{K\beta}{\pi}. \quad (114)$$

The thickness of the brush or its width along the commutator circumference may be a determining factor in choosing the commutator diameter. Formula 96 shows that the thickness of the brush and the commutator bar pitch are factors which determine the width of the commutating zone. The thickness of the brush or the number of commutator bars covered by the brush determines the number of coils short-circuited at one time.

The length of the commutator depends upon the space required by the brushes and upon the surface required to dissipate the heat generated by the commutator losses. If w_b is the width of the brush or its length along the axis of the machine, and n_b is the number of brushes per brush arm, then the length of the commutator

$$l_c = n_b(w_b + \tfrac{1}{8}) + c_2, \quad (115)$$

where $\frac{1}{8}$ in. is the clearance between brushes and depends upon the construction of the brush holder, and c_2 is a clearance allowed to stagger the brushes, as explained on page 100. This clearance will vary somewhat with the size of the commutator, but will generally be from 0.5 in. for small machines to approximately 1.5 in. for large machines. Formula 115 gives the minimum length of commutator, the length required for the brushes. If this length gives too small a radiating surface, so that the commutator temperature rise exceeds the permissible value, then l_c must be increased to give sufficient radiating surface, to dissipate the heat generated by the commutator losses.

The total brush contact surface (positive and negative brushes)

$$S_b = \frac{2I_a}{A_b}. \quad (116)$$

From the standpoint of commutation, the current density at the brush contact should be as high as possible, because the brush contact drop increases with increasing current density, Fig. 75. To keep the brush contact I^2R losses small, the current density must be as low as possible. The higher the current density the smaller will be the brush contact surface and also the brush friction losses. There is therefore one current density for which the total losses at the commutator will be a

minimum. The following table gives the current density in amperes

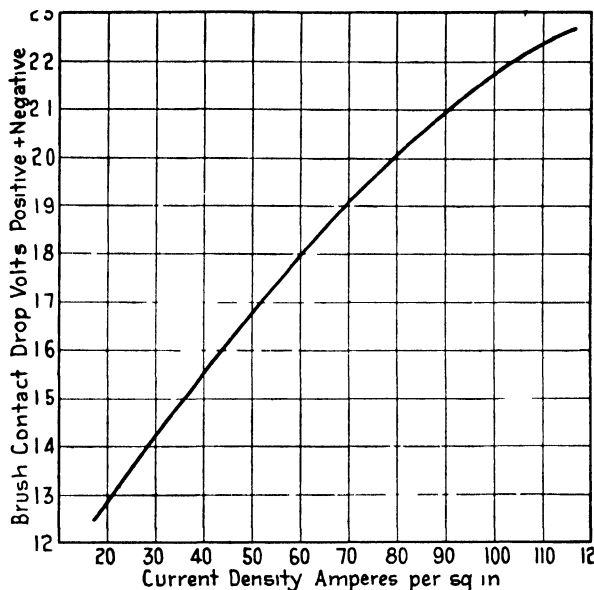


FIG. 75.—Approximate brush contact drop-carbon brushes.

per square inch for various kinds of brushes used for direct current machines:

TABLE VI

Kind of Brush	Sclero- scope Hardness	Amperes per Square Inch	Contact Drop Volts	Coefficient of Friction	Maximum Peripheral Speed
Carbon .	80	35	High	High	3,500
	50	45	Medium	High	3,500
	65	45	Low	Medium	4,500
Carbon graphite	32	50	Medium	Medium	4,000
	49	55	Very high	Low	5,500
	30	45	Low	Medium	4,000
Graphite.	55	50	High	Low	5,500
	40	50	High	Low	5,500
	16	65	Very high	Low	10,000
	17	65	Low	Low	6,000
Metal graphite	12	100	Very low	Very low	4,000
	11	125	Exceptionally low	Very low	4,500
	8	125	Exceptionally low	Very low	4,000

	Contact Drop	Coefficient of Friction
Very high.....	2.6 and over	0.27 and over
High.....	2.0 to 2.5	0.22 to 0.26
Medium.....	1.4 to 1.9	0.17 to 0.21
Low.....	1.0 to 1.3	0.12 to 0.16
Very low.....	0.7 to 0.9	0.07 to 0.11
Exceptionally low.....	0.3 to 0.6	

The current densities given in the table are for normal load and normal operating conditions. The brush contact drops are the voltage drops at both brushes (positive and negative) at rated carrying capacity, for a brush pressure of 3 lb. per sq. in., and a peripheral speed of 3000 ft. per min. The values given for the coefficient of friction are for a brush pressure of 3 lb. per sq. in. and a peripheral speed of 3000 ft. per min.

The thickness of the brush or its width along the commutator circumference is determined from the number of bars covered by the brush. To reduce the length and cost of the commutator, it would be desirable to use a thick brush. But this is not possible, because of the effect of the brush thickness upon commutation and upon the commutating-pole width. The thickness of the brush is generally from 1 to $3\frac{1}{2}$ times the commutator bar pitch. For very low voltage machines with wide commutator bars, the thickness of the brush may be even less than the commutator bar pitch. For multiplex windings the brush should cover more than μ commutator bars to insure even distribution of line current.

The total width of the brushes per brush arm

$$n_b w_b = \frac{S_b}{n_a b_t} \cdot \quad (117)$$

A small area of contact between commutator and each brush generally gives a better contact. The contact surface for each brush is generally from 1 to 2 sq. in., and the width of each brush is generally not over 2 in. When determining the thickness and width of the brush, the standards recommended by the A.I.E.E.⁵ should be followed.

FOR WIDTH OF BRUSHES AND DIAMETER OF ROUND BRUSHES

Up to $\frac{1}{4}$ in. inclusive, increase by steps of $\frac{1}{16}$ in.

Over $\frac{1}{4}$ in. to $2\frac{1}{2}$ in. inclusive, increase by steps of $\frac{1}{8}$ in.

Over $2\frac{1}{2}$ in., increase by steps of $\frac{1}{4}$ in.

Diameter of all round brushes, increase by steps of $\frac{1}{16}$ in.

NOTE.—For widths, $\frac{1}{4}$ in. steps are to be used whenever possible.

⁵ A.I.E.E. Proc., July, 1917, Vol. 36, p. 606.

FOR THICKNESS OF BRUSHES

Up to $\frac{1}{8}$ in. inclusive, increase by steps of $\frac{1}{16}$ in.

Over $\frac{1}{8}$ in., increase by steps of $\frac{1}{8}$ in.

NOTE.—Whenever possible, $\frac{1}{8}$ in. steps are to be used above $\frac{1}{2}$ in. in thickness.

Sample Design: *Design of Commutator and Commutating Poles.*—

The commutator diameter is generally from 60 to 80 per cent of the armature diameter. Choosing 65 per cent, in order that the peripheral speed will not be too high,

$$D_c = 0.65D = 0.65 \times 25 = 16.25 \text{ in.}; \text{ use } 16.0 \text{ in.}$$

The armature winding for this design has four conductors per slot and one turn per coil. Each conductor is, therefore, one-half of a coil and the number of armature coils and commutator bars,

$$K = 2 \times 81 = 162.$$

The commutator bar pitch,

$$\beta = \frac{\pi D_c}{K} = \frac{\pi \times 16}{162} = 0.31 \text{ in.}$$

and

$$\beta_r = 0.31 \frac{25}{16} = 0.485 \text{ in. of armature circumference.}$$

If the brush covers 2.5 commutator bars, the thickness of the brush,

$$b_t = 2.5 \times 0.31 = 0.775 \text{ in.}$$

Use a brush 0.75 in. thick, and the number of bars covered,

$$b = \frac{0.75}{0.31} = 2.42.$$

The armature winding is not a full pitch winding, therefore,

$$\begin{aligned} \varphi &= \frac{K}{p} - \frac{1}{2}(Y_1 - 1) = \frac{162}{6} - \frac{1}{2}(53 - 1) \\ &= 1.0. \end{aligned}$$

The width of the commutating zone is calculated by formula 96,

$$\begin{aligned} w_c &= \left(b + m + \varphi - \frac{a}{p} \right) \beta_r = \left(2.42 + 2 + 1 - \frac{6}{6} \right) 0.485 \\ &= 2.14 \text{ in. of armature circumference.} \end{aligned}$$

The width of the neutral zone, or the space between adjacent pole tips

$$= (1 - \psi)\tau = (1 - 0.66)13.1 = 4.45 \text{ in.}$$

The ratio of the commutating zone to the neutral zone

$$= \frac{2.14}{4.45} = 0.481 \text{ or } 48.1 \text{ per cent.}$$

The brush thickness selected is therefore satisfactory, as it is generally desirable to keep the ratio of commutating zone to neutral zone equal to or less than 0.50.

The mica of the commutator is to be under-cut, so that a medium hard or soft brush with self-lubricating qualities will be satisfactory. Choosing a current density of 65 amperes per sq. in., the total brush contact surface

$$S_b = \frac{2I_a}{A_b} = \frac{2 \times 1207}{65} = 37.1 \text{ sq. in.}$$

The total width of the brushes per brush arm

$$n_b w_b = \frac{S_b}{n_a b_i} = \frac{37.1}{6 \times 0.75} = 8.25 \text{ in.}$$

With a brush width equal to 1.5 in., 6 brushes per arm are required, and the length of the commutator

$$\begin{aligned} l_c &= n_b(w_b + \tfrac{1}{8}) + c_2 = 6(1.5 + \tfrac{1}{8}) + 1.0 \\ &= 10.75 \text{ in.; use } 11 \text{ in.} \end{aligned}$$

This commutator length will be satisfactory if the radiating surface is large enough to dissipate the heat generated by the commutator losses. The method of calculating the commutator radiating surface is given in Chapter VII.

The length of the commutating-pole air gap

$$\begin{aligned} \delta_i &= (1 \text{ to } 2)\delta = (1 \text{ to } 2)0.20 \\ &= 0.20 \text{ to } .40; \text{ use } 0.25 \text{ in.} \end{aligned}$$

The width of the commutating pole

$$\begin{aligned} w_i &= w_c - (1.5 \text{ to } 2)\delta_i = 2.14 - (0.375 \text{ to } 0.50) \\ &= 1.765 \text{ to } 1.64 \text{ in.} \end{aligned}$$

$$w_i \geq \frac{1 - \psi}{2}\tau = \frac{1 - 0.66}{2}13.1 = 2.23 \text{ in.}$$

$$w_i \geq 1.5t_1 = 1.5 \times 0.97 = 1.45 \text{ in.}$$

The commutating-pole shoe is therefore made 1.75 in. wide and the pole body is the same width.

Since as many commutating as main poles are used, the length of the commutating poles

$$\begin{aligned} l_i &= (0.60 \text{ to } 0.80)l_1 = (0.60 \text{ to } 0.80)10.5 \\ &= 6.3 \text{ to } 8.4 \text{ in.}; \text{ use } 7.0 \text{ in.} \end{aligned}$$

The reactance voltage per coil is calculated by formula 101. The data required for this formula are:

$$\text{ATP}_a = 5440, \quad p = 6, \quad t_a = 1.0, \quad n_s = 15, \quad m = 2, \quad b = 2.42,$$

$$A = b + 1 - \frac{a}{p} = 2.42 + 1 - \frac{6}{6} = 2.42, \quad \varphi = 1.0,$$

$$l = 10.5, \quad d_s = 1.56, \quad w_s = 0.31, \quad l_i = 7.0, \quad t_1 = 0.97,$$

$$w_i = 1.75, \quad \delta_i = 0.25, \quad l_s = L_a - l = 27.1 - 10.5 = 16.6$$

$$4.25l \frac{d_s}{w_s} = 4.25 \times 10.5 \frac{1.56}{0.31} = 224$$

$$9.35(l - l_i) \log_{10} \frac{2t_1 - w_s}{w_s} = 9.35(10.5 - 7) \log_{10} \frac{2 \times 0.97 - 0.31}{0.31} = 23.6$$

$$2.03l_i \frac{w_i - w_s}{\delta_i} = 2.03 \times 7 \frac{1.75 - 0.31}{0.25} = 81.9$$

$$8.12l_s = 8.12 \times 16.6 = 135$$

$$2 - \frac{\varphi}{A + m - 1} = 2 - \frac{1.0}{2.42 + 2 - 1} = 1.708$$

$$M = 1.708(224 + 23.6 + 81.9) + 135 = 698$$

$$\begin{aligned} e_r &= \frac{\text{ATP}_a p t_a n_s}{10^8} \frac{m}{A + m - 1} M \\ &= \frac{5440 \times 6 \times 1 \times 15}{10^8} \frac{2}{2.42 + 2 - 1} 698 \\ &= 2.01 \text{ volts.} \end{aligned}$$

The flux density in the commutating-pole air gap

$$\begin{aligned} B_{ai} &= \frac{e_r \times 60 \times 10^8}{2l_a l_v \times 12} \quad \frac{2.01 \times 60 \times 10^8}{2 \times 1 \times 7 \times 5890 \times 12} \\ &= 12,200 \text{ lines per sq. in.} \end{aligned}$$

The air gap coefficient for the commutating-pole air gap is calculated by formula 46, in the same way as for the main-pole air gap:

$$k = \frac{t_1}{w_{i1} + (y\delta_i)} = \frac{0.97}{0.66 + (1.0 \times 0.25)} = 1.065.$$

The ampere-turns for the commutating-pole air gap

$$\text{AT}_{gi} = \frac{B_{gi}\delta_i k}{3.2} = \frac{12,200 \times 0.25 \times 1.065}{3.2} = 1015 \text{ ampere-turns.}$$

These are the ampere-turns required for the commutating-pole air gap, to obtain straight-line commutation at normal load. When the ampere-turns for the remainder of the magnetic circuit are neglected when calculating the commutating-pole ampere-turns, and especially for machines designed for overload capacity, practice has shown that it is desirable to increase the commutating-pole air gap ampere-turns from 1.5 to 2 times. For normal loads, slight over-commutation will then result. If the commutating field is found to be too strong, it may be reduced by increasing the commutating-pole air gap length or by means of a shunt across the commutating field winding.

The ampere-turns per pole for the commutating field winding

$$\begin{aligned} \text{ATP}_i &= \text{ATP}_a + 1.5 \text{AT}_{gi} \\ &= 5440 + 1.5 \times 1015 \\ &= 6960. \end{aligned}$$

The number of turns per pole for the commutating field coil

$$t_i = \frac{\text{ATP}_i}{I_a} = \frac{6960}{1207} = 5.76; \text{ use } 5.5.$$

The section area of the conductor, for a current density of 1300 amperes per square inch,

$$s_i = \frac{I_a}{A_i} = \frac{1207}{1300} = 0.93 \text{ sq. in.}$$

Three strap copper conductors, 0.25×1.25 in., wound in parallel, will be used. Each conductor has an area of 0.305 sq. in. The current density for the commutating field winding

$$A_i = \frac{1207}{3 \times 0.305} = 1320 \text{ amperes per sq. in.}$$

The coil is wound, as shown in Fig. 76, and the mean-turn

$$\begin{aligned} L_i &= 2 \times 7 + \pi(1.25 + 1.75 + \frac{1}{8}) + 1.0. \\ &= 24.8 \text{ in.}, \end{aligned}$$

where 1.0 in. per turn is allowed for the connection between poles.

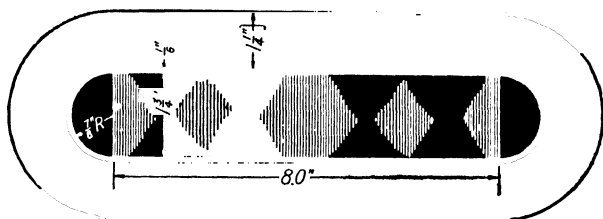


FIG. 76.

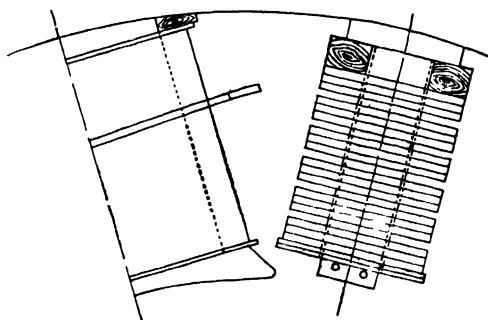


FIG. 77.

The resistance of the commutating field winding at 75° C.

$$\begin{aligned} R_i &= \frac{L_i t_{pr}}{s_i \times 10^6} = \frac{24.8 \times 5.5 \times 6 \times 0.826}{0.915 \times 10^6} \\ &= 0.00074 \text{ ohm}; \end{aligned}$$

and the voltage drop

$$I_a R_i = 1207 \times 0.00074 = 0.892 \text{ volts,}$$

or 0.357 per cent of full-load terminal voltage.

The weight of the commutating field copper

$$\begin{aligned} G_i &= L_i t_{ps_i} \times 0.321 \\ &= 24.8 \times 5.5 \times 6 \times 0.915 \times 0.321 \\ &= 241 \text{ lb.} \end{aligned}$$

The sketch of Fig. 77 shows the clearance between the series and commutating field windings in the interpolar space.

CHAPTER VII

LOSSES, EFFICIENCY, AND TEMPERATURE RISE

THE losses to be considered in direct-current motors and generators are:

- (1) Copper losses in armature and field windings.
- (2) Core or iron losses in the armature teeth and yoke.
- (3) Brush contact (I^2R) losses.
- (4) Field and armature rheostat losses (when present).
- (5) Mechanical losses—bearing friction, brush friction, and windage.

In addition to the losses given above, there are the indeterminate load losses, which may be of importance and which vary with the design of the machine. Because there is no satisfactory method available by which to determine these losses, the Standards of the A.I.E.E. recommend that they be taken equal to 1 per cent of the output for direct-current generators and motors, except for motors 200 hp, 575 r.p.m. and smaller, in which cases they shall be omitted.

In accordance with the Standards of the A.I.E.E., the copper losses for all windings are to be calculated for a temperature of 75° C. for all loads.

Armature Copper Losses.—The resistance of the armature winding has been calculated, page 63, Chapter III. The armature copper loss

$$W_a = I_a^2 R_a. \quad (118)$$

For a generator the armature current is equal to the terminal current plus the shunt field current, and for a motor it is equal to the terminal current minus the shunt field current. For a motor the armature copper losses will then vary with the square of the load, whereas for a generator they will not do so because of the shunt field current, which does not vary directly with the load. Except for machines for which the shunt field current is a large percentage of the load current, the armature copper losses may be taken as varying with the square of the load for both generator and motor.

Commutating Field Copper Loss.—The commutating field winding and the compensating winding, when used, are connected in series with the armature winding, so that the armature current flows in the commutating field winding and compensating winding. The resistance of the commutating field winding has been calculated, page 119, Chapter VI. The copper loss in the commutating field winding

$$W_i = I_a^2 R_i, \quad (119)$$

and varies with the square of the load.

Series Field Copper Loss.—The series field winding is connected in series with the armature winding and commutating field winding. For the long shunt connection the series field current is equal to the armature current, I_a , whereas for the short shunt connection it is equal to the line current, I . The series field resistance was calculated, page 97, Chapter V. The series field copper loss for long shunt,

$$W_s = I_a^2 R_s, \quad (120)$$

and for short shunt,

$$W_s = I^2 R_s. \quad (120a)$$

Shunt Field Copper Loss.—The shunt field resistance was calculated, page 96, Chapter V, and the shunt field copper loss

$$W_f = i_f^2 R_f. \quad (121)$$

When a rheostat is connected in series with the shunt field winding, the rheostat losses must be included with the shunt field copper losses, when calculating the efficiency. For the long shunt connection the voltage across the shunt field is equal to the terminal voltage, but for the short shunt connection it is equal to the terminal voltage plus the drop in the series field winding. The drop in the series field winding is generally quite small and for either long or short shunt connection the shunt field copper loss plus the rheostat losses

$$W_f + W_r = i_f E_t.$$

Brush Contact Losses.—The brush contact ($I^2 R$) losses depend upon the condition of the commutator and upon the quality of commutation obtained. It is therefore very difficult to predetermine accurately the brush contact ($I^2 R$) losses. The A.I.E.E. Standards recommend that 2 volts shall be assumed for the drop at the brush contacts, for both positive and negative brushes, for carbon and graphite brushes with pig-tails attached. A total drop of 3 volts is recommended for brushes with

no pigtails attached. The brush contact loss for brushes with pigtails is then,

$$W_b = I_a^2. \quad (122)$$

Core Loss.—The iron losses in electric sheet steels consist of the hysteresis losses and the eddy current losses. In rotating electric machines, there are, in addition to the hysteresis and eddy current losses in the laminated armature core, pole face losses that are due to the flux pulsations produced by the armature slots, band losses, losses due to punching and bending strains in the laminations, losses due to imperfect insulation between the laminations (caused by burs or slot filing), and losses in the endframes due to stray fluxes. Since these additional losses cannot be easily calculated, the core loss calculations should be based upon the results obtained from tests on similar machines.

A variety of electric sheet steels are available for the armature laminations of direct-current machines. Silicon in steel increases its specific resistance and decreases the eddy current losses, but also decreases its permeability for high flux densities; it also makes it non-aging. Sheet steel, alloyed with silicon, is more expensive than open-hearth steel, and the cost increases as the thickness of the sheet decreases. More complete information on the properties and testing of electric sheet steels can be obtained from Thomas Spooner's splendid book.¹ The efficiency and cost will therefore generally determine the kind of steel to be used for the armature laminations.

Curves showing the total loss per pound, due to the fundamental frequency fluxes, are given in the Appendix for various grades of electric sheet steel. These curves are the results of tests conducted on samples in the Electrical Engineering Laboratories of the University of Minnesota. The standard method of the American Society for Testing Materials was used.

The iron loss for the armature teeth and yoke must be calculated separately, because the flux densities are not the same. For the armature yoke, the flux density is assumed to be uniformly distributed over the section area, and the flux density is calculated as shown on page 69, Chapter IV. The frequency of the flux reversals is calculated by formula 15. From the proper curve in the Appendix, the iron loss per pound can be found which, when multiplied by the weight of iron in the armature yoke and frequency correction factor, gives the core loss in the armature yoke due to the fundamental frequency flux.

The flux density is not the same for all sections of the armature teeth

¹ "Properties and Testing of Magnetic Materials," McGraw-Hill Book Co., New York.

because of the tooth taper. The loss in the armature teeth is calculated for the density, at a section $\frac{1}{3}$ slot depth from the minimum tooth width. The loss per pound, taken from the proper curve in the Appendix, multiplied by the weight of iron in the armature teeth and the frequency correction factor, gives the core loss in the armature teeth, due to the fundamental frequency fluxes. The sum of the loss in the teeth plus the loss in the yoke, calculated as just explained, is the total armature core loss, due to the fundamental frequency fluxes only, and does not include the additional losses. The total armature core loss can be found by multiplying the sum of the tooth and yoke losses (due to the fundamental frequency flux) by a factor which is generally between 1.8 and 3.5. This factor should be determined from tests of similar machines. When such data are not available, 2.5 may be used.

Brush Friction Loss.—The brush friction loss depends upon the brush pressure, the peripheral speed of the commutator, and the coefficient of friction between commutator and brush. It may be calculated approximately by the following formula:

$$W_{bf} = PS_b c_f v_c \times 0.0226 \text{ watt,} \quad (123)$$

where P is the brush pressure in pounds per square inch and is generally from 1.5 to 2 lb. per sq. in., and c_f is the coefficient of friction and is generally from 0.15 to 0.25 for carbon and graphite brushes. Tests on new machines show wide variations in brush friction loss, because the commutator and brushes do not have the smooth surfaces that come after continued operation. For this reason, the American Institute has adopted conventional values for the brush friction loss, based upon tests of a large number of machines, which are to be used in calculating efficiencies. For carbon and graphite brushes, the brush friction loss is to be taken as 8 watts per square inch of brush contact per 1000 ft. per min. peripheral speed, and for metal graphite it is to be taken as 5 watts per square inch of brush contact per 1000 ft. per min. peripheral speed.

Friction and Windage Loss.—Like the brush friction, the bearing friction depends upon the pressure on the bearing, the peripheral speed of the shaft at the bearing, and the coefficient of friction between bearing and shaft. The bearing friction can be calculated² when the bearing dimensions are known. The windage losses cannot be calculated separately; they depend largely upon the construction of the armature.

²“Die Gleichstrommaschine,” Vol. 1, p. 607, Julius Springer, Berlin, and “Electric Machine Design,” by Gray, p. 97, McGraw-Hill Book Co., New York.

The friction and windage losses are generally not separated and are determined from tests of similar machines. When such data

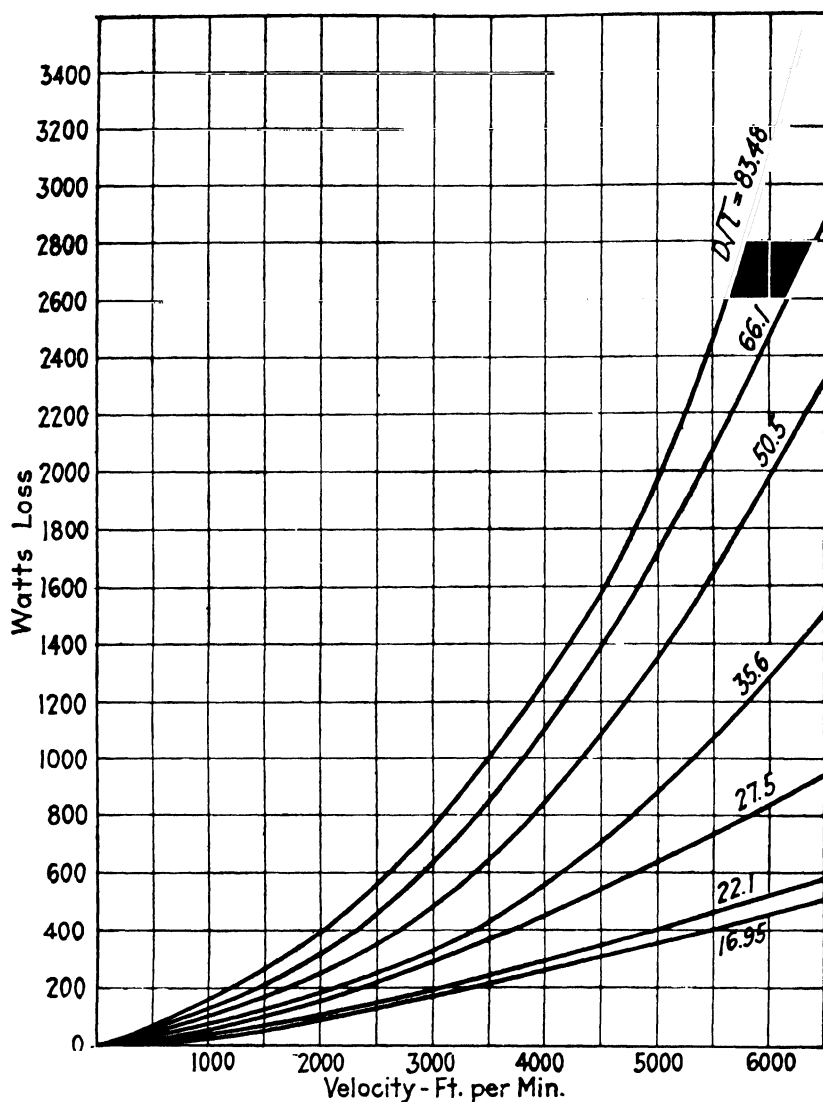


FIG. 78.—Approximate friction and windage losses for d.c. generators and motors.

are not available, they can be estimated with the help of the curves, Fig. 78.

Efficiency.—The efficiency is the ratio of the output to the output plus all the losses. It is expressed as follows:

$$\text{eff.} = \frac{\text{Output} \times 100}{\left\{ \begin{array}{l} \text{Output} + W_a + W_i + W_s + W_f + W_r \\ + W_c + W_b + W_{bf} + W_{fw} + W_s \end{array} \right\}} \text{ per cent.}$$

TABLE VII

COMMUTATING-POLE GENERATOR EFFICIENCIES

Kilowatts	Speed, Revolutions per Minute	Efficiencies		
		Full Load	$\frac{3}{4}$ Load	$\frac{1}{2}$ Load
3½	1750	80.0	79.5	78.0
3½	1150	79.5	79.0	76.0
12	1750	86.0	84.5	81.5
12	750	83.0	82.5	81.0
15	575	83.6	83.5	81.2
20	900	86.6	86.0	83.5
20	750	85.1	84.9	83.3
20	575	85.5	85.2	83.5
25	900	86.7	86.5	84.7
25	750	86.1	86.0	84.5
25	575	86.5	86.5	84.7
30	1150	88.0	87.7	85.0
30	750	87.5	87.0	85.8
30	575	87.5	87.1	85.9
50	1150	89.1	88.6	87.3
50	750	88.3	88.0	86.4
75	1150	90.2	89.6	87.6
75	725	89.6	89.2	88.0
100	1150	90.6	90.2	88.6
100	725	90.2	90.0	88.3
125	1000	91.0	90.5	88.8
125	725	90.2	90.0	88.4
150	1000	91.0	90.0	88.5
175	1000	91.2	90.3	88.5

For constant-speed and constant-potential machines, the efficiency will be a maximum for that load for which the sum of the constant losses is equal to the sum of the variable losses. Direct-current generators and motors are designed, whenever possible, to have maximum efficiency at from $\frac{3}{4}$ to full-load. Usual efficiencies for 250-volt, compound-

TABLE VIII
CONSTANT-SPEED D-C. MOTOR EFFICIENCIES

Rated Horsepower	Rated Full-load Speed, Revolu- tions per Minute	Efficiencies		
		$\frac{1}{4}$ Load	$\frac{1}{2}$ Load	$\frac{3}{4}$ Load
5	1750	83 0	82 0	77 0
5	1150	82 5	81 5	77 0
5	850	80 0	80 0	76 0
10	1750	84 0	83 0	78 0
10	1150	86 0	86 0	81 0
10	850	85 5	85 0	81 0
20	1750	86 5	86 0	84 0
20	1150	88 5	88 5	84 0
20	850	88 0	87 5	83 0
30	1750	88 0	88 0	85 0
30	1150	89 5	89 5	85 0
30	850	88 4	88 2	86 5
50	1750	90 0	88 0	86 0
50	1150	90 1	90 0	88 3
50	850	90 5	90 5	88 9
75	1150	91 6	91 4	89 9
75	850	91 5	91 2	89 7
100	1150	91 4	91 0	89 2

wound, commutating-pole, direct-current generators are given in Table VII. Table VIII gives the efficiencies for 230-volt, commutating-pole, constant-speed, general-purpose, direct-current motors.

Temperature Rise.—The temperature rise of each of the various parts of continuous or short-time rated direct-current machines, above the temperature of the cooling medium, shall not exceed the values given in Table IX.³

³ From A.S.A. Standards, C50, March, 1943. The complete Standard, C50, may be obtained from American Standards Association, 70 East 45 St., New York 17, N. Y.

TABLE IX
LIMITING OBSERVABLE TEMPERATURE RISE

Item	Machine Part	Method of Temperature Determination to be Employed	General-Purpose Motors and Generators Class A Insulation	Totally Enclosed Motors and Generators		Continuous-Duty Generators and Motors	
				Class A Insulation	Class B Insulation	Class A Insulation	Class B Insulation
1	Armature windings and all windings other than 2 and 3	Thermometer	40	55	75	50	70
		Thermometer	40	—	—	50	70
2	Shunt field windings	Resistance	50	60	80	60	80
3	Single-layer field windings with exposed uninsulated surfaces and bare copper windings	Thermometer	50	65	85	60	80
4	Cores and mechanical parts in contact with or adjacent to insulation	Thermometer	40	—	—	50	70
5	Commutators and collector rings	Thermometer	55	65	85	65	85

Class A insulation consists of cotton, silk, paper, and similar organic materials when impregnated or immersed in oil; also enamel, as applied to conductors.

Class B insulation consists of inorganic materials, such as mica, asbestos, and fiber glass or combinations of these. If Class A material is used in small quantities in conjunction, for structural purposes only, the combined material may be considered as Class B, provided the electrical and mechanical properties of the insulated winding are not impaired by the application of the temperature permitted for Class B materials.

It is therefore important that the designer be able to predetermine accurately the maximum temperature rise for all parts of the machine, in order that maximum output for a given amount of material may be obtained. The temperature rise, however, is not the limiting factor

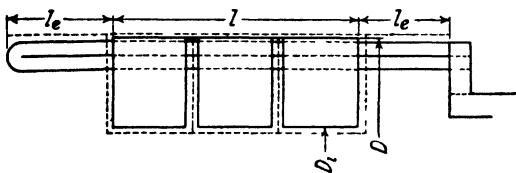


FIG. 79.

for the output, for all machines. For reasonably well ventilated machines, commutation or efficiency, or both, may be the limiting factor rather than temperature.

The losses in the various parts of electrical machinery are converted into heat, which produces a temperature rise above that of the surrounding air. The value of the final temperature depends upon the heat capacity of the various insulating materials used and upon the rate at which the heat is conducted through the materials to the cooling medium. The final temperature is reached when the heat is dissipated as fast as it is generated. The theory of the heat flow in electrical machinery has been given by a number of authors.⁴ The temperature rise can be determined with reasonable accuracy with the aid of test data on machines of similar construction. The general formula for the temperature rise is

$$T = \frac{C_e}{S/W}.$$

⁴ "Die Gleichstrommaschine," Vol. 1, 3rd ed., p. 666, Julius Springer, Berlin; "Electric Machine Design," by Gray, Chapter XI, McGraw-Hill Book Co., New York; "The Cooling of Electrical Machines" and bibliography, by George E. Luke, A.I.E.E. Trans., Vol. 42, 1923, p. 636; "The Thermal Time Constants of Dynamo Electric Machines," by A. E. Kennelly, A.I.E.E. Trans., Vol. 44, 1923, p. 137.

Armature Temperature Rise.—For armatures up to about 16 in. in diameter with axial ventilating ducts on the inside of the armature, the radiating surface is taken as indicated by the dotted line, Fig. 79, and for larger diameters, as shown in Fig. 80. The cooling surface per watt loss for Fig. 79 is

$$\frac{S_a}{W_a} = \frac{\left[\frac{\pi D(l + 2l_e) + \pi Dd + \frac{\pi}{4}(D^2 - D_i^2)(2 + n_d)}{(1 + 0.00051v)} \right]}{W_a + W_c + W_s}, \quad (124)$$

and for Fig. 80,

$$\frac{S_a}{W_a} = \frac{\left[\frac{\pi D(l + 4l_e) + \pi Dd + \frac{\pi}{4}(D^2 - D_i^2)(2 + n_d)}{(1 + 0.00051v)} \right]}{W_a + W_c + W_s}. \quad (124a)$$

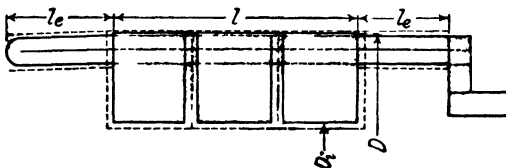


FIG. 80.

The factor $(1 + 0.00051v)$ is given by Dr. Arnold and compensates for the increased radiating capacity of the armature, due to rotation.

The temperature rise of the armature

$$T_a = \frac{C_{ca}}{S_a/W_a} \text{ degrees C.} \quad (125)$$

The value of C_{ca} , the cooling coefficient, can be determined only by test and will not be the same for any two machines. In the absence of accurate test data, the following values may be used:

$C_{ca} = 45$ to 55 for open-type machines, Fig. 1, Chapter I

$C_{ca} = 55$ to 65 for open-type machines, Fig. 16, Chapter I.

Field Winding Temperature Rise.—The radiating surface for the shunt field winding (see Fig. 60)

$$S_f = 2(d_f + h_f)L_f p,$$

and the surface per watt loss

$$\frac{S_f}{W_f} = \frac{2(d_f + h_f)L_f p}{W_f}. \quad (126)$$

When ventilated field coils are used, as shown in Fig. 61, Chapter V, the surface of the ducts must be included when calculating the total cooling surface.

When the series field winding is wound at either end of the shunt field coil or wound of insulated wire on top of the shunt field coil, the two windings may be treated as one winding and the combined cooling surface calculated. The losses for the calculation of the surface per watt must then be the sum of the shunt field and series field losses.

The cooling surface for the commutating field winding is calculated as explained for the shunt and series field winding.

The cooling constant for the field winding depends upon the insulation used, the thickness of the field coil, the construction of the machine, the temperature of the armature, the number of commutating poles used, etc., and can be determined only by test. The cooling coefficient for the shunt field winding can be determined as explained on page 88.

Commutator Temperature Rise.—The cooling surface of the commutator per watt loss

$$\frac{S_c}{W_c} = \frac{\pi D_c l_c (1 + 0.00051 v_c)}{W_b + W_{bf}}, \quad (127)$$

and the commutator temperature rise

$$T_c = \frac{C_{cc}}{S_c/W_c}. \quad (128)$$

For commutating-pole machines with no sparking at the brushes,

$$C_{cc} = 15 \text{ to } 20.$$

When there is sparking at the brushes, it is not possible to calculate the commutator losses and the commutator temperature rise.

Sample Design: *Losses, Efficiency, and Temperature Rise.*—The armature copper losses for full-load

$$\begin{aligned} W_a &= I_a^2 R_a = 1207^2 \times 0.00307 \\ &= 4460 \text{ watts,} \end{aligned}$$

or 1.49 per cent of the rated output.

The resistance of the commutating field winding is given on page 119,

Chapter VI, and the commutating field copper losses for full-load

$$\begin{aligned} W_i &= I_a^2 R_i = 1207^2 \times 0.00074 \\ &= 1080 \text{ watts,} \end{aligned}$$

or 0.36 per cent of rated output.

The full-load series field copper loss

$$\begin{aligned} W_s &= I_a^2 R_s = 1207^2 \times 0.000564 \\ &= 820 \text{ watts,} \end{aligned}$$

or 0.273 per cent of rated output.

The copper loss for the shunt field

$$\begin{aligned} W_f &= i_f^2 R_f = 7.06^2 \times 25.4 \\ &= 1265 \text{ watts,} \end{aligned}$$

or 0.423 per cent of rated output.

Assuming 2 volts drop for positive and negative brushes, the brush contact loss for full-load

$$\begin{aligned} W_b &= I_a 2 = 1207 \times 2 \\ &= 2414 \text{ watts, or } 0.805 \text{ per cent.} \end{aligned}$$

The maximum and minimum width of the armature tooth have been calculated (page 68, Chapter IV), and the average tooth width

$$\begin{aligned} w_{ta} &= \frac{w_{t1} + w_{t2}}{2} = \frac{0.66 + 0.54}{2} \\ &= 0.60 \text{ in.} \end{aligned}$$

The weight of the iron in the armature teeth

$$\begin{aligned} G_{ct} &= w_{ta}(l - n_a w_a) k_1 S d_s \times 0.278 \\ &= 0.60(10.5 - 3 \times \frac{3}{8}) 0.92 \times 81 \times 1.56 \times 0.278 \\ &= 182 \text{ lb.,} \end{aligned}$$

where 0.278 is the weight per cubic inch of open-hearth sheet steel. The flux density at a section $\frac{1}{3}$ slot depth from the minimum tooth width is used to calculate the iron losses in the teeth and is equal to 120 kilo-

lines (page 75, Chapter IV). The loss per pound for this density is found from the loss curve for open-hearth steel in the Appendix and is 8 watts. The frequency of the flux reversals is 45 cycles per sec., and the loss in the armature teeth due to the fundamental frequency flux

$$\begin{aligned} W_{ct} &= 8 \times 0.71 \times 182 \\ &= 1033 \text{ watts.} \end{aligned}$$

The weight of the iron in the armature yoke

$$\begin{aligned} G_{ay} &= \frac{\pi}{4} [(D - 2d_s)^2 - D_i^2] (l - n_d w_d) k_1 \times 0.278 \\ &= \frac{\pi}{4} [(25 - 2 \times 1.56)^2 - 13.5^2] (10.5 - 3 \times \frac{3}{8}) 0.92 \times 0.278 \\ &= 559 \text{ lb.} \end{aligned}$$

The flux density for the armature yoke is 74 kilo-lines (page 77, Chapter IV), and the loss per pound is 3.5 watts. The loss in the armature yoke due to the fundamental frequency flux

$$\begin{aligned} W_{cy} &= 3.5 \times 0.71 \times 559 \\ &= 1390 \text{ watts.} \end{aligned}$$

The total core loss (see page 123)

$$\begin{aligned} W_c &= (1033 + 1390) 2.5 \\ &= 6060 \text{ watts,} \end{aligned}$$

or 2.02 per cent of rated output.

The brush friction loss will be calculated in accordance with the A.I.E.E. recommendation:

$$\begin{aligned} W_{bf} &= 8 \times 40.5 \times 3.77 \\ &= 1220 \text{ watts} = 0.407 \text{ per cent} \end{aligned}$$

From the curves, Fig. 78, the friction and windage loss is found to be 3000 watts = 1.0 per cent of rated output.

The stray load losses will be taken equal to 1 per cent of the output rating, which is in accordance with the A.S.A. Standards.

The calculations for the efficiency are shown in Table X, and the efficiency curve is shown in Fig. 81.

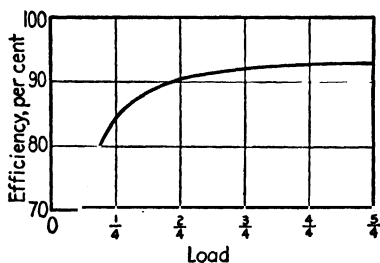


FIG. 81.—Efficiency of 300-kw., 250-volt, 900-r.p.m. generator.

The surface per watt loss for the armature is calculated by formula 124a:

$$\begin{aligned}
 \frac{S_a}{W_a} &= \frac{\left[\pi D(l + 4l_e) + \pi D_i l + \frac{\pi}{4}(D^2 - D_i^2)(2 + n_d) \right] (1 + 0.00051v)}{W_a + W_c + W_{sl}} \\
 &= \frac{\left\{ \frac{\pi \times 25(10.5 + 4 \times 5.17) + \pi \times 13.5 \times 10.5 + \frac{\pi}{4}(25^2 - 13.5^2)(2 + 3)}{(1 + 0.00051 \times 5900)} \right\}}{4460 + 6060 + 3000} \\
 &= 1.375 \text{ sq. in. per watt,}
 \end{aligned}$$

TABLE X

	Load				
	1	2	3	4	5
Armature copper	0.28	1.12	2.51	4.46	7.00
Stray load	0.75	1.50	2.25	3.00	3.75
Commutating field	0.07	0.27	0.61	1.08	1.69
Series field	0.05	0.21	0.46	0.82	1.30
Brush I^2R	0.61	1.21	1.82	2.42	3.02
Shunt field	1.27	1.27	1.27	1.27	1.27
Core	6.06	6.06	6.06	6.06	6.06
Brush friction	1.22	1.22	1.22	1.22	1.22
Friction and windage	3.00	3.00	3.00	3.00	3.00
Total losses	13.31	15.86	19.20	23.33	28.31
Output	75.00	150.00	225.00	300.00	375.00
Output plus losses	88.31	165.86	244.20	323.33	403.31
Efficiency	84.9	90.5	92.1	92.8	93.0

and the estimated full-load temperature rise

$$T_a = \frac{C_{ca}}{\frac{S_a}{W_a}} = \frac{55}{1.375} = 40^\circ \text{ C.}$$

The surface per watt for the shunt field winding has been calculated (page 96, Chapter V), and the temperature rise

$$T_f = \frac{C_{cf}}{\frac{S_f}{W_f}} = \frac{88.1}{2.21} = 39.8^\circ \text{ C.}$$

DIRECT-CURRENT DESIGN SHEET

GENERATOR

Hp. Kw. 300 Volts 230-250 Amps 1200 R p m 900 Poles 6
 Watts/r p m 333 Output constant 1.97×10^4 Type Compound-wound Commutating-pole

Outside diameter 25
 Inside diameter 13.5
 Total length 10.5
 Ducts number size 3×1
 Length gross 9.1 L effective 8.62
 Number of slots 81
 Slots per pole 13.5
 Type of winding Simplex lap
 Number of coils 162
 Turns per coil 1
 Conductors total 324
 Conductors per slot 4
 Total flux 48 300 K L
 Distribution constant 0.0665
 Flux per pole 5350 k l
 Conductor dimensions 0.109×0.625
 Conductor section 0.0656
 Current density 3070
 I qua -conn no, size 27.078×0.5
 Coils in slots ... 1 and 14
 Coils in bar 1 and 2
 One-half mean turn 27.1
 Resistance 25°C 0.00258
 Resistance 75°C 0.00317
 Square inch per watt 1.375
 Cal temperature rise 405°C
 Ampere conductors per inch 830
 Ampere-turns per pole 5440

COMMUTATOR AND BRUSH

Diameter 16.0
 Length 11.0
 Peripheral speed 3770
 Number of bars 162
 Bar pitch 0.31
 Thickness of mica 0.03
 Volts bar average 9.63 Max 18.8
 Number of arms 6
 Amperes per arm 402
 Brushes per arm 6
 Size of brush 0.75×1.50
 Current density 5.96
 Square inch per watt 0.444

WEIGHTS

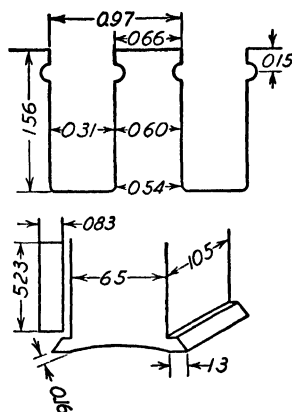
Armature copper 185
 Shunt field copper 213
 Series field copper 241
 Commutating field copper 182
 Armature yoke 559

FULL-LOAD LOSSES

Friction and windage 3000
 Brush friction 1220
 Core 6060
 Stray load 3000
 Armature copper 4460
 Shunt field 1265
 Series field 820
 Commutating field 1080
 Brush contact I^2R 2414
 Total losses 23 330

FULL-LOAD RESISTANCE DROP

Armature $3.71 \times 1.48\%$
 Series field 0.68 0.27
 Commutating field 0.89 0.35
 Brushes 2.00 0.80
 Total 7.28 2.91
 Shunt field I^2R 179



POLES AND YOKE	MAIN	COMM
Material sheet steel	0.023	0.023
Body length and width	101×6	7×1.75
Shoe length and width	10×8.1	
Pole pitch	13.1	
Percentage of pole embrace	65.8	
Pole arc	8.1	
Total air gap length	2×0.20	2×0.25

Material yoke Cast Steel
 Outside diameter of yoke 45.0
 Inside diameter of yoke 38.5
 Length of yoke 15.6
 Magnetic section 6.5×15.5 100.7

FIELD WINDING	SHUNT	SERIES	COMM
Size of conductor No. 13 sq	3 - 0.219	1×0.3	0.25×1.25
Conductor section 0.00465	3×0.216	3×0.305	3×0.305
Amperes 7.06	1207	1207	1207
Current density 1518	181.0	1320	1320
Turns per pole 620	1.5	5.5	5.5
Length of mean turn 38.4	49.2	24.8	24.8
Resistance 25°C 21.3	0.000473	0.00062	0.00062
Resistance 75°C 25.4	0.000564	0.00074	0.00074
Watts loss 1265			
Square inch per watt 2.21			

Field leakage constant 1.20

MAGNETIC CIRCUIT

	Volts 260	R P M 900	
	Section	Density	Length
Gap	825	58.5	1.067
Teeth	404	120	1.56
A yoke	72.8	74	1.6
Pole	68.2	94.1	6.55
I yoke	100.7	63.7	10.9
Total			4990

Shunt AT per pole full load 4370
 Series A I per pole full load 1810
 Commutating A I per pole full load 6640

COMMUTATION

Bars covered by brush 2.42
 Commutating zone at arm surface 2.14
 Commutating zone per cent neutral zone 48.1
 Reactance volts 2.01
 Density in commutating pole air gap 12 200

Remarks Armature laminations 0.014 open hearth sheet steel

The surface per watt loss for the commutator for full-load

$$\begin{aligned}\frac{S_c}{W_c} &= \frac{\pi D_c l_c (1 + 0.00051 v_c)}{W_b + W_{bf}} \\ &= \frac{\pi \times 16 \times 11 (1 + 0.00051 \times 3770)}{2414 + 1220} \\ &= 0.444 \text{ sq. in. per watt,}\end{aligned}$$

and the full-load temperature rise

$$T_c = \frac{C_{cc}}{\frac{S_c}{W_c}} = \frac{20}{0.444} = 45.0^\circ \text{ C.}$$

An assembly drawing of the generator is shown in Fig. 1.

CHAPTER VIII

SAMPLE DESIGN

Sample Design 2: *Design of a Constant-Speed, Direct-Current Motor.*
 —A 20-hp., 1150-r.p.m., 230-volt, constant-speed, commutating-pole, direct-current motor is to be designed. The motor is to be of the general-purpose class, with 40° C. continuous-duty rating. The efficiency of the motor should not be less than 88.5 per cent for rated load, voltage, and speed. (See Table VIII, page 126.)

The motor output

$$Kw = hp \times 746 = 20 \times 0.746 = 14.9 \text{ kw}$$

$$\frac{Kw}{n} \times 10^3 = \frac{14.9}{1150} \times 10^3 = 12.96$$

From the curve of output constants, Fig. 22, Chapter II,

$$C = 3.8 \times 10^4.$$

This motor will be designed with 4 poles, and

$$D = \sqrt[3]{\frac{Kw_a C p}{n(1.5 \text{ to } 3.14)}} = \sqrt[3]{\frac{14.9 \times 3.8 \times 10^4 \times 4}{1150(1.5 \text{ to } 3.14)}} \\ = 10.95 \text{ to } 8.70 \text{ in.}$$

Choose an armature diameter of 10 in., and

$$l = \frac{Kw_a C}{D^2 n} = \frac{14.9 \times 3.8 \times 10^4}{10^2 \times 1150} \\ = 4.90; \text{ use } 5.0 \text{ in.}$$

The peripheral speed,

$$v = \frac{\pi D n}{12} = \frac{3.14 \times 10 \times 1150}{12} \\ = 3010 \text{ ft. per min.}$$

The frequency of the flux reversals in the armature core

$$f = \frac{pn}{2 \times 60} = \frac{4 \times 1150}{2 \times 60} = 38.3 \text{ cycles per sec.}$$

The pole pitch

$$\tau = \frac{\pi D}{p} = \frac{3.14 \times 10}{4} = 7.85 \text{ in.},$$

and for 66 per cent pole embrace the pole arc

$$B = 0.66\tau = 0.66 \times 7.85 = 5.18 \text{ in.}$$

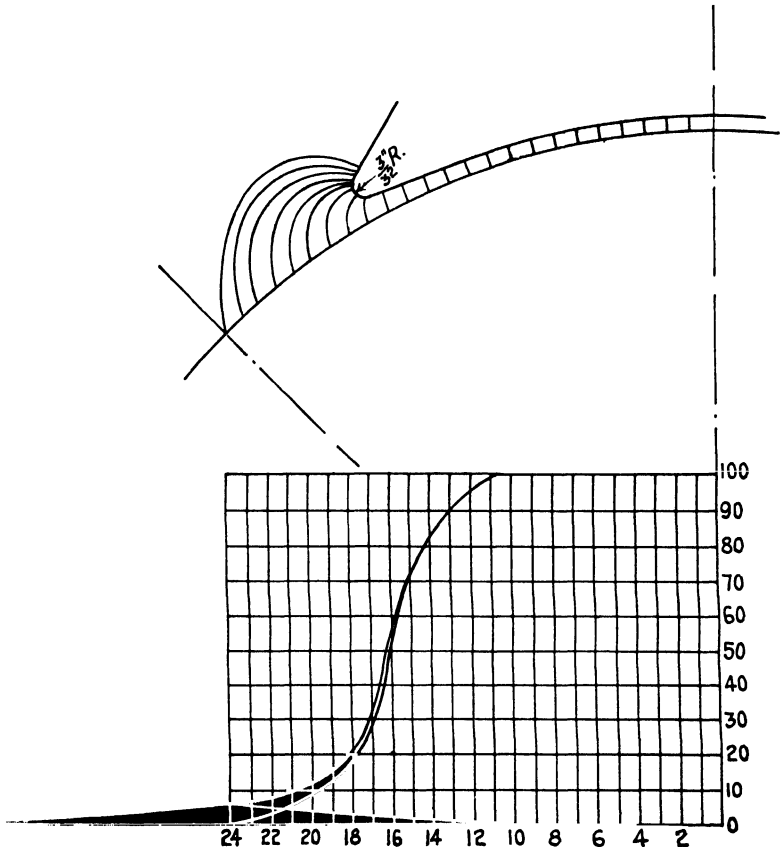


FIG. 82.

The length of the air gap is estimated with the help of the curve, Fig. 25, and the pole shoe is designed as indicated in Fig. 23. The approximate method has been used for making the flux plot, which is shown in Fig. 82, and the air gap flux distribution factor

$$f_d = 0.671$$

From the curve, Fig. 20, the air gap density should be approximately 42.5 kilo-lines per sq. in. The total flux

$$\begin{aligned}\phi_t &= \pi D l B_g = 3.14 \times 10 \times 5.0 \times 42.5 \\ &= 6670 \text{ kilo-lines.}\end{aligned}$$

For a motor the no-load induced voltage, which is equal to the terminal voltage, is used in making the calculations for the magnetic circuit. The no-load speed must then be used, which is assumed to be 1200 r.p.m.

The induced voltage per conductor

$$\begin{aligned}e_i &= \frac{\phi_t n f_d}{60 \times 10^8} = \frac{6670 \times 1200 \times 0.671}{60 \times 10^8} \\ &= 0.896 \text{ volt.}\end{aligned}$$

Since this is quite low, a simplex wave winding can be used to advantage, and the total number of conductors

$$N = \frac{Ea}{e_i} = \frac{230 \times 2}{0.896} = 514.$$

The minimum number of armature slots should be 9 per pole, or 36. The number of armature slots corresponding to the usual tooth pitch, 0.70 to 1.30 in., is

$$S = \frac{\pi D}{t_1} = \frac{\pi \times 10}{0.7 - 1.3} = 44.9 \text{ to } 24.2.$$

Table III, page 40, Chapter III, shows that, in order to avoid dead coils in the armature winding, 2 or 6 coil sides per slot must be used. The number of conductors per slot must be a multiple of 2, and if 6 coil sides per slot are to be used, a multiple of 6. With 6 conductors per slot, too many slots and commutator bars will be necessary; therefore 12 conductors per slot, with 2 turns per coil, will be used. The total number of slots

$$S = \frac{514}{12} = 42.8.$$

Formula 22 shows that 40 slots can be used only with a dead coil. With 39 slots, or $9\frac{3}{4}$ slots per pole, it will be necessary to short chord the armature coils $\frac{3}{4}$ of a slot pitch, which is undesirable for commutating-pole machines, or to over chord $\frac{1}{4}$ of a slot pitch, which should be avoided whenever possible. Forty-one armature slots, or $10\frac{1}{4}$ slots per pole, will therefore probably be most desirable.

The total number of armature conductors

$$N = 12 \times 41 = 492,$$

and

$$\phi_t = \frac{230 \times 2 \times 60 \times 10^8}{492 \times 1200 \times 0.671} = 6970 \text{ kilo-lines.}$$

The armature is therefore simplex wave wound, with 41 slots, 12 conductors per slot, and 2 turns per coil.

The back pitch

$$Y_1 = C_s Y_s + 1 = 6 \times 10 + 1 = 61.$$

The number of commutator bars

$$K = 3 \times 41 = 123,$$

and

$$Y_c = 2 \frac{K \pm 1}{p} = 2 \frac{123 \pm 1}{4} = 62.$$

The front pitch

$$\begin{aligned} Y_2 &= 2Y_c - Y_1 = 2 \times 62 - 61 \\ &= 63. \end{aligned}$$

The average voltage between adjacent commutator bars

$$e_{sa} = \frac{Ep}{K} = \frac{230 \times 4}{123} = 7.48 \text{ volts,}$$

and the maximum voltage

$$e_{sm} = \frac{Ep}{K f_d} 1.30 = \frac{230 \times 4}{123 \times 0.671} 1.3 = 14.5 \text{ volts.}$$

The voltage per turn

$$e_t = \frac{ae_{sm}}{p l_a} = \frac{2 \times 14.5}{4 \times 2} = 3.62 \text{ volts.}$$

The full-load terminal current

$$\begin{aligned} I &= \frac{\text{hp} \times 746}{E_t \times \text{eff.}} = \frac{20 \times 746}{230 \times 0.885} \\ &= 73.4 \text{ amperes.} \end{aligned}$$

From Fig. 48, for $n \times \text{kw.} = 1.94 \times 10^4$, the shunt field current should be approximately 1.0 per cent of the armature terminal current, or 0.70 ampere.

$$I_a = 73.4 - 0.70 = 72.7 \text{ amperes.}$$

$$Q = \frac{I_a N}{\pi D a} = \frac{72.7 \times 492}{\pi \times 10 \times 2} = 570.$$

For $v = 3010$ ft. per min. and $D = 10$ in., QA_a from Fig. 49 is equal to 16.7×10^5 , and

$$A_a = \frac{16.7 \times 10^5}{570} = 2930 \text{ amperes per sq. in.}$$

$$s_a = \frac{I_a}{A_a a} = \frac{72.7}{2930 \times 2} = 0.0124 \text{ sq. in.}$$

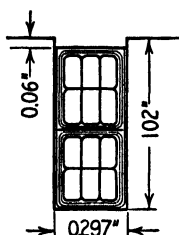


FIG. 83.

The conductors are arranged in the slot as shown in Fig. 83, and the coils are held in the slot by binding bands. From the copper table, a d.c.c. copper ribbon is selected which has the following insulated dimensions: 0.079 in. \times 0.216 in. = 0.0125 sq. in. area. The corrected current density

$$A_a = \frac{72.7}{2 \times 0.0125} = 2900 \text{ amperes per sq. in.}$$

The dimensions of the slot are then (see Table IV):

$$w_s = (3 \times 0.079) + 0.060 = 0.297 \text{ in.}$$

$$d_s = (4 \times 0.216) + 0.160 = 1.024; \text{ use } 1.02 \text{ in.}$$

These slot dimensions will be satisfactory if the resulting tooth densities do not exceed the limits given in Chapter IV.

The net core length with no radial ventilating ducts

$$l_n = 0.92 \times 5.0 = 4.60 \text{ in.}$$

The total net section area at the root of the teeth is

$$\begin{aligned} S_{t2} &= 4.60[\pi(10 - 2 \times 1.02) - 41 \times 0.297] \\ &= 59.0 \text{ sq. in.} \end{aligned}$$

$$B_{t2} = \frac{6970}{59.0} = 118 \text{ kilo-lines per sq. in.}$$

This value is well below the maximum given in Chapter IV.

The calculations for the length of one-half the mean-turn of the armature coil are (see Fig. 50):

$$\begin{aligned}\sin \alpha &= \frac{d}{t_1} = \frac{0.297 + 0.10}{0.766} = 0.518 \\ \alpha &= 31.2^\circ \text{ and } \cos \alpha = 0.855, \tan \alpha = 0.605 \\ L_a &= \frac{\pi(D - d_s)}{p \times \cos \alpha} + 2b + d_s + l \\ &= \frac{3.14(10 - 1.02)}{4 \times 0.855} + 1.5 + 1.02 + 5.0 \\ &= 15.77 \text{ in.}\end{aligned}$$

The axial length of the armature end connections

$$l_e = \frac{\pi(10 - 1.02)}{2 \times 4} 0.605 + 0.75 + 1.02 = 3.90 \text{ in.}$$

The resistance of the armature winding at 75° C.

$$\begin{aligned}R_a &= \frac{L_a N r}{s_a a^2 \times 10^6} = \frac{15.77 \times 492 \times 0.826}{0.0125 \times 2^2 \times 10^6} \\ &= 0.128 \text{ ohm,}\end{aligned}$$

and the voltage drop

$$I_a R_a = 72.7 \times 0.128 = 9.3 \text{ volts,}$$

or 4.04 per cent of rated terminal voltage.

The weight of the armature copper

$$\begin{aligned}G_a &= L_a N s_a \times 0.321 = 15.77 \times 492 \times 0.0125 \times 0.321 \\ &= 31.1 \text{ lb.}\end{aligned}$$

Open-hearth electric steel 29 gauge is to be used for the armature laminations.

$$\begin{aligned}l S t_3 &= 5.0 \pi (10 - \frac{4}{3} 1.02) = 135.5 \\ l_n S w_{t3} &= 4.6 [\pi (10 - \frac{4}{3} 1.02) - 41 \times 0.297] = 68.6 \\ k_t &= 3.2 \left(\frac{135.5}{68.6} - 1 \right) = 3.12 \\ B_{t3}' &= B_{t3} + 3.12 \text{ at.}\end{aligned}$$

The curve below is for open-hearth sheet steel for $k_t = 3.12$ and shows the relation between the apparent tooth density, B_{t3} , and the ampere-turns per inch. For 230 volts, the apparent tooth density

$$B_{t3}' = \frac{\phi_t}{l_n Sw_{t3}} = \frac{6970}{68.6} = 101.5 \text{ kilo-lines per sq. in.}$$

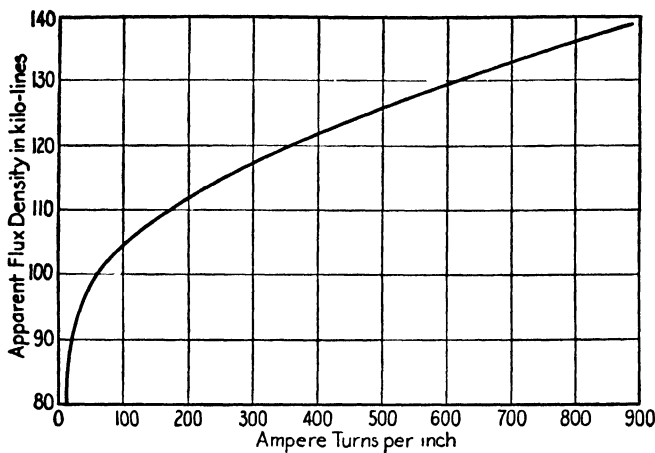


FIG. 83a.

from the curve above for $k_t = 3.12$, at = 66, and $AT_t = 1.02 \times 66 = 67.4$. For various voltages,

E	200	230	260	290
B_{t3}'	88.3	101.5	114.7	128
at _t	18.0	66	245	560
AT_t	18	67	250	570

The armature ampere-turns per pole

$$ATP_a = \frac{72.7 \times 492}{2 \times 2 \times 4} = 2240.$$

The ratio of gap + teeth ampere-turns per pole is to be approximately 0.75 times the armature ampere-turns per pole for rated voltage.

$$AT_g + AT_t = 0.75 \times 2240 = 1680$$

$$AT_g = 1680 - 67 = 1613 = \frac{B_g \delta k}{3.2}$$

$$B_g = \frac{\phi_t}{\pi D l_g} = \frac{6970}{\pi \times 10 \times 5.0} = 44.3 \text{ kilo-lines per sq. in.}$$

Assume $k = 1.20$ and

$$\delta = \frac{3.2 \times 1613}{1.2 \times 44.3} = 0.097; \text{ use } 0.10 \text{ in.}$$

The coefficient

$$k = \frac{t_1}{w_{t1} + (y \times \delta)} = \frac{0.766}{0.469 + (1.8 \times 0.10)} = 1.18,$$

and the ampere-turns per pole for the air gap

$$\text{AT}_g = \frac{44.3 \times 0.10 \times 1.18}{3.2} = 1635.$$

For other voltages,

E	200	230	260	290
B_g	38.6	44.3	50.1	55.9
AT_g	1420	1635	1850	2060

The flux per pole

$$\begin{aligned} \phi &= \frac{\phi_t f_d}{p} = \frac{6970 \times 0.671}{4} \\ &= 1170 \text{ kilo-lines.} \end{aligned}$$

For the flux density in the armature yoke 65 kilo-lines is assumed, and

$$\begin{aligned} d_{ya} &= \frac{\phi}{(l - n_d w_d) k_1 B_{ya}} = \frac{1170}{5.0 \times 0.92 \times 65} \\ &= 3.88 \text{ in.} \end{aligned}$$

The inside diameter of the armature

$$\begin{aligned} D_i &= 10 - 2 \times 1.02 - 3.88 \\ &= 4.08 \text{ in.; use } 4.0 \text{ in.;} \end{aligned}$$

then

$$\begin{aligned} B_{ya} &= \frac{1170}{5.0 \times 0.92 \times 3.96} \\ &= 64.3 \text{ kilo-lines per sq. in.} \end{aligned}$$

The length of the flux path

$$l_{ya} = \frac{(10 - 2 \times 1.02 - 0.5 \times 3.96)\pi}{2 \times 4} = 2.35 \text{ in.,}$$

and the ampere-turns per pole for the armature yoke

$$\begin{aligned} AT_{ya} &= at_{ya}l_{ya} = 6.7 \times 2 \ 35 \\ &= 15.75. \end{aligned}$$

For other voltages,

E	200	230	260	290
B_{ya}	55.8	64.3	72.7	81
at_{ya}	4.95	6.7	9.3	13.3
AT_{ya}	12	16	22	31

The main poles will be built up of hot-rolled sheet steel punchings. The density must not be chosen too high because the commutating-pole flux passes through the main poles for machines having one-half as many commutating poles as main poles. A density of 85 kilo-lines per sq. in. is assumed, and 1.20 is used for the leakage factor. If the length of the pole is equal to the armature length,

$$\begin{aligned} w_p &= \frac{\phi \lambda}{l_1 B_p} = \frac{1170 \times 1 \ 20}{5 \times 85.0} \\ &= 3.3 \text{ in.}; \text{ use } 3.0 \text{ in.}, \end{aligned}$$

then

$$B_p = 93.6 \text{ kilo-lines per sq. in.}$$

From Table V the current density in the field winding conductor should be approximately 1330 amperes per sq. in. The value of the field current has already been determined as 0.70 amperes.

$$s_f = \frac{0.70}{1330} = 0.000526 \text{ sq. in.}$$

A No. 22 B. & S. gauge, heavy Formvar copper wire, with section area of 0.000507 sq. in. and a space factor of 0.66, should be satisfactory. From Table V the ampere-turns per inch of h_f is 790. The field winding ampere-turns per pole,

$$\begin{aligned} ATP_f &= AT_g + AT_l + AT_{ya} + 30\tau \\ &= 1635 + 66 + 16 + 30 \times 7.85 = 1952 \\ l_p &= \frac{1952}{790} + 0.10 \times 7.85 = 3.26 \text{ in.} \end{aligned}$$

This value of l_p is satisfactory for the shunt field winding but does not allow sufficient space for the commutating-pole winding. The radial

pole length is, therefore, increased 25 per cent. Then $l_p = 1.25 \times 3.26 = 4.1$ in., and the inside diameter of the field yoke

$$D_{y_i} = 10 + 2 \times 0.10 + 2 \times 4.1 = 18.4 \text{ in.}$$

Use 18.5 in. and

$$l_p = 4.15 \text{ in.}$$

The ampere-turns for the pole, for hot-rolled sheet steel

$$\begin{aligned} AT_p &= at_p l_p = 45 \times 4.15 \\ &= 187. \end{aligned}$$

For other voltages,

E	200	230	260	290
B_p	81 5	93 6	106	118
at_p	27 5	45	98	250
AT_p	114	187	407	1038

The field yoke will be hot-rolled steel, and a flux density of 60 kilo-lines per sq. in. is assumed.

$$\begin{aligned} s_{yf} &= \frac{\phi \lambda}{B_{yf}} = \frac{1170 \times 1.20}{60} \\ &= 23.4 \text{ sq. in.} \end{aligned}$$

This motor is to be of the bracket type shown in Figs. 16 and 18, Chapter I. The axial length of the yoke is taken equal to 10 in., and the thickness

$$d_{yf} = \frac{23.4}{10} = 2.34.$$

Make this 2.5 in., and

$$\begin{aligned} D_{y_o} &= D_{y_i} + d_{yf} = 18.5 + 2.5 \\ &= 21.0 \text{ in.} \end{aligned}$$

The density

$$\begin{aligned} B_{yf} &= \frac{1170 \times 1.20}{10 \times 2.5} \\ &= 56.1 \text{ kilo-lines per sq. in.} \end{aligned}$$

The length of the flux path

$$l_{yf} = \frac{(18.5 + 1.25)\pi}{2 \times 4} = 7.75 \text{ in.,}$$

and the ampere-turns for hot-rolled steel

$$\begin{aligned} AT_{vf} &= at_{vf} l_{vf} = 12.8 \times 7.75 \\ &= 99. \end{aligned}$$

For various voltages,

E	200	230	260	290
B_{vf}	48.8	56.1	63.5	70.8
at_{vf}	10.7	12.8	15.8	20
AT_{vf}	83.0	99	122	155

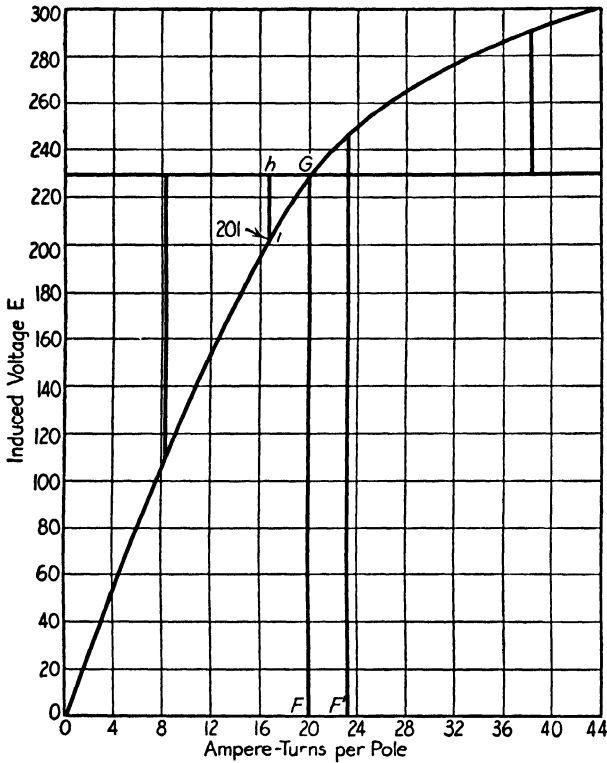


FIG. 84.—Open-circuit saturation curve.

The total ampere-turns per pole for various voltages are summed up below, and the open-circuit saturation curve is shown in Fig. 84.

E	200	230	260	290
AT_t	18	67	250	570
AT_g	1420	1635	1850	2060
AT_{ya}	12	16	22	31
AT_p	114	187	407	1038
AT_{vf}	83	99	122	155
ATP_f	1647	2004	2651	3854

The ratio

$$\frac{ATP_f}{ATP_a} = \frac{2004}{2240} = 0.894,$$

which shows that the assumed air gap length is satisfactory (see page 84).

The shunt field ampere-turns are taken from the open-circuit saturation curve, Fig. 84, for 230 volts.

$$ATP_f = 2004 \text{ ampere-turns.}$$

The length of the mean-turn for the shunt field coil is calculated as explained on page 87:

$$\begin{aligned} L_f &= 2 \times 5.00 + 2(3 - 2 \times 0.125) + \pi[0.60 + 2(0.125 + 0.10)] \\ &= 18.8 \text{ in.,} \end{aligned}$$

and the section area of the conductor

$$\begin{aligned} s_f &= \frac{ATP_f L_f \rho}{E_t \times 10^6} = \frac{2004 \times 18.8 \times 4 \times 0.826}{230 \times 10^6} \\ &= 0.00054 \text{ sq. in.} \end{aligned}$$

This conductor area falls between the area of a No. 21 and No. 22 B. & S gauge. To meet the required field winding resistance, part of each field coil is wound with No. 21 and the other part with No. 22 h.f. copper wire.

For a current density of 1330 amperes per sq. in.,

$$\begin{aligned} i_f &= s_f A_f = 0.00054 \times 1330 \\ &= 0.72 \text{ ampere;} \end{aligned}$$

and the number of turns per pole

$$t_f = \frac{ATP_f}{i_f} = \frac{2004}{0.72} = 2780$$

From Fig. 85, the height of the winding space $h_f = 3.37$ in. The insulated diameter of No. 21 h.f. wire is 0.0314 in., and for No. 22 h.f. wire it is 0.0281 in. The number of turns per layer for No. 21 wire

$$= \frac{3.37}{0.0314} = 107; \text{ use } 106;$$

and for No. 22 the turns per layer

$$= \frac{3.37}{0.0281} = 120; \text{ use } 118.$$

Each coil is wound with 8 layers, 106 turns each, of No. 21 wire on the inside and 16 layers, 118 turns each, of No. 22 wire on the outside of the coil. The turns per pole

$$t_f = t_{f1} + t_{f2} = 8 \times 106 + 16 \times 118 = 2736.$$

The resultant conductor section

$$S_f = \frac{s_{f1}t_{f1} + s_{f2}t_{f2}}{t_{f1} + t_{f2}} = \frac{0.000638 \times 848 + 0.000507 \times 1888}{2736} \\ = 0.000548 \text{ sq. in.}$$

The depth of the field coil

$$d_f = 8 \times 0.0314 + 16 \times 0.0281 = 0.702 \text{ in.}$$

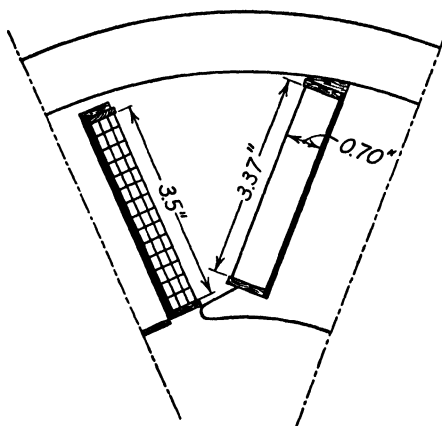


FIG. 85.

The corrected mean-turn is 19.12 in. The resistance of the shunt field winding at 75° C.

$$R_f = \frac{L_f t_f p r}{s_f \times 10^6} = \frac{19.12 \times 2736 \times 4 \times 0.826}{0.000548 \times 10^6} \\ = 316 \text{ ohms.}$$

With 230 volts applied to the shunt field terminals,

$$i_f = \frac{230}{316} = 0.728 \text{ ampere,}$$

and the ampere-turns

$$\text{ATP}_f = 0.728 \times 2736 = 1990$$

The copper loss in the shunt field winding

$$\begin{aligned} W_f &= i_f^2 R_f = 0.728^2 \times 316 \\ &= 167 \text{ watts.} \end{aligned}$$

The cooling surface

$$\begin{aligned} S_f &= 2(0.702 + 3.37) 19.12 \times 4 \\ &= 625 \text{ sq. in.,} \end{aligned}$$

and

$$\frac{S_f}{W_f} = \frac{625}{167} = 3.72,$$

which is satisfactory (see page 88).

The weight of the copper

$$\begin{aligned} G_f &= L_f t_f p s_f \times 0.321 = 19.12 \times 2736 \times 4 \times 0.000548 \times 0.321 \\ &= 36.8 \text{ lb.} \end{aligned}$$

The commutator diameter (see page 111)

$$D_c = 7.25 \text{ in.}$$

The number of commutator bars

$$K = 3 \times 41 = 123,$$

and the bar pitch

$$\begin{aligned} \beta &= \frac{\pi D_c}{K} = \frac{3.14 \times 7.25}{123} = 0.185 \text{ in.} \\ \beta_r &= 0.185 \frac{10}{7.25} = 0.255. \end{aligned}$$

For a brush thickness of $\frac{3}{8}$ in.,

$$b = \frac{0.375}{0.185} = 2.03 \text{ bars.}$$

The phase difference in commutation

$$\begin{aligned} \varphi &= \frac{K}{p} - \frac{1}{2} (Y_1 - 1) = \frac{123}{4} - \frac{1}{2} (61 - 1) \\ &= 0.75, \end{aligned}$$

and the width of the commutating zone

$$\begin{aligned} w_c &= \left(b + m + \varphi - \frac{a}{p} \right) \beta_r = \left(2.03 + 3 + 0.75 - \frac{2}{4} \right) 0.255 \\ &= 1.35 \text{ in.} \end{aligned}$$

The width of the neutral zone

$$= (1 - \psi)\tau = (1 - 0.66)7.85 = 2.67 \text{ in.},$$

and the ratio of commutating zone to neutral zone

$$= \frac{1.35}{2.67} = 0.505,$$

which shows that the thickness of brush selected is satisfactory (see page 103).

The mica is to be under-cut, and a medium hard brush is to be used. A current density of 50 amperes per sq. in. of brush contact is assumed, and

$$S_b = \frac{2I_a}{A_b} = \frac{2 \times 72.7}{50} = 2.91 \text{ sq. in.}$$

The total width of all the brushes per arm

$$n_b w_b = \frac{S_b}{n_a b_t} = \frac{2.91}{4 \times 0.375} = 1.94 \text{ in.}$$

A brush $\frac{3}{8}$ in. thick by 5 in. wide will be used, with 3 brushes per arm. The total contact surface

$$S_b = 0.625 \times 0.375 \times 3 \times 4 = 2.81 \text{ sq. in.}$$

The correct value of the current density at the brush contact

$$A_b = \frac{2 \times 72.7}{2.81} = 51.8 \text{ amperes per sq. in.}$$

The length of the commutator

$$l_c = n_b(w_b + 0.125) + c_2 = 3(0.625 + 0.125) + 0.75 \\ = 3.0 \text{ in.}$$

The commutating-pole air gap length is chosen equal to the length of the main-pole air gap,

$$\delta_i = 0.10 \text{ in.}$$

The width of the commutating pole

$$w_i = w_c - (1.5 \text{ to } 2)\delta_i = 1.35 - (1.5 \text{ to } 2)0.10 \\ = 1.2 \text{ to } 1.15 \text{ in.}$$

$$w_i \leq \frac{1 - \psi}{2} \tau = \frac{1 - 0.66}{2} 7.85 = 1.34 \text{ in.}$$

$$w_i \geq 1.5t_1 = 1.5 \times 0.766 = 1.15 \text{ in.}$$

Make

$$w_i = 1.25 \text{ in.}$$

and

$$l_i = l_1 = 5 \text{ in.}$$

The reactance voltage per coil is calculated by formula 102.

$$\text{ATP}_a = 2240, p = 4, t_a = 2, n_s = 19.2, m = 3, b = 2.03,$$

$$A = b + 1 - \frac{a}{p} = 2.03 + 1 - \frac{2}{4} = 2.53, \varphi = 0.75,$$

$$l = 5, d_s = 1.02, w_s = 0.297, l_i = 5, t_1 = 0.766,$$

$$w_i = 1.25, \delta_i = 0.10, l_s = L_a - l = 15.77 - 5 = 10.77$$

$$4.25l \frac{d_s}{w_s} = 4.25 \times 5 \frac{1.02}{0.297} = 73$$

$$4.66(2l - l_i) \log_{10} \frac{2t_1 - w_s}{w_s}$$

$$= 4.66(2 \times 5 - 5) \log_{10} \frac{2 \times 0.766 - 0.297}{0.297} = 14.4$$

$$1.02l_i \frac{w_i - w_s}{\delta_i} = 1.02 \times 5 \frac{1.25 - 0.297}{0.10} = 48.6$$

$$8.12l_s = 8.12 \times 10.77 = 87.5$$

$$2 - \frac{\varphi}{A + m - 1} = 2 - \frac{0.75}{2.53 + 3 - 1} = 1.835$$

$$M = 1.835(73 + 14.4 + 48.6) + 87.5 = 337.5$$

$$e_r = \frac{\text{ATP}_a t_a p n_s}{10^8} \frac{m}{A + m - 1} M$$

$$= \frac{2240 \times 2 \times 4 \times 19.2}{10^8} \frac{3}{2.53 + 3 - 1} 337.5$$

$$= 0.77 \text{ volt.}$$

The flux density in the commutating-pole air gap

$$B_{oi} = \frac{e_r \times 60 \times 10^8}{t_a l_i v \times 12} = \frac{0.77 \times 60 \times 10^8}{2 \times 5.0 \times 3010 \times 12}$$

$$= 12,800 \text{ lines per sq. in.}$$

The air gap coefficient will be the same as for the main pole because the air gap length is the same.

$$k = 1.18$$

and

$$\begin{aligned} \text{AT}_{g_1} &= \frac{B_{g_1} \delta_1 k}{3.2} = \frac{12,800 \times 0.10 \times 1.18}{3.2} \\ &= 470 \text{ ampere-turns.} \end{aligned}$$

The ampere-turns for the iron parts of the magnetic circuit will not be calculated separately, but will be taken care of by increasing the commutating-pole air gap ampere-turns (see page 111). The total ampere-turns per commutating pole

$$\begin{aligned} \text{ATP}_1 &= \text{ATP}_a + 2\text{AT}_{g_1} \\ &= 2240 + 2 \times 470 \\ &= 3180. \end{aligned}$$

The turns per pole

$$t_1 = \frac{\text{ATP}_1}{I_a} = \frac{3180}{72.7} = 43.7.$$

For a current density of 1330 amperes per sq. in.,

$$s_1 = \frac{I_a}{A_1} = \frac{72.7}{1330} = 0.0547 \text{ sq. in.}$$

A rectangular d.c.c. ribbon with insulated dimensions 0.163×0.222 in. and area 0.0286 sq. in. will be used, two conductors in parallel. The current density is then

$$A_1 = \frac{72.7}{0.0572} = 1270 \text{ amperes per sq. in.}$$

The height of the winding space is taken from Fig. 85 and is equal to 3.5 in. The coil is wound with 3 layers of 14 turns each, so that

$$t_1 = 3 \times 14 = 42 \text{ turns.}$$

The mean-turn

$$\begin{aligned} L_1 &= 2 \times 5.0 + 2(1.25 - 2 \times 0.125) + \pi[0.978 + 2(0.125 + 0.10)] \\ &= 16.5 \text{ in.} \end{aligned}$$

The resistance of the commutating field winding at 75° C.

$$R_i = \frac{L_i t_i p r}{s_i \times 10^6} = \frac{16.5 \times 42 \times 2 \times 0.826}{0.0572 \times 10^6} \\ = 0.02 \text{ ohm,}$$

and the voltage drop

$$I_a R_i = 7.27 \times 0.02 = 1.45 \text{ volts,}$$

or 0.63 per cent of the rated terminal voltage.

The copper loss

$$I_a^2 R_i = 72.7^2 \times 0.02 \\ = 106 \text{ watts,}$$

and the cooling surface

$$S_i = 2(0.98 + 3.5)16.5 \times 2 \\ = 296 \text{ sq. in.}$$

The cooling surface per watt loss is, then,

$$\frac{S_i}{W_i} = \frac{296}{106} = 2.79,$$

which shows that the temperature rise of the commutating field winding should not be excessive.

The weight of the commutating field copper

$$G_i = L_i t_i p s_i \times 0.321 \\ = 16.5 \times 42 \times 2 \times 0.0572 \times 0.321 \\ = 25.4 \text{ lb.}$$

The expression for the speed of a direct-current motor is

$$n = \frac{E_a \times 60 \times 10^8}{\phi_i N f_d}.$$

For any given motor,

$$n = \frac{E}{\phi_i} C_1 \tag{129}$$

$$C_1 = \frac{a \times 60 \times 10^8}{N f_d}.$$

The induced voltage decreases with increasing load because of the resistance drop in the armature, commutating field, and brush contacts. If the flux remains constant, the speed of the motor will drop in direct proportion with the induced voltage. The flux does not remain constant, however, but is decreased by armature reaction. The full-load speed of the motor will be lower than the no-load speed if the voltage drop is greater than the decrease in flux, and it will be higher than the no-load speed if the decrease in flux is greater than the voltage drop. To obtain an economical field winding and low field losses, the commutating-pole shunt motor is designed with small air gap and a ratio of field ampere-turns per pole to armature ampere-turns less than 1.0. A small series field winding, called stabilizing winding, must be used to obtain stable operation under load. The method of determining the ampere-turns required on the series field to compensate for the demagnetizing effect of the armature cross-magnetizing field is given on page 83. Figure 84 shows the construction for this design. The voltage drop, caused by armature reaction, is equal to hi , Fig. 84, Gh being equal to FF' . In Fig. 84, hi is equal to 29 volts and the full-load flux is proportional to 201 volts. The voltage drop in the armature winding, commutating field winding, and brush contacts = 12.8 volts, giving for the induced voltage 217.2 volts. The full-load speed without series field winding

$$n_1 = n_o \frac{E}{E_1} = 1200 \frac{217.2}{201} = 1300 \text{ r.p.m.}$$

To obtain a full-load speed of 1150 r.p.m., E_1 , the voltage proportional to the full-load flux, must be

$$E_1 = \frac{1200}{1150} 217.2 = 226 \text{ volts.}$$

The series field winding must, therefore, be provided with 300 ampere-turns per pole; see Fig. 84.

The number of turns per pole

$$t_s = \frac{300}{72.7} = 4.12; \text{ use } 4.$$

For a current density of 1500 amperes per sq. in.,

$$s_s = \frac{I_a}{A_s} = \frac{72.7}{1500} = 0.0485 \text{ sq. in.}$$

A rectangular d.c.c. copper ribbon with insulated dimensions 0.185×0.345 in. and area 0.0518 sq. in. will be used. This winding is wound in one layer over the shunt field winding.

The mean-turn

$$L_s = 2 \times 5.0 + 2(3 - 2 \times 0.125) + \pi[0.185 + 2(0.7 + 0.125 + 0.10)] \\ = 21.9 \text{ in.}$$

The resistance of the series field winding at 75°C .

$$R_s = \frac{L_s t_s \rho r}{s_s \times 10^6} = \frac{21.9 \times 4 \times 4 \times 0.826}{0.0518 \times 10^6} \\ = 0.0056 \text{ ohm.}$$

The copper loss

$$I_a^2 R_s = 72.7^2 \times 0.0056 \\ = 29.6 \text{ watts.}$$

The weight of series field copper

$$G_s = L_s t_s \rho s_s \times 0.321 \\ = 21.9 \times 4 \times 4 \times 0.0518 \times 0.321 \\ = 5.82 \text{ lb.}$$

The armature copper loss for full-load

$$W_a = I_a^2 R_a = 72.7^2 \times 0.128 \\ = 676 \text{ watts,}$$

or 4.54 per cent of rated output.

The full-load copper loss for the commutating field winding

$$W_i = I_a^2 R_i = 72.7 \times 0.02 \\ = 106 \text{ watts,}$$

which is 0.71 per cent of rated output.

The series field copper loss for full-load

$$W_s = I_a^2 R_s = 72.7 \times 0.0056 \\ = 29.6 \text{ watts,}$$

or 0.199 per cent of rated output.

The shunt field copper loss

$$\begin{aligned} W_f &= i_f^2 R_f = 0.728^2 \times 316 \\ &= 167 \text{ watts or } 1.12 \text{ per cent.} \end{aligned}$$

Assuming 2 volts drop for positive and negative brushes, the brush contact loss for full-load

$$\begin{aligned} W_b &= I_a 2 = 72.7 \times 2 \\ &= 145.4 \text{ watts} = 0.98 \text{ per cent.} \end{aligned}$$

The average armature tooth width

$$w_{ta} = 0.391$$

and

$$\begin{aligned} G_{ct} &= w_{ta}(l - n_d w_d) k_1 S d_s \times 0.278 \\ &= 0.391(5.0)0.92 \times 41 \times 1.02 \times 0.278 \\ &= 21 \text{ lb.} \end{aligned}$$

The armature tooth density at a point $\frac{1}{3}$ slot depth from the minimum tooth width = 101.5 kilo-lines per sq. in., and the loss per pound for open-hearth steel = 5.8 watts. The frequency of the flux reversals is 38.3 cycles per sec., and the loss in the armature teeth due to the fundamental frequency flux

$$\begin{aligned} W_{ct} &= 5.8 \times 21 \times 0.60 \\ &= 73 \text{ watts.} \end{aligned}$$

The weight of the iron in the armature yoke

$$\begin{aligned} G_{cy} &= \frac{\pi}{4} [(D - 2d_s)^2 - D_i^2](l - n_d w_d) k_1 \times 0.278 \\ &= \frac{\pi}{4} [(10 - 2 \times 1.02)^2 - 4^2](5.0)0.92 \times 0.278 \\ &= 47.8 \text{ lb.} \end{aligned}$$

The flux density in the armature yoke is 64.3 kilo-lines, and the loss per pound for open-hearth steel is 2.65 watts. The loss in the armature

yoke due to the fundamental frequency flux

$$\begin{aligned} W_{cy} &= 2.65 \times 47.8 \times 0.60 \\ &= 76 \text{ watts.} \end{aligned}$$

The total core loss (see page 123),

$$\begin{aligned} W_c &= (73 + 76)2.5 \\ &= 372 \text{ watts} = 2.5 \text{ per cent.} \end{aligned}$$

The brush friction loss

$$\begin{aligned} W_{bf} &= 8 \times 2.81 \times 2.18 \\ &= 49.0 \text{ watts} = 0.329 \text{ per cent.} \end{aligned}$$

From the curves of Fig. 78, the friction and windage loss

$$W_{fw} = 200 \text{ watts} = 1.34 \text{ per cent.}$$

The stray load losses are taken equal to zero, which is in accordance with the A.S.A. Standards.

The calculations for the efficiency are shown in Table XII, and the efficiency curve is shown in Fig. 86.

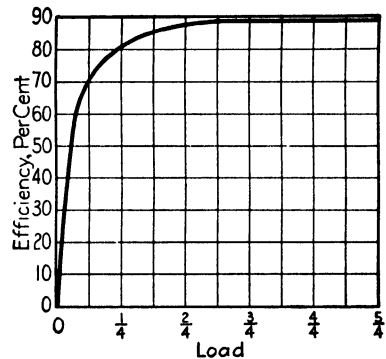


FIG. 86.—Efficiency of 15-hp., 1150-r.p.m., 230-volt, constant-speed motor.

TABLE XII

Losses	Load				
	$\frac{1}{4}$	$\frac{2}{4}$	$\frac{3}{4}$	$\frac{4}{4}$	$\frac{5}{4}$
Armature copper.....	42.2	169.0	380.0	676.0	1056.0
Commutating field.....	6.6	26.5	59.6	106.0	165.8
Series field.....	1.9	7.4	17.7	29.6	46.3
Brush I^2R	36.3	72.5	109.0	145.4	181.3
Shunt field.....	167.0	167.0	167.0	167.0	167.0
Core.....	372.0	372.0	372.0	372.0	372.0
Brush friction.....	49.0	49.0	49.0	49.0	49.0
Friction and windage....	200.0	200.0	200.0	200.0	200.0
Total losses.....	865.0	1063.4	1,354.3	1,705.0	2,257.4
Output.....	3730.0	7450.0	11,200.0	14,900.0	18,650.0
Output plus losses.....	4595.0	8513.4	12,554.3	16,605.0	20,907.4
Efficiency, per cent.....	81.1	87.5	89.1	89.7	89.2

The armature surface per watt loss

$$\begin{aligned}\frac{S_a}{W_a} &= \frac{\left[\pi D(l + 2l_c) + \pi D_c l + \frac{\pi}{4} (D^2 - D_c^2)(2 + n_d) \right] (1 + 0.00051v)}{W_a + W_c} \\ &= \frac{\left[3.14 \times 10(5.0 + 2 \times 3.9) + \pi 4.0 \times 5.0 + \frac{\pi}{4} (10^2 - 4^2) \times 2 \right] (1 + 0.00051 \times 3010)}{676 + 372} \\ &= 1.45 \text{ sq. in. per watt,}\end{aligned}$$

and the full-load temperature rise

$$T_a = \frac{C_{ca}}{\frac{S_a}{W_a}} = \frac{55}{1.45} = 37.9^\circ \text{C.}$$

The surface per watt loss for the commutating field winding (see page 153) is

$$\frac{S_c}{W_c} = 2.8 \text{ sq. in. per watt,}$$

and the temperature rise is calculated as explained on page 88. From Fig. 62, $C_c = 97$ for a peripheral speed of 3010 ft. per min. The space factor for the commutating field winding conductor

$$f_s = \frac{0.0572}{2 \times 0.163 \times 0.222} = 0.79.$$

Then,

$$\begin{aligned}C_{ca} &= C_c + 70(1 - f_s)d_f \\ &= 97 + 70(1 - 0.79)0.98 \\ &= 111.4.\end{aligned}$$

The full-load temperature rise

$$T_c = \frac{111.4}{2.8} = 39.8^\circ \text{C.}$$

For the shunt field (see page 149),

$$\frac{S_f}{W_f} = 3.72 \text{ sq. in. per watt}$$

and

$$\begin{aligned} C_{ef} &= C_c + 70(1 - f_s)d_f \\ &= 97 + 70(1 - 0.645)0.70 \\ &= 114.4. \end{aligned}$$

The temperature rise for the shunt field,

$$T_f = \frac{114.4}{3.72} = 30.8^\circ \text{C}.$$

For the commutator,

$$\begin{aligned} \frac{S_c}{W_c} &= \frac{\pi D_c l_c (1 + 0.00051 v_c)}{W_b + W_{bf}} \\ &= \frac{3.14 \times 7.25 \times 3.0(1 + 0.00051 \times 2180)}{145.4 + 49.0} \\ &= 0.74 \text{ sq. in. per watt,} \\ T_c &= \frac{20}{0.74} = 27^\circ \text{C.} \end{aligned}$$

A resistance must always be used in series with the armature of direct-current motors when starting. The armature current

$$I_a = \frac{E_t - E}{R_c + R_r}; \quad (130)$$

R_c is the resistance of the armature circuit, resistance of armature, commutating field, brush contacts, and series field when present, and R_r is the resistance of the starting rheostat.

The starting resistance is generally so designed that the motor will start full-load, with a starting current not to exceed approximately 150 per cent of full-load current. The resistance necessary to meet these requirements can be calculated by formula 130,

$$R_r = \frac{E_t - (E + I_a R_c)}{I_a}. \quad (131)$$

The starting box for the 20-hp. motor is to be so designed that the starting current will not exceed 150 per cent of the full-load current. The resistance of the armature circuit, $R_c = 0.181$ ohm. At zero speed, the induced voltage, E , is zero, and the resistance that must be connected in series with the armature to limit the current to 150 per cent

of full-load value

$$R_{r1} = \frac{230 - (0 + 109 \times 0.181)}{109}$$

$$= 1.93 \text{ ohms.}$$

If the motor is starting full-load, the current will drop to approximately the rated value after it has accelerated its load, and the induced voltage

$$E = E_t - I_a(R_c + R_r)$$

$$= 230 - 72.7(0.181 + 1.93)$$

$$= 77 \text{ volts.}$$

To increase further the speed of the motor, the resistance of the rheostat must be reduced to

$$R_{r2} = \frac{230 - (77 + 109 \times 0.181)}{109}$$

$$= 1.22 \text{ ohms.}$$

The induced voltage

$$E = 230 - 72.7(0.181 + 1.22)$$

$$= 128 \text{ volts,}$$

and

$$R_{r3} = \frac{230 - (128 + 109 \times 0.181)}{109}$$

$$= 0.76 \text{ ohm.}$$

The calculations are carried out in this manner until the induced voltage is approximately equal to the terminal voltage. The value of the resistance between the first and second buttons of the rheostat = $R_{r1} - R_{r2}$, etc. The starting rheostat for this motor will have 7 buttons, and the resistance of each step is as follows:

Step	Resistance	Ohms
1	$R_{r1} - R_{r2} = 1.93 - 1.22$	$= 0.71$
2	$R_{r2} - R_{r3} = 1.22 - 0.76$	$= 0.46$
3	$R_{r3} - R_{r4} = 0.76 - 0.45$	$= 0.31$
4	$R_{r4} - R_{r5} = 0.45 - 0.24$	$= 0.21$
5	$R_{r5} - R_{r6} = 0.24 - 0.10$	$= 0.14$
6	$R_{r6} - R_{r7} = 0.10 - 0.00$	$= 0.10$
		<u>1.93</u>

DIRECT-CURRENT DESIGN SHEET

MOTOR

Hp 20 Kw Volts 230 Amps 72.5 R p m 1150 Poles 4
 Watts/r p m 12.96 Output constant 3.8×10^4 Type Shunt-wound Commutating pole

Outside diameter 10
 Inside diameter 4
 Total length 5
 Ducts number size none
 Length—gross 5 effective 4.6
 Number of slots 41
 Slots per pole 10.1
 Type of winding Simplex wave
 Number of coils 123
 Turns per coil 2
 Conductors total 492
 Conductors per slot 12
 Total flux 6970 k l
 Distribution constant 0.671
 Flux per pole 1170
 Conductor dimensions 0.079 × 0.216
 Conductor section 0.0125
 Current density 2900
 Equiv. conn. number size none
 Coils in slots 1 and 11
 Coils in bar 1 and 13
 One-half mean turn 1.77
 Resistance 25° C 0.107
 Resistance 75° C 0.128
 Square inch per watt 1.45
 Cal. temperature rise 37
 Ampere conductors per inch 5.4
 Ampere-turns per pole 2240

COMMUTATOR AND BRUSH

Diameter 7.25
 Length 3.0
 Peripheral speed 2180
 Number of bars 123
 Bar pitch 0.18
 Thickness of mica 0.03
 Volts bar average 7.18 max 14.5
 Number of arms 4
 Amps per arm 33
 Brushes per arm 3
 Size of brush 1 × 1
 Current density 51.8
 Square inch per watt 0.74

WEIGHTS

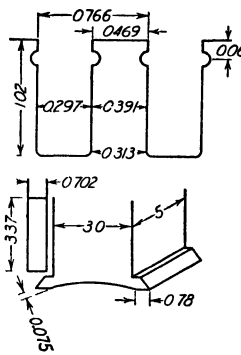
Armature copper 31.1
 Shunt field copper 3.8
 Series field copper 5.8
 Commutating field copper 25.4
 Armature teeth 21
 Armature yoke 47.4

FULL-LOAD LOSSES

Friction and windage 200
 Brush friction 41
 Core 37
 Stray load
 Armature copper 171
 Shunt field copper + rheo 117
 Series field copper 217
 Comm. field copper 106
 Brush contact I²R 11.4
 Total losses 170.1

FULL-LOAD RESISTANCE DROP

Armature 9.3-4.04
 Series field 0.4 0.18
 Commutating field 1.4 0.63
 Brushes 2.00 0.87
 Total 13.15 5.7
 Shunt field IR 230



PILES AND YOKES	MAIN	COMM
Material	Sheet steel	Sheet steel
Body length and width	5 × 3	5 × 1.25
Shoe length and width	5 × 5.18	5 × 1.25
Pole pitch	7.85	
Contact of pole embrace	66	
Pole arc	5.18	
Total air gap length	2 × 0.10	2 × 0.10

Material yoke	Hot rolled steel
Outside diameter of yoke	21
Inside diameter of yoke	18.5
Length of yoke	10
Magnetic section	2.5 × 10 = 25

FIELD WINDING	SHUNT	SERIES	COMM
Size of conductor	No. 21 No. 22	185 × 345	2 163 × 222
Conductor section	0.000638 0.000507	0.0518	2 × 0.0286
Amps per	0.728	71.8	71.8
Current density	1140 1435	138	1270
Turns per pole	848 1588	4	42
Length of mean turn	1.12	21.9	16.5
Resistance 25° C	26.5	0.0047	0.168
Resistance 75° C	316	0.0056	0.20
Watts loss	167	29.6	106
Square inch per watt	3.72		2.8
Field leakage constant			1.20

MAGNETIC CIRCUIT

Volts 230	PERCENT	DEPTH	LENGTH	A I
Cap	157	44.3	1 18 × 0.1	1635
Teeth	18.6	101.5	1.02	67
Yoke	18.2	4.3	2.3	16
Pole	15	93.6	4.15	187
Yoke	25	31	7.75	99
Total				2004

Shunt A I per pole full load 1990
 Series A I per pole full load 287
 Commutating A I per pole full load 3020

COMMUTATION

Bars covered by brush 2.03
 Commutating zone at armature surface 1.35
 Commutating zone per cent neutral zone 50.5
 Reactance volts 0.77
 Density in commutating pole air gap 12.800

Remarks Armature laminations—0.014 in open-heart sheet steel

II—SYNCHRONOUS MACHINES

CHAPTER IX

CONSTRUCTION

THERE are two types of synchronous machines in general use today, the salient-pole machine and the non-salient-pole machine. The salient-pole type is used for generators and motors of large and small capacities of high and very slow speeds. The non-salient-pole type is used for medium and very large capacity generators for high speeds. The latter type is generally known as the turbo-generator. Figure 87 is an assembly drawing of a non-salient-pole type of generator and shows the type of construction in general use. An assembly drawing of a small horizontal salient-pole machine is shown in Fig. 88. A vertical type salient-pole machine is shown in Fig. 89.

Armature.—Modern synchronous machines are of the revolving-field type, that is, the armature is the stationary member and the field rotates. The armature core is built up of sheet-steel laminations, generally from 0.014 to 0.0188 in. thick. The laminations are punched out and carefully annealed to remove shearing and punching strains. They are then coated with an insulating varnish in the manner described for the armature punchings of direct-current machines, page 3. The insulated punchings are next assembled in the armature frame on keys riveted to the frame or in dove-tailed grooves milled into ribs of the frame. Because the armature diameters are usually rather large for all synchronous machines, the laminations are generally punched in segments. The number of segments per circle will depend upon the number of slots, the method of punching, etc. For large-capacity machines, the number of segments per circle must be so chosen that no shaft currents will be produced.¹ One segment with spot-welded tooth supports or duct spacers is shown in Fig. 90.

¹ "Die Wechselstromtechnik," by E. Arnold and J. L. LaCour, Vol. 4, 2nd ed., p. 509, Julius Springer, Berlin; "Shaft Currents in Electrical Machines," by P. L. Alger and H. W. Samson, Trans. A. I.E.E., Vol. 43, 1924, p. 235; "Bearing Currents," by E. G. Merrick, General Electric Review, Vol. 17, Oct., 1914, p. 936; "Bearing Currents—Their Origin and Prevention," by C. T. Pearce, Electric Journal, Vol. 24, Aug., 1927, p. 374.

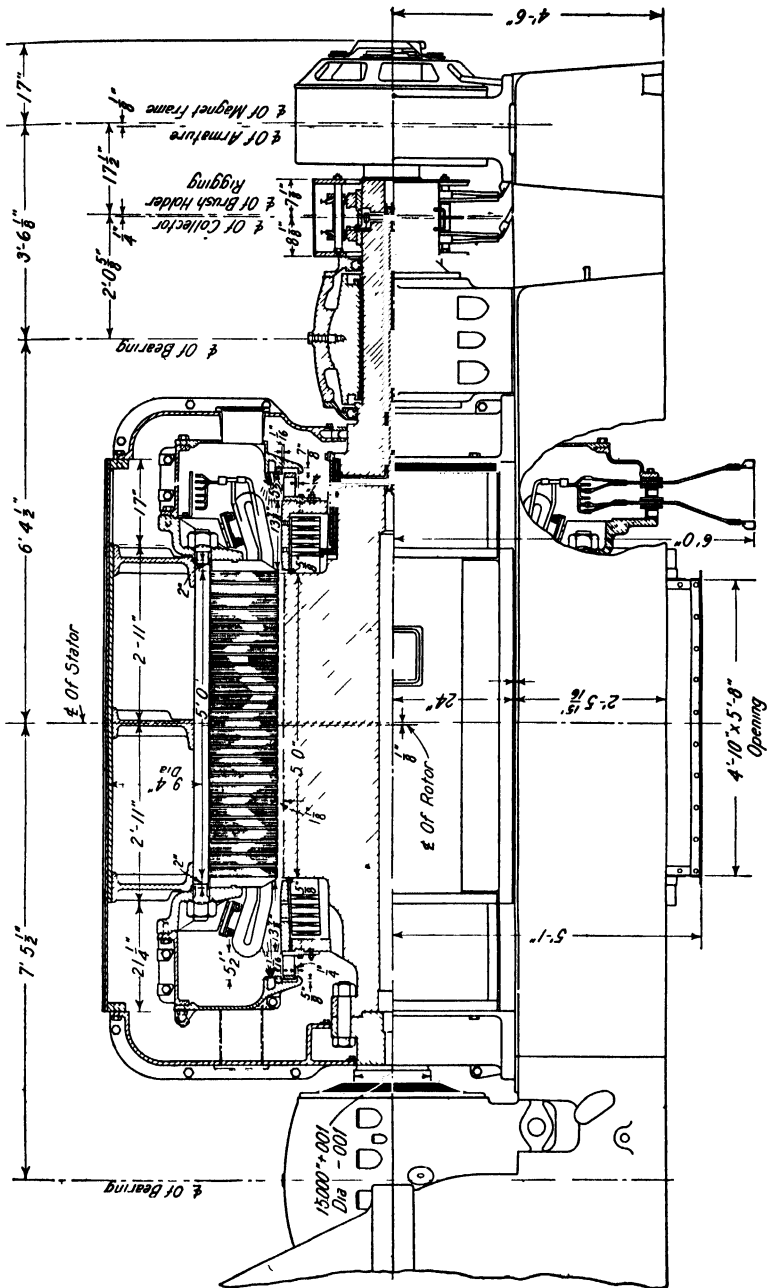


Fig. 87.—Sectional assembly of turbo-generator 12,500 kva, 1800 r.p.m., 13,200 volts

The core is clamped between two follower rings, which are held in place by a key, as shown in Fig. 88, or by long bolts passing through the frame back of the armature core, as shown in Figs. 87 and 89. The teeth are supported by a finger, or tooth support, which extends from the top of the tooth to the inside of the armature core. This tooth support is generally a piece of rolled steel, spot-welded to the last lamination (Fig. 90).

The length of the armature core must be divided into small sections

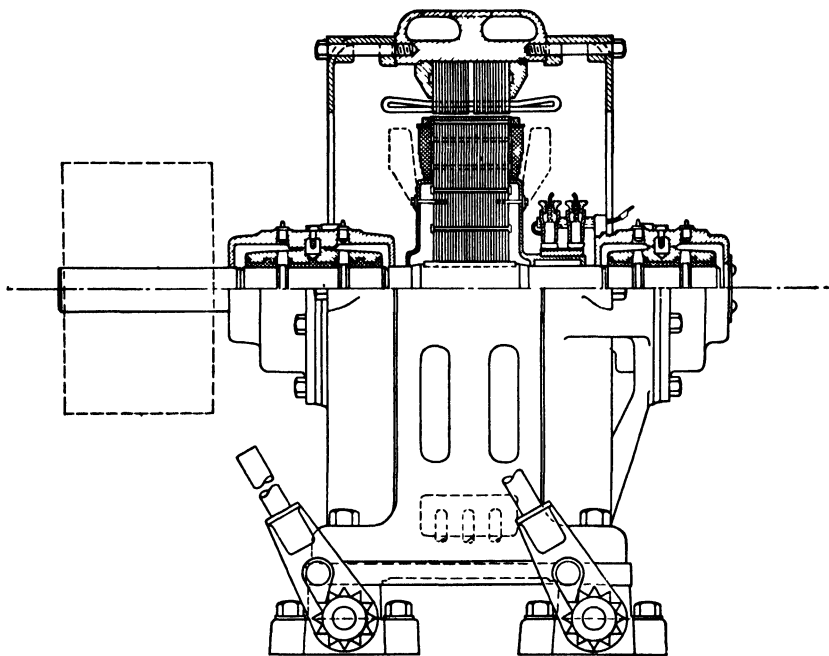


FIG. 88.—Assembly drawing of 115-hp., 1200-r.p.m., bracket-type synchronous motor.

by radial ventilating ducts, to insure proper ventilation of all parts of the armature. These ducts are usually $\frac{3}{8}$ in. wide for small and medium-size machines, and $\frac{1}{2}$ in. for large machines. The distance between centers of ducts should not exceed 3 in. The ventilating duct spacer is generally a rolled-steel piece of I-beam or T section, and like the tooth support is spot-welded to one punching (Fig. 90).

American practice favors the open type of armature slot for synchronous machines, with the two-layer type of winding. The armature coils are so formed that one side will be in the top of one slot and the

other side in the bottom of another slot, approximately a pole pitch away. The coils are completely insulated before they are placed into the slots.

The method of placing the armature coils into the slots is clearly

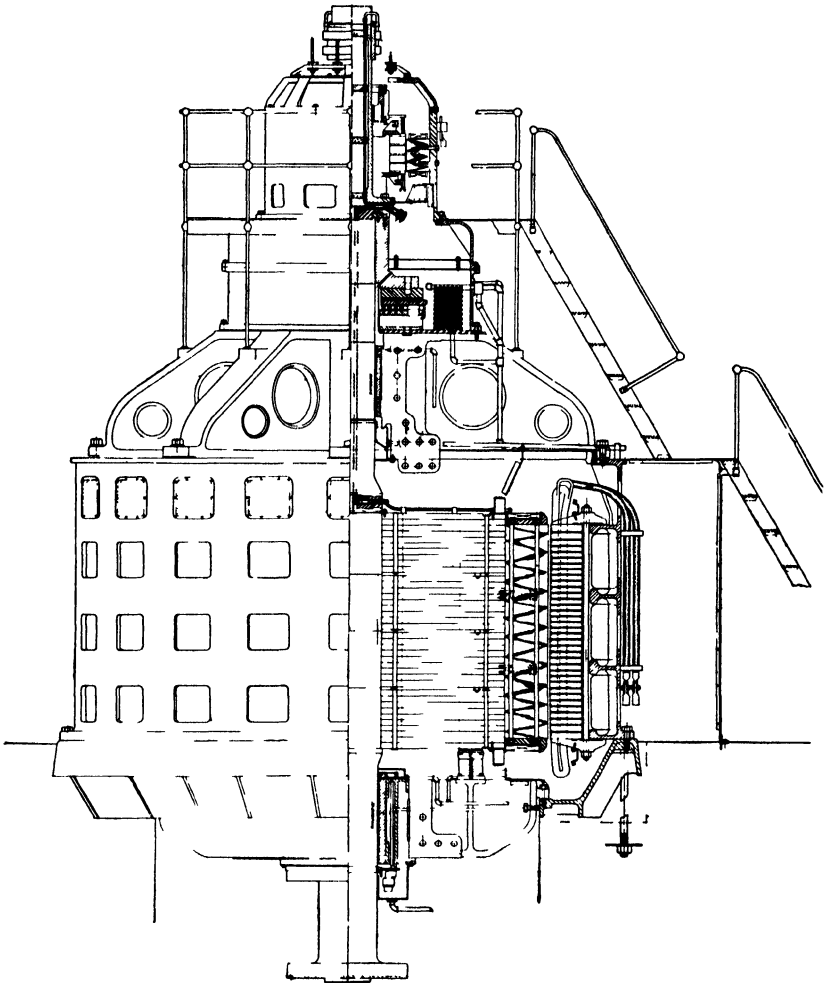


Fig 89—Vertical waterwheel-driven generator with direct connected exciter—
30,000 kva, 300 r p m , 24 poles, 11,000 volts

shown in Fig 91, which is a portion of a partly wound armature for a small-capacity, slow-speed machine. For turbo-generators, the armature coil end-connections are very long and the coils must be supported

to prevent distortion caused by heavy over-loads or short-circuits. Figure 92 shows a partly wound armature for a turbo-generator and

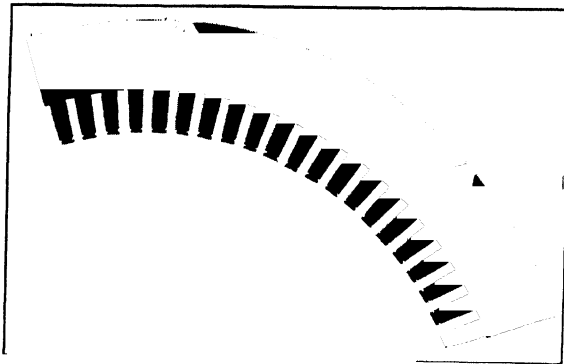


FIG. 90.—One segment with spot-welded tooth supports

shows the method of bracing the armature coil end-connections. For large-capacity salient-pole machines, the armature coil end-connections must be supported in a similar manner.

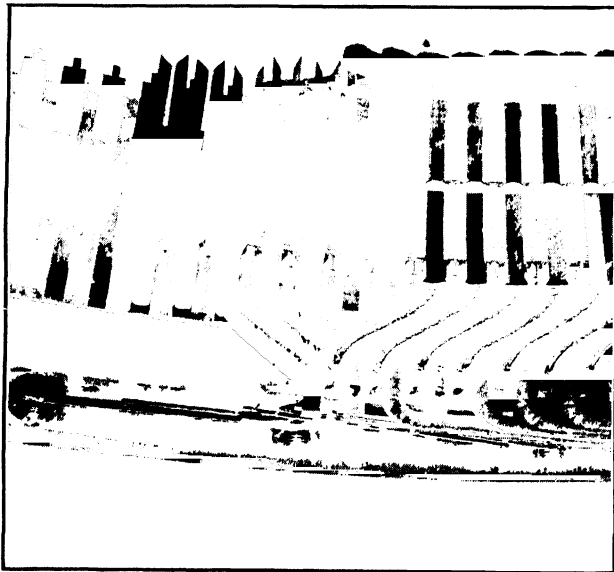


FIG. 91.—Portion of partially wound armature.

Armature Frame.—The type of construction generally employed for the armature frame of synchronous machines is shown in Fig. 93. Large

ventilating passages are provided in the frame back of the armature core. The armature frame is either of cast iron or built up of welded rolled steel.²

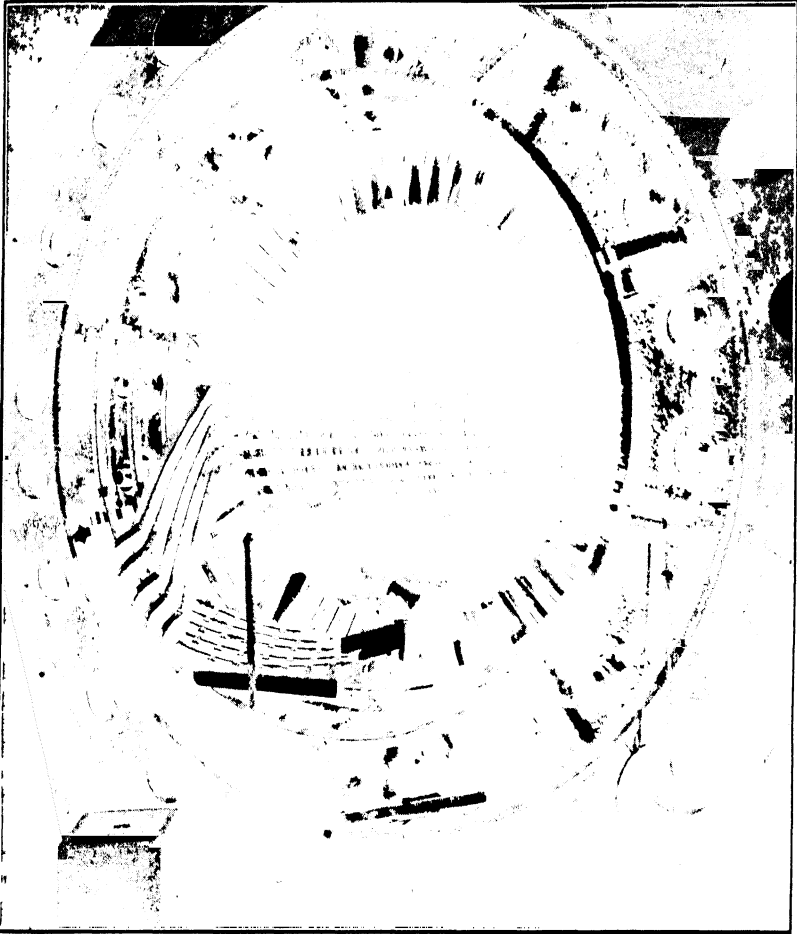


Fig. 92.—Partly wound turbo-generator armature—25,000 kva, 1800 r.p.m., 13,200 volts.

Field: *Non-Salient-Pole Machines.*—For large machines the rotor is often a solid steel forging with slots milled into it for the field winding. A completely machined, forged-steel rotor, without the field winding, for a 12,500-kva, turbine generator is shown in Fig. 94. For small machines,

² General Electric Review, July, 1927, Vol. 30, p. 330.

the rotor is often built up of sheet-steel punchings assembled on the shaft. Figure 95 shows a detail drawing of a rotor punching for a 375-kva, 2-pole turbine generator.

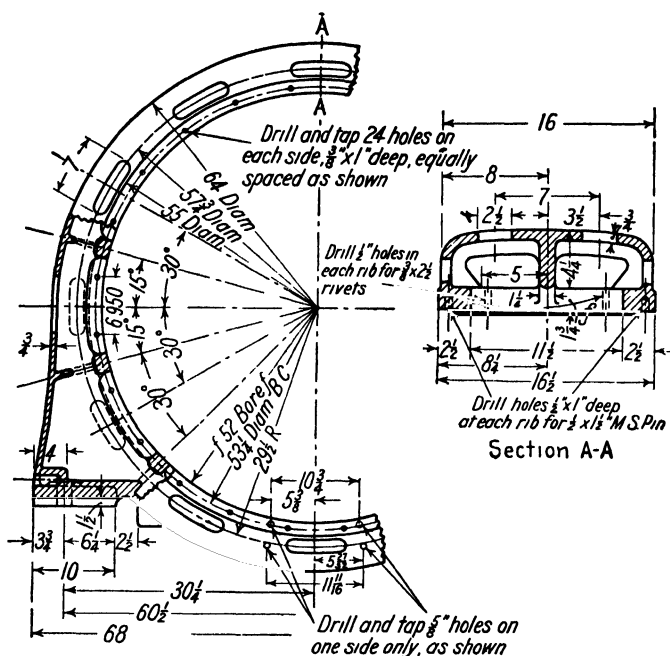


FIG. 93.—Detail drawing of armature frame.

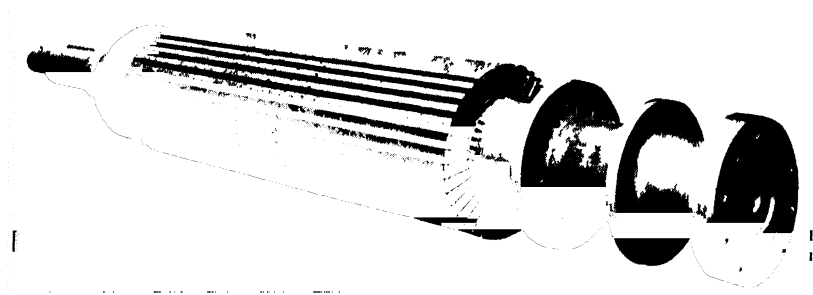


FIG. 94.—Completely machined rotor without winding for 12,500-kva turbo-generator.

The field winding is built up of bare ribbon copper, with mica insulation between turns and between field core and coils. The method of

placing the field winding into the slots is shown in Fig. 96. Because of the high peripheral speeds, heavy metal wedges are used to seal the rotor

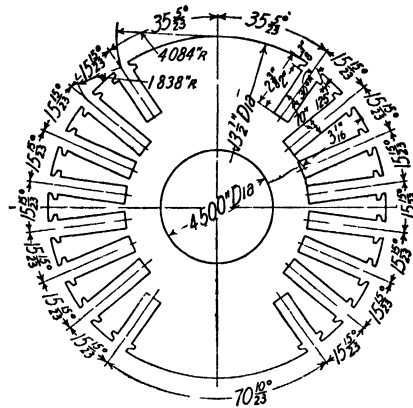


FIG. 95.—Rotor-punching, 375-kva, 3600-r.p.m. turbine generator.

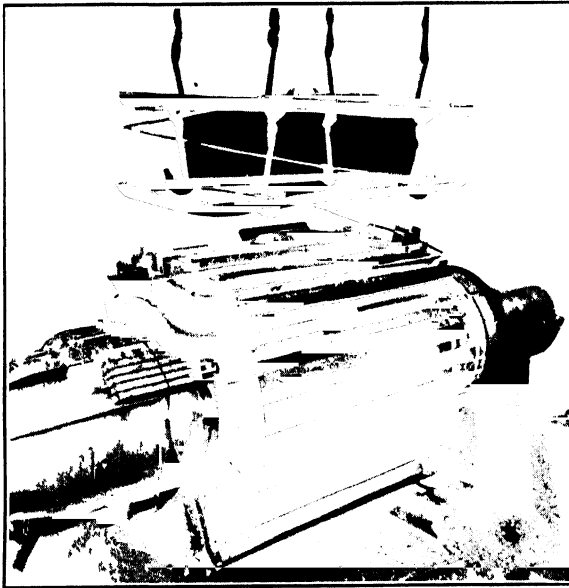


FIG. 96 —Method of placing field coils into slots of turbo-rotor.

slots. The end-connections of the field windings are insulated with mica tape and covered with aluminum saddles, as shown in Fig. 97.

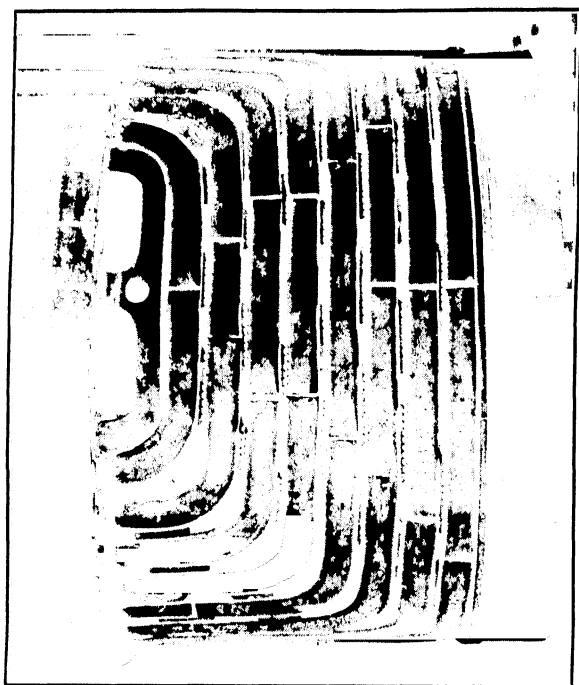


FIG. 97.—Field winding end-connections with aluminum saddles in place.

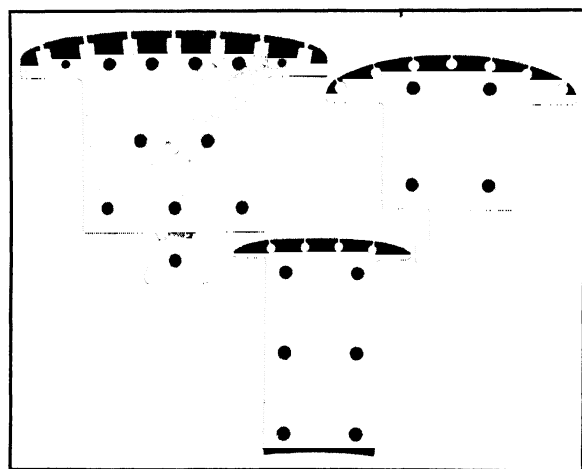


FIG. 98.—Field pole punchings.

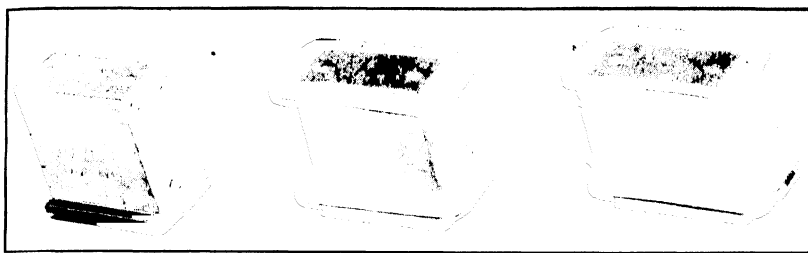


FIG. 99 —Bare pole, insulated pole, and complete wire-wound pole for a 219-kva, 48-pole generator

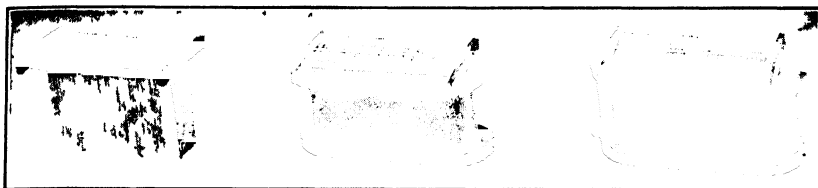


FIG 100 —Bare pole, insulated pole, and complete ribbon-wound pole for 375-kva 36-pole generator.

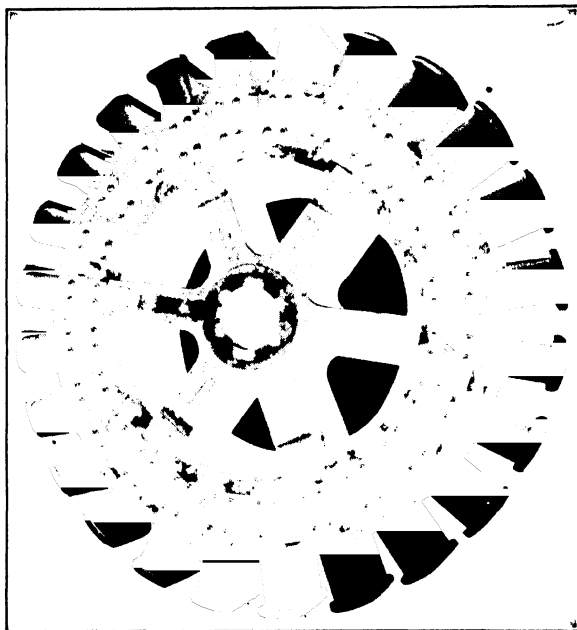


FIG. 101.—Rotor spider with laminated rim

To hold the field coils in place, steel coil retaining rings are shrunk over the aluminum-covered end-connections, as shown in Fig. 87.

Salient-Pole Machines.—The field poles of salient-pole machines are built up of sheet-steel punchings riveted together. The thickness of the sheet used is generally 0.019 to 0.050 in. The poles are either bolted or keyed to the field spider. Figure 98 shows a number of pole punchings and illustrates the methods used to fasten the field poles to the spider. The holes near the surface of the pole shoe are for the squirrel cage starting winding for synchronous motors.

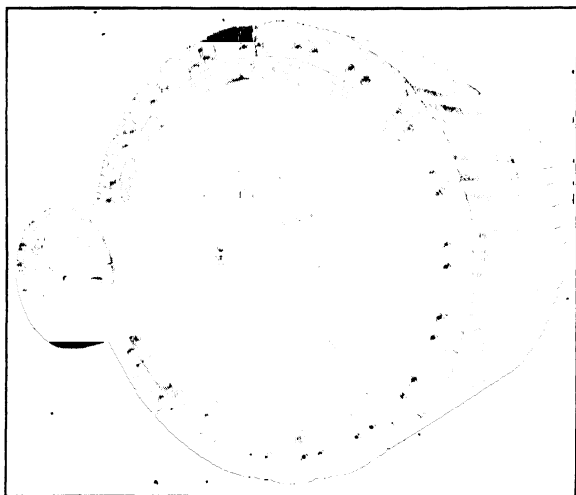


FIG. 102.—Spider built up of $\frac{1}{4}$ -in. steel plate punchings for 33,000-kva, 360-r.p.m., vertical type generator.

The field windings are wound either with d.c.c. copper wire or with bare copper strap wound on edge. A bare pole, insulated pole, and wound pole for a d.c.c. copper wire field winding are shown in Fig. 99. Figure 100 shows the same details but for a strap copper field winding.

Spider.—The spider, on which the field poles are mounted, is either of cast iron, cast steel, rolled steel, or built up of steel plates. The rim of the spider must carry the flux which passes between poles and must therefore have a high permeability besides good mechanical strength. It is, as a rule, difficult to get uniform steel castings, free from flaws, and for that reason rolled steel or built-up spider rims are preferred. A spider with cast-steel hub and arms but with rim built up of $\frac{1}{4}$ -in. steel plate is shown in Fig. 101. The complete spider for a 30,000-kva, 360-r.p.m., 20-pole generator built up of punched steel plates, is shown

in Fig. 102. For small-capacity synchronous motors and for generators with small number of poles, the spider is punched from sheet steel of the same thickness as used for the pole punching. A spider punching and

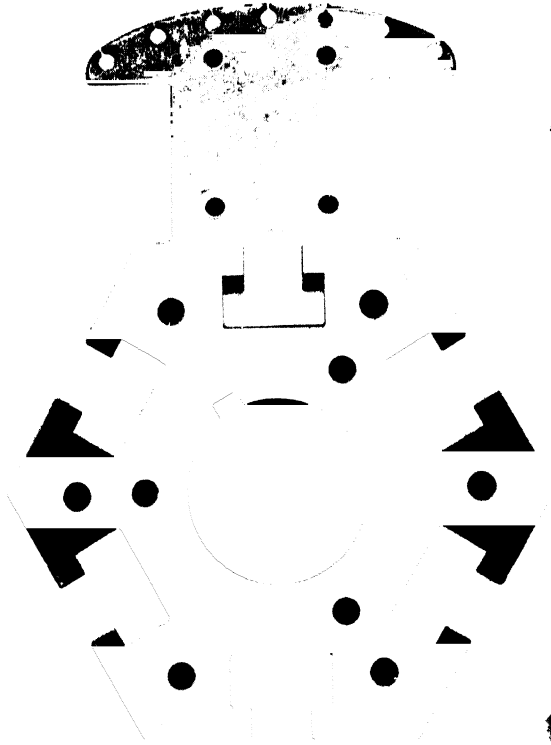


FIG 103 —Spider punching and one-pole punching for 55-hp , 1200-r p m , synchronous motor

one pole punching for a 55-hp., 6-pole, 1200-r.p.m. synchronous motor are shown in Fig. 103.

CHAPTER X

VOLTAGE FORMULA AND OUTPUT EQUATION

Voltage Formula.—The effective value of the voltage induced in each phase of a winding with one slot per pole and phase with pitch coils is given by the equation:

$$E = 4ffaw\phi \times 10^{-8} \text{ volt.}$$

Armature windings of synchronous machines always have more than one slot per pole per phase. The voltages induced in the coils per pole and phase lying in adjacent slots are then not in phase and cannot be added algebraically but must be added vectorily. The ratio of the vector sum to the algebraic sum is called the winding distribution factor, k_d . The two sides of the coils are not always placed in slots a pole pitch or 180 electrical degrees apart but are often chorded one or more slots. The voltage induced in one coil of the armature winding is proportional to the sine of the half-angle, in electrical degrees, which it subtends. The sine of the half-angle in electrical degrees embraced by a coil is called the pitch factor or chord factor, k_p .

The general formula for the effective value of the induced voltage per phase is then:

$$E = 4ffbk_dk_paw\phi \times 10^{-8} \text{ volt.} \quad (132)$$

Just as for direct-current machines, it is often convenient to use the hypothetical total flux instead of the flux per pole (see page 14). The hypothetical total flux

$$\phi_t = \frac{\phi p}{f_d} \text{ lines.}$$

From formula 132,

$$\phi = \frac{E \times 10^8}{4ffbk_pk_daw}$$

and

$$\phi_t = \frac{Ep \times 10^8}{4ffbk_pk_d f_d aw} \text{ lines.}$$

It is generally more convenient to use conductors in series per phase

instead of turns in series per phase and synchronous r.p.m. instead of frequency.

$$w = \frac{N}{2}$$

and

$$f = \frac{np}{2 \times 60}.$$

Making these substitutions,

$$\phi_t = \frac{E \times 60 \times 10^8}{nNk_p f_b k_d f_d}.$$

The form factor f_b , winding distribution factor k_d , and flux distribution factor depend only upon the number of slots and the shape of the air gap flux distribution curve and are not affected by changes in the number of conductors per phase or the coil throw. These factors can therefore be combined into one factor, called the winding constant,

$$C_u = f_b k_d f_d, \quad (133)$$

and then

$$\phi_t = \frac{E \times 60 \times 10^8}{nNk_p C_u} \text{ lines.} \quad (134)$$

Output Equation.—For alternating-current machinery, the terminal current I is equal to the armature current I_a . The armature output for a 3-phase generator expressed in kilovolt-amperes is

$$Kva = EIm \times 10^{-3}. \quad (135)$$

From formula 134,

$$E = \frac{\phi_t n N k_p C_u}{60 \times 10^8} \text{ volts.}$$

Substituting into equation 135,

$$Kva = \frac{\phi_t n N k_p C_u Im}{60 \times 10^{11}}.$$

The hypothetical total flux may be expressed in terms of the gap area times the air gap density,

$$\phi_t = \pi D l B_g.$$

If Q equals the ampere conductors per inch of armature circumference, then

$$INk_p m = \pi DQ$$

and

$$Kva = \frac{\pi D l B_g n \pi D Q C_u}{60 \times 10^{11}}$$

or

$$\frac{D^2 l n}{Kva} = \frac{6.08 \times 10^{11}}{C_u Q B_g}. \quad (136)$$

The total flux is directly proportional to the air gap density and, as has been shown for the direct-current machine, page 16, the tooth density is directly proportional to the air gap density. For high-voltage machines, it will therefore be necessary to use a lower air gap density than for low-voltage machines, because of the greater amount of slot space required for insulation. A high air gap density will lead to high densities in the magnetic circuit and high armature tooth losses. Too low an air gap density will, of course, lead to an uneconomical use of the magnetic circuit. The density for the air gap for 60-cycle synchronous machines will generally lie between the limits:

$$B_g = 35,000 \text{ to } 55,000 \text{ lines per sq. in.}$$

When beginning a design of a motor or generator, an air gap density of 43,000 lines per sq. in. is generally a satisfactory value to assume. For frequencies below 60 cycles per sec., the above values may be increased slightly. For 25-cycle machines, the values of B_g given above may generally be increased from 10 to 15 per cent.

The ampere conductors per inch of armature circumference determine armature reaction and, for a given type of construction, they determine the armature temperature rise. A large value of Q leads to a high leakage reactance and to a large value of armature cross and demagnetizing ampere-turns. Since the voltage regulation of a generator depends upon armature reaction, it follows that low values of Q must be used when good voltage regulation is desired. Modern power systems are generally operated with some form of automatic voltage regulator and only reasonably good regulation is required. Also, generators designed for very good regulation are sensitive to rapid load changes and are difficult to operate in parallel with other machines. For well-designed synchronous generators the voltage regulation is about 15 to 25 per cent, at 100 per cent power factor. The curves, Fig. 104, give average values of Q for 60-cycle synchronous generators for voltages of 3000 volts and less. For higher voltages, lower values of Q must be used; for frequencies below 60 cycles per sec. they may be increased.

For synchronous motors, the ampere conductors per inch of armature circumference given in Fig. 104 may be increased from 10 to 15 per cent.

By substituting average values for C_w , Q , and B_g , equation 136 becomes

$$\frac{D^2 l n}{Kva} = C \quad (137)$$

$$C = \frac{6.08 \times 10^{11}}{C_w Q B_g}$$

in which C is called the output constant. Average values of the output constant are given by the curves in Fig. 105 for 60-cycle, salient-pole, synchronous machines, for 3000 volts and below.

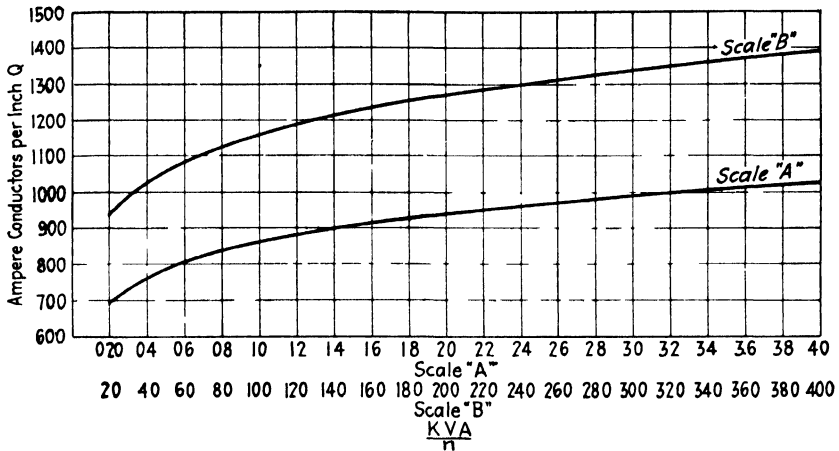


FIG. 104.—Ampere conductors per inch of armature gap circumference for 60-cycle synchronous machines for 3000 volts and below.

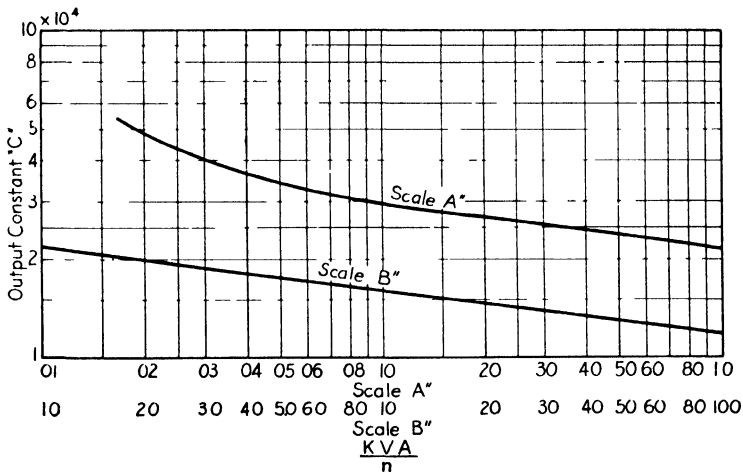


FIG. 105.—Approximate output constants 60-cycle, salient-pole, synchronous machines, 3000 volts and below

In formula 137, Kva is the armature kilovolt-ampere output. Since the armature resistance drop is only a very small percentage of the terminal voltage for synchronous machines, the rated Kva output may be used in this formula for a generator. For 0.8 power factor synchronous motors the Kva input is used, and for unity power factor motors the Kw output.

Armature Diameter and Length.—With the output constant known, the product, D^2l , can be easily calculated by formula 137. Either the diameter or the length may be assumed and the other dimension calculated.

For high-speed machines, the diameter may be limited by the peripheral speed. For synchronous machines, peripheral velocities as high as safe mechanical construction will permit may be used. Peripheral speeds of 20,000 to 25,000 ft. per min. are commonly employed for turbo-generators. For salient-pole machines the peripheral speed is generally much lower, but values as high as 12,000 to 15,000 ft. per min. are possible.

The ratio of armature length to pole pitch is generally about as follows:

$$\frac{l}{\tau} = 0.80 \text{ to } 2.5.$$

The small values apply to small-capacity machines and the large values to the large capacities. For large-capacity turbo-generators larger values than given above may be required, to avoid excessive peripheral speeds.

The pole pitch

$$\begin{aligned}\tau &= \frac{\pi D}{p} \\ \frac{l}{\tau} &= (0.80 \text{ to } 2.5) \\ l &= \frac{\pi D}{p}(0.80 \text{ to } 2.5).\end{aligned}$$

Substituting this expression for l into equation 137,

$$D^2 \frac{\pi D}{p} (0.80 \text{ to } 2.5) = \frac{K_{va}}{n} C'$$

or

$$D = \sqrt[3]{\frac{K_{va} p C'}{\pi(0.80 \text{ to } 2.5)n}}. \quad (138)$$

The values of the ratio armature length to pole pitch are not intended to give the limits for the armature dimensions, but are intended primarily to help the beginner to choose suitable armature dimensions. When in doubt as to the most suitable armature diameter and length for a given K_{va} and speed, the only satisfactory method is to make preliminary calculations for two or more machines with different dimensions and

choose the one that will give good operating characteristics for a reasonable cost of construction.

The diameter found from the output constant curves, Fig. 105, is the armature gap diameter. It is usually desirable to be able to determine the outside diameter of the armature core in order to select the standard frame a given rating of generator or motor is suited for. The tabulation gives the usual ratios of outside diameter to inside diameter for synchronous machines.

Poles	Ratio $\frac{D_o}{D}$	Poles	Ratio $\frac{D_o}{D}$	Poles	Ratio $\frac{D_o}{D}$	Poles	Ratio $\frac{D_o}{D}$
4	1 48	14	1 20	24	1 13	36	1 10
6	1 37	16	1 18	26	1 13	40	1 10
8	1 30	18	1 15	28	1 13	48	1 10
10	1 26	20	1 15	30	1 12	60	1 09
12	1 23	22	1 15	32	1 11	72	1 09

Design of Pole Shoe. The shape of the air gap flux distribution curve depends upon the shape of the pole shoe and the per cent pole embrace. The harmonics present in the voltage wave of synchronous machines depend largely upon the flux distribution in the air gap. There are also harmonics present in the voltage wave produced by the pulsations of the air gap flux caused by the armature slots. A flux distribution curve which decreases gradually to zero on the center line between two poles can be obtained by gradually increasing the air gap from the center or near the center of the pole to the pole tips. Poles not carefully beveled at the pole tips with a large per cent pole embrace may lead to magnetic noises. This is not the only cause of noise in synchronous machines; the number of armature slots per pole or per pole arc has an important effect upon the noise, as will be discussed later.

The per cent pole embrace for synchronous machines is generally from 65 to 75. In general, 70 to 72 per cent pole embrace is most satisfactory for both generators and motors; higher values lead to excessive field leakage. For synchronous motors with heavy pole shoes to accommodate the squirrel-cage starting winding, it may sometimes be necessary to use the lower value of per cent pole embrace, to avoid excessive field leakage.

A satisfactory air gap flux distribution curve is generally obtained when the pole shoe is shaped as indicated in Fig. 106. For generators

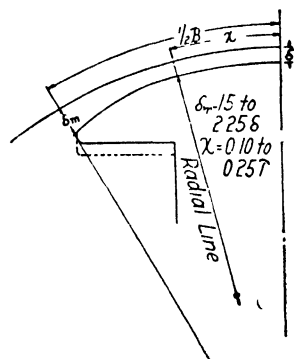


FIG. 106.

requiring no damper winding in the pole faces, the tip of the pole may be rounded off, as shown by the full line, Fig. 106. For synchronous motors and generators with damper windings, a heavier pole tip is generally required. A larger radius can then be used to round off the tip, or the tip may be shaped as indicated by the dotted line, Fig. 106.

Construction of No-load Field Form.—The flux distribution curve in the air gap of synchronous machines is derived from the flux plot in exactly the same way as described for direct-current machines (page 24). The air gap length can be estimated with the help of the curves, Fig. 107,

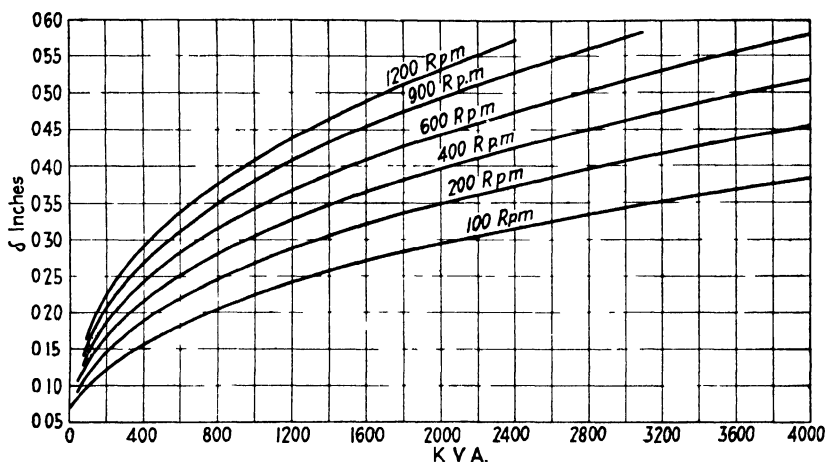


FIG. 107.—Approximate air gap lengths for 60-cycle, salient-pole, synchronous machines.

which give average values of air gap length for salient-pole, synchronous machines. For the flux plot, a full-scale drawing should be made of one-half of the pole shoe, with proper air gap clearance between pole and armature surface. To obtain the flux distribution on the armature surface, the space between pole face and armature must be divided into approximately equal squares by flux and equipotential lines. The method of plotting magnetic fields, with practical applications to salient-pole synchronous machines, is well explained in three excellent papers presented at a winter convention of the A.I.E.E.¹

The flux plot for a 2500-kva, 225-r.p.m. sample generator design is shown in Fig. 108. From this flux plot, the air gap flux distribution curve shown in Fig. 109 is obtained, in the manner described on page

¹ "Graphical Determination of Magnetic Fields," presented at winter convention, A.I.E.E., New York City, Feb. 7-11, 1927.

25. For some purposes, the approximate method of mapping the magnetic field, described on page 26, is sufficiently accurate.

When making the flux plot, the armature is assumed to be a smooth surface. Open armature slots produce deep notches in the top of the

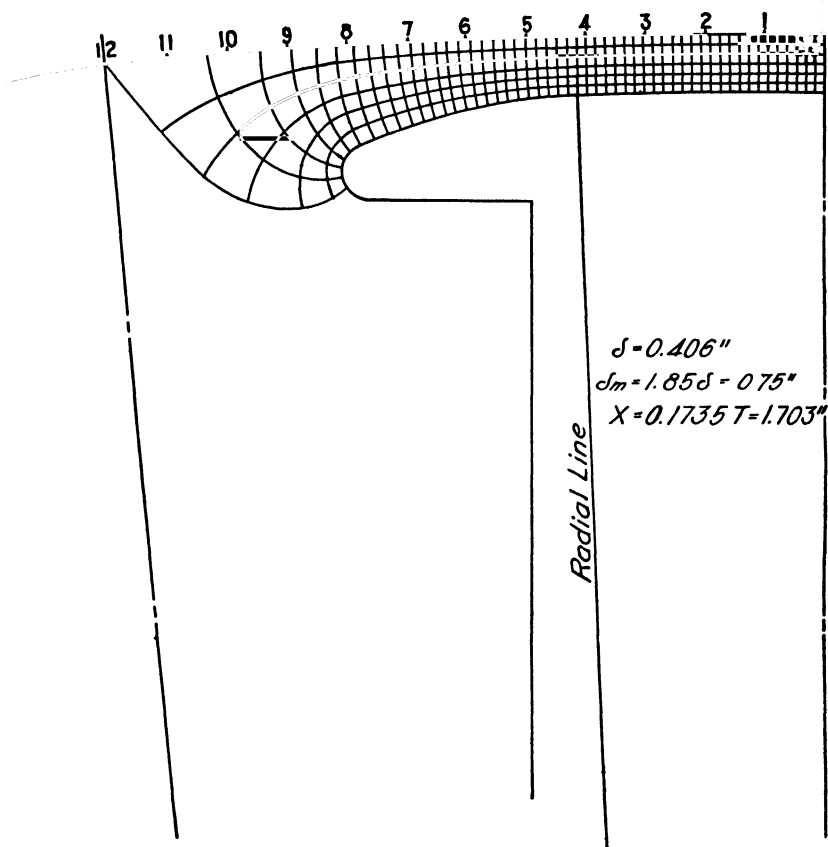


FIG. 108.—Flux plot for 2500-kva, 225-r.p.m., 32-pole generator.

field form, as shown in Fig. 110, which is the no-load air gap flux distribution curve of a 55-hp, 1200-r.p.m. synchronous motor, taken with an oscillograph.

Flux Distribution Factor and Form Factor.—The ratio of the area under the flux distribution curve to the area of a rectangle with same base and maximum ordinate is called the air gap flux distribution factor. This factor can be found by either of the two methods given on

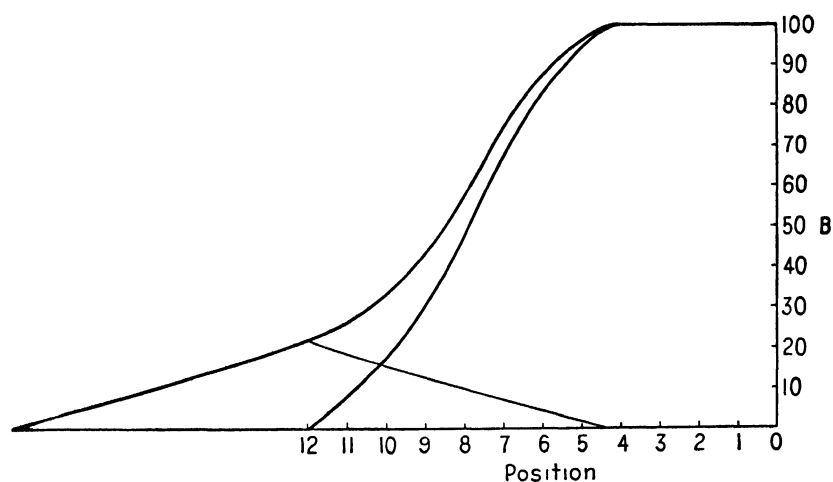


FIG. 109.—Air gap flux distribution curve for 2500-kva, 225-r.p.m., 32-pole generator.

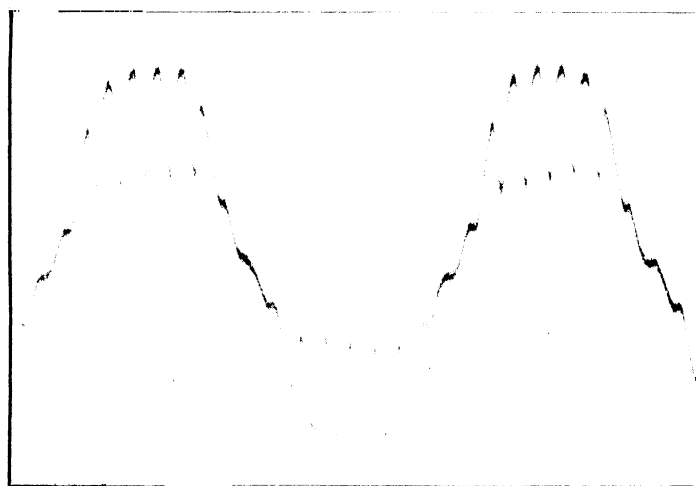


FIG. 110.—Air gap flux distribution curve of 55-hp., 1200-r.p.m., synchronous motor.

page 27, or by analyzing the flux wave by the Fourier series.² The calculations for the analysis of the field form are made as shown in Table XIII, which are for the flux wave shown in Fig. 109. The flux distribution curve is plotted with abscissas in electrical degrees, the ordinates B_{x1} , B_{x2} , etc., being read for every 7.5 electrical degrees. Since

TABLE XIII

B_x	$\sin x$	$\sin 3x$	$\sin 5x$	$\sin 7x$	$B_x \sin x$	$B_x \sin 3x$	$B_x \sin 5x$	$B_x \sin 7x$
$B_{x11} = 7.5$	0.130	0.383	0.609	0.793	0.98	2.88	4.57	5.94
$B_{x10} = 17.6$	0.259	0.707	0.966	0.966	4.56	12.45	17.00	17.00
$B_{x9} = 30.5$	0.383	0.924	0.924	0.383	11.69	28.20	28.20	11.69
$B_{x8} = 48.0$	0.500	1.000	0.500	-0.500	24.00	48.00	24.00	-24.00
$B_{x7} = 68.0$	0.609	0.924	-0.130	-0.991	41.40	62.80	-8.83	-67.40
$B_{x6} = 83.0$	0.707	0.707	-0.707	-0.707	58.70	58.70	-58.70	-58.70
$B_{x5} = 94.0$	0.793	0.383	-0.991	0.130	74.60	36.00	-93.10	12.22
$B_{x4} = 100.0$	0.866	0.000	-0.866	0.866	86.60	00.00	-86.60	86.60
$B_{x3} = 100.0$	0.924	-0.383	-0.383	0.924	92.40	-38.30	-38.30	92.40
$B_{x2} = 100.0$	0.966	-0.707	0.259	0.259	96.60	-70.70	25.90	25.90
$B_{x1} = 100.0$	0.991	-0.924	0.793	-0.609	99.10	-92.40	79.30	-60.90
$B_{x0} = 100.0$	0.500	-0.500	0.500	-0.500	50.00	-50.00	50.00	-50.00
					640.63	-2.37	-56.56	-0.25

the flux distribution curve is symmetrical about the center line of the pole, the even harmonics drop out. The equations for the fundamental, third, fifth, and seventh harmonics then are

$$B_1 = \frac{1}{8}(B_{x11} \sin 7.5^\circ + B_{x10} \sin 15^\circ + \cdots + \frac{1}{2}B_{x0} \sin 90^\circ),$$

$$B_3 = \frac{1}{8}(B_{x11} \sin 22.5^\circ + B_{x10} \sin 45^\circ + \cdots + \frac{1}{2}B_{x0} \sin 3 \times 90^\circ),$$

$$B_5 = \frac{1}{8}(B_{x11} \sin 37.5^\circ + B_{x10} \sin 75^\circ + \cdots + \frac{1}{2}B_{x0} \sin 5 \times 90^\circ),$$

$$B_7 = \frac{1}{8}(B_{x11} \sin 52.5^\circ + B_{x10} \sin 105^\circ + \cdots + \frac{1}{2}B_{x0} \sin 7 \times 90^\circ);$$

$$B_1 = \frac{640.63}{6} = 106.8,$$

$$B_3 = \frac{-2.37}{6} = -0.40,$$

$$B_5 = \frac{-56.56}{6} = -9.41,$$

$$B_7 = \frac{-9.25}{6} = -1.54;$$

$$B_x = B_1 \sin x + B_3 \sin 3x + B_5 \sin 5x + B_7 \sin 7x.$$

² See also "Graphical and Mechanical Computations," by J. Lipka.

The flux wave, fundamental, third, fifth, and seventh harmonics are shown in Fig. 111.

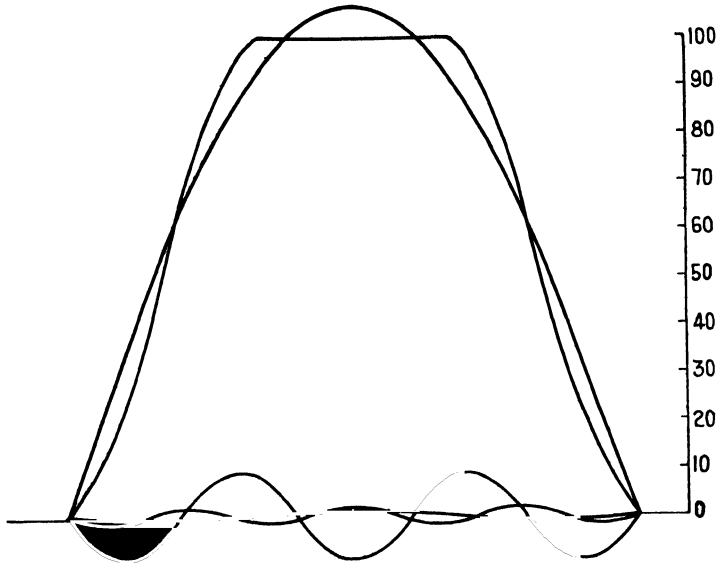


FIG. 111.—Air gap flux wave, fundamental, third, fifth, and seventh harmonics for 2500-kva., 225-r.p.m. generator.

The average value, effective value, and maximum value of the flux wave are calculated from the equation for B_x as follows:

$$\begin{aligned}
 B_a &= \frac{1}{\pi} \int_0^\pi B_x dx = \frac{2}{\pi} (B_1 + \frac{1}{3}B_3 + \frac{1}{5}B_5 + \frac{1}{7}B_7) \\
 &= \frac{2}{\pi} \left(106.8 - \frac{1}{3}0.40 - \frac{1}{5}9.41 - \frac{1}{7}1.54 \right) \\
 &= 66.6; \\
 B_e &= \sqrt{\frac{1}{\pi} \int_0^\pi B_x^2 dx} = \sqrt{\frac{1}{2}(B_1^2 + B_3^2 + B_5^2 + B_7^2)} \\
 &= \sqrt{\frac{1}{2}(106.8^2 + 0.40^2 + 9.41^2 + 1.54^2)} \\
 &= 75.8; \\
 B_m &= B_{x0} = 100.
 \end{aligned}$$

The flux distribution factor

$$f_d = \frac{B_a}{B_m} = \frac{66.6}{100} = 0.666.$$

The value of f_a , calculated by the method explained on page 27, is 0.667, which checks the value found by the method given above.

The form factor of the flux wave has been defined as the ratio of the effective or root-mean-square ordinate to the average ordinate. From the analysis of the flux wave, the effective and average values are calculated as shown above:

$$f_b = \frac{B_e}{B_a} = \frac{75.8}{66.6} = 1.14.$$

The root-mean-square ordinate can be calculated also from the flux distribution curve, by dividing the base line into a number of equal divisions. The sum of the squares of the mean ordinates of each division divided by the number of ordinates gives the mean-square ordinate. The square root of the mean-square ordinate is the root-mean-square or effective ordinate.

By properly choosing the per cent pole embrace and the level of the pole tips, a flux wave with small harmonics can be obtained. Sev-

TABLE XIV

Pole Arc, Per Cent.	δ	δ_m	x	Maximum Fundamental	Maximum Third	Maximum Fifth	Maximum Seventh
71 3	0 390	1 605 = 0 623	0 214 τ = 2 10	112 50	+8 95	-7 17	-4 28
70 0	0 406	1 625 = 0 660	0 187 τ = 1 83	110 04	+5 22	-7 25	-2 32
68 75	0 406	1 775 = 0 720	0 185 τ = 1 813	108 50	+2 23	-9 53	-3 08
68 75	0 406	2 005 = 0 813	0 185 τ = 1 813	104 80	-2 36	-10 92	+0 450
68 75	0 406	1 855 = 0 75	0 174 τ = 1 71	106 80	-0 40	-9 41	-1 54

eral flux plots were made for the sample design. The dimensions of the pole shoe and the results of the analysis of the flux wave are given in Table XIV.

In the A.I.E.E. paper ³ referred to above, Mr. R. W. Wieseman has given a set of curves from which the maximum value of the third harmonic in per cent of the fundamental can be found when the dimensions of the pole shoe and the per cent pole embrace are known. These curves apply to a pole shoe beveled from the center of the pole instead of from a point at a distance x from the center of the pole, as shown in Fig. 106.

Sample Design: Diameter and Length.—A 2500-kva, 225-r.p.m., 3-phase, 60-cycle, 2400-volt, salient-pole, synchronous generator is to be designed. The generator is to be of the vertical, waterwheel type and

³ "Graphical Determination of Magnetic Fields—Practical Applications to Salient Pole Synchronous Machine Design," A.I.E.E. Journal, Vol. 46, May, 1927, p. 433.

is to have an efficiency at full-load, 100 per cent power factor, rated speed, and voltage not less than 95.6 per cent. The efficiency is to be calculated from the losses in accordance with the A.I.E.E. Standards. The temperature rise of no part of the machine shall exceed 50° C. when operating continuously at rated load, voltage, and speed.

$$\frac{Kva}{n} = \frac{2500}{225} = 11.1.$$

The output constant is taken from the curve, Fig. 105.

$$C = 1.58 \times 10^4.$$

The number of poles

$$p = \frac{f \times 2 \times 60}{n} = \frac{60 \times 2 \times 60}{225} = 32.$$

The diameter and length are calculated for several values of l/τ , as given in Table XV. The calculations for $l/\tau = 2.0$ are as follows:

$$D = \sqrt[3]{\frac{KvapC}{\pi \times 2 \times n}} = \sqrt[3]{\frac{2500 \times 32 \times 1.58 \times 10^4}{3.14 \times 2 \times 225}} = 96.4 \text{ in.}$$

$$l = \frac{KvaC}{nD^2} = \frac{2500 \times 1.61 \times 10^4}{225 \times 96.4^2} = 18.9 \text{ in.}$$

$$\tau = \frac{\pi D}{p} = \frac{\pi \times 96.4}{32} = 9.45 \text{ in.}$$

For other values of l/τ , the dimensions are as given in Table XV.

TABLE XV

l/τ	D	l	τ
1.00	121.5	11.9	11.90
1.50	106.1	15.6	10.40
1.75	100.5	17.3	9.86
2.00	96.4	18.9	9.45
2.25	92.6	20.5	9.10

For this design, the following dimensions are selected:

$$D = 100 \text{ in. and } l = 17.5 \text{ in.}$$

The pole pitch

$$\tau = \frac{\pi D}{p} = \frac{3.14 \times 100}{32} = 9.82 \text{ in.}$$

The per cent pole embrace is made 68.75 per cent (see page 179); and the pole arc

$$B = 0.6875 \times 9.82 = 6.75 \text{ in.}$$

The length of air gap is estimated at 0.406 in. (see curves Fig. 107). The flux plot is shown in Fig. 108, and the flux distribution curve in Fig. 109. The flux distribution factor and form factor have been calculated on page 184; they are

$$f_d = 0.666 \text{ and } f_b = 1.14.$$

CHAPTER XI

ARMATURE WINDING AND INSULATION

THE armature windings used for modern synchronous machines and induction motors are:

1. Chain windings.
2. Double-layer windings.

Chain Windings.—Chain windings have only one coil side per slot, and the number of armature coils is equal to one-half of the number of slots. The number of conductors per slot may be any integer, even or odd. The coils cannot all have the same shape because the end-connections must lie in different planes. A variety of methods are used to shape the coil end-connections. Figure 112¹ shows a two-bank, 3-phase chain winding, with 4 slots per pole per phase; Fig. 113¹ shows the same winding with the end-connections arranged in three banks. The armature coils for chain windings must be form-wound. More than one winding form is required for each machine because the coils are not all of the same shape. Large clearances can be allowed between the armature coil end-connections, which are very effective in cooling the winding. American practice has discontinued the use of chain windings; they are still used by many European manufacturers.²

Double-Layer Windings.—Each slot has two coil sides. The number of conductors per slot must therefore be a multiple of two. All coils have the same shape, and the number of coils is equal to the number of slots.

When the coils are so formed that the two sides lie a pole pitch apart, they are called pitch coils. Very often the armature coils are so constructed that the sides lie in slots less than a pole pitch apart, in which case they are called chorded coils. Chorded coils are used whenever possible for armature windings of synchronous machines and induction motors.

¹ Figures 112 and 113 are reproduced from "Die Wechselstromtechnik," by E. Arnold, Vol. III, 2nd ed., pp. 65 and 66, Julius Springer, Berlin.

² For further information on chain windings see "Die Wechselstromtechnik," by E. Arnold, Vol. III, 2nd ed., Julius Springer, Berlin, and "Ankerwicklungen für Gleich- und Wechselstrommaschinen," by R. Richter, Julius Springer, Berlin.

The advantages of chorded windings are:³

(1) Chording the armature coils has the effect of changing the number of conductors in the armature winding. By formula 134, page 175, the number of conductors in series per phase

$$N = \frac{E \times 60 \times 10^8}{\phi_i n C_w k_p}.$$

The conductors in series per phase are therefore inversely proportional to the chord factor, k_p . The chord factor is defined as the sine of the

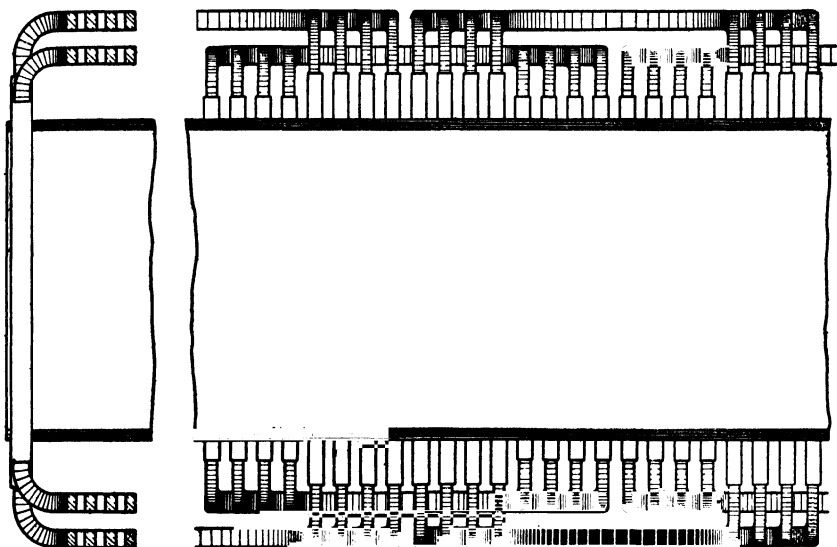


FIG. 112*.—Two-bank, three-phase chain winding with four slots per pole per phase.

* From "Die Wechselstromtechnik," by Dr. Arnold, Vol. III, p. 65, Julius Springer, Berlin.

half-angle, in electrical degrees, spanned by the coil. The pitch coil, which spans 180 electrical degrees, will therefore have as chord factor $k_p = \sin \frac{1}{2} 180^\circ = \sin 90^\circ = 1$ and will have the maximum possible voltage induced. Of the two coils shown in Fig. 114 with 9 slots per pole, the one with a coil throw from slot 1 to 10 spans 9 slots or 180 electrical degrees and $k_p = 1$. The other, with a coil throw from slot 1 to 8, spans 7 slots or $\frac{7}{9} \times 180 = 140$ electrical degrees, and $k_p = \sin \frac{1}{2} 140^\circ = \sin 70^\circ = 0.94$.

When designing the armature winding, one often finds that an odd number of conductors per slot will give the best results. But an odd

³ A.I.E.E. Trans., Vol. 26, Part 2, 1907, pp. 1485-1503; also, A.I.E.E. Trans., Vol. 27, Part 2, 1908, p. 1077.

number of conductors per slot can not be used for double-layer windings. The equivalent of an odd number of conductors per slot can, however, be obtained by using the next larger even number with chorded coils. For

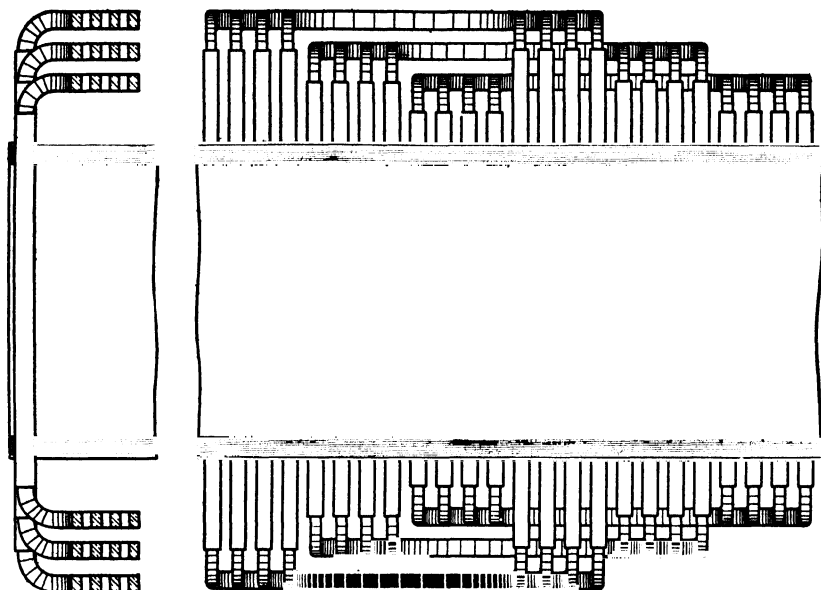


FIG. 113*. —Three-bank, three-phase chain winding with four slots per pole per phase.

*From "Die Wechselstromtechnik," by Dr. Arnold, Vol III, p 66, Julius Springer, Berlin.

example, the calculations for the armature winding of a 36-pole, 3-phase generator showed that 189 slots, with 13 conductors per slot, would give the best results. With 12 conductors per slot, the magnetic densities were found to be too high for best results, and with 14 too low. The desired results were obtained by using 14 conductors per slot, with the coils chorded 76.2 per cent of pitch.

(2) The length of the mean-turn and the overall length of the armature coil, parallel to the shaft, are reduced by chording. Figure 114 shows two coils for a winding, with 9 slots per pole, the one with a coil throw from slot 1 to 10 and the other with a coil throw from slot 1 to 8. It is apparent from the figure that the coil with the shorter throw has a shorter mean-turn and a smaller overall length. Reducing the mean-turn of the coils produces a direct saving in

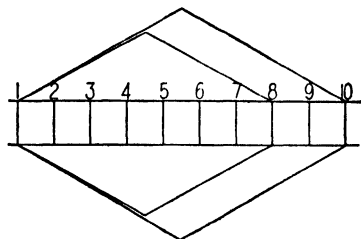


FIG. 114.

copper and reduces the armature resistance. Because of the reduced resistance, the efficiency is higher and armature heating is reduced, since heating depends upon the total losses to be dissipated.

(3) For machines with a small number of poles and small diameter, machine-wound, "pulled type" armature coils can be used. For 2-pole turbo-generators, for example, a pitch coil will have its sides in slots diametrically opposite. Specially constructed end-connections are required for such a design. By chording the coils, the standard "pulled type" of coil, to be described later, can be used.

(4) By chording the coils, the leakage reactance of the armature

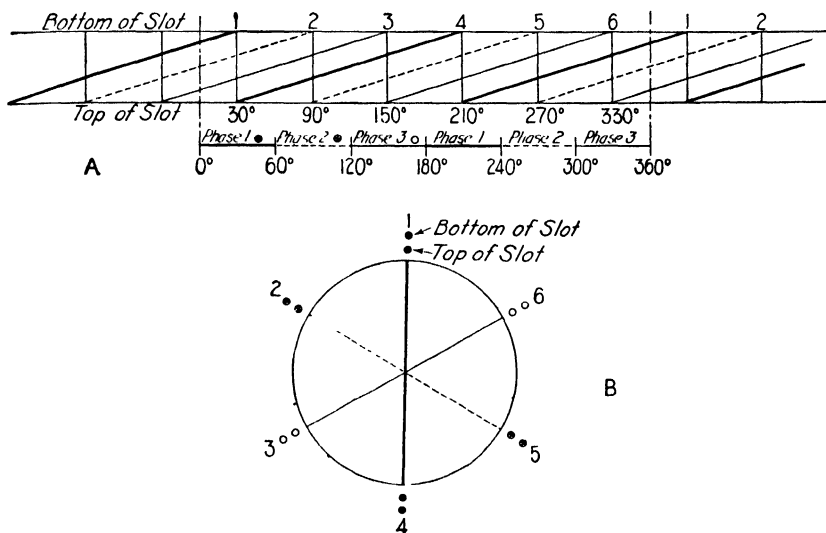


FIG. 115.—Diagram of three-phase winding—one slot per pole per phase—coil throw, slot 1 4, $k_d = 1$, $k_p = 1$.

winding is reduced, as can be seen from the leakage reactance formulas, Chapter XIII.

(5) Chording the armature coils improves the generated voltage wave form of synchronous generators.

Graphic Method of Laying Out the Armature Winding.—The armature coils are placed into the slots in 60° phase belts for 3-phase machines and in 90° phase belts for 2-phase machines. The diagram to determine the sequence of the coils is made as shown in Fig. 115A, which is a developed end-view of the armature slots and coil end-connections. The two horizontal lines represent the top and bottom of the slots, and the vertical lines joining them represent the slots. The diagonal lines passing from top to bottom of slot are the coil end-connections. The

figures at the top of the slots are the electrical degrees for each slot. The zero or starting point for the diagrams shown is chosen on the center line between two slots. The diagram, Fig. 115, is for a 3-phase winding, with 1 slot per pole per phase or 3 slots per pole with pitch coils. The number of electrical degrees between slots is $180 \div 3 = 60$. It is apparent from the diagram that after passing through 360 electrical degrees, which corresponds to 6 slots or 2 poles, the winding repeats, that is, slot 7 is the same as slot 1. The diagram, therefore, need not be extended beyond 6 slots or 2 poles. The minimum number of poles the winding can be used for is therefore 2. For a pitch winding the coils must span 3 slots and the coil throw is from the top of slot 1 to the bottom of slot 4, etc. All slots from zero to and including 60° must have coil sides in the top belonging to phase 1, all slots from 60° to and including 120° must have coil sides in the top belonging to phase 2, and all slots from 120° to and including 180° must have coil sides in the top belonging to phase 3, and so on, as shown in the diagram. The sequence of the coil sides in the bottom of the slots is automatically taken care of by the coil throw.

From the diagram of the winding, a vector diagram of the voltages induced in the coils is made, as shown in Fig. 115*B*. The circle is drawn with any convenient radius and divided into as many equal parts as there are slots required to make the winding repeat. For the diagram in Fig. 115*A*, the circle must be divided into 6 equal parts because 6 slots are necessary to make the winding repeat. The numbers in Fig. 115*B* are slot numbers. The coil sides in top and bottom of the slots are taken from Fig. 115*A*. The length of the line joining the coil side in the top of slot 1 with the coil side in the bottom of slot 4 is proportional to the voltage induced in coil 1 to 4. Similarly, the length of the line joining the coil side in the top of slot 4 with the coil side in the bottom of slot 1 is proportional to the voltage induced in coil 4 to 1. The vectors 1 to 4 and 4 to 1, Fig. 115*B*, must pass through the center of the circle because the coils are pitch coils and have the maximum possible voltage induced. There are two vectors, both occupying the same position, one for each pole. The vectors for the three phases make an angle of 60° with each other, because the coils are placed into the slots in 60° belts.

Figure 116*A* and *B* shows the winding diagram for the same winding as shown in Fig. 115 but shows the coils chorded one slot. The coil sides in the top of the slots are the same as those in Fig. 115, but those in the bottom of the slots are not the same, because of the different coil throw. The voltage vectors do not pass through the center of the circle but are chords of the circle, which shows that the voltage induced is less than for the pitch coils. If the diameter of the circle is assumed to be 1,

then the voltage induced in each of the coils in Fig. 115 is proportional to 1. For the winding shown in Fig. 116, the voltage induced in the coils is less than the voltage induced in the pitch coils by the ratio of the length of the chords 1 to 3 and 4 to 6 to the diameter of the circle. The length of a chord of a circle is equal to the sine of the half angle which it subtends times the diameter. The chords 1 to 3 and 4 to 6 subtend 120° and the length of each is equal to $\sin \frac{1}{2} 120^\circ = \sin 60^\circ = 0.866$, which is equal to the chord factor $k_p = \sin \frac{2}{3} 90^\circ = 0.866$. The voltage induced in the chorded winding is, therefore, 86.6 per cent of the voltage induced in the pitch winding.

For the windings shown in Figs. 115 and 116 the winding distribution

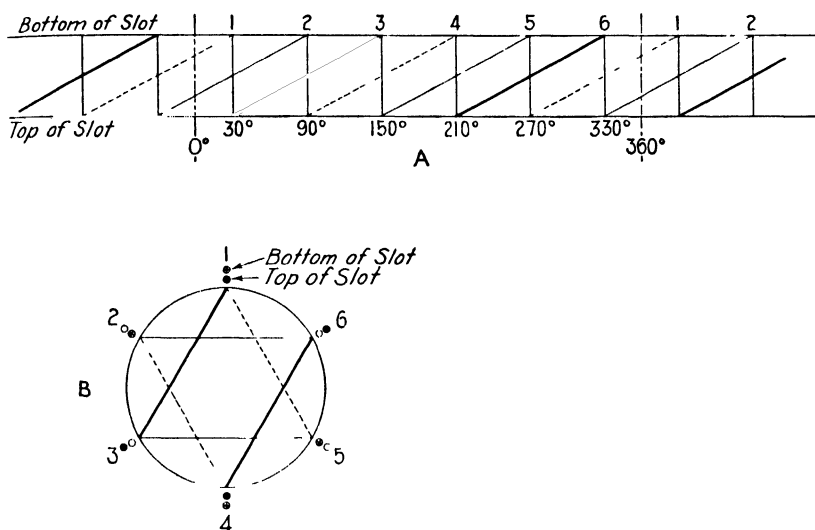


FIG. 116. —Diagram of three-phase winding—one slot per pole per phase—coil throw, slot 1-3.

factor is 1, because there is only one slot per pole and phase. Figure 117 shows the diagram for a 3-phase winding with 2 slots per pole and phase, with pitch coils. This winding also repeats every two poles and can therefore be used on a 2-pole machine. There are now 4 voltage vectors for each phase in the vector diagram, one for each of the 4 coils per phase. Since this is a pitch winding, the vectors representing the voltage induced in each coil must pass through the center of the circle. The voltage induced in the two coils for each pole and phase connected in series is not equal to the arithmetical sum of the voltages induced in each of the coils, but is equal to the vector sum of the voltages induced in the two coils, because, as the diagram shows, the voltages in the two coils are

not in phase but differ by 30 electrical degrees. It is obvious from the vector diagram, Fig. 117*B*, that the vector sum of the voltages induced in the two coils 1 to 7 and 2 to 8 is equal to the sum of the lengths of the two chords 1 to 8 and 2 to 7. The vectors for the two coils under the second pole occupy the same position as the vectors for the first pole. The voltage induced in the 4 coils of each phase is therefore proportional to $4 \sin \frac{1}{2} 150^\circ = 4 \sin 75^\circ = 4 \times 0.966$. The arithmetical sum of the voltage induced in the 4 coils is proportional to 4. Since the chord factor is 1.0, the winding distribution factor, $k_d = \frac{4 \times 0.966}{4} =$

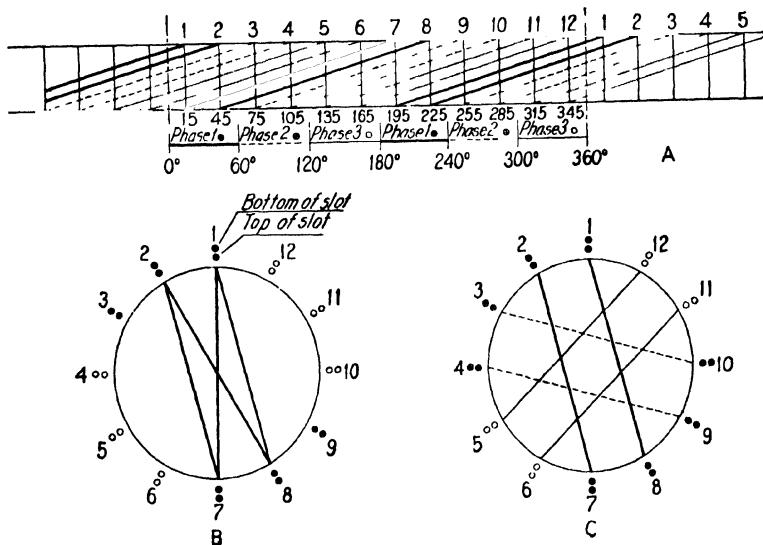


FIG. 117.—Diagram of three-phase winding—two slots per pole per phase—coil throw, slot 1-7.

0.966. The voltage vectors and chords for only one phase are shown in Fig. 117*B*; the complete vector diagram showing the chords for the three phases is that of Fig. 117*C*. The chords must always be so drawn that they connect coil sides in the top of a slot belonging to one phase with coil sides in the bottom of a slot on the opposite side of the circle belonging to the same phase. The chords for each phase must be parallel and must make an angle of 60° with the other phases.

Figure 118 shows the vector diagram for the same winding shown in Fig. 117, but with chorded coils. The coil sides in the top of the slots are the same as for the pitch winding. In the bottom of the slot they are not the same because of the shorter coil throw. For the diagram, Fig.

117, the chord factor is 1. The winding distribution factor is then equal to the sum of the lengths of the chords divided by the number of chords. The voltage induced in a winding varies directly with $k_d k_p$. The ratio of the sum of the lengths of the chords to the number of the chords is therefore equal to $k_d k_p$. For Fig. 118,

$$k_d k_p = \frac{1-6 + 2-5 + 7-12 + 8-11}{4} = \frac{2 \sin 45^\circ + 2 \sin 75^\circ}{4} = 0.836.$$

The chord factor can easily be calculated when the coil throw is known. For a coil throw slot 1 to 5 with 6 slots per pole,

$$k_p = \sin \left(\frac{1}{3} \times 90^\circ \right) = 0.866$$

and

$$k_d = \frac{0.836}{0.866} = 0.966.$$

Figure 119 shows the layout for a 2-phase winding, with 4 slots per pole per phase and coil throw slot 1 to 7. The coils are placed in 90° phase belts, and the chords for each phase are parallel and make an angle of 90° with the other phase. The chord factor

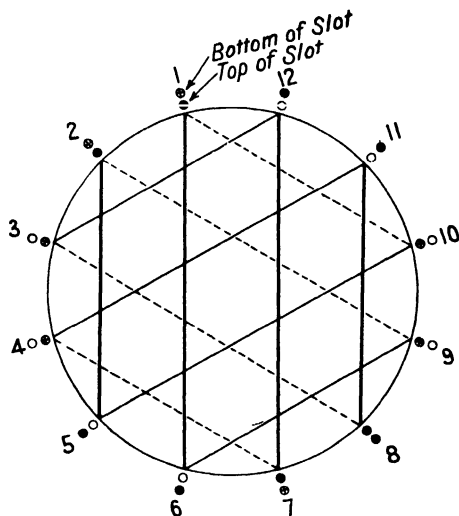


FIG. 118 — Vector diagram of three-phase winding two slots per pole per phase—coil throw, slot 1-5.

$$k_p = \sin \left(\frac{\pi}{6} \times 90^\circ \right) = 0.924.$$

From Fig. 119B, the winding distribution factor is calculated as follows:

$$k_p k_d = \frac{2 \sin 33.75^\circ + 2 \sin 56.25^\circ + 4 \sin 78.75^\circ}{8} = 0.837$$

$$k_d = \frac{0.837}{0.924} = 0.906.$$

For the windings shown above, the total number of slots is a multiple of the number of poles times the number of phases; that is, the number of slots per pole per phase is an integer. The total number of slots need not

always be a multiple of the number of poles times the number of phases, neither need the number of slots per pole per phase be an integer. It may be a mixed number, for example, $2\frac{1}{4}$, $3\frac{1}{3}$, etc.

The method of laying out a winding with a mixed number of slots per pole and phase is exactly the same as for the windings shown above. The windings for which the number of slots per pole per phase is not an integer do not always repeat every two poles. It may be necessary to lay out the winding for 4 or more poles. Figure 120 shows a 3-phase winding, with $2\frac{1}{4}$ slots per pole per phase. The number of slots per pole $= 3 \times 2\frac{1}{4} = 6\frac{3}{4}$, and the electrical degrees between slots

$$\frac{180}{6\frac{3}{4}} = 26\frac{2}{3} \text{ electrical degrees.}$$

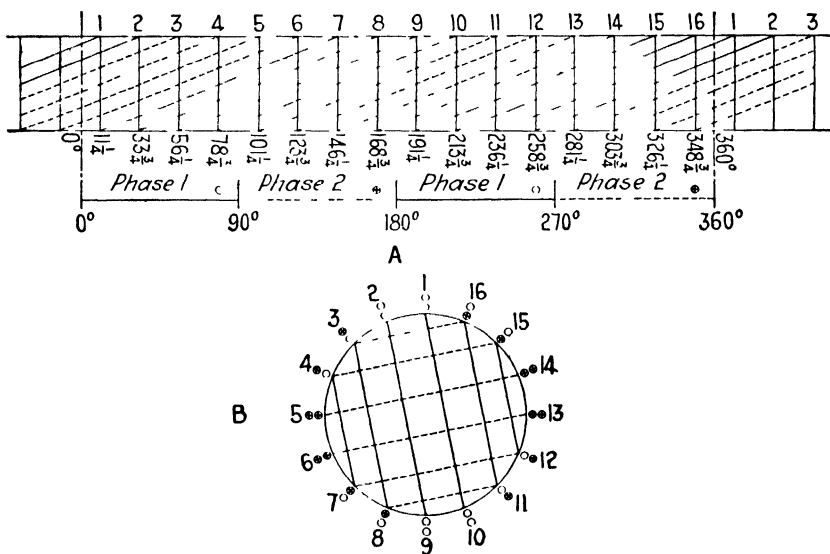


FIG. 119.—Diagram of two-phase winding—4 slots per pole per phase—coil throw, slot 1-7.

The electrical degrees are shown at the top of the slot in Fig. 120A, with the zero or starting point on the center line between two slots. The diagram shows that the winding repeats after passing over 27 slots or 4 poles, that is, slot 28 is the same as slot 1. In the vector diagram, Fig. 120B, the circle is divided into 27 equal parts because there are 27 slots necessary before the winding repeats. The calculations for the winding distribution factor are given in Fig. 120B.

A 2-phase winding with $2\frac{1}{3}$ slots per pole per phase is shown in Fig.

121. The number of slots per pole $= 2 \times 2\frac{1}{2} = 4\frac{1}{2}$, and the electrical degrees per slot $= \frac{180}{4\frac{1}{2}} = 38\frac{1}{2}$ electrical degrees. The vector diagram and the calculations for the winding distribution factor are shown in Fig. 121B.

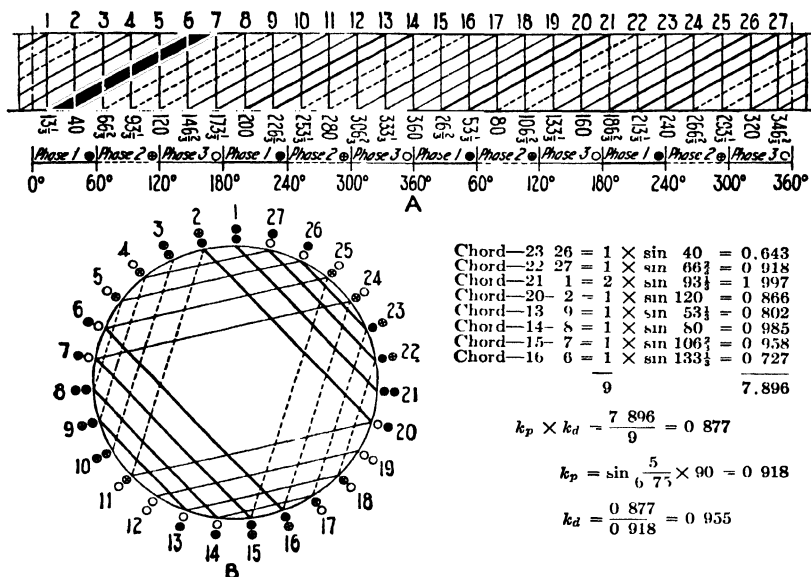


FIG. 120.—Diagram of three-phase winding— $2\frac{1}{2}$ slots per pole per phase—coil throw, slot 1-6.

Not all values of slots per pole per phase can be used for 3-phase and 2-phase windings. When the number of slots per pole and phase is a mixed number, a balanced winding can be obtained only when the denominator of the fraction is not a multiple of the number of phases. For example, $2\frac{1}{2}$ slots per pole per phase can not be used for a 2-phase winding, because 4, the denominator of the fraction, is a multiple of 2. A winding with $2\frac{2}{3}$ slots per pole per phase, for example, can be used for either 2- or 3-phase, because the denominator of the fraction is not a multiple of 2 or 3. This winding repeats every 14 poles, and the minimum number of poles for which it can be used is 14.

The general equation for the winding distribution factor for the fundamental

$$k_d = - \frac{\sin \frac{180^\circ}{2m}}{q \sin \frac{180^\circ}{\alpha}}$$

For windings with mixed number of slots per pole per phase the equivalent number of slots per pole per phase must be used for q . A fractional-slot⁴ armature winding may be represented by

$$f + \frac{g}{h} = \frac{fh + g}{h}.$$

This indicates that there are $fh + g$ slots per phase for every h poles. The winding is equivalent to an integral slot winding with $fh + g$ slots

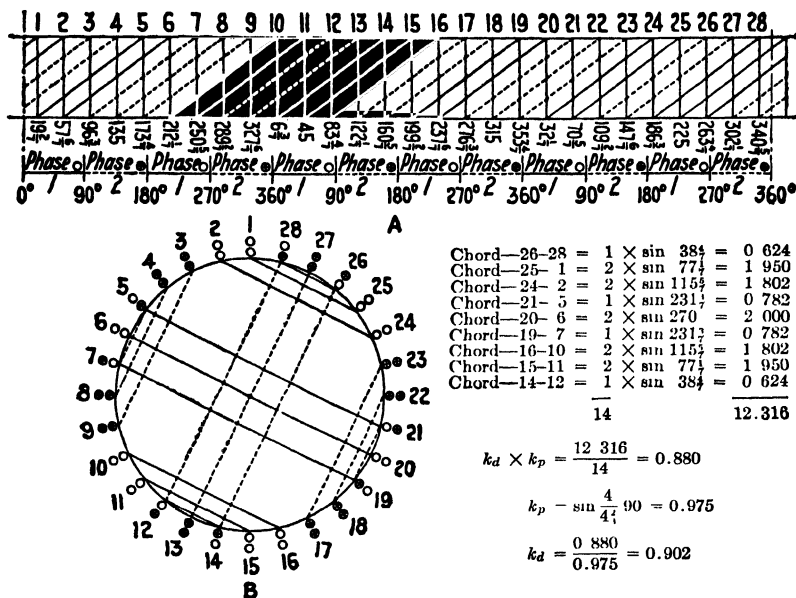


FIG. 121.—Diagram of two-phase winding— $2\frac{1}{2}$ slots per pole per phase—coil throw, slot 1-5.

per pole per phase. For a $2\frac{1}{4}$ -slot-per-pole-per-phase 3-phase winding, Fig. 120, the equivalent integral slot winding would have

$$2 + \frac{1}{4} = \frac{2 \times 4 + 1}{4} = \frac{9}{4},$$

or 9 slots per pole per phase. The winding distribution factor

$$k_d = \frac{\sin \frac{180^\circ}{2 \times 3}}{9 \sin \frac{180^\circ}{2 \times 3 \times 9}} = 0.955.$$

⁴ "Alternating Current Machinery," by J. M. Bryant and E. W. Johnson, McGraw-Hill Book Co., New York.

Connections.—Three-phase windings may be either star or delta-connected. For synchronous generators, only the star connection is used. The advantages of the star connection have been explained by T. S. Eden;⁵ they are as follows: (1) Currents of triple frequency or multiples of triple frequency can not flow in star-connected windings with ungrounded neutral. (2) In general the e.m.f. wave form is nearer a true sine wave. (3) It is possible to bring out a lead from the neutral

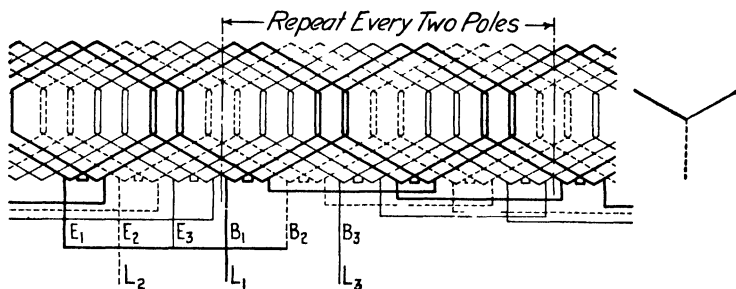


FIG. 122.—Connection diagram for three-phase winding—two slots per pole per phase—one-circuit star.

point, which is useful for various purposes. (4) Grounding the neutral reduces the potential strain on the insulation of the winding, permitting reduced thickness of insulation.

The coils per phase of both 2-phase and 3-phase windings can always be connected in series, and usually they can also be connected in parallel, to form more than one circuit. For high-voltage machines,

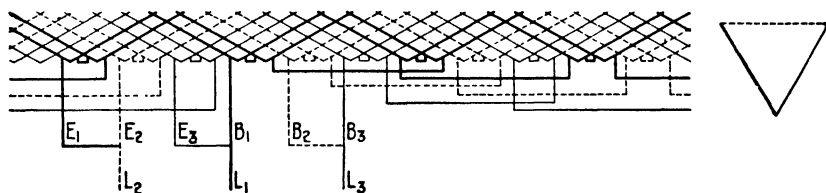


FIG. 123.—Connection diagram for three-phase winding—two slots per pole per phase—one-circuit delta.

the one circuit winding, with all the coils per phase connected in series, should always be used so that the voltage per turn will not be too high. The connection diagram for the winding laid out in Fig. 117 is shown in Fig. 122, with star connection and one circuit. The ends of phases 1 and 3 and the beginning of phase 2 form the neutral. The beginning of phases 1 and 3 and the end of phase 2 are the line leads. The one-cir-

⁵ A.I.E.E. Trans., Vol. 33, Part I, 1914, p. 803.

cuit delta-connection for this same winding is shown in Fig. 123. In this diagram only the coil leads are shown. The two-circuit star-connection is shown in Fig. 124. When more than two circuits are used,

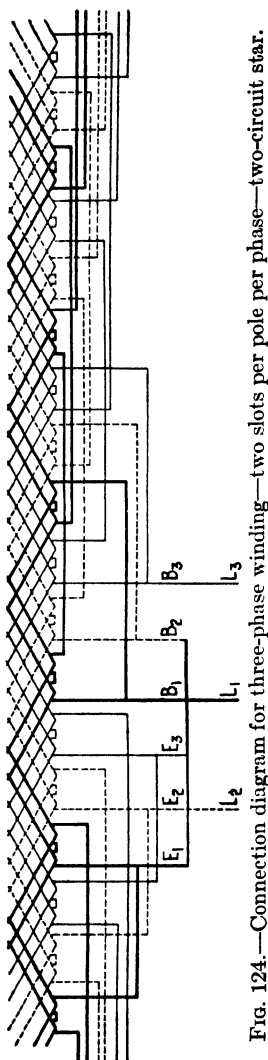


Fig. 124.—Connection diagram for three-phase winding—two slots per pole per phase—two-circuit star.

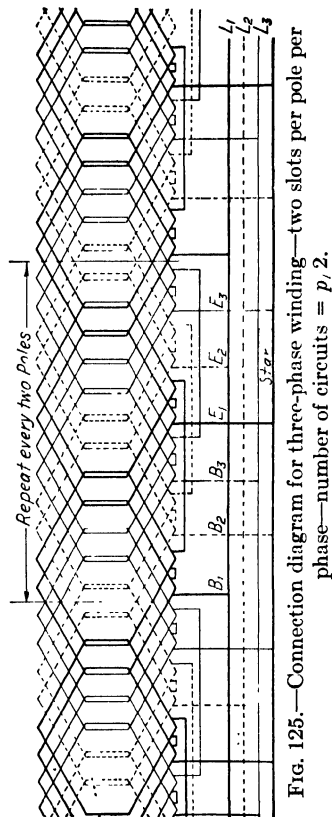


Fig. 125.—Connection diagram for three-phase winding—two slots per pole per phase—number of circuits = $p/2$.

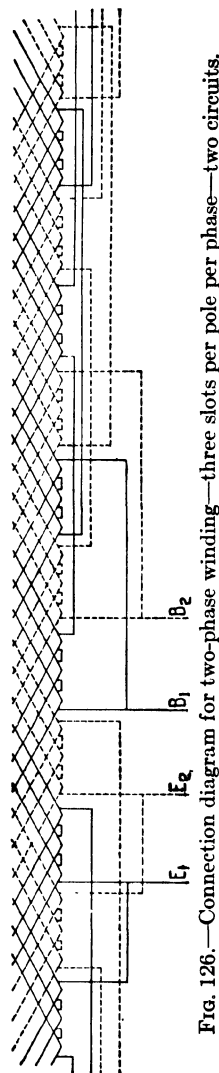


Fig. 126.—Connection diagram for two-phase winding—three slots per pole per phase—two circuits.

the connections are made as shown in Fig. 125, which is the connection diagram for the two-slot-per-pole-per-phase winding laid out in Fig. 117, with as many circuits as there are pairs of poles. For windings with a

mixed number of slots per pole per phase, the number of circuits possible is often very much limited. For example, a winding with $2\frac{1}{4}$ slots per pole per phase does not repeat until 4 poles have been passed over. The minimum number of poles that this winding can be used for is therefore 4, and only one circuit is possible. On an 8-pole machine, the maximum number of parallel circuits possible with this winding is 2, etc. It is for this reason that windings for which the number of slots per pole is an integer are often chosen in preference to fractional slot windings. Small synchronous motors and induction motors are generally designed for two voltages, that is, 110 and 220 volts or 220 and 440 volts. To accomplish this, the windings must be so chosen that two circuits can be used for the low voltage and one for the high voltage. As shown above, this is not always possible with fractional slot windings.

The connection diagram for a 2-circuit, 2-phase winding with 3 slots per pole per phase is shown in Fig. 126.

Number of Armature Slots.—The number of armature slots must be an integer and must be such a number that a balanced winding can be obtained. The total number of slots will always be satisfactory for a given number of poles and phases when the numerator of the fraction $\frac{\text{slots}}{\text{poles}}$, reduced to its lowest terms, is a multiple of the number of phases. For example, with 126 slots on a 14-pole machine,

$$\frac{\text{slots}}{\text{poles}} = \frac{126}{14} = \frac{9}{1}$$

and a balanced 3-phase winding is possible, because 9 is a multiple of the number of phases. With 120 slots on a 14-pole machine,

$$\frac{\text{slots}}{\text{poles}} = \frac{120}{14} = \frac{60}{7}$$

and a balanced 2-phase or 3-phase winding is possible, because 60 is a multiple of both 2 and 3.

With a small number of armature slots, a smaller number of coils will be required than with a larger number, but the number of turns per coil and, therefore, the slot size will be larger. A small number of slots might therefore lead to a slight saving, because there are fewer coils to wind, form, insulate, place into the slots, and connect. The armature slots affect the flux wave which the armature conductors cut. The ripples in the flux wave induce harmonics in the voltage wave of generators and produce eddy-current losses in the pole faces of motors and generators. The effect of the armature slots upon the flux

wave can generally be reduced by using a large number of narrow slots.

The tooth pitch at the armature surface is

$$t_1 = \frac{\pi D}{S}.$$

It may serve as a guide when choosing the number of armature slots. The slot width is generally equal to or slightly less than the tooth width. For a small tooth pitch, the armature tooth will be narrow. This condition might lead to difficulties in construction, for the reason that it is difficult to support the armature teeth at the ventilating ducts and at the ends of the armature core without obstructing the ventilation. For synchronous motors and generators, the tooth pitch at the armature surface is generally 0.80 to 2.0 in. With a small tooth pitch, the armature coil end-connections are close together, with no space for ventilation between the coils. For high-voltage machines, which are generally built in large capacities, it is, as a rule, desirable to use a large tooth pitch. The effect of the armature slots upon the air gap flux distribution curve is generally quite small for large machines because the air gap length is large.

Armature Coil Construction and Insulation.—The armature coils for synchronous motors and generators are wound with round, square, or rectangular copper wire. For small-capacity, high-voltage machines, which require a large number of turns of small wire, round conductors are often necessary. Whenever possible, square or rectangular conductors are used because they make mechanically stronger coils with smaller air spaces between turns. For large-capacity machines requiring large conductor sections, each conductor is built up of a number of small wires in parallel. By subdividing large conductors, a more flexible coil is obtained, which can be easily formed. The eddy current losses present in large solid conductors are thereby reduced.

For some machines, form-wound coils are used. A winding form with wire-wound coil is shown in Fig. 127. The pulled type of armature coil is used for most machines. This coil is wound on a bobbin, as shown in Fig. 128, and then pulled out to the required shape on a coil-pulling machine. Whenever possible, the coils should be wound in such manner that there is only one turn per layer. Fig. 129A shows a section of a coil wound with rectangular conductors with only one turn per layer. When the section area of the conductor exceeds approximately 0.100 sq. in. or when it is not possible to obtain satisfactory slot dimensions with one conductor, the arrangement shown in Fig. 129B is used. Each conductor is subdivided by using several small wires in parallel.

arranged in such manner that the conductors per layer are connected in parallel. The line through the conductor of each layer indicates the

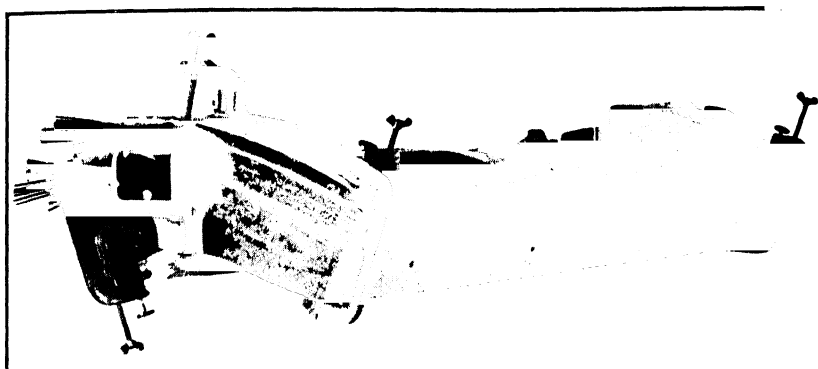


FIG 127 —Winding form with coil.

parallel wires. Figure 130 shows a large armature coil wound with 12 wires, 0.080×0.145 in., in parallel.

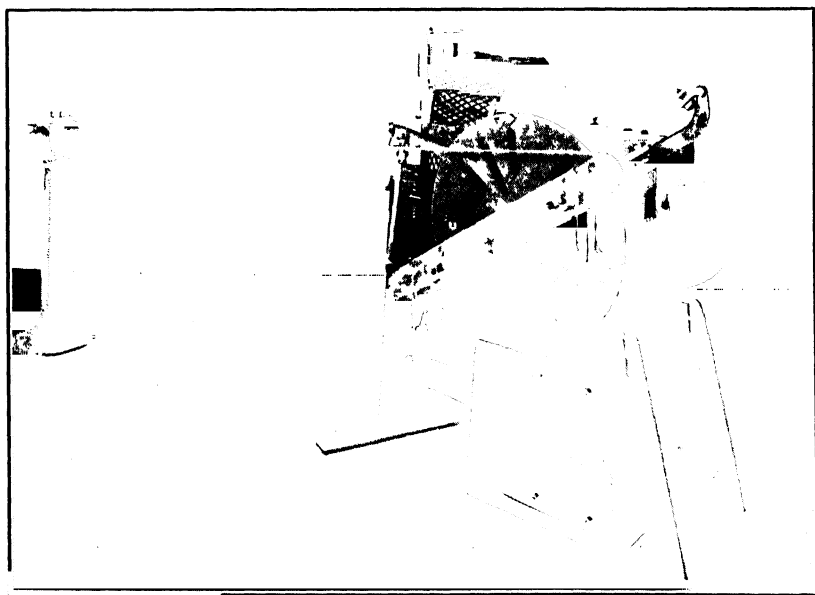


FIG. 128.—Coil-winding machine.

For machines requiring a large number of turns of small wire, the arrangement of conductors shown in Fig. 129A and B cannot always be

used. For such machines the coils should be wound as shown in Fig. 131A. With this arrangement, one half of the coil must be wound backwards, that is, in opposite direction to the other half. The two halves of the coil must be insulated from each other, because of the high voltage between the beginning and ending lead.

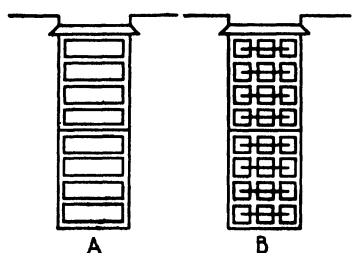
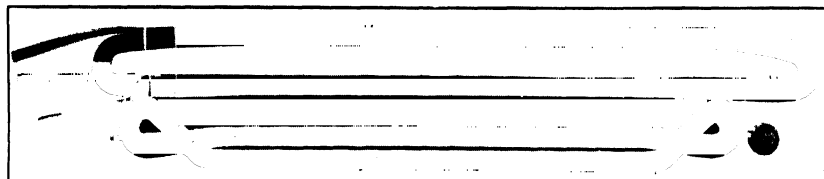


FIG. 129.

Coils with many turns may also be wound as shown in Fig. 131B. For this method of winding the coils, the turns of each layer cross each other, and experience has shown that short circuits often occur at these cross-over points. This method should be used only with round wire and in sizes 0.0163 sq. in. area and smaller.

Double-cotton-covered conductors are generally used for the armature coils. For machines to operate at high temperatures or for heavy overloads for short periods, asbestos-covered

FIG. 130.—Armature coil with 12 wires, 0.08 in. \times 0.145 in. in parallel.

wire is sometimes used. The straight part of the bobbin-wound coil is molded in a steam or electrically heated mold and is then pulled out on a coil-pulling machine to the required shape. For high-voltage, large-capacity machines, the pulled-out coil is treated by the vacuum process,⁶ to fill all interstices with an insulating, moisture-resisting, heat-conducting compound. To maintain a smooth surface on the outside of the coil, it is wrapped with a sacrifice tape before it is impregnated. This tape is removed after the coil has been treated. For moderate-voltage machines, the coils are often given a varnish treatment instead of the vacuum treatment. In the varnish treatment, the coils

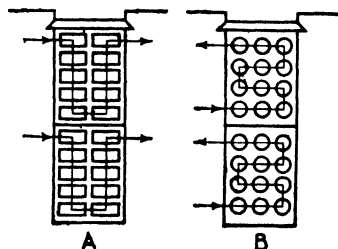


FIG. 131.

⁶ "Insulation and Design of Electrical Windings," by A. P. M. Fleming and R. Johnson, p. 68, Longmans, Green and Co., London; Electric Journal, Vol. 22, Feb., 1925, p. 95

are first dried and then dipped into a bath of insulating varnish. After removal from the varnish bath they are allowed to drain and are then baked at a temperature of 100° C. until dry. This treatment is repeated two or three times, depending upon the voltage, size, and type of machine.

After the varnish or impregnating treatment, the coils are ready for the insulation, which consists of wrappings or tapings of varnished cam-

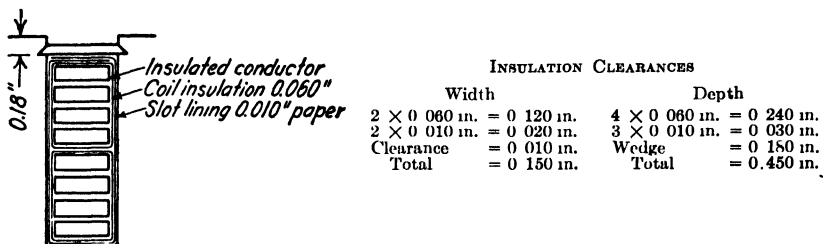


FIG. 132.—Thickness of coil insulation and slot clearances for a 2400-volt armature winding for 40-in. diameter or larger.

TABLE XVI

CLEARANCE ALLOWANCE FOR SLOT INSULATION FOR ARMATURE WINDINGS
OF SYNCHRONOUS MACHINES WITH OPEN-TYPE SLOTS

Volts	s	2b	Slot Depth			Slot Width		
			Gap Diameter			Gap Diameter		
			10 In. and Less	20 In.	40 In. and Over	10 In. and Less	20 In.	40 In. and Over
0- 300	0 10	1 50	0 24	0 25	0 31	0 060	0 065	0 080
300 600	0 12	1 75	0 27	0 29	0 34	0 075	0 085	0 095
600- 1,500	0 14	2 00	0 30	0 31	0 37	0 090	0 095	0 110
1,500 3,000	0 16	2 25	0 34	0 36	0 45	0 110	0 120	0 150
3,000- 5,000	0 18	2 50		0 42	0 51		0 150	0 180
5,000- 8,000	0 20	3 00		0.52	0 65		0 200	0 250
8,000 12,000	0 25	3 50			0 80			0 32
12,000 15,000	0 30	4 00			1 00			0 42

bric, mica, or combinations of both, depending upon the size of the coil and the voltage for which it is to be insulated. The standard test voltage for which the armature windings of synchronous machines must be insulated is given in the Standardization ⁷ Rules of the A.S.A. It is

⁷ A.S.A. Standards C50, 1943.

twice the rated voltage of the winding, plus 1000. The high-voltage test is to be made when the windings are at operating temperature.

The insulating materials generally used are: cotton and linen tape, mica and mica tape, glass and glass tape, varnished cambric, and insulating varnishes. Figure 132 shows how the insulation clearances for width and depth of slot are determined. Table XVI gives the insulation clearances usually required for width and depth of slot for synchronous machine armature windings for various voltages. In the allowance for the depth in this table 0.15 in. is allowed for the wedge for gap diameters less than 40 in. and 0.18 in. for gap diameters over 40 in. For partly closed slots the insulation allowances are taken into account as explained on page 310.

Conductor Section and Slot Size.—The armature copper loss

$$W_a = I^2 R_a \text{ watts.}$$

The current in the armature winding

$$I = A_a s_a,$$

and the resistance of the armature winding

$$R_a = \frac{Lr}{s_a \times 10^6}.$$

Here L is the total length of the armature conductor.

Making the substitutions,

$$W_a = A_a^2 s_a^2 \frac{Lr}{s_a \times 10^6} = A_a^2 s_a Lr \times 10^{-6}.$$

The weight of the armature copper

$$G_a = L s_a \times 0.321$$

and

$$L s_a = \frac{G_a}{0.321}.$$

For 25° C., $r = 0.692$ and

$$W_a = A_a^2 G_a \times 2.15 \times 10^{-6} \text{ watt.} \quad (139)$$

For 75° C., $r = 0.826$ and

$$W_a = A_a^2 G_a \times 2.58 \times 10^{-6} \text{ watt.} \quad (139a)$$

To obtain the effective alternating-current resistance the equations for W_a must be multiplied by the stray-loss factor. This factor depends upon the ratio of the stray load losses to the armature copper losses.

This equation shows that the armature copper loss varies directly with the current density squared and the weight of the copper. Since the armature copper loss is a large percentage of the total losses and since the temperature rise of the armature copper depends upon the copper losses, it follows that temperature rise or efficiency or both will generally limit the value of A_a . The number of armature conductors required for a given voltage and flux increases as the speed of the machine decreases. The copper loss for a given current density will therefore generally be higher for slow-speed machines than for high-speed machines. To obtain an economical design, the current density

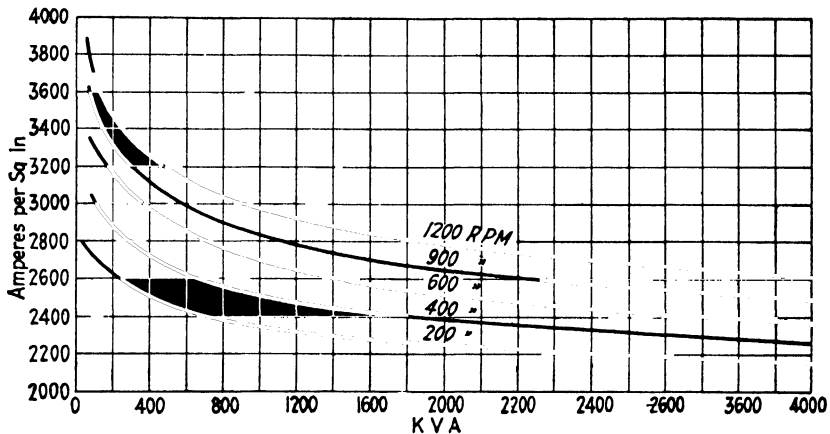


FIG. 133.—Approximate current densities for armature windings of 50° C. salient-pole synchronous machines.

should be chosen as high as good operating characteristics will permit. The curves in Fig. 134 give average values for the armature current density for various capacities and speeds.

The section area of the armature conductor

$$s_a = \frac{I}{A_a a} \text{ sq. in.} \quad (140)$$

The open type of armature slot is generally used for armatures of synchronous machines. For open-type armature slots, the leakage flux is not equally distributed over the entire slot depth, and, as a result, a difference of potential is produced between the top and bottom of any conductor in the slot. If the conductor is large, this difference of potential will set up equalizing currents in the conductor, which may lead to copper losses several times greater than the copper loss due to the normal load current alone. These eddy-current losses may be reduced to a

negligible value by subdividing the individual conductors. This is done by using several small wires in parallel or by using pressed cable. For large-capacity machines, transposed⁸ conductors or inverted turn coils must be used in addition to subdividing the conductors. Figure 134 shows a portion of an armature coil for a 12,500-kva. turbo-generator. The coil has two turns, and each turn is inverted in the end-connection. The armature conductor for synchronous machines is therefore generally built up of a number of small insulated wires in parallel.



FIG. 134.—Part of turbo-generator coil showing transportation in end-connection.

The dimensions of the slot can be found by adding, to the space required by the insulated conductors in the width and depth of the slot, the insulation clearance necessary. The insulation clearances for width and depth of slot are given, for various voltages, in Fig. 132.

Mean-Turn, Resistance, and Weight of Armature Winding.—The shape of the armature coils for synchronous machines is approximately the same as that of the armature coils for direct-current machines. The angle α , Fig. 135, which the straight part of the end-connection makes with the edge of the armature core can be calculated as follows:

$$\sin \alpha = \frac{d}{t_1} \quad (141)$$

Here t_1 is the tooth pitch at the armature surface and d is the thickness of one coil at the end-connections plus the clearance between adjacent

⁸ "Reduction of Armature Copper Losses," by I. H. Summers, *A I E E. Journal*, Vol. 46, May, 1927, p. 451, "Additional Losses of Synchronous Machines," by C. M. Laffoon and J. F. Calvert, *A I E E. Journal*, Vol. 46, June, 1927, p. 573, "Transposed Armature Coils in Alternating Current Generators," by S. L. Henderson, *Electric Journal*, Vol. 23, July, 1926, p. 348.

end-connections. The thickness of the coil at the end-connections may be taken equal to the slot width. The clearance, s , Fig. 135, is given in Table XVI.

The coil pitch is calculated on a diameter through the mean of the slot depth. It is

$$= \frac{\pi(D + d_s)}{p} P \text{ in.}$$

P is the per unit pitch of the coil. The length of the straight part of the end-connection for one end of the coil

$$2C = \frac{\pi(D + d_s)}{p \cos \alpha} P \text{ in.}$$

The part of the armature coil which is embedded in the slot is allowed to extend beyond the edge of the armature core a distance b , Fig. 135.

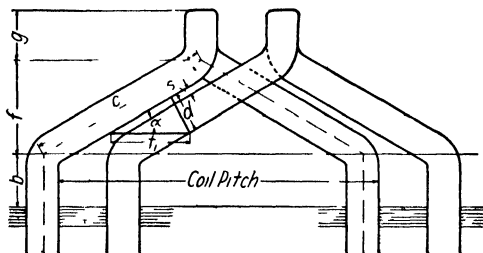


FIG. 135.—Armature coil end-connections.

The length of this coil extension depends upon the voltage of the winding. It is given in Table XVI.

The loop at each end of the coil has a mean length approximately equal to the slot depth.

The complete expression for the length of one-half the mean-turn of an armature coil

$$L_a = \frac{\pi(D + d_s)}{p \cos \alpha} P + 2b + d_s + l \text{ in.} \quad (142)$$

The horizontal extension of the armature coil beyond the armature core is equal to the sum of $b + f + g$, Fig. 135.

$$f = C \sin \alpha \text{ in.}$$

The horizontal extension of the armature coil beyond the armature core on each side is then

$$\begin{aligned} &= C \sin \alpha + b + d_s = \frac{1}{2} \frac{\pi(D + d_s)}{p \cos \alpha} P \sin \alpha + b + d_s \\ &= \frac{\pi(D + d_s)}{2p} P \tan \alpha + b + d_s \text{ in.,} \end{aligned}$$

and g is approximately equal to the slot depth.

The resistance per phase of the armature winding

$$R_a = \frac{L_a N r}{a s_a \times 10^6} \text{ ohms.} \quad (143)$$

$r \times 10^{-6}$ is the resistance of copper per inch of 1-sq. in. section. For 25°C. , $r = 0.692$ and for 75°C. , $r = 0.826$. When the armature conductor is built up of several small wires in parallel, s_a in formula 143 must be the section area of the group of parallel wires. The resistance of the winding at any other temperature, T_2 , can be calculated by formula 37, page 59.

The bare weight of the armature copper

$$G_a = L_a N a m s_a \times 0.321 \text{ lb.} \quad (144)$$

Here s_a is the section area of the group of parallel wires, when the armature conductor is built up of several small wires in parallel. The approximate insulated weight can be calculated from the data given in the copper tables.

Sample Design: *Design of Armature Winding.*—From the data given on page 176, an air gap density of 42,000 lines per sq. in. is assumed.

$$\begin{aligned} \phi_t &= \pi D l B_g = \pi \times 100 \times 17.5 \times 42,000 \\ &= 231,000 \text{ kilo-lines.} \end{aligned}$$

The design of the pole shoe is given on page 179. The air gap flux distribution curve is shown in Fig. 109. The form factor $f_b = 1.14$, and the flux distribution factor $f_d = 0.666$. The winding distribution factor may be taken equal to 0.956.

$$\begin{aligned} C_w &= f_b f_d k_d = 1.14 \times 0.666 \times 0.956 \\ &= 0.725. \end{aligned}$$

For a pitch winding, the number of conductors in series per phase

$$\begin{aligned} N &= \frac{E \times 60 \times 10^8}{\phi_t n k_p C_w} = \frac{1390 \times 60 \times 10^8}{231,000 \times 10^3 \times 225 \times 1 \times 0.725} \\ &= 221. \end{aligned}$$

For a winding with one circuit per phase, the total number of conductors. = $221 \times 3 = 663$.

With 3 slots per pole and phase, the total number of slots

$$S = 3 \times 3 \times 32 = 288,$$

and the tooth pitch at the air gap surface

$$t_1 = \frac{\pi D}{S} = \frac{3.14 \times 100}{288} = 1.09 \text{ in.}$$

The number of conductors per slot

$$= \frac{663}{288} = 2.3.$$

As stated above, this number must be an integer and must be a multiple of 2. If a one-circuit winding is to be used, 2 conductors per slot will be required. But decreasing the number of conductors to this value will produce too large an increase in the total flux. If a 2-circuit winding is used, the conductors per slot must be doubled. With a 2-circuit winding and 6 conductors per slot, the total flux will be too small. It may be increased by using a chorded winding, but this would require a chord factor of about 0.75, which is not satisfactory for a 32-pole machine. The number of slots should therefore either be decreased, so that a 2-circuit winding with 6 conductors per slot can be used, or increased to permit a 2-circuit winding with 4 conductors per slot.

With $3\frac{1}{2}$ slots per pole per phase, the total number of armature slots

$$S = 3\frac{1}{2} \times 3 \times 32 = 336.$$

The tooth pitch at the air gap surface

$$t_1 = \frac{\pi D}{S} = \frac{3.14 \times 100}{336} = 0.935 \text{ in.}$$

The armature windings for synchronous machines are generally designed with more than one turn per coil. Large-capacity turbo-generators, for which coils with transposed conductors are used, require only one turn per coil. A 2-circuit winding will therefore be used. The total number of armature conductors required = $2 \times 663 = 1326$. The conductors per slot

$$= \frac{1326}{336} = 3.95 \text{ or } 4.$$

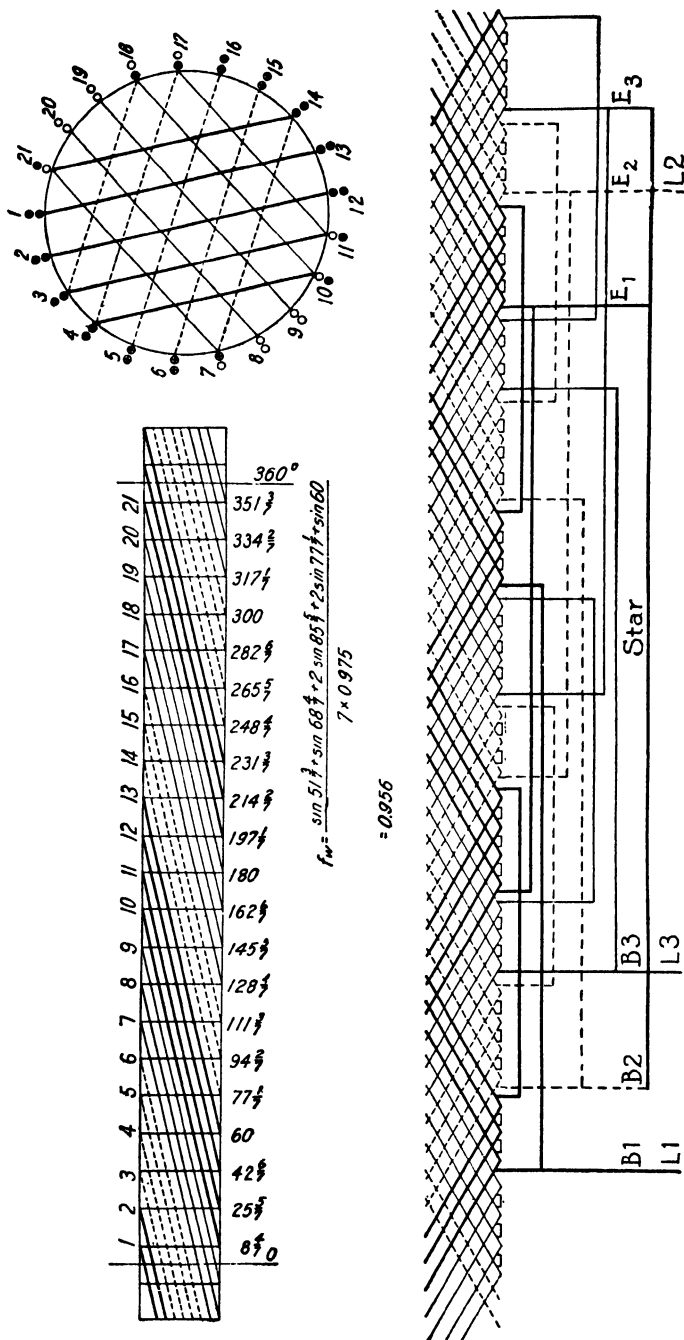


FIG. 136.—Winding lay-out and connection diagram— $3\frac{1}{2}$ slots per pole per phase—three-phase, two-circuit star.

For this winding, with 10.5 slots per pole, a pitch coil can not be used. A coil throw, slot 1 to 10, will be used,

$$k_p = \sin \frac{9}{10.5} 90 = 0.975.$$

The diagrams for the winding are shown in Fig. 136.

The final value of the total flux

$$\begin{aligned} \phi_t &= \frac{E \times 60 \times 10^8}{N n C_w k_p} = \frac{1390 \times 60 \times 10^8}{224 \times 225 \times 0.725 \times 0.975} \\ &= 234,000 \text{ kilo-lines.} \end{aligned}$$

The armature current

$$\begin{aligned} I &= \frac{Kva \times 10^3}{E \times 3} = \frac{2500 \times 10^3}{1390 \times 3} \\ &= 600. \end{aligned}$$

The section area of the armature conductor

$$\begin{aligned} s_a &= \frac{I}{a A_a} = \frac{600}{2 \times 2200} \\ &= 0.136 \text{ sq. in.} \end{aligned}$$

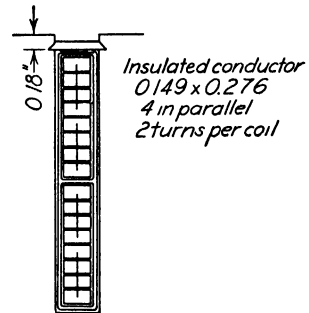


FIG 137.

The tooth pitch at the air gap surface has been calculated above; it is equal to 0.935 in. The width of the slot should not be greater than one-half of 0.935 in., or 0.4675 in. The coils will be wound with 4 d.c.c. copper ribbon conductors in parallel and arranged in the slot as shown in Fig. 137. The insulated dimensions of each conductor are (see copper tables):

Width 0.276 in., thickness 0.149 in., area 0.0325 sq. in.

The slot dimensions required are (see Table XVI):

$$\text{Width} = 1 \times 0.276 + 0.15 = 0.426 \text{ in.}$$

$$\text{Depth} = 16 \times 0.149 + 0.45 = 2.83 \text{ in.}$$

The current density for this conductor

$$A_a = \frac{600}{2 \times 4 \times 0.0325} = 2310 \text{ amperes per sq. in.}$$

This winding will be satisfactory provided that the densities for the various parts of the magnetic circuit do not exceed the limits given in Chapter XII.

The length of the half mean-turn of the armature coil is calculated as follows (see Fig. 135):

$$\sin \alpha = \frac{d}{l_1} = \frac{0.426 + 0.15}{0.935} = 0.616$$

$$\alpha = 38^\circ \text{ and } \cos \alpha = 0.788, \quad \tan \alpha = 0.781.$$

The per unit pitch

$$P = \frac{9}{10.5} = 0.857,$$

$$\begin{aligned} L_a &= \frac{\pi(D + d_s)}{p \cos \alpha} P + 2b + d_s + l \\ &= \frac{3.14(100 + 2.83)}{32 \times 0.788} \cdot 0.857 + 2.5 + 2.83 + 17.5 \\ &= 33.78 \text{ in.} \end{aligned}$$

The resistance per phase of the armature winding at 75°C .

$$\begin{aligned} R_a &= \frac{L_a N r}{a s_a \times 10^6} = \frac{33.78 \times 224 \times 0.826}{2 \times 4 \times 0.0325 \times 10^6} \\ &= 0.024 \text{ ohm.} \end{aligned}$$

The alternating-current resistance of the armature winding is taken equal to 1.30 times the direct-current resistance (see page 255)

$$R_{a.c.} = 1.30 \times 0.024 = 0.0312 \text{ ohm.}$$

The bare weight of the armature copper

$$\begin{aligned} G_a &= L_a N a m s_a \times 0.321 \\ &= 33.78 \times 224 \times 2 \times 3 \times 4 \times 0.0325 \times 0.321 \\ &= 1890 \text{ lb.} \end{aligned}$$

The approximate insulated weight equals 1950 lb.

CHAPTER XII

MAGNETIC CIRCUIT

THE fundamental formulas for the magnetic circuit are given on page 64, Chapter IV. The magnetic circuit for a pair of poles for a salient-pole synchronous machine with revolving field is shown in Fig. 138. The path of the magnetic flux comprises the air gap, armature teeth, armature yoke, field pole, and field yoke or spider rim. The material and flux densities are not the same for all parts of the magnetic circuit; therefore, the ampere-turns must be calculated separately for each part. The symbols used for these calculations are the same as those used for direct-current machines, page 65. The total ampere-turns per pole for no-load and normal voltage

$$ATP_o = AT_g + AT_t + AT_{ya} + AT_p + AT_{yf}.$$

Ampere-Turns for Air Gap. The maximum value of the flux density in the air gap

$$B_g = \frac{\phi_t}{s_g}.$$

The section area of the air gap

$$s_g = \pi D l_g.$$

When the length of the armature core stack exceeds from 5 to 6 in. it is usually divided into sections by radial ventilating ducts. These ventilating ducts reduce the permeance of the air gap section, necessitating a greater magnetomotive force to send the flux through the air gap. The effective length of the air gap section can be determined by equation 46, page 67, by using for the tooth pitch t_1 , the length of a lamination stack plus a ventilating duct, for the slot width w_s , the width of a duct, and for the tooth width the width of a stack of laminations. Then the effective length of the air gap section

$$l_g = \frac{l}{k}. \quad (145)$$

For machines with stack lengths not over 12 to 14 in. this correction is usually small and l_g can be taken equal to l .

The ampere-turns per pole for the air gap

$$AT_g = \frac{B_g \delta k}{3 \cdot 2}.$$

The air gap coefficient, k , is calculated by formula 46, page 67.

Ampere-Turns for Armature Teeth.—Slots with parallel sides are most common for synchronous machines. The tooth width is therefore smaller at the armature surface than at the bottom of the slot. The section area of the teeth at the armature surface

$$s_{t1} = w_{t1}(l - n_d w_d)k_1 S. \quad (146)$$

The number of ventilating ducts is always so chosen that the space between ducts does not exceed 3 to 4 in. The width of the ducts is $\frac{3}{8}$ in. for small and medium-size machines and $\frac{1}{2}$ in. for large-capacity machines. The lamination factor, k_1 , depends upon the method of insulating the laminations and upon the kind and thickness of the sheet. For silicon sheet steel 0.014 in. thick and insulated with core plate varnish, $k_1 = 0.90$. For sheet steel 0.019 in. thick, k_1 may be taken equal to 0.93.

The maximum flux density

$$B_{t1} = \frac{\phi_t}{s_{t1}}.$$

The maximum flux density in the armature teeth should generally not exceed 100,000 lines per sq. in. High tooth densities produce high iron losses and require a large number of ampere-turns on the field winding. Low tooth densities, on the other hand, result in an uneconomical use of magnetic material. The density at the armature surface will generally lie between the limits

$$B_{t1} = 75,000 \text{ to } 95,000 \text{ lines per sq. in.}$$

To take into account the effect of the tooth taper, the ampere-turns for the teeth are calculated for the density at a section $\frac{1}{3}$ tooth length from the minimum section.

$$s_{t3} = w_{t3}(l - n_d w_d)k_1 S$$

and

$$B_{t3} = \frac{\phi_t}{s_{t3}}.$$

The method of calculating w_{t3} is shown in the sample design, page 221.

From the standard saturation curves for the material used in the armature laminations, the ampere-turns per inch corresponding to the

density B_{t3} are found. Then

$$AT_t = at_t l_t.$$

The length of the flux path for the armature teeth, l_t , is equal to the slot depth.

Ampere-Turns for Armature Yoke.—The flux of each pole passes through the armature teeth into the yoke and divides, one-half return-

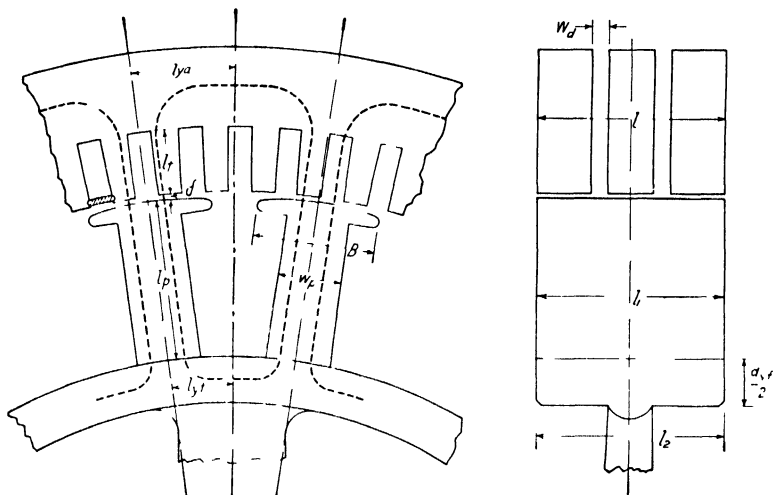


FIG. 138.—Magnetic circuit of salient-pole synchronous machine.

ing through each of the adjacent poles as shown in Fig 138. The flux per pole

$$\phi = \frac{\phi_t f_d}{p}.$$

The depth of the iron below the slots, d_{ya} , is calculated by formula 57 in the same way as described for direct-current machines. The flux density in the armature yoke depends upon the grade of sheet steel used for the armature laminations and upon the frequency of the flux reversals. The losses in the armature iron increase with the frequency and the density. The weight of the iron in the armature yoke is the largest part of the total iron weight; therefore low flux densities will generally be required to avoid high core losses. For 60-cycle synchronous machines, the flux densities in the armature yoke will generally lie between the limits 50,000 to 85,000 lines per sq. in. For lower frequencies, slightly higher values may be used.

The ampere-turns per pole for the armature yoke

$$AT_{ya} = at_{ya}l_{ya}.$$

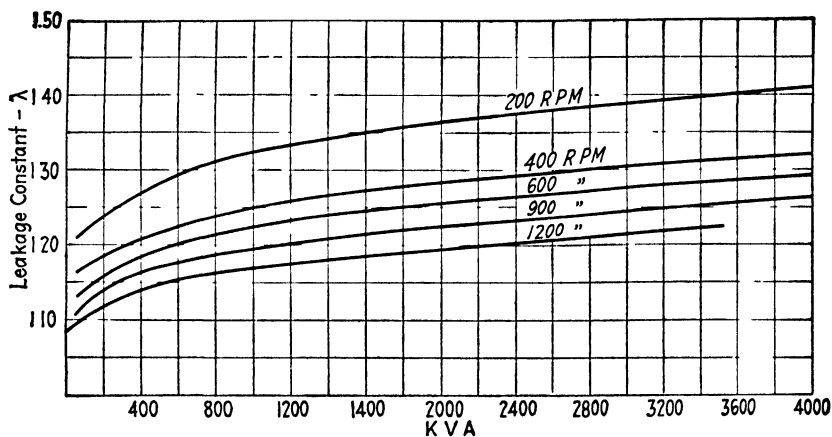


FIG. 139.—Approximate field leakage constants for salient-pole synchronous machines.

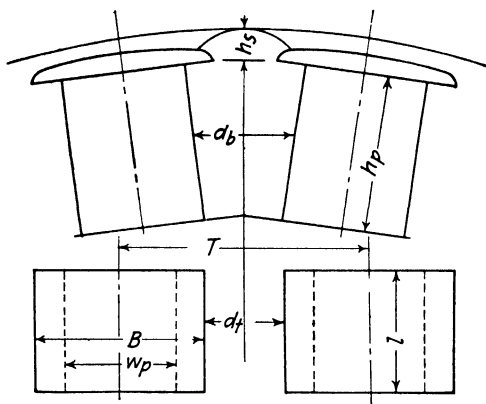


FIG. 140.

The length of the flux path for the yoke is taken equal to one-half the pole pitch on the mean diameter of the yoke.

$$l_{ya} = \frac{\pi(D + 2d_s + \frac{1}{2}d_{ya})}{2p}. \quad (147)$$

Ampere-Turns for the Pole.—The flux in the poles is equal to the useful flux which crosses the air gap and enters the armature, plus the

leakage flux. The pole body density

$$B_p = \frac{\phi \lambda}{s_p}.$$

The leakage flux can not be calculated until the dimensions of the pole are known. The flux density in the pole will depend upon the kind of material used. For laminated poles,

$$B_p = 85,000 \text{ to } 100,000 \text{ lines per sq. in.}$$

For cast-steel poles slightly lower values are necessary because of the non-uniformity of this material. The field leakage constant, λ , may be estimated with the help of the curves, Fig. 139. The section area of the pole body can then be calculated by the formula above. The axial length of the pole may be made slightly less than the armature length, but, more often, l_1 will be equal to l .

The field leakage flux may be calculated approximately by the following formulas ¹ (see Fig. 140):

$$\phi_{11} = X \ 13 \frac{l_1 h_s}{d_t}.$$

$$\phi_{12} = X \ 19 h_s \log_{10} \left(1 + \frac{\pi B}{2 d_t} \right).$$

$$\phi_{13} = X \ 6.5 \frac{l_1 h_p}{d_b}.$$

$$\phi_{14} = X \ 9.5 h_p \log_{10} \left(1 + \frac{\pi w_p}{2 d_b} \right).$$

$$X = AT_g + AT_t + AT_{ya}.$$

$$\phi_l = \phi_{11} + \phi_{12} + \phi_{13} + \phi_{14}.$$

$$\lambda = \frac{\phi + \phi_l}{\phi} = 1 + \frac{\phi_l}{\phi}.$$

The ampere-turns per pole for the pole

$$AT_p = at_p l_p.$$

The length of the flux path, l_p , is equal to the radial height of the pole. This value depends upon the space required by the field winding. The ratio of the radial length of the pole to the pole pitch is generally equal to 0.30–1.50. The small value is for machines with a small number of

¹The development of these formulas is given on page 73. See, also, "Field Leakage in Synchronous Machines," by Theo. Schou, Electrical Review, Vol. 77, p. 281.

poles, or large pole pitch; and the large value for machines with a large number of poles, or small pole pitch.

Ampere-Turns for the Field Yoke.—The field yoke or spider rim, to which the field poles are either bolted or keyed, is either of cast iron, cast steel, rolled steel, or built up of rolled steel plate (see page 172). For cast-iron spiders, the density in the field yoke should not exceed 30,000 lines per sq. in., and for cast-steel spiders it should not exceed 60,000 lines per sq. in. With rolled steel and laminated field yoke, higher densities may be used. For large-capacity high-speed machines, the spider rim section must be checked also for mechanical strength. Generally, however, the section that satisfies the magnetic requirements will be large enough to meet the mechanical requirements for strength. Synchronous motors and generators are often designed to have a large inherent flywheel effect. For this purpose the section area of the spider rim is larger than is necessary to meet the magnetic requirements given above.

The section area of the field yoke

$$s_{yf} = \frac{\phi \lambda}{B_{yf}}.$$

The length of the yoke section parallel to the shaft is generally equal to the length of the pole, l_1 . When extra large yoke sections are used to obtain large flywheel effect, l_2 is often made larger than l_1 .

The depth of the spider rim

$$d_{yf} = \frac{s_{yf}}{l_2}.$$

The ampere-turns for the field yoke

$$AT_{yf} = at_{yf} l_{yf}.$$

The length of the flux path is shown in Fig. 138, and is taken equal to one-half of the pole pitch on the mean circumference of the spider rim.

The open-circuit saturation curve is calculated as explained on page 75. The calculations for the sample generator design are given on page 224.

Sample Design: Magnetic Circuit.—Five ventilating ducts, each $\frac{1}{2}$ in. wide, are used in the armature. The length of the air gap section

$$l_g = \frac{l}{k} = \frac{17.50}{1.038} = 16.9 \text{ in.,}$$

$$\text{where } k = \frac{2.92}{2.42 + (0.406 \times 0.97)} = 1.038.$$

The air gap density

$$B_g = \frac{\phi_t}{\pi D l_g} = \frac{234,000 \times 10^3}{3.14 \times 100 \times 16.9}$$

$$= 44.1 \text{ kilo-lines per sq. in.}$$

The length of the air gap has been estimated at 0.406 in., and the air gap coefficient

$$k = \frac{t_1}{w_{t1} + (\delta y)} = \frac{0.935}{0.509 + (0.406 \times 0.90)}$$

$$= 1.07.$$

The ampere-turns per pole for the air gap

$$\text{AT}_g = \frac{B_g \delta k}{3.2} = \frac{44,100 \times 0.406 \times 1.07}{3.2}$$

$$= 5980 \text{ ampere-turns.}$$

The maximum density in the armature teeth

$$B_{t1} = \frac{\phi_t}{w_{t1}(l - n_d w_d) k_1 S} = \frac{234,000 \times 10^3}{0.509(17.5 - 5 \times \frac{1}{2})0.93 \times 336}$$

$$= 98 \text{ kilo-lines per sq. in.}$$

The width of the armature tooth at a section $\frac{1}{3}$ tooth from the minimum section

$$w_{t3} = \frac{\pi(D + \frac{2}{3}d_s)}{S} - w_s = \frac{\pi(100 + \frac{2}{3}2.83)}{336} - 0.426$$

$$= 0.526.$$

$$B_{t3} = \frac{\phi_t}{w_{t3}(l - n_d w_d) k_1 S} = \frac{234,000 \times 10^3}{0.526(17.5 - 5 \times \frac{1}{2})0.93 \times 336}$$

$$= 95 \text{ kilo-lines per sq. in.}$$

From the standard saturation curve for dynamograde silicon steel, $\text{at}_t = 50$ ampere-turns per inch, and

$$\text{AT}_t = \text{at}_t l_t = 50 \times 2.83$$

$$= 142 \text{ ampere-turns.}$$

The flux per pole

$$\phi = \frac{\phi_d f_d}{p} = \frac{234,000 \times 10^3 \times 0.666}{32}$$

$$= 4870 \text{ kilo-lines.}$$

The depth of the armature yoke

$$d_{ya} = \frac{\phi}{(l - n_d w_d) h_1 B_{ya}} = \frac{4870 \times 10^3}{(17.5 - 5 \times \frac{1}{2}) 0.93 \times 60,000}$$

$$= 5.82 \text{ in.}$$

The outside diameter of the armature core

$$D_0 = D + 2d_s + d_{ya} = 100 + (2 \times 2.83) + 5.82$$

$$= 111.48; \text{ make this } 112 \text{ in.,}$$

and

$$d_{ya} = D_0 - (D + 2d_s) = 112 - (100 + 2 \times 2.83)$$

$$= 6.34 \text{ in.}$$

The flux density in the armature yoke

$$B_{ya} = \frac{\phi}{(l - n_d w_d) h_1 d_{ya}} = \frac{4870 \times 10^3}{(17.5 - 5 \times \frac{1}{2}) 0.93 \times 6.34}$$

$$= 55 \text{ kilo-lines per sq. in.}$$

The length of the flux path

$$l_{ya} = \frac{\pi(D + 2d_s + \frac{1}{2}d_{ya})}{2p} = \frac{3.14(100 + 2 \times 2.83 + \frac{1}{2} \times 6.34)}{2 \times 32}$$

$$= 5.34 \text{ in.}$$

The ampere-turns per inch, from the standard saturation curve for dynamo-grade silicon steel, $at_{ya} = 3.6$ ampere-turns per in., and

$$AT_{ya} = at_{ya} l_{ya} = 3.6 \times 5.34$$

$$= 19 \text{ ampere-turns.}$$

The field leakage constant is taken equal to 1.38, and the section area of the pole body

$$s_p = \frac{\phi \lambda}{B_p} = \frac{4870 \times 10^3 \times 1.38}{95,000}$$

$$= 70.7 \text{ sq. in.}$$

The length of the pole parallel to the shaft is 17.5 in., and

$$w_p = \frac{70.7}{17.5} = 4.05 \text{ in.}; \text{ use } 4 \text{ in.}$$

The radial height of the pole depends upon the space required by the field winding. It is estimated at 7.0 in. (see page 219).

The leakage flux is calculated by the formulas given on page 219.

$$l_1 = 17.5, \quad h_s = 1.125, \quad d_t = 3.06, \quad B = 6.75,$$

$$h_p = 6.25, \quad d_b = 5.0, \quad w_p = 4.0.$$

$$(1) \quad 13 \frac{l_1 h_s}{d_t} = 13 \frac{17.5 \times 1.125}{3.06} = 83.60.$$

$$(2) \quad 19 h_s \log \left(1 + \frac{B\pi}{2d_t} \right) = 19 \times 1.125 \times \log \left(1 + \frac{6.75 \times \pi}{2 \times 3.06} \right) \\ = 13.90.$$

$$(3) \quad 6.5 l_1 \frac{h_p}{d_b} = 6.5 \frac{17.5 \times 6.25}{5.0} = 142.00.$$

$$(4) \quad 9.5 h_p \log \left(1 + \frac{\pi w_p}{2d_b} \right) = 9.5 \times 6.25 \log \left(1 + \frac{\pi \times 4.0}{2 \times 5.0} \right) = 21.0.$$

$$X = 6280 + 199 + 14 = 6493.$$

$$\phi_l = X \times 260.50 = 6493 \times 260.50 = 1,690,000.$$

$$\lambda = \frac{\phi_l}{\phi} + 1 = \frac{1,690,000}{4,870,000} + 1 = 1.347.$$

The flux density in the pole body is, then,

$$B_p = \frac{4,870,000 \times 1.347}{4 \times 17.5} = 93,600 \text{ lines per sq. in.}$$

The ampere-turns per inch, $at = 45$. The length of the flux path $l_p = 7.0$ (see Fig. 138), and

$$AT_p = l_p at_p = 7.0 \times 45 = 315 \text{ ampere-turns.}$$

The section area of the spider rim

$$s_{sf} = \frac{\phi \lambda}{B_{sf}} = \frac{4,870,000 \times 1.347}{65,000} \\ = 101 \text{ sq. in.}$$

If the length of the spider rim parallel to the shaft is made equal to the armature length,

$$d_{yf} = \frac{101}{17.5} = 5.77 \text{ in.}$$

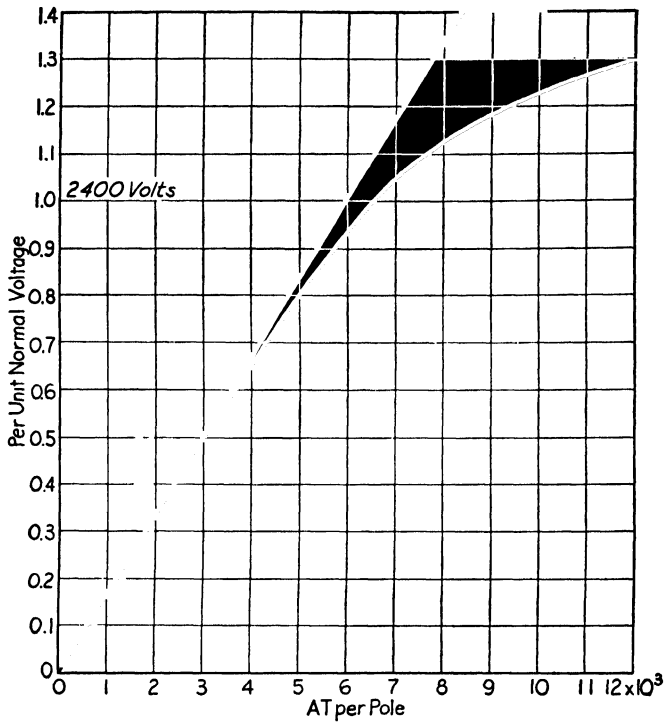


FIG. 141.—Open-circuit saturation curve.

TABLE XVII

Path	Length	90% E			100% E			115% E			125% E		
		B	at	AT	B	at	AT	B	at	AT	B	at	AT
Air gap . .				5380	43.6		5980			6880			7,480
Teeth	2.83	85.5	19.	54	95.0	50 0	142	109.2	230	650	118.8	460.0	1,300
Armature yoke . . .	5.34	49.5	3	16	55.0	3.6	19	63.2	5	27	68.8	6.0	32
Pole	7.00	84.3	30 5	214	93.6	45.0	315	107.8	110	770	117.0	240.0	1,680
Field yoke	4.05	58.5	14.	57	65.0	16.0	65	74.8	22	89	81 3	27.5	111
Total				5721			6521			8416			10,603

The length of the flux path in the field yoke (see Fig. 138)

$$l_{yf} = 4.05 \text{ in.}$$

The ampere-turns per inch for hot-rolled steel, $at = 16$, and

$$AT_{yf} = 4.05 \times 16 = 65 \text{ ampere-turns.}$$

The calculations for the open-circuit saturation curve are given in Table XVII. The data in the table are plotted in Fig. 141.

CHAPTER XIII

ARMATURE REACTIONS IN SYNCHRONOUS MACHINES

WHEN an alternator is carrying load, the armature current produces an alternating current field, which may be divided into two parts. One part passes through the magnetic circuit, and its effect is called armature reaction. The other part, called armature leakage field, does not pass through the magnetic circuit. Its effect is called armature leakage reactance.

Armature Leakage Reactance.—The number of interlinkages between the armature leakage flux per unit of current, times the rate of change of the flux, is called the leakage reactance of the armature. The following method of calculating the armature leakage reactance was presented by P. L. Alger¹ before the American Institute of Electrical Engineers.

For convenience in calculating the reactance, the armature leakage flux is divided into four parts:

- (1) The slot leakage flux, Fig. 143, which has its path through the slot and through the iron of the teeth and below the teeth.

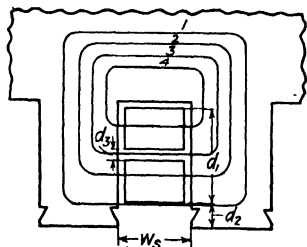


FIG. 142.

- (2) The end-connection leakage flux, which encircles the armature coils at the end-connections.

- (3) The zig zag leakage flux, which has its path in the air gap.

- (4) The belt leakage flux, which has its path in the air gap.

The slot reactance in ohms per phase, due to the slot leakage flux, is equal to the permeance of the path across a unit length of the slot, times the length of the slot, times the number of slots in series per phase, times the number of conductors in series per slot squared, times the rate of change of flux, times 10^{-8} ohm.

The slot leakage flux path, Fig. 142, is partly through air and partly

¹ "The Calculation of the Armature Reactance of Synchronous Machines," by P. L. Alger, A.I.E.E. Trans., Vol. 47, April, 1928, p. 493.

through iron. The reluctance of the part of the path in the teeth and yoke is negligible compared to the reluctance of the part in air; therefore the length of the path of the slot leakage flux is taken equal to the slot width. The permeance of the path for flux (1), Fig. 142, interlinking all the conductors per slot is

$$0.4\pi \frac{d_2}{w_s}.$$

For a pitch winding, for which the currents in the two coil sides per slot are identical in magnitude and phase, the linkages per ampere produced by the flux in paths 2 and 4 are

$$0.4\pi \frac{d_1 - d_3}{3w_s}$$

because, with uniform current distribution over the height d_1 , the flux density distribution is linear and the linkage distribution is parabolic; and the average height of a parabola is one-third its maximum height. The flux through path 3 links one-half the total current. The linkages due to it are therefore one-fourth as much as they would be if this flux linked all of the current. The linkages due to the flux of path 3 are

$$0.4\pi \frac{d_3}{4w_s}.$$

The total permeance for the slot per unit length is

$$0.4\pi \left(\frac{d_1}{3w_s} + \frac{d_2}{w_s} - \frac{d_3}{12w_s} \right).$$

For fractional pitch windings, the currents in the two coil sides in some of the slots are not in phase, and the expression for the slot permeance must be corrected to take this into account. This is done as explained in the paper referred to above; thus the final expression for the slot reactance per phase

$$\begin{aligned} X_s &= \frac{0.8\pi^2}{10^8} fl \frac{S_s}{m} \left(\frac{mN}{S_s} \right)^2 \left[K_s \left(\frac{d_1}{3w_s} + \frac{d_2}{w_s} \right) \right] \\ &= \frac{0.79flmN^2}{10^7 S_s} \left[K_s \left(\frac{d_1}{3w_s} + \frac{d_2}{w_s} \right) \right] \text{ ohms.} \end{aligned}$$

For dimensions in inches, the constant 0.79 must be changed to 2.0.

The third factor in the expression for the permeance is generally so small that it can be neglected. The factor K_s is shown in Fig. 143 plotted against per cent pitch.

The end-connection leakage reactance

$$X_e = \frac{0.79flmN^2}{10^7 S_e} \left[\frac{0.30(3P - 1)DS_e}{p^2 l} \right].$$

The zig zag leakage reactance

$$X_z = \frac{5}{8} \left(\frac{p}{S_e} \right)^2 X_{ad}.$$

The belt leakage reactance

$$X_b = 0$$

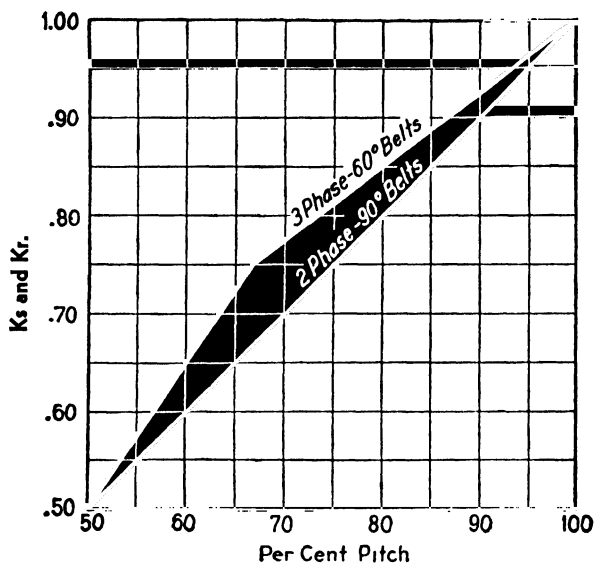


FIG. 143.

for a machine with squirrel-cage winding in the pole faces and integral number of slots per pole per phase

$$X_b = \frac{3}{4} X_{ad} K_b$$

for salient-pole synchronous machines without squirrel-cage winding in the pole faces and with integral number of slots per pole per phase, and

$$X_b = \frac{5}{8} \left(\frac{p}{S_e} \right)^2 X_{ad}$$

for salient-pole synchronous machines with fractional number of slots per pole per phase. The belt leakage constant, K_b , is shown in Fig. 144.

The total leakage reactance per phase for synchronous machines with fractional number of slots per pole per phase with dimensions in inches

$$X_l = \frac{2.0flmN^2}{10^7 S_s}$$

$$\left[K_s \left(\frac{d_1}{3w_s} + \frac{d_2}{w_s} \right) + \frac{0.3(3P-1)DS_s}{p^2 l} + \frac{0.53Dk_p^2 k_d^2}{S_s \delta k} \right] \text{ ohms. } (148)$$

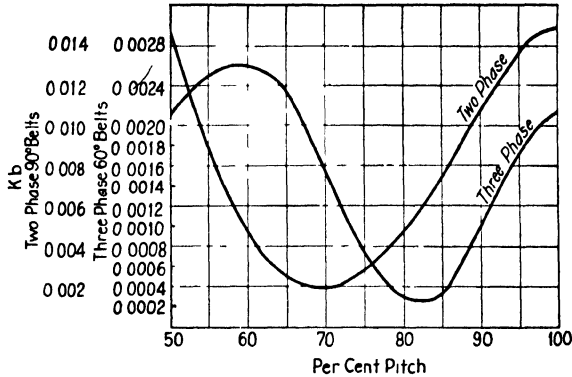


FIG. 144.—Belt leakage constants.

For machines with integral number of slots per pole and with squirrel-cage winding in the pole faces,

$$X_l = \frac{2.0flmN^2}{10^7 S_s}$$

$$\left[K_s \left(\frac{d_1}{3w_s} + \frac{d_2}{w_s} \right) + \frac{0.3(3P-1)DS_s}{p^2 l} + \frac{0.266Dk_p^2 k_d^2}{S_s \delta k} \right] \text{ ohms. } (149)$$

For machines with integral slots per pole but without squirrel-cage winding in the pole faces,

$$X_l = \frac{2.0flmN^2}{10^7 S_s}$$

$$\left[K_s \left(\frac{d_1}{3w_s} + \frac{d_2}{w_s} \right) + \frac{0.3(3P-1)DS_s}{p^2 l} + \frac{0.266Dk_p^2 k_d^2}{S_s \delta k} + \frac{0.319Dk_p^2 k_d^2 S_s K_b}{p^2 \delta k} \right] \text{ ohms. } (150)$$

The per cent reactance drop due to full-load current equals

$$\frac{X_l I}{E} \times 100.$$

The formulas given above are for salient-pole, synchronous machines with two-layer windings and with the coils in 60° belts.

The standstill reactance of a synchronous motor with open field winding can be calculated by adding to the formulas given above the squirrel-cage reactance.

The squirrel-cage reactance of a salient-pole, synchronous motor is rather difficult to calculate accurately, because of the unequal distribution of the current between the bars of each pole. It is divided into slot, end-connection, and zigzag leakage reactance.

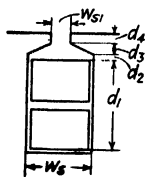


FIG. 145.

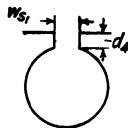


FIG. 146.

The slot reactance is calculated by assuming the bars uniformly distributed, as in a squirrel-cage induction motor. The equivalent rotor slot reactance (see Fig. 145)

$$X_{sr} = \frac{2.0flmN^2}{10^7 S_s} \frac{k_p^2 k_d^2 S_s}{S_r} \left(\frac{d_1}{3w_s} + \frac{d_2}{w_s} + \frac{2d_3}{w_s \times w_{s1}} + \frac{d_4}{w_{s1}} \right) \text{ ohms.} \quad (151)$$

If round bars are used in the squirrel-cage, as shown in Fig. 146, then the rotor slot reactance

$$X_{sr} = \frac{2.0flmN^2}{10^7 S_s} \frac{k_p^2 k_d^2 S_s}{S_r} \left(0.62 + \frac{d_4}{w_{s1}} \right) \text{ ohms.} \quad (152)$$

The end-connection reactance for the squirrel-cage winding is generally small and will be taken equal to zero.

The rotor zigzag leakage reactance

$$X_{sr} = \frac{5}{6} X_m \left(\frac{p}{S_r} \right)^2 \text{ ohms.}$$

The magnetizing reactance of a synchronous machine

$$X_m = \frac{2.0flmN^2}{10^7 S_s} \left(\frac{0.319k_p^2 k_d^2 D S_s}{p^2 \delta k} \right) \text{ ohms.} \quad (153)$$

Then

$$X_{sr} = \frac{2.0flmN^2}{10^7 S_s} \left(\frac{0.266k_p^2 k_d^2 D S_s}{S_r^2 \delta k} \right) \text{ ohms.} \quad (154)$$

The standstill reactance of a synchronous motor with open field winding is then equal to the sum of the stator reactance, as calculated by formulas 148, 149, or 150, plus the rotor slot and zigzag reactances given by formulas 151 and 154.

Synchronous motors are generally started with the field winding short-circuited through a resistance, to limit the voltage induced in the

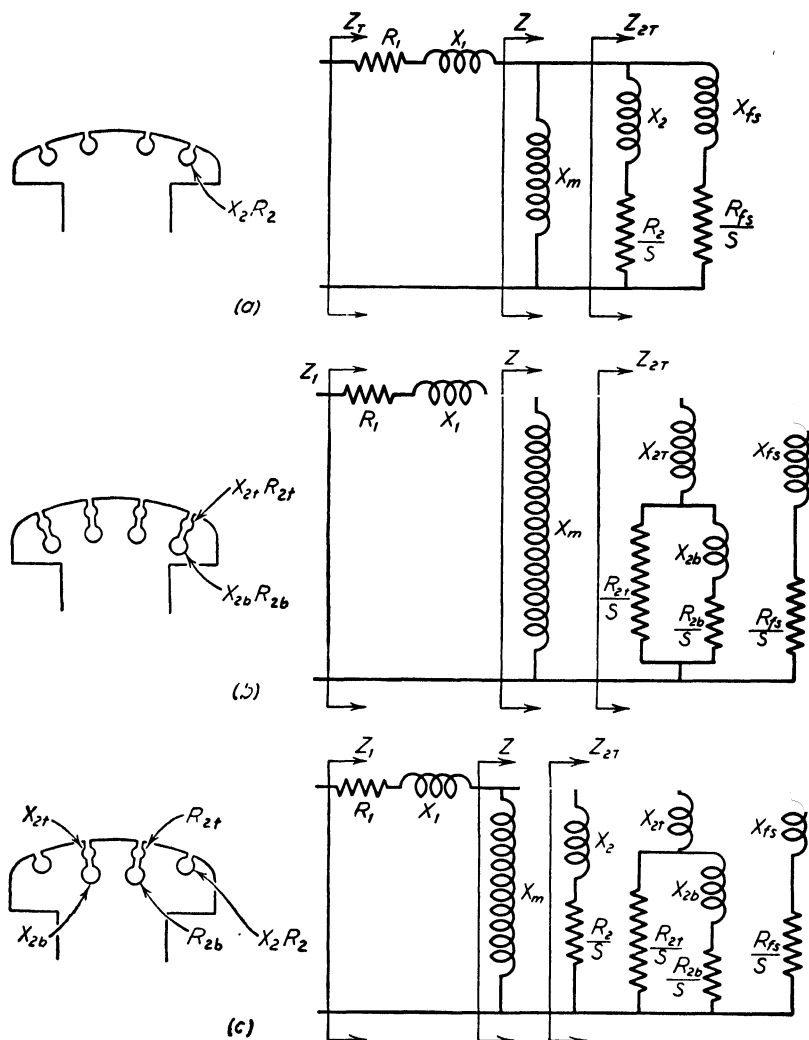


FIG. 147.—Equivalent circuits for self-starting synchronous motors: (a) single squirrel-cage, (b) double squirrel-cage, (c) double squirrel-cage with single cage bars at each pole tip. X_{fs} and R_{fs} are the reactance and resistance of the field winding in terms of the stator winding.

field winding during starting. The standstill reactance of a synchronous motor with short-circuited field winding is equal to the standstill reactance with open field winding plus the field reactance. The total field

reactance can be calculated as explained by R. H. Park and B. L. Robertson in "The Reactances of Synchronous Machines."²

The squirrel-cage winding of self-starting synchronous motors is active only during the starting period and must be designed to give the

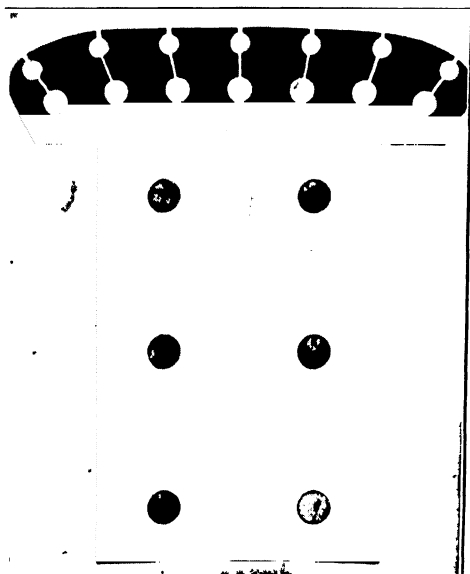


FIG. 148.—Pole punching for synchronous motor with double-squirrel-cage starting winding.

required starting and pull-in torque. Synchronous motors will generally pull into synchronism when the field excitation is applied, if the speed is approximately 95 per cent of synchronous speed. The torque the motor produces at this speed is called the pull-in torque. To obtain high starting torque a high-resistance squirrel-cage winding is required, for high pull-in torque the resistance of the squirrel-cage winding must be low. For both high starting torque and high pull-in torque with low starting current, a double squirrel-cage winding³ as shown in Fig.

148 is often used. The performance of a self-starting synchronous motor during the starting period can be calculated by the same methods used for the squirrel-cage induction motor. The method of calculating the reactances of the stator and rotor winding are given on pages 229 and 230. The resistance of the squirrel-cage winding in terms of the stator winding

$$R_r = \frac{k_p^2 k_d^2 N^2 m r}{10^6} \left(\frac{l_b}{s_b N_b} + \frac{0.64 D_{er}}{p^2 s_{er}} \right) \text{ ohms.} \quad (155)$$

² A.I.E.E. Trans., Vol. 47, April, 1928, Appendix F, p. 531.

³ "The Development of Low Starting Current Induction Motors," by P. L. Alger, General Electric Review, Vol. 28, July, 1925, p. 499; "Starting Performance of Synchronous Motors," by H. V. Putman, A.I.E.E. Trans., Vol. 46, 1927, p. 39; "Starting Performance of Salient-Pole Synchronous Motors," by T. M. Linville, A.I.E.E. Trans., Vol. 49, 1930, p. 531; "Pull-in Characteristics of Synchronous Motors," by D. R. Shoults, S. B. Crary, and A. H. Lander, A.I.E.E. Trans., Vol. 54, 1935, p. 1385; "Starting Performance of Salient-Pole Synchronous Motors," by M. Liwschitz, A.I.E.E. Trans., Vol. 59, 1940, p. 913.

The equivalent circuits used to calculate the torques developed during the starting period are shown in Fig. 147*a*, *b*, and *c*. The method of calculating the torque at starting and at various values of slip including 5 per cent slip is shown in the example motor design.

Armature Reaction.—The current flowing in the armature winding produces an alternating-current field, which passes through the magnetic circuit. The action of this armature field upon the magnetic circuit is called armature reaction.

When the armature current is 90° out of phase with the induced voltage, the maximum ampere-turns of armature reaction ⁴

$$AT_a = \frac{0.45mN I_k p k_d}{p}. \quad (156)$$

The equivalent field ampere-turns per pole are found by multiplying AT_a by the ratio of the fundamental of the flux wave produced by a sinusoidally distributed armature m.m.f., when its axis coincides with the pole center, to the fundamental of the flux wave produced by the field winding. R. W. Wieseman ⁵ has derived coefficients by flux plotting for the calculation of the fundamental sine wave of flux produced in a salient-pole machine by the field winding and by a sinusoidally distributed armature m.m.f. The ratio of the fundamental of the air gap flux wave produced by a sinusoidally distributed armature m.m.f. to the fundamental of the flux wave produced by the concentrated field winding is called the armature reaction factor, K_a . Dr. Arnold ⁶ gives the following formula by which the armature reaction factor can be calculated:

$$K_a = \frac{\pi f_d + \sin \pi f_d}{4 \sin f_d \frac{\pi}{2}}. \quad (157)$$

The air gap flux distribution factor, f_d , is found from the flux plot as explained in Chapter X.

The equivalent field ampere-turns per pole of armature reaction for

⁴ For a discussion of this equation, see "Alternating Current Machines," Chapter VII, by A. F. Puchstein and T. C. Lloyd, 2nd ed., John Wiley & Sons, New York.

⁵ "Graphical Determination of Magnetic Fields," A.I.E.E. Journal, Vol. 46, 1927, pp. 141-148.

⁶ "Die Wechselstromtechnik," Vol. 4, p. 31, Julius Springer, Berlin. See also "Principles of Alternating Current Machinery," by R. R. Lawrence, Vol. 2, 2nd ed., p. 107, McGraw-Hill Book Co., New York; "Electric Machinery," by Liwischitz-Garik and Wipple, Vol. 2, pp. 316-322, D. Van Nostrand Co., New York.

salient-pole synchronous machines

$$AT_{af} = \frac{0.45 K_a m N I k_p k_d}{p}. \quad (158)$$

Synchronous Reactance.—The magnetizing reactance of a cylindrical rotor machine with uniform air gap, such as an induction motor, and with polyphase winding is equal to

$$X_m = \frac{6.38 l_g m N^2 k_p^2 k_d^2 D}{p^2 \delta k \times 10^8} \text{ ohms per phase,}$$

where l_g is the length of the air gap section. To obtain the armature reaction reactance in the direct and quadrature axis for salient-pole machines, this expression must be multiplied by a flux distribution coefficient, A_{d1} for the direct axis and A_{q1} for the quadrature axis. A_{d1} is the ratio of the maximum value of the fundamental to the maximum value of the air gap flux wave when a salient-pole synchronous machine is excited only by a sine-wave armature m.m.f. in the direct axis. Similarly, A_{q1} is the ratio of the maximum value of the fundamental to the maximum value of the air gap flux wave when a salient-pole synchronous machine is excited only by a sine-wave armature m.m.f. in the quadrature axis.

$$A_{d1} = K_a \times A_1,$$

where A_1 is the ratio of the maximum value of the fundamental to the maximum value of the air gap flux wave when the field is excited only, and K_a is as defined on page 233.

These flux coefficients can be found accurately by flux plotting, as shown by Mr. R. W. Wieseman⁵ in his A.I.E.E. paper referred to above. For the pole shoe form generally used for standard machines, K_a can be calculated with satisfactory accuracy by equation 157. A_1 is found from the analysis of the air gap flux distribution curve as explained on page 184. The quadrature axis coefficient can be calculated for machines with normal pole shoe design by the equation given by Mr. Kilgore.⁷

$$A_{q1} = \frac{4\psi + 1}{5} - \frac{\sin \psi \pi}{\pi}.$$

The direct-axis armature reaction reactance in the per unit system

$$X_{ad} = X_m \frac{I}{E} A_{d1},$$

⁷ "Calculation of Synchronous Machine Constants," by L. A. Kilgore, A.I.E.E. Trans., Vol. 50, Dec., 1931, p. 1201.

and the quadrature-axis armature reaction reactance in the per unit system

$$X_{aq} = X_m \frac{I}{E} A_{q1}.$$

The unsaturated synchronous reactance in the direct and quadrature axis in the per unit system

$$X_d = X_l + X_{ad},$$

$$X_q = X_l + X_{aq}.$$

X_l is the armature leakage reactance in the per unit system.

To calculate the operating characteristics of power systems⁸ under both steady and transient state, the transient reactances, negative-sequence and zero-sequence reactance, and the time constants of the generator must be known. In his A.I.E.E. paper referred to above,⁷ Mr. Kilgore gives a method of calculating these constants.

Short-Circuit Characteristic.—The direct-axis synchronous impedance curve shows the relation between the field ampere-turns or field current and the armature current when the generator is driven at normal speed with the armature terminals short-circuited. For the short-circuit condition, the armature current is practically 90° out of phase with the voltage, and the armature m.m.f. has a demagnetizing action upon the field. The voltage induced in the armature when short-circuited is equal to the impedance voltage, IZ_a . The field ampere-turns required to generate this voltage with the short-circuited armature are found from the open-circuit saturation curve, OB , Fig. 149. The armature, when short-circuited, has a demagnetizing action upon the field, and BC , Fig. 149, is equal to the equivalent field ampere-turns per pole of armature reaction. If CD equals the armature current, I , then D is one point on the direct-axis synchronous impedance curve, which is a straight line for normal values of load current. OC equals the field ampere-turns per pole required to circulate the current, I , in the short-circuited armature winding.

In Fig. 149, OF equals the field ampere-turns required to generate normal terminal voltage at no-load. The ratio of OF to OC is called the short-circuit ratio. This ratio is an important factor in the design of synchronous machines; it may be called the ratio of the field strength to the armature strength. A low short-circuit ratio means a small air gap, poor regulation, a small amount of field copper, and, in general, an

⁸ "First Report of Power System Stability," Elec. Eng., Feb., 1937, p. 261; "Calculation of Short-Circuit Currents in A-C Networks," by W. M. Hanna, G. E. Review, March, April, June, and August, 1937.

inexpensive field winding. On the other hand, a large short-circuit ratio means a large air gap, good regulation, a large amount of field copper, and a more expensive field winding. A generator with low short-circuit ratio will require a large change in field excitation for small load changes.

In general the short-circuit ratio of synchronous generators is from 0.8 to 1.20.

The pull-out torque of a synchronous motor varies directly with its short-circuit ratio. A unity power factor synchronous motor will have

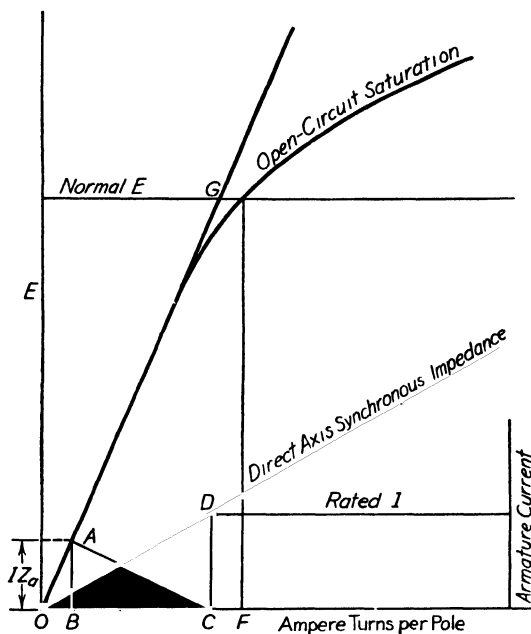


FIG. 149.

a pull-out torque of 1.43 times the full-load torque if the short-circuit ratio is 1.0, and 1.62 times the full-load torque if the short-circuit ratio is 1.20. A 0.80 leading power factor synchronous motor will have a per unit pull-out torque of 2.23 for a short-circuit ratio of 0.8, and a per unit pull-out torque of 2.71 for a short-circuit ratio of 1.20. With a high short-circuit ratio the motor will have a small displacement angle and a high synchronizing power. For 0.80 leading power factor synchronous motors the short-circuit ratio is usually 0.80 to 1.0, and for unity power factor synchronous motors from 1.0 to 1.2.

The short-circuit ratio can also be used to calculate the direct-axis synchronous reactance and armature reaction reactance. If the ratio of OG to OC in Fig. 149 is used to determine the short-circuit ratio

instead of OF to OC , the unsaturated value of short-circuit ratio is obtained. From Fig. 149 it is obvious that the per unit unsaturated direct-axis synchronous reactance⁶

$$X_d = \frac{1}{\text{scr}},$$

where scr is the unsaturated value of short-circuit ratio. The armature reaction reactance or magnetizing reactance in the direct axis

$$X_{ad} = \frac{1}{\text{scr}} - X_l = X_d - X_l.$$

Displacement Angle.—The A.S.A. Standards⁹ define displacement angle as the lag or lead in electrical radians of the rotor, with respect to the line voltage.

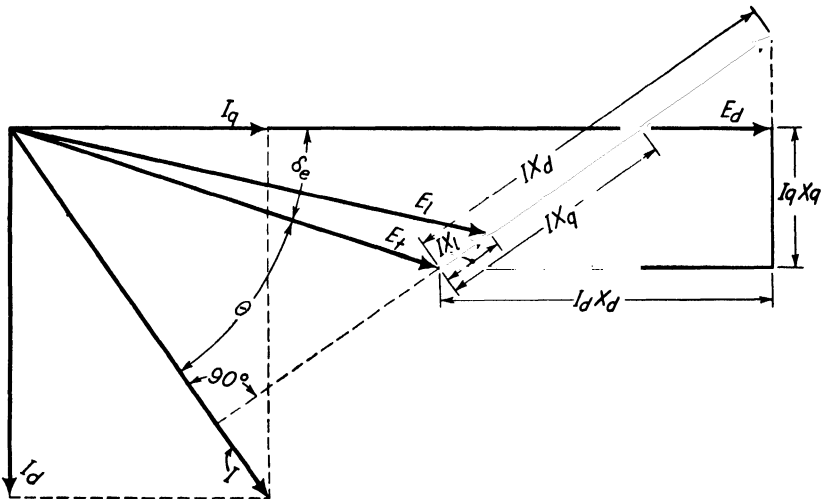


FIG. 150.

In the vector diagram, Fig. 150, the angle δ_e is the rotor displacement angle in electrical degrees. It is the angle between the terminal voltage and the nominally induced voltage, E_d . In general the armature resistance is so small in synchronous machines that it can be neglected with negligible error. In Fig. 150 the armature resistance drop is omitted.

The nominally induced voltage from Fig. 150 in the per unit system

$$E_d = \cos \delta_e + X_d \sin (\theta + \delta_e).$$

⁹ A.S.A. Standards C50, 1943.

The displacement angle in electrical degrees, using the per unit system,

$$\delta_e = \sin^{-1} \frac{X_q \cos \theta}{\sqrt{1 + X_q^2 + 2X_q \sin \theta}}.$$

Since one electrical radian equals 57.3 electrical degrees, the displacement angle can easily be expressed in radians.

Synchronizing Power.—The A.S.A. Standards define synchronizing power as follows: "Synchronizing power is the power at synchronous speed corresponding to the synchronizing torque tending to restore the rotor to the no-load position. P_r is the rate of change of the steady state synchronizing power with respect to the displacement angle at normal voltage and rated load, power factor and frequency. It is expressed in kw. at synchronous speed corresponding to the torque exerted on the rotor per radian displacement."

The synchronizing power P_r must be known to calculate the natural frequency of synchronous machines direct-connected to reciprocating machinery, to determine the proper flywheel¹⁰ for generators, and to calculate the flywheel required for synchronous motors¹¹ direct-connected to compressors.

The relation between power and displacement angle has been derived by Doherty and Nickle.¹² In the per unit system,

$$P = \frac{E_d}{X_d} \sin \delta_e + \frac{(X_d - X_q)}{2X_d X_q} \sin 2\delta_e,$$

armature resistance has only a very small effect on the power-angle characteristic and has been neglected. Core loss and friction and windage losses are also omitted. These are practically constant and may be included by making a correction in the final result.

¹⁰ "Design of Flywheels for Reciprocating Machinery Connected to Synchronous Generators and Motors," by R. E. Doherty and R. F. Franklin, A.S.M.E. Trans., Vol. 42, 1920; "Flywheels for A-C Generating Units," Elec. Eng., Sept., 1937, p. 1156.

¹¹ A.S.A. Standards C50, 1943; "The Flywheel Problem in Compressors Direct Connected to Synchronous Motors," by A. R. Stevenson, Jr., Refrigerating Engineering, Vol. 11, 1924, p. 123; "Flywheel Requirements for Unbalanced Air and Ammonia Compressors," by C. W. Cutler, Refrigerating Engineering, Vol. 12, 1925, p. 75; "Calculation of Flywheels for Air Compressors," by H. R. Goss and H. V. Putman, A.S.M.E. Trans., 1929.

¹² "Synchronous Machines, Part 2, Steady State Power Angle Characteristics," A.I.E.E. Trans., Vol. 45, p. 927, and Part 3, "Torque Angle Characteristics under Transient Conditions," A.I.E.E. Trans., Vol. 46, p. 1; see, also, "Synchronizing Power in Synchronous Machines under Steady and Transient Conditions," by H. V. Putman, A.I.E.E. Trans., Vol. 45, 1926, p. 1116.

For the steady-state condition, when the load on the machine changes very slowly, the synchronizing power, or rate of change of power with displacement angle, is determined by the slope of the tangent to the power-displacement-angle curve at the angle corresponding to rated load. Steady-state synchronizing power is, therefore, the derivative of the power-angle equation with respect to δ_e . For the transient condition, when the load fluctuates, as in a generator driven by a reciprocating prime mover or a motor driving a compressor, the synchronizing power is no longer determined by the slope of the tangent to the power-displacement-angle curve but by the slope of some other line passing through the rated load point with greater slope. When the load is suddenly increased on a motor or generator there is a sudden increase in armature reaction which tends to reduce and distort the field flux. The field flux can not decrease immediately, however, and for the first instant the effect of armature reaction on the field is practically offset by a momentary increase in field current, produced by an induced voltage due to the changing flux. This gives rise to a greater ratio of field strength to armature strength with a resultant increase in synchronizing power. The rate of load fluctuation, therefore, plays an important part in the calculation of synchronizing power under transient state. An approximate method, which has been used in practice for some time with satisfactory results, is to divide the full-load rotor output in kilowatts by the displacement angle for rated load. This corresponds to the slope of a line through zero and the full-load point on the power-displacement-angle curve and lies between the steady state and transient slope lines.

By this method, synchronizing power for a motor

$$P_r = \frac{57.3 \times 0.746 \times \text{hp.}}{\delta_e};$$

and for a generator

$$P_r = \frac{57.3 \times \text{kw.}}{\delta_e \times \text{eff.}}$$

For unity power factor synchronous motors the displacement angle generally lies between 29° and 35° ; for 80 per cent power factor synchronous motors, δ_e is generally equal to 17 to 22 electrical degrees.

Excitation for Any Load and Power Factor.—The method used here to determine the excitation required for a given load and power factor is the one adopted by the A.I.E.E. and the A.S.A. In Fig. 151, ATP_r are the field ampere-turns per pole for rated terminal voltage for an unsaturated magnetic circuit and are read from the air gap line at rated

terminal voltage. ATP_s , in Fig. 151, are the field ampere-turns per pole corresponding to rated armature current from the direct-axis synchronous impedance curve. The full-load ampere-turns per pole at a given power factor are found by adding these two quantities vectorially as shown in Fig. 152. ATP_o is laid off on the horizontal and ATP_s added at an angle corresponding to the power-factor angle

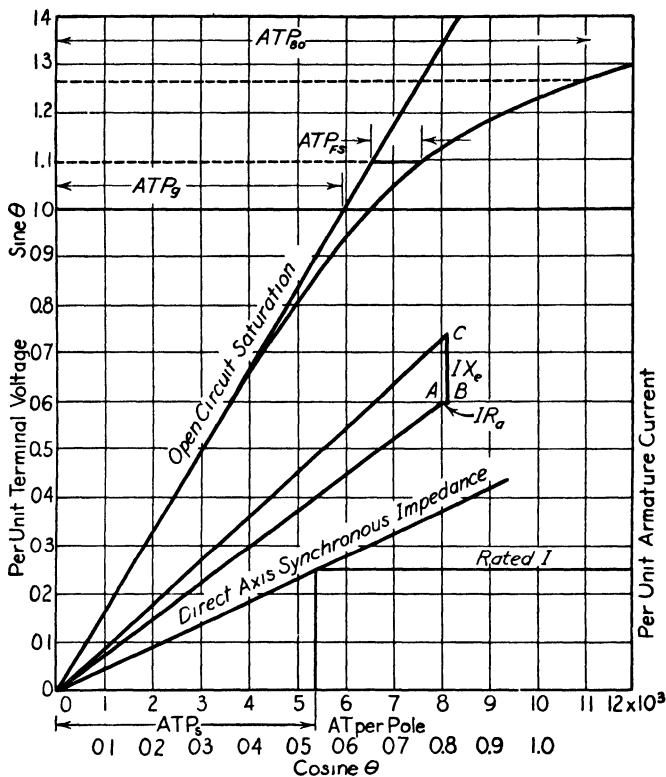


FIG. 151.

of the load with the vertical. The resultant gives the load ampere-turns per pole for an unsaturated magnetic circuit. To this resultant the ampere-turns per pole required to compensate for magnetic saturation, ATP_{FS} , must be added. ATP_{FS} is determined for the internal voltage of the generator as shown in Fig. 151. For convenience a cosine scale is added to the horizontal and a sine scale to the vertical axis. A load power factor of 0.8 is assumed, and OA is the terminal voltage at 0.8 power factor. The internal voltage of the generator, OC , is found by adding the armature resistance drop, AB , parallel to the horizontal

The ampere-turns, ATP_f , are the maximum ampere-turns required on the field winding. The standard exciter voltages are 125 volts for medium- and small-capacity machines and 250 volts for large-capacity machines. The field winding should be designed for a voltage E_f from 15 to 20 per cent less than the exciter voltage to allow for the drop in voltage between generator field and exciter and to allow for variations in the reluctance of the magnetic circuit.

The wire-wound field coil is generally used for machines with a small number of poles. Figure 153 is a sketch of a pole with wire-wound

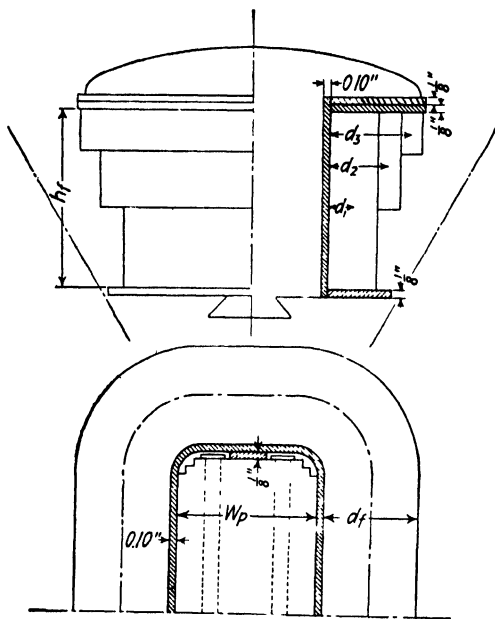


FIG. 153.—Wire-wound field pole.

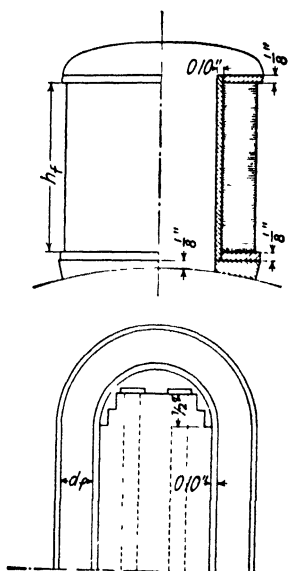


FIG. 154.—Ribbon-copper wound field pole.

field coil and shows how the coils are wound and insulated. The coils are generally wound in steps, because of the large clearance between adjacent poles at the pole shoe. The weighted mean-turn for the coil shown in Fig. 153 is calculated as follows:

$$L_{f1} = 2l_1 + 2(w_p - 0.25) + \pi(0.45 + 2d_1),$$

$$L_{f2} = 2l_1 + 2(w_p - 0.25) + \pi(0.45 + 2d_2),$$

$$L_{f3} = 2l_1 + 2(w_p - 0.25) + \pi(0.45 + 2d_3),$$

$$L_f = \frac{L_{f1}t_{f1} + L_{f2}t_{f2} + L_{f3}t_{f3}}{t_f} \text{ in.} \quad (160)$$

For machines with large number of poles, the field coils are generally wound with bare strap copper wound on edge, with paper insulation, 0.005 in. thick, between turns. The method of winding the coils is shown in Fig. 154. For very large-capacity machines with wide pole body, the coils are wound as shown in Fig. 155. The length of the mean-turn for the type of coil shown in Fig. 154

$$L_f = 2(l_1 - 1.0) + \pi(w_p + 0.20 + d_f) \text{ in.} \quad (161)$$

The number of turns per pole must be proportioned to give the required ampere-turns without an excessive temperature rise. The field current can be estimated by assuming the current density; then

$$i_f = s_f A_f \text{ amperes.} \quad (162)$$

For revolving-field-type synchronous machines,

$$A_f = 1500 \text{ to } 2500 \text{ amperes per sq. in.}$$

For wire-wound field coils with a large number of turns of fine wire with deep windings, the lower values of A_f apply. In general, A_f may

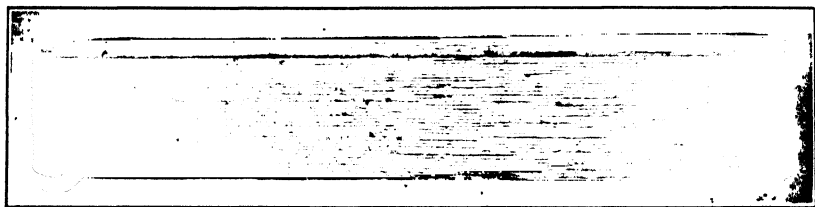


FIG. 155. Ribbon-copper field coil for 65,000-kva., 107-r.p.m., 28-pole generator

be taken equal to 2000 amperes per sq. in. for the first approximation.

The turns per pole

$$t_f = \frac{ATP_f}{i_f}.$$

The correct value for the number of turns will depend upon the temperature rise, which, in turn, depends upon the losses and the cooling surface of the field coils. A high temperature rise indicates too small a number of turns and a high current density, whereas a low temperature rise indicates too large a number of turns and an uneconomical use of field copper.

An approximate check of the temperature rise of the field winding can be obtained from the cooling surface per watt loss. The total cooling surface for the field winding (see Figs. 153 and 154)

$$S_f = 2(d_f + h_f)L_f p \text{ sq. in.,} \quad (163)$$

and the surface per watt loss

$$\frac{S_f}{W_f} = \frac{2(d_f + h_f)L_f p}{i_f^2 R_f} \text{ sq. in. per watt.} \quad (164)$$

For revolving-field synchronous generators with wire-wound field coils, the surface per watt should generally be larger than 1.0 for the maximum condition of load for the field winding, full-load 80 per cent power factor. For bare strap-copper field coils, the surface per watt loss should generally be larger than 0.75.

The resistance of the field winding at 75° C.

$$R_f = \frac{L_f l_f p}{s_f \times 10^6} \text{ ohms.}$$

The copper loss

$$W_f = i_f^2 R_f \text{ watts.}$$

The exciter capacity

$$W_e = \frac{E_c^2}{R_f \times 10^3} \text{ kilowatts.} \quad (165)$$

The weight of copper in the field winding

$$G_f = L_f l_f p s_f \times 0.321 \text{ lb.}$$

Sample Design: *Field Winding Design.*—The data required for the calculation of the leakage reactance are as follows:

$f = 60,$	$d_1 = 2.5 \text{ in.},$	$k_p = 0.975,$
$l = 17.5 \text{ in.},$	$d_2 = 0.26 \text{ in.},$	$k_d = 0.956,$
$m = 3,$	$w_s = 0.126 \text{ in.},$	$\delta = 0.406,$
$N = 224,$	$P = 0.857,$	$k = 1.07,$
$S = 336,$	$D = 100 \text{ in.},$	
$K_s = 0.88,$	$p = 32,$	

Formula 148 must be used, because the armature winding has a fractional number of slots per pole per phase.

$$\begin{aligned} K_s \left(\frac{d_1}{3w_s} + \frac{d_2}{w_s} \right) &= 0.88 \left(\frac{2.5}{3 \times 0.426} + \frac{0.25}{0.126} \right) = 2.26 \\ \frac{0.3(3P - 1)DS_s}{p^2 l} &= \frac{0.30(3 \times 0.857 - 1)100 \times 336}{32^2 \times 17.5} = 0.882 \\ \frac{0.53Dk_p^2 k_d^2}{S_s \delta k} &= \frac{0.53 \times 100 \times 0.975^2 \times 0.956^2}{336 \times 0.406 \times 1.07} = 0.315 \\ X_l &= \frac{2.0flmN^2}{10^7 S_s} (2.26 + 0.882 + 0.315) \\ &= \frac{2.0 \times 60 \times 17.5 \times 3 \times 224^2}{10^7 \times 336} (2.26 + 0.882 + 0.315) = 0.324 \text{ ohm.} \end{aligned}$$

The per cent reactance drop due to full-load current

$$\frac{IX_t \times 100}{E} = \frac{0.324 \times 600 \times 100}{1390} = 14.0 \text{ per cent.}$$

The a-c. resistance of the armature winding is given on page 214.
The per cent resistance drop due to full-load current

$$\frac{IR_a \times 100}{E} = \frac{0.0312 \times 100 \times 600}{1390} = 1.35 \text{ per cent.}$$

The per cent impedance drop

$$\frac{IZ_a \times 100}{E} = \sqrt{14^2 + 1.35^2} = 14.1 \text{ per cent.}$$

The synchronous reactances are calculated as explained on page 234.

$$\begin{aligned} K_a &= \frac{\pi f_d + \sin \pi f_d}{4 \sin f_d \frac{\pi}{2}} \\ &= \frac{\pi \times 0.666 + \sin \pi \times 180}{4 \sin 0.666 \frac{180}{2}} \\ &= 0.852. \end{aligned}$$

A_1 is equal to 1.068 from page 183.

$$A_{d1} = 0.852 \times 1.068 = 0.91.$$

The per unit armature reaction reactance in the direct axis

$$\begin{aligned} X_{ad} &= \frac{6.38 f m l_g N^2 k_p^2 k_d^2 D}{p^2 \delta k \times 10^8} \frac{I}{E} A_{d1} \\ &= \frac{6.38 \times 60 \times 3 \times 16.9 \times 224^2 \times 0.975^2 \times 0.956^2 \times 100}{32^2 \times 0.406 \times 1.07 \times 10^8} \frac{600}{1390} \times 0.91 \\ &= 0.752. \end{aligned}$$

$$\begin{aligned} A_{q1} &= \frac{4\psi + 1}{5} - \frac{\sin \psi \pi}{\pi} \\ &= \frac{4 \times 0.6875 + 1}{5} - \frac{\sin 0.6875 \times 180}{\pi} \\ &= 0.485. \end{aligned}$$

The per unit armature reaction reactance in the quadrature axis

$$X_{aq} = X_{ad} \frac{A_{q1}}{A_{d1}} = 0.752 \frac{0.485}{0.91} = 0.40.$$

246 ARMATURE REACTIONS IN SYNCHRONOUS MACHINES

The per unit unsaturated synchronous reactance in the direct axis

$$\begin{aligned} X_d &= X_l + X_{ad} \\ &= 0.14 + 0.752 = 0.892, \end{aligned}$$

and the per unit unsaturated synchronous reactance in the quadrature axis

$$\begin{aligned} X_q &= X_l + X_{aq} \\ &= 0.14 + 0.40 = 0.54. \end{aligned}$$

The vector diagram for this machine for 80 per cent power factor inductive load is shown in Fig. 150.

The equivalent field ampere-turns per pole of armature reaction for full-load current

$$\begin{aligned} AT_{af} &= \frac{0.45 K_a m N I k_p k_d}{p} \\ &= \frac{0.45 \times 0.852 \times 3 \times 224 \times 600 \times 0.975 \times 0.956}{32} \\ &= 4500 \text{ ampere-turns.} \end{aligned}$$

The direct axis synchronous impedance is shown in Fig. 156 and is determined as explained on page 236. The short-circuit ratio

$$\frac{ATP_o}{ATP_s} = \frac{6521}{5340} = 1.22.$$

The unsaturated value of short-circuit ratio is 1.12 from Fig. 156 and per unit

$$X_d = \frac{1}{1.12} = 0.893.$$

Per unit

$$X_{ad} = 0.893 - 0.14 = 0.753.$$

The ampere-turns per pole required on the field winding for full-load at 80 per cent lagging power factor are found graphically as explained on page 240. The construction for the sample design is shown in Figs. 152 and 156 for unity and 80 per cent lagging power factor. For unity power factor full-load,

$$ATP_{100} = 8620 \text{ ampere-turns,}$$

and for 80 per cent lagging power factor,

$$ATP_{80} = 11,180 \text{ ampere-turns.}$$

The per unit regulation at 80 per cent power factor (see Fig. 156)

$$= 1.27 - 1.0 = 0.27,$$

and at 100 per cent power factor

$$= 1.165 - 1.0 = 0.165.$$

The field current for any load and power factor can also be calculated by means of the two-reaction theory. From the vector diagram,

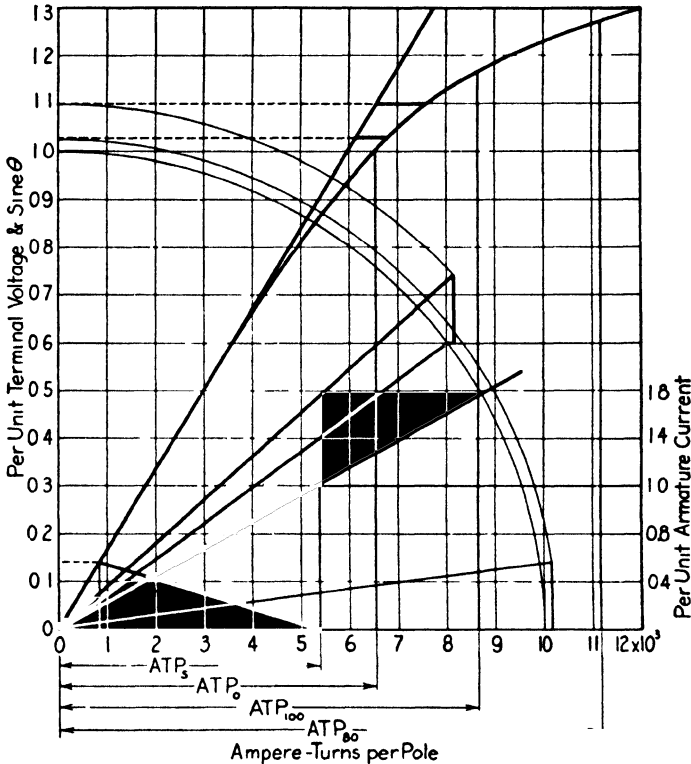


FIG. 156. —Open-circuit and short-circuit characteristics.

Fig. 150, the displacement angle for full-load and 80 per cent power factor

$$\begin{aligned} \delta_e &= \sin^{-1} \frac{X_q \cos \theta}{\sqrt{1 + X_q^2 + 2X_q \sin \theta}} \\ &= \sin^{-1} \frac{0.54 \times 0.80}{\sqrt{1 + 0.54^2 + 2 \times 0.54 \times 0.60}} \\ &= 18.05^\circ. \end{aligned}$$

The induced voltage for no saturation, that is, straight-line saturation curve in per unit system,

$$\begin{aligned} E_d &= \cos \delta_e + X_d \sin (\theta + \delta_e) \\ &= 0.95 + 0.892 \times 0.819 \\ &= 1.68. \end{aligned}$$

From Table XVII the air gap ampere-turns per pole for 100 per cent voltage are equal to 5980. For 168 per cent of normal voltage they will be $5980 \times 1.68 = 10,060$ ampere-turns.

To this value must be added the difference between the air gap ampere-turns per pole and the ampere-turns per pole from the satura-

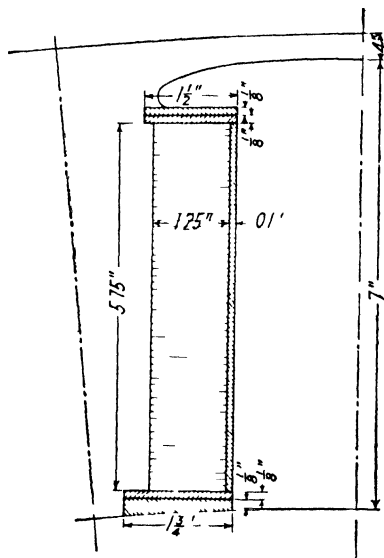


FIG. 157.

tion curve corresponding to the voltage E_d , Fig. 150. From the saturation curve, Fig. 156, this value is equal to 1100 ampere-turns, and

$$\begin{aligned} \text{ATP}_{80} &= 10,060 + 1100 \\ &= 11,160 \text{ ampere-turns.} \end{aligned}$$

For full-load at 100 per cent power factor this method gives

$$\text{ATP}_{100} = 8550 \text{ ampere-turns.}$$

The length of the mean-turn for the field winding must first be estimated. The bare strap-copper field winding, shown in Fig. 154,

will be used for this design. The length of the mean-turn for a copper strap 1.25 in. wide

$$\begin{aligned} L_f &= 2(l_1 - 1.0) + \pi(w_p + 0.20 + d_f) \\ &= 2(17.5 - 1.0) + \pi(4.0 + 0.20 + 1.25) \\ &= 50.1 \text{ in.} \end{aligned}$$

The section-area of the conductor

$$\begin{aligned} s_f &= \frac{\text{ATP}_{80} L_f p \times 0.826}{E_f \times 10^6} \\ &= \frac{11,180 \times 50.1 \times 32 \times 0.826}{110 \times 10^6} \\ &= 0.135 \text{ sq. in.} \end{aligned}$$

From the sketch, Fig. 157, the space available for the field winding

$$h_f = 5.75 \text{ in.}$$

A conductor 0.109 in. \times 1.25 in., area 0.134 sq. in., is selected from the copper table. The insulation between turns consists of paper 0.005 in. thick. If 0.005 in. is allowed for buckling of the conductor in the process of winding, then the total space occupied by one turn = $0.005 + 0.005 + 0.109 = 0.119$ in. The number of turns that can be wound on each pole

$$t_f = \frac{5.75}{0.119} = 48.$$

The field current for full-load and 80 per cent lagging power factor

$$i_{f80} = \frac{\text{ATP}_{80}}{t_f} = \frac{11,180}{48} = 233 \text{ amperes,}$$

and the current density

$$A_f = \frac{233}{0.134} = 1740 \text{ amperes per sq. in.}$$

The resistance at 75°C .

$$\begin{aligned} R_f &= \frac{L_f t_f p \times 0.826}{s_f \times 10^6} \\ &= \frac{50.1 \times 48 \times 32 \times 0.826}{0.134 \times 10^6} = 0.474 \text{ ohm,} \end{aligned}$$

250 ARMATURE REACTIONS IN SYNCHRONOUS MACHINES

and the copper loss for a field current of 233 amperes

$$W_f = 233^2 \times 0.474 = 25,700 \text{ watts.}$$

The radiating surface

$$\begin{aligned} S_f &= 2(d_f + h_f)L_f p \\ &= 2(1.25 + 5.75)50.1 \times 32 = 22,500 \text{ sq. in.,} \end{aligned}$$

and the surface per watt loss

$$\frac{S_f}{W_f} = \frac{22,500}{25,700} = 0.875 \text{ sq. in. per watt.}$$

The voltage drop in the field winding for the full-load 80 per cent lagging power factor field current

$$E_f = 233 \times 0.474 = 111 \text{ volts.}$$

The maximum field current for 120 volts across the field winding, allowing 5 volts drop in exciter leads and brushes, is

$$i_{f \text{ max.}} = \frac{120}{0.474} = 253 \text{ amperes.}$$

The exciter capacity

$$\begin{aligned} W_e &= \frac{E_f^2}{R_f \times 10^3} = \frac{125^2}{0.474 \times 10^3} \\ &= 33 \text{ kilowatts.} \end{aligned}$$

The weight of the field copper

$$\begin{aligned} G_f &= L_f p s_f \times 0.321 \\ &= 50.1 \times 48 \times 32 \times 0.134 \times 0.321 \\ &= 3310 \text{ lb.} \end{aligned}$$

CHAPTER XIV

LOSSES, EFFICIENCY, AND TEMPERATURE RISE

THE losses in synchronous machines are:

- (1) Copper losses in armature and field winding.
- (2) Field rheostat losses.
- (3) Core losses.
- (4) Mechanical losses; bearing friction, and windage.
- (5) Stray load-losses.

Armature Copper Losses.—The method of calculating the armature resistance is given on page 209. The armature copper loss

$$W_a = I^2 R_a m \text{ watts.} \quad (166)$$

The A.I.E.E. Standards specify that the copper losses are to be calculated for a temperature of 75° C. for all loads; therefore, R_a must be the armature resistance per phase at 75° C. The armature current varies directly with the load for a given power factor; therefore the copper loss will vary as the square of the load.

Field Copper Losses.—The resistance of the field winding is calculated as shown on page 244, and the field current for any load and power factor is determined as explained on page 240. The loss in the field winding at 75° C.

$$W_f = i^2 R_f \text{ watts.} \quad (167)$$

A field rheostat is generally connected in series with the field winding of synchronous generators. Unity power factor synchronous motors are often operated without a field rheostat; the field winding of the motor is then designed to give the required field current when normal exciter voltage is applied.

Core Losses.—The losses in the armature core consist of the hysteresis and eddy-current losses in the teeth and yoke and the additional losses. The additional losses consist of losses in the pole face and surface of the armature teeth due to the flux pulsations in the air gap produced by the armature slots, losses due to punching and bending strains in the laminations, losses due to imperfect insulation between laminations caused by burrs or slot filing, and losses in the end-frames due to stray fluxes.

The method of calculating core losses for direct-current generators and motors can also be used for synchronous machines. The curves in the Appendix give the loss per pound per cycle due to the fundamental frequency flux for various grades of sheet steel. These curves were obtained from tests of samples in accordance with the standards of the American Society for Testing Materials.

The armature cores of small and medium size machines are generally built up of an open-hearth electric sheet steel with very little or no silicon and in thickness from 0.014 to 0.019 in. For machines with large armature cores, the core losses can be materially reduced by using a sheet steel alloyed with silicon. The following quotation from an A.I.E.E. paper¹ bears this out:

To illustrate the reduction in core loss that results from the use of these higher grade steels, if the loss in non-silicon steel is represented by 100, the loss with 2 per cent silicon steel will be 70, and 45 with 4 per cent silicon steel. The use of 4 per cent silicon steel improves the efficiency slightly more than 1 per cent of full load, and 2½ per cent at half load, as compared with the efficiency of machines using non-silicon steel. When this steel is used, the core loss is reduced from 50 per cent of the total loss to 30 per cent of the total loss.

The additional losses may also include a no-load damper winding loss² if a squirrel-cage winding is present in the pole faces. This loss is produced by the stator slot harmonics and is large when the squirrel-cage has a much larger number of slots than the stator and neither stator nor rotor slots are skewed. The total core losses for synchronous machines are generally from 1.8 to 3.0 times the sum of the losses in the teeth and yoke due to the fundamental frequency flux. The multiplying factor should be determined from tests of machines of similar design. When such data are not available 2 to 2.5 may be used.

Friction and Windage Losses.—The loss due to bearing friction can be calculated when the dimensions of the bearing, the peripheral speed of the shaft at the bearing, the load on the bearing, and the coefficient of friction are known. The windage losses are very difficult to calculate and depend largely upon the type of construction. The combined friction and windage loss is therefore generally taken from tests of machines of the same construction. When such data are not available, the friction and windage loss may be estimated with the help of the curves, Figs. 158 and 159.

¹ "Recent Improvements in Turbine Generators," by S. L. Henderson and C. R. Soderberg, A.I.E.E. Trans., Vol. 47, No. 2, p. 549.

² "Calculation of No-Load Damper Winding Loss in Synchronous Machines," by E. I. Pollard, A.I.E.E. Trans., Vol. 51, June, 1932, p. 477; "Parasitic Losses in Synchronous-Machine Damper Windings," by J. H. Walker, Journal of the Institution of Electrical Engineers, Vol. 94, Part II, Feb., 1947, p. 13.

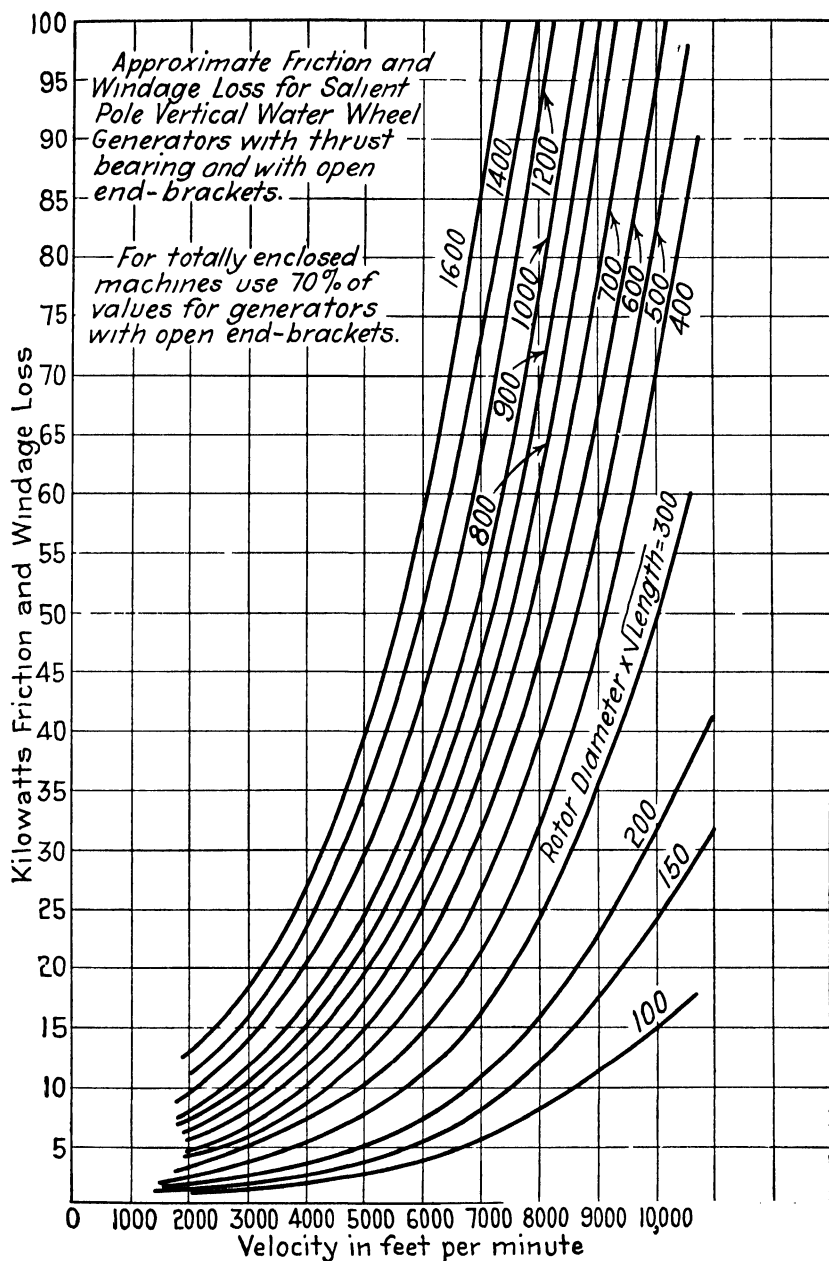


FIG. 158.

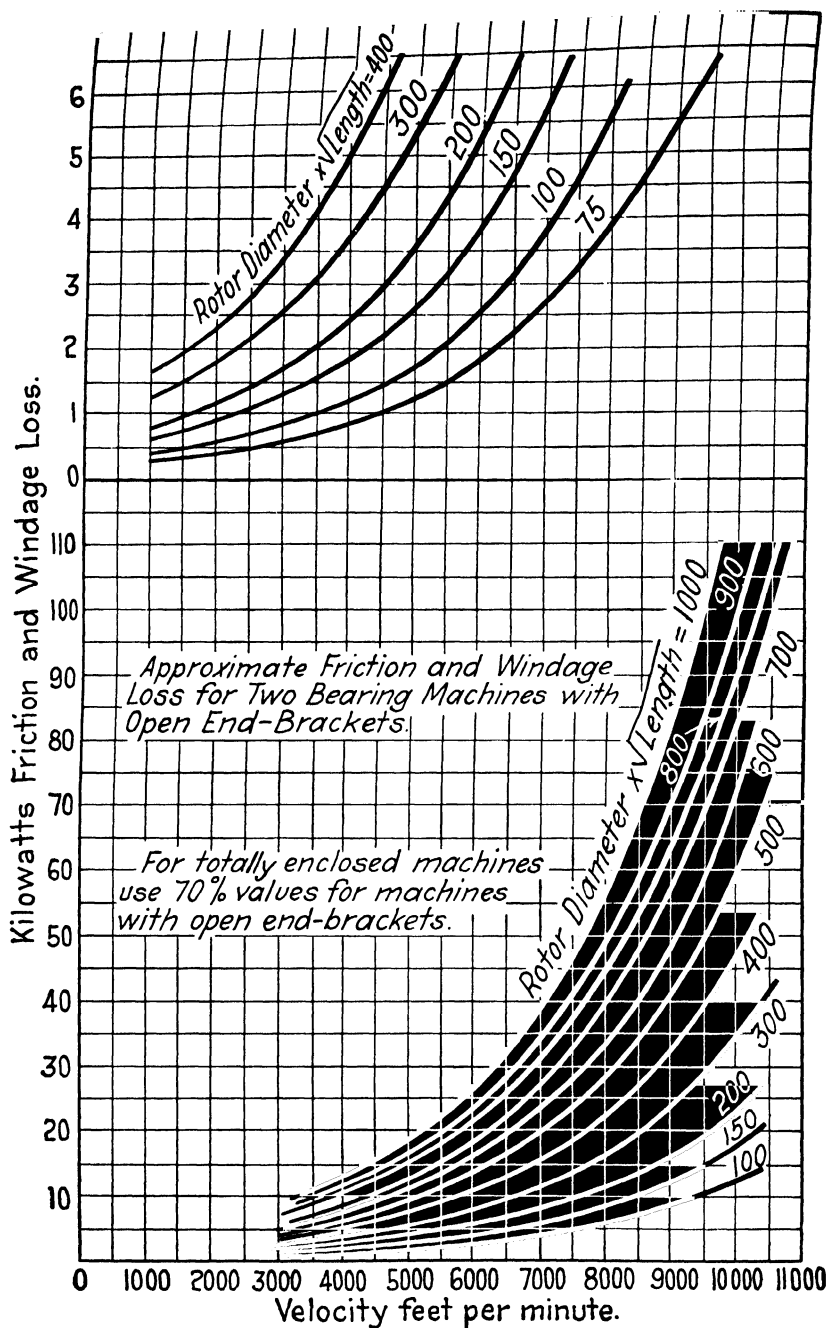


FIG. 159.

Bearing failures have been found to occur on large-capacity machines, caused by currents flowing between shaft and bearing. The designer of large-capacity generators and motors must take the proper precautions to limit to a negligible value the current between shaft and bearing. Careful studies have been made to determine the origin and method of preventing shaft currents. The results of these investigations have been published in various technical journals.³

Stray Load-Losses.—The Standards of the A.S.A. define the stray load-losses as follows: "These include iron losses and eddy-current losses in the copper, due to fluxes varying with the load and also saturation."

For large machines, the eddy-current losses in the copper are large because of the large conductor sections and deep slots. For these reasons, most large-capacity machines are now being built with transposed⁴ conductors in the armature coils. Large conductor sections must therefore be avoided in armature windings and the conductors built up of a number of small wires in parallel.

It is difficult to calculate the stray load-losses accurately; they must therefore be assumed based on test values from machines of similar design. From the short-circuit test specified in the A.S.A. Standards, the effective alternating-current armature resistance can be found by dividing the total loss on short circuit, after deducting the friction and windage loss, by the current squared. If this resistance is used to calculate the armature copper loss, the result will be I^2R plus stray load-losses. Dr. Arnold⁵ states that the effective alternating-current resistance is generally from 1.5 to 2.5 times the resistance measured by direct current in single-phase machines and 1.3 to 2.0 in polyphase machines.

Efficiency.—The efficiency of a motor or generator is the ratio of the output to the output plus all the losses. It is generally expressed as a percentage as follows:

$$\text{eff.} = \frac{\text{Kva output} \times \text{PF} \times 100}{(\text{Kva output} \times \text{PF}) + W_a + W_f + W_{sl} + W_{fw} + W_c} \text{ per cent.}$$

For engine-type generators and motors to be direct-connected to steam or internal-combustion engines, or air or ammonia compressors, the electrical manufacturer does not furnish the bearings, and the

³ See footnote, page 162.

⁴ "Reduction of Armature Copper Losses," by J. H. Summers, A.I.E.E. Journal, Vol. 46, May, 1927, p. 451; "Transposed Armature Coils in Alternating Current Generators," by S. L. Henderson, Electric Journal, Vol. 23, July, 1926, p. 348.

⁵ "Die Wechselstromtechnik," Vol. 4, p. 54, Julius Springer, Berlin.

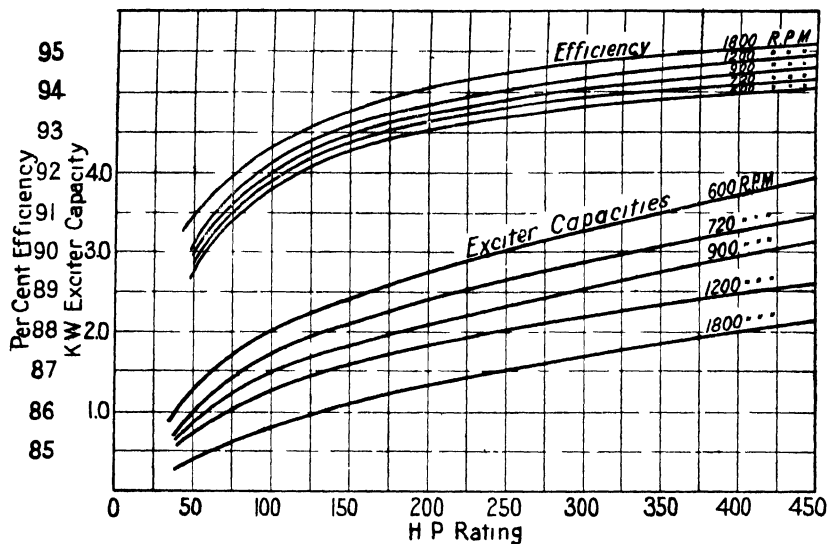


FIG. 160.—Approximate full-load efficiencies and exciter capacities for 60-cycle, unity power factor, synchronous motors.

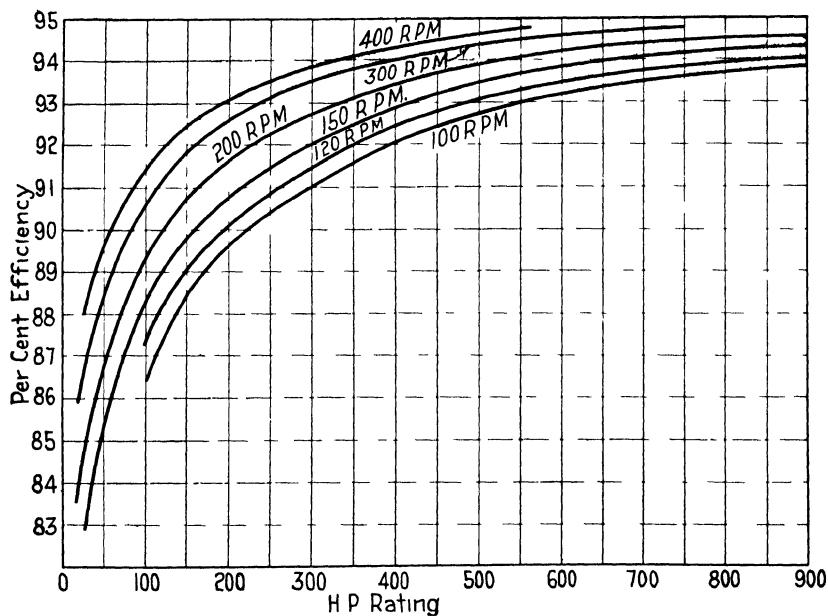


FIG. 161.—Approximate full-load efficiencies for engine-type synchronous motors—60 cycles, unity power factor.

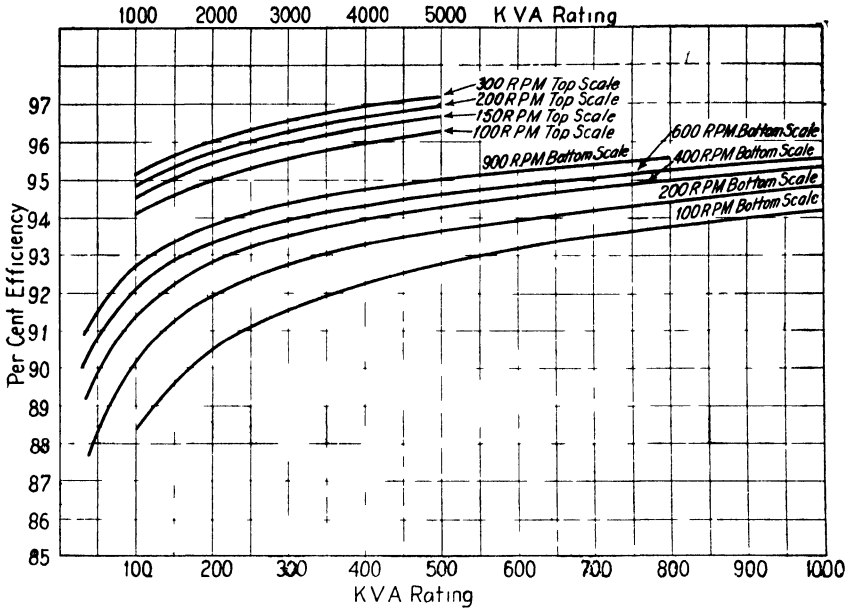


FIG. 162 Approximate full-load, unity power factor efficiencies of 60-cycle, salient-pole synchronous generators.

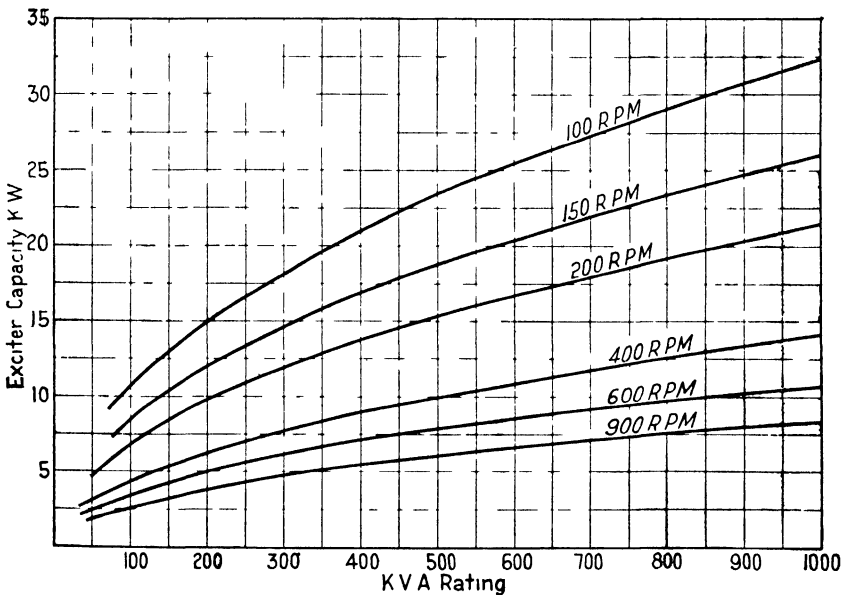


FIG. 163.—Approximate exciter capacities for 60-cycle, 80 per cent power factor, salient-pole generators.

friction and windage losses are not included when calculating the efficiency.

When specifying the efficiency of electric machines, it is important to specify by what method the efficiency is to be determined, because marked variations⁶ in efficiency are obtained by various methods.

The curves in Fig. 160 show the approximate full-load efficiency and exciter capacity for high-speed, unity power factor, synchronous motors, for voltages including 2200 volts. The approximate full-load efficiencies for unity power factor, 50°-rated, engine-type synchronous motors are shown in Fig. 161. The approximate efficiency of standard, 50°-rated, synchronous generators is shown in Fig. 162 for full-load at 100 per cent power factor. The exciter capacities required are shown in Fig. 163.

Temperature Rise.—The losses in the armature copper and core and in the field winding are converted into heat, which increases the temperature of the machine above that of the surrounding air. The value of the final temperature depends upon the heat capacity of the various insulating materials used and upon the rate at which heat is conducted through the material to the cooling medium. The final temperature is reached when the rate at which heat is generated becomes equal to the rate at which the heat is dissipated. Tests on various kinds of insulating materials have shown that for each material there is a safe continuous operating temperature which can not be exceeded without impairing the life of the material. The maximum continuous operating temperatures specified by the American Standards Association for synchronous machines are given in Tables XVIII and XIX.

The temperature rise of each of the various parts of steam turbine generators, above the temperature of the cooling medium, shall not exceed the values given in Table XVIII and for salient-pole motors and generators, the values given in Table XIX. The temperatures should be determined by the methods specified in the tables.

The various kinds of insulating materials included in the different classes referred to in the tables are given on page 127, Chapter VII.

The output that can be obtained from a given frame may or may not be limited by the safe operating temperature. For salient-pole synchronous machines of the revolving-field type, satisfactory ventilation of the armature winding can generally be obtained; and operating characteristics, efficiency, regulation, etc., may be the limiting factors rather than temperature. The designer must, however, make ample

⁶ "A Comparison of the Efficiency of Synchronous Machines as Determined by Various Methods," by P. L. Alger, *General Electric Review*, Vol. 29, Nov., 1926, pp. 765-774.

TABLE XVIII *

LIMITING TEMPERATURE RISES FOR STEAM-TURBINE-
DRIVEN ALTERNATORS

Item	Description of Part	Method of Temperature Determi- nation Required	Limiting Temperature Rise in Degrees Centigrade	
			Class A Insulation	Class B Insulation
1	Insulated armature windings on sta- tors of machines of 500 kva and below.	Thermometer	50	70
		Resistance	60	80
2	Insulated armature windings with 2 coil sides per slot on stators of machines above 500 kva.	Embedded detector	60	80
3	Insulated field windings.	Resistance	.	90
4	Collector rings. (The class of insula- tion refers to insulation affected by the heat from the collector rings, which insulation is employed in the construction of the collector rings or is adjacent thereto.)	Thermometer	65	85
5	Cores and mechanical parts in con- tact with or adjacent to insulation.	Thermometer	50	70
6	Miscellaneous parts (such as brushholders, brushes, pole tips, etc.), other than those whose temperatures affect the temperature of the insulating material, may attain such temperatures as will not be injurious.			

* A.S.A. Standards C50, 1943.

provisions for ventilation in large-capacity machines to avoid local hot spots. The radiating surfaces are usually quite large for slow-speed machines, and the problems of temperature control are generally less difficult than for high-speed machines. The field windings⁷ of high-speed machines are particularly difficult to ventilate properly.

⁷ "Recent Improvements in Turbine Generators," by S. L. Henderson and C. R. Soderberg, A.I.E.E. Trans., Vol. 47, No. 2, p. 549; "The Multiple Path Radial Ventilation of Large Turbo-Alternators," by M. D. Ross, Electric Journal, Vol. 21, Dec., 1924, p. 540; "Temperatures in Large Alternating Generators," by W. J. Foster, General Electric Review, Vol. 23, July, 1920, p. 560; General Electric Review, Vol. 23, Feb., 1920, pp. 99-108 and 147-152. See also references, page 128.

TABLE XIX *

LIMITING TEMPERATURE RISES FOR SYNCHRONOUS MACHINES OTHER
THAN STEAM-TURBINE-DRIVEN ALTERNATORS

Item	Description of Part	Method of Temperature Determi- nation Required	Limiting Temperature Rise in Degrees Centigrade	
			Class A Insulation	Class B Insulation
1	Insulated armature windings with 2 coil sides per slot on stators of machines of 1500 kva and below.	Thermometer	50	70
		Resistance	60	80
2	Insulated armature windings with 2 coil sides per slot on stators of machines above 1500 kva.	Embedded detector	60	80
3	Insulated field windings.	Resistance	60	80
4	Collector rings. (The class of insulation refers to insulation affected by the heat from the collector rings, which insulation is employed in the construction of the collector rings or is adjacent thereto.)	Thermometer	65	85
5	Cores and mechanical parts in contact with or adjacent to Class A or B insulation.	Thermometer	50	70
6	Amortisseur windings may attain such temperature as will not occasion mechanical injury to the machine.			
7	Miscellaneous parts (such as brushholders, brushes, pole tips, etc.) other than those whose temperatures affect the temperature of the insulating material may attain such temperatures as will not be injurious.			

* A.S.A. Standards C50, 1943.

The radiating surface of the armature core may be taken equal to the perimeter of the core section, plus one surface for each duct (see Fig. 164),

$$S_a = \frac{\pi}{4} (D_0^2 - D^2) (2 + n_a) + \pi l (D + D_0). \quad (168)$$

The losses that must be dissipated by this surface are the core loss and the armature copper loss for that part of the armature coil embedded in the slots.

The radiating surface per watt loss

$$\frac{S_a}{W} = \frac{\frac{\pi}{4} (D_0^2 - D^2) (2 + n_d) + \pi l (D_0 + D)}{W_c + W_a \frac{l}{L_a}} \quad (169)$$

For a temperature rise not to exceed 50° C., the radiating surface per watt for the armature should generally be greater than 0.70.

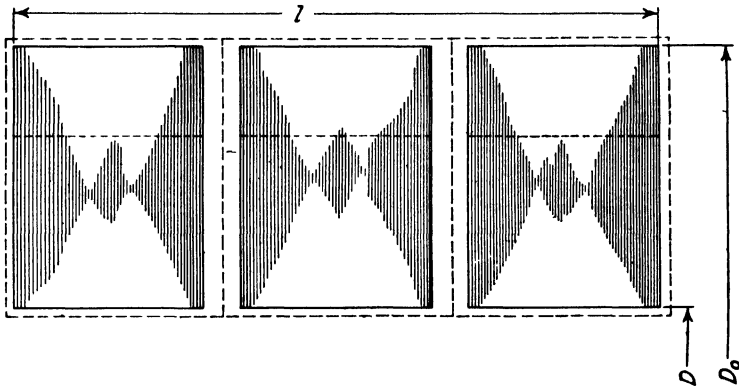


FIG. 164.—Section of armature core showing radiating surfaces.

The method of calculating the radiating surface for the field winding and the safe values for the surface per watt loss have been given on page 244.

Sample Design: Losses, Efficiency, and Temperature Rise.—The armature resistance is given on page 214. The copper loss at full-load

$$\begin{aligned} W_a &= I^2 R_{am} = 600^2 \times 0.024 \times 3 \\ &= 25,900 \text{ watts.} \end{aligned}$$

The field ampere-turns per pole for full-load and unity power factor, $ATP_{100} = 8620$, and the field current (see Fig. 156),

$$i_f = \frac{8620}{48} = 180 \text{ amperes.}$$

The field copper loss plus rheostat loss for full-load at unity power factor

$$W_f = 180^2 \times 0.474 = 15,350.$$

The average armature tooth width

$$w_{ta} = \frac{\pi(D + d_s)}{S} - w_s = \frac{\pi(100 + 2.83)}{336} - 0.426$$

$$= 0.534 \text{ in.}$$

The weight of the armature teeth

$$G_{ct} = w_{ta}(l - n_d w_d) k_1 S d_s \times 0.278$$

$$= 0.534(17.5 - 5 \times \frac{1}{2}) 0.93 \times 336 \times 2.83 \times 0.278$$

$$= 1970 \text{ lb.}$$

The weight of the armature yoke

$$G_{cy} = \frac{\pi}{4} [D_0^2 - (D + 2d_s)^2] (l - n_d w_d) k_1 \times 0.278$$

$$= \frac{\pi}{4} [112^2 - (100 + 2 \times 2.83)^2] (17.5 - 5 \times \frac{1}{2}) 0.93 \times 0.278$$

$$= 4260 \text{ lb.}$$

From the iron loss curve in the Appendix for 26 gauge dynamograde silicon steel, the loss per pound for the tooth density, $B_{t3} = 95$ kilo-lines per sq. in., is equal to 2 watts. The loss in the armature teeth due to the fundamental frequency flux

$$W_{ct} = 2 \times 1970 = 3940 \text{ watts.}$$

The loss per pound for the yoke density, $B_{y3} = 55$ kilo-lines per sq. in., equals 0.7 watt, and the loss in the yoke due to the fundamental frequency flux

$$W_{cy} = 0.7 \times 4260 = 2980 \text{ watts.}$$

The total core loss

$$W_c = (3940 + 2980) 2.0 = 13,840 \text{ watts.}$$

The friction and windage losses are taken equal to 15,000 watts, from the curves, Fig. 158, for vertical waterwheel generators with open end-brackets.

The stray load-losses are estimated at 30 per cent of the armature I^2R losses. The efficiencies and losses for unity power factor for various loads are given in Table XX.

TABLE XX
LOSSES AND EFFICIENCIES

	Load				
	$\frac{1}{4}$	$\frac{2}{4}$	$\frac{3}{4}$	$\frac{4}{4}$	$\frac{5}{4}$
Armature I^2R	1.62	6.48	14.55	25.90	40.50
Stray load.....	1.95	3.90	5.85	7.80	9.75
Field I^2R	12.60	13.45	14.35	15.35	16.20
Core losses.....	13.84	13.84	13.84	13.84	13.84
Friction and windage losses...	15.00	15.00	15.00	15.00	15.00
Total losses.....	45.91	52.67	63.59	77.89	95.29
Output.....	625.00	1250.00	1875.00	2500.00	3125.00
Output + losses.....	670.91	1302.67	1938.59	2577.89	3220.29
Efficiency, per cent.....	93.00	95.80	96.75	97.00	97.10

The radiating surface of the armature

$$\begin{aligned}
 S_a &= \frac{\pi}{4} (D_0^2 - D^2)(2 + n_d) + \pi l(D + D_0) \\
 &= \frac{\pi}{4} (112^2 - 100^2)(2 + 5) + \pi 17.5(100 + 112) \\
 &= 25,650 \text{ sq. in.}
 \end{aligned}$$

The radiating surface per watt loss for full-load

$$\frac{S_a}{W} = \frac{25,650}{13,840 + 33,700 \times \frac{17.50}{33.78}} = 0.82.$$

The radiating surface and surface per watt loss for the field winding are given on page 250.

The synchronizing power for full-load and 80 per cent power factor

$$\begin{aligned}
 P_r &= \frac{57.3 \times \text{kw.}}{\delta_c \times \text{eff.}} \\
 &= \frac{57.3 \times 2000}{18.05 \times 0.958} \\
 &= 6640 \text{ kilowatts.}
 \end{aligned}$$

The efficiency is for full-load at 80 per cent power factor.

SYNCHRONOUS MACHINE DESIGN SHEET

GENERATOR-MOTOR

Hp. . . Kva 2500 Volts 2400 Phase 3 Amperes 600 Cycles 60 Poles 32
 R p m 225 Kva / r p m 111 Output constant 1.58×10^4

ARMATURE

FIELD

Sheet steel	0 019 Dynamo grade
Outside diameter	112.0
Gap diameter	100.0
Total length	17.5
Ducts number and size	5 $\frac{1}{2}$
Gross length	15.0
Effective length	14.0
Slots per pole per phase	$3\frac{1}{2}$
Total number of slots	336
Type of winding	2 layer star
Circuits per phase	2
Coil throw	Slots 1 and 10
Per cent pitch	85.7
Conductors	
Per slot	4
Dimensions	$0.149 \times 0.276 - 4$
Area	4×0.0325
In series per phase	224
Total	1326
Current density	2310
Length one half mean turn	33.78
Resistance per phase 25°C	0.0202
Resistance per phase 75°C	0.024
Resistance drop volts	18.7
Resistance drop per cent	1.35
Reactance drop volts	195
Reactance drop per cent	14
Impedance drop volts	196
Impedance drop per cent	14.1
Armature reaction A I per pole	5280
Armature reaction factor	0.852
Armature reaction eq fld A I	4500
Square inches per watt	0.82
Amper conductors per inch	1.200
Short circuit ratio	1.22
$\frac{D^2 l n}{kva}$	1.58×10^4
ATP ₉₀	8620
ATP ₉₅	11 180
Regulation 80% P f	27.0 %
Regulation 100% P f	16.5%

Total air gap length	2×0.406
Rotor diameter	99.188
Peripheral speed	5840
Pole pitch	9.82
Pole arc	6.75
Material spider	Hot rolled steel
Damper bars per pole	
Size of bar	
Material of bar	
Section end ring	
Material end ring	
Air gap coefficient	1.07
Effective length of gap	0.435
Leakage constant	1.35
$f_d = 0.666 f_b = 1.14 k_l = 0.956 C_s = 0.725 k_p = 0.975$	
Total flux 234 000 k L Flux per pole 4870 k L	

	Section	Density	Length	Amp turns
Air gap	5310	44.1	1.07×0.406	5980
Teeth	2470	95	2.83	142
Armature yoke	88.5	55	5.34	19
Poles	70	93.6	7.00	315
Field yoke	101	63.0	4.05	65
Total ampere turns per pole				6521

Size of conductor	0.109×1.25
Turns per pole	48
Amperes no load	136 Maximum 253
Length of mean turn	50.1
Resistance 25°C	0.398
Resistance 75°C	0.474
I_a no load	53.8 Maximum 120
$I_a R$ no load	7360 Maximum 30 400
Square inch per watt maximum I	0.74
Kva	2500
Power factor	80%
Amperes	233.0
$I_a R 75^\circ \text{C}$	110.0
$I_a R 75^\circ \text{C}$	25 700
Square inch per watt	0.875
Exciter voltage	125.0
Exciter capacity	33.0

FULL LOAD LOSSES 100% P f

Friction and windage	15 000
Core	13 840
Stray load	7 800
Armature copper	25 900
Field copper	15 350
Total losses	77 890
Flywheel effect WR^2	159 800 lb-ft ²

WEIGHTS

Armature copper	1890
Field copper	3310.0
Armature teeth	1970
Armature yoke	4260.0
Field poles	4300.0

Remarks Vertical Water wheel Type $X_d = 0.892 \lambda_g = 0.54$
 $\delta_{eff} = 0.80 \text{ p f} = 18.05 P_r f l = 0.80 \text{ p f} = 6640 \text{ kw}$

$P_f = 1985 \text{ lbs } P_d = 5870 \text{ lbs}$

CHAPTER XV

SAMPLE DESIGN OF SYNCHRONOUS MOTOR

To design a synchronous motor for leading power factor calculate the kva input and proceed as for a generator. The input

$$Kva = \frac{hp \times 0.746}{\text{eff.} \times PF}.$$

Design of 200-Hp Synchronous Motor.— The motor to be designed is to have the following rating: 200 hp, 440 volts, 3-phase, 60 cycles, 900 r.p.m. It is to be a self-starting synchronous motor for direct connection to a centrifugal pump and is to operate at 100 per cent power factor at full-load without field rheostat. The temperature rise for continuous full-load operation must not exceed 50° C., and the full-load efficiency must not be less than 93.3 per cent.

The output

$$Kva = \frac{hp \times 0.746}{PF} = \frac{200 \times 0.746}{1.00} = 149.$$

The number of poles

$$p = \frac{f \times 2 \times 60}{n} = \frac{60 \times 2 \times 60}{900} \\ = 8.$$

$$\frac{Kva}{n} = \frac{149}{900} = 0.166.$$

The output constant from Fig. 105,

$$C = 2.75 \times 10^4.$$

For $l/\tau = 1.0$,

$$D = \sqrt[3]{\frac{Kva p C}{\pi l / \tau n}} = \sqrt[3]{\frac{149 \times 8 \times 2.75 \times 10^4}{\pi \times 1 \times 900}} \\ = 22.6 \text{ in.} \\ l = \frac{Kva C}{D^2 n} = \frac{149 \times 2.75 \times 10^4}{22.6 \times 900} \\ = 8.93 \text{ in.}$$

For other values of l/τ the dimensions are:

l/τ	D	l	τ
1.0	22.6	8.93	8.87
0.9	23.5	8.25	9.21
0.8	24.4	7.65	9.56
0.7	25.5	7.00	10.00

The following dimensions are selected:

$$D = 25.0 \text{ in.}, \quad l = 7.0 \text{ in.}$$

The pole pitch

$$\tau = \frac{\pi D}{p} = \frac{3.14 \times 25}{8} = 9.81 \text{ in.}$$

For 70 per cent pole embrace the pole arc

$$B = 0.70 \times 9.81 = 6.875 \text{ in.}$$

The method of shaping the pole shoe suggested by R. W. Wieseman¹ will be used.

From the curves Fig. 107, the minimum air gap length should be

$$\delta = 0.188 \text{ in.}$$

$$\frac{\delta_m}{\delta} = 1.75, \quad \frac{\delta}{\tau} = 0.0192, \quad \frac{B}{\tau} = 0.70.$$

The shape of the pole shoe is shown in Fig. 165, and the air gap flux distribution curve is shown in Fig. 166. The calculations for the fundamental, third, fifth, and seventh harmonic are given in Table XXI.

$$B_1 = \frac{598.00}{6} = 99.3, \quad B_3 = \frac{-25.61}{6} = -1.77.$$

$$B_5 = \frac{-31.16}{6} = -3.46, \quad B_7 = \frac{-10.15}{6} = -3.71.$$

The average ordinate for the flux wave

$$\begin{aligned} B_a &= \frac{2}{\pi} \left(99.3 - \frac{1}{3} \times 1.77 - \frac{1}{5} \times 3.46 - \frac{1}{7} \times 3.71 \right) \\ &= 62, \end{aligned}$$

¹ See reference, page 185.

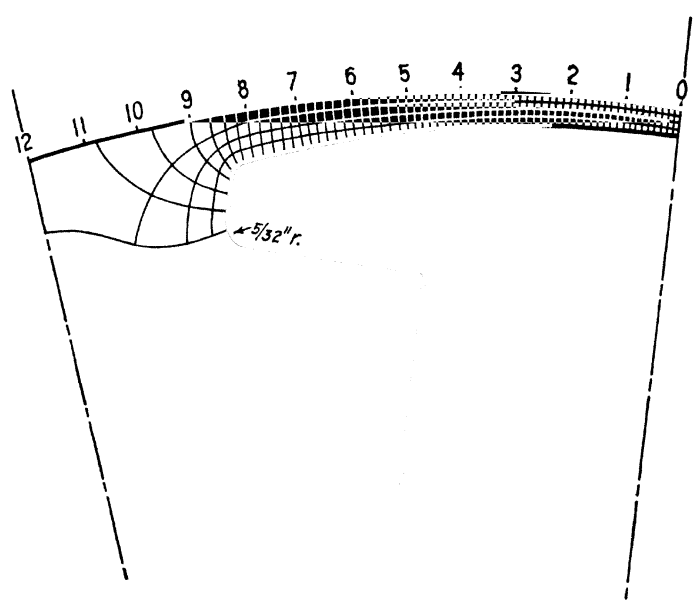


Fig. 165.—Flux plot.

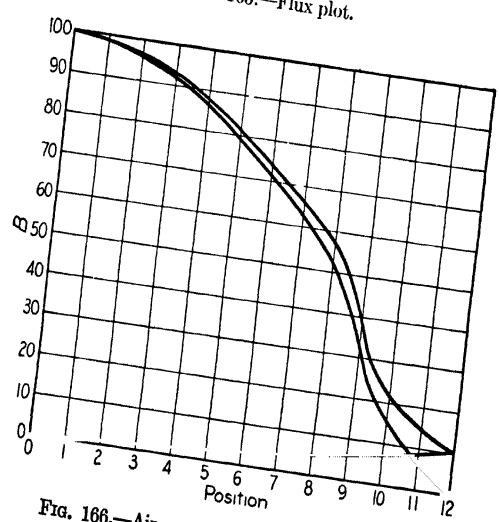


Fig. 166.—Air gap flux-distribution curve.

TABLE XXI

B_x	$\sin x$	$\sin 3x$	$\sin 5x$	$\sin 7x$	$B_x \times \sin x$	$B_x \times \sin 3x$	$B_x \times \sin 5x$	$B_x \times \sin 7x$
$B_{x11} = 6.0$	0.130	0.383	0.609	0.793	0.78	2.30	3.65	4.76
$B_{x10} = 14.5$	0.259	0.707	0.966	0.966	3.76	10.25	14.00	14.00
$B_{x9} = 32.2$	0.383	0.924	0.924	0.383	12.33	29.70	29.70	12.33
$B_{x8} = 52.5$	0.500	1.000	0.500	-0.500	26.25	52.50	26.25	-26.25
$B_{x7} = 62.5$	0.609	0.924	-0.130	-0.991	38.10	57.70	-8.12	-62.00
$B_{x6} = 71.0$	0.707	0.707	-0.707	-0.707	50.20	50.20	-50.20	-50.20
$B_{x5} = 79.5$	0.793	0.383	-0.991	0.130	64.00	30.45	-78.80	10.34
$B_{x4} = 86.2$	0.866	0.000	-0.866	0.866	74.70	00.00	-74.70	74.70
$B_{x3} = 92.0$	0.924	-0.383	-0.383	0.924	85.00	-35.20	-35.20	85.00
$B_{x2} = 96.0$	0.966	-0.707	0.259	0.259	92.80	-67.90	24.85	24.85
$B_{x1} = 98.2$	0.991	-0.924	0.793	-0.609	97.40	-90.60	77.80	-59.80
$B_{x0} = 100.0$	0.500	-0.500	0.500	-0.500	50.00	-50.00	50.00	-50.00
					595.32	-10.60	-20.77	-22.27

and the root-mean-square ordinate

$$B_e = \sqrt{\frac{1}{2}(99.3^2 + 1.77^2 + 3.46^2 + 3.71^2)}$$

$$= 70.7.$$

The flux distribution factor

$$f_d = \frac{B_a}{B_m} = \frac{62}{100} = 0.62.$$

The form factor

$$f_b = \frac{B_e}{B_a} = \frac{70.7}{62} = 1.14.$$

The air gap density is assumed equal to 43,000 lines per sq. in.

$$\phi_t = \pi D l B_g = \pi \times 25 \times 7.0 \times 43,000$$

$$= 23,600 \text{ kilo-lines.}$$

The winding constant

$$C_w = f_d f_b k_d = 0.62 \times 1.14 \times 0.956$$

$$= 0.676.$$

The number of conductors in series per phase are, for a star-connected winding with pitch coils,

$$N = \frac{E \times 60 \times 10^8}{n\phi_t k_p C_w} = \frac{254 \times 60 \times 10^8}{900 \times 23,600 \times 10^3 \times 1.0 \times 0.676}$$

$$= 106.$$

For one circuit per phase, the total number of conductors = $106 \times 3 = 318$. The number of armature slots will be 72 for 3 slots per pole per phase and 84 for $3\frac{1}{2}$ slots per pole per phase. The corresponding values for the tooth pitch at the armature surface

$$t_1 = \frac{\pi \times 25}{72} = 1.09 \text{ in.}, \quad t_1 = \frac{\pi \times 25}{84} = 0.935 \text{ in.}$$

The winding with 84 slots is selected. The conductors per slot will be 3.79 if the chord factor is 1.0. The number of conductors per slot must be an even integer; therefore 4 conductors per slot are used and the coils chorded $66\frac{2}{3}$ per cent of pitch. The coil throw will then be slot 1 and 8, and the chord factor

$$k_p = \sin \frac{7}{10} 90 = 0.866.$$

The final value of the total flux

$$\phi_t = \frac{254 \times 60 \times 10^8}{112 \times 900 \times 0.866 \times 0.676}$$

$$= 25,900 \text{ kilo-lines.}$$

The armature current per phase

$$I = \frac{\text{Kva} \times 10^3}{E \times 3} = \frac{160 \times 10^3}{254 \times 3}$$

$$= 210 \text{ amperes.}$$

The current density in the armature copper should be approximately 3400 amperes per sq. in., from the curves of Fig. 133. The section area of the armature conductor

$$s_a = \frac{I}{aA_a} = \frac{210}{1 \times 3400}$$

$$= 0.0618 \text{ sq. in.}$$

From the copper table a d.c.c., copper ribbon conductor is selected which has following dimensions: 0.129×0.258 in. bare, 0.149×0.276 in. insulated, area 0.0325 sq. in. Two conductors are wound in parallel and arranged in the slot as shown in Fig. 167. The slot dimensions are:

$$\text{Width} = (1 \times 0.276) + 0.085 = 0.361 \text{ in.}$$

$$\text{Depth} = (8 \times 0.149) + 0.31 = 1.50 \text{ in.}$$

The current density for this conductor

$$A_a = \frac{210}{2 \times 0.0325} = 3230 \text{ amperes per sq. in.}$$

The length of the half-mean-turn of the armature coil is calculated as follows (see Fig. 135):

$$\sin \alpha = \frac{d}{t_1} = \frac{0.361 + 0.12}{0.935} = 0.515$$

$$\alpha = 31^\circ \text{ and } \cos \alpha = 0.857.$$

The per unit pitch for the armature coils

$$P = \frac{7}{10.5} = 0.667,$$

$$L_a = \frac{\pi(D + d_s)}{p \cos \alpha} P + 2b + d_s + l$$

$$= \frac{\pi(25 + 1.50)}{8 \times 0.857} 0.667 + 1.75 + 1.50 + 7.0$$

$$= 18.35 \text{ in.}$$

The resistance per phase of the armature winding at 75° C.

$$R_a = \frac{L_a N r}{a s_a \times 10^6} = \frac{18.35 \times 112 \times 0.826}{1 \times 0.065 \times 10^6}$$

$$= 0.0262 \text{ ohm per phase.}$$

The bare weight of the armature copper

$$G_a = L_a N a m s_a 0.321 = 18.35 \times 112 \times 1 \times 3 \times 0.065 \times 0.321$$

$$= 129 \text{ lb.}$$

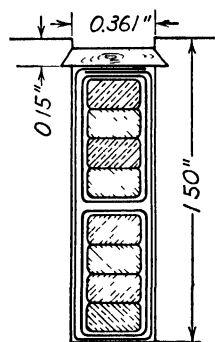


FIG. 167.

This motor is designed with two ventilating ducts each $\frac{1}{2}$ in. wide; ducts $\frac{3}{8}$ in. wide are the more common practice.

The length of the gap section is taken equal to the total armature length, and the air gap density

$$B_g = \frac{\phi_t}{\pi D l} = \frac{25,900 \times 10^3}{3.14 \times 25 \times 7.0}$$

$$= 47.2 \text{ kilo-lines.}$$

The air gap coefficient for an air gap length $\delta = 0.22$ in.

$$k = \frac{l_1}{w_{t1} + (\delta \times y)} = \frac{0.935}{0.574 + (0.22 \times 1.22)}$$

$$= 1.11.$$

The air gap ampere-turns per pole

$$\text{AT}_g = \frac{B_g \delta k}{3.2} = \frac{47,200 \times 0.22 \times 1.11}{3.2}$$

$$= 3600 \text{ ampere-turns.}$$

The maximum tooth density

$$B_{t1} = \frac{\phi_t}{w_{t1}(l - n_d w_d) k_1 S} = \frac{25,900 \times 10^3}{0.574(7.0 - 2 \times 0.5) 0.93 \times 84}$$

$$= 96.5 \text{ kilo-lines.}$$

The width of the armature tooth at a section $\frac{1}{3}$ tooth length from the minimum width

$$w_{t3} = \frac{\pi(D + \frac{2}{3}d_s)}{S} - w_s = \frac{\pi(25 + \frac{2}{3} \times 1.5)}{84} - 0.361$$

$$= 0.611 \text{ in.}$$

$$B_{t3} = \frac{\phi_t}{w_{t3}(l - n_d w_d) k_1 S} = \frac{25,900 \times 10^3}{0.611(7.0 - 2 \times 0.5) 0.93 \times 84}$$

$$= 90.5 \text{ kilo-lines.}$$

From the standard saturation curve for 1 per cent silicon steel, $\text{at}_t = 27$ ampere-turns per inch.

$$\text{AT}_t = \text{at}_t l_t = 27 \times 1.5$$

$$= 41 \text{ ampere-turns.}$$

The flux per pole

$$\begin{aligned}\phi &= \frac{\phi f_d}{p} = \frac{25,900 \times 10^3 \times 0.62}{8} \\ &= 2010 \times 10^3 \text{ lines.}\end{aligned}$$

If the flux density in the armature yoke is taken equal to 80,000 lines per sq. in., then

$$\begin{aligned}d_{ya} &= \frac{\phi}{(l - n_d w_d) k_1 B_{ya}} = \frac{2010 \times 10^3}{(7.0 - 2 \times 0.5) 0.93 \times 80,000} \\ &= 4.5 \text{ in.}\end{aligned}$$

The outside diameter of the armature core

$$\begin{aligned}D_0 &= D + 2d_s + d_{ya} = 25 + 2 \times 1.5 + 4.5 \\ &= 32.5 \text{ in.}\end{aligned}$$

Make the outside diameter 32.5 in., and the armature yoke density

$$B_{ya} = 80 \text{ kilo-lines.}$$

The length of the flux path

$$\begin{aligned}l_{ya} &= \frac{\pi(D + 2d_s + \frac{1}{2}d_{ya})}{2p} = \frac{\pi(25 + 2 \times 1.5 + \frac{1}{2} \times 4.5)}{2 \times 8} \\ &= 5.93 \text{ in.}\end{aligned}$$

$$\text{at}_{ya} = 11 \text{ ampere-turns per in.}$$

$$\text{AT}_{ya} = \text{at}_{ya} l_{ya} = 11 \times 5.93 = 65 \text{ ampere-turns.}$$

From the curves, Fig. 139, the leakage constant will be approximately 1.14. The section area of the pole body

$$\begin{aligned}s_p &= \frac{\phi \lambda}{B_p} = \frac{2010 \times 10^3 \times 1.14}{85,000} \\ &= 27.0 \text{ sq. in.,}\end{aligned}$$

if the flux density, B_p , is assumed equal to 85,000 lines per sq. in. The length of the pole parallel to the shaft is equal to the armature length, and

$$w_p = \frac{27.0}{7.0} = 3.86 \text{ in.; use 3.5 in.}$$

The radial length of the pole is estimated at 5.0 in. (see page 219). The leakage flux is calculated as shown below for machines with a small

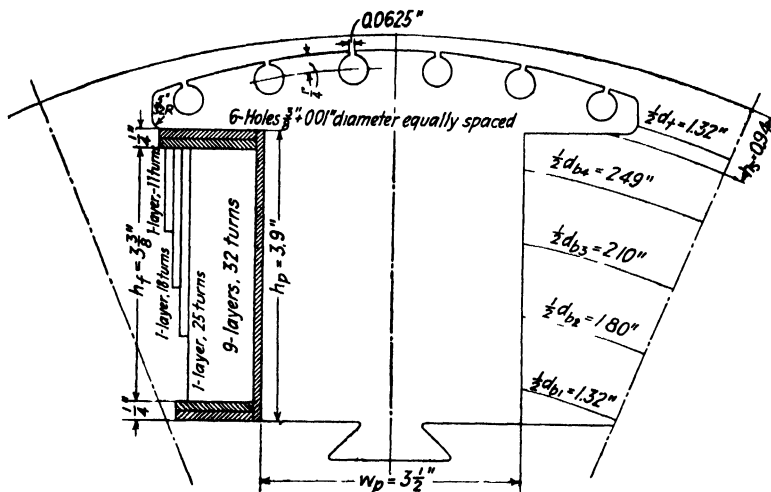


FIG. 168.

number of poles for which the sides of the poles cannot be assumed to be parallel.² The data for these calculations are taken from Fig. 168:

$$l = 7.0, \quad h_s = 0.94, \quad d_t = 2.64, \quad B = 6.875,$$

$$h_p = 3.90, \quad d_{b1} = 2.64, \quad d_{b2} = 3.60, \quad d_{b3} = 4.2,$$

$$d_{b4} = 4.98, \quad w_p = 3.50, \quad X = 3600 + 41 + 65 = 3706.$$

$$(1) \quad 13 \frac{lh_s}{d_t} = 13 \frac{7.0 \times 0.94}{2.64} = 32.5$$

$$(2) \quad 19h_s \log \left(1 + \frac{\pi B}{2d_t} \right) = 19 \times 0.94 \log \left(1 + \frac{\pi \times 6.875}{2 \times 2.64} \right) = 12.7.$$

$$(3) \quad 0.4h_{pl}\left(\frac{1}{d_{b1}} + \frac{3}{d_{b2}} + \frac{5}{d_{b3}} + \frac{7}{d_{b4}}\right) = 0.4 \times 3.9 \times 7.0$$

$$\left(\frac{1}{2.64} + \frac{3}{3.60} + \frac{5}{4.2} + \frac{7}{4.98}\right) = 41.5.$$

² "Field Leakage in Synchronous Machines," by Theo. Schou, *Electrical Review*, Vol. 77, Aug. 21, 1920, p. 281.

$$\begin{aligned}
 (4) \quad & 0.58h_p \left[\log \left(1 + \frac{\pi w_p}{2d_{b1}} \right) + 3 \log \left(1 + \frac{\pi w_p}{2d_{b2}} \right) \right. \\
 & \quad \left. + 5 \log \left(1 + \frac{\pi w_p}{2d_{b3}} \right) + 7 \log \left(1 + \frac{\pi w_p}{2d_{b4}} \right) \right] \\
 & = 0.58 \times 3.9 \left[\log \left(1 + \frac{\pi \times 3.5}{2 \times 2.64} \right) + 3 \log \left(1 + \frac{\pi \times 3.5}{2 \times 3.6} \right) \right. \\
 & \quad \left. + 5 \log \left(1 + \frac{\pi \times 3.5}{2 \times 4.2} \right) + 7 \log \left(1 + \frac{\pi \times 3.5}{2 \times 4.98} \right) \right] = 13.1.
 \end{aligned}$$

$$\phi_i = 3706(32.5 + 12.7 + 41.5 + 13.1) = 370,000 \text{ lines.}$$

$$\lambda = \frac{\phi_i}{\phi} + 1 = \frac{370,000}{2,010,000} + 1 = 1.184.$$

The flux density in the pole body will then be

$$B_p = \frac{2010 \times 10^3 \times 1.184}{3.5 \times 7.0} = 97.2 \text{ kilo-lines per sq. in.}$$

TABLE XXII

Path	Length	90 Per Cent E			100 Per Cent E			115 Per Cent E			125 Per Cent E		
		B	at	AT	B	at	AT	B	at	AT	B	at	AT
Air gap				3240	47.2		3600			4150			4500
Teeth	1.50	81.5	12.0	1890	5.27	0.41	104.0	100.0	150.1	113.1	260.0		390
Armature yoke	5.93	72.0	7.1	4280	0.11	0.65	92.0	31.5	187	100.0	68.0		404
Pole	5.00	87.5	34.0	17097	2.55	0.275	112.0	157.0	78.5	121.5	340.0		1700
Field yoke	2.86	35.7	7.2	2139	7.8	0.23	45.6	9.0	26	49.6	10.8		.31
Total				3491			4004			5298			7025

The length of the flux path in the pole is equal to the radial length of the pole, which has been estimated at 5.0 in. The ampere-turns per pole for hot-rolled sheet steel,

$$AT_p = at_p l_p = 55 \times 5.0 = 275 \text{ ampere-turns.}$$

The field spider is punched from sheet steel, and the poles are assembled as shown in Fig. 103. If the shaft diameter is taken equal to 6.0 in., two times the radial depth of the spider

$$= 25.0 - 2 \times 0.22 - 2 \times 5.0 - 6.0 = 8.56 \text{ in.}$$

The flux density

$$B_{yf} = \frac{2010 \times 10^3 \times 1.184}{8.56 \times 7.0} = 39.7 \text{ kilo-lines per sq. in.}$$

The length of the flux path

$$l_{vf} = \frac{(25 - 2 \times 0.22 - 2 \times 5.0)\pi}{2 \times 8} = 2.86 \text{ in.}$$

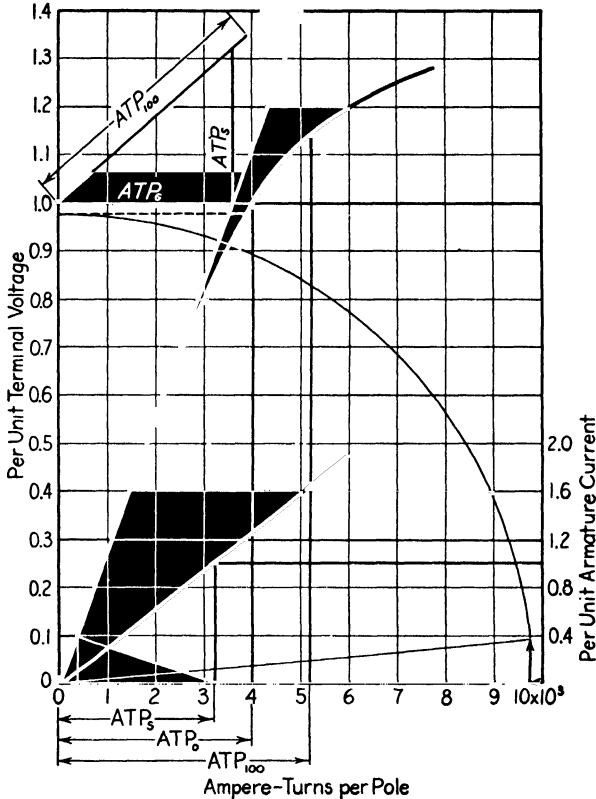


FIG. 169.

From the standard saturation curve for open-hearth sheet steel for field poles, $at_{yf} = 8$ ampere-turns per in.

$$\text{AT}_{yf} = \text{at}_{yf} l_{yf} = 8 \times 2.86 = 23 \text{ ampere-turns.}$$

The calculations for the open-circuit saturation curve are given in Table XXII, and the curve is shown in Fig. 169.

The armature leakage reactance is calculated by formula 148 for a fractional slot winding. The data required are:

$$\begin{aligned} f &= 60, & S_s &= 84, & P &= 0.667, & k_d &= 0.956, \\ l_g &= 7.0, & d_1 &= 1.25, & D &= 25, & \delta &= 0.22, \\ m &= 3, & d_2 &= 0.20, & p &= 8, & K_s &= 0.75, \\ N &= 112, & w_s &= 0.361, & k_p &= 0.866, & k &= 1.11. \end{aligned}$$

$$X_l = \frac{2.0 flmN^2}{S_s \times 10^7}$$

$$\left[K_s \left(\frac{d_1}{3w_s} + \frac{d_2}{w_s} \right) + \frac{0.3(3P - 1)DS_s}{p^2 l} + \frac{0.53Dk_p^2 k_d^2}{S_s \delta k} \right],$$

$$K_s \left(\frac{d_1}{3w_s} + \frac{d_2}{w_s} \right) = 0.75 \left(\frac{1.25}{3 \times 0.361} + \frac{0.20}{0.361} \right) = 1.28.$$

$$\frac{0.3(3P - 1)DS_s}{p^2 l} = \frac{0.3(3 \times 0.667 - 1)25 \times 84}{8^2 \times 7.0} = 1.41.$$

$$\frac{0.53Dk_p^2 k_d^2}{S_s \delta k} = \frac{0.53 \times 25 \times 0.866^2 \times 0.956^2}{84 \times 0.22 \times 1.11} = 0.443.$$

$$X_l = \frac{2.0 \times 60 \times 7.0 \times 3 \times 112^2}{84 \times 10^7} (1.28 + 1.41 + 0.443)$$

$$= 0.118 \text{ ohm per phase.}$$

The per cent reactance drop due to full-load current

$$\frac{IX_l}{E} 100 = \frac{210 \times 0.118}{254} 100 = 9.75 \text{ per cent.}$$

The full-load a-c. resistance drop of the armature winding, using a stray loss factor, $k_5 = 1.25$ (see page 255),

$$\frac{IR_a}{E} 100 = \frac{210 \times 0.0262 \times 1.25}{254} 100 = 2.71 \text{ per cent.}$$

The per cent impedance drop

$$= \sqrt{2.71^2 + 9.75^2} = 10.1 \text{ per cent.}$$

From equation 157, $K_a = 0.86$, and A_1 is equal to 0.993 from page 266.

$$A_{d1} = 0.86 \times 0.993 = 0.855.$$

The equivalent field ampere-turns per pole of armature reaction in the direct axis for full-load current at zero per cent power factor

$$\begin{aligned} AT_{af} &= \frac{0.45K_a m N I_k k_d}{p} \\ &= \frac{0.45 \times 0.86 \times 3 \times 112 \times 210 \times 0.866 \times 0.956}{8} \\ &= 2830 \text{ ampere-turns.} \end{aligned}$$

The direct axis synchronous impedance curve is shown in Fig. 169, and the short-circuit ratio

$$\frac{ATP_o}{ATP_s} = \frac{4000}{3200} = 1.25.$$

The unsaturated short-circuit ratio

$$\text{scr} = \frac{3600}{3200} = 1.124.$$

The per unit unsaturated direct-axis synchronous reactance

$$X_d = \frac{1}{1.124} = 0.89.$$

The per unit armature reaction reactance

$$X_{ad} = 0.89 - 0.098 = 0.792.$$

When calculating the per unit resistance and reactance for a leading power factor synchronous motor the in-phase component of the input current is used instead of the total input current.

For the pole shoe form used for this design it is probably more accurate to use f_d instead of ψ in the calculation of A_{q1} .

$$\begin{aligned} A_{q1} &= \frac{4 \times 0.62 + 1}{5} - \frac{\sin 0.62 \times 180}{\pi} \\ &= 0.40. \end{aligned}$$

The per unit armature reaction reactance in the quadrature axis

$$X_{aq} = X_{ad} \frac{A_{q1}}{A_{d1}} = 0.792 \frac{0.400}{0.855} = 0.37.$$

The per unit unsaturated synchronous reactance in the quadrature axis

$$X_q = 0.098 + 0.37 = 0.468.$$

The field ampere-turns per pole for full-load at unity power factor are found graphically as shown in Fig. 169,

$$\text{ATP}_{100} = 5220.$$

The field winding for this machine will be of the wire-wound type. The average depth of the coil is estimated at 1.0 in. (see Fig. 168), and the approximate mean length of turn

$$\begin{aligned} L_f &= 2 \times 7.0 + 2(3.5 - 0.25) + \pi(0.45 + 1.0) \\ &= 25.05 \text{ in.} \end{aligned}$$

The section area of the conductor

$$\begin{aligned} s_f &= \frac{\text{ATP}_{100} L_{fp} \times 0.826}{E_f \times 10^6} = \frac{5220 \times 25.05 \times 8 \times 0.826}{120 \times 10^6} \\ &= 0.0072 \text{ sq. in.} \end{aligned}$$

A number 11 square conductor is selected. The dimensions are: bare diameter 0.091 in., insulated diameter 0.103 in., area 0.00775 sq. in. For a current density of 2000 amperes per sq. in., the field current

$$\begin{aligned} i_f &= s_f A_f = 0.00775 \times 2000 \\ &= 15.5 \text{ amperes,} \end{aligned}$$

and the turns per pole

$$t_f = \frac{\text{ATP}_{100}}{i_f} = \frac{5220}{15.5} = 337.$$

From the sketch, Fig. 168, the height of the winding space $h_f = 3.4$ in. The number of turns per layer $= \frac{3.4}{0.103} = 33$. In winding the field coils, the space of one turn is required in passing from one layer to the next; therefore 32 turns per layer are used. At the base of the pole, the depth of the field coil can be approximately 0.90 in., which will permit 9 layers. The remainder of the turns are wound as shown in Fig. 168, making a total of 342 turns.

The corrected length of mean-turn

$$\begin{aligned} L_{f1} &= 2l_1 + 2(w_p - 0.25) + \pi(0.45 + 2d_1) \\ &= 2 \times 7.0 + 2(3.5 - 0.25) + \pi(0.45 + 2 \times 0.464) = 24.83 \text{ in.} \end{aligned}$$

$$\begin{aligned} L_{f2} &= 2l_1 + 2(w_p - 0.25) + \pi(0.45 + 2d_2) \\ &= 2 \times 7.0 + 2(3.5 - 0.25) + \pi(0.45 + 2 \times 0.98) = 28.07 \text{ in.} \end{aligned}$$

$$L_{f3} = 2l_1 + 2(w_p - 0.25) + \pi(0.45 + 2d_3) \\ = 2 \times 7.0 + 2(3.5 - 0.25) + \pi(0.45 + 2 \times 1.08) = 28.70 \text{ in.}$$

$$L_{f4} = 2l_1 + 2(w_p - 0.25) + \pi(0.45 + 2d_4) \\ = 2 \times 7.0 + 2(3.5 - 0.25) + \pi(0.45 + 2 \times 1.18) = 29.33 \text{ in.}$$

$$L_f = \frac{L_{f1}t_{f1} + L_{f2}t_{f2} + L_{f3}t_{f3} + L_{f4}t_{f4}}{t_f} \\ = \frac{24.83 \times 288 + 28.07 \times 25 + 28.70 \times 18 + 29.33 \times 11}{342} \\ = 25.4 \text{ in.}$$

The resistance of the field winding at 75° C.

$$R_f = \frac{L_f t_f p \times 0.826}{s_f \times 10^6} = \frac{25.4 \times 342 \times 8 \times 0.826}{0.00775 \times 10^6} \\ = 7.4 \text{ ohms.}$$

If 5 volts drop is allowed for the exciter leads and brush contacts, the field current

$$i_f = \frac{120}{7.4} = 16.2 \text{ amperes,}$$

and the field copper loss

$$W_f = i_f^2 R_f = 16.2^2 \times 7.4 = 1940 \text{ watts.}$$

The radiating surface

$$S_f = 2(d_f + h_f)L_f p = 2(1.24 + 3.38)25.4 \times 8 \\ = 1880 \text{ sq. in.}$$

The surface per watt loss

$$\frac{S_f}{W_f} = \frac{1880}{1940} = 0.97.$$

The exciter capacity required

$$W_e = \frac{E_f^2}{R_f \times 10^3} = \frac{125^2}{7.4 \times 10^3} = 2.11 \text{ kilowatts.}$$

The weight of field copper

$$G_f = L_f t_f p s_f \times 0.321 \\ = 25.4 \times 342 \times 8 \times 0.00775 \times 0.321 \\ = 173 \text{ lb.}$$

The squirrel-cage winding for synchronous motors is placed in the pole shoe and is designed to produce the required starting and pull-in torque with minimum starting kva.³ To avoid dead points, that is, points of low or zero torque in the speed torque curve, it is important that the rotor bar pitch and the stator tooth pitch be not the same. The rotor bar pitch should be 15 to 20 per cent larger or smaller than the stator tooth pitch. The resistance of the squirrel-cage winding determines the torque and kva during the starting period. The squirrel-cage winding resistance depends upon the length, section area, and material of the bars. Two starting windings are designed for this motor, a single-cage and a double-cage. The single-cage winding has six $\frac{3}{8}$ -in.-diameter round copper bars placed in the pole shoe as shown in Fig. 168. The section area of the end-ring is calculated as explained on page 321.

$$s_{er} = \frac{0.32s_b N_b}{p} = \frac{0.32 \times 0.111 \times 48}{8} = 0.213 \text{ sq. in.}$$

A rolled copper strap is used for the end-ring, $\frac{3}{16}$ in. by 1.25 in., with section area 0.234 sq. in. The bars are allowed to extend 2.0 in. beyond the pole iron on each end to provide room for the end-ring. The length of the bars is then 11.0 in.

The per unit constants for the equivalent circuit shown in Fig. 147a for a single-cage winding are calculated as shown below. The stator reactance has been calculated on page 276, and the per unit value

$$X_1 = 0.118 \frac{210}{254} = 0.098.$$

The per unit rotor reactance in terms of the stator winding (see page 230)

$$\begin{aligned} X_2 &= \frac{2.0 f l m N^2}{S_s 10^7} \frac{k_p^2 k_d^2 S_s}{S_r} \left[\left(0.62 + \frac{d_4}{w_{s1}} \right) + \frac{0.266 D}{S_s \delta k} \right] \frac{I}{E} \\ &= \frac{2.0 \times 60 \times 7 \times 3 \times 112^2}{84 \times 10^7} \frac{0.866^2 \times 0.956^2 \times 84}{48} \times \\ &\quad \left[0.62 + \frac{0.063}{0.063} + \frac{0.266 \times 25}{48 \times 0.22 \times 1.11} \right] \frac{210}{254} \\ &= 0.0816. \end{aligned}$$

³ For the starting and pull-in torque requirements for synchronous motors see A.S.A. Standards C50, March, 1943, p. 25. These standards may be obtained from the American Standards Association, 70 East 45 Street, New York 17, N.Y.

The per unit magnetizing reactance is calculated from the unsaturated short-circuit ratio given on page 277.

$$X_m = \frac{1}{\text{scr}} - X_1 = \frac{1}{1.124} - 0.098 = 0.792.$$

The per unit reactance of the field winding in terms of the stator winding

$$X_{fs} = \frac{2.0flmN^2}{S_s \times 10^7} k_p^2 k_d^2 S_s \frac{\phi_l}{10X_{pl}} \frac{I}{E}.$$

Here, ϕ_l is the field leakage flux in lines calculated on page 274, and X is the sum of the field ampere-turns per pole for gap, armature teeth, and yoke.

$$\begin{aligned} X_{fs} &= \frac{2.0 \times 60 \times 7 \times 3 \times 112^2}{84 \times 10^7} 0.866^2 \times \\ &\quad 0.956^2 \times 84 \frac{370,000}{10 \times 3706 \times 8 \times 7} \frac{210}{254} \\ &= 0.32. \end{aligned}$$

The resistance of the armature winding is given on page 270 for 75° C. For starting performance calculations the resistance of the windings at 25° C. is used. The per unit armature resistance at 25° C.

$$R_1 = 0.022 \frac{210}{254} = 0.0182.$$

The per unit field winding resistance plus the field discharge resistance equal to 4 times R_f in terms of the stator winding at 25° C.

$$\begin{aligned} R_{fs} &= \frac{0.70 k_p^2 k_d^2 N^2 R_f}{p^2 t_f^2} \frac{I}{E} \\ &= \frac{0.70 \times 0.866^2 \times 0.956^2 \times 112^2 \times 31.2}{8^2 \times 342^2} \frac{210}{254} \\ &= 0.0208. \end{aligned}$$

The per unit squirrel-cage winding resistance in terms of the stator winding at 25° C.

$$\begin{aligned} R_2 &= \frac{k_p^2 k_d^2 N^2 m r}{10^6} \left[\frac{l_b}{s_b N_b} + \frac{0.64 D_{cr}}{p^2 s_{rr}} \right] \frac{I}{E} \\ &= \frac{0.866^2 \times 0.956^2 \times 112^2 \times 3 \times 0.692}{10^6} \times \\ &\quad \left[\frac{11.0}{0.111 \times 48} + \frac{0.64 \times 24}{8^2 \times 0.234} \right] \frac{210}{254} \\ &= 0.0455. \end{aligned}$$

The constants are now put into the equivalent circuit of Fig. 147a and the per unit input current and torque calculated for a slip of 1.0 and 0.05. When the slip is 1.0, that is, at starting, the per unit current and torque are calculated as follows:

$$\begin{aligned}
 Z_{fs} &= 0.0208 + j0.32 = 0.32 / 86.3^\circ, & Y_{fs} &= 0.203 - j3.12 = 3.125 / -86.3^\circ. \\
 Z_2 &= 0.0455 + j0.0816 = 0.0934 / 61.6^\circ, & Y_2 &= 5.22 - j9.37 = 10.70 / -60.9^\circ. \\
 Z_{2T} &= 0.0293 + j0.0673 = 0.0735 / 66.5^\circ, & Y_{2T} &= 5.423 - j12.49 = 13.6 / -66.5^\circ. \\
 X_m &= j0.792, & Y_m &= 0 - j1.26. \\
 Z &= 0.0246 + j0.0644 = 0.069 / 68.5^\circ, & Y &= 5.423 - j13.75 = 14.79 / -68.5^\circ. \\
 Z_1 &= 0.0182 + j0.098. \\
 Z_T &= 0.043 + j0.1609 = 0.1665 / 75^\circ. \\
 I_1 &= \frac{1}{Z_T} = \frac{1}{0.1665} = 6.0. \\
 I_2 &= I_1 \frac{Z}{Z_{2T}} = 6.0 \frac{0.0677}{0.0735} = 5.53. \\
 T &= I_2^2 R_{2T} \frac{1}{\text{rated pf}} = 5.53^2 \times 0.0293 = 0.895.
 \end{aligned}$$

When the slip is 0.05, that is, at pull-in, the per unit current and torque calculations are made as shown below:

$$\begin{aligned}
 Z_{fs} &= 0.415 + j0.32 = 0.524 / 37.6^\circ, & Y_{fs} &= 1.51 - j1.165 = 1.91 / -37.6^\circ. \\
 Z_2 &= 0.91 + j0.0816 = 0.915 / 5.2^\circ, & Y_2 &= 1.095 - j0.0987 = 1.10 / -5.2^\circ. \\
 Z_{2T} &= 0.31 + j0.150 = 0.345 / 25.9^\circ, & Y_{2T} &= 2.605 - j1.264 = 2.90 / -25.9^\circ. \\
 X_m &= j0.792, & Y_m &= 0 - j1.26. \\
 Z &= 0.198 + j0.192 = 0.276 / 44.1^\circ, & Y &= 2.605 - j2.524 = 3.63 / -44.1^\circ. \\
 Z_1 &= 0.0182 + j0.098. \\
 Z_T &= 0.2162 + j0.29 = 0.362 / 53.3^\circ. \\
 I_1 &= \frac{1}{Z_T} = \frac{1}{0.362} = 2.76. \\
 I_2 &= I_1 \frac{Z}{Z_{2T}} = 2.76 \frac{0.276}{0.345} = 2.21. \\
 T &= I_2^2 R_{2T} \frac{1}{\text{rated pf}} = 2.21^2 \times 0.31 = 1.52.
 \end{aligned}$$

For the double squirrel-cage-winding design the outer bars at the pole shoe surface are brass, $\frac{5}{16}$ in. in diameter and set $\frac{1}{16}$ in. below the pole shoe face with $\frac{1}{16}$ -in.-wide reluctance slots. Two $\frac{1}{2}$ -in.-diameter copper bars are used for the lower cage and placed $\frac{1}{8}$ in. below the two center bars with a $\frac{1}{16}$ -in.-wide reluctance slot between them. The end-ring has the same dimensions as the one for the single-cage design and is common to both windings. The equivalent circuit for a combination single- and double-cage winding is shown in Fig. 147c, and the per unit constants are calculated as shown below:

The per unit stator reactance

$$X_1 = 0.098.$$

The per unit reactance of the four single-cage bars in the tips of the pole shoe

$$X_2 = \frac{2.0 \times 60 \times 7 \times 3 \times 112^2}{84 \times 10^7} \frac{0.866^2 \times 0.956^2 \times 84}{32} \times \left[0.62 + \frac{0.063}{0.063} + \frac{0.266 \times 25}{32 \times 0.22 \times 1.11} \right] \frac{210}{254} = 0.138.$$

The per unit magnetizing reactance

$$X_m = 0.792.$$

The per unit reactance for the two top cage bars

$$X_{2t} = \frac{2.0 \times 60 \times 7 \times 3 \times 112^2}{84 \times 10^7} \frac{0.866^2 \times 0.956^2 \times 84}{16} \times \left(0.62 + \frac{0.063}{0.063} + \frac{0.266 \times 25}{16 \times 0.22 \times 1.11} \right) \frac{210}{254} = 0.372.$$

The per unit reactance of the two lower cage bars

$$X_{2b} = \frac{2.0 \times 60 \times 7 \times 3 \times 112^2}{84 \times 10^7} \frac{0.866^2 \times 0.956^2 \times 84}{16} \times \left(0.62 + \frac{0.063}{0.063} + \frac{0.266 \times 25}{16 \times 0.22 \times 1.11} \right) \frac{210}{254} = 0.484.$$

The per unit reactance of the field winding

$$X_{fs} = 0.32.$$

The per unit stator resistance at 25° C.

$$R_1 = 0.0182.$$

The per unit field winding resistance plus the discharge resistance of 25 ohms at 25° C.

$$R_{fs} = 0.0208.$$

The per unit squirrel-cage winding resistance for the four single-cage brass bars at 25° C.

$$R_2 = \frac{0.866^2 \times 0.956^2 \times 112^2 \times 3 \times 0.692}{10^6} \times \left(\frac{11.0 \times 4}{32 \times 0.0766} + \frac{0.64 \times 24}{8^2 \times 0.234} \right) \frac{210}{254} = 0.281.$$

The per unit resistance of the two brass bars of the upper cage winding at 25° C.

$$R_{2t} = \frac{0.866^2 \times 0.956^2 \times 112^2 \times 3 \times 0.692}{10^6} \times \left(\frac{11 \times 4}{16 \times 0.0766} + \frac{0.64 \times 24}{8^2 \times 0.234} \right) \frac{210}{254} = 0.546.$$

The per unit resistance of the two copper bars of the lower cage winding at 25° C.

$$R_{2b} = \frac{0.866^2 \times 0.956^2 \times 112^2 \times 3 \times 0.692}{10^6} \times \left(\frac{11.0}{16 \times 0.197} + \frac{0.64 \times 24}{8^2 \times 0.234} \right) \frac{210}{254} = 0.067.$$

When the slip is 1.0, that is, at starting, the calculations for per unit current and torque are carried out as shown below:

$$\begin{aligned} Z_{2b} &= 0.067 + j0.484 = 0.484 / \underline{82.1^\circ}, & Y_{2b} &= 0.285 - j2.06 = 2.08 / \underline{-82.1^\circ}, \\ R_{2t} &= 0.546, & g_{2t} &= 1.83, \\ Z_{2b} + R_{2t} &= 0.243 + j0.236 = 0.339 / \underline{43.9^\circ}, & Y_{2b} + g_{2t} &= 2.115 - j2.06 = 2.95 / \underline{-43.9^\circ}, \\ X_{2t} &= j0.372, \\ Z_{2bt} &= 0.243 + j0.608 = 0.655 / \underline{68.3^\circ}, & Y_{2bt} &= 0.566 - j1.42 = 1.53 / \underline{-68.3^\circ}, \\ Z_2 &= 0.281 + j0.138 = 0.314 / \underline{26.2^\circ}, & Y_2 &= 2.86 - j1.41 = 3.19 / \underline{-26.2^\circ}, \\ Z_{fs} &= 0.0208 + j0.32 = 0.32 / \underline{86.3^\circ}, & Y_{fs} &= 0.203 - j3.12 = 3.13 / \underline{-86.3^\circ}, \\ Z_{2T} &= 0.0747 + j0.1225 = 0.1435 / \underline{58.6^\circ}, & Y_{2T} &= 3.629 - j5.95 = 6.97 / \underline{-58.6^\circ}, \\ X_m &= j0.792, & Y_m &= 0 - j1.26, \\ Z &= 0.057 + j0.1115 = 0.1252 / \underline{63^\circ}, & Y &= 3.629 - j7.11 = 7.98 / \underline{-63^\circ}, \\ Z_1 &= 0.0182 + j0.098, \\ Z_T &= 0.0752 + j0.2095 = 0.222 / \underline{70.3^\circ}, \\ I_1 &= \frac{1}{Z_T} = \frac{1}{0.222} = 4.5, \\ I_2 &= I_1 \frac{Z}{Z} = 4.5 \frac{0.1252}{0.1435} = 3.93, \\ T &= I_2^2 R_{2T} \frac{1}{\text{rated pf}} = 3.93^2 \times 0.0747 = 1.16. \end{aligned}$$

The calculations for per unit current and torque from the equivalent circuit of Fig. 147c for a slip of 0.05, at pull-in, are shown below:

$$\begin{aligned} Z_{2b} &= 1.34 + j0.484 = 1.426 / \underline{19.8^\circ}, & Y_{2b} &= 0.661 - j0.238 = 0.702 / \underline{-19.8^\circ}, \\ R_{2t} &= 10.9, & g_{2t} &= 0.917. \end{aligned}$$

$$\begin{aligned}
Z_{2b} + R_{2t} &= 1.21 + j0.382 = 1.267 / 17.6^\circ, & Y_{2b} + g_t &= 0.7527 - j0.238 = 0.79 / -17.6^\circ, \\
X_{2t} &= j0.372, \\
Z_{2bt} &= 1.21 + j0.754 = 1.425 / 31.9^\circ, & Y_{2bt} &= 0.596 - j0.371 = 0.702 / -31.9^\circ, \\
Z_2 &= 5.62 + j0.138 = 5.62 / 1.4^\circ, & Y_2 &= 0.178 - j0.00437 = 0.178 / -1.4^\circ, \\
Z_{fs} &= 0.415 + j0.32 = 0.524 / 37.6^\circ, & Y_{fs} &= 1.51 - j1.165 = 1.91 / -37.6^\circ, \\
Z_{2T} &= 0.301 + j0.203 = 0.364 / 34^\circ, & Y_{2T} &= 2.284 - j1.54 = 2.75 / -34^\circ, \\
X_m &= +j0.792, & Y_m &= 0 - j1.26, \\
Z &= 0.175 + j0.214 = 0.277 / 50.8^\circ, & Y &= 2.284 - j2.80 = 3.61 / -50.8^\circ, \\
Z_1 &= 0.0182 + j0.098, \\
Z_T &= 0.1932 + j0.312 = 0.367 / 58.2^\circ, \\
I_1 &= \frac{1}{Z_T} = \frac{1}{0.367} = 2.725, \\
I_2 &= I_1 \frac{Z}{Z_{2T}} = 2.725 \frac{0.277}{0.364} = 2.075, \\
T &= I_2^2 R_{2T} \frac{1}{\text{rated pf}} = 2.075^2 \times 0.301 = 1.295.
\end{aligned}$$

The results of the current and torque calculations are summed up below.

Winding	Starting $s = 1$		Pull-in $s = 0.05$	
	p.u. Current	p.u. Torque	p.u. Current	p.u. Torque
Single-cage	6.0	0.895	2.76	1.52
Double-cage	4.5	1.16	2.725	1.295

The armature copper loss for full-load

$$\begin{aligned}
W_a &= R_a I_a^2 = 0.0262 \times 210^2 \times 3 \\
&= 3460 \text{ watts.}
\end{aligned}$$

The field current for full-load at 100 per cent power factor = 16.2 amperes. With 125 volts applied at the collector rings,

$$\begin{aligned}
W_f &= i_f E_c = 16.2 \times 125 \\
&= 2020 \text{ watts.}
\end{aligned}$$

The weight of the armature teeth

$$\begin{aligned}
G_{ct} &= 0.63(7 - 2 \times 0.5)0.93 \times 84 \times 1.50 \times 0.278 \\
&= 123 \text{ lb.}
\end{aligned}$$

The weight of the armature yoke

$$\begin{aligned}
G_{cy} &= \frac{\pi}{4} [32.5^2 - (25 + 3)^2](7 - 2 \times 0.5)0.93 \times 0.278 \\
&= 334 \text{ lb.}
\end{aligned}$$

The loss per pound in the armature teeth, due to the fundamental frequency flux for the density, $B_{t3} = 90.5$ kilo-lines = 2.82 watts for 1 per cent silicon steel, 26 gauge. The loss in the teeth

$$W_{ct} = 2.82 \times 123 = 347 \text{ watts.}$$

The loss per pound in the armature yoke due to the fundamental frequency flux = 2.18 watts for 1 per cent silicon steel. The loss in the yoke $W_{cy} = 2.18 \times 334 = 728$ watts. The total core loss

$$W_c = (347 + 728)2 = 2150 \text{ watts.}$$

The friction and windage losses are taken from the curves in Fig. 159 and are equal to 1200 watts.

The stray load-losses will be estimated at 25 per cent of the armature I^2R loss.

The efficiency calculations in Table XXIII are for unity power factor at all loads.

TABLE XXIII

Losses	$\frac{1}{4}$	$\frac{2}{4}$	$\frac{3}{4}$	$\frac{4}{4}$	$\frac{5}{4}$
Armature I^2R	0 22	0 86	1 95	3 46	5.40
Stray load.	0 22	0 13	0 65	0 87	1.08
Field winding.	1 21	1 44	1 68	2 02	2.22
Core.	2 15	2.15	2 15	2 15	2.15
Friction and windage. . .	1 20	1.20	1 20	1.20	1.20
Total.	5 00	6.08	7 63	9.70	12.05
Output.	37 30	74 60	112 00	149 00	186 50
Output + losses.	42 30	80 68	119 63	158 70	198 55
Efficiency, per cent.	89 1	92.4	93 8	94 0	94 0

The effective radiating surface of the armature

$$\begin{aligned}
 S_a &= \frac{\pi}{4} (D_0^2 - D^2)(2 + n_d) + \pi l(D + D_0) \\
 &= \frac{\pi}{4} (32.5^2 - 25^2)(2 + 2) + \pi \times 7(32.5 + 25) \\
 &= 2625 \text{ sq. in.}
 \end{aligned}$$

The radiating surface per watt loss

$$\frac{S_a}{W} = \frac{2625}{2150 + 4330 \frac{7}{18.35}} = 0.691 \text{ sq. in. per watt.}$$

The radiating surface per watt loss for the field winding has been calculated on page 279.

For motors driving centrifugal pumps and in general for high-speed motors it is not necessary to calculate the displacement angle and synchronizing power. For slow-speed synchronous motors direct-connected to periodic fluctuating loads, such as air and ammonia compressors, these calculations must be made to determine the proper flywheel to limit the armature current pulsations⁴ to safe values.

For full-load and unit power factor

$$\begin{aligned}\delta_e &= \sin^{-1} \frac{X_q \cos \theta}{\sqrt{1 + X_q^2 + 2X_q \sin \theta}} \\ &= \sin^{-1} \frac{0.468 \times 1}{\sqrt{1 + 0.468^2}} \\ &= 26.2^\circ. \\ P_r &= \frac{57.3 \times 0.746 \times \text{hp.}}{\delta_e} \\ &= \frac{57.3 \times 0.746 \times 200}{26.2} \\ &= 327 \text{ kw.}\end{aligned}$$

The shafts for electric machinery must be rigid to guard against flexing due to unbalanced magnetic pull between rotor and stator. When the rotor is perfectly centered inside the stator, that is, uniform air gap length around entire rotor periphery, the pull of each pole is balanced by an equal pull diametrically opposite. When the air gap is slightly smaller on one side of the rotor a large unbalanced pull is produced. For purposes of shaft design the unbalanced magnetic pull is calculated for a rotor displacement of $\frac{1}{32}$ inch.

The magnetic pull between each field pole and stator core

$$P_p = \frac{f_d^2 S_p B_p^2}{8\pi 2.54^2 \times 445,000} = \frac{f_d^2 B_p \phi_p}{720 \times 10^6} \text{ pounds.}$$

For $\frac{1}{32}$ -in. rotor displacement the unbalanced pull on the rotor

$$P_d = \frac{B_p \phi_p f_d^2 p}{1920\delta \times 10^6} \text{ pounds.}$$

⁴ See reference, page 238.

III — INDUCTION MOTORS

CHAPTER XVI

CONSTRUCTION

POLYPHASE motors are built in sizes from $\frac{1}{2}$ hp. to very large sizes, several thousand horse-power. There are two types of polyphase induction motors in general use: (1) the polyphase squirrel-cage motor,

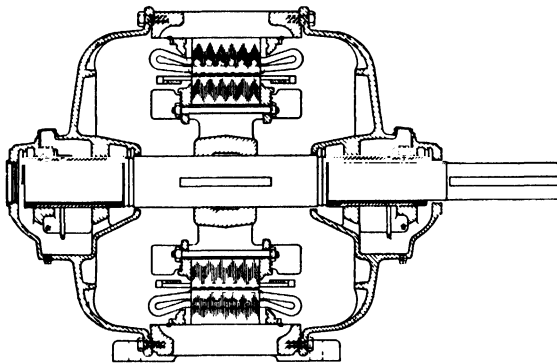


FIG. 170.—Cross-section of squirrel-cage induction motor.

and (2) the polyphase wound-rotor, or slip-ring motor.

The types of construction generally employed are shown in Figs. 170, 171, and 172.

Stator.—The construction of the stator or field of the induction motor is generally the same as the armature of synchronous machines. For small

machines, the same stator is often used for either a synchronous machine or an induction motor.

The stator laminations are punched from electric sheet steel with from 1 to 3.0 per cent silicon. The thickness of the sheet is usually from 0.014 in., for machines for which low core loss is important, to 0.019 in. For small-diameter machines, the stator laminations are often punched in one piece. For the larger diameters, segmental punchings are always used. Figure 173 shows a one-piece stator punching with partially closed slots and two segmental punchings, one with open slots and one with partially closed slots. The punchings are assembled in the stator frame as shown in Figs. 170, 171, and 172. When the length of the stator core exceeds 4 or 5 in., it must be divided into sections by radial ventilating ducts to insure proper ventilation of

the core and winding. The ventilating ducts are $\frac{3}{8}$ in. wide for moderate sized machines and $\frac{1}{2}$ in. for large machines. The distance between centers of ducts should not exceed 3 in. A ventilating duct is generally provided at each end of the stator by the tooth supports. An assembled stator core with part of the stator coils in place is shown in Fig. 174.

For small-diameter motors partly closed stator slots are used and the teeth, instead of the slots, have parallel sides. Figure 175 shows one punching for a 1-hp, 3-phase, 4-pole, 1800-r.p.m. motor.

The stator frames for very large motors are as a rule built up of welded rolled steel plate just as the armature frames of synchronous machines (see Fig. 176).

Rotor.—The rotor is built of sheet steel laminations, generally punched from the same material as that used for the stator. For small motors, the rotor punchings are punched in one piece and assembled on the shaft. Figure 177 shows one rotor punching for a 1-hp, 4-pole, squirrel-cage motor. One-piece punchings are used for medium diameters; for large diameters segmental punchings must be used. These are assembled on a spider and clamped between two end-plates by through-bolts, as shown in Fig. 178.

When ventilating ducts are required in the stator, an equal number of ducts of the same size are used in the rotor. For squirrel-cage rotors, the slots are generally shallow and the tooth supports and venti-

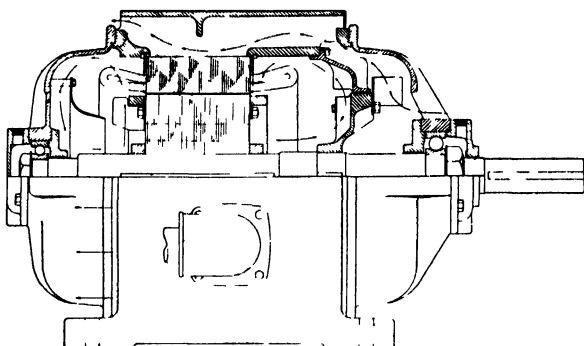


FIG. 171 Sectional assembly of totally enclosed squirrel-cage motor with ball bearings

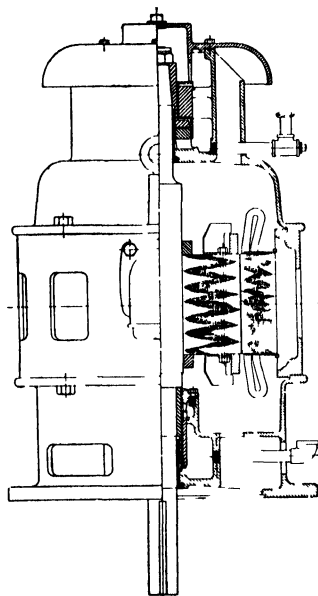


FIG. 172.—Cross-section of vertical squirrel-cage motor.

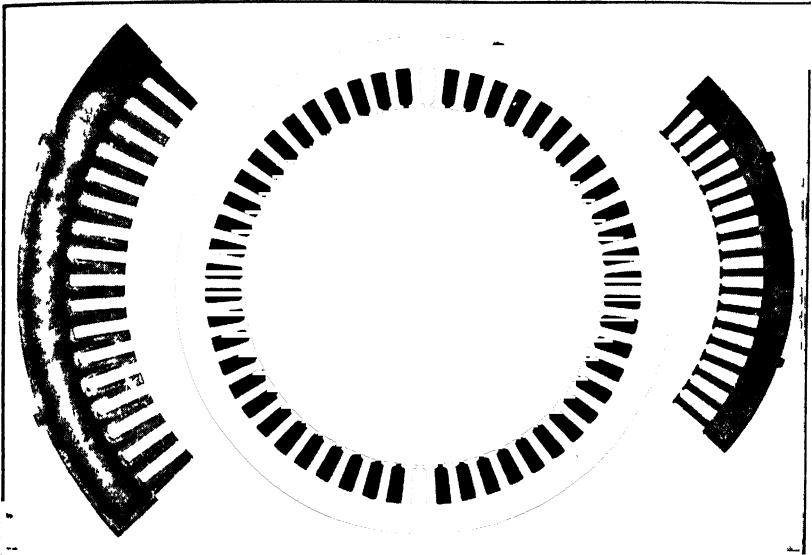


FIG. 173.—Induction motor stator punchings.

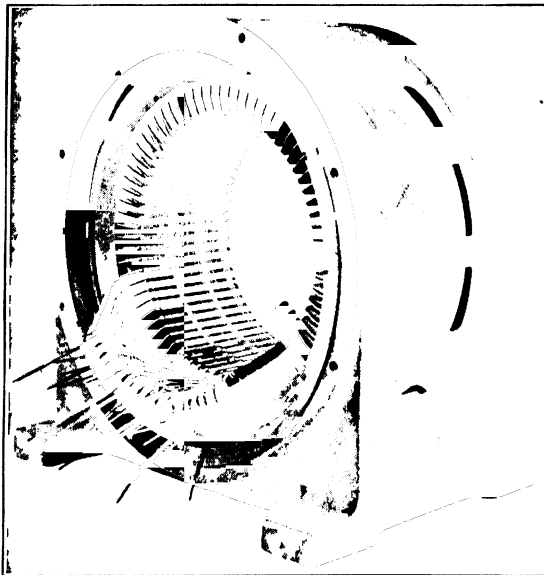


FIG. 174.—Partially wound stator with open slots.

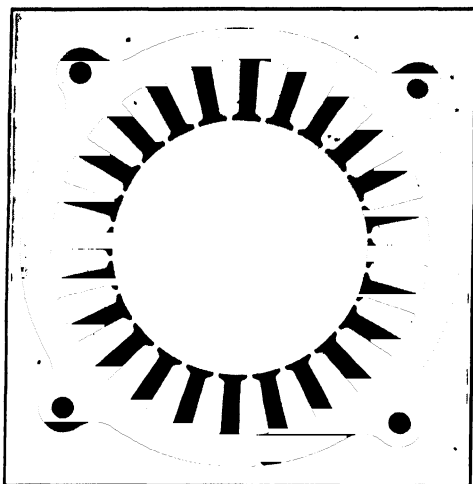


Fig. 175.—Stator punching for 1-hp, 1800-r.p.m., three-phase, 60-cycle motor.

Outside diameter $7\frac{1}{4}$ in.
 Inside diameter $4\frac{1}{2}$ in.
 Slot opening 0.11 in.

Slot width $\begin{cases} \text{top } 0.35 \text{ in.} \\ \text{bottom } 0.50 \text{ in.} \end{cases}$
 Slot depth 1.0 in.

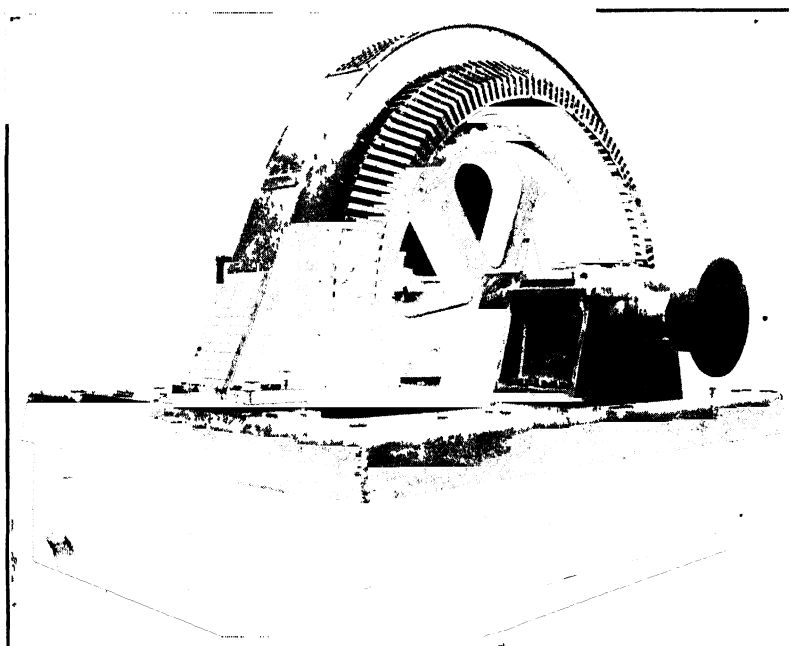


Fig. 176.—1500-hp, 36-pole, 200-r.p.m., 6600-volt mill type induction motor with welded rolled-steel stator frame.

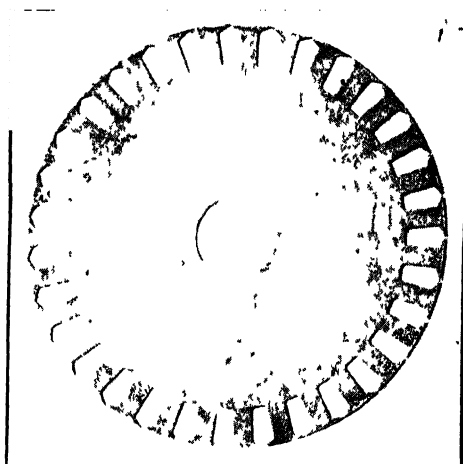


FIG. 177.—Rotor punching for 1-hp, 1800-r.p.m., three-phase, 60-cycle motor.

Outside diameter 4 22 in.

Shaft diameter $\frac{1}{2}$ in.

Slot width $\left\{ \begin{array}{l} \text{top 0.22 in.} \\ \text{bottom 0.16 in.} \end{array} \right.$

Slot depth 0.41 in.

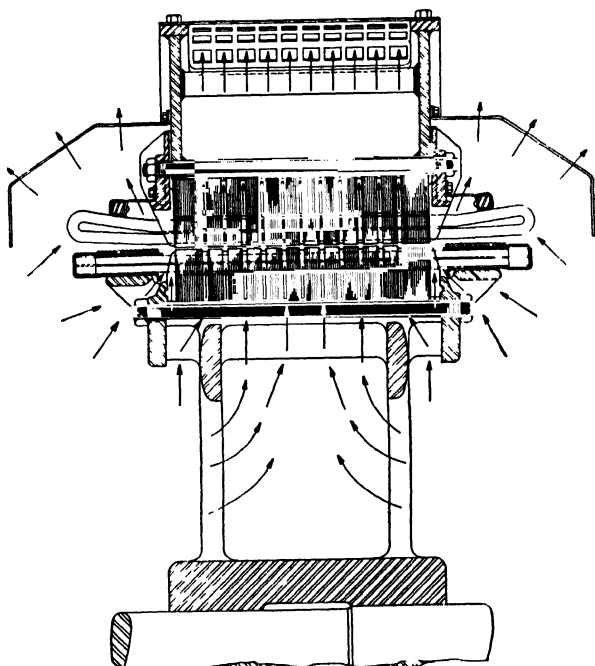


FIG. 178.—Sectional view of stator and rotor.

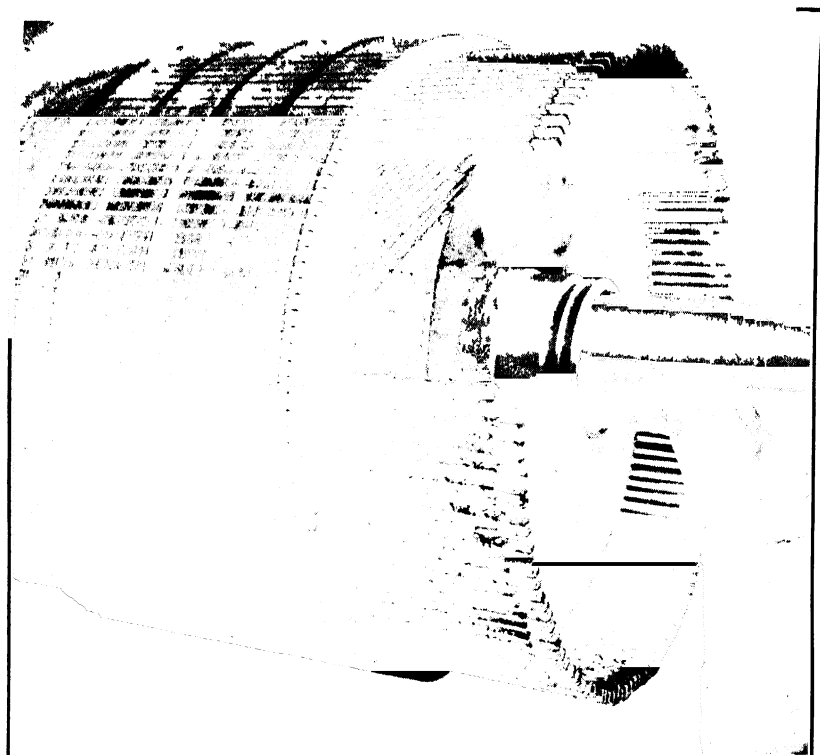


FIG. 179—Partially wound slip ring rotor

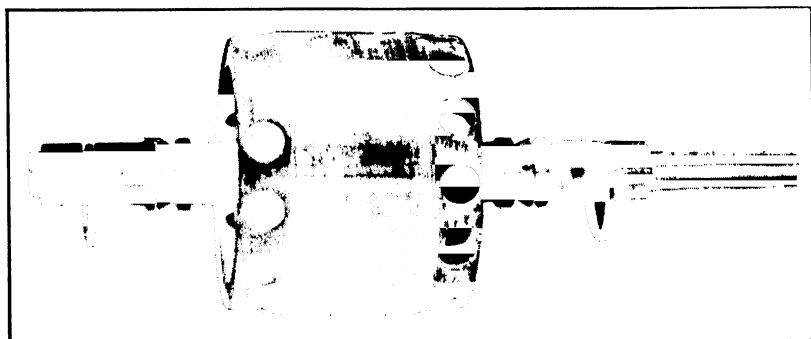


FIG. 180—Complete rotor with cast squirrel-cage winding.

lating ducts at each end of the armature core are often omitted. For the slip-ring motor, insulated windings must be used in the rotor, which require deep slots and tooth supports at each end of the rotor core, similar to those used for the stator. A sectional view of stator and rotor for a large-capacity, wound-rotor motor is shown in Fig. 178, and a partially wound slip-ring rotor is shown in Fig. 179.

The squirrel-cage winding is generally built up of rectangular or round copper bars joined at each end by a copper end-ring. A cast squirrel-cage winding is used by several manufacturers. The metal used is aluminum and is cast into the assembled rotor core. With this method of construction, it is possible to use a large number of rotor slots on small-diameter rotors without excessive tooth densities, because teeth with parallel sides can be used with trapezoid-shaped slots. The rotor punching shown in Fig. 177 is for a cast squirrel-cage rotor. A complete rotor with cast squirrel-cage winding is shown in Fig. 180.

CHAPTER XVII

THE STATOR

THE design of the stator of an induction motor is carried out in the same way as the armature design of a synchronous motor or generator. The voltage induced in the stator winding

$$E = \frac{\phi n N k_p C_w}{60 \times 10^8} \text{ volts per phase.} \quad (170)$$

This formula is explained on page 174.

A sine-wave flux distribution is generally assumed for the induction motor, because the distributed stator winding produces an air gap flux wave which is very nearly sinusoidal. The form factor and flux-distribution factor have been explained on page 181. They are equal to 1.11 and 0.637 respectively for a sine wave. The winding-distribution factor has been carefully explained on page 193. It may be taken equal to 0.956 for 3-phase windings and 0.91 for 2-phase windings. The winding constant

$$C_w = f_i f_d k_d = 1.11 \times 0.637 \times 0.956 = 0.677 \text{ for 3-phase,}$$

$$C_w = f_i f_d k_d = 1.11 \times 0.637 \times 0.91 = 0.643 \text{ for 2-phase.}$$

The voltage induced in a coil is proportional to the sine of the half-angle which the coil spans. The sine of the half-angle spanned by the coil is called the chord factor.

$$k_p = \sin (P \times 90^\circ).$$

For a given voltage the total flux

$$\phi_t = \frac{E \times 60 \times 10^8}{n N k_p C_w} \text{ lines.}$$

In this equation E is the induced voltage per phase and is equal to the terminal voltage per phase times $(1 - \text{per unit } I_m \times \text{per unit } X_1)$. The product of per unit I_m and X_1 generally lies between the limits 0.02 and 0.04 and can for most designs be taken equal to 0.03. Then $E = E_T \times 0.97$.

Induction motor magnetic circuit calculations are often more conveniently made by using flux per pole instead of total flux, and frequency instead of synchronous r.p.m. The flux per pole

$$\phi = \frac{\phi_t \times f_d}{p}$$

Substituting the equation above for ϕ_t and $\frac{2 \times 60 \times f}{p}$ for synchronous r.p.m.,

$$\phi = \frac{E_T \times 0.97 \times 10^8}{2 \times 22Nfk_p k_d} \text{ lines.}$$

Output Constant.—If E is the terminal voltage per phase, the output of an induction motor

$$\text{hp.} = \frac{EIm \times \text{eff.} \times \text{PF}}{746} \text{ horsepower,}$$

$$E = \frac{\phi_t n N k_p C_w}{60 \times 10^8} \text{ volts, approximately.}$$

The total flux $\phi_t = \pi D l_g B_g$, and the total ampere-conductors on the stator $ImNk_p = \pi DQ$. Substituting into the output equation above,

$$\begin{aligned} \text{hp.} &= \frac{\pi D l_g B_g \pi D Q n C_u \times \text{eff.} \times \text{PF}}{44 \times 75 \times 10^{11}} \\ &= \frac{D^2 l_g n B_g Q C_u \times \text{eff.} \times \text{PF}}{4 \times 54 \times 10^{11}} \\ \text{hp.} &= \frac{D^2 l_g n B_g Q C_u \times \text{eff.} \times \text{PF}}{4 \times 54 \times 10^{11}} \end{aligned} \quad (171)$$

Air Gap Density.—In an induction motor the magnetizing current or the current required to maintain the flux in the magnetic circuit is drawn from the alternating-current lines to which the motor is connected. This magnetizing current lags the voltage by 90° and must be small if reasonable operating characteristics are to be obtained. For air gap lengths as short as practicable, the reluctance of the air gap is greater than that of the remainder of the magnetic circuit. To avoid excessive magnetizing currents moderate densities are therefore required. The density in the stator teeth is directly proportional to that in the air gap. High tooth densities produce high core losses and increase the magnetizing current. The flux density in the air gap of induction

motors generally lies between the limits 25,000 and 45,000 lines per sq. in. The high values are for large-capacity, high-speed motors. For general-purpose motors, air gap densities from 30,000 to 40,000 lines per sq. in. are most satisfactory.

Ampere-Conductors.—The value of the ampere-conductors per inch of stator gap circumference depends upon the size of the motor, the voltage of the stator winding, the type of ventilation, and the permissible leakage reactance. Average values of Q for open-type, 40° C.-rated motors for voltages up to 2500 volts are given by the curve in Fig. 181.

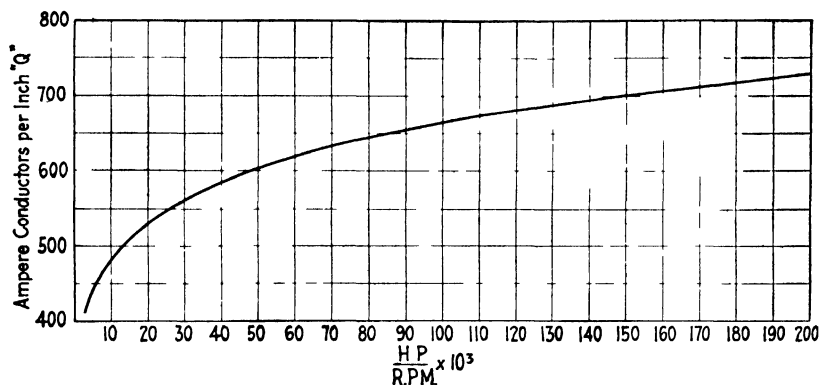


FIG. 181.—Ampere conductors per inch of stator gap circumference for polyphase induction motors

Efficiency and Power Factor. The operating characteristics shown in Table XXIV are for normal polyphase, 60-cycle, constant-speed, 40° , squirrel-cage motors for voltages up to 600 volts, and those in Table XXV are for normal polyphase, 60-cycle, constant-speed, 40° , slip-ring motors for voltages up to 600 volts.

For 2200-volt motors, the full-load efficiency is approximately 1 per cent lower and the full-load power factor approximately 2 per cent lower than the values given in Tables XXIV and XXV.

It is apparent from equation 171 that a series of constants can be derived for various ratings and speeds which can be used to calculate the stator diameter and length. The length, l_g , in equation 171 is the length of the stator core minus the ventilating ducts. It is generally convenient to calculate the total stator length instead of the length of the air gap section. The diameter used in the output equation 171 is the inside diameter or gap bore of the stator. It is usually desirable to be able to determine the outside diameter of the stator, which is the inside frame diameter, from the output equation in order to select the standard

TABLE XXIV

OPERATING CHARACTERISTICS OF 3-PHASE, 60-CYCLE, CONSTANT-SPEED
HORIZONTAL SQUIRREL-CAGE MOTORS

Hp.	Speed, R.p.m.		Eff., Full- Load	PF, Full- Load	Current in Amperes, 220 Volts		Torque in Pounds at 1-Ft. Radius		
	Syn.	Full- Load			Full- Load	Locked Rotor	Full-Load at Full- Load Speed (Approximate)	Starting (With Full Voltage) Per Cent Full-Load	Maximum Running Per Cent Full-Load
½	1200	1120	73	65	2.07	11.0	2.38	150	250
	900	840	68	63	2.29	12	3.13	150	250
¾	1800	1735	78	78	2.41	15.0	2.27	175	275
	1200	1140	77	72	2.65	15.0	3.46	175	275
1	900	850	73	64	3.15	15	4.64	150	250
	1800	1720	78.5	79	3.16	24	3.06	175	300
1	1200	1145	78.5	74	3.38	24	4.58	175	275
	900	855	74.5	68	4.1	24	6.15	150	250
1½	3600	3475	79	81	4.60	35	2.27	175	275
	1800	1730	82	81	4.43	35	4.55	175	275
1½	1200	1140	79.5	75	4.94	35	6.90	175	275
	900	860	79	68	5.48	35	9.16	150	250
2	3600	3490	81	81.5	5.95	45	3.01	175	250
	1800	1735	82	82	5.84	45	6.06	175	250
2	1200	1110	81	76	6.36	45	9.22	175	250
	900	860	82	69	6.94	45	12.2	150	225
3	3600	3450	82	85	8.45	60	4.55	175	250
	1800	1725	82	85	8.45	60	9.14	175	250
3	1200	1145	82.5	78	9.14	60	13.8	175	250
	900	860	83	72	9.85	60	18.3	150	225
5	3600	3460	83	83	14.2	90	7.6	150	225
	1800	1735	84	85	13.7	90	15.2	185	225
5	1200	1150	84	82	14.2	90	22.9	160	225
	900	865	84.5	72	16.1	90	30.4	130	225
7½	3600	3500	85.5	87	19.8	120	11.3	150	215
	1800	1735	85	83.5	20.1	120	22.7	175	215
7½	1200	1160	85	82	21.2	120	33.9	150	215
	900	865	85	75	22.8	120	45.5	125	215
10	3600	3480	86	89	25.6	150	15	150	200
	1800	1740	86	86	26.4	150	30.2	175	200
10	1200	1160	85.5	83	27.6	150	45.3	150	200
	900	875	86	73	29.6	150	60.4	125	200
15	3600	3480	88	89	37.6	220	22.5	150	200
	1800	1745	87	86	39.2	220	45.1	165	200
15	1200	1170	87	85	39.6	220	67.3	140	200
	900	875	87	78	43.4	220	90.4	125	200
20	3600	3490	88.0	90	49.5	290	30.1	150	200
	1800	1760	88	87	51.0	290	59.8	150	200
20	1200	1170	88.0	86	52.0	290	89.7	135	200
	900	875	88.0	80	55.8	290	121.0	125	200
20	720	700	88.0	73	61.0	290	150.0	120	200
	600	580	86.0	70	65.0	290	181.0	115	200
25	3600	3540	88	89	62.6	365	37	150	200
	1800	1760	89.5	87.5	62.6	365	74.5	150	200

TABLE XXIV—Continued

Hp.	Speed, R.p.m.		Eff., Full- Load	PF, Full- Load	Current in Amperes, 220 Volts		Torque in Pounds at 1-Ft. Radius		
	Syn.	Full- Load			Full- Load	Locked Rotor	Full-Load at Full- Load Speed (Approximate)	Starting (With Full Voltage) Per Cent Full-Load	Maximum Running Per Cent Full-Load
25	1200	1170	89.0	87	63.0	365	111	135	200
	900	875	88.5	82	67.8	365	150	125	200
	720	700	88.5	76	73.0	365	188	120	200
	600	580	80	70	79.2	365	226	115	200
30	1800	1760	90.0	88	74.2	435	89.2	150	200
	1200	1170	89.5	88	74.6	435	134	135	200
	900	875	89.0	83	79.6	435	180	125	200
	720	700	89	78	84.5	435	225	120	200
	600	580	88	76	88	435	271	115	200
40	1800	1765	90	88.5	98.6	580	119	150	200
	1200	1175	89.5	88	99.6	580	178	135	200
	900	875	89.5	84	104	580	240	125	200
	720	700	89.5	82	106.8	580	300	120	200
	600	580	89	76	112.8	580	362	115	200
50	1800	1765	90.5	89	120	725	148	150	200
	1200	1175	90.0	88	123	725	223	135	200
	900	875	90.0	86	127	725	300	125	200
	720	700	90	84	129.5	725	375	120	200
	600	580	88.0	77	145	725	453	115	200
60	1800	1770	90.5	89	146	870	178	150	200
	1200	1175	91	88	147	870	268	135	200
	900	875	90.5	88	148	870	360	125	200
	720	700	88.5	81	164	870	450	120	200
	600	580	88.5	77	173	870	543	115	200
75	1800	1770	91.0	89	182	1085	222	150	200
	1200	1175	92.0	88	182	1085	335	135	200
	900	875	90.0	86	190	1085	450	125	200
	720	700	89.0	82	201	1085	563	120	200
	600	580	89.0	80	207	1085	679	115	200
100	1800	1770	91.5	89	241	1450	297	125	200
	1200	1180	91.5	86	249	1450	445	125	200
	900	875	90.5	86	252	1450	600	125	200
	720	700	90.0	83	259	1450	750	120	200
	600	580	89.5	81	271	1450	905	115	200
125	1800	1770	92	89	300	1810	370	110	200
	1200	1180	92.0	87	306	1815	556	125	200
	900	875	90.5	87	311	1815	748	125	200
	720	700	90.5	86	314	1815	938	120	200
	600	580	90.0	82	333	1815	1131	115	200
150	1800	1770	92	90	356	2170	445	110	200
	1200	1180	92	88	363	2170	668	125	200
	900	875	91.0	88	367	2170	900	125	200
	720	700	90.5	86	376	2170	1126	120	200
	600	580	90	83	386	2170	1360	115	200
200	1800	1770	92.5	90	470	2900	593	100	200
	1200	1180	92.0	88	484	2900	890	125	200
	900	875	91.5	88.0	487	2900	1200	125	200
	720	700	91	87	491	2900	1500	120	200
	600	580	91.5	85	500	2900	1800	115	200

TABLE XXV

OPERATING CHARACTERISTICS OF 3-PHASE, 60-CYCLE, CONSTANT-SPEED
HORIZONTAL WOUND ROTOR MOTORS

Hp.	Speed, R.p.m.		Eff. Full- Load	PF, Full- Load	Full-Load Current in Amperes, 220 Volts		Torque in Pound at 1-Ft. Radius	
	Syn.	Full- Load			Stator	Rotor per Lead	Full-Load at Full-Load Speed (Approximate)	Maximum Running
½	900	825	70	59	3.56	8.3	4.78	9.7
1	1200	1100	73	70	3.84	10	4.78	9.2
	900	845	73	69	3.84	10	6.21	16.4
1½	900	845	74	69	6.13	14.5	9.32	27.7
2	1800	1700	78	82	6.14	17.2	6.18	14
	1200	1115	77	72	7.06	18	9.43	19
	900	850	76	67	7.7	18	12.35	31.3
3	1800	1690	81	83	8.76	21	9.32	19
	1200	1140	80	78	9.44	21	13.84	28
	900	855	80	68	10.8	22	18.4	40.7
5	1800	1700	84	86	13.6	30.5	15.46	33
	1200	1140	82	81	14.8	27.3	22.95	46
	900	855	83	72	16.4	30	30.7	62
7½	1800	1700	85	87	19.9	28	23.2	47
	1200	1145	85	83	20.9	27.6	34.4	72
	900	870	86	64	26.8	29.2	45	99
10	1800	1725	88	86	25.9	28	30.5	90
	1200	1145	85	84	27.4	30	45.9	91
	900	840	83	78	30	53.5	62	150
15	1800	1700	87.0	86.5	43	57	46.3	110
	1200	1125	85	83	41.6	60.5	70	160
	900	840	84.5	79	44	64	94	200
20	1800	1720	87.0	87.0	52	61	61.1	150
	1200	1145	86.5	85	53	62.5	91	220
	900	835	85	81	57	104	126	220
25	1800	1720	86.0	87.5	64	66	76.3	195
	1200	1130	86	85	67	97	116	300
	900	840	86	82	70	103	158	225
30	1800	1740	86	88	78	69.5	90	300
	1200	1145	87	85.5	79	93	137	350
	900	850	86	83	82	132	185	375
40	1800	1735	87.5	88.5	101	79	121	360
	1200	1140	87	88	102	138	184	400
	900	850	86.5	85	106	141	245	500
50	1800	1720	87.5	91	123	98.5	152	360
	1200	1170	90	85	128	129	224	750
	900	870	89	81.5	135	79	301	850
	720	685	87	80	140	148	383	960
	600	570	86.5	75	150	114	461	1150
60	1800	1755	89	86	150	147	180	450
	1200	1170	90.5	86	151	129	269	850

TABLE XXV—*Continued*

OPERATING CHARACTERISTICS OF 3-PHASE, 60-CYCLE, CONSTANT-SPEED
HORIZONTAL WOUND ROTOR MOTORS

Hp.	Speed, R.p.m.		Eff. Full- Load	PF, Full- Load	Full-Load Current in Amperes, 220 Volts		Torque in Pound at 1-Ft. Radius	
	Syn.	Full- Load			Stator	Rotor per Lead	Full-Load at Full-Load Speed (Approximate)	Maximum Running
60	900	870	88.5	83	160	150	361	950
	720	690	87	82	165	150	457	1000
	600	575	87	76	171	141	547	1200
75	1800	1755	90	89	183	145	225	560
	1200	1165	90	87	188	178	338	900
	900	870	89	85	193	145	453	1200
	720	695	88.5	80	200	146	567	1350
	600	580	88	77	215	150	680	1500
100	1800	1760	90.5	90	214	142	298	750
	1200	1165	90.5	88	246	192	451	1050
	900	870	90.0	85	256	150	603	1500
	720	695	88.5	83	265	207	755	1520
	600	580	89.0	73	314	164	905	2000
125	1800	1760	90.5	90	304	131	372	1100
	1200	1170	91.0	88	306	200	561	1300
	900	875	90.0	86	316	210	750	1700
	720	695	89.0	84	325	228	945	1900
	600	580	89.5	79	350	170	1130	2400
150	1800	1760	90.5	90	360	131	448	1200
	1200	1170	91.0	88	367	152	673	1500
	900	875	90.5	87	373	217	900	2000
	720	695	90.0	84	387	220	1134	2280
	600	580	89.5	80	400	225	1350	3000
200	1800	1760	90.5	90	480	175	597	1300
	1200	1170	91.5	88	484	173	897	2000
	900	875	91	88	490	237	1201	2500
	600	580	90.5	87	500	240	1795	4200

frame a given motor rating is suited for. For this purpose the output equation is written

$$\frac{D_o^2 l n}{\text{hp.}} = C. \quad (172)$$

The output constants given in Fig. 182 fit average present-day design practice and are for 60-cycle, constant-speed, squirrel-cage motors for voltages up to 600 volts. For 2200-volt motors and for wound-rotor induction motors the output constants of Fig. 182 must be increased approximately 5 per cent. The dimensions of the motor¹ can also be

¹ See also "Output of Induction Motor Depends on Total Active Material," by P. H. Trickey, *Product Engineering*, Dec., 1946, p. 114.

determined by plotting the product of D_o^2l instead of the output constant C against hp./r.p.m. The data for such a curve can be taken from Fig. 182.

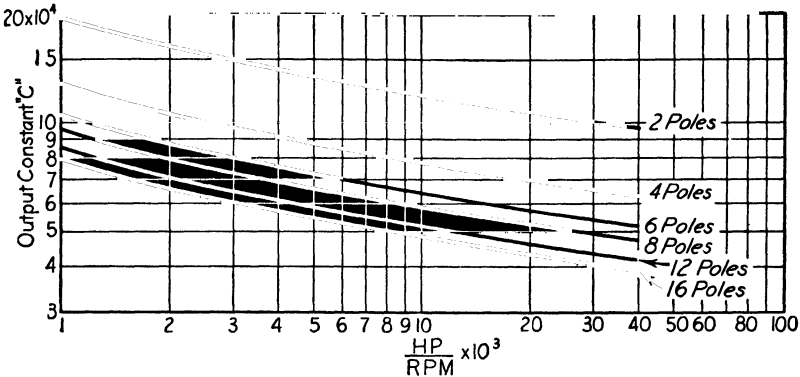


FIG. 182a. —Output constants for 60-cycle polyphase induction motors up to 600 volts with partly closed stator slots.

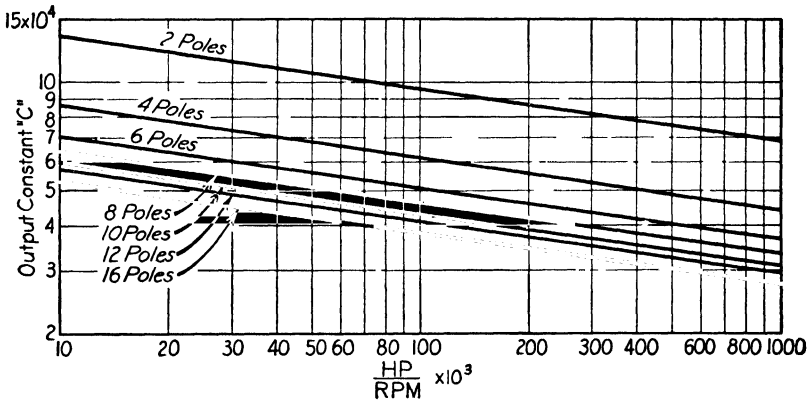


FIG. 182b. —Output constants for 60-cycle polyphase induction motors up to 600 volts with open stator slots.

Diameter and Length.—With the product of D_o^2l known, the diameter and length must be so proportioned that satisfactory operating characteristics can be obtained with minimum cost. The gap diameter or inside diameter is found with the help of the table, which gives the ratio, r , outside diameter to inside diameter of stator for various numbers of poles.

The operating characteristics of induction motors vary with the ratio of the length of the stator core to the pole pitch at the gap circum-

ference. For best power factor l/τ should be equal to from 1.0 to 1.25, and for best efficiency, about 1.5. For minimum cost l/τ should be equal to 1.5 to 2.0. The power factor of induction motors varies with the pole pitch; that is, a motor with large pole pitch and small number of poles will have a higher power factor than a motor with small pole

Poles	$r = \frac{D_o}{D}$	Poles	$r = \frac{D_o}{D}$	Poles	$r = \frac{D_o}{D}$	Poles	$r = \frac{D_o}{D}$
2	1.85 to 1.95	6	1.35 to 1.43	10	1.23 to 1.27	14	1.20
4	1.45 to 1.55	8	1.28 to 1.33	12	1.22	16	1.18

pitch. For motors with large pole pitch the diameter and length are selected to give minimum cost, and for motors with small pole pitch the diameter and length are proportioned to give good power factor at reasonable cost. A value of l/τ equal to 1.0 can not always be used for small motors, below approximately 15 hp., because the resulting small diameter will necessitate too small a number of stator slots. In general, the ratio of stator core length to pole pitch

$$\frac{l}{\tau} = 0.60 \text{ to } 2.0.$$

The pole pitch

$$\tau = \frac{\pi D}{p},$$

and

$$l = \frac{\pi D}{p} (0.60 \text{ to } 2.0).$$

The output constants, Fig. 182, are for the outside diameter of the armature D_o . Usual values of r , the ratio of stator outside diameter to inside diameter, are given in the table. The core length in terms of the outside diameter

$$l = \frac{\pi D_o}{r \times p} (0.60 \text{ to } 2.0) \text{ in.}$$

Substituting into the output equation,

$$D_o = \sqrt[3]{\frac{pC \text{ hp. } r}{\pi(0.60 \text{ to } 2.0)n}} \text{ in.} \quad (173)$$

$$l = \frac{C \text{ hp.}}{D_o^2 n} \text{ in.} \quad (174)$$

The outside diameter of the stator can also be found, when the product of $D_o^2 l$ is known, by use of the equation

$$D_o^4 = \frac{\text{hp.}}{n} 2.5 \times 10^6 \text{ in.}$$

The safe peripheral speed may be the determining factor in the choice of the dimensions. Standard constructions can generally be used for peripheral speeds up to 12,000 ft. per min. Peripheral speeds of 15,000 ft. per min. are possible with special rotor construction and increased cost.

Windings.—The windings used for the stator or field of induction motors are the same as the armature windings of synchronous machines. The method of laying out these windings has been explained in Chapter XI. Concentric-coil windings are generally used for the stators of single-phase² motors. Sometimes concentric-coil windings³ are used for polyphase motors, but they have been replaced by the double-layer winding by most manufacturers because of the saving in cost of manufacture.

General-purpose induction motors are built for both 2-phase and 3-phase and for a variety of voltages. To keep the cost of manufacture as low as possible, the number of stator slots should be so chosen for each frame that the maximum number of combinations of poles, phases, and voltages is possible. For integral number of slots per pole per phase, the slots per pole will be an integer, and the total number of slots will be satisfactory for both 2-phase and 3-phase when the number of slots per pole is a multiple of both 2 and 3. Standard induction motors are generally designed with stator windings for 220 or 440 volts. This can be done by using a 1-circuit winding for 440 volts and a 2-circuit winding for 220 volts, or, if a 2-circuit winding is required for 440 volts, then a 4-circuit winding must be used for 220 volts.

Fractional slot windings may be used also for induction motors. For these windings, the denominator of the fraction must not be a multiple of the number of phases for which the winding is intended. For example: A winding with $2\frac{1}{2}$ slots per pole per phase is satisfactory for a 3-phase winding but not for a 2-phase winding. Similarly $2\frac{2}{3}$ slots per pole per phase is satisfactory for 2-phase but not for 3-phase. The use of $3\frac{3}{7}$ slots per pole per phase, however, is satisfactory for both

² "Winding and Connecting of Small Single Phase Motors," by C. A. M. Weber, *Electric Journal*, Vol. 21, Aug., 1924, p. 377.

³ "The Automatic-Start Polyphase Induction Motor," and discussion by J. L. Hamilton, *A.I.E.E. Journal*, Vol. 41, Oct., 1922, pp. 772-795; "Connecting Induction Motors," by A. M. Dudley, pp. 37-40, McGraw-Hill Book Co., New York.

2-phase and 3-phase. The number of parallel circuits is very much limited with fractional slot windings because these windings do not repeat every pole as the windings with integral slots per pole and phase do. For these reasons, standard induction motors are generally designed with the number of stator slots equal to a multiple of the number of poles, times the number of phases.

Chorded windings are also used for induction motors. The advantages of chording discussed in Chapter XI apply also to induction motors. A complete discussion of the advantages of fractional pitch windings for induction motors has been given by D. F. Alexander.⁴

Number and Size of Slots.—The number of conductors per slot must be an even integer for double-layer windings, because one-half of the conductors per slot belong to the coil side in the top of the slot and the other half to the coil side in the bottom of the slot. The number of conductors in series per phase can be determined by formula 170,

$$N = \frac{E_T 0.97 \times 60 \times 10^8}{n \phi k_p C_u}.$$

The flux density in the air gap may generally be taken equal to 35,000 lines per sq. in. for the preliminary calculations. Then the total flux

$$\phi_t = \pi D l_g B_g \text{ lines.}$$

The flux per pole for polyphase induction motors can be determined from the following relationship:

$$\frac{\phi}{\sqrt{\text{hp.} \times \frac{60}{f}}} = C_1 \times 10^5.$$

The limits for C_1 are given below.

	Poles	2	4	6	8	10	12	14	16
C_1	Maximum	3.7	2.45	2.10	1.90	1.80	1.70	1.65	1.60
	Minimum	2.55	1.95	1.70	1.55	1.45	1.40	1.33	1.30

The effective conductors in series per phase

$$N k_p k_d = \frac{E_T \times 0.97 \times 10^8}{2.22 \times f \phi}.$$

⁴ "Fractional Pitch Windings for Induction Motors," *Electric Journal*, Vol. 25, Feb., 1928, p. 77.

The total stator conductors = Nam .

The number of stator slots must, therefore, be selected to meet the requirements of the number of poles and phases with an even number of conductors per slot of such value that a satisfactory air gap density can be obtained with chord factor between the limits 0.707 and 1.0. It is generally not desirable to chord induction motor windings more than $\frac{2}{3}$ of pitch. For two-pole motors, however, a chord factor as low as 0.707 may be necessary.

For motors with open stator slots, the slot openings have an appreciable effect on the air gap reluctance. The stator and rotor slots should be so proportioned that the minimum variations in air gap reluctance will result when the rotor slots move by the stator slots. The effect of variations in air gap reluctance is to produce pulsations in the air gap flux, which produce additional core losses and noise. These effects of the stator slots can generally be kept small by using a large number of narrow slots. The larger the number of slots for a given diameter, the smaller will be the tooth pitch. The minimum tooth pitch

$$t_{1s} = \frac{\pi D}{S_s}.$$

The width of the stator slots is generally one-half or slightly less than one-half of the tooth pitch on the gap circumference. If the tooth pitch is small, the width of the tooth is also small, and difficulties in construction often arise; that is, it becomes difficult to support the stator teeth at the ventilating ducts and at the ends of the stator core without obstructing the ventilation. Figure 183 shows a part of a stator lamination with ventilating duct spacers and minimum tooth pitch equal to 0.406 in. The cost of manufacture is also higher for motors with a large number of slots, because there are more coils to wind, insulate, and place into the slots. In general the number of stator slots should be selected to give an integral number of slots per pole per phase and a tooth pitch at the air gap circumference for open-type slots between the limits 0.60 and 1.0. For partly closed slots the tooth pitch may be less than 0.60 in. For such slots the tooth usually has parallel sides and the slot depth is less than for open-type slots.

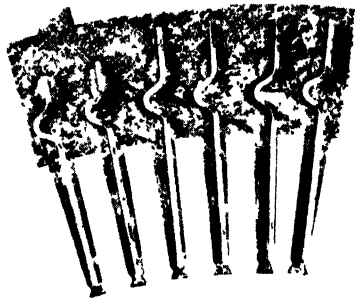


FIG. 183.—Portion of stator lamination with duct spacer.

The current per phase in the stator winding,

$$I = \frac{\text{hp.} \times 746}{Em_s \times \text{eff.} \times \text{PF}} \quad (175)$$

The section area of the stator conductor,

$$s_s = \frac{I}{aA_s} \quad (176)$$

The copper losses in any winding vary directly with A^2 . The temperature rise depends upon the losses for a given type of construction. The stator current density must be so chosen that a satisfactory efficiency can be obtained without excessive temperature rise. For the stator windings of standard induction motors with open-type frame construction as shown in Fig. 170, current densities from 2000 to 3400 amperes per sq. in. are satisfactory. The lower value is used for slow-speed motors, and the larger one is for the higher ratings at high speed.

The conductors per slot must be arranged in the slots to occupy the minimum amount of space, with the proper insulation between turns and between core and coils. Open-type stator slots are generally used for induction motors larger than approximately 25 hp., and the conductors are generally d.c.c. square wire or d.c.c. copper ribbon. For all polyphase motors, the windings are designed to have more than one

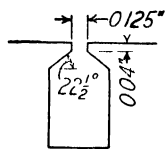


FIG. 184.

turn per coil and the turns should, whenever possible, be so arranged that there is only one turn per layer, as shown in Fig. 129A and B. Large conductor sections are built up of two or more small wires in parallel, to prevent excessive eddy-current losses⁵ (see Fig. 129B). For windings requiring many turns per coil, it is not always possible to use only one turn per layer; for such cases the coils should be wound as shown in Fig. 131A and B. For small motors, less than approximately 25 hp., partially closed stator slots are as a rule required because of the adverse effects of open slots. The slot opening is then generally $\frac{1}{8}$ in., as shown in Fig. 184, and the shape of the slots is as shown in Fig. 175. For this type of slot, the coils are random-wound round d.c.c. wire or with heavy Formex or Formvar insulated wire. When the diameter of wire required is larger than $\frac{1}{8}$ in., two or more smaller wires in parallel can be used.

The size of the stator slot depends upon the number of conductors per slot, the size of conductor, and the insulation thickness required. The insulation on the conductors is either double cotton, Formvar, or

⁵ See references, page 208.

for class B insulation double fiber glass. The insulation between core and coils is varnished cambric, cotton tape, insulating varnish, and paper for class A insulation, and mica, fiber glass cloth, and tape for class B insulation. The method of determining the insulation clearances for open slots is the same as for synchronous machines and is shown in Fig. 132. Table XXVI gives the insulation clearances required for width and depth of slot for induction-motor stator windings for various voltages.

TABLE XXVI

CLEARANCE ALLOWANCE FOR SLOT INSULATION FOR STATOR WINDINGS OF
INDUCTION MOTORS WITH OPEN AND PARTLY CLOSED SLOTS

Volts	<i>s</i>	<i>2b</i>	Slot Depth			Slot Width		
			Gap Diameter, Inches			Gap Diameter, Inches		
			15 and Less	15 to 40	40 and over	15 and less	15 to 40	40 and over
0 300	0.08	1.00	0.24	0.25	0.31	0.060	0.065	0.080
300 600	0.10	1.50	0.25	0.29	0.34	0.075	0.085	0.095
600 1500	0.12	1.75		0.31	0.37		0.095	0.110
1500 3000	0.14	2.00		0.36	0.45		0.120	0.150

In this table the allowances for width and depth for gap diameters 15 in. and less are for partly closed slots. The allowance for the wedge for open slots for gap diameters 15 to 40 in. is 0.15; for 40 in. and larger it is 0.18 in. The end connection clearance, *s*, is very small for partly closed slots and may be taken equal to zero.

For open-type slots the insulation is wrapped on the coil with a 0.010-in. paper slot lining to protect the coil while it is placed into the slot. The coils are carefully layer wound, and the slot width is found by multiplying the insulated conductor dimension in the width of the slot by the number of conductors wide and adding the insulation clearance from Table XXVI. Similarly the depth of the slot is the insulated dimension of the conductor in the depth multiplied by the number of conductors deep plus the insulation clearance from Table XXVI. The width of the stator slot is generally approximately 50 per cent of the minimum stator tooth pitch and should seldom if ever exceed 60 per cent of the minimum tooth pitch. To avoid a high leakage reactance and consequent poor operating characteristics, the stator slot should generally not be deeper than 6 times the slot width.

For partly closed slots, the insulation is placed in the slot instead of around the coil, because the narrow slot opening makes it necessary

to place the conductors into the slot one by one. Partly closed slots are used for induction motors with gap diameter 15 in. and less and for voltages 600 volts and below. The slot opening, w_{s1} , Fig. 185, is 0.10 in. for gap diameters 8.0 in. and less and 0.125 in. for gap diameters 8.0 to 15.0 in. The total flux, total number of conductors, and number of slots are determined as explained above, and the tooth width is found by equation 177. For partly closed slots the tooth usually has parallel sides, and

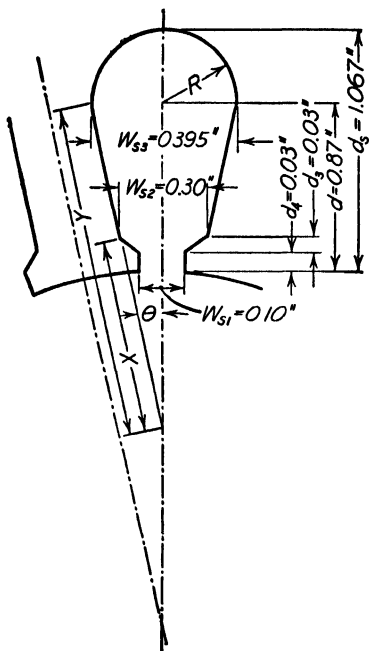


FIG. 185.

$$w_{ts} = \frac{\phi_t}{B_t(l - n_d w_d) k_1 S_s}.$$

The dimensions d_3 and d_4 , Fig. 185, are usually 0.03 in. for small gap diameters to 0.06 in. for the larger gap diameters. The ratio of the insulated copper area in the slot to the net slot space available for winding is called the space factor or fill factor. The insulated copper area per slot is the insulated diameter of the conductor squared times the number of conductors per slot. For

heavy Formvar insulated wire the space factor should not be larger than 0.85, and for quantity production not over 0.70 to 0.75. The net slot area for round bottom slots (see Fig. 185)

$$SA = \left(\frac{w_{s2} + w_{s3}}{2} - i_w \right) \left(d - i_d + \frac{i_w}{2} \right) + \frac{\pi}{2} \left(R - \frac{i_w}{2} \right)^2 \text{ sq. in.},$$

and for flat bottom slots the net slot area

$$SA = \left(\frac{w_{s2} + w_{s3}}{2} - i_w \right) (d_s - i_d) \text{ sq. in.}$$

Here i_w and i_d are the insulation and clearance allowances for the width and depth of slot respectively from Table XXVI. From the copper area per slot and the space factor the required slot area can be determined and the slot width w_{s2} can be calculated as soon as the tooth width is determined. The slot dimensions to give the desired slot area can be

determined as shown below (see Fig. 185).

$$\theta = \frac{180}{S_s}, \quad X = \frac{w_{s2}}{2 \sin \theta}, \quad K = \frac{w_{s2}}{2} - i_w,$$

$$a = d_3 - X - i_d + d_4, \quad b = \frac{\frac{K}{\sin \theta} + a - \pi \frac{i_w}{2}}{1 + \frac{\pi}{2} \sin \theta},$$

$$c = \frac{Ka - SA + \frac{\pi}{2} \left(\frac{i_w}{2} \right)^2}{\sin \theta \left(1 + \frac{\pi}{2} \sin \theta \right)}, \quad Y = \frac{-b + (b^2 - 4c)^{1/2}}{2},$$

$$R = Y \sin \theta, \quad d = Y - X + d_4 + d_3, \quad d_s = d + R.$$

For flat bottom slots the π terms drop out and $d = d_s$.

Stator Tooth and Yoke Densities.— For a given total flux, the dimensions of the slots determine the tooth density. For high tooth densities, the losses in the teeth are high, and a large number of ampere-turns are required to send the flux through the teeth. The maximum value of the stator tooth density for the minimum section

$$B_{ts1} = \frac{\phi_t}{w_{ts1}(l - n_d w_d) k_1 S_s}. \quad (177)$$

The width of the tooth for the minimum section

$$w_{ts1} = t_{1s} - w_{ss}. \quad (178)$$

The maximum value of the stator tooth density for the minimum section should generally not exceed

$$B_{ts1} = 100,000 \text{ lines per sq. in. for 60 cycles,}$$

$$B_{ts1} = 110,000 \text{ lines per sq. in. for 25 cycles.}$$

The depth of the stator laminations below the slots depends upon the flux density in the yoke. The iron losses in the yoke and the ampere-turns required to send the flux through the yoke determine the density. The flux density should not exceed

$$B_{ys} = 95,000 \text{ lines per sq. in. for 60 cycles,}$$

$$B_{ys} = 110,000 \text{ lines per sq. in. for 25 cycles.}$$

Generally B_{ys} is equal to 50,000 to 85,000 lines per sq. in. for 60 cycles and 60,000 to 100,000 lines per sq. in. for 25 cycles.

The flux per pole

$$\phi = \frac{\phi_t f_d}{p}.$$

The depth of the iron below the slots for both sides of the diameter

$$d_{ys} = \frac{\phi}{B_{ys}(l - n_d w_d)k_1}. \quad (179)$$

The outside diameter of the stator laminations

$$D_0 = D + 2d_{ss} + d_{ys}. \quad (180)$$

Sample Design: *Design of Stator for a 15-Hp., 3-Phase, 60-Cycle, 1200-R.p.m., 220-Volt, Squirrel-Cage General-Purpose Motor.*—The full-load efficiency and power factor are to be not less than 87.0 per cent and 85.0 per cent, respectively. The motor must have a starting torque not less than 135 per cent of full-load torque for normal voltage and a maximum running torque not less than 200 per cent of full-load torque. The temperature rise of no part of the motor should exceed 40° C. for continuous full-load operation.

The number of poles

$$p = \frac{f \times 2 \times 60}{n} = \frac{60 \times 2 \times 60}{1200} = 6$$

$$\frac{\text{hp.}}{n} \times 10^3 = \frac{15}{1200} \times 10^3 = 12.5.$$

From the curve in Fig. 182a, the output constant

$$C = 6 \ 16 \times 10^4.$$

For the ratio $l/\tau = 0.90$ and $r = 1 \ 36$

$$D_0 = \sqrt[3]{\frac{C \text{ hp. } pr}{\text{R.p.m.} \times \pi \times 0 \ 9}} = \sqrt[3]{\frac{6 \ 16 \times 10^4 \times 15 \times 6 \times 1.36}{1200 \times \pi \times 0 \ 9}}$$

$$= 13.02; \text{ use } 13 \ 0 \text{ in.}$$

$$l = \frac{C \text{ hp.}}{D_0^2 n} = \frac{6 \ 16 \times 10^4 \times 15}{13 \ 0^2 \times 1200}$$

$$= 4.56; \text{ use } 4 \ 5 \text{ in.}$$

$$\text{The gap diameter } D = \frac{13}{1.36} = 9.56; \text{ use } 9 \ 5 \text{ in.}$$

The following dimensions are selected:

$$D = 9.5 \text{ in.}, \quad l = 4.5 \text{ in.}, \quad \tau = 4.97 \text{ in.}, \quad l/\tau = 0.905.$$

For the diameter and length selected, it will not be necessary to use radial ventilating ducts in the stator core. The length of the air gap section will then equal the total length of the stator core

$$l_g = l = 4.5 \text{ in.}$$

For $C_1 = 1.70$ the flux per pole

$$\phi = 1.70 \times 10^3 \sqrt{15 \frac{60}{60}} = 658 \text{ kilo-lines.}$$

If the star-connected winding is chosen, the phase voltage

$$E_T = \frac{220}{1.73} = 127 \text{ volts.}$$

The product

$$Nk_p k_d = \frac{E_T \times 0.97 \times 10^8}{2.22 \times f \times \phi} = \frac{127 \times 0.97 \times 10^8}{2.22 \times 60 \times 658 \times 10^3} = 141.$$

It will be desirable to use two parallel circuits per phase; the winding can then be reconnected to one circuit per phase for 440 volts.

With 3 slots per pole per phase, the total number of slots

$$S_s = 3 \times 3 \times 6 = 54;$$

and the minimum tooth pitch

$$t_{1s} = \frac{\pi D}{S_s} = \frac{\pi \times 9.5}{54} = 0.552 \text{ in.}$$

The winding distribution factor

$$k_d = \frac{\sin 30^\circ}{3 \sin 10^\circ} = 0.96,$$

and the pitch factor for a coil throw, slot 1 and 9,

$$k_p = \sin \left(\frac{8}{9} \times 90 \right) = 0.985.$$

The number of conductors per slot

$$= \frac{141 \times 2 \times 3}{0.96 \times 0.985 \times 54} = 16.6.$$

This must be an even integer, so 18 conductors per slot are used.

The conductors in series per phase

$$N = \frac{18 \times 54}{2 \times 3} = 162,$$

and the flux per pole is

$$\begin{aligned} \phi &= \frac{E_T \times 0.97 \times 10^8}{2.22 \times f N k_p k_d} = \frac{127 \times 0.97 \times 10^8}{2.22 \times 60 \times 162 \times 0.96 \times 0.985} \\ &= 604 \text{ kilo-lines.} \end{aligned}$$

The final value of the air gap density

$$\begin{aligned} B_g &= \frac{\phi_t}{\pi D l_g} = \frac{604 \times 10^3 \times 6}{\pi \times 9.5 \times 4.5 \times 0.637} \\ &= 42.3 \text{ kilo-lines.} \end{aligned}$$

The stator current per phase

$$I = \frac{\text{hp. } 746}{E m_s \times \text{eff.} \times \text{PF}} = \frac{15 \times 746}{127 \times 3 \times 0.87 \times 0.85} = 39.7 \text{ amperes.}$$

For a current density of 3000 amperes per sq. in.,

$$s_s = \frac{I}{a A_s} = \frac{39.7}{2 \times 3000} = 0.00662 \text{ sq. in.}$$

Two No. 14 round heavy Formvar insulated wires in parallel will be used. The insulated diameter is 0.0678 in., and the area = 0.00322 sq. in. The current density for this conductor

$$A_s = \frac{39.7}{2 \times 2 \times 0.00322} = 3080 \text{ amperes per sq. in.}$$

The shape of the slot selected for this design is shown in Fig. 185, and $d_3 = d_4 = 0.03$ in. The width of the stator tooth is made 0.26 in., and the tooth density

$$B_{ts} = \frac{604 \times 6}{0.637 \times 54 \times 0.26 \times 4.5 \times 0.93} = 97.0 \text{ kilo-lines per sq. in.}$$

The slot width

$$w_{s2} = \frac{\pi(9.5 + 2 \times 0.06)}{54} - 0.26 = 0.30 \text{ in.}$$

The insulation allowances for the width and depth of the slot from Table XXVI are $i_w = 0.075$ in. and $i_d = 0.25$ in. The slot area for a

space factor of 0.80

$$SA = \frac{2 \times 18 \times 0.0678^2}{0.80} = 0.207 \text{ sq. in.}$$

The slot dimensions can now be calculated.

$$\theta = \frac{180}{54} = 3.33; \quad X = \frac{0.30}{2 \sin 3.33} = 2.58; \quad K = \frac{0.30}{2} - 0.075 = 0.075.$$

$$a = 0.03 - 2.58 - 0.25 + 0.03 = -2.77.$$

$$b = \frac{\frac{0.075}{\sin 3.33} - 2.77 - \pi \frac{0.075}{2}}{1 + \pi/2 \sin 3.33^\circ} = \frac{-1.598}{1.092} = -1.46.$$

$$c = \frac{0.075 \times -2.77 - 0.207 + \frac{\pi}{2} \left(\frac{0.075}{2} \right)^2}{\sin 3.33 \left(1 + \frac{\pi}{2} \sin 3.33 \right)} = -6.51.$$

$$Y = \frac{1.46 + (-1.46^2 - 4 \times -6.51)^{1/2}}{2} = 3.39 \text{ in.}$$

$$R = 3.39 \times \sin 3.33^\circ = 0.197 \text{ in.}$$

$$d = 3.39 - 2.58 + 0.03 + 0.03 = 0.87 \text{ in.}$$

$$d_s = 0.87 + 0.197 = 1.067 \text{ in.}$$

$$w_{s3} = \frac{\pi(9.5 + 2 \times 0.87)}{51} - 0.26 = 0.395 \text{ in.}$$

The effective radial depth of the stator yoke for round-bottom slots is equal to the radial depth of yoke below the slots plus one-third the radius of the bottom of the slot.

$$d_{ys} = 13.0 - 9.5 - 2 \times 0.87 - \frac{4}{3} \times 0.197 = 1.497 \text{ in.}$$

The flux density in the stator yoke

$$B_{ys} = \frac{604}{4.5 \times 0.93 \times 1.497} = 96.5 \text{ kilo-lines per sq. in.}$$

CHAPTER XVIII

THE ROTOR

Air Gap Length.—The ampere-turns required to send the flux through the air gap are directly proportional to the density and the length of the gap. Even with low air gap densities and short air gap lengths, the gap ampere-turns are larger than the ampere-turns for the remainder of the magnetic circuit. The air gap density and length, therefore, determine the magnetizing current. To obtain good operating characteristics, the magnetizing current should be as small as possible and the length of the air gap should be as small as mechanical construction will permit. The approximate minimum air gap length can be determined by the following empirical formula,

$$\delta = 0.125 - \frac{10.17}{D + 90}. \quad (181)$$

The rotor diameter

$$D_r = D - 2\delta.$$

Rotor Windings.—Squirrel-cage windings are built up of bar conductors short-circuited at each end by end-rings. The bars are either round or rectangular in shape and are of either copper, brass, or aluminum. The end-ring is generally of the same material as that used for the bars and may have any convenient shape. Various methods¹ have been used to join the end-ring to the bars. Because of the large temperature changes from no-load to full-load, the best possible connection between bars and end-ring is necessary to avoid high contact resistance at the joints. The cast squirrel-cage winding, shown in Fig. 180, is very desirable in this respect, because there are no joints. For large motors the end-ring is generally brazed or welded to the bars, and the methods of construction shown in Fig. 186 are generally used.

For wound-rotor motors, 3-phase, double-layer windings are used on the rotor, which are modified wave windings.² They may be con-

¹“Connecting Induction Motors,” by A. M. Dudley, p. 58, McGraw-Hill Book Co., New York.

²“Connecting Induction Motors,” by A. M. Dudley, pp. 69-75, McGraw-Hill Book Co., New York.

nected star or delta and may be either full pitch or chorded. The windings can be laid out to determine the proper coil sequence by the method explained in Chapter XI for armature windings of synchronous machines. Figure 187 shows the winding diagram for a 3-phase, 6-pole, 1-circuit, star-connected, modified wave winding with 54 slots and 4 conductors per slot. In this figure, all the coils are shown for one phase. For

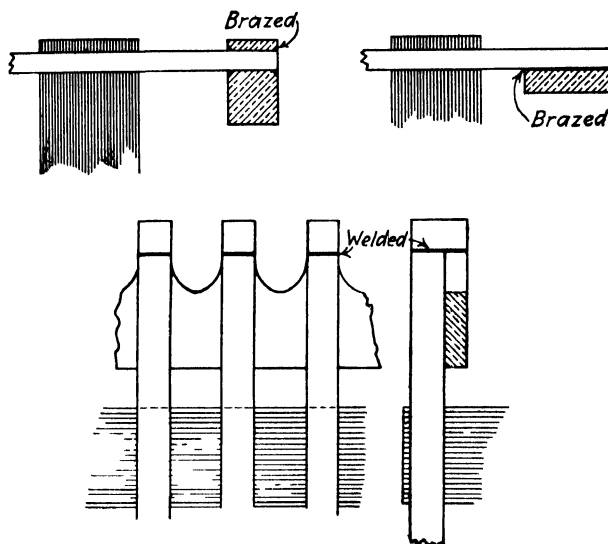


FIG. 186.

the other two phases only the beginning and ending coils are shown. A 3-phase, 8-pole, 1-circuit, delta-connected rotor winding with 96 slots and two conductors per slot is shown in Fig. 188.

Number and Size of Rotor Slots.— For squirrel-cage motors careful design of the rotor is necessary to avoid vibration and noise, cogging or locking torque, and synchronous cusps in the speed torque curve. Cogging or locking torque is a condition of varying torque at starting for different rotor positions. The cycle of high and low torque repeats as the rotor is moved through a rotor slot pitch. Synchronous cusps are points on the speed-torque curve where the motor locks into step at low speed and runs as a synchronous motor over a wide range of torque values. The minimum point on the torque curve may be so low that the rotor cannot come up to full speed even at no-load. These undesirable characteristics are largely due to the harmonics in the air

gap flux wave.³ Since the stator and rotor slots produce harmonics in the air gap flux wave it is important that the proper number of rotor slots be chosen in relation to the number of stator slots to avoid these

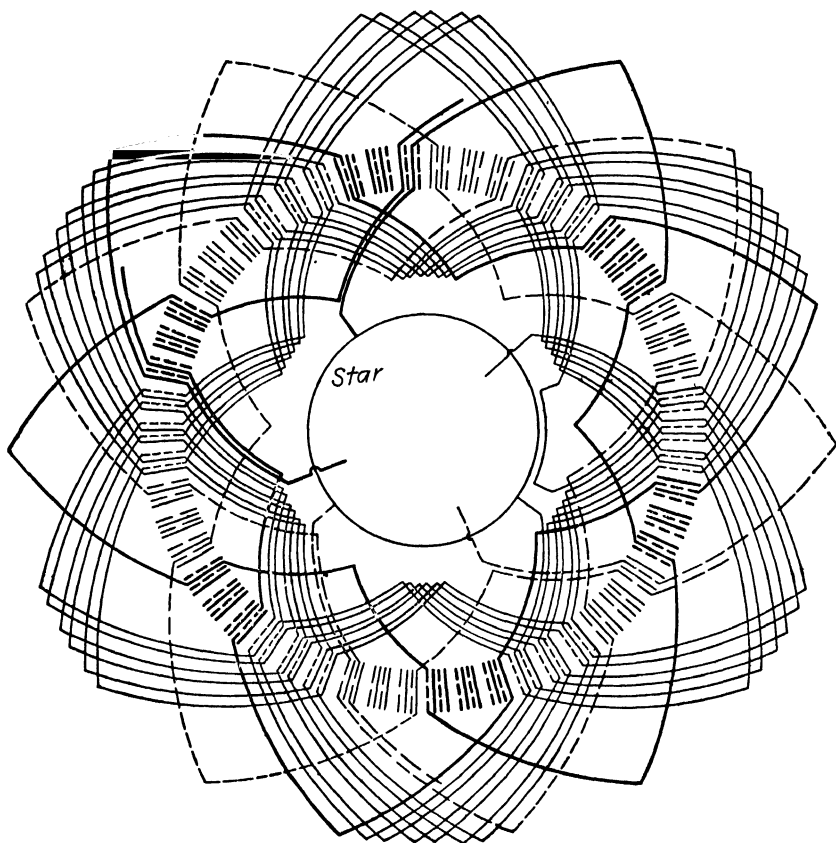


FIG. 187.—Rotor winding diagram—3-phase, 6 poles, 54 slots, 4 conductors per slot, 1-circuit star.

undesirable characteristics. The number of rotor slots must never be equal to the number of stator slots but must be either larger or smaller. Satisfactory results are usually obtained when the number of rotor slots

³ "Synchronous Motor Effects in Induction Machines," by E. E. Drees, A.I.E.E. Trans., Vol. 49, July, 1930, p. 1033; "Induction Motor Slot Combination," by G. Kron, A.I.E.E. Trans., Vol. 50, June, 1931, p. 757; "Dead Points in Squirrel-Cage Motors," by Q. Graham, A.I.E.E. Trans., Vol. 59, 1940, p. 637; "Harmonic Theory of Noise in Induction Motors," by W. J. Morrill, A.I.E.E. Trans., Vol. 59, 1940, p. 474; "Electric Machinery," Vol. II, by Lievschitz-Garik and Wipple, p. 236, D. Van Nostrand Co., New York.

is from 15 to 30 per cent larger or smaller than the number of stator slots. It is obviously impossible to give here a complete analysis of all the undesirable slot combinations for squirrel-cage induction motors. Only a few of the slot combinations most certain to give trouble are

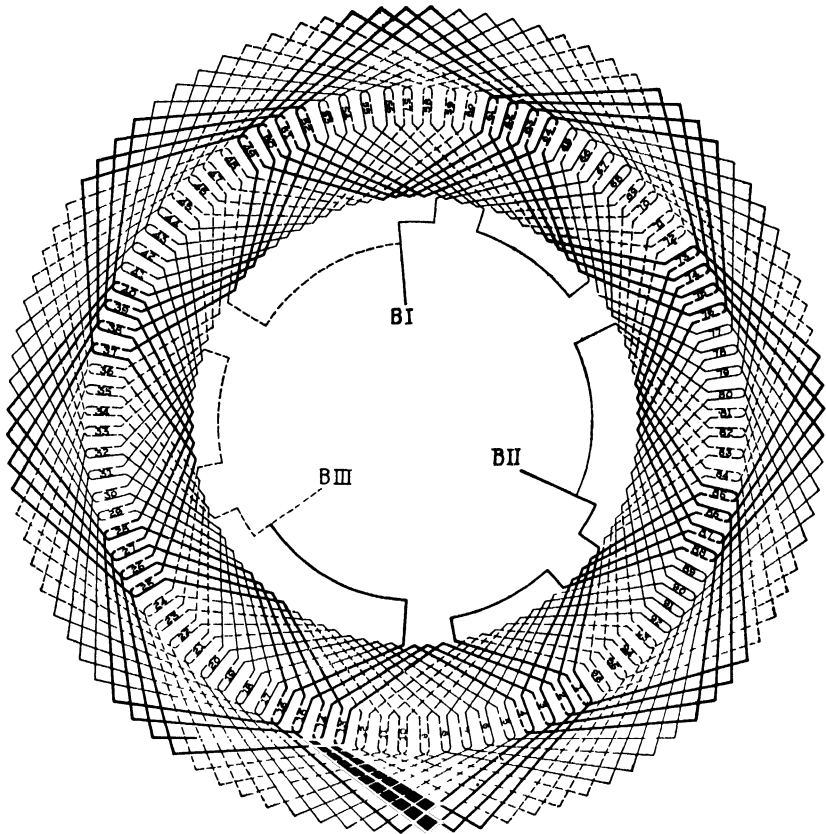


FIG. 188.—Rotor winding diagram—3-phase, 8 poles, 96 slots, 2 conductors per slot, 1-circuit delta.

listed. The student who wishes to investigate a given stator and rotor slot combination more fully should study the references below.

Noise and vibration are usually reduced to a satisfactory level if the number of rotor slots is selected so that $S_s - S_r$ is not equal to ± 1 , ± 2 , $\pm(p \pm 1)$, or $\pm(p \pm 2)$. To avoid dead points or cogging, $S_s - S_r$ must not be equal to $\pm 3p$ or any multiple of $3p$ for 3-phase motors and $\pm 2p$ or any multiple of $2p$ for 2-phase machines. To avoid cusps in the speed-torque curve, $S_s - S_r$ should not be equal to $\pm p$ for 3-phase and 2-phase motors or be equal to $-2p$ or $-5p$ for 3-phase motors.

Dead points, noise, and cusps in the speed-torque curve can be reduced or even eliminated entirely by skewing either stator or rotor slots with proper stator coil throw. For small motors, the rotor slots are usually skewed, because the most desirable stator and rotor slot proportions are not always possible on small diameters. When diagonal slots are used the skew is approximately one stator or rotor slot pitch, whichever is the larger.

The rotor windings for wound-rotor motors are 3-phase windings, and the number of rotor slots must permit a balanced winding. Generally, windings with an integral number of slots per pole per phase are used for the rotor. Fractional slot windings may also be used, but usually only those will be satisfactory for which the number of slots is a multiple of the number of phases times the number of pairs of poles. Wound-rotor motors are started with normal voltage applied to the stator winding and enough resistance in the rotor circuit to give full-load torque with full-load current. The main field is therefore of normal strength during the starting period. To avoid magnetic noises and excessive flux pulsations in the air gap, however, the ratio of the stator slots to the rotor slots should, whenever possible, lie within the limits given above.

If the total rotor ampere-turns are assumed to be 10 per cent less than the total stator ampere-turns, the ratio of the total copper section of the rotor to the total stator copper section

$$\frac{S_{rr}}{S_{rs}} = 0.90 \frac{I_s}{A_r} \quad (182)$$

For squirrel-cage windings, the current density may be higher than for the stator winding because the mean length of turn is shorter and the ventilation is better. For a current density of 2500 amperes per sq. in. in the stator winding and 5000 amperes per sq. in. in the bars of the squirrel-cage winding, the ratio of the total rotor copper section to the total stator copper section

$$\frac{S_{er}}{S_{cs}} = 0.9 \frac{2500}{5000} = 0.45.$$

The total rotor copper section must be selected, in relation to the length of the bar and the end-ring section, so that the proper rotor resistance can be obtained to meet the starting torque requirements. It is generally from 50 to 80 per cent of the total stator copper section.

For wound-rotor windings, the length of the mean-turn is approximately equal to the length of the mean-turn of the stator coils. Con-

sequently, to avoid excessive rotor copper losses, the rotor current density can not be made much higher than the stator current density. The total rotor copper section is therefore generally from 80 to 95 per cent of the total stator copper section.

The distribution of the current in the bars and end-rings of a squirrel-cage winding⁴ is shown in Fig. 189. It is apparent from Fig. 189 that the current in each bar divides in the end-ring, one-half returning through a bar a pole pitch to the right and the other half through a bar

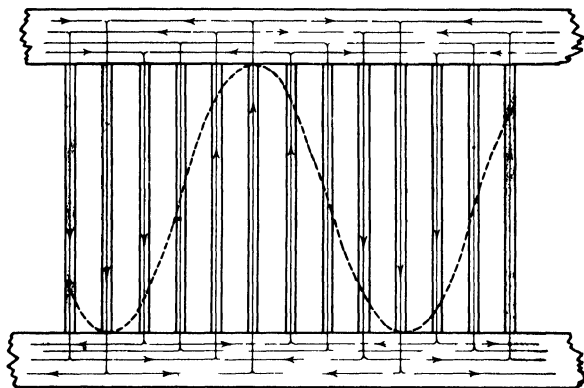


FIG. 189.—Section of squirrel-cage winding showing distribution of current.

a pole pitch to the left. If the maximum value of the current in each bar is I_m and if the current is maximum in all the bars at the same time, then the maximum value of the current in the end-ring

$$= \frac{I_m}{2} \times \frac{N_b}{p}.$$

The current is not maximum in all the bars per pole at the same instant, but varies according to the sine law; hence, the maximum value of the current in the end-ring

$$= -\frac{I_m}{2} \times \frac{N_b}{p} \times \frac{2}{\pi},$$

and the effective value of the current in the end-ring

$$= \frac{I_m}{2} \times \frac{N_b}{p} \times \frac{2}{\pi} \times \frac{\sqrt{2}}{2}.$$

⁴ "Turns and Phases in Squirrel-Cage Windings," Bulletin 5, Engineering Experiment Station, University of Minnesota, by G. F. Corcoran and H. R. Reed.

The effective value of the current in each bar, $I_b = I_m/\sqrt{2}$, and the end-ring current

$$= \frac{0.32I_b N_b}{p}. \quad (183)$$

The section area of each end-ring

$$s_{er} = \frac{0.32I_b N_b}{p A_{er}}, \quad (184)$$

and the total bar section

$$S_{cr} = \frac{I_b N_b}{A_r}. \quad (185)$$

By combining these two equations and simplifying, the section area of each end-ring in terms of the total rotor copper section

$$s_{er} = \frac{0.32 S_{cr}}{p} \frac{A_r}{A_{er}}. \quad (186)$$

The ventilation is generally better for the end-rings than for the bars, and the current density can be made equal to the current density in the bars or slightly higher.

The rotor slots are always of the partially closed type as shown in Figs. 190 and 191. The rectangular-shaped bar and slot is generally preferred, because the higher reactance of the lower part of the bar

during the starting period forces the current to the top of the bar, thereby increasing slightly the resistance of the rotor winding. Deep rotor slots, however, increase the leakage reactance and lead to small tooth widths and high density at the root of the teeth. When deep bars are used for the

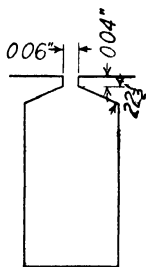


FIG. 190.

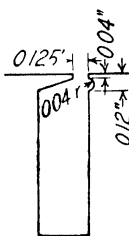
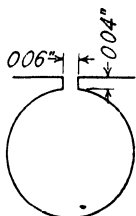


FIG. 191.

squirrel-cage winding the rotor slot is usually from 4 to 6 times as deep as it is wide. Motors with deep bar windings are called Class B motors in the Test Code of the A.I.E.E. for Induction Machines and are defined as normal-torque, low-starting-current squirrel-cage motors. Squirrel-cage motors for high starting torque and low starting current are called Class C motors in the A.I.E.E. Test Code and usually have a double squirrel-cage winding on the rotor. The double squirrel-

cage winding⁵ may be constructed in a number of different ways. Basically it consists of a high-resistance winding placed near the air gap surface of the rotor and a low-resistance winding placed well below the surface. The effectiveness of the lower winding at starting will depend upon how deep it is placed below the rotor surface. During starting, the reactance of the lower winding is high and only the high-resistance winding near the surface is active. After the rotor has attained full speed, the reactance of the lower winding is small and it will carry the largest portion of the rotor current.

The section area of each bar

$$s_b = \frac{S_{cl}}{N_b} \quad (187)$$

No insulation is used between the bars and rotor core. A small clearance, 0.005 to 0.015 in., depending upon whether the slots are skewed or not, must be allowed between the bar and core.

The number of rotor conductors for a wound-rotor motor depends upon the voltage between slip rings when the rotor is stationary, with the rings open, and normal voltage applied to the stator winding. For general-purpose motors, the rotor voltage between slip rings will generally not exceed about 400 volts. For large motors, higher rotor voltages are necessary to avoid large conductor sections. The rotor voltage

$$E_r = \frac{N_r k_p k_d}{N_k p k_d} k_2 E. \quad (188)$$

For star-connected rotor windings, $k_2 = 1.73$, and for delta-connected rotor windings, $k_2 = 1.00$.

Rectangular bar conductors are used for the rotor winding. When the rectangular type of slot shown in Fig. 190 is used, the coils are only partly formed before placing into the slots as shown in Fig. 179, Chapter XVI. For the type of slot shown in Fig. 191, the coils are insulated and formed before they are placed into the slots.

The insulation thickness required depends upon the rotor voltage. A slot lining consisting of 0.010-in. horn fiber is placed into the slot, and the remaining insulation is placed on the coils. The single thickness of insulation on the coils is generally 0.025 in. for voltages up to 600 and 0.035 in. for voltages up to 2500. The coil insulation is built up of varnished cambric, cotton tape, and insulating varnish. The

⁵ "The Development of Low Starting Current Induction Motors," by P. L. Alger, General Electric Review, Vol. 28, July, 1925, pp. 499-508.

allowance for the wedge for closing the slot is generally as shown in Figs. 190 and 191.

The area of each conductor

$$s_r = \frac{S_{cr}}{N_r m_a} \quad (189)$$

Rotor Tooth and Yoke Densities.—The maximum density for the rotor teeth

$$B_{t2} = \frac{\phi_t}{w_{t2}(l - n_d w_d) k_1 S_r}.$$

The minimum tooth width

$$w_{t2} = \frac{(D_r - 2d_{s1})\pi}{S_r} - w_{sr}. \quad (190)$$

For constant-speed induction motors, the frequency of the flux reversals in the rotor are very small, per cent slip times the stator frequency. The core losses in the rotor iron will therefore be small even if the densities are high. The maximum density in the rotor teeth can generally be only slightly higher than the maximum stator tooth density, because of the ampere-turns required to send the flux through the teeth.

The rotor yoke density is generally equal to or only slightly higher than the stator yoke density and can be calculated as explained for the stator yoke (see page 312).

Sample Design: *Design of Squirrel-Cage Rotor.*—The length of the air gap

$$\begin{aligned} \delta &= 0.125 - \frac{10}{D + 90} = 0.125 - \frac{10.17}{110 + 90} \\ &= 0.0228 \text{ in.}; \text{ use } 0.022 \text{ in.} \end{aligned}$$

The rotor diameter

$$D_r = D - 2\delta = 9.5 - 0.044 = 9.456 \text{ in.}$$

The number of rotor slots (see page 317)

$$S_r = 1.20 \times 54 = 64.8; \text{ use } 65.$$

The total stator copper section

$$\begin{aligned} S_{cs} &= N m_s a s_s = 162 \times 3 \times 2 \times 0.00644 \\ &= 6.26 \text{ sq. in.} \end{aligned}$$

If the rotor copper section is taken equal to 75 per cent of the total stator copper section (see page 320), then

$$S_{cr} = 0.75 \times 6.26 = 4.70 \text{ sq. in.},$$

and the area of each bar

$$s_b = \frac{4.70}{65} = 0.0723 \text{ sq. in.}$$

The rotor tooth pitch at the gap

$$t_{1r} = \frac{\pi D_r}{S_r} = \frac{\pi \times 9.456}{65} = 0.457 \text{ in.}$$

To avoid a very narrow tooth width at the bottom of the slot, it is generally necessary to make the rotor slot width less than half of t_{1r} . Copper bars, 0.141×0.531 in., 0.075 sq. in. in area, will be used for the squirrel-cage winding. The slot dimensions are (see Fig. 192): width 0.156 in., depth 0.616 in.

If the current density in the end-ring is equal to the current density in the bars, the end-ring section (see page 322)

$$s_{er} = \frac{0.32 \times 4.70}{6} \times 1 = 0.25 \text{ sq. in.}$$

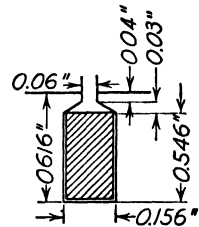


FIG. 192.

A copper end-ring, 0.25×0.875 in., or 0.219 sq. in. in area, will be used and will be brazed to the inside of the bars (see Fig. 186).

The minimum rotor tooth width

$$w_{tr2} = \frac{\pi(D_r - 2d_{sr})}{S_r} - w_{sr} = \frac{\pi(9.456 - 2 \times 0.616)}{65} - 0.156 = 0.241 \text{ in.}$$

The maximum density in the rotor teeth

$$B_{tr2} = \frac{\phi_t}{w_{tr2}(1 - n_d w_d) k_1 S_r} = \frac{604 \times 6}{0.241(4.5 - 0.093 \times 65 \times 0.637)} = 87.0 \text{ kilo-lines.}$$

For a flux density of 70,000 lines per sq. in. in the rotor yoke

$$d_{yr} = \frac{\phi}{B_{yr}(1 - n_d w_d) k_1} = \frac{604 \times 10^3}{70,000(4.5 - 0.093)} = 2.06 \text{ in.}$$

and the inside diameter of the rotor core

$$\begin{aligned} D_i &= D_r - 2d_{sr} - d_{yr} = 9.456 - 2 \times 0.616 - 2.06 \\ &= 6.164 \text{ in.}; \text{ make this } 6.25 \text{ in.} \end{aligned}$$

Then

$$d_{yr} = 1.97 \text{ in.}$$

and

$$B_{yr} = \frac{604 \times 10^3}{1.97(4.5 - 0)0.93} = 73.3 \text{ kilo-lines per sq. in.}$$

CHAPTER XIX

MOTOR CHARACTERISTICS

The Magnetizing Current.—Figure 193 shows the magnetic circuit for a 4-pole motor. The flux set up by the stator ampere-turns passes through the air gap into the rotor and through the rotor teeth into the rotor yoke. There the flux of each pole divides, one-half returning through the rotor teeth, air gap, stator teeth, and yoke of each of the adjacent poles.

Air Gap Ampere-Turns.—The ampere-turns per pole required on the stator to send the flux through the air gap

$$AT_g = B_g \delta k_s k_r \times 0.313. \quad (191)$$

The slot openings of both stator and rotor increase the reluctance of the air gap. Their effect may be taken into account by assuming that the air gap section is reduced a given amount, thereby increasing the density, or by assuming that the slot openings are equivalent to an increased length of air gap. F. W. Carter¹ derived an equation by which the air gap coefficient can be calculated. A similar equation is given by Dr. Arnold.² R. W. Wieseman³ obtained air gap coefficients by plotting graphically the flux distribution around a tooth. His results check very well with those obtained by the formulas given by Dr. Arnold and F. W. Carter. The air gap coefficient for the stator slot openings, assuming a smooth rotor without slots,

$$k_s = \frac{t_{1s}}{w_{t_{s1}} + (\delta y)}. \quad (192)$$

Similarly, the air gap coefficient for the rotor slot openings, assuming a smooth stator without slots,

$$k_r = \frac{t_{1r}}{w_{t_{r1}} + (\delta y)}. \quad (193)$$

¹ Electrical World, Vol. 38, p. 884, 1901.

² "Die Wechselstromtechnik," by Dr. Arnold, Vol. 4, pp. 78 and 79.

³ "Graphical Determination of Magnetic Fields," by R. W. Wieseman, A.I.E.E. Journal, Vol. 46, May, 1927, p. 431.

The value for y in equations 192 and 193 is taken from the curve in Fig. 53.

The air gap coefficient from Carter's work for open slots

$$k = \frac{t_1(5\delta + w_{s1})}{t_1(5\delta + w_{s1}) - w_{s1}^2}, \quad (192a)$$

and for partially closed slots

$$k = \frac{t_1(4.4\delta + 0.75w_{s1})}{t_1(4.4\delta + 0.75w_{s1}) - w_{s1}^2}. \quad (193a)$$

To calculate k_s , the stator slot opening and tooth pitch at the gap are used in the equations 192a or 193a, and to calculate k_r for the rotor, the rotor values are used.

$$AT_g = B_g \delta k_s k_r \times 0.313. \quad (194)$$

Ampere-Turns Stator and Rotor Yoke.—The method of calculating the flux density in the yoke for the stator and rotor has been given above. This is the maximum value of the flux density in the yoke. For induction motors the flux does not enter the stator and rotor yoke at a point; therefore, the yoke density can not be constant over the length of the flux path. If the air gap flux distribution curve is assumed to be a sine wave, then the flux density in the yoke will vary sinusoidally with maximum value in the interpolar space. The ampere-turns per pole for the stator and rotor yoke can be calculated by the following method.⁴ For a given maximum value of sinusoidally varying yoke density the ampere-turns per inch are determined for various points along the wave. The average value of the ampere-turns per inch is determined for this curve by graphical integration. By repeating such calculations for a number of maximum values of B_{ys} , a curve can be plotted of B_{ys} against average ampere-turns per inch. Such a curve is shown in Fig. 202 for electrical-grade sheet steel and is used for calculating ampere-turns per pole for stator and rotor yoke. The length of the flux path in the yokes may be taken equal to one-half the pole pitch on the mean diameter of the yoke. For the stator

$$l_{ys} = \frac{(D + 2d_{ss} + \frac{1}{2}d_{rs})\pi}{2p}, \quad (195)$$

⁴ See, also: "Elektrische Maschinen," R. Richter, Vol. 2, p. 69, Julius Springer, Berlin; "Experimentelle Bestimmung der Magnetisierungs-Kurve für hohe Inductionen," by K. O. Lehmann: "Archiv für Electrotechnik," Vol. 24, 1930, p. 804; "Flux Distribution in the Core of a Turbo-Alternator," by Fechheimer, A.I.E.E. Journal, Vol. 39, 1920, p. 669.

and for the rotor

$$l_{yr} = \frac{(D_r - 2d_{sr} - \frac{1}{2}d_{yr})\pi}{2p} \quad (196)$$

The ampere-turns per pole for the stator yoke

$$AT_{ys} = at_{ys}l_{ys},$$

and for the rotor yoke

$$AT_{yr} = at_{yr}l_{yr}.$$

Ampere-Turns Stator and Rotor Teeth.—For tapered stator and rotor teeth, the density varies along the length of the tooth. Various methods have been proposed for calculating the ampere-turns required to send the flux through tapered teeth. Satisfactory results are generally obtained by calculating the ampere-turns for the density at a section $\frac{1}{3}$ tooth length from the minimum section. From a curve derived as explained for Fig. 202 the ampere-turns per inch are found and multiplied by 1.57, and

$$AT_{ts} = at_{ts}l_{ts}.$$

For the rotor teeth

$$AT_{tr} = at_{tr}l_{tr}.$$

The length of the flux path in the teeth is equal to the depth of the slot.

The total ampere-turns per pole required to send the flux through the magnetic circuit

$$ATP = AT_g + AT_{ts} + AT_{tr} + AT_{ys} + AT_{yr}.$$

The effective value of the magnetizing current ⁵ per phase

$$I_m = \frac{2.22pATP}{m_s N k_d k_p} \quad (197)$$

$$\text{The per cent magnetizing current} = \frac{I_m}{I} 100.$$

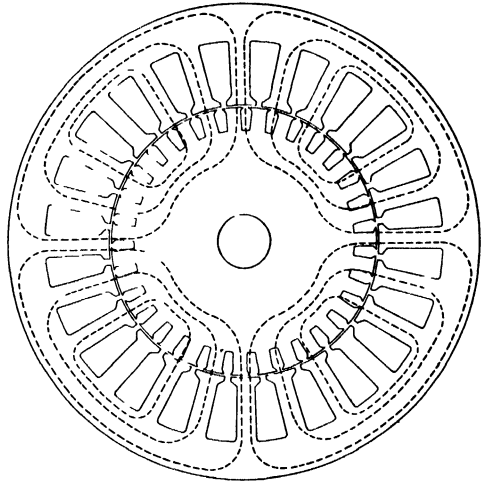


FIG. 193. —Magnetic circuit—1 hp, 1800 r.p.m., 4 pole, three-phase motor (for dimensions see Figs. 175 and 177).

⁵ "Wechselstromtechnik," Vol. 5-1, Julius Springer, Berlin.

No-Load Current.—The no-load current of an induction motor is made up of two components: one, the magnetizing current, which is 90° out of phase with the voltage; two, the watt component of the no-load current, which is in phase with the voltage. The in-phase component of the no-load current is the current required by the no-load losses. These consist of core losses, friction and windage losses, and armature copper losses due to the no-load current.

Core Losses.—The losses⁶ in the cores of induction motors consist of the hysteresis and eddy-current losses in the teeth and yokes due to the fundamental frequency flux plus additional losses. The additional losses comprise surface losses in the teeth due to variations in the air gap density, tooth pulsation losses due to variations in the tooth density, losses due to slot filing, losses due to non-uniform flux distribution, and losses in the end-plates and end-brackets. In the stator core, the frequency of the flux reversals is equal to line frequency; in the rotor it is equal to line frequency times the per cent slip. For wound-rotor motors operating at reduced speed, the rotor core losses must be included when calculating the operating characteristics. The loss in the stator teeth due to the fundamental frequency flux is equal to the loss per pound for the stator tooth density times the weight of the iron in the teeth. The loss per pound for various flux densities and for several grades of sheet steel is given by the curves in the Appendix. These curves are obtained from tests on samples in accordance with the American Society for Testing Materials. The loss in the stator yoke due to the fundamental frequency flux is calculated as explained for the teeth.

The additional losses are difficult to calculate. The surface losses in the teeth and the tooth pulsation losses can be calculated by the method proposed by T. Spooner⁷ and I. F. Kinard.

Tooth pulsation loss

$$= CB_g^{2.3} \left(\frac{f}{p} \right)^{1.55} D^{20.5} \left(\frac{w_{s1}}{\delta} \right)^{1.22} \sqrt{S_s} (l - n_d w_d) k_1 10^{-8} \text{ watts.}$$

Here $C = 1.85$ for 26-gauge electrical-grade sheet steel, 1.36 for 26-gauge dynamo grade, and B_g is the air gap density in kilo-lines per square inch. The additional losses may also include a no-load loss in

⁶ "Induction Motor Core Losses," by P. L. Alger and R. Eksbergian, A.I.E.E. Journal, Vol. 39, Oct., 1920, pp. 906-920.

⁷ "Tooth Pulsation in Rotating Machines," by T. Spooner, Trans. A.I.E.E., Vol. 43, 1924, p. 252; "Surface Iron Losses with Reference to Laminated Materials," by T. Spooner and I. F. Kinard, A.I.E.E. Trans., Vol. 43, 1924, p. 262; "No-Load Induction Motor Core Losses," by T. Spooner and C. W. Kincaid, presented at winter convention A.I.E.E., Jan. 28 to Feb. 1, 1929.

the squirrel-cage winding. (See footnote, page 252.) The total core losses for induction motors are generally 1.5 to 2.5 times the sum of the stator tooth and yoke losses due to the fundamental frequency flux. The multiplying factor should be obtained from tests of motors of similar design. When such data are not available 1.75 to 2.2 may be used.

Friction and Windage Losses.—The bearing friction losses can be calculated when the bearing dimensions are known. The windage losses depend upon the type of construction and are very difficult to calculate. The combined friction and windage losses should be determined from tests of machines of similar design and construction. These losses are generally equal to from 3.5 per cent of the kilowatt output for 5-hp., 1800-r.p.m. motors to 1.0 per cent for 200- to 300-hp., 450-r.p.m. motors.

No-Load Stator Copper Loss.—The length of the half mean-turn of the stator coils is calculated as explained for the armature coils of synchronous machines, page 208. The coil extension and the clearance between coils at the end-connections are generally smaller than those used for the armature windings of synchronous machines. Table XXVI gives suitable values for induction motor stator and rotor windings.

The length of the half mean-turn of a stator coil (see Fig. 135 and Table XXVI)

$$L_s = \frac{\pi(D + d_s)}{p \cos \alpha} P + 2b + d_{ss} + l \text{ in.} \quad (198)$$

$$\sin \alpha = \frac{w_s + s}{t_{1s}}.$$

The horizontal extension of the stator coil beyond each end of the core is calculated as explained on page 210. The length of the half mean-turn of a rotor coil for wound-rotor type motors (see Fig. 50 and Table XXVI, page 309)

$$L_r = \frac{\pi(D_r - d_s)}{p \cos \alpha} P + 2b + d_{sr} + l \text{ in.} \quad (199)$$

$$\sin \alpha = \frac{w_r + s}{t_{1r}}.$$

The resistance per phase of the stator winding

$$R_s = \frac{L_s N r}{as_s \times 10^6} \text{ ohms.} \quad (200)$$

This is the direct-current resistance of the stator winding; the effective, also called alternating-current, resistance, R_{se} , is usually from 1.15 to 1.30 times the direct-current resistance. The lower value will apply to the smaller ratings with small conductor section area in the stator winding, and the higher value to the larger ratings.

The resistance of the rotor winding for a wound-rotor motor in terms of the stator winding

$$R_r = \frac{k_d^2 k_p^2 N^2}{k_{dr}^2 k_{pr}^2 N_r^2} - \frac{L_r N_r r}{a s_r \times 10^6} \text{ ohms per phase,} \quad (201)$$

or

$$R_r = \frac{k_d^2 k_p^2}{k_{dr}^2 k_{pr}^2} \frac{L_r}{L_s} \frac{S_{cs}}{S_{cr}} R_s \text{ ohms per phase.} \quad (201a)$$

For a temperature of 25° C., $r = 0.692$, and for 75° C., $r = 0.826$. The stator copper losses due to the no-load current are, approximately,

$$W_{sc0} = I_m^2 m R, \text{ watts.} \quad (202)$$

The in-phase component of the no-load current

$$I_w = \frac{W_r + W_{fu} + W_{sc0}}{mE} \text{ amperes,} \quad (203)$$

and the no-load current

$$I_0 = \sqrt{I_m^2 + I_w^2} \text{ amperes.} \quad (204)$$

The power factor of the motor at no-load

$$\text{PF}_0 = \frac{I_w}{I_0}. \quad (205)$$

Short-Circuit Current.—The current that an induction motor will draw from the line when the rotor is blocked depends upon the applied voltage and the total impedance of the motor at standstill. The total impedance comprises the stator and rotor resistance and the stator and rotor leakage reactance.

Rotor Resistance.—The method of calculating the resistance of the rotor winding for wound-rotor motors has been given above. Figure 189 shows the distribution of the current in a squirrel-cage winding. The total resistance of the squirrel-cage bars

$$= \frac{l_b N_{br}}{10^6 s_b} \text{ ohms,}$$

and that of the two end-rings

$$= \frac{2\pi D_{er} r}{10^6 s_{er}} \text{ ohms.}$$

The total resistance of the squirrel-cage winding is equal to the total copper loss divided by the current squared, and is

$$= \frac{l_b N_b r}{10^6 s_b} + \frac{N_b^2}{\pi^2 p^2} \frac{2\pi D_{er} r}{10^6 s_{er}} = N_b^2 \left(\frac{l_b r}{10^6 s_b N_b} + \frac{0.64 D_{er} r}{10^6 s_{er} p^2} \right) \text{ ohms.}$$

The rotor resistance must be expressed in terms of the stator winding before it can be added to the stator resistance to give the total resistance of the motor. At standstill, the induction motor is simply a polyphase transformer; the equivalent resistance of the rotor is therefore equal to the total rotor resistance times the square of the ratio of the effective stator turns to the effective rotor turns. The number of phases in a squirrel-cage winding is equal to the number of bars per pole = N_b/p , and the number of turns in series per phase is equal to the number of pole pairs = $p/2$. The total resistance of a squirrel-cage winding in terms of the stator winding is, then,

$$\begin{aligned} &= \left[\frac{(N/2) k_p k_d m}{(p/2)(N_b/p)} \right]^2 \frac{r}{10^6} N_b^2 \left(\frac{l_b}{s_b N_b} + \frac{0.64 D_{er}}{p^2 s_{er}} \right) \\ &= \left(\frac{N^2 k_p^2 k_d^2 m^2 r}{10^6} \right) \left(\frac{l_b}{s_b N_b} + \frac{0.64 D_{er}}{p^2 s_{er}} \right). \end{aligned}$$

When the radial width of the end-ring is large, as it often is in small motors, the end-ring resistance must be corrected to take into account the effect of non-uniform current distribution in the ring. P. H. Trickey,⁸ in his paper "Induction Motor Resistance Ring Width," has developed a constant by which the end-ring resistance must be multiplied to include the effect of non-uniform current distribution. The equivalent rotor resistance per phase

$$R_r = \frac{N^2 k_p^2 k_d^2 m r}{10^6} \left(\frac{l_b}{s_b N_b} + \frac{0.64 D_{er}}{p^2 s_{er}} K_{ring} \right) \text{ ohms.} \quad (206)$$

K_{ring} is taken from the curves of Fig. 194, and m , the number of phases, is equal to 2 for single-phase machines. In this formula, $r \times 10^{-6}$ is the resistance of copper per square inch section, 1 in. long; $r = 0.826$ for 75° C. and 0.692 for 25° C. If a material other than copper is used for the squirrel-cage winding the corresponding value of r must be used. Standard brass has a resistance about 4 times, and aluminum about 2 times, that of copper.

To calculate the leakage reactance of any winding it is necessary to

⁸ "Induction Motor Resistance Ring Width," by P. H. Trickey, *Electrical Engineering*, Vol. 55, Feb., 1936, p. 144.

calculate first the leakage flux per unit of current flowing in the winding, which is equal to the magnetomotive force acting on the leakage path times the permeance of the path.

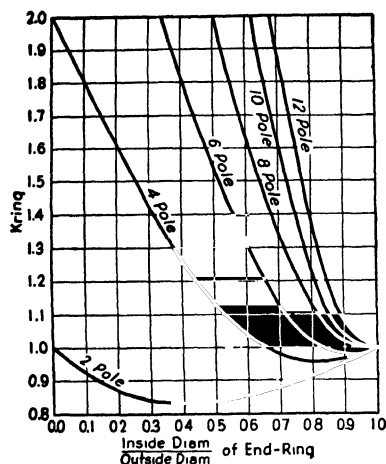


FIG. 194.

The flux per unit of current times the turns with which it is inter-linked gives the inductance and the reactance is $2\pi fL$. The leakage reactance of rotating machinery windings is calculated by assuming that the leakage flux flows in definite paths for which the area and length can be calculated. For induction motors it is common practice to divide the total leakage flux into stator and rotor slot leakage flux, end-connection leakage, zigzag leakage or differential leakage, belt leakage, and skew leakage. The reactance calculations are made on the assumption that these leakage paths are not saturated. The large

current drawn by the motor during the starting period produces saturation in the tooth tips which has the effect of reducing the total leakage reactance. To calculate the starting performance a corrected total leakage reactance must, therefore, be used. The method of calculating the slot permeance is given by various authors.⁹ For a pitch winding the inductance per phase for the slot leakage flux

$$L_s = 0.4\pi n_s^2 \frac{m}{S} l_g 2.54(F_{st} + F_{sb}) 10^{-8} \text{ henry.}$$

For fractional pitch windings the current in the two coil sides in some of the slots is not in phase and the inductance is less than for a pitch

⁹ "The Design of Induction Motors," by C. A. Adams, A.I.E.E. Trans., Vol. 24, 1905, p. 649; "Zigzag Leakage of Induction Motors," by R. E. Hellmund, A.I.E.E. Trans., Vol. 26, 1907, p. 1505; "The Calculation of the Armature Reactance of Synchronous Machines," by P. L. Alger, A.I.E.E. Trans., Vol. 47, 1928, p. 493; "Analytical Determination of Magnetic Fields," by B. L. Robertson and I. A. Terry, A.I.E.E. Trans., Vol. 48, 1929, p. 1242. "Calculation of Synchronous Machine Constants," by L. A. Kilgore, A.I.E.E. Trans., Vol. 50, 1931, p. 1201. "Electric Machinery," by Liwshitz-Garik and Wipple, Vol. 1, p. 63, D. Van Nostrand Co., New York; "Calculation of Slot Constants," by A. F. Puchstein, A.I.E.E. Trans., Vol. 66, 1947, p. 1315; "The Air Gap Reactance of Polyphase Machines," by P. L. Alger and H. R. West, A.I.E.E. Trans., Vol. 66, 1947, p. 1331, "Reactances of Induction Motors," by V. C. Lloyd, V. F. Giusti, and S. S. L. Chang, A.I.E.E. Trans., Vol. 66, 1947, p. 1349.

winding. This effect is taken into account by multiplying the equation for inductance by a reduction factor which is given by Fig. 143. Substituting $\frac{Nm}{S_s}$ for n_s , the series conductors per slot, and multiplying by $2\pi f$, the slot leakage reactance

$$X_{ss} = \frac{N^2 m f}{10^7} \frac{2 \text{ } 0l_g K_s}{S_s} (F_{sst} + F_{ssb}) \text{ ohm.}$$

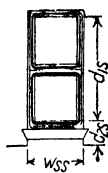


FIG. 195.

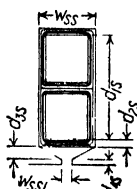


FIG. 196.

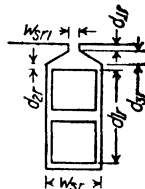


FIG. 197.

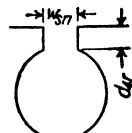


FIG. 198.

Here F_{sst} is the stator slot factor for the top of the slot and F_{ssb} the slot factor for the bottom of the slot. For open stator slots, Fig. 195,

$$F_{sst} + F_{ssb} = \frac{d_{1s}}{w_{ss}} + \frac{d_{1s}}{3w_{ss}}.$$

For partly closed stator slots, Fig. 196,

$$F_{sst} + F_{ssb} = \left(\frac{d_{1s}}{w_{ss}} + \frac{2d_{1s}}{w_{ss} + w_{ss1}} \right) + \left(\frac{d_{2s}}{w_{ss}} + \frac{d_{1s}}{3w_{ss}} \right).$$

The rotor slot leakage reactance

$$X_{sr} = \frac{N^2 m f}{10^7} \frac{2 \text{ } 0l_g (h_p h_d)^2 K_r}{(h_p h_d)^2 S_r} (F_{srt} + F_{srb}) \text{ ohm.}$$

For rectangular partly closed rotor slots, Fig. 197,

$$F_{srt} + F_{srb} = \left(\frac{d_{1r}}{w_{sr}} + \frac{2d_{1r}}{w_{sr} + w_{sr1}} \right) + \left(\frac{d_{2r}}{w_{sr}} + \frac{d_{1r}}{3w_{sr}} \right).$$

For round rotor slots, Fig. 198,

$$F_{srt} + F_{srb} = \frac{d_{1r}}{w_{sr}} + 0.625.$$

For trapezoidal slots on either stator or rotor the slot factor for top and bottom of slot is calculated as shown in Figs. 213 and 214, pp. 369, 370.

The stator zigzag⁹ leakage reactance

$$X_{sz} = \frac{5}{6} X_m \left(\frac{p}{S_s} \right)^2 \text{ ohms;}$$

and the rotor zigzag leakage reactance

$$X_{rz} = \frac{5}{6} X_m \left(\frac{p}{S_r} \right)^2 \text{ ohms.}$$

The magnetizing reactance of an induction motor in ohms per phase is approximately equal to the terminal voltage per phase divided by the magnetizing current per phase corresponding to the air gap ampere-turns. The total stator and rotor zigzag leakage reactance

$$X_z = \frac{E}{1.2 I_{m_g}} \left[\left(\frac{p}{S_s} \right)^2 + \left(\frac{p}{S_r} \right)^2 \right] \text{ ohms.}$$

The belt leakage reactance is equal to zero for motors with squirrel-cage rotor windings and integral number of slots per pole. For wound-rotor motors, the total belt leakage reactance for stator and rotor

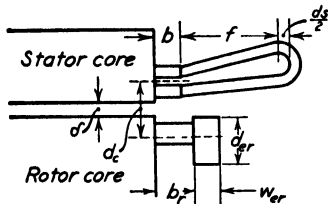


FIG. 199.

$$X_b = \frac{E}{I_{m_g}} (K_{bs} + K_{br}).$$

The belt leakage constants, K_{bs} and K_{br} , vary with the per cent pitch of the respective windings. They are shown in Fig. 144. They have been derived

by P. L. Alger in his A.I.E.E. paper referred to above.

The stator end-connection leakage reactance may be calculated by the method suggested by L. A. Kilgore,⁹

$$X_{se} = \frac{N^2 m_f}{10^7} \frac{0.8 (k_p k_d)^2}{p} \left[b + 0.5 \left(f + \frac{d_{ss}}{2} \right) \right].$$

The stator coil end-connection is shown in Fig. 199. Values for b are given in Table XXVI, and f may be calculated as shown on page 309. For the end-connection leakage reactance of wound-rotor induction motors the rotor values are used and the entire equation multiplied by the effective turns ratio squared to convert to stator terms.

$$\begin{aligned} X_{re} &= \frac{N_r^2 m_f}{10^7} \frac{0.8 (k_{pr} k_{dr})^2}{p} \left[b_r + 0.5 \left(f_r + \frac{d_{sr}}{2} \right) \right] \frac{N^2 k_p^2 k_d^2 m_s}{N_r^2 k_{pr}^2 k_{dr}^2 m_r} \\ &= \frac{N^2 m_f}{10^7} \frac{0.8 (k_p k_d)^2}{p} \left[b_r + 0.5 \left(f_r + \frac{d_{sr}}{2} \right) \right]. \end{aligned}$$

The values of b in Table XXVI can also be used for the rotor winding, and f_r can be calculated as explained for direct-current armature windings, page 59.

The rotor end-connection leakage reactance for squirrel-cage rotor windings

$$X_{re} = \frac{N^2 m f}{10^7} \frac{c_r (k_p k_d)^2}{p^2} \left(2pb_r + \frac{\pi D d_c}{1.7w_{er} + 1.2d_{er} + 1.4d_c} \right) \text{ ohm.}$$

For brazed rotor windings for which the bars extend beyond the rotor core $c_r = 0.4$, and for die-cast rotor windings with end-ring adjacent to rotor core $c_r = 0.58$. The dimension d_c , Fig. 199, is the radial distance from the center of the end-ring to the center of the filled part of the stator slot.

The skew leakage reactance

$$X_{sl} = \frac{E}{I_{m0}} \frac{\theta_{sk}^2}{12} \text{ ohm,}$$

where θ_{sk} is the skew expressed in radians and is equal to π times the ratio of the number of slots skew to the number of slots per pole of the skewed member.

The total leakage reactance of the stator plus the rotor in terms of the stator winding in ohms per phase

$$X_{l \text{ run}} = X_{ss} + X_{sr} + X_{se} + X_{re} + X_z + X_b + X_{sk} \text{ ohms.} \quad (207)$$

The per unit reactance $= \frac{I_p X_l}{E_T}$. I_p is the in-phase component of the motor input current. The stator reactance per phase

$$X_{1 \text{ run}} = X_{ss} + X_{se} + 0.5(X_z + X_{sk} + X_b) \text{ ohms,}$$

and the rotor reactance per phase

$$X_{2 \text{ run}} = X_{rs} + X_{re} + 0.5(X_z + X_{sk} + X_b) \text{ ohms.}$$

The magnetizing reactance

$$X_m = \frac{E_T - I_m X_1}{I_m} = \frac{E_T}{I_m} - X_1,$$

and

$$b_m = \frac{1}{X_m}.$$

The resistance to represent the core loss in the equivalent circuit

$$R_m = \frac{\text{Core loss}}{m J_m^2},$$

and the conductance

$$g_m = \frac{\text{Core loss}}{mE_1^2} = \frac{\text{Core loss}}{m(E_T - I_m X_1)^2}.$$

The equivalent-circuit method¹⁰ is generally used to calculate induction-motor performance characteristics. For the single squirrel-cage winding the equivalent circuit is shown in Fig. 204, and for the double squirrel-cage winding in Fig. 205. For any slip up to and including the slip at maximum torque, the performance characteristics are calculated as shown below. For full-load output R_r/s is approximately equal to E_T/I .

$$Z_2 = R_r/s + jX_2 = Z_2/\theta^\circ. \quad Y_2 = g_r - jb_2 = Y_2/(-\theta^\circ).$$

$$Z = R + jX = Z/\theta^\circ. \quad Y_m = q_m - jb_m$$

$$Z_1 = R_s + jX_1. \quad Y = G - jB = Y/(-\theta^\circ).$$

$$Z_T = R_T + jX_T = Z_T/\theta^\circ.$$

$$I = E_T \div Z_T; I_r = \frac{Z}{Z_2} I; \text{PF} = R_T : Z_T.$$

The stator copper loss = $I^2 m R_s$ watts (1).

The rotor copper loss = $I_r^2 m R_r$ watts (2).

The gross secondary output = $(1 - s)I_r^2 m R_r/s$ watts (3).

The input = (1) + (2) + (3) + core loss + stray load-loss.

The shaft output = (3) - friction and windage loss.

$$\text{Efficiency} = \frac{\text{shaft output}}{\text{input}}.$$

$$\text{R.p.m.} = (1 - s) \times \text{syn. r.p.m.}$$

$$\text{Torque} = \frac{7.04 \times \text{shaft output}}{\text{R.p.m.}}$$

The slip at maximum torque

$$s_m = \frac{R_r}{\sqrt{R_s^2 + X_{1 \text{ run}}^2}}.$$

¹⁰ "Theoretical Elements of Electrical Engineering," by C. P. Steinmetz, McGraw-Hill Book Co., New York; General Electric Review, Vol. 22, April, 1919, p. 230; Electric Journal, Vol. 24, Nov., 1927, pp. 569-573; "Induction Motor Performance Calculations," by P. L. Alger, A.I.E.E. Trans., Vol. 49, July, 1930, p. 1055; "Poly-phase Induction Motors," by W. J. Branson, A.I.E.E. Trans., Vol. 49, Jan., 1930, p. 319; "Performance Calculations on Induction Motors," by C. G. Veinott, A.I.E.E. Trans., Vol. 51, Sept., 1932, p. 743.

The effect of magnetic saturation in the leakage flux path and the effect of unequal current distribution in deep rotor bars during starting can be determined with satisfactory accuracy by the methods proposed by H. M. Norman¹¹ and M. Liwschitz.¹¹ The constant R_c , by which

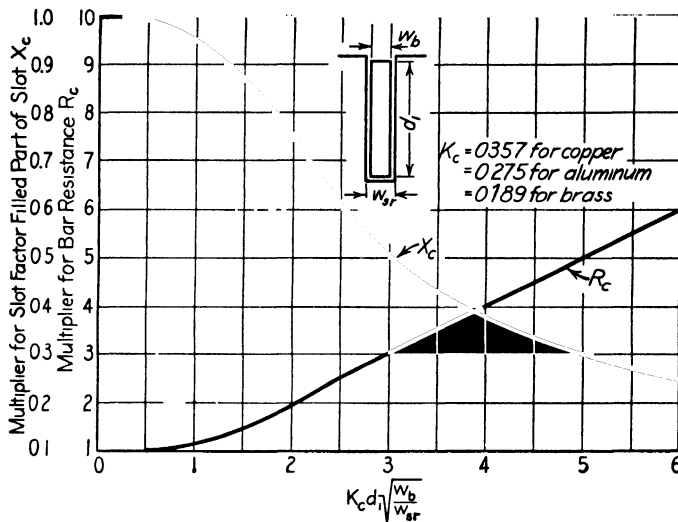


FIG. 200.

the embedded portion of the rotor bar must be multiplied to correct for skin effect, is shown in Fig. 200 and varies with

$$K_c d_1 \sqrt{f \frac{w_b}{w_{sr}}}.$$

Here d_1 is the depth of the bar, w_b the width of the bar, w_{sr} the slot width, f the line frequency for the stator and slip frequency for the rotor, and K_c a constant equal to 0.357 for copper, 0.275 for aluminum, and 0.189 for brass. The squirrel-cage winding resistance at starting

$$R_{r \text{ start}} = \frac{N^2 k_p^2 k_d^2 m r}{10^6} \left(\frac{l_b}{s_b \times N_b} R_c + \frac{0.64 D_r}{p^2 s_{r}} K \text{ ring} \right).$$

When the rotor bar extends beyond the core, the bar resistance must be calculated in two steps since only the embedded part of the bar is multiplied by the correction factor R_c .

¹¹ "Induction Motor Locked Saturation Curves," by H. M. Norman, *Electrical Engineering*, April, 1934, pp. 536-541; "Asynchronous Motors with Squirrel-Cage Armature for High Starting Torque and Low Starting Current," by M. Liwschitz, *Siemens Zeitschrift*, Feb. and March, 1925.

The determination of the effect of saturation in the leakage paths of squirrel-cage motors on the reactance at starting is difficult, and very little work has been done on this subject. The method given here is based on H. M. Norman's A.I.E.E. paper referred to above. It is the author's hope that the presentation of a method of calculating the effect of saturation upon leakage reactance might encourage some students to carry on further investigations as a thesis or special design problem.

The ampere-turns per slot for the locked rotor current

$$AT_s = I_s \frac{t_a \times c_s}{a} 0.707 \left[K_s + k_p \times k_d^2 \times \frac{S_s}{S_r} \right] \sqrt{\frac{E}{E_T}}.$$

Here t_a is the number of turns per coil, c_s the number of coil sides per slot, K_s the stator winding pitch correction factor for slot leakage given

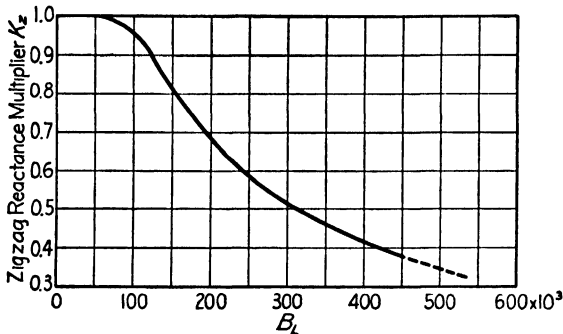


FIG. 201.

in Fig. 143, and I_s the short-circuit or locked rotor current input which is assumed.

$$\beta = \sqrt{\frac{6.25\delta}{t_{1s} + t_1}} + 0.64$$

and

$$B_L = \frac{AT_s}{0.628\delta\beta}.$$

From Fig. 201 the multiplying factor K_z is found, and

$$C_{ss} = (t_{1s} - w_{s1})(1 - K_z)$$

for the stator slot opening and

$$C_{sr} = (t_{1r} - w_{r1})(1 - K_z)$$

for the rotor slot opening. The reduction of the slot factor for the top of the slot for open slots, Fig. 195,

$$\Delta F_{sst} = \frac{d_{2s}}{w_{ss}} \left(\frac{C_{ss}}{C_{ss} + w_{ss}} \right)$$

For partly closed slots, Fig. 196,

$$\Delta F_{sst} = \frac{d_{4s} + 0.58d_{3s}}{w_{s1}} \left(\frac{C_{ss}}{C_{ss} + 1.5w_{s1}} \right).$$

The corresponding values for the rotor slot are calculated by using rotor slot dimensions instead of the stator slot values. A correction is also applied to the slot factor for the bottom of the rotor slot when deep bars are used; this factor X_c is given in Fig. 200. The leakage reactances at starting

$$X_{ss \text{ start}} = X_{ss \text{ run}} \left(\frac{F_{sst} - \Delta F_{sst} + F_{ssb}}{F_{sst} + F_{ssb}} \right).$$

$$X_{sr \text{ start}} = X_{sr \text{ run}} \frac{F_{srt} - \Delta F_{srt} + (F_{srb} \times X_c)}{F_{srt} + F_{srb}}.$$

$$X_z \text{ start} = X_z \text{ run} \times K_z.$$

$$X_l \text{ start} = X_{ss \text{ start}} + X_{sr \text{ start}} + X_{sc} + X_{re} + X_z \text{ start}.$$

$$X_1 \text{ start} = X_{ss \text{ start}} + X_{sc} + 0.5X_z \text{ start}.$$

From the calculations of the equivalent circuit for $s = 1$ the input current and equivalent rotor current are calculated.

$$\text{Starting torque} = \frac{\text{rotor copper loss } (s = 1) 7.04}{s \text{ r.p.m.}} \text{ lb.-ft.}$$

Rheostat Data.—Wound-rotor motors are started by inserting a resistance into the rotor circuit, which is generally star-connected and of such value as to give full-load torque at starting. The voltage across the slip-rings at standstill, with normal voltage applied to the stator, is calculated by formula 188 and is

$$E_r = \frac{N_r k_p k_{dr}}{N k_p k_d} k_2 E \text{ volts.}$$

At synchronous speed, the rate of change of the primary flux through the rotor coils is the same as that produced by the alternations of the primary flux at standstill. The counter e.m.f. at synchronous speed is therefore equal to E_r . The counter e.m.f. varies directly with the

speed; for any load it is then equal to $E_r(1 - \text{slip})$. The motor output in watts is equal to the counter voltage times the rotor current. Neglecting the phase displacement between rotor voltage and current, which is negligible for normal speeds, the rotor current per phase for 3-phase rotor windings

$$I_r = \frac{\text{hp. } 746k_2}{E_r(1 - \text{slip})3} \text{ amperes.} \quad (208)$$

For a star-connected rotor winding, $k_2 = 1.73$; and for delta-connected rotor winding, $k_2 = 1.0$. This formula does not take into account all the factors affecting the rotor current, but it is sufficiently accurate for design calculations.

The rheostat resistance per phase when star-connected for full-load starting torque

$$R_{rh} = \frac{E_r(1 - \text{slip})}{I_r k_2} \text{ ohms.} \quad (209)$$

For star-connected rotor winding, $k_2 = 1.73$; and for delta-connected rotor winding, $k_2 = 1$.

Temperature Rise.—The limiting observable temperature rise for the various windings of induction motors should not exceed the values specified by the American Standards Association and given in Table XXVII.¹² The heat-dissipating surface should include all those surfaces of the core and windings swept by the cooling air. This means that the surface area exposed to the cooling air will depend upon the frame construction and methods used to direct the cooling air through the motor. For open-type motors, the radiating surface usually will include the back and end surfaces of the stator core plus one surface for each ventilating duct, the surface around the stator winding end connections, and the end surfaces of the rotor core plus the surface around the end connections of the rotor winding. The losses that must be dissipated are stator and rotor copper loss, stray load-losses, and stator core loss. Since the type of frame construction determines in a large measure the radiating surface, it is difficult to specify exact limits of radiating surface per watt required for different values of temperature rise. In general, the square inch radiating surface per watt loss for open-type motors should be approximately 1.0 for a 40° C. temperature rise. For totally enclosed motors with cast-iron frame and end brackets without fan cooling the total outside surface area of the motor per watt loss must be greater than 2.5 for a temperature rise not to exceed 55° C.

¹² See American Standard Rotating Electrical Machinery, C50, March, 1943. These standards may be obtained from the American Standards Association, 70 East 45 Street, New York 17, New York.

Sample Design: Operating Characteristics.—The ratio of stator slot opening to air gap length

$$= \frac{0.10}{0.022} = 4.55.$$

From the curve in Fig. 53, $y = 2.26$, and the air gap coefficient for the stator slots

$$k_s = \frac{t_{1s}}{w_{ts1} + (\delta y)} = \frac{0.552}{0.452 + (0.022 \times 2.26)} = 1.10.$$

TABLE XXVII
LIMITING OBSERVABLE TEMPERATURE RISE
INDUCTION MOTORS

Item	Machine Part	Method of Temperature Determination to be Employed	General-Purpose Motors		Totally Enclosed Motors		Other Motors	
			Class A Insulation	Class B Insulation	Class A Insulation	Class B Insulation	Class A Insulation	Class B Insulation
1	Windings	Thermometer Resistance	40	—	55	75	50	70
			50	—	60	80	60	80
2	Cores and mechanical parts in contact with or adjacent to insulation	Thermometer	40	—	55	75	50	70
3	Collector rings and commutators	Thermometer	55	75	65	85	65	85
4	Squirrel-cage windings and miscellaneous parts (such as brush holders, brushes, pole tips, etc.) may attain such temperatures as will not injure the machine in any respect.							

For the rotor slot, the ratio of slot opening to gap length

$$= \frac{0.06}{0.022} = 2.7$$

and $y = 1.71$. The air gap coefficient is then

$$k_r = \frac{t_{1r}}{w_{tr1} + \delta y} = \frac{0.457}{0.397 + 0.022 \times 1.71} = 1.06.$$

The flux density in the air gap is given on page 314. The air gap ampere-turns per pole

$$\begin{aligned} AT_g &= B_g \delta k_s k_r \times 0.313 = 42,300 \times 0.022 \times 1.10 \times 1.06 \times 0.313 \\ &= 340 \text{ ampere-turns.} \end{aligned}$$

The stator tooth width is constant, and

$$w_{ts} = 0.26.$$

The flux density

$$\begin{aligned} B_{ts} &= \frac{\phi_t}{w_{ts}(l - n_d w_d) k_1 S_s} = \frac{604 \times 6}{0.26(4.5 - 0) 0.93 \times 54 \times 0.637} \\ &= 97.0 \text{ kilo-lines per sq. in.} \end{aligned}$$

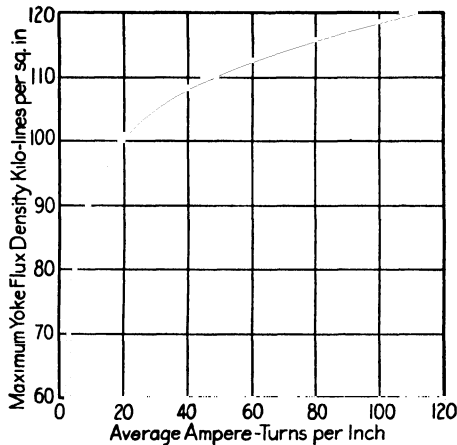


FIG. 202.

From the saturation curve, Fig. 202, for 1 per cent silicon steel, at $l_{ts} = 24$ ampere-turns per in., and the ampere-turns per pole for the stator teeth

$$AT_{ts} = 24 \times 0.991 = 23.8 \text{ ampere-turns.}$$

l_{ts} from Fig. 185 is equal to $d + \frac{2}{3}R$.

The rotor tooth width at a point $\frac{1}{3}$ tooth length from the minimum width

$$\begin{aligned} w_{tr} &= \frac{\pi(D_r - 1\frac{1}{3}d_{ar})}{S_r} - w_{ar} = \frac{\pi(9.45 - 1\frac{1}{3} \times 0.616)}{65} - 0.156 \\ &= 0.261 \text{ in.,} \end{aligned}$$

and

$$B_{ts} = \frac{\phi_t}{w_{ts}(l - n_d w_d) k_1 S_r} = \frac{604 \times 6}{0.261(4.5 - 0) 0.93 \times 65 \times 0.637}$$

$$= 80.0 \text{ kilo-lines per sq. in.}$$

$$AT_{tr} = 11.0 \times 0.616 = 6.8 \text{ ampere-turns.}$$

The length of the flux path in the stator yoke

$$l_{ys} = \frac{\pi(D_o - \frac{1}{2}d_{ys})}{2p} = \frac{\pi(13.0 - \frac{1}{2} \times 1.497)}{2 \times 6}$$

$$= 3.20 \text{ in.}$$

For the flux density in the stator yoke (see page 315), $at_{ys} = 14$ ampere-turns per in. from Fig. 202.

$$AT_{ys} = 14 \times 3.2 = 44.8.$$

The length of the flux path in the rotor yoke

$$l_{yr} = \frac{\pi(D_r - 2d_{sr} - \frac{1}{2}d_{yr})}{2p} = \frac{\pi(9.456 - 2 \times 0.616 - \frac{1}{2} \times 1.97)}{2 \times 6}$$

$$= 1.89 \text{ in.}$$

$$AT_{yr} = 4.0 \times 1.89 = 7.6 \text{ ampere-turns.}$$

The total ampere-turns per pole

$$ATP = 340 + 23.8 + 6.8 + 44.8 + 7.6 = 422.$$

The magnetizing current per phase

$$I_m = \frac{2.22 ATP \times p}{m N f_c f_w} = \frac{2.22 \times 422 \times 6}{3 \times 162 \times 0.96 \times 0.985}$$

$$= 12.3 \text{ amperes} = 31 \text{ per cent.}$$

The width of a stator tooth is 0.26 in., and the weight of the iron in the teeth

$$G_{ct} = 0.26 \times 4.5 \times 0.93 \times 54 \times 0.936 \times 0.278$$

$$= 15.3 \text{ lb.}$$

The loss per pound for the stator tooth density

$$B_{ts} = 97.0 \text{ kilo-lines per sq. in.}$$

is equal to 3.3 watts for 1 per cent silicon steel, 0.0185 in. thick. The loss in the stator teeth due to the fundamental frequency flux

$$W_{ct} = 3.3 \times 15.3 = 50.5 \text{ watts.}$$

The weight of the iron in the stator yoke

$$\begin{aligned} G_{cy} &= \frac{\pi}{4} [D_o^2 - (D_o - d_{ys})^2] l_y \times 0.92 \times 0.278 \\ &= \frac{\pi}{4} [13.0^2 - (13.0 - 1.497)^2] 4.5 \times 0.93 \times 0.278 \\ &= 33.2 \text{ lb.} \end{aligned}$$

The loss per pound for the stator yoke density

$$B_{ys} = 96.5 \text{ kilo-lines per sq. in.}$$

is equal to 3.25 watts, and the loss in the stator yoke due to the fundamental frequency flux

$$\begin{aligned} W_{cy} &= 3.25 \times 33.2 \\ &= 108 \text{ watts.} \end{aligned}$$

The total core loss (see page 330)

$$W_c = (50.5 + 108) 2.0 = 317 \text{ watts.}$$

The friction and windage losses are estimated at 2.0 per cent of the output in watts, 224 watts.

The length of the half mean-turn of a stator coil (see page 331 and Table XXVI)

$$\begin{aligned} L_s &= \frac{\pi(9.5 + 1.067)}{0.828 \times 6} 0.889 + 1.5 + 1.067 + 4.5 \\ &= 12.95 \text{ in.} \end{aligned}$$

The resistance per phase of the stator winding at 65° C.

$$R_s = \frac{L_s N r}{a_s \times 10^6} = \frac{12.95 \times 162 \times 0.80}{2 \times 0.00644 \times 10^6} = 0.13 \text{ ohm.}$$

The loss in the stator winding due to the magnetizing current

$$= 12.3 \times 3 \times 0.13 = 65.0 \text{ watts.}$$

The watt component of the no-load current

$$I_w = \frac{317 + 224 + 65.0}{3 \times 127} = 1.59 \text{ amperes.}$$

The no-load current

$$\begin{aligned} I_0 &= \sqrt{I_m^2 + I_w^2} = \sqrt{12.3^2 + 1.59^2} \\ &= 12.4 \text{ amperes.} \end{aligned}$$

The no-load power factor

$$\text{PF}_0 = \frac{I_w}{I_0} = \frac{1.59}{12.4} = 12.8 \text{ per cent.}$$

The leakage reactance is calculated as explained on page 334. The following data are required:

$$\begin{aligned} f &= 60. & d_{1s} &= 0.87. & w_{s2} &= 0.30. & k_d &= 0.96. & d_{4r} &= 0.04. & k_{dr} &= 1.0. \\ l_g &= 4.5. & d_{is} &= 0.03 & w_{s1} &= 0.10 & S_r &= 65 & w_{sr} &= 0.156. & D &= 9.5. \\ m &= 3. & d_{4s} &= 0.03. & P &= 0.889 & d_{1r} &= 0.531. & w_{sr1} &= 0.06. & p &= 6. \\ N &= 162 & w_{ss1} &= 0.395. & K_s &= 0.92 & d_{2r} &= 0. & K_r &= 1.0. & \tau &= 4.97. \\ S_s &= 54. & & & k_p &= 0.985. & d_{1r} &= 0.03 & k_{1r} &= 1.0. \end{aligned}$$

The stator slot factor from Fig. 214

$$\begin{aligned} F_{sst} + F_{ssb} &= \left(\frac{d_{4s}}{w_{s1}} + \frac{d_{3s} \times 2}{w_{s1} + w_{s2}} \right) + \phi \\ &= \left(\frac{0.03}{0.10} + \frac{0.03 \times 2}{0.10 + 0.30} \right) + 1.10 = 0.45 + 1.10, \end{aligned}$$

and the stator slot reactance per phase

$$\begin{aligned} X_{ss} &= \frac{N^2 m f}{10^7} \frac{2 l_g K_s}{S_s} (F_{sst} + F_{ssb}) \\ &= \frac{162^2 \times 3 \times 60}{10^7} \frac{2 \times 4.5 \times 0.92}{54} 1.55 = 0.112 \text{ ohm.} \end{aligned}$$

The rotor slot factor

$$\begin{aligned} F_{srt} + F_{srb} &= \left(\frac{d_{4r}}{w_{r1}} + \frac{2d_{3r}}{w_{r1} + w_{s1}} \right) + \left(\frac{d_{2r}}{w_{sr}} + \frac{d_{1r}}{3w_{sr}} \right) \\ &= \left(\frac{0.04}{0.06} + \frac{2 \times 0.03}{0.156 + 0.06} \right) + \left(\frac{0}{0.156} + \frac{0.531}{3 \times 0.156} \right) \\ &= 0.914 + 1.132 = 2.076, \end{aligned}$$

and the rotor slot reactance per phase

$$\begin{aligned} X_{sr} &= \frac{N^2 m f}{10^7} \frac{2 l_g (k_p k_d)^2 K_r}{(k_{pr} k_{dr})^2 S_r} (F_{srt} + F_{srb}) \\ &= \frac{162^2 \times 3 \times 60}{10^7} \frac{2.0 \times 4.5 (0.985 \times 0.96)^2 1.0}{65} \times 2.076 \\ &= 0.121 \text{ ohm.} \end{aligned}$$

The magnetizing current per phase due to the air gap ampere-turns

$$I_{m_g} = \frac{2.22AT_g p}{mNk_pk_d} = \frac{2.22 \times 340 \times 6}{3 \times 162 \times 0.985 \times 0.96} \\ = 9.85 \text{ amperes.}$$

The stator and rotor zigzag leakage reactance

$$X_s = \frac{E}{1.2I_{m_g}} \left[\left(\frac{p}{S_s} \right)^2 + \left(\frac{p}{S_r} \right)^2 \right] \\ = \frac{127}{1.2 \times 9.85} \left[\left(\frac{6}{54} \right)^2 + \left(\frac{6}{65} \right)^2 \right] = 0.226 \text{ ohm per phase.}$$

For the stator end-connection, the length

$$f = \frac{\pi(9.5 + 1.067)}{2 \times 6} 0.889 \times 0.68 = 1.67 \text{ in.,}$$

and the stator end-connection leakage reactance per phase

$$X_{se} = \frac{N^2 m f}{10^7} \frac{0.8(k_pk_d)^2}{p} \left[b + 0.5 \left(f + \frac{d_{ss}}{2} \right) \right] \\ = \frac{162^2 \times 3 \times 60}{10^7} \frac{0.8(0.985 \times 0.96)^2}{6} \times \\ \left[0.75 + 0.5 \left(1.67 + \frac{1.067}{2} \right) \right] \\ = 0.104 \text{ ohm.}$$

The length of the bar in the squirrel-cage winding is 7.0 in. The horizontal extension between core and end-ring, b_r , Fig. 199, is 1.23 in. on each end, and the bar is skewed one stator slot pitch. The end-ring has a radial depth of 0.875 in. and a horizontal width of 0.25 in. The rotor end-connection leakage reactance per phase

$$X_{re} = \frac{N^2 m f}{10^7} \frac{c_r(k_pk_d)^2}{p^2} \left(2pb_r + \frac{\pi D d_e}{1.7w_{er} + 1.2d_{er} + 1.4d_e} \right) \\ = \frac{162^2 \times 3 \times 60}{10^7} \frac{0.4(0.985 \times 0.96)^2}{6^2} \\ \left(2 \times 6 \times 1.23 + \frac{\pi \times 9.5 \times 1.03}{1.7 \times 0.25 + 1.2 \times 0.875 + 1.4 \times 1.03} \right) \\ = 0.119 \text{ ohm.}$$

The skew leakage reactance per phase

$$X_{sk} = \frac{E}{I_{m0}} \frac{\theta_{sk}^2}{12} = \frac{127}{9.85} \frac{0.35^2}{12} = 0.133 \text{ ohm.}$$

The total reactance per phase of the motor at normal running speeds

$$X_{i \text{ run}} = 0.112 + 0.121 + 0.226 + 0.104 + 0.119 + 0.133 = 0.815.$$

The stator reactance per phase

$$X_{1 \text{ run}} = 0.112 + 0.104 + 0.5(0.226 + 0.133) = 0.396 \text{ ohm,}$$

and the rotor reactance per phase

$$X_{2 \text{ run}} = 0.121 + 0.119 + 0.5(0.226 + 0.133) = 0.42 \text{ ohm.}$$

The magnetizing reactance per phase

$$X_m = \frac{E_T}{I_m} - X_1 = \frac{127}{12.3} - 0.396 = 9.904 \text{ ohms,}$$

$$b_m = \frac{1}{9.904} = 0.101,$$

and the conductance per phase

$$g_m = \frac{317}{3(127 - 12.3 \times 0.396)^2} = 0.0071 \text{ mho.}$$

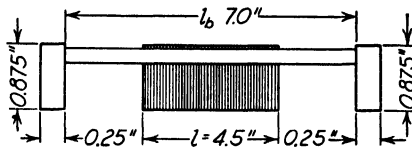


FIG. 203.

The length of the bars in the squirrel-cage winding is 7.0 in. (see Fig. 203). The rotor resistance in terms of the stator winding at 65° C.

$$\begin{aligned} R_r &= \frac{k_p^2 k_d^2 N^2 m r}{10^6} \left[\frac{l_b}{s_b N_b} + \frac{0.64 D_r}{p^2 s_r} K_{ring} \right] \\ &= \frac{0.985^2 \times 0.96^2 \times 162^2 \times 3 \times 0.80}{10^6} \times \\ &\quad \left[\frac{7.0}{0.075 \times 65} + \frac{0.64 \times 8.58}{6^2 \times 0.219} 1.0 \right] \\ &= 0.12 \text{ ohm per phase, or } 0.104 \text{ ohms at } 25^\circ \text{ C.} \end{aligned}$$

The equivalent circuit of Fig. 204 is used for calculating the performance characteristics. The stray load losses at full load are usually equal to 3.0 per cent of the watt output for small motors to 0.5 per cent

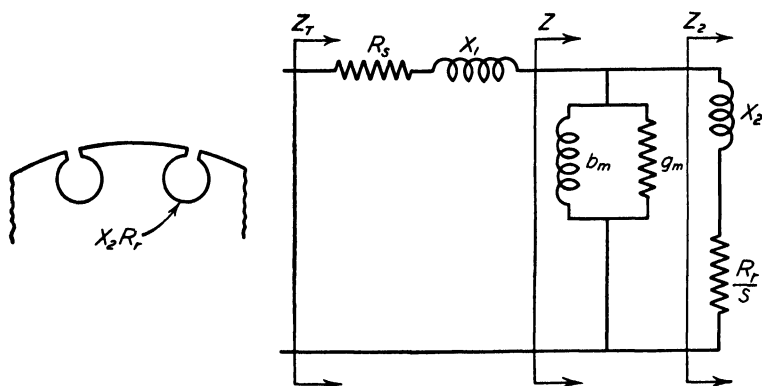


FIG. 204.—Equivalent circuit for induction motors with single squirrel-cage.

for large motors. For calculating the running performance, the stator and rotor resistance at 65° C. must be used for a 40° C. rated motor,

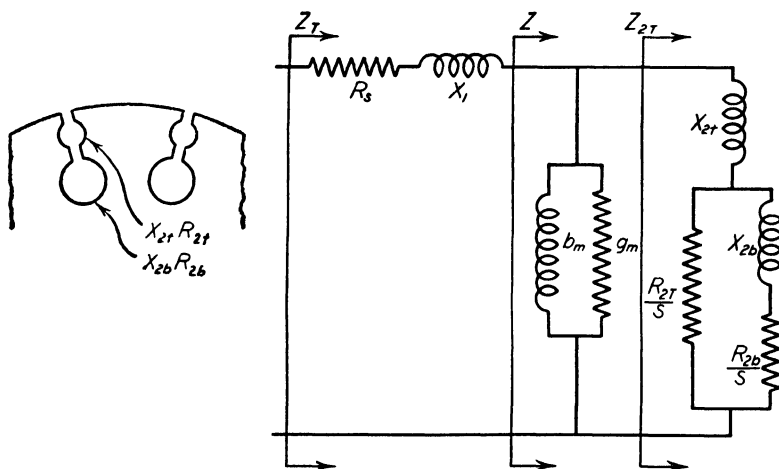


FIG. 205.—Equivalent circuit for induction motors with double squirrel-cage.

and for the starting performance calculations the cold resistance at 25° C. is used. For a full-load slip of 0.037:

$$\frac{R_r}{s} = \frac{0.12}{0.037} = 3.24.$$

$$Z_2 = 3.24 + j0.420 = 3.27. \quad Y_2 = 0.303 - j0.0393.$$

$$Y_m = 0.0071 - j0.101.$$

$$Z = 2.68 + j1.215 = 2.93. \quad Y = 0.31 - j0.1403 = 0.34.$$

$$Z_1 = 0.13 + j0.396.$$

$$Z_t = 2.81 + j1.611 = 3.23.$$

$$I \text{ input} = 127 \div 3.23 = 39.3 \text{ amperes.}$$

$$I_r \text{ rotor current} = \frac{2.93}{3.27} 39.3 = 35.2 \text{ amperes.}$$

$$\text{Power factor} = R_t \div Z_t = \frac{2.8}{3.23} = 0.87.$$

$$\text{Stator } I^2R = 3 \times 39.3^2 \times 0.13 = 602 \text{ watts.}$$

$$\text{Rotor } I^2R = 3 \times 35.2^2 \times 0.12 = 446 \text{ watts.}$$

$$\text{Gross secondary output} = (1 - 0.037) 35.2^2 \times 3 \times 3.24 = 11,580 \text{ watts.}$$

$$\text{Input} = 602 + 446 + 11,580 + 317 + 112 = 13,057 \text{ watts.}$$

$$\text{Shaft output} = 11,580 - 224 = 11,356 \text{ watts or 15.2 hp.}$$

$$\text{Efficiency} = 11,356 \div 13,057 = 0.87.$$

$$\text{Full-load speed} = (1 - 0.037) 1200 = 1157 \text{ r.p.m.}$$

$$\text{Torque} = (7.04 \times 11,356) \div 1157 = 69.0 \text{ lb.-ft.}$$

The slip at maximum torque

$$s_m = \frac{0.12}{\sqrt{0.13^2 + 0.815^2}} = 0.145,$$

and

$$\frac{R_r}{s_m} = \frac{0.12}{0.145} = 0.827.$$

$$Z_2 = 0.827 + j0.42 = 0.927. \quad Y_2 = 0.962 - j0.488.$$

$$Y_m = 0.0071 - j0.101.$$

$$Z = 0.75 + j0.459 = 0.88. \quad Y = 0.969 - j0.589 = 1.135.$$

$$Z_1 = 0.13 + j0.396.$$

$$Z_t = 0.88 + j0.855 = 1.23.$$

$$I \text{ input} = 127 \div 1.23 = 103 \text{ amperes.}$$

$$I_r \text{ rotor current} = \frac{0.88}{0.927} \times 103 = 97.8.$$

$$\text{Gross secondary output} = (1 - 0.145) 97.8^2 \times 3 \times 0.827 = 20,300 \text{ watts.}$$

$$\text{Shaft output} = 20,300 - 224 = 20,076 \text{ watts.}$$

$$\text{Speed} = (1 - 0.145) 1200 = 1026 \text{ r.p.m.}$$

Torque = $(7.04 \times 20,076) \div 1026 = 137.2$ lb.-ft. or 200 per cent of full-load torque.

$$K_c d_1 \sqrt{f \frac{w_b}{w_{sr}}} = 0.357 \times 0.531 \sqrt{60 \frac{0.141}{0.156}} = 1.40.$$

From Fig. 201, $R_c = 1.32$.

The rotor resistance per phase at starting in terms of the stator winding

$$R_{r \text{ start}} = \frac{162^2 \times 0.985^2 \times 0.96^2 \times 3 \times 0.692}{10^6} \times \left(\frac{4.53 \times 1.32 + 2.47}{0.075 \times 65} + \frac{0.64 \times 8.58}{6^2 \times 0.219} \times 1.0 \right) \\ = 0.1185 \text{ ohm at } 25^\circ \text{ C.}$$

To calculate the effect of saturation upon the leakage reactance, it is necessary to estimate the value of the starting or blocked rotor current.

For this purpose $X_{l \text{ start}}$ may be taken equal to $\frac{X_{l \text{ run}}}{1.4}$; then

$$Z_{\text{start}} = \sqrt{(R_s + R_{r \text{ start}})^2 + \left(\frac{X_{l \text{ run}}}{1.4} \right)^2} \\ = \sqrt{(0.13 + 0.119)^2 + \left(\frac{0.815}{1.4} \right)^2} \\ = 0.634 \text{ ohm.}$$

The starting current

$$I_s = \frac{127}{0.634} = 200 \text{ amperes.}$$

$$AT_s = I_s \frac{t_a \times c_s}{a} 0.707 \left[K_s + k_p \times k_d^2 \times \frac{S_s}{S_r} \right] \sqrt{\frac{E}{E_t}} \\ = 200 \frac{9 \times 2}{2} 0.707 \left[0.92 + 0.985 \times 0.96^2 \times \frac{54}{65} \right] \sqrt{\frac{121.4}{127}} \\ = 2090.$$

$$\beta = \sqrt{\frac{6.25\delta}{t_{1s} + t_{1r}}} + 0.64 = \sqrt{\frac{6.25 \times 0.022}{0.552 + 0.457}} + 0.64 = 1.01.$$

$$B_L = \frac{AT_s}{0.628\beta} = \frac{2090}{0.628 \times 0.022 \times 1.01} = 150,000.$$

From Fig. 201, $K_z = 0.811$ and $C_{ss} = (0.552 - 0.10)(1 - 0.811) = 0.0853$.

$$C_{sr} = (0.457 - 0.06)(1 - 0.811) = 0.075.$$

$$\begin{aligned}\Delta F_{sst} &= \frac{d_{4s} + 0.58d_{3s}}{w_{s1}} \left(\frac{C_{ss}}{C_{ss} + 1.5w_{s1}} \right) \\ &= \frac{0.03 + 0.58 \times 0.03}{0.10} \left(\frac{0.0853}{0.0853 + 1.5 \times 0.10} \right) \\ &= 0.172\end{aligned}$$

$$\Delta F_{srt} = \frac{0.04 + 0.58 \times 0.03}{0.06} \left(\frac{0.075}{0.075 + 1.5 \times 0.06} \right) = 0.436$$

$$\begin{aligned}X_{ss \text{ start}} &= X_{ss \text{ run}} \left(\frac{F_{sst} - \Delta F_{sst} + F_{ssb}}{F_{sst} + F_{ssb}} \right) \\ &= 0.112 \left(\frac{0.45 - 0.172 + 1.10}{0.45 + 1.10} \right) = 0.0995 \text{ ohm.}\end{aligned}$$

From Fig. 200, $X_c = 0.891$.

$$\begin{aligned}X_{sr \text{ start}} &= X_{sr \text{ run}} \frac{F_{srt} - \Delta F_{srt} + (F_{srb} \times X_c)}{F_{srt} + F_{srb}} \\ &= 0.121 \frac{0.944 - 0.436 + (1.132 \times 0.891)}{0.944 + 1.132} \\ &= 0.0884 \text{ ohm.}\end{aligned}$$

$$X_{z \text{ start}} = X_{z \text{ run}} \times K_z = 0.226 \times 0.811 = 0.183 \text{ ohm.}$$

$$X_{\text{start}} = 0.0995 + 0.0884 + 0.104 + 0.119 + 0.183 = 0.594 \text{ ohm.}$$

$$X_{1 \text{ start}} = 0.0995 + 0.104 + 0.5 \times 0.183 = 0.295 \text{ ohm.}$$

$$X_{2 \text{ start}} = 0.0884 + 0.119 + 0.5 \times 0.183 = 0.299 \text{ ohm.}$$

For $s = 1.0$:

$$Z_2 = 0.1185 + j0.299 = 0.322.$$

$$Y_2 = 1.145 - j2.89.$$

$$Z = 0.112 + j0.291 = 0.312.$$

$$Y_m = 0.0071 - j0.101.$$

$$Z_1 = 0.113 + j0.295.$$

$$Y = 1.1521 - j2.991 = 3.21.$$

$$Z_t = 0.225 + j0.586 = 0.627.$$

$$I_s = 127 \div 0.627 = 202 \text{ amperes.}$$

$$I_{sr} = \frac{0.312}{0.322} \times 202 = 196 \text{ ampères.}$$

UNIVERSITY OF MINNESOTA
ELECTRICAL ENGINEERING DEPARTMENT

Hp 15 S R p m 1200 Cycles 60 Poles 6 Phases 3 Volts 220 Amps Line 39.2
Amperes per Phase 39.2 Volts per Phase 127 Apparent Efficiency

STATOR		CONDUCTORS	
Sheet steel	0 019—1% Si	Per slot	
Outside diameter	13 0	Size	
Gap diameter	9 5	Material	
Total length	4 5	Section total	
Ducts number and size	None	In series per phase	
Gross iron length	4 5	Insulation allowance	
Effective length	4 18	Depth	
Slots		Width	
Number	54	Circuits per phase	
Depth	round bottom 1 067	Connections	
Width	0 30 0 395	Coil throw	
Opening	0 10	Per cent pitch	
Minimum tooth width	0 26	End ring	
Conductors		Section	0 25 × 0 875 = 0 219 sq in
Per slot	18	Material	Copper
Size	2 14 rd in parallel	Length of bar	7 0
Area	0 00644	Resistance per phase	65° C = 0 12 or 0 104 @ 25° C
Total section	6 26	Conductor weight	
In series per phase	162		
Amperes per square inch	3080		
Conductors arranged in slot	random		
Insulation allowance			
Depth	0 25		
Width	0 075		
Circuits per phase	2 0		
Connections	Star		
Coil throw	Slots 1 and 9		
Per cent pitch	0 889		
Length half mean turn	12 95		
Resistance per phase 65° C	0 13		
Copper weight			
ROTOR		STATOR AND ROTOR	
Sheet steel	0 019—1% Si	Total resistance per phase	0 15 + 0 12 = 0 27
Gap diameter	9 456	Total reactance per phase	0 39 + 0 42 = 0 81
Inside diameter	6 25	Short circuit power factor	38 4
Total length	4 50	Short circuit current	202
Ducts number and size	None	Friction and windage loss	224
Effective length	4 18	No load stator I _h	65 0
Slots		Magnetizing current	12 3 31%
Number	65	Watt component of I	1 59
Depth	0 616	No load current	12 4
Width	0 136	No load power factor	12 5
Opening	0 06	Full load current	39 2
Minimum tooth width	0 241	Full load slip	0 037
		Full load speed	1157
		Full load torque	69 0
		Starting torque	80 0
		Maximum torque	137 2

Total flux 5690 × 10⁸ $k_p = 0.985$ Flux per pole 604 × 10 $k_l = 0.96$ $C = 0.679$

	Length	Section	Density	Ampere turns	Weight	Core loss
Stator teeth	0 936	58 7	97 0	23 8	15 3	50 5
Stator yoke	3 20	6 26	96 5	44 8	33 2	108 0
Rotor teeth	0 616	71 0	80 0	6 8		158 5
Rotor yoke	1 89	8 25	73 3	7 6		2
Air gap	0 022 × 1 155	134 0	42 3	340 0		317 0
				4.2		

Rheostat data

Open-circuit volts across rings
Amperes per phase
Starting resistance per phase
Remarks

Designed by J H Kuhlmann

Date

Fig. 206.—Induction motor design sheet.

$$\text{Starting torque} = \frac{7.04 \times 3 \times 196^2 \times 0.1185}{1200} = 80.0 \text{ lb.-ft., or 116 per}$$

cent of full-load torque, which does not meet the minimum requirements. The student should study the proportions chosen for this design and make the necessary changes so that the running performance characteristics will remain approximately the same but give a starting torque of 135 per cent of full-load torque. What temperature rise will the stator of this motor be likely to have?

CHAPTER XX

FRACTIONAL-HORSEPOWER SINGLE-PHASE MOTOR DESIGN

THE procedure in the design of single-phase motors is in general the same as for polyphase motors. The more important differences will be discussed before proceeding with the examples.

Windings.—The stator windings of single-phase induction motors are generally of the concentric coil type shown in Fig. 207. There are

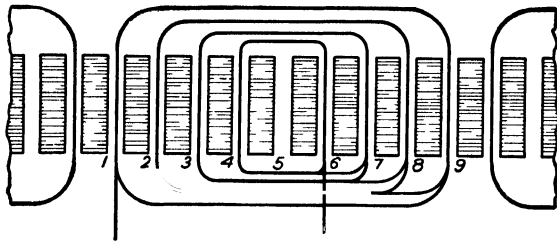


FIG. 207.

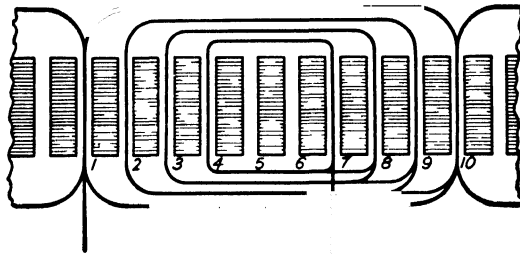


FIG. 208.

usually 3 or more coils per pole each having the same or different number of turns. The winding arrangement shown in Fig. 207 is for a stator with 9 slots per pole. The inside coil spans 2 slots and the outside coil 8. The coils can also be arranged as shown in Fig. 208, that is, the inside coil spans 3 slots and the outside coil 9 or full pitch. With this arrangement the number of turns in the outside coil must be one-half of the conductors in slot 1, the other half belonging to the outside coil of the adjacent pole.

The current in the stator and rotor windings does not produce a pure sine wave of flux in the air gap but rather harmonic fluxes in addition to the fundamental. Mr. Appleman¹ has shown how to determine these harmonic fluxes and the effect of winding distribution upon them.

$$\text{Harmonic poles} = 2 \left(\frac{p}{2} \pm S \right).$$

$$\text{The harmonic order} = \frac{\text{Harmonic poles}}{\text{Fundamental poles}},$$

or

$$\text{Harmonic order} = \frac{2 \left(\frac{p}{2} \pm S \right)}{p} = 1 \pm 2 \frac{S}{p}.$$

Mr. Appleman suggests calculating the number of harmonic poles for stator and rotor slots and for the difference between them and has found that a quiet-running motor will generally result if there are no harmonic fields with numbers of poles differing by less than 4. The number of stator slots is usually fixed by winding arrangement, number of poles, etc. The number of rotor slots must, therefore, be adjusted to meet the requirements given above. For motors with more than 2 poles quiet operation can generally be expected when the number of rotor slots is divisible by the number of pairs of poles of the fundamental and when the number of rotor slots differs from the number of stator slots by more than the number of poles. The stator and rotor slot openings, length of air gap, etc., also have an effect upon noise. The number of rotor slots must also be selected with regard to locking or points of low torque at starting (see page 317). In general that number of rotor slots should be selected that meets the requirements given above and has the smallest possible number of rotor teeth in line with stator teeth for any position of the rotor.

Proper winding distribution will reduce harmonics of low order so that their effect will be small. The tooth harmonics, however, are not affected by winding distribution. To reduce their effect the rotor slots must be skewed, that is, the rotor slots pass from one end of the rotor core to the other diagonally instead of parallel to the shaft. If it is desired to have no voltage induced in the rotor bars from a given harmonic in the air gap flux wave, the rotor slots must be skewed so that both ends of the bar will cut flux from like harmonic poles. With 36 slots on a 4-pole stator the air gap flux wave will have the seventeenth and nine-

¹ "The Cause and Elimination of Noise in Small Motors," by W. R. Appleman, *Electrical Engineering*, Nov., 1937, p. 1359.

teenth tooth harmonics, which have 68 and 76 poles, respectively. To skew out the effect of these harmonics for a rotor with 26 slots, the bars must be skewed $1/34 \times 26 = 0.765$ bar or $1/38 \times 26 = 0.685$ bar. Since more than one harmonic is always present in the flux wave a compromise must usually be made. Noise in electrical machinery is caused by the flux variations in the air gap which set the frame into vibration. Mr. Mikina² lists four modes of frame vibrations for electrical machinery and has found that modes 1, 2, and 4 are eliminated if the rotor is skewed any integral number of slot pitches and that mode 3 can be eliminated by skewing 1.43 slot pitches or by making the rotor bars a multiple of the number of poles.

The number of turns per pole may be distributed according to the sine law. The turns¹ required in each coil can then be found as follows:

For Fig. 207,

$$\begin{aligned}\text{Coil 4-6 sin of } 1/2 \text{ coil span} &= \sin 2/9 \times 90 = 0.342 \\ \text{Coil 3-7 sin of } 1/2 \text{ coil span} &= \sin 4/9 \times 90 = 0.643 \\ \text{Coil 2-8 sin of } 1/2 \text{ coil span} &= \sin 6/9 \times 90 = 0.866 \\ \text{Coil 1-9 sin of } 1/2 \text{ coil span} &= \sin 8/9 \times 90 = 0.985 \\ &\underline{2.836}\end{aligned}$$

$$\text{Per cent turns per pole in coil 4-6} = 0.342/2.836 \times 100 = 12.10.$$

$$\text{Per cent turns per pole in coil 3-7} = 0.643/2.836 \times 100 = 22.70.$$

$$\text{Per cent turns per pole in coil 2-8} = 0.866/2.836 \times 100 = 30.60.$$

$$\text{Per cent turns per pole in coil 1-9} = 0.985/2.836 \times 100 = 34.60.$$

The same procedure can be used for the winding arrangement of Fig. 208 except in determining the base for the per cent turn calculations one-half the sine of 90° must be used for coil 1-10. The per cent turns per pole required with this arrangement to give sinusoidal distribution are,

$$\text{Coil 4-7} = 18.5.$$

$$\text{Coil 3-8} = 28.3.$$

$$\text{Coil 2-9} = 34.7.$$

$$\text{Coil 1-10} = 18.5.$$

While sinusoidal distribution of the winding reduces the harmonics in the air gap flux wave to a minimum, good results are also obtained with non-sinusoidal distribution. For example: In Fig. 207 coils 3-7 and 2-8 may have two times and coil 1-9 three times as many turns as

² "Effect of Skewing and Pole Spacing on Magnetic Noise in Electrical Machinery," by S. J. Mikina, A.S.M.E. Trans., Vol. 56, Oct., 1934, p. 711; see also "Harmonic Theory of Noise in Induction Motors," by W. J. Morrill, to be presented before the A.I.E.E.

coil 4-6, or coil 4-6 may be omitted and the remaining three coils wound with the same number of turns.

The winding distribution factor for concentric-type single-phase windings is a weighted mean chord factor or pitch factor and is calculated by multiplying the chord factor of each coil per pole group by the turns in the coil and dividing the sum of these products by the total number of turns. The chord factor or pitch factor has been defined on page 296. For the winding in Fig. 207 with 9 slots per pole (see also sample design page 363),

$$f_c \text{ coil 4-6} = \sin 2/9 \times 90 = 0.342,$$

$$f_c \text{ coil 3-7} = \sin 4/9 \times 90 = 0.643,$$

$$f_c \text{ coil 2-8} = \sin 6/9 \times 90 = 0.866,$$

$$f_c \text{ coil 1-9} = \sin 8/9 \times 90 = 0.985.$$

$$C_w = \frac{0.342 t_{4-6} + 0.643 t_{3-7} + 0.866 t_{2-8} + 0.985 t_{1-9}}{t_{4-6} + t_{3-7} + t_{2-8} + t_{1-9}}.$$

Split-phase and capacitor motors³ require an auxiliary winding on the stator in addition to the main winding. This winding is placed at 90° with the main winding and has a smaller conductor. In the split phase and capacitor start motors it is cut out by a centrifugal switch after the rotor has attained approximately 75 per cent of full-load speed. The auxiliary winding can be arranged and distributed as explained for the main winding. That winding arrangement and distribution will generally be used that gives the required starting torque at minimum cost.

The repulsion start motor³ has only the main winding on the stator. The rotor winding is the same as the armature winding on direct-current machines.

Core Diameter and Length.—For fractional-horsepower motors it is probably more satisfactory to use output in watts instead of horsepower in the output equation 172.

$$C = \frac{D^2 l n}{\text{watts output}}.$$

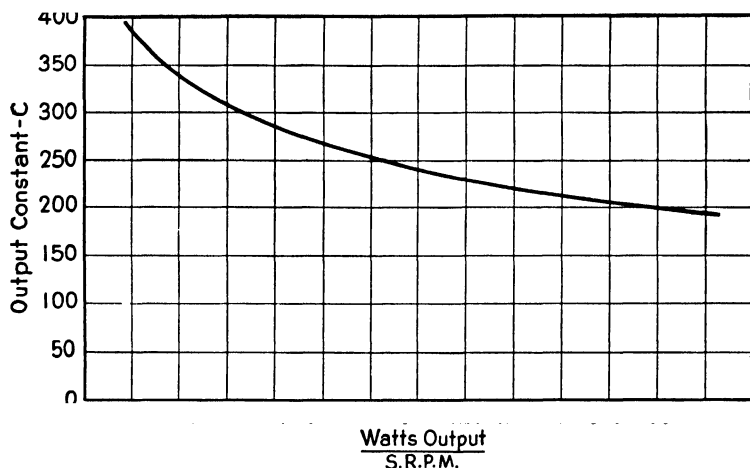
The output constants shown in Fig. 209 are only approximate to provide a starting point when laying out a new design. The final dimensions should be determined after making preliminary calculations for two or more values of core dimensions to determine that gap diameter and

³ "Rewinding Small Motors," by D. H. Braymer and A. C. Roe, McGraw-Hill Book Co., Inc., New York; "Fractional Horsepower Electric Motors," by C. G. Veinott, McGraw-Hill Book Co., Inc., New York.

core length that will give the desired operating characteristics at minimum cost. The ratio of core length to gap diameter is generally from 0.50 to 0.75.

The flux per pole, assuming sine wave flux distribution in the air gap,

$$\phi = \frac{E 45 \times 10^6}{fNC_w} \text{ lines,}$$



Approximate Output Constants for Split-Phase and Capacitor-Start Induction Motors for Continuous Duty

FIG. 209.—Output constants single-phase motors.

where E is the induced voltage and can in most cases be assumed equal to $0.95 E_t$ for fractional-horsepower single-phase induction motors. The total flux

$$\begin{aligned} \phi_t &= \frac{p\phi}{f_d} \\ &= \frac{pE 45 \times 10^6}{fN \times C_w \times f_d} \text{ lines,} \end{aligned}$$

where f_d , the flux distribution constant, is equal to 0.637 for sine-wave flux distribution.

Many different types of single-phase motors for a variety of ratings and speeds are available today. Mr. C. G. Veinott³ describes the performance and construction of the various types in his book.

Sample Design 1: Design of a 1/4-Hp., 110-Volt, 1725-R.p.m., 60-Cycle, Single-Phase Resistance Split-Phase Induction Motor.—The full-load efficiency and power factor should not be less than 62.0 and 60.0 per cent, respectively. The motor must have a locked rotor torque

at rated voltage not less than 90 per cent of full-load torque with a locked rotor current not to exceed 23 amperes. The maximum or breakdown torque must be not less than 185 per cent of full-load torque. The motor is to be of the open type, and the temperature rise of the windings must not exceed 40° C. for continuous full-load operation.

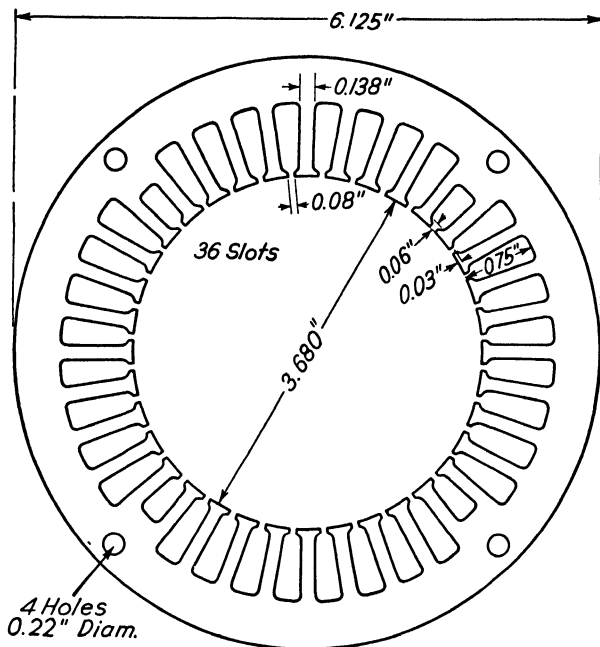


FIG. 210.—Stator punching, $\frac{1}{4}$ -hp. split-phase induction motor.

Stator.—The stator is to be designed with the punching shown in Fig. 210. The watt output = $0.25 \times 746 = 186.5$ watts, and the number of poles for 1800 s.r.p.m.

$$p = \frac{f \times 2 \times 60}{n} = \frac{60 \times 2 \times 60}{1800} = 4.$$

The output constant from Fig. 209 is 303, and the core length,

$$l = \frac{\text{watts } C}{D^2 n} = \frac{186.5 \times 303}{3.68^2 \times 1800} = 2.32 \text{ in.}$$

Preliminary calculations showed that reasonable magnetic densities could be obtained with a 2.0-in. core length. The stator tooth density can generally be from 90,000 to 110,000 lines per sq. in. for 60 cycles. If low losses and noise are important or if the motor is to be totally

enclosed then lower densities must be used. The grade and thickness of electric sheet steel must also be taken into account when determining stator tooth and yoke densities. For fractional-horsepower motors 24-gauge 0.025-in., or 26-gauge 0.0185-in. armature or electrical grade are commonly used.

The tooth width from Fig. 210 is 0.138 in., and the total tooth section

$$\begin{aligned} S_t &= w_t S_s l \times 0.95 = 0.138 \times 36 \times 2.0 \times 0.95 \\ &= 9.44 \text{ sq. in.} \end{aligned}$$

The stacking factor may be taken equal to 0.95 for 24-gauge sheet steel.

For a tooth density of 95,000 lines per sq. in. the total flux,

$$\begin{aligned} \phi_t &= B_t \times S_t = 95,000 \times 9.44 \\ &= 896,000 \text{ lines.} \end{aligned}$$

The winding constant can not be calculated until the distribution of the winding is known. For the usual winding distributions, C_w will lie between 0.75 and 0.85. For sinusoidal distribution and the winding arrangement of Fig. 207, $C_w = 0.795$.

The total number of conductors in series for the main winding

$$\begin{aligned} N_m &= \frac{pE_t \times 0.95 \times 45 \times 10^6}{f\phi_t C_{wm} f_d} \\ &= \frac{4 \times 110 \times 0.95 \times 45 \times 10^6}{60 \times 896,000 \times 0.795 \times 0.637} \\ &= 690. \end{aligned}$$

The turns in series per pole

$$t_p = \frac{N_m}{2 \times p} = \frac{690}{2 \times 4} = 86.2.$$

The winding arrangement shown in Fig. 207 must be used for the main winding. The shallow slots will then lie in the pole centers of the main winding. For sinusoidal distribution the number of turns for each coil will be as follows:

$$\text{Coil 4-6} = 0.121 \times 86.2 = 10.42; \text{ use 10.}$$

$$\text{Coil 3-7} = 0.227 \times 86.2 = 19.60; \text{ use 20.}$$

$$\text{Coil 2-8} = 0.306 \times 86.2 = 26.40; \text{ use 26.}$$

$$\text{Coil 1-9} = 0.346 \times 86.2 = 29.90; \text{ use 30.}$$

Total 86 turns.

The winding constant is then

$$\sin 2/9 \times 90 = 0.342 \times 10 = 3.42$$

$$\sin 4/9 \times 90 = 0.643 \times 20 = 12.86$$

$$\sin 6/9 \times 90 = 0.866 \times 26 = 22.50$$

$$\sin 8/9 \times 90 = 0.985 \times 30 = 29.60$$

$$C_{wm} = \frac{68.38}{86} = 0.795.$$

Since no change has been made in the total number of conductors and winding constant, the total flux will remain as above.

For the efficiency and power factor to be met the input current

$$\begin{aligned} I &= \frac{\text{hp.} \times 746}{E_t \times \text{eff.} \times \text{P.F.}} = \frac{0.25 \times 746}{110 \times 0.62 \times 0.60} \\ &= 4.56 \text{ amperes.} \end{aligned}$$

For economical reasons the current density in the stator conductor is made as high as temperature or efficiency guarantees will permit. It depends upon whether the motor is open or enclosed and if open what kind of ventilation it has, the method of insulating the winding, etc. For open-type motors split-phase, capacitor and repulsion start, the current density can usually be from 2500 to 3000 amperes per sq. in. For enclosed motors much lower values must be used. For a current density of 2800 amperes per sq. in. and a one-circuit winding the section area of the stator conductor for main winding

$$s_{sm} = \frac{I}{a \times A_{sm}} = \frac{4.56}{1 \times 2800} = 0.00163 \text{ sq. in.}$$

A No. 17 round wire has an area of 0.00159 sq. in. With this conductor and the number of turns given above the motor can be used only on 110 volts. If the winding is to be arranged so that it can be used on 220 volts also, the number of turns must be doubled and a conductor of one-half the section area must be used. The winding was carried out in this way. The total number of turns per pole are, then, $2 \times 86 = 172$, and the conductor No. 20 round single cotton-covered enamel wire which has a section area of 0.000804 sq. in. The current density with this conductor

$$\begin{aligned} A_{sm} &= \frac{I}{a \times s_{sm}} = \frac{4.56}{2 \times 0.000804} \\ &= 2840 \text{ amperes per sq. in.} \end{aligned}$$

The stator slots do not all have the same number of conductors, and some contain both main winding and auxiliary winding conductors. The auxiliary winding conductor has a small section area, and its effect on the size of the slot is small. Generally the main winding coil with the largest number of turns will determine the size of the stator slot. For partly closed slots the insulation between core and coils is placed in the slot as slot lining. For 110- and 220-volt motors this slot lining consists of a treated paper or of a paper and varnished cloth combination 0.015 in. thick. Small motors are quite commonly wound with plain enamel wire; enamel single cotton-covered, cellophane-covered or paper-covered wire is also used. For high-temperature applications spun-glass-insulated wire should make an excellent conductor. The ratio of the insulated conductor area to the slot area can generally not exceed 0.35. It is possible to get the conductors into the slot with a ratio greater than 0.35, but the added time required to wind the stator makes the use of higher ratios impractical. The insulated area of No. 20 s.c.c.e. wire = $0.039^2 \times 0.785 = 0.001195$ sq. in., and the total conductor area per slot = $60 \times 0.001195 = 0.0716$ sq. in. The slot area for this purpose is calculated by multiplying the mean width by the depth. The average slot width

$$w_{sa} = \frac{(D + d_{vs})\pi}{S_s} - w_t = \frac{(3.68 + 0.75)\pi}{36} - 0.138$$

$$= 0.249 \text{ in.},$$

and the slot area

$$= 0.249 \times 0.75 = 0.187 \text{ sq. in.}$$

The ratio of insulated conductor area to slot area

$$= \frac{0.0716}{0.187} = 0.383.$$

This ratio is higher than given above, and considerable difficulty was experienced when placing the conductors in the slots.

The double radial depth of the stator yoke

$$d_{vs} = D_0 - (D + 2d_{ss}) = 6.125 - (3.68 + 2 \times 0.75)$$

$$= 0.945 \text{ in.}$$

The flux per pole

$$\phi = \frac{E_t \times 0.95 \times 45 \times 10^6}{f N_m C_{wm}} = \frac{110 \times 0.95 \times 45 \times 10^6}{60 \times 688 \times 0.795}$$

$$= 143,000 \text{ lines.}$$

The density in the stator yoke

$$\begin{aligned} B_{ys} &= \frac{\phi}{d_{ys} \times l \times 0.95} = \frac{143,000}{0.945 \times 2.0 \times 0.95} \\ &= 81,400 \text{ lines per sq. in.} \end{aligned}$$

Rotor.—The length of the air gap for fractional-horsepower motors is usually made smaller than the value by equation 181. For fractional-horsepower motors the air gap length can be determined approximately by the following empirical equation,

$$\begin{aligned} &= 0.005 + 0.00035D + 0.001l + 0.003v/1000 \\ &= 0.005 + 0.00035 \times 3.68 + 0.001 \times 2.0 + 0.003 \times 1.66 \\ &= 0.0133 \text{ in.} \end{aligned}$$

The outside diameter of the rotor punching, see Fig. 211, is 3.657 in.; the air gap length is, then,

$$= \frac{1}{2}(3.680 - 3.657) = 0.0115 \text{ in.}$$

The rotor punching, Fig. 211, has 48 slots, which with the 36 stator slots meets all the requirements for a quiet motor.

The total stator copper section for main winding

$$S_{cs} = N_m m_s a_{s_s} = 688 \times 1 \times 2 \times 0.000804 = 1.108 \text{ sq. in.}$$

A high rotor resistance is desirable from the standpoint of starting torque and current but leads to a high slip. The ratio of total rotor copper section to total stator copper section can in general be the same as for polyphase motors (see page 320). Cast aluminum is used for the squirrel-cage winding of this motor. Since the aluminum generally used for this purpose has a conductivity 50 per cent that of copper, the total bar area must be two times the area required for copper. The area of the slot is also the bar area and is, from Fig. 211, 0.0303 sq. in. The ratio of total rotor conductor section to total stator copper section is, then,

$$\frac{S_{cr}}{S_{cs}} = \frac{0.0303 \times 48}{1.108} = 1.315.$$

This is a rather low ratio and will lead to a rather high slip at full load. By using a smaller number of turns in the stator with consequent higher magnetic densities in stator teeth and yoke this ratio can be increased.

The end ring section is calculated as explained on page 321 and for aluminum must be two times as large as for copper. The end ring for this motor is cast integral with the bars and has a section area

$$S_{cr} = 0.124 \text{ sq. in.}$$

The rotor tooth and yoke densities might, from the standpoint of losses, be considerably higher than those of the stator, because the rotor frequency at normal operating speed is very low. Because of the high magnetizing current that would result the rotor magnetic densities are

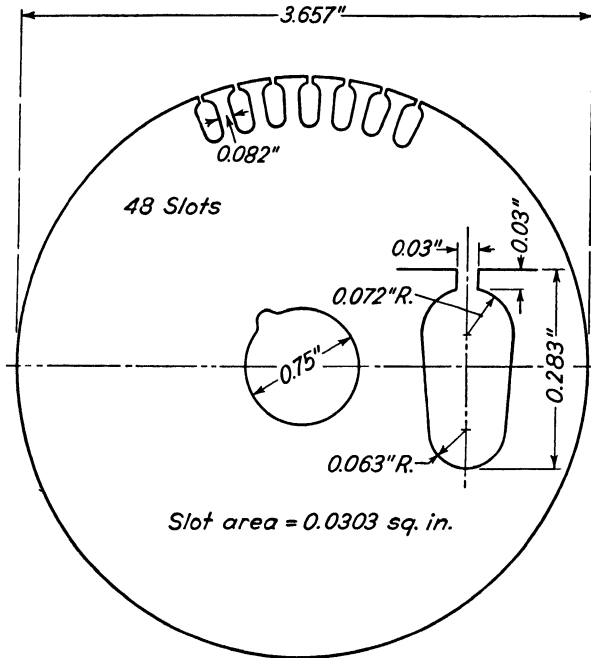


FIG. 211.—Rotor punching, $\frac{1}{4}$ -hp. split-phase induction motor.

only slightly higher than the corresponding stator densities. The section area of the rotor teeth

$$\begin{aligned} s_t &= w_{tr} l_s r 0.95 = 0.082 \times 2 \times 48 \times 0.95 \\ &= 7.48 \text{ sq. in.} \end{aligned}$$

The final value of the total flux

$$\phi_t = \frac{\phi p}{f_d} = \frac{143,000 \times 4}{0.637} = 897,000 \text{ lines.}$$

The flux in the rotor is less than the flux in the stator because of the stator leakage flux. The field leakage flux factor can be taken equal to 0.95, and the rotor tooth density

$$B_{tr} = \frac{897,000 \times 0.95}{7.48} = 114,000 \text{ lines per sq. in.}$$

The radial depth of the rotor yoke

$$\frac{1}{2}d_{yr} = (D_r - 2d_{sr} - D_i)\frac{1}{2}.$$

When ventilating holes are used in the rotor yoke D_i is the diameter of a circle at outside of holes; if these holes are round, one-third the radius should be added to the radial depth. For round-bottom rotor slots one-third of the radius at the bottom of the slot should be added to the radial yoke depth.

$$\begin{aligned}d_{yr} &= 3.657 - (2 \times 0.283 + 0.75) + 0.042 \\ &= 2.383 \text{ in.}\end{aligned}$$

The rotor yoke density

$$\begin{aligned}B_{yr} &= \frac{\phi \times 0.95}{d_{yr}l \times 0.95} = \frac{143,000 \times 0.95}{2.383 \times 2 \times 0.95} \\ &= 30,000 \text{ lines per sq. in.}\end{aligned}$$

The air gap density

$$B_g = \frac{897,000 \times 0.95}{\pi \times 3.68 \times 2.0} = 36,900 \text{ lines per sq. in.}$$

Operating Characteristics.—The ratio of stator slot opening to air gap length

$$= \frac{0.080}{0.0115} = 6.95.$$

From the curve, Fig. 53, $y = 2.77$, and the air gap coefficient for the stator slot

$$\begin{aligned}k_s &= \frac{t_{1s}}{w_{1s_1} + (y\delta)} = \frac{0.321}{0.241 + (2.77 \times 0.0115)} \\ &= 1.175.\end{aligned}$$

For the rotor slot opening,

$$\begin{aligned}k_r &= \frac{t_{1r}}{w_{1s_1} + (y\delta)} = \frac{0.239}{0.209 + (1.66 \times 0.0115)} \\ &= 1.048.\end{aligned}$$

The air gap coefficient

$$k = k_s \times k_r = 1.175 \times 1.048 = 1.23.$$

The saturation factor, which is the ratio of the total ampere-turns for the magnetic circuit to the air gap ampere-turns only, is difficult to predetermine from direct-current magnetization curves. The shape of

the magnetizing current wave is not sinusoidal because of the non-linear nature of the magnetization curve of the core material. By use of alternating-current magnetization curves⁴ the magnetization characteristics can be fairly accurately calculated.

For single-phase induction motors the saturation factor will usually lie between the limits 1.10 and 1.35. When the magnetic densities in the teeth and yoke are low the low value applies, and when high, a higher value must be used. This motor has rather high magnetic densities in the magnetic circuit, and F_s is chosen equal to 1.25.

The length of the half mean-turn for each of the coils per pole of a concentric type winding

$$= \frac{4.2(D + d_s)}{S_s} \text{ slots spanned} + l.$$

In this expression 4.2 is used instead of π to take into account the extension of the coil beyond the stator core. If the coils are wound

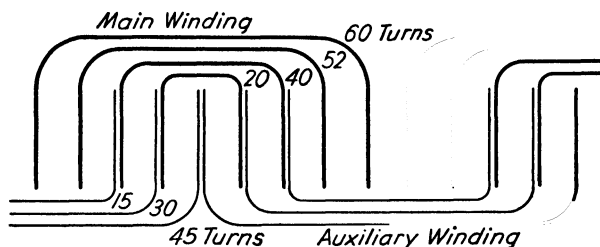


FIG. 212.—Winding distribution, $\frac{1}{4}$ -hp. split-phase induction motor.

close together in the end connections, 4 can be used instead of 4.2. The sum of the products of one-half mean-turn of each coil by turns per coil divided by the turns per pole is the weighted one-half mean-turn of the winding. Figure 212 shows the winding distribution for the $\frac{1}{4}$ -hp. split-phase motor design, and the length of the half mean-turn is calculated as follows:

$$\left[\frac{4.2(3.68 + 0.75)}{36} \times 2 + 2.0 \right] 20 = 60.80$$

$$[0.518 \times 4 + 2.0] 40 = 162.80$$

$$[0.518 \times 6 + 2.0] 52 = 266.00$$

$$[0.518 \times 8 + 2.0] 60 = 368.40$$

$$L_{sm} = \frac{858.00}{172} = 5.0 \text{ in.}$$

⁴ See Technical Bulletin 3, Carnegie-Illinois Steel Corp., for d-c. and a-c. magnetization curves for the grades of electric sheet steel used in electrical apparatus.

The resistance of the main stator winding

$$R_{sm} = \frac{L_{sm} N_m \times 0.692}{a_{sm} \times 10^6} = \frac{5.0 \times 688 \times 0.692}{2 \times 0.000804 \times 10^6}$$

$$= 1.48 \text{ ohms at } 25^\circ \text{ C.}$$

$$= 1.48 \times 1.15 = 1.70 \text{ ohms at } 65^\circ \text{ C.}$$

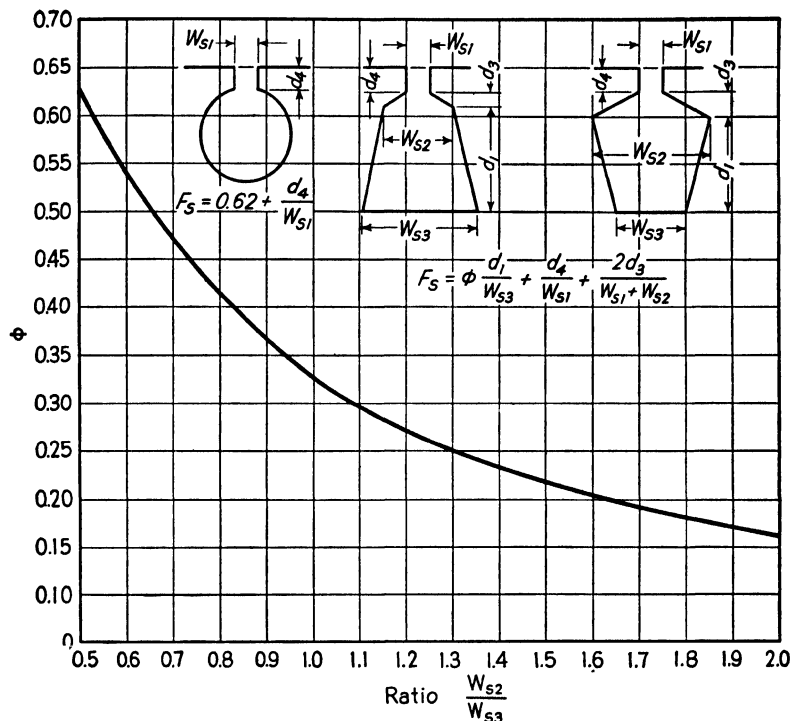


FIG. 213.—Slot reactance factor.

The rotor bars for this motor are skewed 1.85 slot pitches, or $1.85 \times 0.239 = 0.442$ in. The length of the rotor bar is, then,

$$l_b = \sqrt{2.0^2 + 0.442^2} = 2.05 \text{ in.}$$

The inside diameter of the end ring is 3.28 in., and the outside diameter 3.60 in. From Fig. 194, $K_{ring} = 0.97$, and the rotor resistance in terms of the main winding of the stator (see page 333),

$$R_{rm} = \frac{N_m^2 C_{wm}^2 m r}{10^6} \left(\frac{l_b}{s_b N_b} + \frac{0.64 D_{er}}{p^2 s_{er}} K_{ring} \right)$$

$$= \frac{688^2 \times 0.795^2 \times 2 \times 0.692}{10^6} \left(\frac{2.05}{0.0303 \times 48} + \frac{0.64 \times 3.60}{4^2 \times 0.124} 0.97 \right) 2$$

$= 2.12 \text{ ohms at } 25^{\circ} \text{ C.}$
 $= 2.12 \times 1.15 = 2.44 \text{ ohms at } 65^{\circ} \text{ C.}$

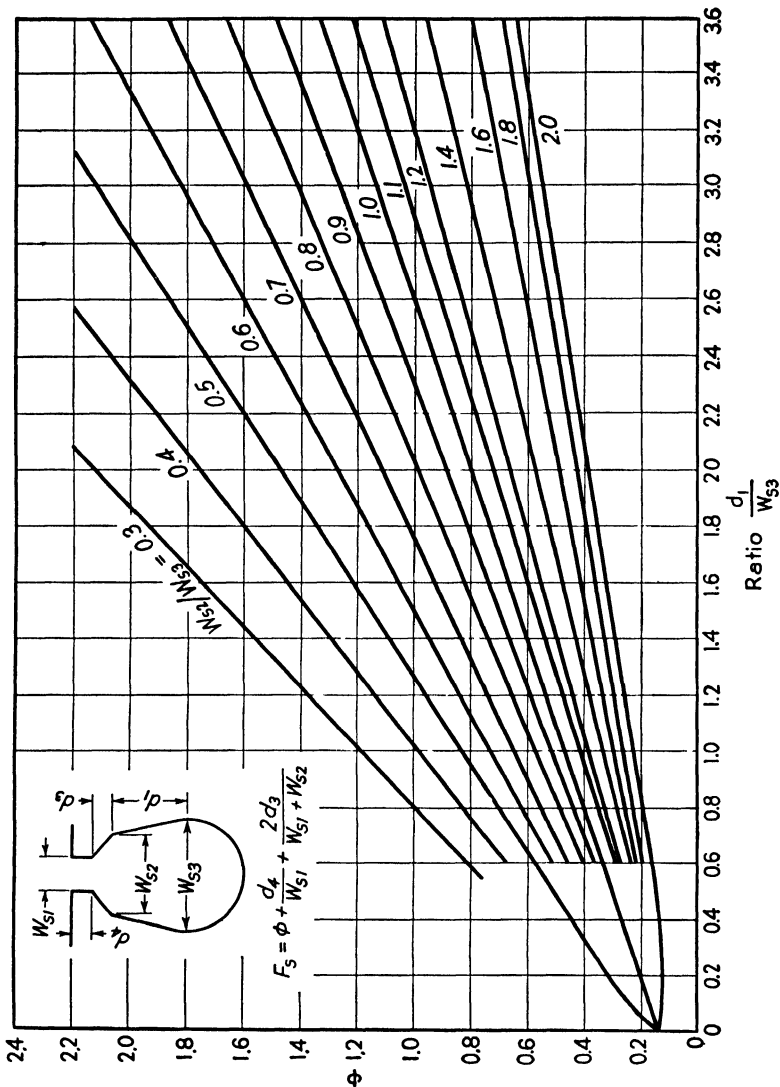


Fig. 214.—Slot reactance factor.

The rotor resistance determined from the locked rotor test will be higher than the calculated value and is the effective resistance of the rotor winding at starting. For normal operating speeds the rotor resistance is very nearly equal to the direct-current resistance. The difference

between the locked rotor resistance and the direct-current resistance is greater for deep rectangular slots than for shallow or round slots. For round slots the locked rotor resistance from test was found to be approximately 10 per cent higher than the calculated direct-current resistance of the rotor winding.

The method of calculating the leakage reactance is in general the same as used for polyphase machines; some changes must, however, be made because of the different type of slot and winding used on single-phase induction motors. Practical design experience has shown that the leakage reactance equations below give sufficiently close results for the design of most fractional-horsepower induction motors.

$$X_s = 2\pi f N_m^2 C_{wm}^2 \times 10^{-8} \left[\frac{6.38l}{S_s} \right] \left[F_{ss} + \frac{S_s}{S_r} F_{sr} \right] \text{ ohms.}$$

The stator and rotor slot factors, F_{ss} and F_{sr} , are calculated as shown in Figs. 213 and 214.

The zigzag leakage reactance for stator and rotor in terms of main winding

$$X_z = 2\pi f N_m^2 C_{wm}^2 10^{-8} \left[\frac{2.13l}{S_s \delta} \right] \left[\frac{(w_{ts1} + w_{tr1})^2}{4(t_{1s} + t_{1r})} \right] \text{ ohms.}$$

The end connection leakage reactance

$$X_e = 2\pi f N_m^2 C_{wm}^2 10^{-8} \left[\frac{\pi(D + d_s) \text{ av. coil span}}{S_s p} \right] \text{ ohms.}$$

The skew leakage reactance

$$X_{sk} = X_m \frac{\theta_{sk}^2}{12} K_p \text{ ohms,}$$

where θ_{sk} is the rotor bar skew expressed in radians and is equal to π divided by rotor slots per pole times number of bars skew, and K_p is the stator leakage flux factor which can be taken equal to 0.95.

The magnetizing reactance ⁵

$$X_m = 2\pi f N_m^2 C_{wm}^2 10^{-8} \frac{0.645l_r}{\delta k p F_s} \text{ ohms.}$$

F_s , the saturation factor, has been explained on page 367. Mr. P. H. Trickey⁶ gives a method of calculating the leakage reactance for the shaded pole motor.

⁵ See also "Characteristic Constants of Single-Phase Induction Motors, Part I: Air Gap Reactances," by W. J. Morrill, Elec. Eng., March, 1937, p. 333.

⁶ "An Analysis of the Shaded Pole Motor," by P. H. Trickey, Elec. Eng., Sept., 1936, p. 1007.

The total leakage reactance of the stator main winding plus rotor in terms of the main winding of the stator

$$X_{lm} = X_s + X_s + X_s + X_{sk} \text{ ohms.}$$

The open-circuit reactance, the reactance of the stator main winding with secondary open,

$$X_0 = X_m + \frac{X_{lm}}{2} \text{ ohms.}$$

The leakage flux factors

$$K_r = \frac{X_0 - X_{lm}}{X_0} \quad \text{and} \quad K_p = \sqrt{\frac{X_0 - X_{lm}}{X_0}}.$$

The constant term for the various reactances

$$= 2\pi \times 60 \times 688^2 \times 0.795^2 \times 10^{-8} = 1.128.$$

For the stator slot

$$\frac{w_{s2}}{w_{s3}} = \frac{0.194}{0.314} = 0.618.$$

From Fig. 213, $\phi = 0.530$, and

$$F_{ss} = 0.530 \frac{0.69}{0.314} + \frac{0.03}{0.08} + \frac{2 \times 0.03}{0.08 + 0.194} = 1.864.$$

For the rotor slot,

$$\frac{w_{s2}}{w_{s3}} = \frac{0.144}{0.126} = 1.14 \quad \text{and} \quad \frac{d_1}{w_{s3}} = \frac{0.118}{0.126} = 0.937.$$

From Fig. 214, $\phi = 0.37$, and

$$F_{sr} = 0.37 + \frac{0.03}{0.03} + \frac{2 \times 0.072}{0.03 + 0.144} = 2.20.$$

$$X_s = 1.128 \left[\frac{6.38 \times 2.0}{36} \right] \left[1.864 + \frac{36}{48} 2.20 \right] = 1.40 \text{ ohms.}$$

$$X_s = 1.128 \left[\frac{2.13 \times 2.0}{36 \times 0.0115} \right] \left[\frac{(0.241 + 0.209)^2}{4(0.321 + 0.239)} \right] = 1.05 \text{ ohms.}$$

$$X_s = 1.128 \left[\frac{3.14 \times 4.43 \times 5}{36 \times 4} \right] = 0.545 \text{ ohm.}$$

$$X_m = 1.128 \left[\frac{0.645 \times 2.0 \times 2.89}{0.0115 \times 1.23 \times 4 \times 1.25} \right] = 59.4 \text{ ohms.}$$

$$X_{sk} = 59.4 \frac{0.484^2}{12} 0.95 = 1.10 \text{ ohms.}$$

The leakage reactance

$$X_{lm} = 1.40 + 1.05 + 0.545 + 1.10 = 4.095 \text{ ohms.}$$

$$X_0 = X_m + \frac{X_{lm}}{2} = 59.4 + \frac{4.10}{2} = 61.45 \text{ ohms.}$$

The leakage flux factors

$$K_r = \frac{61.45 - 4.10}{61.45} = 0.933;$$

$$K_p = \sqrt{K_r} = \sqrt{0.933} = 0.965.$$

The core loss is calculated as explained on page 330 for polyphase machines.

The weight of the stator teeth

$$\begin{aligned} G_{ct} &= 0.138 \times 2.0 \times 0.93 \times 36 \times 0.75 \times 0.278 \\ &= 1.97 \text{ lb.} \end{aligned}$$

The loss per pound for the tooth density, 95,000 lines per sq. in., for the armature-grade 24-gauge electric sheet steel is 4.45, and the loss in the stator teeth due to the fundamental frequency flux

$$W_{ct} = 4.45 \times 1.97 = 8.75 \text{ watts.}$$

The weight of the stator yoke

$$\begin{aligned} G_{cy} &= \frac{\pi}{4} [6.125^2 - (3.68 + 2 \times 0.75)^2] 2.0 \times 0.93 \times 0.278 \\ &= 4.30 \text{ lb.} \end{aligned}$$

For armature-grade 24-gauge electric sheet steel the loss per pound for the stator yoke density is 3.12, and the loss in the yoke due to the fundamental frequency flux

$$W_{cy} = 3.12 \times 4.30 = 13.4 \text{ watts.}$$

The total core loss

$$W_c = (8.75 + 13.4) 2.2 = 48.6 \text{ watts.}$$

The bearing friction and windage loss will depend upon the type of bearing to be used, whether ball bearing or sleeve bearing. For sleeve bearings and 1725 r.p.m. it is usually from 4.0 to 8.0 per cent of the watt output. The high value applies to small motors below $\frac{1}{4}$ -hp.

The friction and windage loss is taken equal to 6.0 per cent of the watt output for this design, or $186.5 \times 0.06 = 11.2$ watts.

The operating characteristics are calculated by the analytical method

prepared by Mr. Veinott.⁷ The speed at maximum torque can be determined from the curve, Fig. 215, which is from this same paper. The calculations are shown for full-load and maximum torque only. By assuming suitable values of slip the operating characteristics can be calculated for any desired load.

Auxiliary Winding.—The purpose of the auxiliary winding or starting winding is to produce a revolving field at starting and thereby provide torque to bring the rotor up to speed. This winding is connected in parallel with the main winding, and when the rotor has attained approximately 75 per cent of normal speed a switch, usually of centrifugal type, opens the auxiliary winding circuit. In order that the

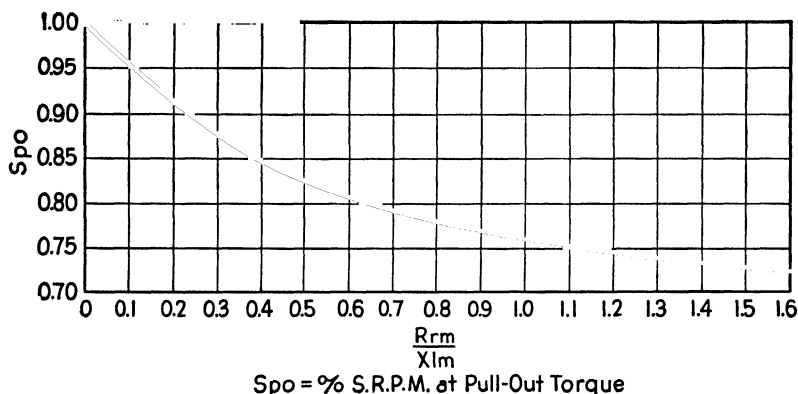


FIG. 215.—Speed at maximum torque, single-phase induction motors.

auxiliary winding can produce a revolving field the flux it sets up must be out of phase with the flux of the main winding. The number of turns of the main winding must satisfy the requirements of the core, and the size of conductor the current requirements of the load. The reactance is, therefore, high with low resistance. The auxiliary winding must then have constants just the reverse of those for the main winding if the flux it produces is to be appreciably out of phase with the main winding. It is not possible to obtain a 90° angle between the two flux waves in a resistance split-phase motor. The phase angle between the auxiliary winding current and voltage should generally be $\frac{2}{3}$ of that for the main winding.

The starting torque of resistance split-phase motors can be cal-

⁷ "Performance Calculations on Induction Motors," by C. G. Veinott, A.I.E.E. Trans., Vol. 51, Sept., 1932, p. 745; see also "Single Phase Induction Motors," by W. J. Branson, A.I.E.E. Trans., Vol. 31, Part II, 1912, p. 1749.

PERFORMANCE CALCULATIONS, SINGLE-PHASE INDUCTION MOTORS

 $\frac{1}{4}$ Hp 110 Volts 1800 S r p m

Motor Constants

Line volts— E	= 110	$F_3 = (I_m R_{rm}) R_{rm} / X_0$	= 0 173
Reactance— X_{lm}	= 4 1	$F_4 = (I_m R_{rm})^2$	= 8 74
X_0	= 61 5	$F_5 = (I_m R_{rm}) K_p$	= 4 21
R_{sm} at 65° C	= 1 70	$F_6 = [(I_m R_{rm}) K_p]^2 R_{rm}$	= 43 2
R_{rm} at 65° C	= 2 44	$F_7 = E K_p$	= 106 2
		$F_8 = (E K_p)^2 R_{rm}$	= 27,500
$K_p = \sqrt{\frac{X_0 - X_{lm}}{X_0}}$	= 0 966	$F_9 = \frac{\text{Core loss } (m)}{E}$	= 0 221
$R_{rm} = 0 595$	$\frac{R_{rm}}{X_0} = 0 0396$	Core loss (m)	= 24 3
$X_{lm} = \frac{E}{I_m} = 1 79$	$I_m R_{rm} = 4 37$	Core loss (c)	= 24 3
$F_1 = (2 - K_p^2) R_{rm}$	= 2 60	Friction and windage loss	= 11 2
$F_2 = (2 R_{sm} + R_{rm}) R_{rm} / X_0$	= 0 232	(Core loss (m) = core loss (c))	= $\frac{1}{2}$ total core loss)

*1	$s = \text{r p m} / \text{s r p m}$	0 966	0 81
*2	s^2	0 933	0 656
*3	$(1 - s^2)$	0 067	0 344
*4	$(1 - s^2) R_{sm}$	0 114	0 585
*5	F_1	2 60	2 60
*6	$U = (4) + (5)$	2 714	3 185
*7	$(1 - s^2) \lambda_{lm}$	0 275	1 41
*8	F_2	0 232	0 232
*9	$W = (7) - (8)$	0 043	1 178
*10	$\sqrt{U^2 + W^2}$	2 714	3 40
11	$(1 - s) E$	7 37	
12	F_3	0 173	
13	$M = (11) - (12)$	7 197	
14	$F_4 U$	0 600	
15	$N = (13) + (14)$	7 797	
16	$\sqrt{N^2 + F_4^2}$	11 700	
17	$I_1 = (16) / (10)$	4 310	
18	$(1 - s) F_7$	7 12	
19	$\sqrt{(18)^2 + F_5^2}$	8 27	
20	$I_2 = (19) / (10)$	3 05	
21	$\sqrt{F_5^2}$	4 06	
22	$I_3 = (21) / (10)$	1 50	
*23	$(1 - s^2) F_8$	1840 00	9460 0
*24	F_6	43 20	43 2
*25	$(23) - (24)$	1796 80	9416 8
26	Prim copper loss = $I_1^2 R_{sm}$	31 60	
27	Sec copper loss (m) = $I_2^2 R_{rm}$	22 70	
28	Sec copper loss (c) = $I_3^2 R_{rm}$	5 50	
29	Core loss (m)	24 30	
*30	$(25) \times (2) / (10)^2$	228 00	535 0
31	Input = $(26) + (27) + (28) + (29) + (30)$	312 10	
*32	Core loss (c) + (F and W)	35 50	35 5
*33	Output = $(30) - (32)$	192 50	499 5
*34	R p m = $s \times \text{s r p m}$	1739 00	1460
*35	Torque = $112 6 \times (33) / (34)$	12 48	38 4
36	Efficiency = $(33) / (31)$	61 70	
37	P f = $(31) / E I_1$	65 80	
38	App eff = $(36) \times (37)$	40 60	
39	Per cent full-load	103	318

* To calculate output and torque only
From A I L L Trans, Vol 51, Sept, 1932

culated by the equation given by Mr. C. R. Boothby⁸ for the capacitor motor by omitting the capacitor terms.

$$T_s = \frac{1.88pE^2KR_{rm}}{f} \frac{R_aX_{lm} - R_mX_{la}}{Z_m^2Z_a^2} \text{ oz-ft.}$$

This equation does not take into account the effect of magnetizing current. Mr. P. H. Trickey gives the following multiplying factor to take this into account:

$$\left[\frac{K_r}{1 + \left(\frac{R_{rm}}{X_0} \right)^2} \right].$$

This factor can for most cases be taken equal to K_r . If the components of R_a and R_m are substituted into the starting torque equation and the derivative⁹ with respect to R_{sa} set equal to zero, the value of auxiliary winding resistance can be found to give maximum starting torque. For given main winding constants the starting torque will be maximum when

$$R_{sa} = K^2(R_{sm} + Z_m).$$

From the ratio,

$$K = \frac{N_a C_{wa}}{N_m C_{wm}},$$

the number of conductors of the auxiliary winding can be determined. The section area of the conductor can then be calculated to give the required resistance when the length of the half mean-turn of the winding is known. The auxiliary winding is similar to the main winding, and the half mean-turn can easily be estimated. It is not always possible to use the auxiliary winding that gives maximum starting torque for a given value of K because of the current capacity of the conductor. Since the auxiliary winding is in service only during the starting period, a few seconds, the current density in the conductor may be very high but should not exceed 42,000 amperes per sq. in. In the books referred to in the footnote on page 359 the methods used for forming the coils for both main and auxiliary winding and of winding small motors are very thoroughly explained.

For the auxiliary winding for the $\frac{1}{4}$ -hp. split-phase motor design a

⁸ Discussion of the papers, "The Condenser Motor," "The Fundamental Theory of the Capacitor Motor," and "The Revolving Field Theory of the Capacitor Motor," by C. R. Boothby, A.I.E.E. Trans., Vol. 48, April, 1929, p. 629; for other methods of calculating starting torque see "Starting Torque of Split-Phase Motors," by A. F. Puchstein and T. C. Lloyd, Product Engineering, Feb., 1938, p. 87.

⁹ See "Alternating Current Machines," by A. F. Puchstein and T. C. Lloyd, John Wiley & Sons, New York.

No. 25 s.c.c.e. wire was used and the value of K determined which would give the desired starting torque with a safe current density in the conductor. This wire size was used because it was available although it is smaller than is common practice. Generally the auxiliary winding conductor is 6 sizes smaller than the main winding conductor. The preliminary calculations to determine the ratio of effective auxiliary winding conductors to effective main winding conductors are not shown here. From these calculations, $K = 1.25$. Then

$$\begin{aligned} N_a C_{wa} &= K N_m C_{wm} \\ &= 1.25 \times 688 \times 0.795 \\ &= 683. \end{aligned}$$

The winding distribution factor, C_{wa} , will be large with the winding arrangement selected and is assumed equal to 0.90. Then

$$N_a = \frac{684}{0.90} = 760.$$

The skein type of winding was selected, which determined the winding arrangement. The inside or short span coil has as many turns as the skein; the next coil, 2 times that number; and the third coil, 3 times the number of turns in the skein. With 15 turns per skein the number of turns per pole will be 90 and $N_a = 90 \times 8 = 720$. The winding constant is found as follows:

$$\begin{aligned} \sin 5/9 \times 90 &= 0.766 \times 15 = 11.50 \\ \sin 7/9 \times 90 &= 0.940 \times 30 = 28.20 \\ \sin 9/9 \times 90 &= 1.00 \times 45 = 45.00 \\ C_{wa} &= \frac{84.70}{90} = 0.942. \end{aligned}$$

$$K = \frac{720 \times 0.942}{688 \times 0.795} = 1.24.$$

The length of the half mean-turn is calculated as explained for the main winding instead of the stator diameter through the middle of the slot; the diameter below the wedge is used because the auxiliary winding occupies only a small space just below the wedge.

$$\begin{aligned} \left[\frac{4.2 \times (3.68 + 0.12)}{36} \times 5 + 2.0 \right] 15 &= 63.2 \\ [0.443 \times 7 + 2.0] 30 &= 153.0 \\ [0.443 \times 9 + 2.0] 45 &= 270.0 \\ L_{sa} &= \frac{486.2}{90} = 5.4 \text{ in.} \end{aligned}$$

The resistance of the auxiliary winding

$$R_{sa} = \frac{5.4 \times 720 \times 0.692}{1 \times 0.000252 \times 10^6} = 10.67 \text{ ohms at } 25^\circ \text{ C.}$$

The rotor resistance in terms of the auxiliary winding

$$R_{ra} = K^2 R_{rm} = 1.24^2 \times 2.12 = 3.26 \text{ ohms at } 25^\circ \text{ C.}$$

The total leakage reactance in terms of the auxiliary winding

$$X_{la} = K^2 X_{lm} = 1.24^2 \times 4.1 = 6.31 \text{ ohms.}$$

For the purpose of calculating the starting current and torque the equivalent rotor resistance is increased 15 per cent to take into account skin effect. The total resistance of the main winding at 25° C.

$$\begin{aligned} R_m &= R_{sm} + R_{rm} \times 1.15 = 1.48 + 2.12 \times 1.15 \\ &= 3.92 \text{ ohms.} \end{aligned}$$

The total impedance of the main winding at 25° C. is, then,

$$Z_m = \sqrt{3.92^2 + 4.1^2} = 5.67 \text{ ohms.}$$

For the auxiliary winding,

$$\begin{aligned} R_a &= R_{sa} + R_{ra} \times 1.15 = 10.67 + 3.26 \times 1.15 \\ &= 14.42 \text{ ohms at } 25^\circ \text{ C.,} \end{aligned}$$

and

$$Z_a = \sqrt{14.42^2 + 6.31^2} = 15.70 \text{ ohms.}$$

The short-circuit or locked rotor current in the main winding

$$I_{sm} = \frac{E}{Z_m} = \frac{110}{5.67} = 19.40 \text{ amperes;}$$

and in the auxiliary winding

$$I_{sa} = \frac{E}{Z_a} = \frac{110}{15.70} = 7.0 \text{ amperes.}$$

The current density for the auxiliary winding at starting is then

$$= \frac{7.0}{0.000252} = 27,800 \text{ amperes per sq. in.}$$

The locked rotor current for both windings in parallel can easily be shown to be equal to

$$\begin{aligned} I_s &= \frac{I_{sm}(Z_m + Z_a)}{Z_a} \\ &= \frac{19.40(5.67 + 15.70)}{15.70} = 26.40 \text{ amperes.} \end{aligned}$$

The starting torque,

$$T_s = \frac{1.88pE^2KR_{rm}}{f} \frac{R_aX_{lm} - R_mX_{la}}{Z_m^2Z_a^2} K_r.$$

$$T_s = \frac{1.88 \times 4 \times 110^2 \times 1.24 \times 2.44}{60} \frac{14.42 \times 4.1 - 3.92 \times 6.31}{5.67^2 \times 15.70^2} 0.933$$

$$= 18.5 \text{ oz-ft.}$$

Full-load torque

$$= \frac{\text{watts output} \times 112.6}{\text{r.p.m.}} = \frac{186.5 \times 112.6}{1725}$$

$$= 12.2 \text{ oz-ft.}$$

The starting torque in per cent of full-load torque is 152.0 per cent.

The tested value of locked rotor current with windings at room temperature is 24.7 amperes with a starting torque of 15.0 oz-ft. The constants of the motor were determined from test by the method proposed by C. G. Veinott.¹⁰ The results from the running light and locked rotor tests are as follows:

$$R_{sm} = 1.67 \text{ ohms } 25^\circ \text{ C.; } R_{sa} = 10.6 \text{ ohms at } 25^\circ \text{ C.}$$

The locked rotor resistance, $R_{rm} = 2.95$ ohms at 25° C.

$$X_{lm} = 3.8 \text{ ohms, } X_0 = 60.9 \text{ ohms,}$$

$$K_r = 0.937, \quad K_p = 0.967.$$

The guaranteed values on the design sheet are the minimum values specified in the N.E.M.A. standards. The test values of efficiency and power factor for full-load are given on the design sheet.

The stator main winding resistance was calculated for form-wound coils; in winding this motor, hand winding was used. This method of winding, unless carefully carried out, will lead to a longer mean-turn and consequent higher resistance than is obtained with a form winding. The difference between calculated and test values of efficiency, starting torque, and current is due to the high main winding resistance.

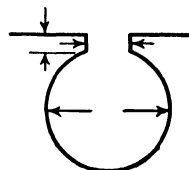
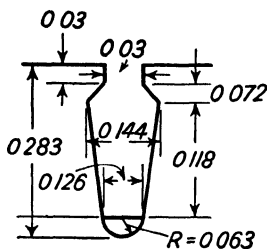
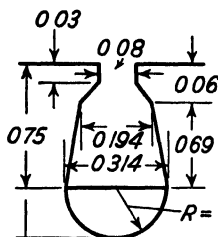
The stator winding design and the calculations for this motor were made by R. W. Saunders for the senior electrical design course. He also wound the stator and tested it. The results of the test are given above.

¹⁰ "Segregation of Losses in Single Phase Induction Motors," by C. G. Veinott, Elec. Eng., Dec., 1935, p. 1302.

380 FRACTIONAL-HORSEPOWER SINGLE-PHASE MOTOR DESIGN

SINGLE-PHASE INDUCTION MOTOR DESIGN SHEET

Hp, ¼	S r p m, 1800	Cycles, 60	Poles, 4	Volts, 110	Amps, 4 3
	Stator	Rotor		Stator	Rotor
Outside diameter	6 125	3 657	tooth face	0 241	0 209
Inside diameter	3 680	0 75	tooth width	0 138	0 082
Length	2 00	2 00	Depth below slot	0 473	1 19
Number of slots	36	48	Slot factor	1 175	1 048
Tooth pitch	0 321	0 239	Total conductor section	1 108	1 455



Slot number	1	2	3	4	5	6	7	8	9	10	11	12	13	14	15	16	17	18	19	20
Stator main	20	40	52	60	60	60	52	40	20		20	40	52	60	60	52	40	20		
Stator auxiliary	45	30	15					15	30	45	30	15					15	30	45	

Winding	Main	Auxiliary	Rotor	
Conductor size	20 s c c e	25 s c c e	Bar section	0 0303
area	0 000804	0 000252	length	2 05
Amps per sq in	2880	27,800	material	aluminum
Half mean-turn	5 0	5 4	skew bars	1 85
Conductors in series	688	720	End ring section	0 124
Cp	0 795	0 942	material	aluminum
Weight, lb	1 80	0 314	diam outside	3 60
			diam inside	3 28

Gap length	0 0115	Gap coefficient	1 23	Pole pitch	2 89
Total flux	897,000	fd	0 637	Flux per pole	143,000

	Section	Density	Weight	Core Loss
Stator teeth	9 44	95,000	1 97	8 75
Stator yoke	1 80	81,400	4 30	13 40
Rotor teeth	7 48	114 000		22 15
Rotor yoke	4 53	30,000		×2 2
Air gap	23 10	36,900		48 60

R _{sm}	1 48 ohms at 25° C	R _{sa}	10 67 ohms at 25° C	X _{lm}	4 1 ohms	X _{la}	6 31 ohms
R _{rm}	2 12 × 1 15 ohms at 25° C	R _{ra}	3 75 ohms at 25° C	Z _m	5 67 ohms	Z _a	15 70 ohms
R _m	3 92 ohms at 25° C	R _a	14 42 ohms at 25° C	K	1 24 ohms	X ₀	61 50 ohms

	Full Load						Torque		Locked
	Amps	Watts	Eff	P F	App Eff	R p m	Max	Start	Amps
Guar	4 6	301	62 0	60 0	37 2	1725	22 5	11 0	23 0
Calc	4 3	302	61 7	65 8	40 7	1739	38 4	18 5	26 4
Test	4 4	327	57 0	67 0	38 2	1726	31 6	15 0	24 7

Designed by R M Saunders

Design 2. Design of a 1/2-Hp., 110-Volt, 1725-R.P.M., 60-Cycle, Single-Phase Capacitor Start Induction Motor.—The full-load efficiency and power factor to be not less than 70 and 70 per cent, respectively. The locked rotor torque should be 200 per cent of full-load torque with a locked rotor current not over 35 amperes. The breakdown torque should be 200 per cent of full-load torque. The motor is to be of the open type with the temperature rise of the windings not above 40° C. for continuous duty.

The author prepared the mechanical as well as electrical design of this motor with drawings and specifications and supervised the making of assembling fixtures and tools for the Department of Mechanical Engineering, Minnesota Institute of Technology. The motor is to be built by electrical and mechanical engineering students as a shop course for instruction in production methods. The dies and tools were designed and made by Eric Rosendahl, tool and instrument maker in the Department of Mechanical Engineering.

Stator.—The watt output = $0.50 \times 746 = 373$ watts. The motor will have 4 poles, and the s.r.p.m. is 1800. The output constant from Fig. 209 is 225, and

$$D^2 l = \frac{373 \times 225}{1800} = 46.6.$$

With a ratio of core length to gap diameter equal to 0.60,

$$D = \sqrt[3]{\frac{46.6}{0.60}} = 4.26 \text{ in.}$$

The core length for this diameter

$$l = \frac{373 \times 225}{4.26^2 \times 1800} = 2.57 \text{ in.}$$

Preliminary calculations were made for gap diameters of 4.25 and 4.50 in. The core dimensions finally selected are

$$D = 4.375 \text{ in., } l = 2.56 \text{ in.}$$

The core laminations are punched from electrical grade sheet steel 26 gauge, 0.0185 in. thick. The stator will have 36 slots, and the tooth width is made 0.13 in. The total stator tooth section

$$\begin{aligned} s_{ts} &= w_{ts} l S_s \times 0.93 = 0.13 \times 2.56 \times 36 \times 0.93 \\ &= 11.12 \text{ sq. in.} \end{aligned}$$

The staking factor is taken equal to 0.93.

For a tooth density of 105,000 lines per sq. in. the total flux

$$\phi_t = B_{ts} \times s_{ts} = 105,000 \times 11.12 = 1,170,000 \text{ lines.}$$

The winding arrangement selected for the main winding is the one shown in Fig. 207. The winding distribution factor with sinusoidal distribution of the turns per pole is then 0.795 (see page 363. The number of series conductors in the main winding

$$\begin{aligned} N_m &= \frac{pE_t \times 0.95 \times 45 \times 10^6}{f\phi_t C_{wm} f_d} \\ &= \frac{4 \times 110 \times 0.95 \times 45 \times 10^6}{60 \times 1,170,000 \times 0.795 \times 0.637} = 530. \end{aligned}$$

To obtain a small conductor size which is easier to wind, and also to make it possible to use the motor on 110- or 220-volt supply, the winding is arranged in 2 parallel circuits. The number of turns per pole

$$t_p = \frac{aN_m}{2 \times p} = \frac{2 \times 530}{2 \times 4} = 132.5.$$

For sinusoidal distribution the number of turns required in each coil are (coil 1 is the inside or short span coil)

$$\text{Coil 1} = 0.121 \times 132.5 = 16.0; \text{ use } 16$$

$$\text{Coil 2} = 0.227 \times 132.5 = 30.1; \text{ use } 30$$

$$\text{Coil 3} = 0.306 \times 132.5 = 40.5; \text{ use } 40$$

$$\text{Coil 4} = 0.346 \times 132.5 = 45.8; \text{ use } 46$$

$$t_p = 132$$

The conductors in series are, then,

$$N_m = \frac{pt_p \times 2}{a} = \frac{4 \times 132 \times 2}{2} = 528,$$

and the final value of the flux per pole

$$\phi = \frac{110 \times 0.95 \times 45 \times 10^6}{60 \times 528 \times 0.795} = 187,000 \text{ lines.}$$

The total flux

$$\phi_t = \frac{187,000 \times 4}{0.637} = 1,172,000 \text{ lines.}$$

The stator tooth density

$$B_{ts} = \frac{1,172,000}{11.12} = 105,200 \text{ lines per sq. in.}$$

To determine the input current of the motor the apparent efficiency or product of power factor and true efficiency must be assumed. For an apparent efficiency of 0.49 the input current

$$I = \frac{0.50 \times 746}{110 \times 0.49} = 6.92 \text{ amperes.}$$

A current density of 2700 amperes per sq. in. is assumed; see page 363. The main winding conductor section

$$s_{sm} = \frac{I}{a \times A_{sm}} = \frac{6.92}{2 \times 2700} = 0.00128 \text{ sq. in.}$$

For the stator main winding conductor No. 18 s.c.c.e. wire will be used. The section area of this wire is 0.00126 sq. in. and the insulated diameter 0.047 in. The current density for this conductor

$$A_{sm} = \frac{6.92}{2 \times 0.00126} = 2750 \text{ amperes per sq. in.}$$

The size of the stator slot is determined as explained on page 364 and must be made large enough to accommodate 46 No. 18 s.c.c.e. conductors with the required amount of insulation. For motors $\frac{1}{2}$ -hp. and larger the dielectric test voltage for the windings is twice rated voltage of the winding plus 1000. For the slot insulation 0.015-in. treated paper is used. The insulated conductor area = $0.047^2 \times 0.785 = 0.001732$ sq. in., and the slot area required

$$= \frac{46 \times 0.001732}{0.30} = 0.266 \text{ sq. in.,}$$

where 0.30 is the ratio of insulated conductor area to slot area. For an assumed slot depth of 0.75 in. the mean width

$$w_{sa} = \frac{(4.375 + 0.75)\pi}{36} - 0.13 = 0.317 \text{ in.,}$$

and the slot area = $0.317 \times 0.75 = 0.238$ sq. in. The ratio of insulated conductor area to slot area is, for this slot depth,

$$= \frac{46 \times 0.001732}{0.238} = 0.334.$$

This slot depth was adopted for this motor. The stator punching is shown in Fig. 216.

The stator yoke radial depth is taken equal to $0.50 [6.75 - (4.375 + 2 \times 0.75)]$ or 0.4375 in., and the yoke density

$$B_{ys} = \frac{187,000}{0.4375 \times 2 \times 2.56 \times 0.93} = 89,600 \text{ lines per sq. in.}$$

Rotor.—The equation for air gap length on page 365 gives larger values than have been found satisfactory with modern construction methods. If low air gap densities are used the length of the air gap can be increased, but this also increases the cost. For this motor,

$$\delta = 0.0135 \text{ in.}$$

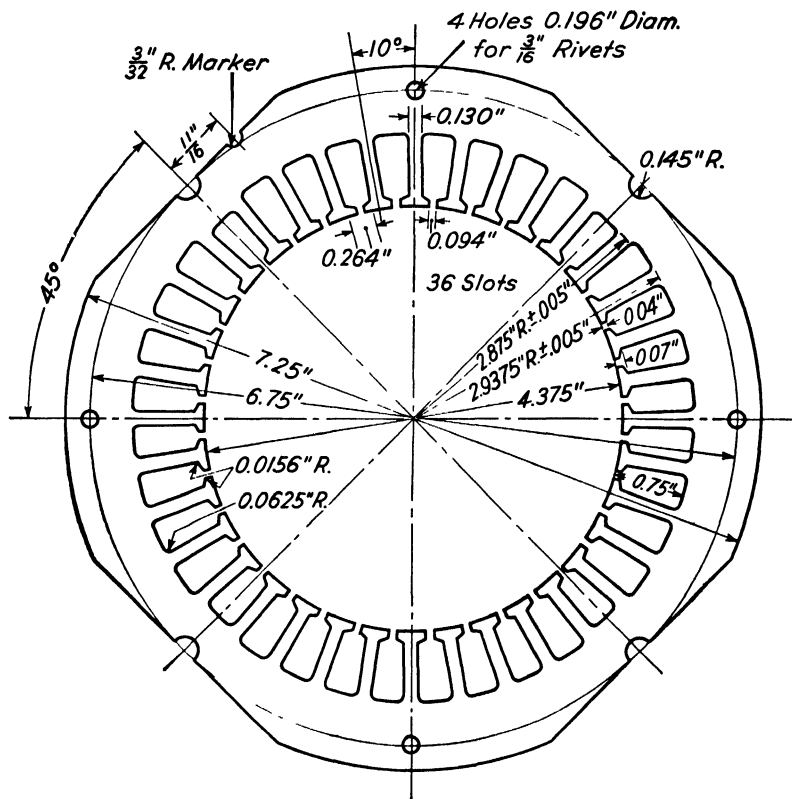


FIG. 216.—Stator punching, $\frac{1}{2}$ -hp. capacitor-start motor.

The gap diameter of the stator is ground true, and the finished diameter is 4.376 in. The rotor diameter is, then,

$$D_r = 4.376 - 2 \times 0.0135 = 4.349 \text{ in.}$$

The number of rotor slots are chosen to satisfy the conditions given on page 319. The number of rotor slots may be either larger or smaller than the number of stator slots. With a smaller number the time required to make the die is materially reduced. The requirements for a quiet motor given on page 319 are satisfied with 26 rotor slots with

The end ring is rolled like a coil spring from $\frac{3}{8} \times \frac{1}{2}$ in. copper bar. The section area is then 0.0938 sq. in. The holes for the bars are drilled near the outside periphery of the ring in a specially designed drilling jig. The outside diameter of the ring is 4.329 in., and the inside diameter 3.329 in.

The minimum width of rotor tooth (see Fig. 217),

$$w_{tr} = \frac{\pi \times 4.051}{26} - 0.238 = 0.252 \text{ in.}$$

The stator leakage flux factor is taken equal to 0.95, and the rotor tooth density

$$B_{tr} = \frac{1,172,000 \times 0.95}{0.252 \times 2.56 \times 0.93 \times 26} = 71,500 \text{ lines per sq. in.}$$

The radial depth of the rotor yoke is calculated as explained on page 354 (see Fig. 217).

$$\frac{1}{2}d_{vr} = (4.349 - 2 \times 0.238 - 2.56) 0.5 + 0.083 = 0.78 \text{ in.}$$

The rotor yoke density

$$B_{vr} = \frac{187,000 \times 0.95}{2 \times 0.78 \times 2.56 \times 0.93} = 47,800 \text{ lines per sq. in.}$$

The air gap density

$$B_g = \frac{1,172,000 \times 0.95}{\pi \times 4.376 \times 2.56} = 31,700 \text{ lines per sq. in.}$$

Operating Characteristics.—The ratio of stator slot opening to air gap length

$$= \frac{0.094}{0.0135} = 6.96.$$

From the curve, Fig. 53, $y = 2.78$, and the air gap coefficient for the stator slot

$$k_s = \frac{t_{1s}}{w_{ts1} + (y\delta)} = \frac{0.382}{0.288 + (2.78 \times 0.0135)} = 1.172.$$

For the rotor slot opening

$$k_r = \frac{t_{1r}}{w_{tr1} + (y\delta)} = \frac{0.524}{0.484 + (1.80 \times 0.0135)} = 1.03.$$

The air gap coefficient

$$k = k_s k_r = 1.172 \times 1.03 = 1.21.$$

The length of the half mean-turn of the stator main winding is calculated as explained on page 368.

$$\begin{aligned} \left[\frac{4.2(4.376 + 0.75)}{36} \times 2 + 2.56 \right] 16 &= 60.00 \\ [0.598 \times 4 + 2.56] 30 &= 148.60 \\ [0.598 \times 6 + 2.56] 40 &= 246.00 \\ [0.598 \times 8 + 2.56] 46 &= 338.00 \\ L_{sm} &= \frac{792.60}{132} = 6.00 \text{ in.} \end{aligned}$$

The resistance of the stator main winding

$$\begin{aligned} R_{sm} &= \frac{L_{sm} N_m \times 0.692}{as_{sm} \times 10^6} = \frac{6.0 \times 528 \times 0.692}{2 \times 0.00126 \times 10^6} \\ &= 0.872 \text{ ohm at } 25^\circ \text{ C.} \\ &= 1.00 \text{ ohm at } 65^\circ \text{ C.} \end{aligned}$$

The bar skew in inches is equal to the rotor tooth pitch or 0.525 in. The length of the rotor bar

$$l_b = \sqrt{2.56^2 + 0.525^2} = 2.61 \text{ in.}$$

For the ratio, inside to outside diameter of end ring equal to 0.77, K_{ring} from Fig. 194 = 0.96.

The rotor resistance in terms of the stator main winding

$$\begin{aligned} R_{rm} &= \frac{N_m^2 C_{wm}^2 m r}{10^6} \left[\frac{l_b}{s_b N_b} + \frac{0.64 D_r}{p^2 s_{er}} K_{ring} \right] \\ &= \frac{528^2 \times 0.795^2 \times 2 \times 0.692}{10^6} \left[\frac{2.61}{0.0412 \times 26} + \frac{0.64 \times 4.329}{4^2 \times 0.0938} 0.96 \right] \\ &= 1.03 \text{ ohms at } 25^\circ \text{ C., or} \\ &1.03 \times 1.15 = 1.19 \text{ ohms at } 65^\circ \text{ C.} \end{aligned}$$

The constant term for the various reactances

$$\begin{aligned} &= 2\pi f N_m^2 C_{wm}^2 10^{-8} = 2\pi \times 60 \times 528^2 \times 0.795^2 \times 10^{-6} \\ &= 0.665. \end{aligned}$$

For the stator slot

$$\frac{w_{s2}}{w_{s3}} = \frac{0.264}{0.383} = 0.689.$$

From Fig. 213, $\phi = 0.48$ and

$$\begin{aligned} F_{ss} &= \phi \frac{d_1}{w_{s3}} + \frac{d_4}{w_{s1}} + \frac{2d_3}{w_{s1} + w_{s2}} \\ &= 0.48 \frac{0.68}{0.383} + \frac{0.04}{0.094} + \frac{2 \times 0.03}{0.094 + 0.264} \\ &= 1.45. \end{aligned}$$

For the rotor slot

$$\begin{aligned} F_{sr} &= 0.62 + \frac{d_4}{w_{s1}} = 0.62 + \frac{0.03}{0.04} = 1.37. \\ X_s &= 0.665 \left[\frac{6.38 \times 2.56}{36} \right] \left[1.45 + \frac{36}{26} 1.37 \right] = 1.01 \text{ ohms.} \\ X_s &= 0.665 \left[\frac{2.13 \times 2.56}{36 \times 0.0135} \right] \left[\frac{(0.288 + 0.485)^2}{4(0.382 + 0.525)} \right] = 1.23 \text{ ohms.} \\ X_s &= 0.665 \left[\frac{\pi(4.375 + 0.75)5}{36 \times 4} \right] = 0.372 \text{ ohm.} \end{aligned}$$

The saturation factor for the calculation of magnetizing reactance is taken equal to 1.20.

$$\begin{aligned} X_m &= 0.665 \frac{0.645 \times 2.56 \times 3.44}{0.0135 \times 1.21 \times 1.20 \times 4} = 48.20 \text{ ohms.} \\ X_{sk} &= 48.2 \frac{0.482^2}{12} 0.95 = 0.89 \text{ ohm.} \end{aligned}$$

The leakage reactance

$$\begin{aligned} X_{lm} &= 1.01 + 1.23 + 0.372 + 0.89 = 3.50 \text{ ohms.} \\ X_0 &= X_m + \frac{X_{lm}}{2} = 48.2 + \frac{3.50}{2} = 49.95 \text{ ohms.} \end{aligned}$$

The leakage flux factors

$$\begin{aligned} K_r &= \frac{X_0 - X_{lm}}{X_0} = \frac{49.95 - 3.50}{49.95} = 0.93. \\ K_p &= \sqrt{\frac{X_0 - X_{lm}}{X_0}} = \sqrt{0.93} = 0.964. \end{aligned}$$

The weight of the stator teeth

$$G_{ct} = 0.13 \times 2.56 \times 0.93 \times 36 \times 0.75 \times 0.278 = 2.32 \text{ lb.}$$

The loss per pound for the stator tooth density, 105,200 lines per sq. in.,

PERFORMANCE CALCULATIONS, SINGLE-PHASE INDUCTION MOTORS

 $\frac{1}{2}$ Hp., 110 Volts. 1800 S.r.p.m.

Motor Constants

Line volts— E	= 110	$F_3 = (I_m R_{rm}) R_{rm} / X_0$	= 0.0624
Reactance— X_{lm}	= 3 5	$F_4 = (I_m R_{rm})^2$	= 5.24
X_0	= 50 0	$F_5 = (I_m R_{rm}) K_p$	= 2.52
R_{sm} at 65° C.	= 1.0	$F_6 = [(I_m R_{rm}) K_p]^2 R_{rm}$	= 7.58
R_{rm} at 65° C.	= 1.19	$F_7 = E K_p$	= 106 0
$K_p = \sqrt{\frac{X_0 - X_{lm}}{X_0}}$	= 0.964	$F_8 = (E K_p)^2 R_{rm}$	= 13,400.0
$\frac{R_{rm}}{X_{lm}} = 0.34$	$\frac{R_{rm}}{X_0} = 0.0238$	$F_9 = \frac{\text{Core loss (m)}}{E}$	= 0.218
$I_m = \frac{E}{X_0} = 2.2$	$I_m R_{rm} = 2.62$	Core loss (m)	= 24
$F_1 = (2 - K_p^2) R_{rm}$	= 1 270	Core loss (c)	= 24
$F_2 = (2 R_{sm} + R_{rm}) R_{rm} / X_0$	= 0.076	Friction and windage loss	= 17
		(Core loss (m) = core loss (c))	= $\frac{1}{2}$ total core loss

*1	$s = \text{r.p.m.} / \text{s.r.p.m.}$	0 970	0 86
*2	s^2	0 941	0.74
*3	$(1 - s^2)$	0 059	0.26
*4	$(1 - s^2) R_{sm}$	0 059	0.26
*5	F_1	1 270	1.27
*6	$U = (4) + (5)$	1 329	1.53
*7	$(1 - s^2) X_{lm}$	0 206	0.91
*8	F_2	0 076	0 076
*9	$W = (7) - (8)$	0.130	0.834
*10	$\sqrt{U^2 + W^2}$	1 333	1 74
11	$(1 - s^2) E$	6 50	
12	F_3	0 0624	
13	$M = (11) - (12)$	6 44	
14	$F_9 U$	0 29	
15	$N = (13) + (14)$	6 73	
16	$\sqrt{N^2 + F_4^2}$	8 53	
17	$I_1 = (16) / (10)$	6 40	
18	$(1 - s^2) F_7$	6 25	
19	$\sqrt{(18)^2 + F_5^2}$	6 74	
20	$I_2 = (19) / (10)$	5 05	
21	$s F_6$	2 45	
22	$I_3 = (21) / (10)$	1 83	
*23	$(1 - s^2) F_8$	790 00	3480 00
*24	F_6	7 58	7 60
*25	$(23) - (24)$	782 42	3472 4
26	Prm. copper loss = $I_1^2 R_{sm}$	41 00	
27	Sec. copper loss (m) = $I_2^2 R_{rm}$	30 40	
28	Sec. copper loss (c) = $I_3^2 R_{rm}$	4 00	
29	Core loss (m)	24 00	
*30	$(25) \times (2) / (10)^2$	413 00	849.0
31	Input = $(26) + (27) + (28) + (29) + (30)$	512 40	
*32	Core loss (c) + (F and W)	41 00	41 0
*33	Output = $(30) - (32)$	372 00	808 0
*34	R.p.m. = $s \times \text{s.r.p.m.}$	1746	1550
*35	Torque = $112.6 \times (33) / (34)$	24 0	58.4
36	Efficiency = $(33) / (31)$	72 6	
37	P.F. = $(31) / E I_1$	72.7	
38	App. eff. = $(36) \times (37)$	52 8	
39	Per cent full-load	99.7	

* To calculate output and torque only
From A I E E Trans., Vol. 51, Sept., 1932.

for 26-gauge electrical grade sheet steel, is 3.7, and the loss in the stator teeth due to the fundamental frequency flux

$$W_{et} = 3.7 \times 2.32 = 8.58 \text{ watts.}$$

The weight of the stator yoke is approximately

$$\begin{aligned} G_{cy} &= \frac{\pi}{4} [6.75^2 - (4.375 + 2 \times 0.75)^2] 2.56 \times 0.93 \times 0.278 \\ &= 5.76 \text{ lb.} \end{aligned}$$

For the stator yoke density, 89,600 lines per sq. in., the loss per pound is 2.7 and the loss in the yoke due to the fundamental frequency flux

$$W_{cy} = 2.7 \times 5.76 = 15.50 \text{ watts.}$$

The laminations used for this motor are core plated and 26 gauge. The additional losses are taken equal to 2.0 times the fundamental frequency loss.

$$W_c = (8.58 + 15.5) 2.0 = 48.16 \text{ watts.}$$

The friction and windage losses will be assumed equal to 4.5 per cent of the watt output or equal to $373 \times 0.045 = 16.8 - 17.0$ watts.

The operating characteristics are calculated by the analytical method prepared by Mr. Veinott (see page 374).

Auxiliary Winding. - For the capacitor-start motor, the capacitor is relied upon to produce the phase displacement between the current in the main and auxiliary winding. The auxiliary winding circuit is opened after the rotor has attained approximately 75 per cent of normal speed. The starting torque can be calculated by the equation given by Mr. C. R. Boothby with the correction by Mr. Trickey to take into account the effect of magnetizing current (see footnote page 363).

$$T_s = \frac{1.88pE^2KR_m}{f} \cdot \frac{R_aX_{lm} - R_m(X_{la} - X_c)}{[R_m^2 + X_{lm}^2][R_a^2 + (X_{la} - X_c)^2]} K_r \text{ oz-ft.}$$

In this equation R_a is the auxiliary winding resistance plus the resistance of the capacitor.

The derivative of this equation with respect to X_c set equal to zero and solved for X_c gives the capacity reactance required for maximum starting torque. This was carried out by Mr. Boothby, and for maximum starting torque

$$X_c = X_{la} + \frac{R_a}{R_m} (Z_m - X_{lm}) \text{ ohms.}$$

The value of X_c required for maximum starting torque for given main winding constants varies directly with X_{la} and R_a , which in turn vary directly with the square of K , the ratio of effective auxiliary winding turns to main winding turns. The curves of Fig. 218 show how maximum torque, capacity, starting current, and current density in the auxiliary winding vary with the ratio K for given main winding constants and an assumed auxiliary winding conductor. For minimum cost of capacitor K should be large, but a large value of K increases the cost of the auxiliary winding. The designer must, therefore, select

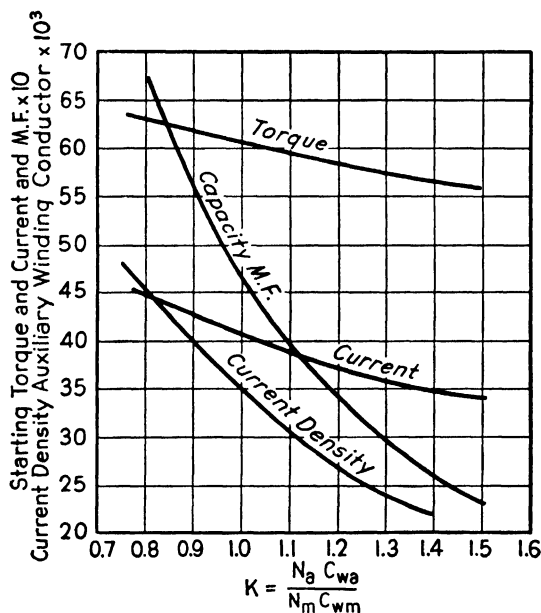


FIG. 218.

that combination that gives the required starting characteristics at reasonable cost.

To obtain a small capacitor and low starting current 1.55 was selected for the ratio K . Then

$$N_a = \frac{KN_m C_{wm}}{C_{wa}} = \frac{1.55 \times 528 \times 0.795}{0.85} = 765.$$

The winding arrangement and distribution for this motor are shown in Fig. 219. The number of turns per pole for a one-circuit winding

$$t_p = \frac{aN_a}{2 \times p} = \frac{1 \times 765}{2 \times 4} = 95.6.$$

For sinusoidal distribution the turns per coil are calculated as follows:

$$\begin{array}{ll} \sin 3/9 \times 90 = 0.500 \text{ per cent turns} = \frac{0.500}{3.206} = 0.156 \times 95.6 = 14.9; \text{ use } 14 \\ \sin 5/9 \times 90 = 0.766 & = 0.239 \times 95.6 = 22.9; \text{ use } 23 \\ \sin 7/9 \times 90 = 0.940 & = 0.293 \times 95.6 = 28.0; \text{ use } 28 \\ \sin 9/9 \times 90 = 1.000 & = 0.312 \times 95.6 = 30.0; \text{ use } 30 \\ \hline & \text{Turns per pole} = 95 \end{array}$$

The winding constant for the auxiliary winding is, then,

$$\begin{array}{l} \sin 3/9 \times 90 = 0.500 \times 14 = 7.50 \\ \sin 5/9 \times 90 = 0.766 \times 23 = 17.60 \\ \sin 7/9 \times 90 = 0.940 \times 28 = 26.30 \\ \sin 9/9 \times 90 = 1.000 \times 30 = 30.00 \\ \hline C_{wa} = \frac{81.40}{95} = 0.856. \end{array}$$

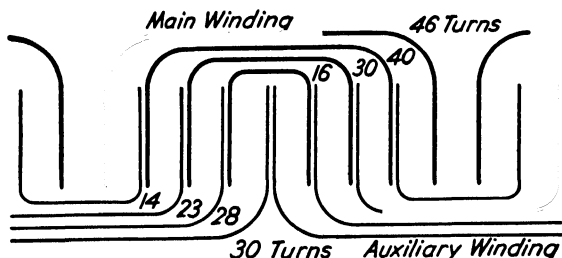


FIG. 219.—Winding distribution for $\frac{1}{2}$ -hp. capacitor-start motor.

The final ratio of effective conductors

$$K = \frac{760 \times 0.856}{528 \times 0.795} = 1.55.$$

The length of the half mean-turn is calculated as follows:

$$\begin{array}{l} \left[\frac{4.2(4.375 + 0.75/2)}{36} \times 3 + 2.56 \right] 14 = 59.2 \\ [0.555 \times 5 + 2.56] 23 = 122.8 \\ [0.555 \times 7 + 2.56] 28 = 180.0 \\ [0.555 \times 9 + 2.56] 30 = 226.0 \\ \hline L_{sa} = \frac{588.0}{95} = 6.20 \text{ in.} \end{array}$$

The starting torque and current were calculated for several conductor sizes, and No. 22 s.c.c.e. wire was chosen. The section area of this conductor is 0.00507 sq. in. The resistance of the auxiliary winding

$$R_{sa} = \frac{6.2 \times 760 \times 0.692}{1 \times 0.00507 \times 10^6} = 6.43 \text{ ohms at } 25^\circ \text{ C.}$$

For starting torque calculations the d-c. rotor resistance in terms of the main winding is increased 10 per cent, and the effective locked rotor resistance

$$R_{rm} = 1.10 \times 1.03 = 1.132 \text{ ohms at } 25^\circ \text{ C.}$$

The total main winding resistance

$$R_m = R_{sm} + R_{rm} = 0.872 + 1.132 = 2.004 \text{ ohms at } 25^\circ \text{ C.}$$

The locked rotor resistance in terms of the auxiliary winding

$$R_{ra} = 1.55^2 \times 1.132 = 2.72 \text{ ohms at } 25^\circ \text{ C.,}$$

and

$$R_a = R_{sa} + R_{ra} = 6.43 + 2.72 = 9.15 \text{ ohms.}$$

The total leakage reactance in terms of the auxiliary winding

$$X_{la} = 1.55^2 \times 3.50 = 8.4 \text{ ohms.}$$

The main winding locked rotor impedance

$$\begin{aligned} Z_m &= \sqrt{X_{lm}^2 + (R_{sm} + R_{rm})^2} \\ &= \sqrt{3.5^2 + (0.872 + 1.132)^2} = 4.03 \text{ ohms at } 25^\circ \text{ C.} \end{aligned}$$

The locked rotor current in the main winding

$$I_{sm} = \frac{110}{4.03} = 27.2 \text{ amperes.}$$

The capacity reactance required for maximum starting torque

$$\begin{aligned} X_c &= X_{la} + \frac{R_a}{R_m} (Z_m - X_{lm}) \\ &= 8.4 + \frac{9.15}{2.00} (4.03 - 3.50) = 10.83 \text{ ohms.} \end{aligned}$$

The capacity in microfarads

$$C = \frac{10^6}{2\pi f X_c} = \frac{10^6}{2\pi \times 60 \times 10.83} = 245 \text{ } \mu\text{f.}$$

A dry electrolytic capacitor with 200-microfarad nominal rating was selected for which the capacity reactance

$$X_c = \frac{10^6}{2\pi fC} = \frac{10^6}{2\pi \times 60 \times 200} = 13.3 \text{ ohms.}$$

The impedance of the auxiliary winding with capacitor in series

$$\begin{aligned} Z_{ac} &= \sqrt{R_a^2 + (X_{la} - X_c)^2} = \sqrt{9.15^2 + (8.4 - 13.3)^2} \\ &= 10.38 \text{ ohms.} \end{aligned}$$

The locked rotor current in the auxiliary winding

$$I_{sa} = \frac{110}{10.38} = 10.60 \text{ amperes.}$$

The current density in the auxiliary winding conductor at starting is then

$$= \frac{10.60}{0.000507} = 20,900 \text{ amperes per sq. in.}$$

The locked rotor current for both windings in parallel

$$\begin{aligned} I_s &= \frac{I_{sm}(\dot{Z}_m + \dot{Z}_{ac})}{\dot{Z}_{ac}} \\ &= 27.2 \frac{\sqrt{(2.004 + 9.15)^2 + [3.5 + (8.4 - 13.3)]^2}}{10.38} \\ &= 29.5 \text{ amperes.} \end{aligned}$$

The starting torque

$$\begin{aligned} T_s &= \frac{1.88 \times 4 \times 110^2 \times 1.55 \times 1.13}{60} \frac{9.15 \times 3.5 - 2.0 \times (8.4 - 13.3)}{[2.0^2 + 3.5^2] [9.15^2 + (8.4 - 13.3)^2]} 0.93 \\ &= 59.0 \text{ oz.-ft.} \end{aligned}$$

Full-load torque

$$= \frac{373 \times 112.6}{1725} = 24.4 \text{ oz.-ft.,}$$

and the per cent starting torque

$$= \frac{59.0}{24.4} \times 100 = 242.$$

The test value of locked rotor current with winding at room temperature is 31.4 amperes with a starting torque of 55 oz-ft. The constants of the motor were determined from test by the method proposed by Mr. C. G. Veinott (see page 379). The results from the running light and locked rotor tests are as follows:

$$R_{sm} = 0.883 \text{ ohm at } 25^{\circ} \text{ C.}; \quad R_{sa} = 6.5 \text{ ohms at } 25^{\circ} \text{ C.}$$

The locked rotor resistance, $R_{rm} = 1.16 \text{ ohms at } 25^{\circ} \text{ C.}$

$$X_{lm} = 3.25 \text{ ohms}, \quad X_0 = 49.7 \text{ ohms.}$$

$$K_r = 0.935, \quad K_p = 0.966.$$

The test values of efficiency and power factor for full-load are from the input-output test made with electric dynamometer and are given on the design sheet. The difference between test and calculated values of starting torque and current is very probably due to the fact that capacitor constants calculated from nominal rating were used in the calculations instead of test values for the particular capacitor on the motor tested. Capacitor resistance was also neglected.

The first motor built from this design, from which the test results given above were obtained, was not built by students. The machine work was done by Eric Rosendahl and Harry Martinson. The stator was wound by the author with form-wound coils. An assembly drawing of the motor is shown in Fig. 220.

Recent theories of noise in rotating electrical machinery indicate that a 28-slot rotor with 36-slot stator should be more desirable than the 26-slot rotor used for this design. The performance of this motor, however, is so satisfactory that it is doubtful that any improvement would be obtained with 28-rotor slots. Noise measurements made with a General Electric Co. noise level meter and frequency analyzer gave the following results:

120	cycles	per	sec.,	58	decibels
780	"	"	"	40	"
900	"	"	"	44	"
1020	"	"	"	42	"

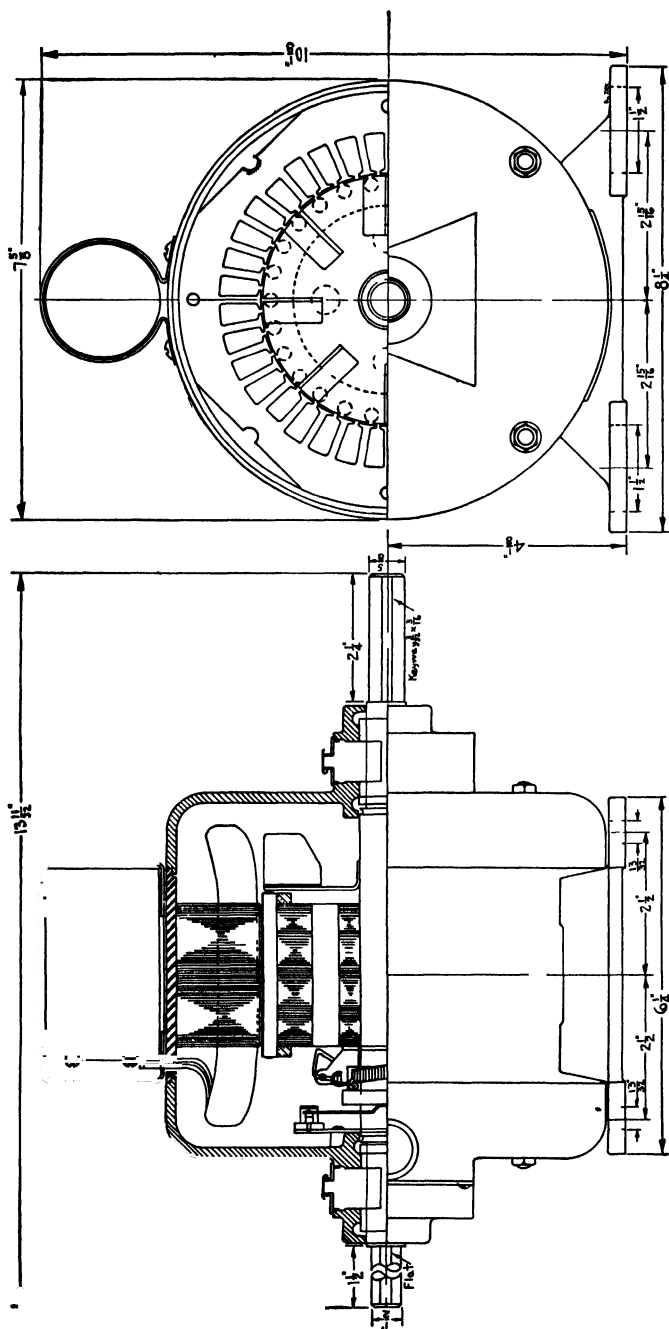
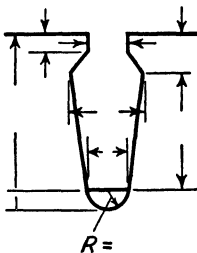
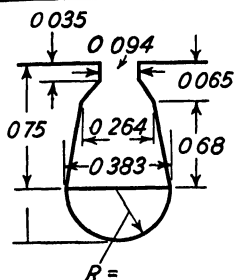


FIG. 220.—Assembly drawing of capacitor-start induction motor, $\frac{1}{2}$ hp., 1725 r.p.m.

SINGLE-PHASE INDUCTION MOTOR DESIGN SHEET

Hp, ½	S r p m, 1800	Cycles, 60	Poles, 4	Volts, 110	Amps 6 4
	Stator	Rotor		Stator	Rotor
Outside diameter	7 25	4 349	Tooth face	0 288	0 485
Inside diameter	4 376	2 56	Tooth width	0 13	0 252
Length	2 56	2 56	Depth below slot	0 4375	0 780
Number of slots	36	28	Slot factor	1 172	1 03
Tooth pitch	0 382	0 525	Total conductor section	1 33	1 07



Slot number	1	2	3	4	5	6	7	8	9	10	11	12	13	14	15	16	17	18	19	20
Stator main	30	28	23	14	46	46	40	30	16	30	30	28	23	14	46	46	40	30	16	30
Stator auxiliary																				

Winding	Main	Auxiliary	Rotor	
Conductor size	18 s c c e	22 s c c e	Bar section	0 0412
area	0 00126	0 000507	length	2 81
Amps per sq in	2540	20 900	material	copper
Half mean turn	6 0	6 20	skew bars	1 0
Conductors in series	528	760	End ring section	0 0938
C_w	0 705	0 856	material	copper
Weight, lb	2 56	0 766	diam outside	4 329
			diam inside	3 329

Gap length	0 0135	Gap coefficient	1 21	Pole pitch	3 44
Total flux	1,172 000	f_d	0 637	Flux per pole	187,000

	Section	Density	Weight	Core Loss
Stator teeth	11 12	10 ⁵ 200	2 32	8 56
Stator yoke	2 08	89 600	5 76	15 50
Rotor teeth	15 60	71,500		24 06
Rotor yoke	3 72	47 800		×2
Air gap	35 20	31,700		48 12

R_{sm} 0 872 ohm at 25° C	R_{sa} 6 43 ohms at 25° C	X_{lm} 3 50 ohms	λ_{la} 8 40 ohms
R_{rm} 1 03 × 1 10 ohms at 25° C	R_{ra} 2 72 ohms at 25° C	Z_m 4 03 ohms	Z_a 10 38 ohms
R_m 2 00 ohms at 25° C	R_a 9 15 ohms at 25° C	K 1 55	λ_c 13 30 ohms

	Full Load						Torque		Locked
	Amps	Watts	Γ ff	P F	App Eff	R p m	Max	Start	Amps
Guar Calc	6 4	512 4	72 6	72 7	52 8	1746	58 4	59 0	29 50
Test	6 6	518 0	72 0	71 8	51 7	1745		55 0	31 40

Test values of starting torque and current approximate only

Designed by J H Kuhlmann

IV—TRANSFORMERS

CHAPTER XXI

CONSTRUCTION

THE transformer is a device for “stepping up” or “down” the voltage or current in an alternating current circuit. The essential parts are: a magnetic circuit, built up of sheet steel; and an electric circuit, consisting of one or more windings. Transformers may be divided into three classes: (1) Instrument transformers, (2) Constant-current transformers, (3) Constant-potential transformers. In the following pages, only the design and construction of constant-potential transformers, such as used to transform power from a high voltage and small current to a lower voltage and large current, or vice versa, will be discussed.

Constant potential transformers are used for light and power service and are generally divided into two groups: (1) distribution transformers, (2) power transformers.

Distribution transformers include sizes 200 Kva and smaller which are used to step down the voltage from the distribution voltage to a standard service voltage, or from the transmission voltage to the distribution voltage. They are built for voltages up to and including 66,000 volts, either single-phase or 3-phase. Standard sizes, voltage ratings, and taps for single-phase and 3-phase distribution transformers for the various system voltages have been adopted by the National Electric Manufacturers Association.¹

Power transformers include those sizes larger than 200 Kva which are used to step up the voltage to the transmission voltage at the generating station, or to step down the voltage at the substation. They also include those transformers in sizes larger than 200 Kva which are used to step down the voltage from either a transmission or a distribution voltage to a standard service voltage. They may be either single-phase or 3-phase and have been built for 220,000 volts star. The

¹ “Handbook of Transformer Standards,” 5th ed., National Electric Manufacturers’ Association, 420 Lexington Avenue, New York.

National Electric Manufacturers Association has adopted standard sizes, voltage ratings, and taps.

Core.—The magnetic circuit of all transformers is built up of silicon sheet-steel laminations. For 60-cycle transformers, a 4 to 4.5 per cent silicon sheet steel 0.014 in. thick is used; for low frequencies, 25 cycles, a 2.5 to 3.0 per cent silicon steel sheet up to 0.019 in. thick is often used. (Silicon steel is used because of its non-aging properties and low losses.

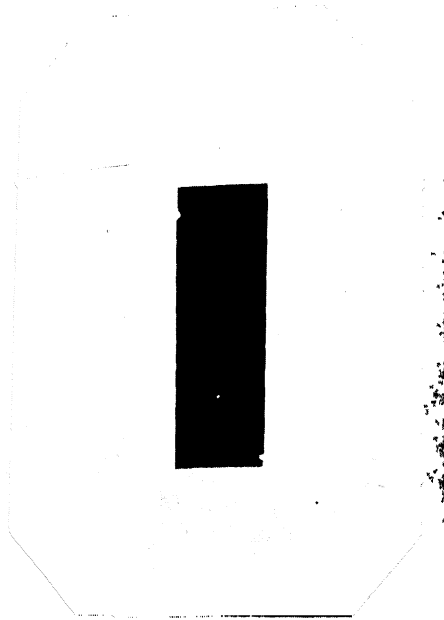


FIG. 221.—Core for small capacity rectangular core type distribution transformer.

For more complete information on the properties of electric sheet steels, the reader is referred to the splendid book by Thomas Spooner, "Properties and Testing of Magnetic Materials."² After the laminations are cut or punched to the proper size, they are carefully annealed to remove all punching or shearing strains, which increase the losses. When the laminations have been annealed, a thin coating of insulating varnish is applied in the same manner as described for armature laminations of direct current machines, page 3. For small distribution

² "Properties and Testing of Magnetic Materials," McGraw-Hill Book Co., New York, N. Y.



FIG 222.—Partially assembled core and coils of a rectangular core type distribution transformer.

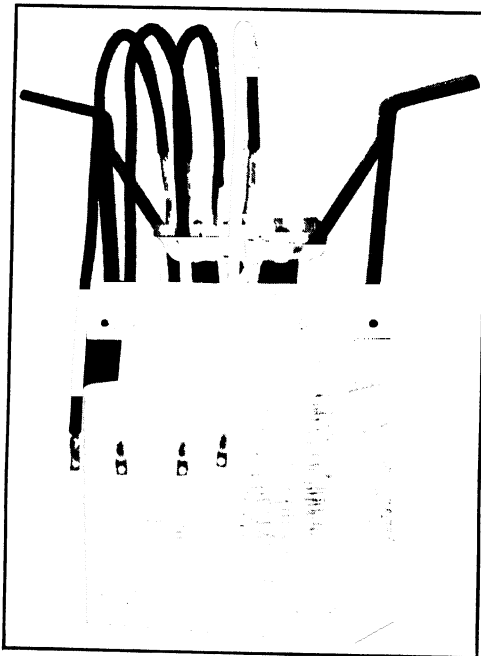


FIG. 223.—Rectangular core type transformer removed from tank.

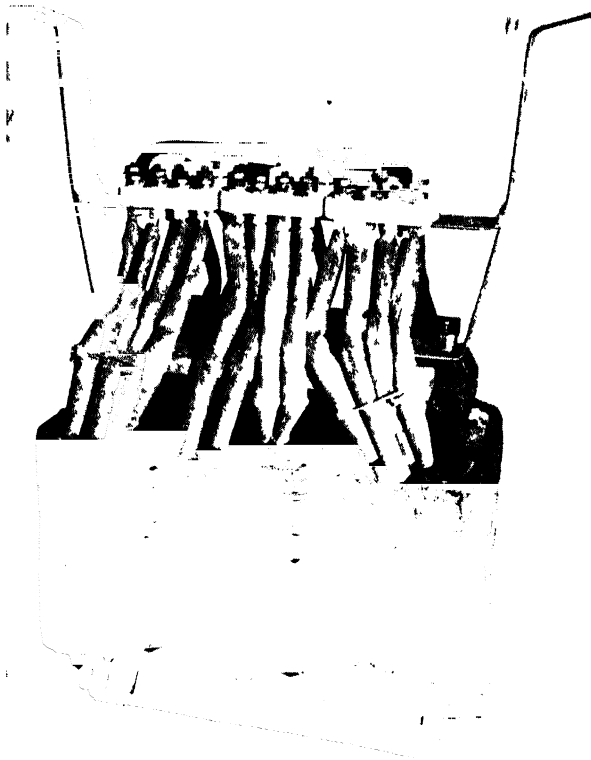


FIG 224 — Three-phase core type distribution transformer removed from tank.

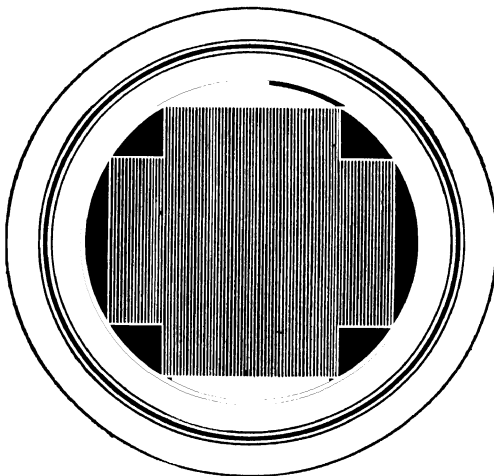


FIG. 225 —Section of cruciform shaped core with circular coils.

transformers, the insulating coating is generally not necessary, as the heavy scale always present on silicon steel offers sufficient insulation.

There are three types of construction in common use: core type, shell type, and distributed core type.

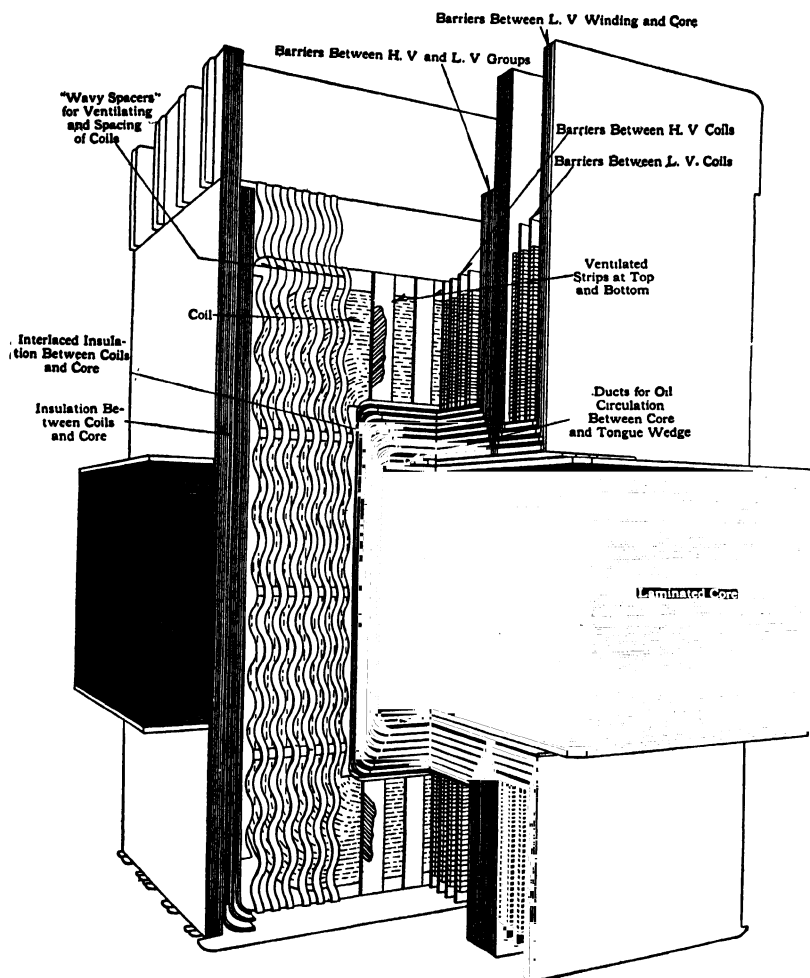


FIG. 226.—Sectional drawing of shell-type transformer.

Core Type.—Figure 221 shows the core for a small core-type distribution transformer. The laminations are L-shaped and are assembled through the coils which are wound on a form, as shown in Fig. 222. Figure 223 shows a completely assembled, 15-kva., 6900-volt, rect-

angular core type distribution transformer removed from tank. A completely assembled, 3-phase rectangular core type distribution transformer is shown in Fig. 224. For high voltages, 22,000 volts and higher, the cruciform-shaped core section with circular coils shown in Fig. 225, is used.

Shell Type.—The shell type of construction is generally best suited for transformers for relatively low voltage or for relatively large capacity, which have a good space factor in the winding. A sectional assembly drawing³ of a shell type transformer is shown in Fig. 226. The windings are built up of "pancake" type coils, as shown in Fig. 226. A completely assembled shell type transformer is shown in Fig. 227.

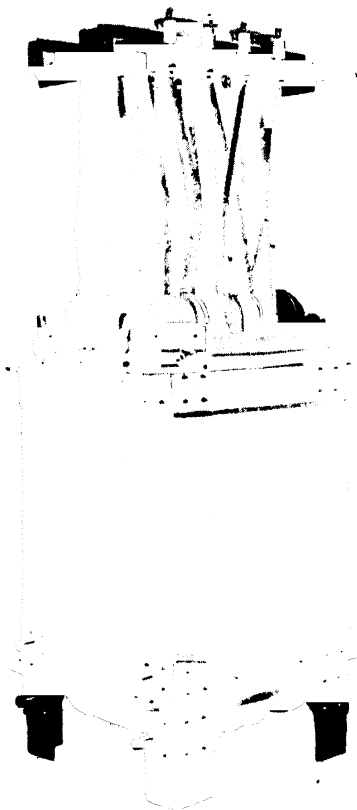


Fig. 227.—Complete shell type transformer removed from tank.

Distributed Core Type.—The distributed core type construction is built with 2-part, 3-part, and 4-part distributed core. The 3-part distributed core type is used for small-capacity distribution transformers for moderate voltages. The 4-part distributed core type is used for distribution transformers and small power transformers. For small capacity and moderate voltage 3-part and 4-part distributed core type transformers, the core is assembled as shown in Fig. 228, and the windings are wound directly on the core. For the larger capacities and higher voltages, the coils are form-wound and assembled on the core, as shown in Fig. 229.

Tank.—Transformers are cooled by either one of the following methods:

(1) *Natural-air-cooled*, for which the natural circulation of the surrounding air is relied upon to carry away the heat generated by the

³ "The Modern Manufacture of Large Power Transformers," by L. H. Hill, *Electric Journal*, Vol. 24, April, 1927, pp. 146 to 151.

losses. This method of cooling is utilized for instrument transformers, constant-current transformers, and auto-transformers that supply reduced voltage for starting alternating-current motors. Since the devel-

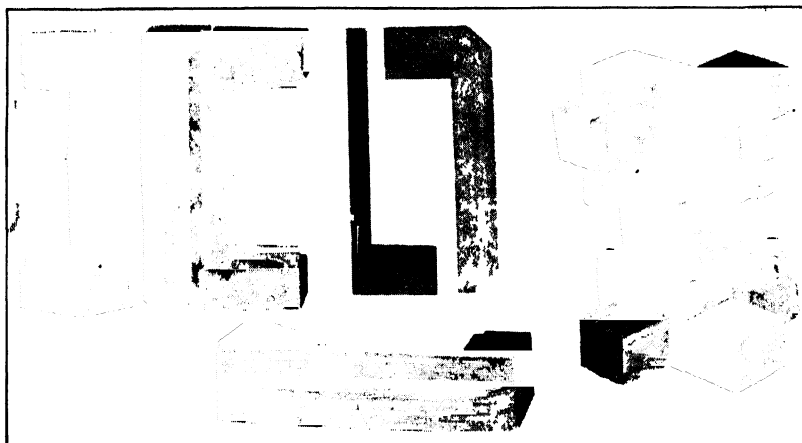


FIG. 228.—Shape of punching and method of assembling core of small four-part distributed-core-type transformer.

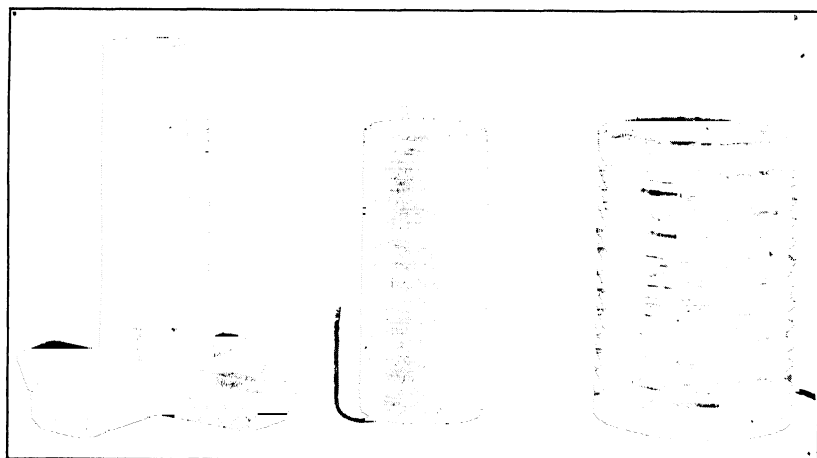


FIG. 229.—Method of assembling core and coils of large-capacity four-part distributed-core-type transformer.

opment of fiber glass insulation and silicone resin insulating varnishes, the dry type of construction is employed for distribution and small power transformers. A sheet-metal enclosure protects the winding from mechanical injury.

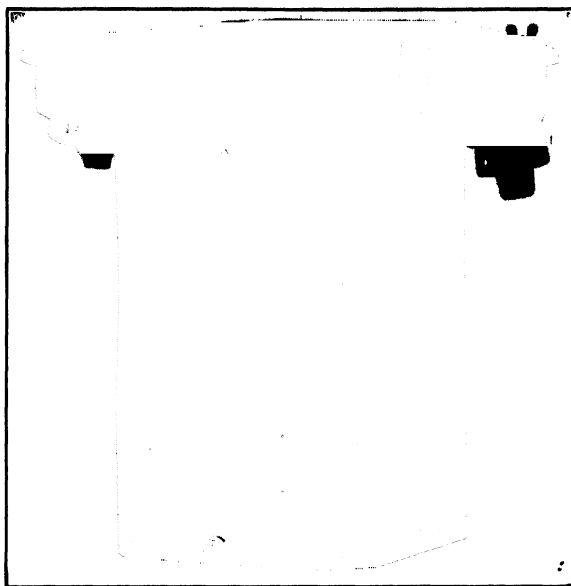


FIG. 230.—Welded sheet steel tank for transformer shown in Fig. 223.

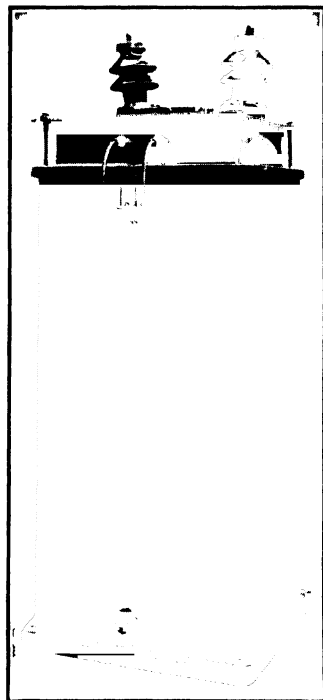




FIG. 232.—Top view of transformer and tank with cover removed.

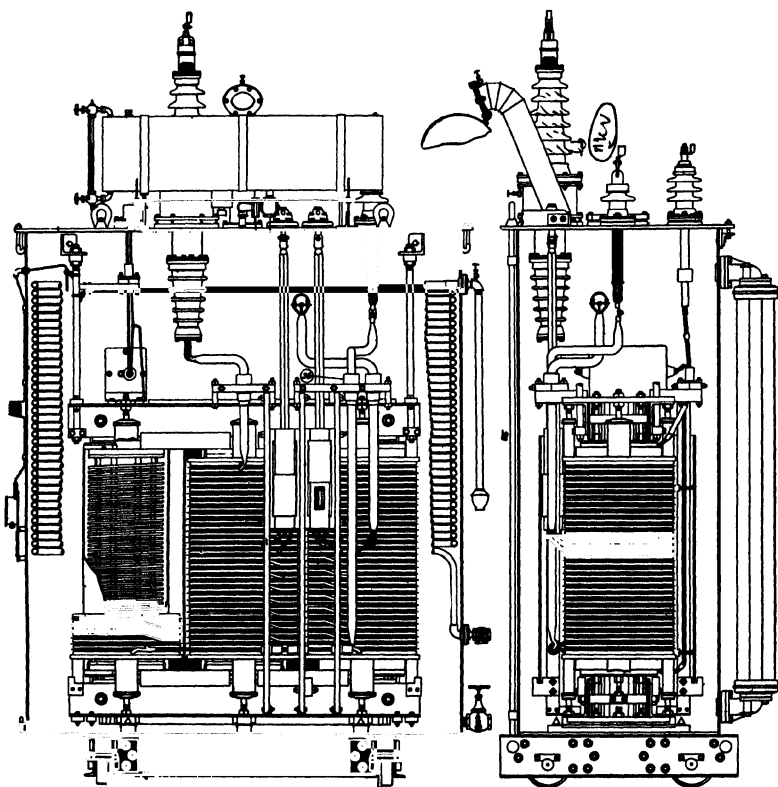


FIG. 233.—Sectional assembly drawing of three-phase transformer oil and water cooled.

(2) *Natural-oil-cooled*, which method is used for all distribution and for power transformers. The transformer is immersed in a transformer oil which carries the heat to the walls of the containing tank.

(3) *Oil and Water Cooled*.—For this method the transformer is immersed in a transformer oil and cooling water is circulated through coils of pipe placed near the top of the tank under the surface of the oil.

(4) *Cooled by Forced Circulation of the Oil*.—For this method the oil is drawn from the tank, passed through cooling coils on the outside of the tank, and returned to the bottom of the tank.

(5) *Cooled by air blast*, for which a continuous stream of cool air is forced through the core and windings.

For small distribution transformers, a plain cast-iron tank has often been used. The welded-sheet-steel tank is, however, used almost exclusively for modern transformers. Figure 230 shows a welded-sheet-steel transformer tank which is for the 15-kva., 6900-volt, core-type transformer shown in Fig. 223. For the larger-capacity distribution transformers, it is difficult to obtain sufficient radiating surface with plain sheet steel tanks to dissipate the heat without excessive temperature rise. To increase the radiating surface, cooling vanes are welded to the tank or corrugated sheet steel tanks are adopted as shown in Fig. 231. Figure 232 is a top view of a tank with cover removed and shows how the transformer is secured in the tank and how the leads are brought out of the tank.

For oil- and water-cooled transformers, plain sheet steel tanks are generally used. A sectional drawing of a 3-phase, oil- and water-cooled transformer is shown in Fig. 233. It shows the position of the transformer and cooling coils in the tank.

Distribution transformers are now being built in the smaller sizes with a wound core of continuous strip steel. The sheet steel used for this purpose is a new development and has particularly good magnetic properties when the flux flows with the grain. This type of construction is explained by Mr. E. D. Treanor⁴ in *Electrical Engineering*.

⁴ "The Wound-Core Distribution Transformer," by E. D. Treanor, *Elec. Eng.*, Vol. 57, Nov., 1938, p. 622.

CHAPTER XXII

CORE AND WINDINGS

TRANSFORMERS may be designed for minimum cost without regard to the losses, or for minimum total losses.

There is a lower limit to the cost for which a given transformer can be designed, because the copper density cannot be worked above a certain value because of heating; also, the core density is fixed by saturation of the magnetic circuit. The lowest-cost transformer will generally be the one for which the cost of iron and cost of copper are approximately equal.

With the densities fixed in core and copper, the minimum total loss transformer is the one for which the core loss is approximately equal to the copper loss at full-load. Such a transformer will have maximum efficiency at full-load.

Transformers intended for lighting load—distribution transformers—should have the core loss as small as possible, because they operate at light-load the greater part of the day and at full-load only a few hours. For such transformers the ratio of the core loss to the copper loss

$$\frac{W_c}{W_k} = 0.30 \text{ to } 0.70.$$

Large power transformers are generally designed with the core loss approximately equal to the copper loss at full-load.

The loss per pound for the core can be found from the loss curves in the Appendix for various grades of sheet steel. The copper loss plus stray-load loss for 75° C. is calculated by formula 139a.

$$W_k = A^2 G_k k_5 \times 2.58 \times 10^{-6} \text{ watt.}$$

The loss per pound

$$w_k = \frac{W_k}{G_k} = A^2 k_5 \times 2.58 \times 10^{-6} \text{ watt.}$$

When the flux density in the core and the current density in the copper have been determined, the loss per pound in core and copper can readily be calculated.

The magnetizing current of a transformer lags the voltage by 90° . It is the current drawn from the line to maintain the flux in the magnetic circuit. In order that this current shall be as small as possible, the flux density in the core must be below the saturation point of the grade of sheet steel used. Silicon steel has a high permeability at low values of induction, but at high values of induction the permeability decreases rapidly (see standard saturation curve in Appendix). For distribution transformers, the flux density in the core is generally

$$B = 55,000 \text{ to } 75,000 \text{ lines per sq. in.}$$

Distributed-core-type transformers are usually designed with densities of 75,000 to 90,000 lines per sq. in. in the center leg and 40,000 to 55,000 lines per sq. in. in the remainder of the magnetic circuit. In this way the length of the mean-turn of the windings can be reduced without sacrifice in core loss, because the central core is only a small part of the entire magnetic circuit. When neither core loss nor magnetizing current but only first cost is important, slightly higher values for B can be used. For large power transformers, the flux densities in the core should generally not exceed 90,000 lines per sq. in.

The current density in the copper is limited by the efficiency and the allowable temperature rise. For distribution and small power transformers, self-oil-cooled,

$$A = 700 \text{ to } 1500 \text{ amperes per sq. in.}$$

The low values apply to the small capacities up to about 50 kva. For large power transformers, self-oil-cooled,

$$A = 1400 \text{ to } 1900 \text{ amperes per sq. in.}$$

The ratio of core loss to copper loss

$$\frac{W_c}{W_k} = \frac{w_c \times G_c}{w_k \times G_k} \quad (210)$$

When the densities in the core and copper are fixed, the loss per pound for core and copper can readily be determined. The ratio of weights for a given ratio of losses can easily be calculated by equation 210. The ratio of core weight to copper weight generally lies between the limits 1.5 and 3.0 for distribution transformers. For small-capacity, single-phase, core-type transformers, the ratio of weights is often less than 1.50. For high-voltage power transformers, it may be twice the values given above.

Design of Core.—The section area of the core is readily determined when the total flux is known. The curve in Fig. 234 gives average values of ϕ_t for distributed-core-type transformers. The reader must not conclude that distributed-core-type transformers are to be designed with values of total flux as given by this curve. These data are given merely to guide the beginner. Satisfactory designs can be obtained with values of ϕ_t either larger or smaller than those given by the curve. For the core type of construction, the best design is generally obtained with a smaller total flux than that used for the distributed-core-type transformer. For single-phase, core-type transformers, multiply the

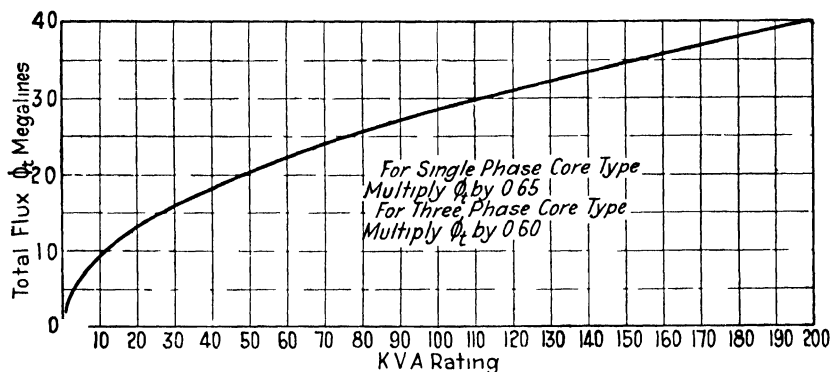


FIG. 234—Total flux for four-part distributed core type transformer.

values of ϕ_t in Fig. 234 by 0.65 and for 3-phase core type by 0.60. The section area of the core

$$A_c = \frac{\phi_t}{B}.$$

Dr. Arnold ¹ has developed the following output equation by which the section area of the core can be calculated when the output constant is known. For a single-phase transformer, the output

$$Kva = EI \cdot 10^{-3}.$$

The induced voltage

$$E = 4.44 f t B A_c \cdot 10^{-8} \text{ volt}$$

and

$$I = A_s c.$$

¹ "Die Wechselstromtechnik," by E. Arnold, Vol. II, 2nd ed., p. 310, Julius Springer, Berlin; see also "The Essentials of Transformer Practice," by Emerson G. Reed, 2nd ed., p. 62, D. Van Nostrand Co., New York.

Therefore,

$$Kva = 4.44fBA_cA_s 10^{-11}. \quad (211)$$

The weight of the core

$$G_c = A_c l_c a_c \text{ lb.}$$

and the weight of the copper

$$G_k = \frac{2ts_c l_k g_k}{\text{cond. section}} \text{ lb.,}$$

if the weights of the high voltage and that of the low voltage winding are assumed to be equal.

The ratio of the core weight to the copper weight

$$\frac{G_c}{G_k} = \frac{A_c l_c g_c}{2ts_c l_k g_k}.$$

If the ratio of the mean length of the magnetic circuit to the mean-turn of the winding is assumed to be constant, which is approximately true for a given type of transformer, then

$$\frac{G_c}{G_k} = C_1 \frac{A_c}{ts_c}$$

and

$$ts_c = \frac{G_k}{G_c} A_c C_1.$$

Substituting this expression into equation 211, the core section

$$A_c = C \sqrt{\frac{Kva \frac{G_c}{G_k} 10^{11}}{BAf}}. \quad (212)$$

The output constants for the various types of construction are given below:

Type of Transformer	C
Distributed core type.....	0.55 to 0.65
Single-phase core type.....	0.40 to 0.55
Three-phase core type.....	0.30 to 0.50
Single-phase shell type.....	0.80 to 1.0

The shape of the core section is rectangular, square, or cruciform. For core-type distribution and small power transformers for moderate

and low voltages, the rectangular-shaped core section shown in Fig. 235 is generally used. The dimensions of the section can be calculated as follows: The long side of the core section is generally from 1.4 to 2.0 times the short side. The notches on the corners of the section shown in Fig. 235 are often omitted on transformers below 25-kva. capacity. For small core sections

$$A_c = abk_1$$

$$b = (1.4 \text{ to } 2.0)a.$$

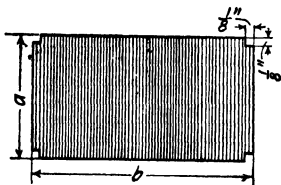


FIG. 235.

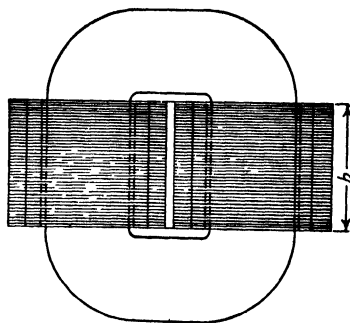
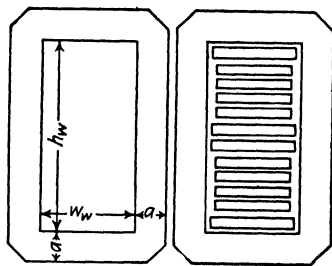


FIG. 236.

Therefore

$$a = \sqrt{\frac{A_c}{(1.4 \text{ to } 2.0)k_1}}. \quad (213)$$

When the corners are notched, as shown in Fig. 235,

$$a = \sqrt{\frac{A_c + 0.064k_1}{(1.4 \text{ to } 2.0)k_1}}. \quad (214)$$

For shell-type transformers (see Fig. 236) the ratio $b/2a$ generally lies between the limits 2 and 3. When there are no ventilating ducts in the core

$$b = \frac{A_c}{2ak_1}$$

$$2a = \sqrt{\frac{A_c}{(2 \text{ to } 3)k_1}}. \quad (215)$$

When circular coils are required for high-voltage distribution and large power transformers, the cruciform-shaped core shown in Fig. 237 is used. The dimensions of the section to give the maximum area of

core for a given diameter are calculated as follows: The gross core area for the section shown in Fig. 237 equals

$$\frac{A_r}{k_1} = 2a2b + (2b - 2a) 2a = 4(2ab - a^2)$$

Then

$$a = \frac{D}{2} \sin \alpha; \quad b = \frac{D}{2} \cos \alpha.$$

$$\frac{A_r}{k_1} = 4 \left(2 \frac{D}{2} \sin \alpha \frac{D}{2} \cos \alpha - \frac{D^2}{4} \sin^2 \alpha \right) = D^2 (2 \sin \alpha \cos \alpha - \sin^2 \alpha).$$

The value of the angle α that will give the maximum core section can be found by differentiating the above equation with respect to α and equating the resultant expression to zero

$$\frac{d \frac{A_r}{k_1}}{d\alpha} = D^2 (2 \cos 2\alpha - 2 \sin \alpha \cos \alpha) = 0$$

$$\tan 2\alpha = 2; \quad \alpha = 31.75^\circ.$$

Therefore

$$a = 0.263D; \quad b = 0.425D.$$

The gross section area of the core is then

$$\frac{A_r}{k_1} = 2a2b + (2b - 2a)2a = 0.618D^2.$$

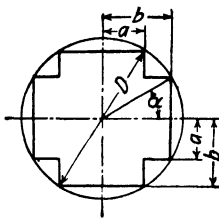


FIG. 237.

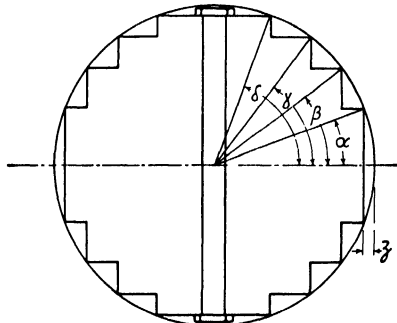


FIG. 238.—Four-step circular core section.

The ratio of the net area of the core to the area of the circumscribed circle is called the core space factor, f_{cs} . The lamination factor, k_1 , can be taken equal to 0.90 for 0.014-in. silicon sheet steel. Then

$$f_{cs} = \frac{0.618D^2 \times 0.90}{(\pi/4)D^2} = 0.70. \quad (216)$$

For large core areas, a section, such as that shown in Fig. 238, with three or more steps is often used. Such cores are expensive to build but

show a saving in copper and copper losses because of the smaller diameter for a given core area. Circular coils are preferred for large power transformers because of their superior mechanical characteristics.²

A transformer coil, under the magnetic stresses produced by excessive leakage flux due to short-circuit, tends to assume a circular form. On circular coils, these forces are radial and there is no tendency for the coil to change its shape; on rectangular coils the forces are perpendicular to the conductor and tend to give the coil a circular form

The values of the various angles for 2-, 3-, 4-, and 5-step cores, to give the maximum area for a given diameter, have been calculated by W. B. Garrett³ and are given in the following table.

The dimension z , Fig. 238, must be large enough to allow for end plates, nuts, etc. The space so required generally varies from 15 per cent of the core diameter in large cores to 25 per cent in small cores, which corresponds to an angle for the most remote step of from 57° to 48° , respectively. Table XXVIII gives the various angles for 2-, 3-, 4-, and 5-step cores in terms of the angle for the most remote step, which is called the fixed angle.

TABLE XXVIII

Angle	2-Step	3-Step	3-Step (1 Duct) *	4-Step	4-Step (1 Duct) *	5-Step (1 Duct) *	5-Step (3 Ducts) †
ϵ	Fixed	Fixed
δ	Fixed	Fixed	0 833 ϵ	0.850 ϵ
γ	Fixed	Fixed	0.785 δ	0.785 δ	0.667 ϵ	0.702 ϵ
β	Fixed	0 712 γ	0 714 γ	0.563 δ	0.570 δ	0.491 ϵ	0 511 ϵ
α	0 553 β	0 400 γ	0 414 γ	0 321 δ	0 337 δ	0 291 ϵ	0 299 ϵ

* Width of duct = 0 030 D .

† Width of duct = 0 015 D .

With the section area of the core determined and the flux density, B , fixed, the total flux

$$\phi_t = BA_c. \quad (217)$$

The number of turns for the high-voltage winding

$$t_h = \frac{E_h \times 10^8}{4.44 f \phi_t}$$

² "Circular-Coil High-Voltage Power Transformers," by Clinton Jones, General Electric Review, Vol. 24, May, 1921, pp. 399-404; "Fundamental Principles of Present-Day Transformer Design," by W. M. McConahey and J. F. Peters, Electrical World, Vol. 69, Jan. 20, 1917, pp. 129-132.

³ "An Investigation into the Sectional Proportions of the Cores of Circular Core Type Transformers," by W. B. Garrett, World Power, Vol. 6, Dec. 1926, pp. 292-298.

and for the low-voltage winding

$$t_l = \frac{E_l}{E_h} t_h.$$

The voltage per turn

$$= \frac{E_h}{t_h}.$$

The current in the high-voltage winding

$$I_h = \frac{Kva \ 10^3}{l_h'} \text{ amperes}$$

and in the low-voltage winding

$$I_l = \frac{t_h}{t_l} I_h \text{ amperes.}$$

The section area of the conductor for the high-voltage winding

$$s_{ch} = \frac{I_h}{A} \text{ sq. in.}$$

and for the low-voltage winding

$$s_{cl} = \frac{I_l}{A} \text{ sq. in.}$$

To obtain the desired ratio of core loss to copper loss, it is necessary to determine the core dimensions that will give the previously fixed ratio of core weight to copper weight. The ratio of the height of the window opening to the width will generally lie between the following limits:

$$h_w/w_w = 2.0 \text{ to } 4.0.$$

The copper space factor, that is, the ratio of the net copper area in the window to the area of the window, varies with the capacity of the transformer and with the voltage of the windings. The curves in Fig. 239 give average values for f_s for the various types of transformers.

For single-phase transformers, the area of the window

$$h_w w_w = \frac{s_{ch} t_h + s_{cl} t_l}{f_s} = \frac{2(s_{ch} t_h)}{f_s} \text{ sq. in.}$$

and for 3-phase core type transformers

$$h_w w_w = \frac{2(s_{cht_h} + s_{cilt_l})}{f_s} = \frac{4(s_{cht_h})}{f_s} \text{ sq. in.}$$

From the expression for the ratio of the dimensions

$$w_w = \frac{h_w}{2.0 \text{ to } 4.0} \text{ in.}$$

Therefore

$$h_w = \sqrt{\frac{(2.0 \text{ to } 4.0) 2 s_{cht_h}}{f_s}} \text{ in. for single-phase,} \quad (218)$$

and

$$h_w = \sqrt{\frac{(2.0 \text{ to } 4.0) 4 s_{cht_h}}{f_s}} \text{ in. for 3-phase.} \quad (219)$$

Before proceeding with the design of the windings, it will be desirable to check the approximate core and copper weight, to determine whether the desired ratio of weight can be obtained with the core dimensions selected. (See sample designs, Chapter XXIV.)

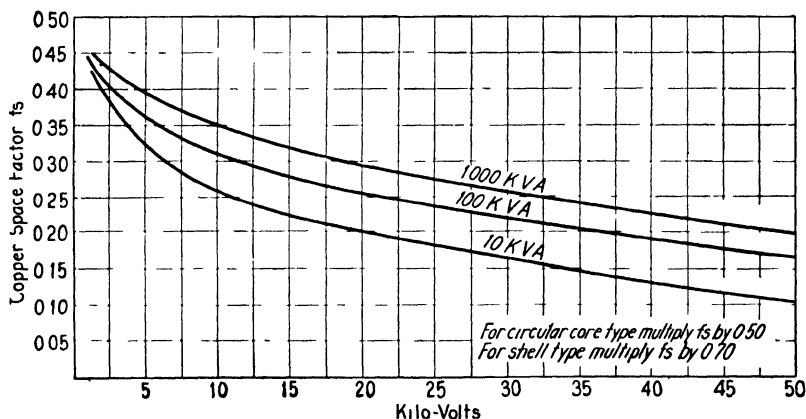


FIG. 239.— Approximate copper space factors.

Design of Windings.—The windings of transformers must be designed to give the best possible electrical characteristics with the proper mechanical strength to withstand the stresses due to short-circuits and with proper ventilation to avoid excessive temperature rise and “hot spots.” The approximate electrical characteristics of single-phase distribution transformers for 2300, 4600, and 6900 volts are given in Tables XXIX and XXX. Similar data are given in Table XXXI for 3-phase, 4600-volt, star-connected, distribution transformers.

TABLE XXIX

ELECTRICAL CHARACTERISTICS OF SELF-OIL-COOLED DISTRIBUTION TRANSFORMERS
SINGLE-PHASE, 60 CYCLES, 2300 AND 4600 TO 115 AND 230 VOLTS

Kva	Losses		Efficiency, Full-Load	Regulation		Per Cent		
	Core	Copper		100% PF	80% PF	IR	IX	IZ
1.5	25	54	95.0	3.61	3.57	3.60	1.15	3.78
3.0	32	85	96.2	2.88	3.25	2.83	1.65	3.27
5.0	46	128	96.6	2.58	3.16	2.56	1.85	3.16
7.5	58	176	96.9	2.39	3.00	2.34	1.89	3.02
10.0	73	226	97.1	2.28	2.77	2.26	1.60	2.77
15.0	96	320	97.3	2.10	3.21	2.13	2.51	3.30
25.0	133	490	97.5	1.98	3.20	1.96	2.72	3.35
37.5	172	570	97.6	1.98	3.25	1.95	2.82	3.43
50.0	210	780	98.0	1.68	3.15	1.56	3.16	3.53
75.0	330	1200	98.0	1.65	3.15	1.60	3.11	3.50
100.0	450	1460	98.1	1.50	3.20	1.46	3.38	3.68
150.0	695	1900	98.3	1.32	3.30	1.27	3.80	4.00
200.0	920	2400	98.3	1.27	3.37	1.20	4.02	4.20

TABLE XXX

ELECTRICAL CHARACTERISTICS OF SELF-OIL-COOLED DISTRIBUTION TRANSFORMERS
SINGLE-PHASE, 60 CYCLES, 6900 TO 115 AND 230 VOLTS

Kva	Losses		Efficiency, Full-Load	Regulation		Per Cent		
	Core	Copper		100% PF	80% PF	IR	IX	IZ
1.5	28	42	95.5	3.00	5.00	2.80	4.60	5.40
3.0	38	85	96.0	3.00	5.00	2.83	4.57	5.37
5.0	49	140	96.3	2.95	5.00	2.80	4.60	5.40
7.5	71	175	96.8	2.45	4.90	2.34	5.05	5.56
10.0	81	220	97.0	2.35	4.85	2.20	5.15	5.60
15.0	106	320	97.2	2.30	4.70	2.13	5.00	5.44
25.0	158	464	97.5	2.05	5.10	1.86	7.02	7.25
37.5	208	595	97.9	1.80	5.00	1.59	6.21	6.41
50.0	280	785	97.9	1.75	4.90	1.57	6.06	6.25
75.0	394	1030	98.1	1.55	4.70	1.38	6.00	6.15
100.0	600	1230	98.2	1.40	4.30	1.23	5.54	5.68
150.0	900	2010	98.1	1.50	4.35	1.34	5.47	5.64
200.0	1100	2650	98.1	1.50	4.40	1.33	5.57	5.72

TABLE XXXI

ELECTRICAL CHARACTERISTICS OF SELF-OIL-COOLED DISTRIBUTION TRANSFORMERS
THREE-PHASE, 60 CYCLES, 4600 TO 230 AND 460 VOLTS

Kva	Losses		Efficiency, Full-Load	Regulation		Per Cent		
	Core	Copper		100% PF	80% PF	IR	IX	IZ
5 0	74	148	95 8	3 00	4 01	2 96	2 73	4 03
7 5	84	203	96 5	2 75	3 85	2 71	2 80	3 89
10 0	96	250	96 6	2 56	3 70	2 50	2 84	3 78
15 0	122	340	97 0	2 30	3 70	2 26	3 15	3 88
25 0	176	510	97 3	2 09	3 65	2 04	3 37	3 94
37 5	227	750	97 4	2 06	3 78	2 00	3 64	4 15
50 0	277	940	97 6	1 95	3 87	1 88	3 95	4 37
75 0	352	1310	97 8	1 81	3 75	1 75	3 92	4 30
100 0	476	1530	98 0	1 60	3 60	1 53	3 97	4 26
150 0	620	2140	98 1	1 51	3 60	1 43	4 10	4 34
200 0	892	2720	98 2	1 48	3 65	1 36	4 27	4 49

The A.S.A. Standards⁴ specify that the temperature rise of transformer windings shall not exceed 55° C. for class A insulation. The temperature is to be determined by the resistance method and checked by thermometer. The types of materials included in class A and class B insulations are given on page 128.

In winding and assembling the coils of a transformer, either of two polarities, subtractive or additive, may be produced. Figure 240 shows an elementary diagram of a loaded transformer.⁵ The direction of the voltage induced in the primary winding at a particular instant is shown by E_p . The flow of current in the primary winding is from the terminal at which the impressed primary voltage is positive to the terminal at which it is negative and is opposed by the induced primary voltage E_p . The load component of the primary current sets up a magnetomotive force which tends to produce a flux in the core in the direction indicated by m.m.f._p. Since the direction of current flow in the secondary must produce a magnetomotive force to oppose m.m.f._p, it must flow in the direction shown in the diagram, producing a flux tendency in the direction indicated by m.m.f._s. The flow of current

⁴ A.S.A. Standards No. C57, Transformers, Induction Regulators and Reactors.

⁵ "Notes on Transformer Polarity and Connections," Part I, by John Anchincloss, General Electric Review, Vol. 29, Nov., 1926, p. 783.

through the load connected across the secondary terminals is, therefore, from left to right, that is, the left-hand terminal of the secondary winding is positive and the right-hand one is negative. The secondary voltage, E_s , has the direction shown in Fig. 240. It will be observed that E_p and E_s have the same direction. Adjacent primary and secondary terminals, therefore, have the same polarity, the left-hand primary and secondary terminals at the instant chosen being positive, and the right terminals negative.

The polarity of the transformer just described is called subtractive. If two adjacent primary and secondary terminals are connected, as shown in Fig. 240b, and voltage applied, say, to the primary winding, the voltage measured by a voltmeter connected across the other adjacent terminals will be the difference between the primary and secondary voltages; hence, the term subtractive polarity.

If the secondary winding in Fig. 240a were wound on the core in the

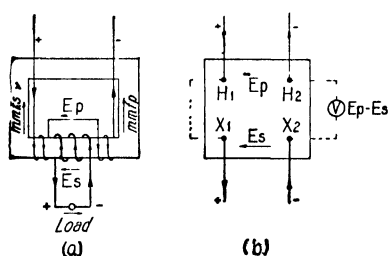


FIG. 240.

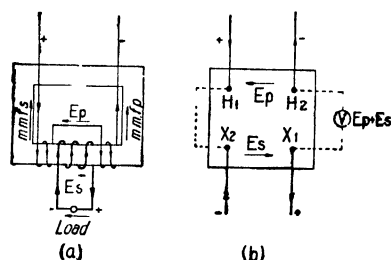


FIG. 241:

opposite direction, as shown in Fig. 241a, the secondary current would have to flow in a direction opposite to that shown in Fig. 240a. Therefore, at the instant when the left-hand primary terminal is positive, the left-hand secondary terminal is negative, and the current flow in the external circuits is in the opposite direction, as are also the voltages E_p and E_s in the internal circuits of the transformer. The polarity for the transformer shown in Fig. 241 is called additive for the reason that, if two adjacent primary and secondary terminals are connected, and voltage is applied to either the high- or low-voltage winding, the voltage measured by a voltmeter connected across the other adjacent terminals will be the sum of the primary and secondary voltages.

The windings of transformers may be arranged concentrically with reference to one another, or they may be arranged in groups of high-voltage and low-voltage coils stacked alternately one upon the other. The former is known as the concentric type of winding and the latter as the interleaved type.

For the concentric type of winding, the low-voltage coils are wound in cylindrical form or in rectangular tubular form and generally have only one layer. Two-layer, low-voltage coils are, however, not uncommon, and more layers may be used if proper ventilating ducts are provided. The high-voltage coils for moderate voltages, 6900 volts and below, are generally wound with several layers and are placed on the outside of the low-voltage coil. To avoid hot spots in the coils, the depth of winding must be kept small. This is done by winding the coils in sections, and separating them by ventilating ducts. Figure 242 shows the coil group for a rectangular-core-type transformer with a

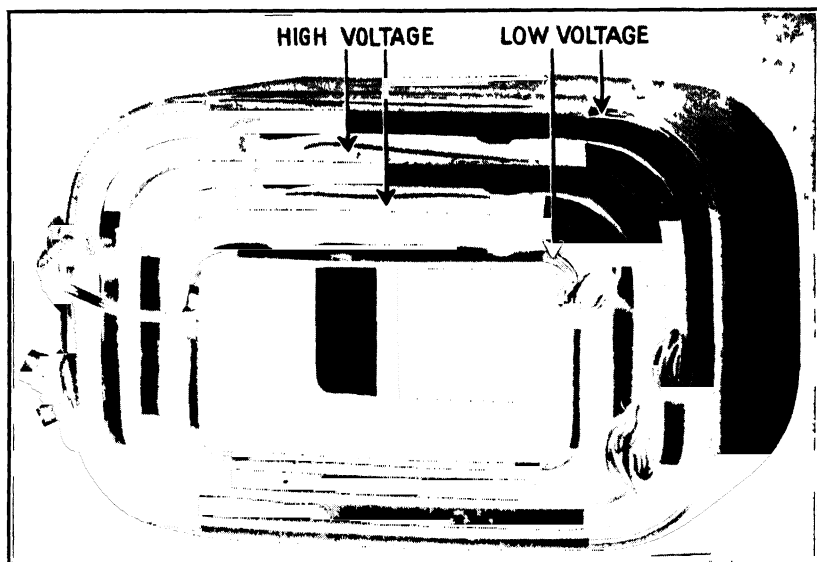


FIG. 242.—Concentric wound coil with two-section low-voltage and high-voltage coils.

two-section, high-voltage winding placed between the two coils of the low-voltage winding. For high-voltage, concentric-coil-type windings, the coils are generally wound and arranged as shown in Fig. 243.

The interleaved type of winding is shown in Fig. 244. It consists of thin circular or rectangular coils arranged in high-voltage and low-voltage groups and stacked alternately one upon the other.

The conductors are either round, square, or rectangular in section and are double-cotton-covered or insulated with a treated paper held in place by bands of cotton thread. To avoid large eddy-current losses, large conductor sections must be built up of several small conductors in parallel. When the parallel conductors are wound on top

of one another in a radial direction, the inside conductor will have a higher reactance than the outside one. Consequently, the current is not equally distributed among the group of parallel conductors. Uniform distribution of the current can be obtained by transposing the conductors, as shown in Fig. 245.

The insulating materials used for transformer windings must have high dielectric and good mechanical strength and must not be soluble in hot transformer oil. The materials generally employed are: cotton

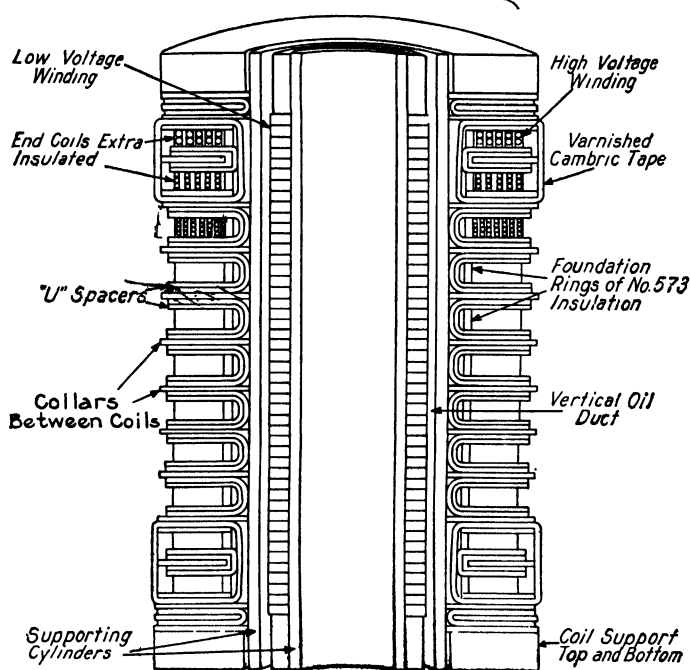


FIG. 243.—Section of concentric type winding with disc-type high-voltage coils.

tape, empire cloth, paper in various forms, insulating varnish, and insulating oils.

Double-cotton-covered conductors, or their equivalent, can generally be used when the voltage per turn does not exceed 25 volts. For layer-wound coils, the maximum voltage between the turns of two layers should not exceed approximately 300 volts. Figure 246 shows four layers of a coil with six turns per layer. It is apparent that the maximum voltage per layer at *b* and *c* is equal to two times the voltage per turn, times the number of turns per layer. Coils with high layer voltage require heavy insulation between layers, which leads to a low

space factor and low heat conductivity. Paper and empire cloth are generally used for the layer insulation. The thickness depends upon the size of the conductor and the voltage stress between layers. For large conductors, the tension required to wind the coils is greater than for small ones; therefore the layer insulation must have greater mechani-

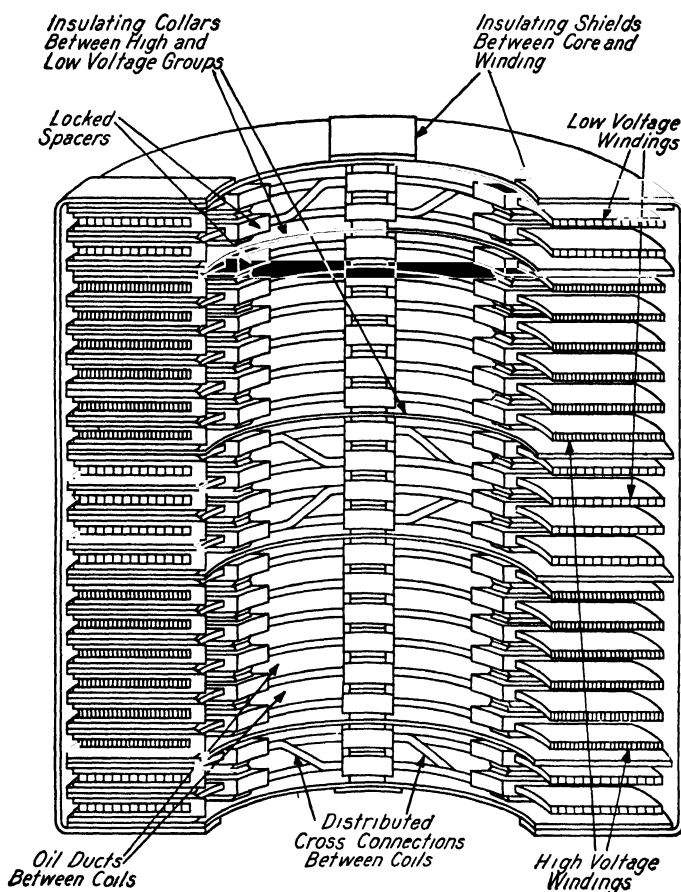


FIG. 244.—Section of interleaved type of winding with disc-type high-voltage and low-voltage coils.

cal strength. For conductors of 0.040-sq. in. area and smaller the thickness⁶ of the insulation between layers may be taken equal to 0.003 in. for each 20 to 30 volts.

⁶ Much useful information on the insulation of transformer windings is given by A. P. M. Fleming and R. Johnson in "Insulation and Design of Electrical Windings," pp. 155 to 176, Longmans, Green & Co., London.

For section-wound coils with only one turn per layer, such as the coils used for the interleaved type of winding arrangement, the voltage per turn may be 70 to 80 volts, because additional insulation can readily be wound between turns.

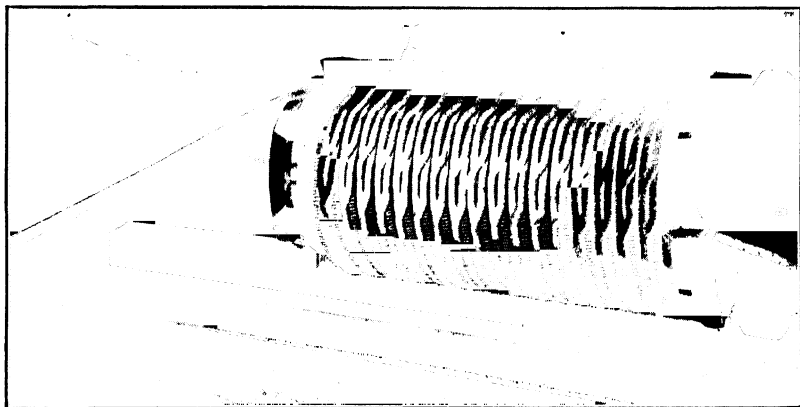


FIG. 245.—Partially wound low-voltage coil with three transposed conductors.

For transformers for 7500 volts and higher, the end turns must be specially insulated because abrupt changes in potential may raise the voltage between the conductors near the terminals to many times the normal value.⁷ The percentage of end turns that must be specially insulated varies from 2.5 per cent for 7500 to 15,000 volts to approximately 15 per cent for 220,000 volts. Messrs. Fleming and Johnson recommend 2.5 per cent for 10,000-volt windings and an additional $\frac{1}{2}$ per cent for every 10,000 volts. Figure 247 shows the end-turn insulation for a 132,000-volt, concentric-type winding.

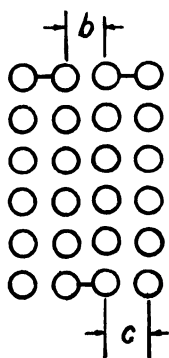


FIG. 246.

The insulation between core and windings and between high-voltage and low-voltage windings of concentric-coil-type transformers generally consists of molded cylinders or rectangular tubes. These tubes have high dielectric and mechanical strength and are

⁷ "Protection of Internal Insulation of a Static Transformer against High Frequency Strains," by W. S. Moody, *Trans. A.I.E.E.*, Vol. 26, Part 2, p. 1173; "Choke-Coils Versus Extra Insulation on the End Windings of Transformers," by S. M. Kintner, *Trans. A.I.E.E.*, Vol. 26, Part 2, p. 1169; "Transformers: Some Theoretical and Practical Considerations," by A. P. M. Fleming and K. M. Fayo-Hansen, *Journal I.E.E. Br.*, Vol. 42, 1908-09, p. 373.

not affected by insulating oils. The dielectric strength of the insulation between the various parts of the winding must be high enough to meet

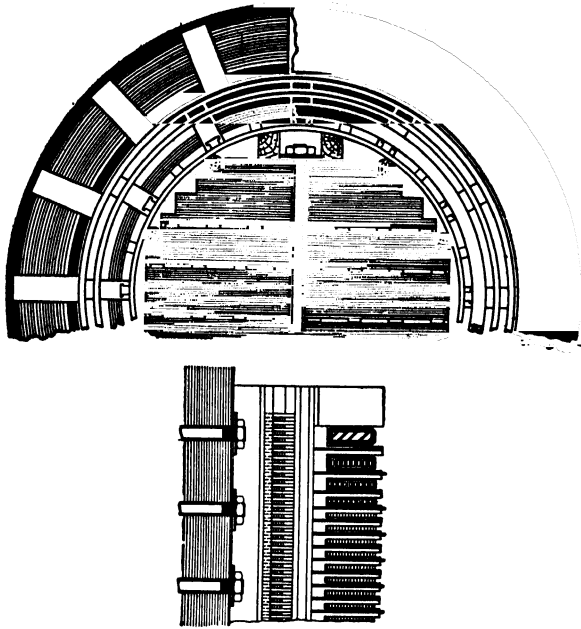


FIG. 247.—Concentric type winding and insulation—132,000 volt transformer.

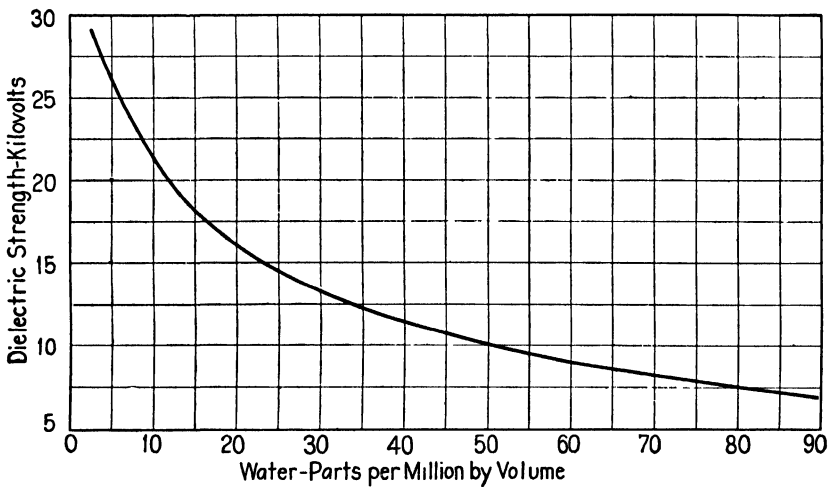


FIG. 248.—Dielectric strength of insulating oil.

the requirements of service with a reasonable factor of safety. The dielectric tests made on transformers consist of standard low-frequency tests, which may be an applied-potential test, an induced-potential test, or both, and an impulse test. The method of making these tests, as well as the values of voltages to be used for them, are given in American Standards for Transformers, Regulators and Reactors⁸ C57, 1948.

The thickness of the insulation between high-voltage and low-voltage coils and between low-voltage and core will depend upon the voltage of the windings and upon the mechanical strength required for winding and assembling the coils. The dielectric strength of molded insulating tubes $\frac{1}{4}$ in. thick is 100 kilovolts. More complete information on the insulation thickness required for transformer windings is given by Messrs. Fleming and Johnson.⁹ In addition to the insulating barriers, ducts are used between low-voltage winding and core, and between high- and low-voltage winding. The width of the ducts is generally $\frac{1}{4}$ in. in small-capacity transformers and $\frac{5}{16}$ to $\frac{1}{2}$ in. in large-capacity, high-voltage, power transformers. These ducts are used primarily for cooling purposes, but for oil-immersed transformers they also have a marked insulation value. Insulating oils, such as used for transformers, have a high dielectric strength when clean and free from moisture. Figure 248 shows the relation between the amount of water in insulating oil and the dielectric strength.¹⁰ The transformer standards of the Electrical Manufacturers Association specify that insulating oil used for transformers must meet the following requirements:

Transformer oils shall be capable of withstanding at commercial frequencies, 22,000 volts between 1-in. disc-terminals spaced 0.10 in. apart.

For voltages above 6900 volts, the insulation between windings and between windings and core is generally arranged as shown in Fig. 249 (see also Figs. 242 and 247).

The thickness of the insulating collars at each end of the windings varies from $\frac{1}{4}$ in. for windings below 500 volts to 6 in. for 70,000-volt windings. Large-capacity, high-voltage power transformers must have rigid supports at the ends of the coils to prevent distortion produced by the short-circuit forces.

For voltages below 6900 volts, the insulation between core and coils,

⁸ These standards are obtainable from the American Standards Association, 70 East 45 Street, New York 17, N. Y.

⁹ "Insulation and Design of Electrical Windings," pp. 155-175, Longmans, Green & Co., London; "Herkolite Insulating Materials in Transformers," General Electric Review, Vol. 29, Feb., 1926, pp. 102-108.

¹⁰ "Electric Insulating Oil," by Dean Harvey, Electric Journal, Vol. 25, Feb. and March, 1928.

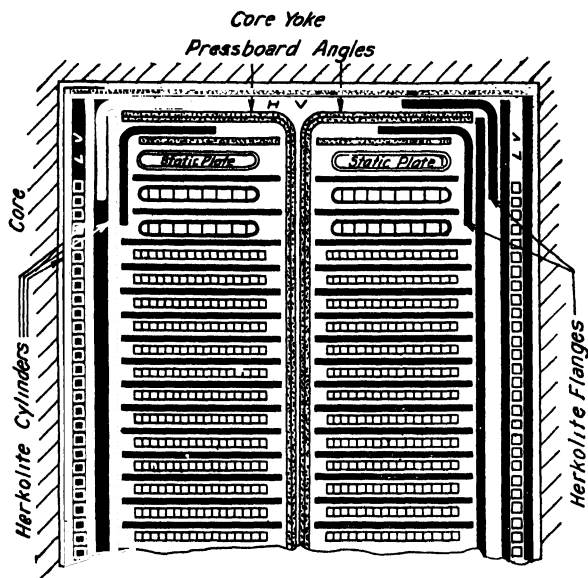


FIG. 249—Sketch showing section through window of a high-voltage concentric disc type transformer

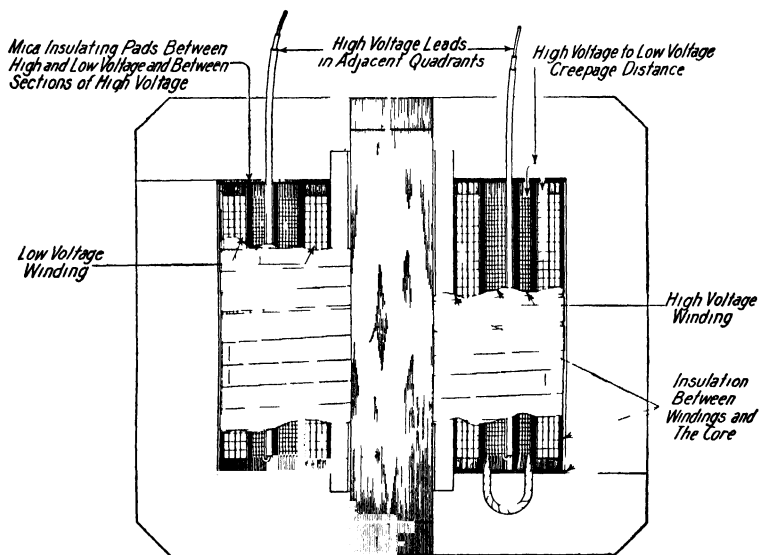


FIG. 250—Section of moderate voltage four-part distributed-core-type transformer.

and between high-voltage and low-voltage winding, is generally a mica pad. Figure 250 is a sectional drawing of a moderate-voltage, distributed-core-type transformer and shows the usual method of arranging and insulating the windings. No ducts are used between high-voltage and low-voltage coils, but one duct is used in the high-voltage coil. To avoid hot spots and to insure uniform temperature, the thickness of the coils from outside to duct, between ducts, or from duct to core should generally not exceed 1.0 in.

Interleaved-type windings are usually insulated as shown in Figs. 226 and 244. Pressboard collars are generally used to insulate the windings from one another. The insulation between core and coils is either molded insulation or pressboard. Ducts are provided between winding and between individual coils. The duct spacers are built up of pressboard, or are of treated wood.

After the coils are wound, they are thoroughly dried and impregnated by the vacuum process or treated with insulating varnish, the method used depending upon the type and size of coil. Small transformers are generally treated by the vacuum process after the core and coils are assembled. The insulating varnish and impregnating compound fill all the crevices of the coils and cement the turns firmly together. The insulation is thereby greatly strengthened, the heat conductivity of the coils increased, and the winding made moisture proof.

CHAPTER XXIII

OPERATING CHARACTERISTICS

Resistance.—The length of the mean-turn of the windings can easily be calculated from a sketch of the coils (see the sample designs in Chapter XXIV).

The weight of the copper in the low-voltage coil is,

$$G_l = L_l t_l s_{cl} \times 0.321 \text{ lb.} \quad (220)$$

and in the high-voltage coil,

$$G_h = L_h t_h s_{ch} \times 0.321 \text{ lb.} \quad (221)$$

The copper loss plus stray load loss for the two windings, at 75° C., are calculated by formula 139*a* (see page 408).

The resistance of each winding at 75° C.

$$R_l = \frac{W_l}{I_l^2} \text{ ohms, and } R_h = \frac{W_h}{I_h^2} \text{ ohms.}$$

The total resistance of the transformer in terms of the high-voltage winding

$$R_t = R_h + R_l \frac{t_h^2}{t_l^2} = \frac{W_l + W_h}{I_h^2} \text{ ohms.}$$

The per cent resistance drop

$$P_r = \frac{I_h R_t}{E_h} 100.$$

Leakage Reactance.—The leakage reactance can be calculated only approximately because certain assumptions must be made as to the length and area of the flux path. Formulas for calculating the reactance of transformers have been developed by various authors.¹ The

¹ "Die Wechselstromtechnik," by Dr. Arnold, Vol. 2, pp. 22–29, Julius Springer, Berlin; "Die Transformatoren," by Dr. Milan Vidmar, pp. 93–114, Julius Springer, Berlin; "Principles of Alternating Current Machinery," by R. R. Lawrence, pp. 186–191, McGraw-Hill Book Co., New York. "The Essentials of Transformer Practice," by E. G. Reed, pp. 115–123, D. Van Nostrand Co., New York.

leakage flux path for a core-type transformer with concentric winding and with the low-voltage coil on the inside and high-voltage winding outside is shown in Fig. 251. The total reactance, high voltage plus low voltage in terms of high voltage, for one leg of a transformer, with windings arranged as shown in Fig. 251,

$$X_l = \frac{21.5ft_h'^2}{h \times 10^8} \left(\frac{d_h + d_l}{3} + d \right) \frac{L_h + L_l}{2} \text{ ohms.}$$

The per cent reactance drop

$$P_x = \frac{X_l I_h}{E_h} 100 = \frac{21.5ft_h'^2 I_h}{h E_h \times 10^6} \left(\frac{d_h + d_l}{3} + d \right) \frac{L_h + L_l}{2}. \quad (222)$$

Here t_h' = the turns per leg of the high-voltage winding.

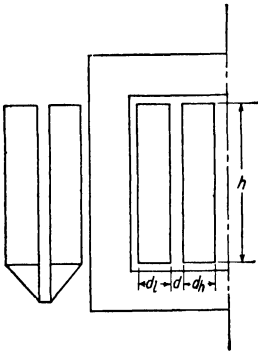


FIG. 251.

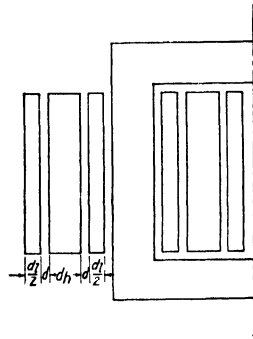


FIG. 252.

When the windings on the two legs are connected in series, the per cent reactance calculated by formula 222 must be multiplied by 2.0, and when connected in parallel it must be multiplied by 0.50. Formula 222 shows that the per cent reactance drop varies directly with the number of turns, the thickness of the coils, the spaces between windings, and the average mean-length of turn, and inversely with the length of the coils.

A lower reactance drop can be obtained, for a given number of turns and core length, by arranging the windings as shown in Fig. 252. The per cent reactance for this arrangement

$$P_x = \frac{10.8ft_h'^2 I_h}{h E_h \times 10^6} \left(\frac{d_h + d_l}{6} + d \right) L_h. \quad (223)$$

The per cent reactance drop for the interleaved type of windings arranged as shown in Fig. 253 is

$$P_z = \frac{11.0 f t_h'^2 I_h x_{hl}}{w_w E_h \times 10^6} \left(\frac{x_h d_{xh} + x_l d_{xl}}{6} + d \right) L_h k_4. \quad (224)$$

The constant

$$k_4 = 1 - \frac{x_h d_{xh} + x_l d_{xl} + 2d}{2\pi w_w}, \quad (225)$$

where x_h and x_l are the number of high-voltage and low-voltage coils per group respectively, t_h' is the number of high-voltage turns per group, and x_{hl} is the number of "high-low" groups.

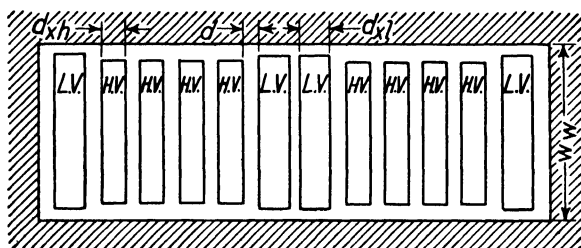


FIG. 253.

This formula does not take into account the leakage flux that passes through the space between the coils of high-voltage and low-voltage groups, which is generally small.²

The per cent impedance drop

$$P_z = \sqrt{P_x^2 + P_r^2}.$$

The sustained short-circuit current for normal primary voltage

$$I_s = \frac{E_h}{Z} = \frac{I \times 100}{P_z} \text{ amperes.} \quad (226)$$

The mechanical forces³ on the windings, set up electromagnetically, vary as the square of the current. On short-circuit, these forces may be large enough to distort the coils and destroy the insulation. The windings of large capacity transformers must therefore be carefully braced to withstand the shocks due to short-circuits.

² "Beitrag zur Berechnung der Streuspannung von Transformatorenwicklungen," by R. Kuechler, E. T. Z., Vol. 45, 1924, pp. 273 and 274.

³ "Die Wechselstromtechnik," by Dr. Arnold, Vol. II, p. 185, Julius Springer, Berlin; "Mechanical Stresses in Transformers," by J. F. Peters, Electric Journal, Vol. 12, Dec., 1915, p. 555.

Regulation.—The voltage regulation of a transformer is most conveniently calculated by the formulas given in the Standards of the A.S.A., which are explained in various textbooks. For unity-power-factor load

$$\text{Per cent regulation} = P_r + \frac{P_z^2}{200} \text{ approximately.}$$

For inductive loads of power factor $\cos \theta$ and reactive factor $\sin \theta$

$$\text{Per cent regulation} = \cos \theta P_r + \sin \theta P_z + \frac{(\cos \theta P_z - \sin \theta P_r)^2}{200}$$

approximately.

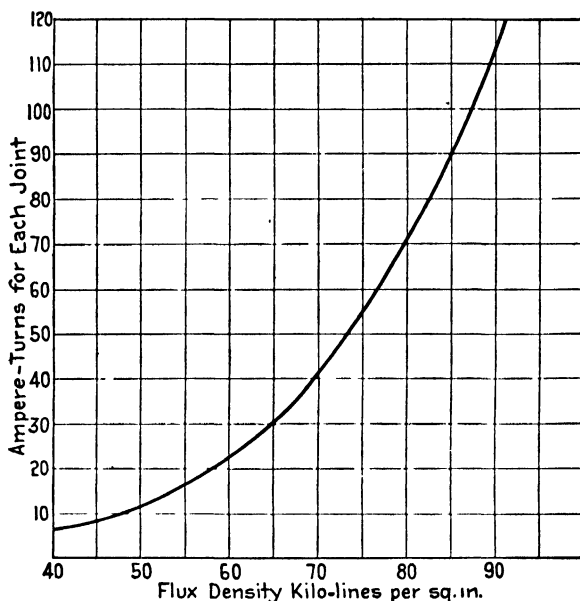


FIG. 254.—Ampere-turns per joint.

Exciting current.—The current that a transformer draws from the line at no-load may be thought of as consisting of two components: (1) the magnetizing current, I_m , which is 90° out of phase with the impressed voltage, and (2) the core-loss current, I_w , which is in phase with the impressed voltage. The curve in Fig. 254 shows the ampere-turns for each joint in the magnetic circuit of a transformer. The method of calculating the magnetizing current and the core-loss current is explained in the sample problems in Chapter XXIV. The exciting current

$$I_0 = \sqrt{I_m^2 + I_w^2} \text{ amperes.}$$

Efficiency.—The losses in a transformer are no-load losses and load losses. The no-load losses include core losses, I^2R losses in the windings due to the exciting current, and dielectric losses. Of the no-load losses, only the core losses are calculated because the remaining losses are generally so small that they may be disregarded. The curves in the Appendix give the loss per pound of transformer steel for various densities. In the finished transformer core, these losses are generally from 10 to 15 per cent larger, due to bending and shearing strains, imperfect insulation between sheets, etc.

The load losses include I^2R losses in the windings and stray losses due to stray fluxes in the windings, core clamps, etc. The I^2R losses for the windings are calculated by formula 139a. (The stray losses are difficult to predetermine accurately. Dr. Arnold⁴ states that they are generally equal to from 5 to 25 per cent of the total copper losses).

$$\text{The efficiency} = \frac{\text{Kva output} \times \text{PF}}{\text{Kva output} \times \text{PF} + \text{Kw losses}}.$$

Temperature Rise.—The Standardization Rules of the A.S.A. specify that the limiting temperature rise of transformer windings insulated with cotton, silk, paper, and similar organic materials, when impregnated or immersed in oil, shall not exceed 55° C. The temperature is to be determined by resistance and checked by thermometer. The temperature rise can be predetermined approximately by calculating the exposed surface of the core and ducts and of the coils and ducts. Practice has shown that the ducts are only half as effective as the outside surfaces; therefore only half of the duct surface is used in calculating the effective radiating surface. For a temperature rise not to exceed 55° C. the radiating surface in square-inches-per-watt loss should be equal to 3 to 4 for natural-air-cooled transformers, from 2.0 to 3.0 for natural-oil-cooled transformers, and from 1.0 to 1.75 for oil-and-water-cooled transformers. The method of calculating the total radiating surface is illustrated by the sample problems in Chapter XXIV.

Design of Tank.—The heat generated by the losses is radiated by the exposed surfaces of the transformer to the cooling medium. When the transformer is immersed in oil, the heat is transmitted by the oil to the tank walls and thence to the surrounding air. Figure 255 shows the results of a test on a small distribution transformer operating at full-load in still air. The temperatures for the various parts of the tank are the values obtained after the temperature has become constant.

⁴ "Die Wechselstromtechnik," Vol. 2, p. 360, Julius Springer, Berlin.

The maximum temperature of the oil, near the surface, is generally from 1.15 to 1.50 times the average temperature and depends upon the depth of oil above the transformer and upon the circulation. The dimensions of the tank are generally so proportioned that the amount of oil required will be as small as possible. The depth of oil above the transformer should never be less than 2 in.

The difference between the temperature of the transformer windings and the average oil temperature is usually from 15° C. to 20° C. This

difference depends upon the insulation on the coils, the thickness of the coils, etc. For a temperature rise of 55° C. for the windings, the average rise of the oil will then be from 35° C. to 40° C.

Plain sheet-steel tanks such as shown in Fig. 230 are generally used for moderate-voltage distribution transformers of 25-Kva capacity and smaller. For a transformer temperature rise not to exceed 55° C., the square inch wetted tank surface (not including top or bottom) per watt loss should be from 4 to 5.5.

For large-capacity and high-voltage distribution transformers and for power transformers, tanks with corrugated sides or with cooling tubes are used. The square inch wetted tank surface re-

quired for each watt will depend upon the type of tank used. For plain steel tanks with cooling tubes, the wetted square inch tank surface for each watt loss should be from 5 to 6. For corrugated sheet-steel tanks,⁵ S/W is generally equal to from 6.0 to 9.0 sq. in. per watt loss and depends upon the pitch and depth of the corrugations.

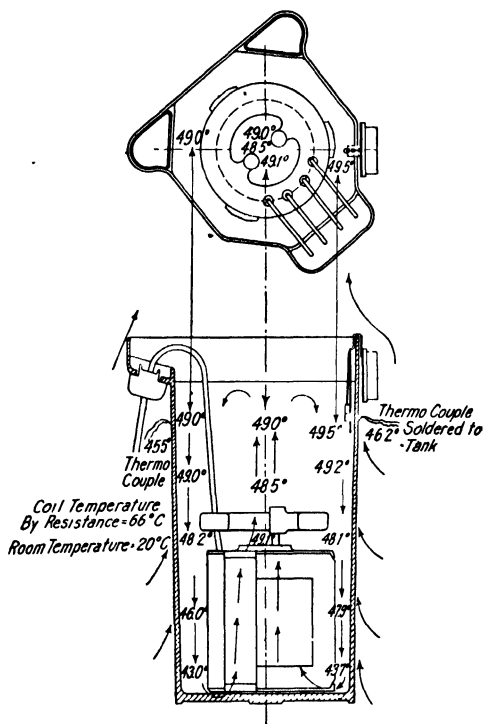


FIG. 255.—Oil temperature in various parts of transformer tank when operating at full load in still air.

⁵ "Dissipation of Heat from Self-Cooled Oil-Filled Transformer Tanks," by J. J. Frank and H. O. Stephens, A.I.E.E. Trans., Vol. 30, Part I, 1911, pp. 447-456.

The heating and cooling curves ⁶ for self-oil-cooled transformers can be predetermined with satisfactory accuracy when the specific heat of the various materials used in their construction is known. These curves are necessary to determine the average temperature rise of a transformer used for intermittent duty.

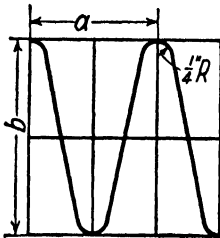


FIG. 256.

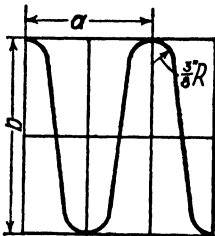


FIG. 257.

Generally, only a small clearance is allowed between the transformer and the walls of the tank (see Figs. 232 and 233. The depth of the oil is then equal to the wetted area of the walls, divided by the perimeter of the tank. The approximate length of the corrugated surface per inch length of center line is given in Table XXXII for several types of corrugated tank walls.

TABLE XXXII

FIGURE 256			FIGURE 257		
<i>a</i>	<i>b</i>	Mean Length of Corrugation per Inch of Center Line	<i>a</i>	<i>b</i>	Mean Length of Corrugation per Inch of Center Line
1½ in.	4 in.	5.75 in.	2.00 in.	4.0 in.	4.45 in.
1½ in.	4 in.	5.00 in.	2.25 in.	4.0 in.	4.05 in.
1½ in.	3 in.	4.50 in.	2.50 in.	4.0 in.	3.66 in.
1½ in.	3 in.	3.86 in.	3.00 in.	4.0 in.	3.42 in.
1½ in.	2 in.	3.75 in.	2.00 in.	3.0 in.	3.51 in.
1½ in.	2 in.	3.17 in.	2.25 in.	3.0 in.	3.12 in.
1½ in.	2 in.	2.73 in.			

The volume of oil required is equal to the volume of the tank, minus the volume of the transformer.

⁶ "Essentials of Transformer Practice," by Emerson G. Reed, 2nd ed., p. 136, D. Van Nostrand Co., New York; and "Cooling of Transformer Windings after Shut-Down," by V. M. Montsinger, General Electric Review, Vol. 22, Dec., 1919, pp. 1056-1066.

CHAPTER XXIV

SAMPLE TRANSFORMER DESIGNS

Design No. 1: *Design of a 400-Kva., Single-Phase, Core-Type Power Transformer.*—The complete rating of the transformer is as follows: 400 kva., single-phase, 60 cycles, 42,000 volts primary to 2400 volts secondary. The transformer is to be of the self-oil-cooled type and must carry its rated load continuously with a temperature rise not to exceed 55° C. The full-load 100 per cent power factor efficiency must not be less than 98.0 per cent and the ratio of losses should be approximately 1.0.

For a ratio of losses equal to 1.0, the flux density in the core can be chosen equal to 90,000 lines per sq. in. From the iron loss curves in the Appendix for 0.014-in., 4.0 per cent silicon steel, the loss per pound for this density $w_c = 1.40 \times 1.12 = 1.57$ watts, if the additional losses are taken equal to 12.0 per cent of the fundamental frequency loss (see page 432).

For an average current density, $A = 1500$ amperes per sq. in., the copper loss per pound (formula 139a)

$$w_k = 2.58A^2k_5 \times 10^{-6} = 2.58 \times 1500^2 \times 1.10 \times 10^{-6} = 6.39 \text{ watts.}$$

The ratio of core weight to copper weight

$$\frac{G_c}{G_k} = \frac{w_k}{w_c} \times \frac{W_c}{W_k} = \frac{6.39}{1.57} \times 1 = 4.07.$$

The output constant is taken equal to 0.45 (see page 411) and the net section area of the core

$$\begin{aligned} A_c &= C \sqrt{\frac{\text{kva} \frac{G_c}{G_k} 10^{11}}{BAf}} = 0.45 \sqrt{\frac{400 \times 4.07 \times 10^{11}}{90,000 \times 1500 \times 60}} \\ &= 63.9 \text{ sq. in.} \end{aligned}$$

The cruciform-shaped core section shown in Fig. 237 will be used for this transformer. The diameter of the core

$$D = \sqrt{\frac{A_c \times 4}{\pi f_{cs}}} = \sqrt{\frac{63.9 \times 4}{3.14 \times 0.70}} = 10.8; \text{ use } 10.875 \text{ in.}$$

The calculations for the core space factor, f_{cs} , are given on page 413.

The dimensions of the core section (see Fig. 258) are:

$$2a = 0.526D = 0.526 \times 10.9 = 5.74; \text{ use } 5.75 \text{ in.}$$

$$2b = 0.85D = 0.85 \times 10.9 = 9.27; \text{ use } 9.25 \text{ in.}$$

The total flux for a density of 90,000 lines per sq. in.

$$\phi = AB = 66.0 \times 90,000 = 5940 \text{ kilo-lines.}$$

The number of turns for high-voltage and low-voltage windings

$$t_h = \frac{E_h \times 10^8}{4.44 f \phi_t} = \frac{42,000 \times 10^8}{4.44 \times 60 \times 5940 \times 10^3} \\ = 2660.$$

$$t_l = \frac{E_l}{E_h} \times t_h = \frac{2400}{42,000} \times 2660 = 152.$$

The full-load current in the two windings

$$I_h = \frac{Kva \times 10^3}{E_h} = \frac{400 \times 10^3}{42,000} = 9.52 \text{ amperes}$$

$$I_l = \frac{t_h}{t_l} I_h = \frac{2660}{152} 9.52 = 166.8 \text{ amperes.}$$

For the average current density assumed above, the section area of the conductors for the high-voltage and low-voltage windings

$$s_{ch} = \frac{I_h}{A} = \frac{9.52}{1500} = 0.00635 \text{ sq. in.}$$

$$s_{cl} = \frac{I_l}{A} = \frac{166.8}{1500} = 0.111 \text{ sq. in.}$$

The area of the window opening

$$h_w w_w = \frac{2s_{ch} t_h}{f_s} = \frac{2 \times 0.00635 \times 2660}{0.105} \\ = 322.0 \text{ sq. in.}$$

The copper space factor, f_s , is taken from the curves of Fig. 239.

For a ratio of window height to window width equal to 3.0, the dimensions of the window are:

$$h_w = \sqrt{3 \times 322} = 31.1 \text{ in.; use } 31.0 \text{ in.}$$

$$w_w = \frac{31.0}{3} = 10.3 \text{ in.; use } 10.5 \text{ in.}$$

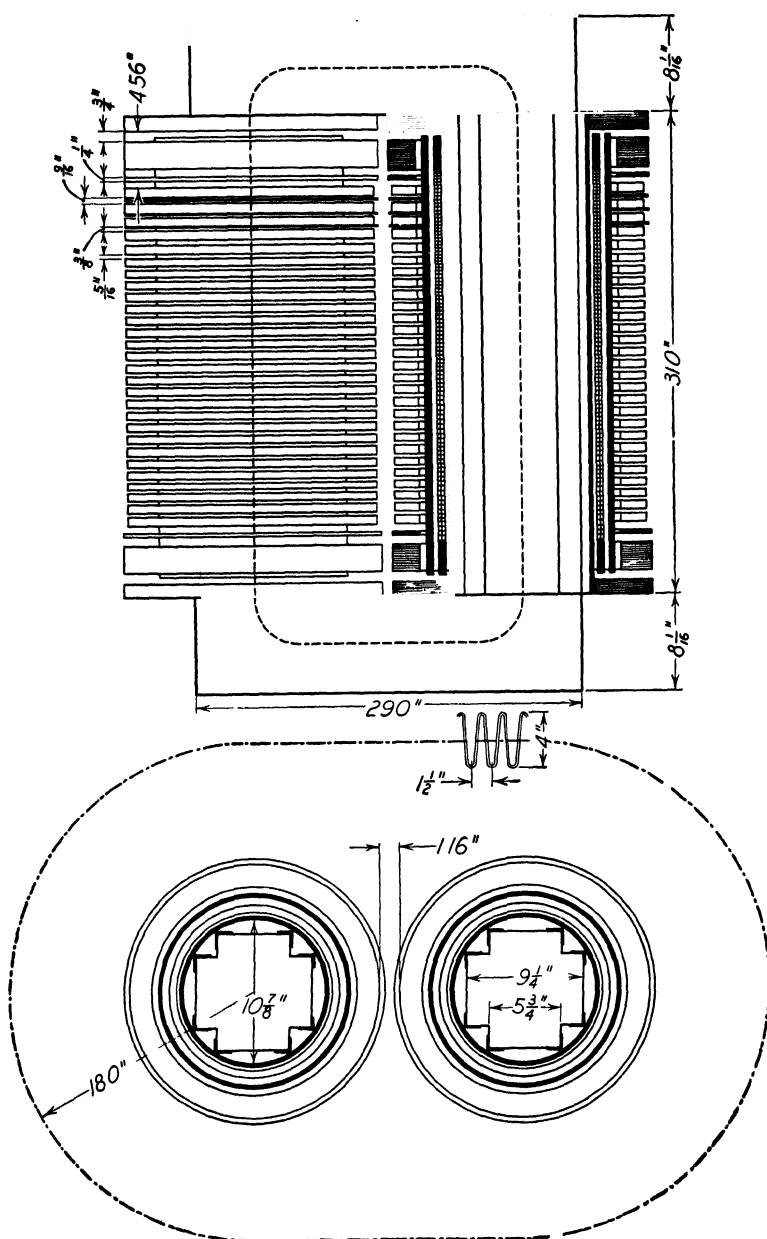


FIG. 258.

It is desirable at this point to calculate the approximate core and copper weight, to determine whether the core dimensions selected above give approximately the ratio of core weight to copper weight desired.

The flux density in the yoke will be made equal to the flux density in the core legs. The height of the yoke section

$$\frac{66}{0.90 \times 9.25} = 8.08 \text{ in.}; \text{ use } 8\frac{1}{8}$$

The length of the yoke

$$l_y = w_w + (2 \times 2b) = 10.5 + (2 \times 9.25) = 29.0 \text{ in.}$$

The total weight of the core

$$\begin{aligned} G_c &= [2l_y A_c + (2h_w A_r)] 0.272 \\ &= [2 \times 29.0 \times 66.0 + (2 \times 31 \times 66.0)] 0.272 = 2155 \text{ lb.} \end{aligned}$$

The clearance, β , between the two coils in the window opening should be approximately 1.25 in. The length of the average mean-turn for the windings

$$L_{av} = \left(D + \frac{w_w - \beta}{2} \right) \pi = \left(10.9 + \frac{10.5 - 1.25}{2} \right) \pi = 48.8 \text{ in.}$$

The approximate total copper weight

$$\begin{aligned} G_k &= 2t_{hsch} L_{av} \times 0.321 \\ &= 2 \times 2660 \times 0.00635 \times 48.8 \times 0.321 = 529.0 \text{ lb.} \end{aligned}$$

The ratio of core weight to copper weight

$$\frac{G_c}{G_k} = \frac{2155.0}{529.0} = 4.07.$$

The dimensions of the window are, then,

$$h_w = 31.0 \text{ in.}, \quad w_w = 10.5 \text{ in.}$$

DESIGN OF WINDINGS

Low-Voltage Winding.—The section area of the low-voltage conductor, $s_{cl} = 0.111$ sq. in. Two conductors, each 0.182×0.289 -in. bare, 0.204×0.310 -in. insulated, 0.0507 sq. in. area, are wound in parallel.

A helical-wound coil with transposed conductors as shown in Fig. 245 is used for the low-voltage winding.

The number of turns per core leg

$$= \frac{152}{2} = 76.$$

The conductor is wound flat, with the two parallel wires on top of each other. The space occupied by the winding in the direction of the window height

$$= 0.31 \times 76 = 23.6 \text{ in.}$$

For a window 31 in. high, there will be a clearance of 3.7 in. at each end of the winding, which is required for insulation and supporting collars.

The insulation between the low-voltage winding and core consists of $\frac{1}{16}$ -in. fuller-board channels placed over the corners of the core, $\frac{3}{16}$ -in. pressed paper cylinder, and a $\frac{1}{4}$ -in. duct as shown in Fig. 258.

High-Voltage Winding.—Disc-type coils will be used for the high-voltage winding. The following conductor is selected from the copper table:

Bare.....	0 025 × 0.258 in.
Insulated.....	0.043 × 0.270 in.
Area.....	0.00632 sq. in.

The number of turns per core

$$= \frac{2660}{2} = 1330.$$

Extra insulation is required on the end-turns of high-voltage transformers (see page 423). Therefore the number of turns in the coils should be so proportioned that the end coils will have a smaller number of turns, to provide space for the extra insulation. Approximately 4.5 per cent of the high-voltage turns on each end of the winding should have extra insulation. Coils with two turns per layer, half of the turns wound backward to avoid cross-over, will be used. Fuller-board 0.020 in. thick is placed between the two sections of the coils. The number of coils and number of turns per layer are as follows:

Number of Coils per Core Leg	Turns per Section	Turns per Coil	Total Turns
21	28	56	1176
1	25	50	50
1	22	44	44
1	18	36	36
1	10 and 14	24	24
Turns per core leg.....	1330

The coils are insulated from each other by $\frac{5}{16}$ -in. oil ducts; between the end coils wider ducts are used, as shown in Fig. 258.

The width of each coil in the direction of the window height

$$= 2 \times 0.27 + 0.020 = 0.560 \text{ in.}$$

The four end coils have extra insulation and therefore require more space. If 10 per cent is allowed for the space required for the extra insulation, the width of each of the four end coils

$$= 0.560 \times 1.10 = 0.616 \text{ in.}$$

The total space occupied by the coils in the direction of the window height

$$= 21 \times 0.560 + 4 \times 0.616 = 14.22 \text{ in.}$$

The total duct space between the coils (see Fig. 258)

$$= 21 \times \frac{5}{16} + 2 \times \frac{3}{8} + \frac{9}{16} = 7.87 \text{ in.}$$

The high-voltage winding therefore occupies 22.09 in. in the direction of the window height. With a window opening 31 in. high, there is a space of 4.56 in. at each end of the winding, which is required for insulation and supporting collars.

The insulation between the high-voltage and low-voltage winding consists of a $\frac{1}{2}$ -in. duct, plus a pressed paper insulating cylinder $\frac{5}{16}$ in. thick, plus $\frac{1}{2}$ -in. duct. The total thickness of the windings

$$= \frac{1}{2}(10.9 - 9.25) + 0.50 + 2 \times 0.204 + 0.50 + 0.3125 + 0.50 + 28(0.043 + 0.015) = 4.67 \text{ in.}$$

The clearance between the coils in the window opening

$$= 10.5 - 2 \times 4.67 = 1.16 \text{ in.}$$

The total flux

$$\phi_t = \frac{E_h \times 10^8}{4.44 f t_h} = \frac{42,000 \times 10^8}{4.44 \times 60 \times 2660} = 5940.0 \text{ kilo-lines.}$$

The flux density in the core

$$B = \frac{5940 \times 10^3}{66.0} = 90,000 \text{ lines per sq. in.}$$

The dimensions of the core have not been changed; therefore the total core weight is the same as given.

The current density in the low-voltage winding

$$A_t = \frac{166.5}{2 \times 0.0507} = 1640 \text{ amperes per sq. in.,}$$

and in the high-voltage winding

$$A_h = \frac{9.52}{0.00632} = 1503 \text{ amperes per sq. in.}$$

The length of the mean-turn for the low-voltage winding

$$L_l = \pi[10.9 + (0.50 \times 2) + (2 \times 0.204)] = 38.6 \text{ in.},$$

and for the high-voltage winding

$$\begin{aligned} L_h &= \pi[10.9 + (2 \times 0.50) + 2(2 \times 0.204) + (2 \times 1.3125) \\ &\quad + 28(0.043 + 0.015)] \\ &= 53.3 \text{ in.} \end{aligned}$$

The copper weight for each of the windings

$$\begin{aligned} G_l &= t_l s_{cl} L_l \times 0.321 \\ &= 152 \times 2 \times 0.0507 \times 38.6 \times 0.321 = 191.0 \text{ lb.}, \\ G_h &= t_h s_{ch} L_h \times 0.321 \\ &= 2660 \times 0.00632 \times 53.3 \times 0.321 = 298.0 \text{ lb.} \end{aligned}$$

The total copper weight

$$G_k = 191 + 298 = 489.0 \text{ lb.}$$

The ratio of core weight to copper weight

$$\frac{G_c}{G_k} = \frac{2155}{489} = 4.41.$$

This value of the ratio of weights is higher than the one calculated above because of the high current density chosen for the low-voltage winding.

The output constant

$$C = \frac{A_c}{\sqrt{\frac{\text{kva } G_c / G_k \times 10^{11}}{BAf}}} = \frac{66.0}{\sqrt{\frac{400 \times 4.41 \times 10^{11}}{90,000 \times 1572 \times 60}}} = 0.466.$$

The copper space factor

$$\begin{aligned} f_s &= \frac{s_{ch} t_h + s_{cl} t_l}{h_w w_w} = \frac{0.00632 \times 2660 + 0.1014 \times 152}{31.0 \times 10.5} \\ &= 0.109. \end{aligned}$$

From the loss curve for 0.014 in., 4.0 per cent silicon steel, the loss per pound for a density of 90 kilo-lines per sq. in.

$$w_c = 1.40 \times 1.12 = 1.57 \text{ watts per lb.}$$

The total core loss

$$W_c = w_c G_c = 1.57 \times 2155 = 3380 \text{ watts.}$$

The I^2R loss plus stray load-loss in each of the windings at 75° C.

$$\begin{aligned} W_l &= 2.58 A_l^2 G_{lk5} \times 10^{-6} \\ &= 2.58 \times 1640^2 \times 191 \times 1.10 \times 10^{-6} = 1460 \text{ watts,} \end{aligned}$$

$$\begin{aligned} W_h &= 2.58 A_h^2 G_{hk5} \times 10^{-6} \\ &= 2.58 \times 1503^2 \times 298 \times 1.10 \times 10^{-6} = 1910 \text{ watts.} \end{aligned}$$

The ratio of losses

$$\frac{W_c}{W_k} = \frac{3380}{3370} = 1.003.$$

The resistance of the low-voltage and high-voltage windings at 75° C.

$$R_l = \frac{W_l}{I_l^2} = \frac{1460}{166.5^2} = 0.0527 \text{ ohm,}$$

$$R_h = \frac{W_h}{I_h^2} = \frac{1910}{9.52^2} = 21.1 \text{ ohms.}$$

The total resistance in terms of the high-voltage winding

$$R_t = \frac{1460 + 1910}{9.52^2} = 37.2 \text{ ohms.}$$

The per cent resistance drop

$$P_r = \frac{I_h R_t}{E_h} 100 = \frac{9.52 \times 37.2}{42,000} 100 = 0.844 \text{ per cent.}$$

Formula 222 gives the per cent reactance drop for one core leg of a core-type transformer with concentric type winding. For our problem, the windings on the two core legs are connected in series; therefore, formula 222 must be multiplied by 2.

$$\begin{aligned} P_x &= 2 \frac{21.5 f t_k^2 I_h \left(\frac{d_h + d_l}{3} + d \right) \frac{L_h + L_l}{2}}{h E_h \times 10^6} \\ &= 2 \frac{21.5 \times 60 \times 1330^2 \times 9.52 \left(\frac{1.624 + 0.408}{3} + 1.313 \right)}{22.09 \times 42,000 \times 10^6} \times \\ &\quad \frac{53.3 + 38.6}{2} = 4.29 \text{ per cent.} \end{aligned}$$

The per cent impedance drop

$$P_z = \sqrt{P_x^2 + P_r^2} = \sqrt{4.29^2 + 0.844^2} = 4.37 \text{ per cent.}$$

The sustained short-circuit current for normal primary voltage

$$I_s = \frac{I \times 100}{P_z} = \frac{9.52 \times 100}{4.37} = 218 \text{ amperes.}$$

To calculate the mechanical stresses on the windings due to the short-circuit current, see references on page 430.

The per cent regulation for 100 per cent power factor load

$$= P_r + \frac{P_z^2}{200} = 0.844 + \frac{4.37^2}{200} = 0.94 \text{ per cent,}$$

and for 80 per cent power factor load, per cent regulation

$$\begin{aligned} &= \cos \theta P_r + \sin \theta P_z + \frac{(\cos \theta P_z - \sin \theta P_r)^2}{200} \\ &= 0.80 \times 0.844 + 0.60 \times 4.37 \\ &\quad + \frac{(0.80 \times 4.37 - 0.60 \times 0.844)^2}{200} \\ &= 3.376 \text{ per cent.} \end{aligned}$$

The mean length of the flux path is shown by the dotted line in Fig. 258 and is

$$= (31.0 + 8.063)2 + (10.5 + 9.25)2 = 117.6 \text{ in.}$$

From the standard magnetization curve for 4.0 per cent silicon steel, the ampere-turns per inch for a density of 90 kilo-lines, at = 30.0. The total ampere-turns necessary to maintain the flux in the iron part of the magnetic circuit

$$= \text{at} \times 117.6 = 30.0 \times 117.6 = 3528.$$

The ampere-turns for each joint for a density of 90.0 kilo-lines = 113.0 (see Fig. 254). With 4 joints in the magnetic circuit, the ampere-turns

$$= 4 \times 113.0 = 452.$$

The magnetizing current

$$I_m = \frac{\text{AT}}{\sqrt{2}t_h} = \frac{3980}{\sqrt{2} \times 2660} = 1.246 \text{ amperes.}$$

The in-phase component of the no-load current

$$I_w = \frac{W_e}{E_h} = \frac{3380}{42,000} = 0.0805 \text{ amperes.}$$

The exciting current

$$I_0 = \sqrt{I_m^2 + I_w^2} = \sqrt{1.246^2 + 0.0805^2} = 1.248 \text{ ampere.}$$

The stray load-losses will be estimated equal to 10 per cent of the total I^2R losses (see page 432). The efficiencies and losses for various loads at 100 per cent and 80 per cent lagging power factor are as follows:

	$\frac{1}{4}$	$\frac{2}{4}$	$\frac{3}{4}$	$\frac{4}{4}$	$\frac{5}{4}$
I^2R + stray load-losses	211	843	1,896	3,370	5,265
Core losses.....	3,380	3,380	3,380	3,380	3,380
Total losses.....	3,591	4,223	5,276	6,750	8,645
Output.....	100,000	200,000	300,000	400,000	500,000
Input.....	103,591	204,223	305,276	406,750	508,645
Efficiency 100% PF...	96.5	97.9	98.3	98.3	98.3
Efficiency 80% PF....	95.6	97.4	97.9	97.9	97.9

The total radiating surface of the transformer winding and core is calculated as follows:

$$\text{Core legs: } (4 \times 5.75 + 4 \times 3.5)2 \times 31 = 2290 \text{ sq. in.}$$

$$\text{Yokes: } (4 \times 8.063 \times 29 + 9.25 \times 29.0 \times 2 + 8.063 \times 9.25 \times 4) = 1769 \text{ sq. in.}$$

$$\text{Low-voltage winding: } (2 \times 38.6 \times 23.6 \times 2) = 3640 \text{ sq. in.}$$

$$\text{High-voltage winding: } 2(0.56 + 1.624)53.3 \times 25 \times 2 = 11,640 \text{ sq. in.}$$

$$\text{Total radiating surface} = 19,339 \text{ sq. in.,}$$

and the surface per watt loss

$$\frac{S}{W} = \frac{19,339}{6750} = 2.87.$$

For a corrugated sheet-steel tank, the surface per watt loss should be approximately 7.5 (see page 433). The total wetted tank surface

$$S_t = (W_e + W_k)S/W = 6750 \times 7.5 = 50,600 \text{ sq. in.}$$

Figure 258 shows the shape of the tank section and the position of the transformer in the tank. The length of the surface of the corrugations

TRANSFORMER DESIGN SHEET

Kva, 400 Phase, Single Cycles 60 Volts $\begin{cases} \text{HV, 42 000} \\ \text{LV, 2,400} \end{cases}$ Phase Volts $\begin{cases} \text{HV} \\ \text{LV} \end{cases}$
 Line Amperes $\begin{cases} \text{HV, 9.52} \\ \text{LV, 166.5} \end{cases}$ Phase Amperes $\begin{cases} \text{HV} \\ \text{LV} \end{cases}$
 Type Circular Core Type of Cooling Self Oil

CORE			Per cent			
Sheet steel	0.014	4% S ₁	Resistance			0.844
Output constant		0.43	Reactance			4.29
Core leg	Center	Outside	Impedance			4.37
Area	66		Power factor	80	100	
Diameter	10.9		Regulation	3.38	0.94	
Dimensions	$2a = 5.75 \quad 2b = 9.25$		Losses			
Density	90.000		Total core			3380
Weight	1115		Stray load			308
Core factor		0.70	Total copper			3062
Yoke			Per cent			
Area		66.0	Load	25	50	75
Dimensions		$8\frac{1}{2} \times 9.25$	Efficiency	96.5	97.9	98.3
Density		90.000	Square inches per watt			2.87
Weight		1040	Ratio of losses			1.0
Copper space factor f_s		0.109	Ratio of weights			4.41
Window dimensions		105×31.0	TANK			
Lamination factor k_1		0.90	Type of tank	corrugated sheet steel	$1\frac{1}{2} \times 4.0$	
CORE AND WINDINGS			Square inches per watt			7.5
Mean length of flux path		117.6	Total wetted surface			50.600
Total ampere-turns		3980	Depth of oil			57.7
Magnetizing current		1.25	Gallons of oil			391
Core loss current		0.0805	Weight of oil			2740
Exciting current			Cooling coils			
Amperes		1.25	Size			
Per cent		13.1	Length			
			Surface			
			Water gallons per minute			

WINDINGS	HIGH VOLTAGE	LOW VOLTAGE
Type of winding	Disc coils	Helical
Connections		
Conductor		
Dimensions	$0.043 \times 0.27 \text{ d c c}$	$0.204 \times 0.31 \text{ d c c}$
Section	0.00632	0.0507
Number in parallel	None	2
Current density	1503	1640
Turns per phase	2660	152
Coils		
Total number	50	2
Per core leg	2	1
Turns		
Per coil	*	76
Per layer	†	76
Number of layers	2 sections	1
Coil		
Connections	Series	Series
Dimensions	0.56×1.74	0.454×25.8
Ducts number and size	$21-\frac{1}{8} \quad 2-\frac{1}{8} \quad 1-\frac{1}{8}$	
Insulation		
Layer	0.015	
Core and coils		
HV and LV	$\frac{1}{2} D + \frac{1}{8} P B + \frac{1}{2} D$	$\frac{1}{8} F B + \frac{1}{8} P B + \frac{1}{2} D$
Voltage per turn	15.8	
Maximum voltage between layers	885	
Length of mean-turn	53.3	38.6
Copper		
Weight	298	191
Loss	1910	1460
Resistance 75°C	21.1	0.0527
Per cent end turns with extra insulation	5.3	

Remarks	* 21 coils 56 turns	† 21 coils 28 turns per section
	1 coil 50 turns	1 coil 25 turns per section
	1 coil 44 turns	1 coil 22 turns per section
	1 coil 36 turns	1 coil 18 turns per section
	1 coil 24 turns	1 coil 10 and 14 turns per section

Designed by J. H. Kuhlmann

Date _____

for each inch of length of the center line equals 5.75 in. The clearance between the outside of the coils and the inside of the tank is 8.7 in., and the length of the center line of the corrugated tank wall

$$= 2(10.5 + 9.25) + \pi \times 36.0 = 152.5 \text{ in.}$$

The depth of the hot oil

$$= \frac{50,600}{152.5 \times 5.75} = 57.7 \text{ in.}$$

The volume of oil required is equal to the volume of the tank minus the volume of the transformer. The volume of the transformer can be calculated approximately from the weight of the active materials. The insulation, core clamps, coil supports, etc., occupy only a small per cent of the space required for the active material. The volume of the tank

$$= \left(\frac{\pi}{4} \times 36.0^2 + 36 \times 19.75 \right) 57.7 = 99,900 \text{ cu. in.}$$

The approximate volume of the transformer

$$= \frac{2155}{0.272} + \frac{489}{0.321} = 9440 \text{ cu. in.}$$

The volume of oil required is therefore equal to 90,460 cu. in. The number of cubic inches in a gallon is 231; therefore 391 gallons of oil are required, or 0.978 gallons per kva. One gallon of transformer oil weighs approximately 7.0 lb.; the total weight of the oil is then

$$7.0 \times 391 = 2740.0 \text{ lb.}$$

In the assembly drawing of the transformer, Fig. 258, the core clamps, coil supports, etc., have been omitted.

Design No. 2: *Design of a 1000-Kva, Three-Phase, Core-Type Power Transformer.*—The complete rating of the transformer is as follows: 1000 kva, three-phase, 60 cycles, 7960 volts primary to 575 volts secondary, with delta-connected primary and secondary windings. The transformer is to be of the self-oil-cooled type and must carry its rated load continuously with a temperature rise not to exceed 50° C. The full-load, 100 per cent power factor efficiency must not be less than 98.2 per cent and the ratio of the core loss to copper loss should be approximately 0.90.

For a ratio of losses equal to 0.9, the flux density in the core can be taken equal to 90,000 lines per sq. in. For this density the core loss

per pound for 2.5 per cent silicon steel, 0.014 in. thick,

$$w_c = 1.55 \times 1.12 = 1.74 \text{ watts per lb.,}$$

if the additional losses are taken equal to 12.0 per cent of the fundamental frequency loss (see page 432).

For an average current density, $A = 1600$ amperes per sq. in., the copper loss per pound plus stray load-losses,

$$\begin{aligned} w_k &= 2.58 A^2 k_5 \times 10^{-6} = 2.58 \times 1600^2 \times 1.10 \times 10^{-6} \\ &= 7.26 \text{ watts per lb.} \end{aligned}$$

The ratio of core weight to copper weight

$$\frac{G_c}{G_k} = \frac{w_k}{w_c} \frac{W_c}{W_k} = \frac{7.26}{1.74} 0.90 = 3.76.$$

With an output constant equal to 0.39 (see page 411) the net core section area

$$\begin{aligned} A_c &= C \sqrt{\frac{\text{Kva } G_c / G_k \times 10^{11}}{B A f}} = 0.39 \sqrt{\frac{1000 \times 3.76 \times 10^{11}}{90,000 \times 1600 \times 60}} \\ &= 81.4 \text{ sq. in.} \end{aligned}$$

The cruciform core section shown in Fig. 237 is chosen. The diameter of the core (see page 413),

$$D = \sqrt{\frac{A_c \times 4}{\pi f_{cs}}} = \sqrt{\frac{81.4 \times 4}{3.14 \times 0.70}} = 12.18 \text{ in.}$$

Make this 12.125 in. and the dimensions of the core section (see Fig. 259) are:

$$2a = 0.526 \times D = 0.526 \times 12.125 = 6.4; \text{ use } 6\frac{3}{8} \text{ in.}$$

$$2b = 0.85D = 0.85 \times 12.125 = 10.3; \text{ use } 10.25 \text{ in.}$$

With these dimensions, the net section of the core

$$A_c = [6\frac{3}{8} \times 10.25 + 6\frac{3}{8}(10.25 - 6\frac{3}{8})] 0.90 = 81.1 \text{ sq. in.}$$

With a density of 90,000 lines per sq. in., the total flux

$$\phi_t = A_c B = 81.1 \times 90,000 = 7300 \text{ kilo-lines.}$$

The number of turns per phase for the high-voltage and low-voltage windings

$$t_h = \frac{E_h \times 10^8}{4.44 f \phi_t} = \frac{7960 \times 10^8}{4.44 \times 60 \times 7300 \times 10^3} = 410; \text{ use } 415.$$

$$t_l = \frac{E_l}{E_h} t_h = \frac{575}{7960} 410 = 29.6; \text{ use } 30.0.$$

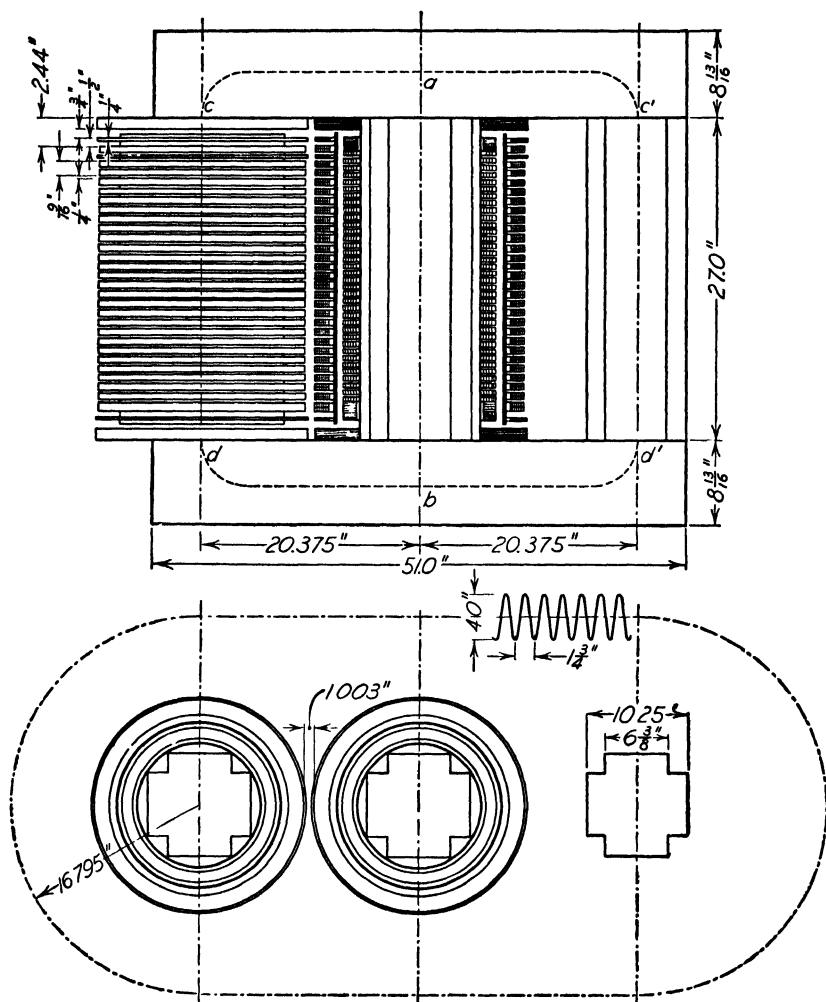


FIG. 259.

Using 30.0 turns per phase on the low-voltage winding, the number of high-voltage turns per phase will be equal to 415.

The voltage per turn

$$= \frac{7960}{415} = 19.2 \text{ volts.}$$

The full-load current per phase for the high-voltage winding

$$I_h = \frac{Kva \times 10^3}{3E_h} = \frac{1000 \times 10^3}{3 \times 7960} = 41.8 \text{ amperes,}$$

and for the low-voltage winding

$$I_l = \frac{Kva \times 10^3}{3E_l} = \frac{1000 \times 10^3}{3 \times 575} = 580.0 \text{ amperes.}$$

For the average current density assumed above, the section area of the conductor for the high-voltage winding

$$s_{ch} = \frac{I_h}{A} = \frac{41.8}{1600} = 0.0261 \text{ sq. in.}$$

The area of the window opening

$$h_w w_w = \frac{4s_{ch} t_h}{f_s} = \frac{4 \times 0.0261 \times 415}{0.18} = 241.0 \text{ sq. in.}$$

The copper space factor, f_s , is taken from the curves (Fig. 239).

If a window height equal to three times the width is chosen, the dimensions of the window are

$$h_w = \sqrt{3 \times 241} = 26.9 \text{ in.; use } 27.0 \text{ in.}$$

$$w_w = \frac{241}{27} = 8.94 \text{ in.; use } 9.0 \text{ in.}$$

With the flux density in the yoke equal to the flux density in the core legs, the height of the yoke

$$= \frac{81.1}{10.25 \times 0.90} = 8.80 \text{ in.; use } 8\frac{1}{8} \text{ in.}$$

The length of the yoke

$$\begin{aligned} l_y &= 2w_w + 3 \times 2b = 2 \times 9.0 + 3 \times 10.25 \\ &= 48.75 \text{ in.} \end{aligned}$$

The total core weight

$$\begin{aligned} G_c &= (2l_y A_c + 3h_w A_c) 0.272 \\ &= (2 \times 48.75 \times 81.1 + 3 \times 27.0 \times 81.1) 0.272 = 3940 \text{ lb.} \end{aligned}$$

With a clearance, β , between adjacent coils in the window opening equal to 1.0 in., the length of the average mean-turn for the windings

$$L_{av} = \left(D + \frac{w_w - \beta}{2} \right) \pi = \left(12.125 + \frac{9.0 - 1.0}{2} \right) \pi = 50.7 \text{ in.}$$

The approximate total copper weight

$$\begin{aligned} G_k &= 2 \times 3 t_h s_{ch} L_{av} \times 0.321 \\ &= 2 \times 3 \times 415 \times 0.0261 \times 50.7 \times 0.321 = 1060 \text{ lb.} \end{aligned}$$

The ratio of active material weight is then

$$\frac{G_e}{G_k} = \frac{3940}{1060} = 3.72.$$

This is approximately the same as the value previously determined.

DESIGN OF WINDINGS

Low-Voltage Winding.—The low-voltage winding is placed close to the core and, consequently, has a shorter mean-turn than the high-voltage coil. A higher current density can therefore be used without excessive copper loss. With a current density equal to 1700 amperes per sq. in.; the conductor section

$$s_{el} = \frac{580.0}{1700} = 0.341 \text{ sq. in.}$$

Five parallel conductors are used, each 0.182×0.365 in. bare, 0.206×0.386 in. insulated, and of 0.0645 sq. in. area. With this conductor, the current density in the low-voltage winding

$$A_l = \frac{580.0}{5 \times 0.0645} = 1800 \text{ amperes per sq. in.}$$

A helical-wound coil with transposed conductors such as shown in Fig. 245 is used. The five parallel conductors are wound on top of one another with a 0.25-in. duct between turns. The height of the low-voltage coil

$$= 30 \times 0.386 + 29 \times 0.25 = 18.83 \text{ in.,}$$

and the thickness of the coil

$$d_l = 5 \times 0.206 = 1.03 \text{ in.}$$

The insulation between the low-voltage winding and core consists of a pressed paper cylinder $\frac{1}{8}$ in. thick and a $\frac{1}{4}$ -in. duct, as shown in Fig. 259.

High-Voltage Winding.—The high-voltage winding is wound over the low-voltage coil and therefore has a large mean-turn. To avoid excessive copper loss, the current density should be less than for the

low-voltage coil. With 1400 amperes per sq. in., the section area of the conductor

$$s_{ch} = \frac{41.8}{1400} = 0.0292 \text{ sq. in.}$$

A conductor 0.114×0.258 in. bare, 0.133×0.276 in. insulated, 0.0286 sq. in. area is selected, and

$$A_h = \frac{41.8}{0.0286} = 1460 \text{ amperes per sq. in.}$$

Disc-type coils with two turns per layer are chosen for the high-voltage winding. One-half of the turns of each coil are wound backward to avoid cross-overs. The two sections of each coil are insulated from each other by fuller-board 0.013 in. thick. The number of coils per core leg and number of turns per coil are as follows:

Number of Coils per Core Leg	Turns per Section	Turns per Coil	Total Turns
25	8	16	400
1	4	8	8
1	4 and 3	7	7
Turns per core leg			<u>415</u>

The coils are insulated from each other by $\frac{1}{4}$ -in. ducts. Between the end coils, a wider duct is used as shown in Fig. 259. The width of the high-voltage coils

$$= 2 \times 0.275 + 0.013 = 0.563 \text{ in.}$$

If 10 per cent is allowed for the space required by the extra insulation on the end coils, then the width of the two end coils

$$= 0.563 \times 1.10 = 0.619 \text{ in.}$$

The total space required for the high-voltage coils in the direction of the window height

$$= 25 \times 0.563 + 2 \times 0.619 = 15.32 \text{ in.}$$

There are twenty-five $\frac{1}{4}$ -in. ducts and one $\frac{9}{16}$ -in. duct between the coils. The total height of the winding is then

$$= 15.32 + 6.81 = 22.13 \text{ in.}$$

A clearance of 2.44 in. at each end of the winding for insulating and supporting collars is satisfactory for a 7960-volt transformer winding.

The window height is therefore reduced to 27.0 in. and the total clearance at both ends of the winding

$$= 27.0 - 22.13 = 4.87 \text{ in.}$$

With the insulation between turns 0.013 in. thick, the thickness of the high-voltage coils

$$= 0.133 \times 8 + 7 \times 0.013 = 1.155 \text{ in.}$$

The insulation between high-voltage and low-voltage windings consists of a $\frac{3}{8}$ -in. duct, plus $\frac{3}{16}$ -in. pressed paper insulating cylinder, plus a $\frac{1}{2}$ -in. duct. The total depth of the windings per core leg is then

$$= 0.938 + 0.375 + 1.03 + 1.063 + 1.155 = 4.561 \text{ in.}$$

The clearance between adjacent coils in the window opening should preferably be about 1.0 in. for a transformer of this size. The window width is therefore increased to 10.125 in., and the clearance between coils equals 1.003 in.

The dimensions of the window are then

$$h_w = 27.0 \text{ in.}, \quad w_w = 10.125 \text{ in.}$$

The total flux

$$\phi_t = \frac{E_h \times 10^8}{4.44 f l_h} = \frac{7960 \times 10^8}{4.44 \times 60 \times 415} = 7200 \text{ kilo-lines.}$$

The flux density in the core

$$B = \frac{7200 \times 10^3}{81.1} = 88.7 \text{ kilo-lines.}$$

Since the dimensions of the window have been changed from the values first determined, it will be necessary to recalculate the weight of the core. The length of the yoke

$$l_y = 2 \times 10.125 + 3 \times 10.25 = 51.0 \text{ in.},$$

and

$$G_c = (2 \times 51.0 \times 81.1 + 3 \times 27.0 \times 81.1) 0.272 = 4010 \text{ lb.}$$

The length of the mean-turn for the low-voltage winding

$$l_l = \pi[12.125 + (2 \times 0.375) + 1.03] = 43.7 \text{ in.},$$

and for the high-voltage winding

$$\begin{aligned} l_h &= \pi[12.125 + (2 \times 0.375) + (2 \times 1.03) + (2 \times 1\frac{1}{8}) + 1.155] \\ &= 57.2 \text{ in.} \end{aligned}$$

The weight of the copper in each winding

$$G_l = 3t_l s_{cl} L_l \times 0.321$$

$$= 3 \times 30 \times 0.3225 \times 43.7 \times 0.321 = 407.0 \text{ lb.},$$

$$G_h = 3t_h s_{ch} L_h \times 0.321$$

$$= 3 \times 415 \times 0.0286 \times 57.2 \times 0.321 = 655.0 \text{ lb.}$$

The total copper weight

$$G_k = 407 + 655 = 1062 \text{ lb.}$$

The final value for the ratio of the weights of the active material is therefore

$$\frac{G_c}{G_k} = \frac{4010}{1062} = 3.77.$$

The design constant for this transformer is then

$$C = \frac{A_c}{\sqrt{\frac{\text{Kva } G_c / G_k \times 10^{11}}{BAf}}} = \frac{81}{\sqrt{\frac{1000 \times 3.77 \times 10^{11}}{88,700 \times 1630 \times 60}}} = 0.391.$$

The copper space factor

$$f_s = \frac{2(s_{ch}t_h + s_{cl}t_l)}{h_w w_w} = \frac{2(0.0286 \times 415 + 0.3225 \times 30)}{27.0 \times 10.125} = 0.158.$$

From the loss curve for 0.014 in., 2.5 per cent silicon sheet steel, the loss per pound for a flux density of 88.7 kilo-lines per sq. in.

$$w_c = 1.52 \times 1.12 = 1.70 \text{ watts.}$$

The total core loss

$$W_c = w_c G_c = 1.70 \times 4010 = 6820 \text{ watts.}$$

The I^2R loss plus stray load-loss in each winding at 75° C.

$$W_l = 2.58 A_l^2 G_l k_5 \times 10^{-6}$$

$$= 2.58 \times 1800^2 \times 407 \times 1.10 \times 10^{-6} = 3740 \text{ watts.}$$

$$W_h = 2.58 A_h^2 G_h k_5 \times 10^{-6}$$

$$= 2.58 \times 1460^2 \times 655 \times 1.10 \times 10^{-6} = 3960 \text{ watts.}$$

The total copper loss plus stray load-loss $W_k = 3740 + 3960 = 7700$.

The ratio of losses

$$\frac{W_c}{W_k} = \frac{6820}{7700} = 0.886.$$

The effective resistance per phase of the windings at 75° C.

$$R_l = \frac{W_l}{3I_l^2} = \frac{3740}{3 \times 580^2} = 0.0037 \text{ ohm per phase,}$$

$$R_h = \frac{W_h}{3I_h^2} = \frac{3960}{3 \times 41.8^2} = 0.756 \text{ ohm per phase.}$$

The total resistance in terms of the high-voltage winding

$$R_t = \frac{3740 + 3960}{3 \times 41.8^2} = 1.47 \text{ ohms per phase.}$$

The per cent resistance drop

$$P_r = \frac{I_h R_t}{E_h} 100 = \frac{41.8 \times 1.47}{7960} 100 = 0.771 \text{ per cent.}$$

Formula 222 must be used to calculate the per cent reactance. gives the reactance drop per phase for three-phase transformers

$$\begin{aligned} P_x &= \frac{21.5 f I_h^2 I_h}{h E_h 10^6} \left(\frac{d_h + d_l}{3} + d \right) \frac{L_h + L_l}{2} \\ &= \frac{21.5 \times 60 \times 415^2 \times 41.8}{22.13 \times 7960 \times 10^6} \left(\frac{1.155 + 1.03}{3} + 1.063 \right) \times \\ &\quad \frac{57.2 + 43.7}{2} \\ &= 4.76 \text{ per cent.} \end{aligned}$$

The per cent regulation for 100 per cent power factor

$$= P_r + \frac{P_x^2}{200} = 0.771 + \frac{4.76^2}{200} = 0.884 \text{ per cent,}$$

and for 80 per cent power factor load

$$\begin{aligned} &= \cos \theta P_r + \sin \theta P_x + \frac{(\cos \theta P_x - \sin \theta P_r)^2}{200} \\ &= 0.80 \times 0.771 + 0.60 \times 4.76 + \frac{(0.80 \times 4.76 - 0.60 \times 0.771)^2}{200} \\ &= 3.53 \text{ per cent.} \end{aligned}$$

An approximate method is used to calculate the magnetizing current for a three-phase transformer. The mean length of the magnetic circuit

(see Fig. 259) is divided into three parts—the length, ab , from the center of the top yoke through the center core leg to the center of the bottom yoke and the length $acdb$ and $ac'd'b$ through the yokes and the outside core legs. The mean length of the path ab

$$= 27.0 + 8.81 = 35.81 \text{ in.},$$

and of the paths $acdb$ and $ac'd'b$

$$= 2(10.125 + 10.25) + 8.81 + 27 = 76.56 \text{ in.}$$

The magnetizing current for the path ab

$$I_m = \frac{35.81 \times 26 + (110 \times 2)}{\sqrt{2} \times 415} = 1.96 \text{ amperes},$$

and for paths $acdb$ and $ac'd'b$

$$I_m = \frac{76.56 \times 26 + (110 \times 2)}{\sqrt{2} \times 415} = 3.77 \text{ amperes.}$$

The core loss current

$$I_w = \frac{W_c}{E_h 3} = \frac{6820}{7960 \times 3} = 0.286 \text{ ampere.}$$

The no-load current for each of the paths

$$= \sqrt{1.96^2 + 0.286^2} = 1.98 \text{ amperes}$$

$$= \sqrt{3.77^2 + 0.286^2} = 3.78 \text{ amperes,}$$

and the no-load current for the transformer

$$I_0 = \frac{2 \times 3.78 + 1.98}{3} = 3.18 \text{ amperes}$$

$$= \frac{3.18}{41.8} 100 = 7.60 \text{ per cent.}$$

The stray load-losses are estimated at 10 per cent of the total I^2R losses (see page 432). The efficiency and losses for various loads at 100 per cent power factor are as follows:

	$\frac{1}{4}$	$\frac{2}{4}$	$\frac{3}{4}$	$\frac{4}{4}$	$\frac{5}{4}$
I^2R + stray load-losses.	481	1,924	4,330	7,700	12,020
Core losses.....	6,820	6,820	6,820	6,820	6,820
Total losses.....	7,301	8,744	11,150	14,520	18,840
Output.....	250,000	500,000	750,000	1,000,000	1,250,000
Input.....	257,301	508,744	761,150	1,014,520	1,268,860
Efficiency.....	97.3	98.3	98.5	98.6	98.6

The total radiating surface of the core and windings is calculated as follows:

$$\text{Core legs: } (4 \times 6.375 + 4 \times 3.875)3 \times 27 = 3,320 \text{ sq. in.}$$

$$\begin{aligned} \text{Yokes: } (4 \times 8.81 \times 51.0) + (10.25 \times 51.0 \times 2) \\ + (4 \times 8.81 \times 10.25) = 3,205 \text{ sq. in.} \end{aligned}$$

$$\text{Low-voltage coils: } 2(18.83 + 1.03) \times 43.7 \times 3 = 5,210 \text{ sq. in.}$$

$$\text{High-voltage coils } 2(0.563 + 1.155) 57.2 \times 27 \times 3 = 15,900 \text{ sq. in.}$$

$$\begin{aligned} \text{The total radiating surface} &= 27,635 \text{ sq in.,} \\ \text{and the surface per watt} \end{aligned}$$

$$\frac{S}{W} = \frac{27,635}{14,520} = 1.90.$$

With a corrugated sheet-steel tank, the surface per watt loss should be from 6.0 to 9.0 (see page 433). If 7.5 is used, the total tank surface

$$S_t = (W_c + W_k) 7.5 = 14,520 \times 7.5 = 109,000 \text{ sq. in.}$$

The shape of the tank section and the position of the transformer in the tank are shown in Fig. 259. A corrugated tank wall with a pitch of 1.75 in., depth of 4.0 in., and a mean length of 5.0 in. is selected. With a clearance of 5.5 in. between the outside of the coils and the inside of the tank, the perimeter of the tank on the center line of the corrugated tank wall

$$= 4(10.125 + 10.25) + \pi \times 29.58 = 174.4 \text{ in.}$$

The depth of the hot oil

$$= \frac{109,000}{174.4 \times 5.0} = 125.0 \text{ in.}$$

The volume of the tank

$$\begin{aligned} &= \left[2(10.125 + 10.25)29.58 + \frac{\pi}{4} 29.58^2 \right] 125.0 \\ &= 236,000 \text{ cu. in.} \end{aligned}$$

The volume of the active materials

$$= \frac{4010}{0.272} + \frac{1062}{0.321} = 18,060 \text{ cu. in.}$$

The volume of oil required = $236,000 - 18,060 = 217,940$ cu. in. This value is slightly high because the volume of the insulating material,

TRANSFORMER DESIGN SHEET

Kva 1000	Phase 3	Cycles 60	Volts {HV 7 960 LV, 575	Phase Volts {HV 7 960 LV 575
Line Amperes {HV 72 6 LV 1005 0			Phase Amperes {HV, 41 8 LV 580 0	
Type Circular Core			Type of Cooling Self Oil	

CORE			Per cent			
Sheet steel		0 014 3 0% Si	Resistance			0 771
Output constant			Reactance			4 76
Core leg	Center	Outside	Impedance			4 81
Area	81 1		Power factor	80	100	
Diameter	12 1		Regulation	3 53	0 884	
Dimensions	2a = 6 1 2b = 10 25		Losses			
Density	88 700		Total core			6820
Weight	1780		Stray load			700
Core factor		0 70	Total copper			7700
Yoke			Per cent			
Area		81 1	Load	25	50	75
Dimensions		8 81 × 10 25	Efficiency	97 3	98 3	98 5
Density		88 700	Square inches per watt			1 90
Weight		2240	Ratio of losses			0 886
Copper space factor f_s		0 158	Ratio of weights			3 77
Window dimensions		10 125 × 27 0				
Lamination factor k_1		0 90				
CORE AND WINDINGS			TANK			
Mean length of flux path		35 81 & 76 56	Type of tank corrugated sheet steel	1 75 × 4 0		
Total ampere turns		1150 & 2210	Square inches per watt			7 5
Magnetizing current		1 96 & 3 77	Total wetted surface			109 000
Core loss current		0 286	Depth of oil			125 0
Exciting current			Gallons of oil			944 0
Amperes		3 18	Weight of oil			6600
Per cent		7 6	Cooling coils			
			Size			
			Length			
			Surface			
			Water gallons per minute			

WINDINGS	HIGH VOLTAGE	LOW VOLTAGE
Type of winding	Disc coils	Helical
Connections	Delta	Delta
Conductor		
Dimensions	0 133 × 0 276 d c c	0 206 × 0 386 d c c
Section	0 0286	0 0645
Number in parallel	None	5
Current density	1460	1800
Turns per phase	415	30
Coils		
Total number	81	3
Per core leg	27	1
Turns		
Per coil	*	30
Per layer	†	30
Number of layers	2-sections	1
Coil		
Connections	Series	
Dimensions	0 563 × 1 155	1 03 × 18 83
Ducts number and size	25 1 & 1 1/4	0 25 Between turns
Insulation		
Layer	0 013	
Core and coil		
HV and LV	1/2 D + 1/4 PB + 1/2 D	1/2 PB + 1/2 D
Voltage per turn	19 2	
Maximum voltage between layers	307	
Length of mean turn	57 2	43 7
Copper		
Weight	655	407
Loss	3960	3740
Resistance 75° C	0 756	0 0037
Per cent end turns with extra insulation	5 08	

Remarks * 25 coils 16 turns † 25 coils 8 turns per section

1 coil 8 turns 1 coil 4 turns per section

1 coil 7 turns 1 coil 3 to 4 turns per section

Designed by J H Kulhmann

Date

core clamps, coil supports, leads, etc., has not been included in calculating the volume of the transformer.

The number of gallons of oil required

$$= \frac{217,940}{231} = 944.0.$$

The total weight of the oil

$$= 7.0 \times 944.0 = 6600.0 \text{ lb.}$$

The core clamps, coil, and lead supports are not shown in the assembly drawing of the transformer, Fig. 259.

Design No. 3: *Design of 10-Kva, Single-Phase, Four-Part Distributed-Core-Type Distribution Transformer.*—The complete rating is as follows: 10 kva, single-phase, 60 cycles, 2300 volts primary to 115 and 230 volts secondary. The transformer is to be of the self-oil-cooled type and must carry its rated load continuously with a temperature rise not to exceed 55° C. The efficiency and regulation at full-load and 100 per cent power factor should be approximately 97.5 per cent and 1.95 per cent respectively. The ratio of the core loss to the full-load copper loss should be approximately 0.40. The transformer must also be suitable for operation at 2400 and 2200 volts.

For the method of punching the laminations and assembling the core of this type of transformer see Fig. 228. The weight of the core is proportioned approximately as follows: center leg 20 per cent, yokes 50 per cent, and outside legs 30.0 per cent of the total weight. The flux densities in the yokes and outside legs are generally 54.0 and 67.0 per cent, respectively, of the density in the center leg. If the flux density in the center leg is assumed equal to 75,000 lines per sq. in., then the density in the yokes and outside legs should be approximately 40,500 and 50,200 lines per sq. in. respectively.

From the curve Fig. 234, the total flux for a 10-kva transformer

$$\phi_t = 900 \text{ kilo-lines.}$$

The section area of the center leg for the assumed density of 75 kilolines per sq. in.

$$A_c = \frac{\phi_t}{B} = \frac{900 \times 10^3}{75 \times 10^3} = 12.0 \text{ sq. in.}$$

The center core section is square, and the dimensions

$$= \sqrt{\frac{12.0}{0.90}} = 3.65; \text{ use } 3.68 \text{ in.}$$

The core punchings are L-shaped and are assembled as shown in Fig. 260. The dimensions for the section of the outside legs are fixed by the center leg dimensions (see Fig. 260) and are

$$= 1.84 \times 2.76 \text{ in.}$$

The flux density in the yoke has been assumed equal to 40,500 lines per sq. in. The section area is then

$$\frac{900,000}{4 \times 40,500} = 5.55 \text{ sq. in.}$$

The height of the yoke section is then

$$= \frac{5.55}{2.76 \times 0.90} = 2.24; \text{ use } 2.25 \text{ in.}$$

The number of turns for the high- and low-voltage winding

$$t_h = \frac{E_h \times 10^8}{4.44 f \phi_t} = \frac{2400 \times 10^8}{4.44 \times 60 \times 900 \times 10^3} = 1000.$$

$$t_l = \frac{E_l}{E_h} t_h = \frac{240}{2400} 1000 = 100.$$

The flux densities assumed above are for the highest voltage at which the transformer is to operate; therefore 2400 volts is used for the calculation of the number of turns in the winding.

To calculate the maximum current in the windings, the lowest voltage at which the transformer is to operate must be used. The full-load current in the windings

$$I_h = \frac{10 \times 10^3}{2200} = 4.55 \text{ amperes,}$$

and

$$I_l = \frac{t_h}{t_l} I_h = \frac{1000}{100} 4.55 = 45.5 \text{ amperes.}$$

A current density of 1000 amperes per sq. in. is assumed. The section area of the conductor for high-voltage and low-voltage winding

$$s_{eh} = \frac{I_h}{A} = \frac{4.55}{1000} = 0.00455 \text{ sq. in.,}$$

$$s_{el} = \frac{I_l}{A} = \frac{45.5}{1000} = 0.0455 \text{ sq. in.}$$

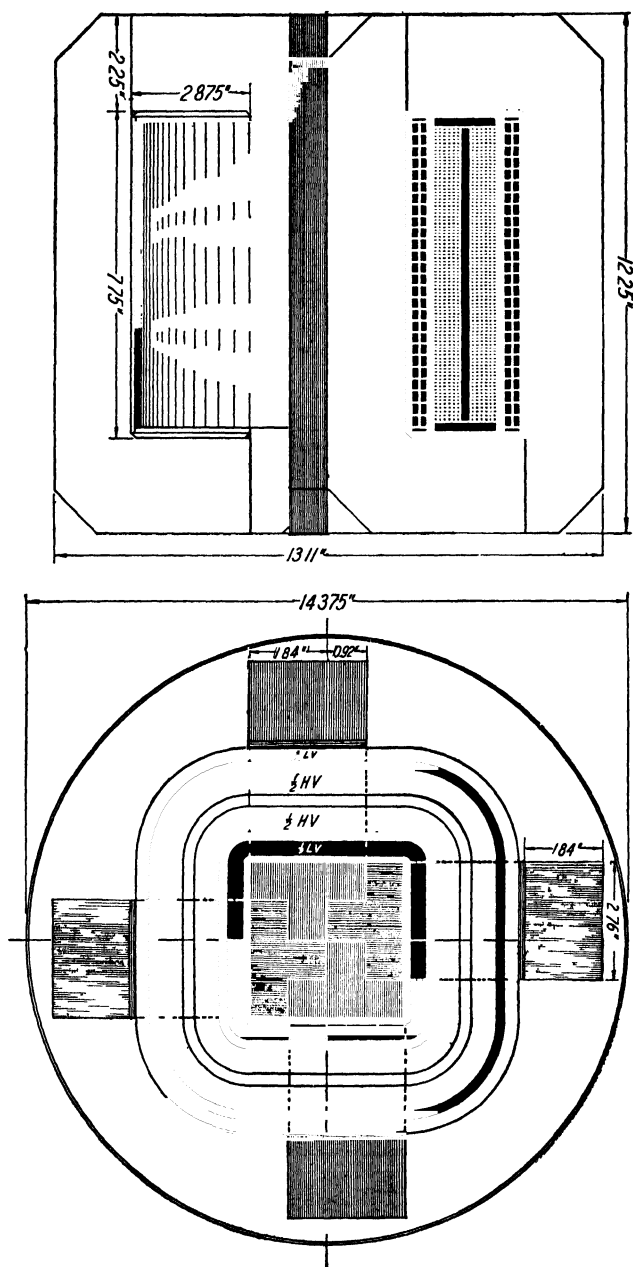


Fig. 260.

The area of the window opening

$$h_w w_w = \frac{2t_{hsch}}{f_s} = \frac{2 \times 1000 \times 0.00455}{0.40}$$

$$= 22.8 \text{ sq. in.}$$

The copper space factor, f_s , is taken from the curves of Fig. 239.

The ratio of window height to width may be taken equal to 3.
The dimensions of the window

$$h_w = \sqrt{3 \times 22.8} = 8.28; \text{ use } 8.25 \text{ in.,}$$

$$w_w = \frac{22.8}{8.25} = 2.76; \text{ use } 2.75 \text{ in.}$$

The mean length of the center and outside leg can be taken equal to the window height. The respective weights are then

$$\text{Center leg} = 8.25 \times 12.2 \times 0.272 = 27.4 \text{ lb.,}$$

$$\text{Outside legs} = 8.25 \times 4.57 \times 4 \times 0.272 = 41.0 \text{ lb.}$$

The mean length of the yoke is 11.64 in. (see Fig. 260), and the weight

$$\text{Yokes} = 11.64 \times 5.59 \times 4 \times 0.272 = 70.8 \text{ lb.}$$

The total core weight

$$G_c = 139.2 \text{ lb.}$$

The mean length of turn for the windings

$$L_{av} = 4 \times 3.68 + \pi(2.75 - 0.25) = 22.56 \text{ in.}$$

The approximate copper weight

$$G_k = 22.56 \times 1000 \times 0.00455 \times 2 \times 0.321 = 65.8 \text{ lb.}$$

The ratio of core weight to copper weight is then

$$\frac{G_c}{G_k} = \frac{139.2}{65.8} = 2.12.$$

	Density, Kilo-lines per Square Inch	Loss per Pound, Watts	Weight, Pounds	Total Loss, Watts
Center legs.....	73.8	1.008	27.4	27.6
Outside legs.....	49.2	0.471	41.0	19.3
Yokes.....	40.2	0.358	70.8	25.3
Total core loss.....				72.2

The losses should now be calculated to determine whether the selected core dimensions will give approximately 0.40 for the ratio of losses. The additional core losses will be assumed equal to 12 per cent of the fundamental frequency losses.

The approximate total copper loss

$$\begin{aligned} W_k &= 2.58A^2G_k \times 10^{-6} \\ &= 2.58 \times 1000^2 \times 65.8 \times 10^{-6} = 169.0 \text{ watts.} \end{aligned}$$

The ratio of loss is then

$$\frac{W_c}{W_k} = \frac{72.2}{169.0} = 0.427.$$

DESIGN OF WINDINGS

Low-Voltage Winding.—The conductor chosen for the low-voltage winding has the following dimensions: 0.162×0.258 in. bare, 0.184×0.278 in. insulated, 0.0410 sq. in. area. The secondary winding must be so arranged that 115 and 230 volts can be obtained at rated capacity. To accomplish this, the low-voltage coil is divided into two equal sections, which are connected in parallel for 115 volts and in series for 230 volts. The total number of low-voltage turns

$$t_l = 100.$$

The low-voltage coils will, therefore, be wound with two layers of 25 turns each, and one of the coils will be placed on the inside of the high-voltage coil and the other on the outside (see Fig. 260).

For layer-wound coils, the space of one turn must be allowed for the start of the winding. The total height of the coils is then

$$= 0.278 \times 26 = 7.22 \text{ in.}$$

With a window height equal to 8.25 in., the space for insulation at each end of the winding equals 0.515 in., which is larger than necessary. The window can not be changed until the space required by the high-voltage winding has been determined.

The voltage per turn

$$= \frac{240}{100} = 2.40 \text{ volts,}$$

and the maximum voltage between layers

$$= 2 \times 25 \times 2.4 = 120 \text{ volts.}$$

Paper insulation 0.024 in. thick will be used between layers of the low-voltage coils.

The depth of each low-voltage coil is then

$$= 2 \times 0.184 + 0.024 = 0.392 \text{ in.}$$

The insulation between the core and winding consists of a paper channel 0.10 in. thick.

High-Voltage Winding.—A No. 13 sq. d.c.c. copper conductor is selected from the copper table. The dimensions of the conductor are: 0.072×0.072 in. bare, 0.083×0.083 in. insulated, 0.00465 sq. in. area. The high-voltage coil is divided into two sections by a $\frac{1}{4}$ -in. duct through which the high-voltage leads are brought out. The total number of turns

$$t_h = 1000.$$

Use 12 layers: 11 of 84 turns each, and one of 76 turns.

The height of the high-voltage coil is then

$$= 0.083 \times 85 = 7.06 \text{ in.}$$

The maximum voltage between layers

$$= 2.40 \times 2 \times 84 = 403.2 \text{ volts.}$$

Two layers of treated paper insulation, each 0.012 in. thick, are used between layers. The depth of the coil plus the duct is then

$$= (12 \times 0.083) + (10 \times 0.024) + 0.25 = 1.486 \text{ in.}$$

The insulation between the yokes and the ends of the coils consists of a mica pad $\frac{1}{8}$ in. thick plus press-board space blocks $\frac{1}{8}$ in. thick for the low-voltage coils, and plus press-board space blocks 0.22 in. thick for the high-voltage coils (see Fig. 260). The height of the coils plus insulation is then:

$$\text{Low-voltage, } 7.22 + 2(0.125 + 0.125) = 7.72 \text{ in.}$$

$$\text{High-voltage, } 7.06 + 2(0.125 + 0.22) = 7.75 \text{ in.}$$

The window height is therefore reduced from 8.25 in. to 7.75 in.

The insulation between the high-voltage and low-voltage windings consists of a mica pad 0.15 in. thick. The total depth of the winding

$$= 0.10 + 0.392 + 0.15 + 1.486 + 0.15 + 0.392 + 0.10 = 2.77 \text{ in.}$$

The clearance between the outside core leg and the winding is too small. The window is therefore made 2.875 in. wide and the clearance = 0.105 in.

OPERATING CHARACTERISTICS

The operating characteristics will be calculated for the normal voltage rating, that is, 2300 volts to 230/115 volts.

The total flux

$$\phi_t = \frac{E_h \times 10^8}{4.44 f t_h} = \frac{2300 \times 10^8}{4.44 \times 60 \times 1000} = 863 \text{ kilo-lines.}$$

The dimensions, flux densities, weights, and losses for the various parts of the magnetic circuit are as follows:

	Section Area, Square Inches	Flux Density, Kilo-lines	Weight, Pounds	Loss per Pound, Watts	Total Loss, Watts
Center leg.....	12.2	70.7	25.7	0.93	23.9
Outside leg.....	4.57	47.2	38.6	0.448	17.3
Yokes.....	5.59	38.6	67.0	0.342	24.7
Total core loss.....					65.9

The additional losses have been estimated at 12 per cent of the fundamental frequency loss.

The secondary winding is symmetrical about the primary winding. The length of the mean-turn of the high-voltage coil is therefore also the average mean-turn for the low-voltage winding.

$$L_h = 4 \times 3.68 + \pi(2 \times 0.10 + 2 \times 0.392 + 2 \times 0.15 + 1.486) \\ = 23.42 \text{ in.}$$

The copper weight for the two windings

$$G_l = 23.42 \times 100 \times 0.041 \times 0.321 = 30.9 \text{ lb.}$$

$$G_h = 23.42 \times 1000 \times 0.00465 \times 0.321 = 35.0 \text{ lb.}$$

The ratio of core weight to copper weight

$$\frac{G_c}{G_k} = \frac{136.5}{65.9} = 2.07.$$

The copper space factor

$$f_s = \frac{s_{ch} t_h + s_{cl} t_l}{h_w w_w} = \frac{0.00465 \times 1000 + 0.041 \times 100}{7.75 \times 2.875} = 0.393.$$

The full-load current in the windings for the normal voltage rating

$I_l = 43.5$ amperes, and $I_h = 4.35$ amperes.

The current densities

$$A_l = \frac{43.5}{0.041} = 1060 \text{ amperes per sq. in.,}$$

$$A_h = \frac{4.35}{0.00465} = 935 \text{ amperes per sq. in.}$$

The I^2R losses plus stray load-losses at 75°C .

$$W_l = 2.58 A_l^2 G_l k_5 10^{-6} = 2.58 \times 1060^2 \times 30.9 \times 1.10 \times 10^{-6} = 98.2 \text{ watts,}$$

$$W_h = 2.58 \times 935^2 \times 35.0 \times 1.10 \times 10^{-6} = 86.4 \text{ watts.}$$

The ratio of losses

$$\frac{W_c}{W_k} = \frac{65.9}{184.6} = 0.357.$$

The effective resistance of the windings at 75°C .

$$R_l = \frac{W_l}{I_l^2} = \frac{98.2}{43.5^2} = 0.052 \text{ ohm,}$$

$$R_h = \frac{W_h}{I_h^2} = \frac{86.4}{4.35^2} = 4.54 \text{ ohms.}$$

The total resistance in terms of the high-voltage winding

$$R_t = \frac{98.2 + 86.4}{4.35^2} = 9.75 \text{ ohms.}$$

The per cent resistance drop

$$P_r = \frac{I_h R_t}{F_{th}} 100 = \frac{4.35 \times 9.75}{2300} 100 = 1.85 \text{ per cent.}$$

Formula 223 must be used to calculate the per cent reactance drop,

$$\begin{aligned} P_x &= \frac{10.8 f k_h^2 I_h}{h E_h \times 10^6} \left(\frac{d_h + d_l}{6} + d \right) L_h \\ &= \frac{10.8 \times 60 \times 1000^2 \times 4.35}{7.06 \times 2300 \times 10^6} \left(\frac{1.51 + 0.784}{6} + 0.15 \right) 23.46 \\ &= 2.17 \text{ per cent.} \end{aligned}$$

The per cent impedance drop

$$P_z = \sqrt{P_r^2 + P_x^2} = \sqrt{1.85^2 + 2.17^2} = 2.85 \text{ per cent.}$$

The per cent regulation for 100 per cent power factor

$$= P_r + \frac{P_x^2}{200} = 1.85 + \frac{2.17^2}{200} = 1.87 \text{ per cent,}$$

and for 80 per cent power factor

$$\begin{aligned} &= \cos \theta P_r + \sin \theta P_x + \frac{(\cos \theta P_x - \sin \theta P_r)^2}{200} \\ &= 0.80 \times 1.85 + 0.60 \times 2.17 + \frac{(0.80 \times 2.17 - 0.60 \times 1.85)^2}{200} \\ &= 2.782 \text{ per cent.} \end{aligned}$$

The approximate mean length of the flux path for the various parts of the magnetic circuit and the corresponding number of ampere-turns are as follows:

	Flux Density, Kilo-lines	Mean Length, Inches	Ampere-turns per Inch	Ampere-turns
Center leg.....	70.7	7.75	7.1	55.0
Outside leg.....	47.2	7.75	2.9	22.5
Yokes.....	38.6	11.89	2.2	26.2
Joints.....	38.6	12.0
Total ampere-turns.....	115.7

The magnetizing current

$$I_m = \frac{AT}{\sqrt{2} \times t_h} = \frac{115.7}{1.42 \times 1000} = 0.0815 \text{ ampere.}$$

The core loss current

$$I_w = \frac{W_c}{E_h} = \frac{65.9}{2300} = 0.0286 \text{ ampere.}$$

The exciting current

$$\begin{aligned} I_0 &= \sqrt{I_m^2 + I_w^2} = \sqrt{0.0815^2 + 0.0286^2} = 0.0864 \text{ ampere} \\ &= \frac{0.0864 \times 100}{4.35} = 1.98 \text{ per cent of the full-load current.} \end{aligned}$$

The stray load-losses are estimated equal to 10 per cent of the total I^2R losses (see page 419). The losses and efficiencies for various loads at 100 per cent power factor are as follows:

	$\frac{1}{4}$	$\frac{2}{4}$	$\frac{3}{4}$	$\frac{4}{4}$	$\frac{5}{4}$
I^2R + stray load-losses.....	11.52	46.10	103.8	184.6	288.2
Core losses.....	65.90	65.90	65.9	65.9	65.9
Total losses.....	77.42	112.00	169.7	250.5	354.1
Output.....	2500.00	5000.00	7500.0	10,000.0	12,500.0
Input.....	2577.42	5112.00	7669.7	10,250.5	12,854.1
Efficiency, per cent.....	97.1	97.8	97.8	97.6	97.2

The total radiating surface of core and coils is calculated as follows:

$$\text{Outside legs: } (1.84 + 2.76)2 \times 7.75 \times 4 = 285.0 \text{ sq. in.}$$

$$\begin{aligned} \text{Yokes: } (2.25 + 2.76)2 \times 11.89 \times 4 + 2.25 \times 2.76 \\ \times 4 \times 2 = 527.0 \text{ sq. in.} \end{aligned}$$

$$\begin{aligned} \text{Windings: } 23.42 \times 7.06 + 32.12 \times 7.22 + 23.42 \\ \times 2.77 \times 2 = \frac{527.0 \text{ sq. in.}}{1339.0 \text{ sq. in.}} \end{aligned}$$

The radiating surface per watt loss

$$\frac{S}{W} = \frac{1339.0}{250.5} = 5.34 \text{ (see page 432).}$$

A plain sheet-steel tank will be used. The surface per watt loss should then be about 4.50 (see page 433). The total area of the tank walls

$$S_t = (W_c + W_k)S/W = 250.5 \times 4.5 = 1130.0 \text{ sq. in.}$$

The tank is circular in section, as shown in Fig. 260. The over-all dimensions of the transformer are:

$$\text{Width: } 3.68 + 2 \times 2.875 + 2 \times 1.84 = 13.11 \text{ in.}$$

$$\text{Height: } 7.75 + 2 \times 2.25 = 12.25 \text{ in.}$$

Make the inside diameter of the tank 14.25 in., then the outside diameter is 14.375 in., if the thickness of the wall is $\frac{1}{8}$ in.

The depth of the hot oil

$$= \frac{1130.0}{\pi \times 14.375} = 25.0 \text{ in.}$$

TRANSFORMER DESIGN SHEET

Kva, 10 Phase Single Cycles 60 Volts $\left\{ \begin{array}{l} \text{HV} \\ \text{LV} \end{array} \right. \begin{array}{l} 2300 \\ 115 \text{ 230} \end{array}$ Phase Volts $\left\{ \begin{array}{l} \text{HV} \\ \text{LV} \end{array} \right. \begin{array}{l} \\ \end{array}$
 Line Amperes $\left\{ \begin{array}{l} \text{HV} \\ \text{LV} \end{array} \right. \begin{array}{l} 4 \text{ 35} \\ 87 \text{ 0-43 5} \end{array}$ Phase Amperes $\left\{ \begin{array}{l} \text{HV} \\ \text{LV} \end{array} \right. \begin{array}{l} \\ \end{array}$
 Type Four Part Distributed Core Type of Cooling Self Oil

CORE			Per cent			
Sheet steel		0 014 4 5% Si	Resistance			1 85
Total flux		863 0 K L	Reactance			2 17
Core leg	Center	Outside	Impedance			2 85
Area	12 2	4 57	Power factor		80	100
Diameter			Regulation		2 78	1 87
Dimensions	3 68 × 3 68	1 84 × 2 76	Losses			
Density	70 7	47 2	Total core			65 9
Weight	25 7	38 6	Stray load			16 77
Core factor			Total copper			167 70
Yoke			Per cent			
Area		5 59	Load	25	50	75
Dimensions		2 25 × 2 76	Efficiency	97 1	97 8	97 8
Density		38 6	Square inches per watt			5 34
Weight		72 2	Ratio of losses			0 357
Copper space factor f_c		0 393	Ratio of weights			2 07
Window dimensions		2 875 × 7 75	TANK			
Lamination factor k_l		0 90	Type of tank	plain sheet steel		
CORE AND WINDINGS			Square inches per watt			4 50
Mean length of flux path		7 75 7 75 11 89	Total wetted surface			1130 0
Total ampere turns		55 0 22 5 26 2	Depth of oil			25 0
Magnetizing current		0 0815	Gallons of oil			14 2
Core loss current		0 0286	Weight of oil			99 4
Exciting current			Cooling coils			
Amperes		0 0864	Size			
Per cent		1 98	Length			
			Surface			
			Water gallons per minute			

WINDINGS	HIGH VOLTAGE	LOW VOLTAGE
Type of winding	Concentric	Concentric
Connections		
Conductor		
Dimensions	0 083 × 0 083 d c c	0 184 × 0 276 d c c
Section	0 00465	0 041
Number in parallel	None	None
Current density	935	1060
Turns per phase	1000	100
Coils		
Total number	1	2
Per core leg	1	2
Turns		
Per coil	1000	50
Per layer	11 84 and 1 76	25
Number of layers	12	2
Coil		
Connections		Series Parallel
Dimensions	1 51 × 7 06	0 392 × 7 22
Ducts number and size	1 1	
Insulation		
Layer	0 024	0 024
Core and coils		0 10 P B
H V and L V	0 15 mica pad	
Voltage per turn	2 4	2 4
Maximum voltage between layers	403 2	120
Length of mean turn	23 42	23 42
Copper		
Weight	35 0	30 9
Loss	78 5	89 2
Resistance 75° C	4 14	0 0472
Per cent end turns with extra insulation		

Remarks

Designed by J H Kuhlmann

Date

The volume of the tank

$$= \frac{\pi}{4} \times 14.25^2 \times 25.0 = 3980.0 \text{ cu. in.}$$

The volume of the transformer, if calculated from the active material weights with no allowance for insulation, core clamps, etc.,

$$= \frac{136.5}{0.272} + \frac{65.9}{0.321} = 707.0 \text{ cu. in.}$$

The volume of oil required

$$= 3980.0 - 707.0 = 3273.0 \text{ cu. in.}$$

The number of gallons of oil

$$= 3273.0 \times 0.00433 = 14.2.$$

The weight of the oil

$$= 14.2 \times 7.0 = 99.4 \text{ lb.}$$

An assembly drawing of the transformer without core clamps and lead supports is shown in Fig. 260.

Design No. 4: *Design of Power-Supply Transformer for Electronic Amplifier.*—The primary winding of this transformer is to be for 115 volts at 60-cycle frequency. The secondary is to have three windings, one for 800 volts with center top and 0.15-ampere capacity, the second for 12.6 volts with center top and 2.0-ampere capacity, and the third for 5 volts and 1.0-ampere capacity. The temperature rise for continuous duty and rated output must not exceed 55° C.

The volt-ampere rating of the transformer

$$VA = 800 \times 0.15 + 12.6 \times 2.0 + 5 \times 1.0 = 150.2.$$

For an efficiency of 90 per cent the input

$$= \frac{150.2}{0.90} = 167 \text{ volt-amperes.}$$

The input or primary current

$$I_p = \frac{167}{115} = 1.45 \text{ amperes.}$$

From the induced voltage equation, the number of turns required in the primary winding

$$t_p = \frac{E_p \times 108}{4.44f \times BA_c k_1}.$$

The flux density in core determines the core losses as well as the magnetizing current. For 2.5 to 3.0 per cent silicon sheet steel not over 0.025 in. thick, the core density can generally be equal to 80 kilo-lines per sq. in. for 60 cycles. For 25 cycles, core densities up to 95 kilo-lines per sq. in. may be used. For 400 cycles, 29 gauge sheet steel should be used, and the core density usually can not exceed 40 kilo-lines per sq. in. If cold reduced sheet steel 0.007 in. thick is used and the core is rolled up so that the flux passes only in the direction in which the sheet has been rolled, the core density may be 80 kilo-lines for 400 cycles. The stacking factor, k_1 , is 0.90 for 29-gauge 0.014-in. sheet steel; for 24-gauge 0.025-in. sheet steel, 0.95 is used.

The core construction may be either core type or shell type. The shell-type core construction has been found most satisfactory for these small transformers and is adopted for this design.

The number of turns that can be placed in a given window opening depends upon the size of wire and the insulation requirements. The copper loss in any winding varies directly with the square of the current density in amperes per square inch and the weight of copper in the winding. Economical considerations require that the minimum-size conductors consistent with temperature rise, voltage regulation, and efficiency be used. Temperature rise rather than voltage drop or efficiency will probably be the controlling factor in most designs. The final operating temperature will depend upon the losses in the transformer, the radiating surface, the method of cooling, and the ambient temperature of the surrounding air. If the transformer is mounted on or adjacent to large metal surfaces or if forced circulation of air is used, greater losses can be dissipated without excessive temperature rise. If, however, the transformer is mounted in the same compartment or adjacent to other hot objects, such as vacuum tubes, considerably higher operating temperatures will be encountered. For dry-type transformers located in free air for which voltage regulation and efficiency are not the controlling factors, the maximum safe current density can be taken equal to 400 circular mils per ampere or 3180 amperes per sq. in. The conductor section

$$s_c = I \times A \text{ circular mils,}$$

where A is the current density in circular mils per ampere.

The windings of these small transformers are usually wound on automatic winding machines with paper insulation between the various layers. To make the coils self-supporting and to provide insulation on each end of the coils, the insulating tube on which the coil is wound as

well as the layer insulation is allowed to extend beyond the winding. The extension of the insulation on each end of the coil is called the margin and varies with the size of wire and the voltage of the winding. Table XXXIII gives the current capacity of various sizes of wire based on 400 circular mils per ampere, the margin allowance for each end of the winding, the turns per inch, and the pile-up. The pile-up is the space required by the insulated wire plus the layer insulation.

TABLE XXXIII

A.W.G. Gauge No.	Current Capacity	Turns per Inch	Margin	Pile-up
15	8.13	15.6	0.250	0.0755
16	6.46	17.5	.187	.0653
17	5.12	19.6	.187	.0592
18	4.06	21.8	.187	.0535
19	3.22	24.3	.156	.0465
20	2.56	27.1	.156	.0421
21	2.02	30.4	.156	.0382
22	1.60	34.0	.125	.0324
23	1.27	37.9	.125	.0294
24	1.01	42.2	.125	.0256
25	0.80	47.2	.125	.023
26	.63	53.0	.125	.0208
27	.50	59	.125	.0184
28	.40	65	.125	.0165
29	.32	72	.125	.0149
30	.25	79	.125	.0133
31	.20	88	.125	.0120
32	.16	100	.094	.0109
33	.125	113	.094	.0099
34	.100	125	.094	.0086
35	.079	141	.094	.0078
36	.0625	158	.094	.0072
37	.0495	178	.094	.0065
38	.0394	195	.062	.006
39	.0312	221	.062	.005
40	.025	245	.062	.0045

Assuming that half of the window width is required for the primary winding, the number of primary turns that can be wound in a given window

$$t_p = \frac{\text{turns}}{\text{inch}} (hw - \text{margin}) \left(0.5 \frac{w_w - i}{\text{pile-up}} \right).$$

For 115-volt primary windings and secondary voltages not over 1000 volts, the insulation allowance, i , can be taken equal to 0.08 in. for a window area less than 0.75 sq. in. and 0.125 in. for larger window areas.

From Table XXXII the minimum size of conductor for the primary

winding should be a No. 22 wire. In order to obtain better than minimum performance characteristics, a No. 21 wire is chosen. For the lamination shown in Fig. 261, the primary turns

$$t_p = 30.4(2\frac{7}{16} - 0.312) \left(0.5 \frac{0.468 - 0.125}{0.0382} \right) = 290 \text{ turns.}$$

For a core density of 80 kilo-lines per sq. in., the gross core area

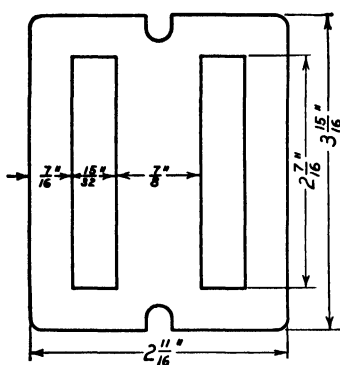


FIG. 261.—Transformer lamination.

$$A_c = \frac{540}{290 \times 0.90} = 2.07 \text{ sq. in.}$$

The length of stack required for a center leg width of 0.875 in.

$$= \frac{2.07}{0.875} = 2.36 \text{ in.}$$

To meet standard core-winding forms and insulating tubes, 2.5 in. is used. The number of primary turns for core density, 80 kilo-lines per sq. in.,

$$t_p = \frac{2.36}{2.50} 290 = 274 \text{ turns.}$$

The number of turns in the secondary windings must then be

$$t_{s5} = \frac{5}{115} 274 = 11.9; \text{ use } 12.$$

$$t_{s12.6} = \frac{12.6}{115} \times 274 = 30.$$

$$t_{s800} = \frac{800}{115} \times 274 = 1910.$$

The size of conductors for the secondary windings are determined with the help of Table XXXIII. For the 5-volt secondary winding, a No. 24 enamel wire is selected and for the 12.6-volt winding, a No. 21 enamel wire. For the 800-volt winding, a No. 31 enamel wire is chosen which is one size larger than the minimum given in Table XXXIII.

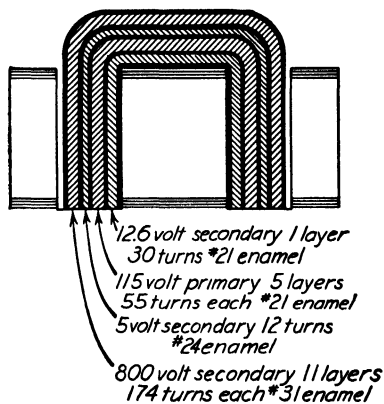


FIG. 262.—Arrangement of transformer windings.

The windings are wound on the core as shown in Fig. 262, and the total winding space in the window width is as follows:

Core insulation	0.025 in.
One layer, 30 turns No. 21 enamel	0.0382 in.
Two layers, 0.003 in. varnished cambric	0.006 in.
Five layers, 55 turns No. 21 enamel	0.191 in.
Three layers, 0.003 in. varnished cambric	0.009 in.
One layer, 12 turns No. 21 enamel	0.0256 in.
Three layers, 0.003 in. varnished cambric	0.009 in.
Eleven layers, 174 turns each No. 31 enamel	0.132 in.
Two layers, 0.003 varnished cambric	0.006 in.
Total	0.4418 in.

The total clearance between the winding and the outside core leg is $0.468 - 0.442 = 0.026$ in. If the manufacturing methods do not permit such close tolerance, the core stack must be increased and the number of turns decreased. If it is desirable to have a more nearly square center core leg, then a lamination with wider center core leg must be selected.

The length of the mean-turn of the various windings is

$$L_{s12.6} = (0.875 + 2.5)2 + \pi[2 \times 0.025 + 0.038] = 7.03 \text{ in.}$$

$$\begin{aligned} L_p &= (0.875 + 2.5)2 \\ &\quad + \pi[2(0.025 + 0.038 + 0.006) + 0.191] \\ &= 7.78 \text{ in.} \end{aligned}$$

$$\begin{aligned} L_{s5} &= (0.875 + 2.5)2 \\ &\quad + \pi[2(0.025 + 0.038 + 0.006 + 0.191 + 0.009) \\ &\quad + 0.026] \\ &= 8.52 \text{ in.} \end{aligned}$$

$$\begin{aligned} L_{s5} &= (0.875 + 2.5)2 \\ &\quad + \pi[2(0.025 + 0.038 + 0.006 + 0.191 \\ &\quad + 0.009 + 0.026 + 0.009) \\ &\quad + 0.132] \\ &= 9.07 \text{ in.} \end{aligned}$$

The resistance of the windings at 75° C. is

$$R_{s12.6} = \frac{7.03 \times 30 \times 0.826}{0.000638 \times 10^6} = 0.273 \text{ ohm.}$$

$$R_p = \frac{7.78 \times 275 \times 0.826}{0.000638 \times 10^6} = 2.77 \text{ ohms.}$$

$$R_{s5} = \frac{8.52 \times 12 \times 0.826}{0.000317 \times 10^6} = 0.267 \text{ ohm.}$$

$$R_{s800} = \frac{9.07 \times 1914 \times 0.826}{0.0000622 \times 10^6} = 231.0 \text{ ohms.}$$

The copper losses at 75° C. in the different windings are

$$W_{s12.6} = 2.0^2 \times 0.273 = 1.09 \text{ watts.}$$

$$W_p = 1.45^2 \times 2.77 = 5.82 \text{ watts.}$$

$$W_{s5} = 1.0^2 \times 0.267 = 0.267 \text{ watt.}$$

$$W_{s800} = 0.15^2 \times 231.0 = 5.20 \text{ watts.}$$

The total copper loss = 1.09 + 5.82 + 0.267 + 5.2 = 12.38 watts.

The core weight is best determined by weighing a given number of finished laminations. If such information is not available, then it must be calculated from the dimensions of the core.

$$\begin{aligned} \text{The outside core legs} &= 0.438 \times 2.438 \times 2.0 \times 2.5 \times 0.90 \times 0.278 \\ &= 1.33 \text{ lb.} \end{aligned}$$

$$\begin{aligned} \text{The center core leg} &= 0.875 \times 2.438 \times 2.5 \times 0.90 \times 0.278 \\ &= 1.33 \text{ lb.} \end{aligned}$$

$$\begin{aligned} \text{The yokes} &= 0.438 \times 2.688 \times 2.0 \times 0.90 \times 0.278 \\ &= 0.59 \text{ lb.} \end{aligned}$$

For 29-gauge electrical-grade sheet steel, the loss per pound is 1.72 watts, and the total core loss, including the additional losses,

$$W_c = 1.72 \times 3.25 \times 1.15 = 6.44 \text{ watts.}$$

The data for the losses of 29-gauge electrical grade sheet steel are not given in the Appendix; they can be found in Engineering Manual 3, U.S.S. Electrical Steel Sheet, U.S. Steel Corporation, Pittsburgh, Pa.

The efficiency for unity power factor load is

$$\frac{150.2}{150.2 + 6.44 + 12.38} = 88.7 \text{ per cent.}$$

The heat-dissipating surfaces are all surfaces exposed to the cooling air.

For the core, the cooling surface is

$$\begin{aligned} \text{Outside legs} &= 0.438 \times 2.438 \times 4 + 2.5 \times 3.312 \times 2 \\ &= 19.87 \text{ sq. in.} \end{aligned}$$

$$\begin{aligned} \text{Yokes} &= 0.438 \times 2.688 \times 4 + 2.688 \times 3.312 \times 2 \\ &= 21.35 \text{ sq. in.} \end{aligned}$$

For the winding, the exposed surfaces are

$$\text{Coil ends} = (0.875 + 0.468) \pi \times 0.468 \times 2 = 3.94 \text{ sq. in.}$$

$$\text{Coil outside} = (0.875 + 0.936) \pi \times 2.438 = 13.90 \text{ sq. in.}$$

The total cooling surface = $19.87 + 21.35 + 3.94 + 13.90 = 59.06$ sq. in. The cooling surface per watt loss

$$= \frac{59.06}{6.44 + 12.38} = 3.14.$$

The surface per watt loss for small dry-type transformers in free air should be over 3 sq. in. per watt for a temperature rise not to exceed 50° C.

This transformer is designed with the turns ratio equal to the no-load voltage ratio. If the load on the transformer is constant, the secondary turns are sometimes increased to compensate for the voltage drop in the windings. The voltage regulation can be calculated by the same methods used for distribution and power transformers. The leakage reactance is usually so small that it can be neglected.

Index

- Additional losses, direct-current machines, 123, 132, 157
 - induction motors, 330, 346, 373, 390
 - synchronous machines, 252, 262, 286
 - transformers, 432, 435, 447, 464, 474
- Air blast transformer, 407
- Air gap, ampere-turns, direct-current machines, 65, 67, 77, 143
 - induction motors, 328, 344
 - synchronous machines, 216, 222, 271
- coefficient, direct-current machines, 66, 77, 143
 - induction motors, 328, 343, 367, 386
 - synchronous machines, 216, 221, 271
- density, average values of, direct-current machines, 16
 - induction motors, 297
 - synchronous machines, 176
- direct-current machines, 65, 77, 143
- induction motors, 314, 367, 386
- synchronous machines, 215, 221, 271
- length, approximate minimum value of direct-current machines, 24, 30, 84
 - induction motors, 316, 324, 365, 384
 - synchronous machines, 180, 235
- section, direct-current machines, 66, 76, 142
 - length of, synchronous machines, 215, 220, 271
 - synchronous machines, 215
- Aluminum, resistance of, 333
- Ampere conductors per inch of, armature circumference, direct-current machines, 16, 56, 61, 140
 - synchronous machines, 176
- stator gap circumference, induction motors, 298
- Ampere-turns, armature teeth, direct-current machines, 67, 76, 142
 - synchronous machines, 217, 221, 271
- Ampere-turns, armature yoke, direct-current machines, 69, 78, 144
 - synchronous machines, 217, 222, 272
- field pole, direct-current machines, 70, 79, 145
 - synchronous machines, 219, 223, 274
- field yoke, direct-current machines, 72, 80, 146
 - synchronous machines, 220, 225, 275
- per commutating pole, 111, 118, 152
- per inch of flux path, 65, Appendix
- per inch height of field coil, direct-current machines, 72
- per joint transformer cores, 431, 443, 455, 466
 - per pole, direct-current machines, 65, 80, 146
 - synchronous machines, 215, 224, 274
- rotor teeth, 329, 345
 - yoke, 328, 345
- stator teeth, 329, 344
 - yoke, 328, 345
- Armature, coil, construction, direct-current machines, 47
 - synchronous machines, 202
- end-connection clearances, direct-current machines, 53, 58
 - synchronous machines, 205
- insulation, direct-current machines, 49 52
 - synchronous machines, 202-205
- conductor section, direct-current machines, 54, 61, 140
 - synchronous machines, 206, 213, 270
- conductors, in series per phase, synchronous machines, 210, 269
 - total, direct-current machines, 60, 138
 - synchronous machines, 211, 269
- construction, direct-current machines, 3
 - synchronous machines, 162
- copper losses, direct-current machines, 121, 130, 155

- Armature, copper losses, synchronous machines, 206, 251, 261, 285**
 cross-magnetizing ampere-turns, 82, 154
 current, direct-current machines, 55, 61, 140
 synchronous machines, 213, 269
 demagnetizing ampere-turns, 81
 diameter and length, direct-current machines, 20, 29, 136
 synchronous machines, 178, 186, 266
 frame, construction of, synchronous machines, 166
 laminations, thickness of, direct-current machines, 3
 synchronous machines, 162
 leakage flux paths, direct-current machines, 103
 reactance, synchronous machines, 226, 229, 244, 276
 length, direct-current machines, 20, 29, 136
 synchronous machines, 178, 186, 266
 peripheral speed, direct-current machines, 20
 synchronous machines, 178
 reaction, synchronous machines, 233
 ampere-turns, maximum value of, 233
 factor, 233, 245, 276
 flux coefficients, 234, 245, 277
 slot dimensions, direct-current machines, 56, 62, 140
 synchronous machines, 208, 213, 270
 slots, effect upon flux wave, direct-current machines, 27, 45
 synchronous machines, 201
 teeth, section of, direct-current machines, 67, 75, 140
 synchronous machines, 216
 tooth density, average values for, direct-current machines, 68, 75, 141
 synchronous machines, 216, 221, 271
 maximum values for, direct-current machines, 68
 synchronous machines, 216, 221, 271
- Armature, tooth support, direct-current machines, 5**
 synchronous machines, 164
 voltage drop, direct-current machines, 55, 60, 63, 141
 windings, direct-current machines, classification of, 31
 synchronous machines, classification of, 188
 connections of, 199
 method of laying out, 191
 parallel circuits of, 199, 211, 269
- Armature yoke section, direct-current machines, 69, 77, 143**
 synchronous machines, 222, 272
- Arrangement of coils, transformer windings, 420**
- Auxiliary winding, single-phase motors, 374, 390**
- Average temperature rise of oil, 433**
- Axial length of field yoke, direct-current machines, 72, 79, 145**
- Back pitch, lap winding, 32, 61**
 wave winding, 37, 139
- Bar pitch squirrel-cage winding, synchronous motors, 280**
- Bar section, squirrel-cage winding, 323, 325, 365, 385**
- Bars per pole squirrel-cage winding, synchronous motors, 280**
- Bearings, direct-current machines, 12**
- Belt leakage, constant, synchronous machines, 229**
 reactance, synchronous machines, 228
- Brass, resistance of, 333**
- Brush, contact, 100**
 drop, 113
 loss, 122, 131, 156
 surface, 112, 116, 150
 friction loss, A.I.E.E. Standards, direct-current machines, 123, 132, 157
 thickness, 101, 112, 114, 115, 149
 width, total per arm, 114, 116, 150
- Brushes, characteristics of, 113**
 lubricating qualities of, 100
 stagger of, 100

- Capacitor-start motor, 381
- Chain windings, 188
- Choice of armature winding, direct-current machines, 53, 60, 138
- Chord factor, calculation of, 189, 195
 - definition of, 174
 - stator winding, 296, 313
- Chorded stator windings, induction motors, 306
- Chorded windings, direct-current machines, 102
 - synchronous machines, 189
 - advantages of, 189
- Circular transformer coils, advantages of, 414
- Coefficient of, mutual induction, 103
 - self-induction, 103
- Coil pitch, 34
 - armature coils, direct-current machines, 58
 - synchronous machines, 209
- Coil support, synchronous machines, 165
- Commutating field, copper loss, 121, 131, 153
 - winding, conductor section, 91, 118, 152
 - design of, 91, 118, 152
 - insulation of, 91, 119
- Commutating pole, air gap, ampere-turns, 109, 118, 152
 - density, 109, 117, 151
 - length, 107, 116, 150
 - design of, 106
 - flux, 110
 - length, 107, 117, 151
 - shoe bevel of, 109
 - width, 106, 117, 151
- Commutating pole machine, 1
 - magnetic circuit, 110
- Commutating zone, maximum width of, 103
- Commutation, 99
 - effect of mechanical condition of commutator and brushes, 100
- Commutator bar, construction, 5
 - diameter, 111, 115, 149
 - length, 112, 116, 150
 - mica, thickness of, 111
 - minimum thickness of, 111
 - peripheral speed, 111
- Commutator bar, pitch, lap winding, 33, 61
 - wave winding, 39, 139
 - segment pitch, 112, 115, 149
 - minimum value of, 112
- Compensated machine, 1
 - advantages of, 1
- Compensating winding, 84
- Concentric-type transformer winding, 420
- Conductor insulation, armature coils, direct-current machines, 49-52
 - synchronous machines, 202-205
 - rotor winding, 323
 - stator winding, 309, 314, 364
 - transformer windings, 420-423
- Conductor section, high-voltage winding, 415, 439, 451, 463
 - low-voltage winding, 415, 438, 450, 462
 - stator winding, induction motors, 308, 314, 363, 377, 383, 393
 - wound rotor winding, 321
- Conductors, in series, per phase, stator winding, 306, 362, 377, 382, 391
 - wound rotor winding, 323
- per slot, armature, direct-current machines, 60, 139
 - synchronous machines, 188, 211, 269
 - arrangement of, 202, 213, 270
- per stator slot, 306, 313
 - arrangement of, 308
 - total stator, induction motors, 307
- Constant potential transformers, 398
- Construction of, armature, direct-current machines, 3
 - synchronous machines, 162
- belt tightener base, 13
- brush holder and brush yoke, 12
- commutating pole winding, 10
- field coil, direct-current machines, 9
 - synchronous machines, 171
- field poles, direct-current machines, 9
 - synchronous machines, 172
- field winding, non-salient pole machines, 167
- field yoke, direct-current machines, 11
- rotor, 290
- stator, 289
- transformer core, 399
 - tank, 403

- Cooling constant, armature, direct-current machines, 129, 133, 158
 - field winding, direct-current machines, 88, 133, 158, 159
- Cooling curves, transformers, 434
- Cooling surface, armature, direct-current machines, 129
 - synchronous machines, 260, 263, 286
 - field winding, synchronous machines, 243, 250, 279
 - shunt field winding, 88, 96, 149
- Copper loss, average values of, transformers, 417, 418
 - per pound, 408
- Copper space factor, average values of, 415
- Copper table, bare copper strap, 482-485
 - double-cotton-covered ribbon, 479
 - round wire, 477
 - square wire, 478
- Copper weight, armature winding, direct-current machines, 59, 63, 141
 - synchronous machines, 210, 214, 270
 - commutating field winding, 91, 119, 153
 - field winding, synchronous machines, 244, 250, 279
 - high-voltage coil, 428, 441, 453, 464
 - low-voltage coil, 428, 441, 453, 464
 - series field winding, 90, 98, 155
 - shunt field winding, 89, 96, 149
- Core loss, average values of, transformers, 417, 418
 - current, 431, 444, 455, 466
 - direct-current machines, 122, 131, 156
 - induction motors, 330, 346, 373, 390
 - per pound, 408
 - electrical sheet steels, 486
 - synchronous machines, 251, 262, 286
- Core space factor, 413
- Core-type transformers, construction of, 402
- Current, in high-voltage winding, 415, 436, 448, 460
 - in low-voltage winding, 415, 436, 449, 460
 - per path, direct-current armature winding, 55
 - per phase, induction motors, 308, 314, 363, 383
- Current density, armature conductor, direct-current machines, 55, 61, 140
 - synchronous machines, 206, 213, 270
- brush contacts, 112, 113, 116, 150
- commutating field conductor, 91, 118, 152
- field winding, synchronous machines, 243, 249, 278
- in copper, of transformers, 409, 440, 450, 451, 465, 471
- series field conductor, 90, 97, 154
- shunt field conductor, 72, 95, 144
- squirrel-cage winding, 320
- stator windings, induction motors, 308, 314, 363, 378, 383
- Dead coil, 41
- Dead-points, squirrel-cage motors, 317
- Density, armature yoke, direct-current machines, 69, 77, 143
 - synchronous machines, 217, 222, 272
- field pole, direct-current machines, 70, 78, 144
 - synchronous machines, 219, 223, 274
- field yoke, direct-current machines, 72, 79, 145
 - synchronous machines, 220, 224, 275
- Depth of oil, 434, 446, 456, 467
- Design of, pole shoe, direct-current machines, 22
 - synchronous machines, 179
 - shunt field rheostat, 91, 98
- Design sheet, direct-current generator, 134
 - motor, 161
 - distributed core-type transformer, 468
 - single-phase core-type transformer, 445
 - single-phase induction motors, 380, 397
 - squirrel-cage motor, 354
 - synchronous generator, 264
 - motor, 288
 - three-phase core-type transformer, 457
- Difference between temperature of windings and average oil temperature, 433
- Direct-current machines, classification of, 1
- Displacement angle, 237, 247, 287

- Distributed core-type transformer, construction of, 403
 - core design, 458
 - operating characteristics, 464
 - tank design, 467
 - winding design, 462
- Distribution of current in, squirrel-cage windings, 321
- transformers, 398
- Double-layer windings, synchronous machines, 188
- Double squirrel-cage winding, induction motors, 322, 350
 - synchronous motors, 231, 282
- Ducts in, transformer core, 414
 - transformer windings, 425
- Eddy current losses in, armature coils, synchronous machines, 207
 - stator copper, induction motors, 308
 - transformer windings, 420
- Effect of, slot openings upon air gap flux, induction motors, 307
 - undercutting mica, 100
- Effective value of current, in end rings, squirrel-cage winding, 321
 - per bar, squirrel-cage winding, 321
- Efficiency, average values of, direct-current generators, 125
 - direct-current motors, 126
 - slip-ring motors, 301
 - squirrel-cage motors, 299
 - synchronous machines, 256, 257
 - transformers, 417, 418
- direct-current machines, 125, 132, 157
 - synchronous machines, 255, 262, 286
 - transformers, 432, 444, 455, 467
- Electronic amplifier power supply transformer, core design, 472
 - operational characteristics, 474
 - winding design, 472
- End-connection leakage reactance, induction motors, 336, 348, 371, 372, 388
 - synchronous machines, 228
- End-ring section, squirrel-cage winding, induction motors, 322, 325, 365, 385
 - synchronous motors, 280
- End-turn insulation, transformers, 423, 439, 451
- Equalizer connections, conductor section, 43
 - multiplex windings, 44
 - number, 43, 44, 63
- Equalizer pitch, 42
- Equivalent circuit of induction motors, 338, 350
 - double cage winding, 231, 282
- Equivalent field ampere-turns of armature reaction, 233, 246, 277
- Excitation for any load and power factor, 239
- Exciter capacity, synchronous machines, 244, 250, 257, 279
- Exciter voltage, synchronous machines, 242
- Field current, synchronous machines, 243, 249, 278
 - leakage, constant, synchronous machines, 219, 223, 274
 - factor, direct-current machines, 71, 74
 - flux, calculation of, direct-current machines, 73
 - synchronous machines, 219, 223, 273
- Field pole, punchings, thickness of, synchronous machines, 172
 - winding, conductor section, synchronous machines, 241, 249, 278
 - copper loss, synchronous machines, 250, 251, 261, 279
 - design, synchronous machines, 241
 - rheostat loss, synchronous machines, 251, 261
 - windings, synchronous machines, 172
- Flux density, in transformer core, 409, 440, 452, 464, 472
 - distribution curve, analysis of, 180, 268
 - average ordinate of, 184, 266
 - construction of, 23, 180
 - effective ordinate of, 184, 268
 - harmonics of, 183, 266
 - maximum ordinate of, 184
 - distribution factor, direct-current machines, 27, 30, 137
 - induction motors, 296

- Flux density, distribution factor, synchronous machines, 181, 268
 Flux per pole, direct-current machines, 69, 77
 induction motors, 297, 306, 314, 360, 364, 382
 synchronous machines, 217, 222, 272
 Flux plot, construction of, direct-current machines, 24, 137
 synchronous machines, 181, 267
 Forced oil-cooled transformers, 407
 Forces on transformer windings, 430
 Form factor, induction motors, 296
 synchronous machines, 181, 268
 Fractional slot, rotor windings, 320
 stator windings, 305
 synchronous machine windings, 196
 Frequency, direct-current machines, 21, 29, 136
 Friction and windage loss, direct-current machines, 123, 132, 157
 induction motors, 331, 346
 synchronous machines, 252, 262, 286
 Frogleg winding, 45
 Front pitch, lap winding, 32, 61
 wave winding, 37, 139
 Full-load, current, induction motors, 299, 351, 375, 389
 efficiency, induction motors, 299, 351, 375, 389
 power factor, induction motors, 299, 351, 375, 389
 speed, direct-current motors, 154
 induction motors, 299, 351, 375, 389
 Heating curves of transformers, 434
 High mica, 100
 Impedance, at standstill, induction motors, 332, 341, 353, 378
 average values of transformers, 417, 418
 Impregnation of transformer coils, 427
 Induced voltage, in armature winding, direct-current machines, 14, 54, 60, 138
 synchronous machines, 174
 in stator winding, induction motors, 296
 in transformer windings, 410
 Induction motors, construction of, 289
 Inside diameter, of field yoke, direct-current machines, 77, 145
 of rotor core, 326, 367, 386
 Insulating collars, thickness of, 425, 440, 451
 Insulating materials for transformer windings, 421
 Insulating oil, dielectric strength of, 425
 Insulation, allowances, stator windings, induction motors, 309, 364, 383
 between core and windings, transformers, 423, 439, 450, 463
 between high-voltage and low-voltage windings, transformers, 423, 440, 453, 463
 of transformer laminations, 399
 stator coils, induction motors, 309
 test, A.I.E.E. Standards, armature windings, direct-current machines, 50
 synchronous machines, 205
 thickness, wound rotor coils, 323
 Interleaved type of transformer winding, 420
 Lamination factor, 68, 216, 413
 Lap winding, multiplex, 43
 progressive, 33
 retrogressive, 33
 Layer insulation, thickness of transformer windings, 422, 439, 451
 Leakage reactance, induction motors, 334, 348, 371, 388
 synchronous machines, 226, 229, 244, 276
 transformers, 428, 442, 454, 465
 Length of, bars, squirrel-cage windings, 349, 369, 387
 corrugated tank surface per inch of center line, 434
 field pole, axial, direct-current machines, 66, 78, 144
 synchronous machines, 219, 223, 272
 field yoke, axial, direct-current machines, 72, 79, 145
 synchronous machines, 220, 224, 275
 flux path, armature teeth, direct-current machines, 69, 76, 142
 synchronous machines, 217, 221, 271

- Length of, flux path, armature yoke,
 - direct-current machines, 70, 77, 143
 - synchronous machines, 218, 222, 272
- field pole, direct-current machines, 71, 79, 145
 - synchronous machines, 219, 223, 273
- field yoke, direct-current machines, 79, 145
 - synchronous machines, 220, 225, 275
- rotor yoke, 329, 345
- stator yoke, 329, 345
- mean-turn, commutating field coil, 91, 119, 152
 - field coil, synchronous machines, 243, 249, 278
 - series field coil, 90, 97, 155
 - shunt field coil, 87, 95, 147
- one-half mean-turn, armature coil, direct-current machines, 59, 62, 141
 - synchronous machines, 209, 214, 270
- rotor coil, 331
- stator coil, 331, 346, 368, 387
- Limiting temperature rise, salient pole synchronous generators and motors, 260
- steam-turbine-driven synchronous generators, 259
- transformers, A.I.E.E. Standards, 432
- Load losses in transformers, 432
- Losses in, direct-current machines, 120
 - synchronous machines, 251
 - transformers, 432
- Magnetic circuit, commutating pole machines, 110
 - induction motors, 327
 - non-commutating pole machines, 66
 - salient pole synchronous machines, 215
 - transformers, construction of, 399
- Magnetic pull per pole, 287
- Magnetization curve, cast iron, 486
 - cast steel, 486
 - electrical sheet steels, 486-489
 - hot rolled steel, 486
- Magnetizing current, 431
 - calculation of, distributed core-type transformer, 466
 - induction motors, 329, 345, 375, 389
 - single-phase core-type transformer, 443
 - three-phase core-type transformer, 455
 - induction motors, 297, 316
- Magnetizing force, 65
- Magnetizing reactance, 234, 371
- Maximum torque, induction motors, 351, 375, 389
- Method of, forming direct-current armature coils, 47, 48
 - insulating armature punchings, 3
 - measuring transformer temperature, A.I.E.E. Standards, 432
 - sealing slots, direct-current machines, 5
- Minimum cost transformers, 408
- Minimum loss transformers, 408
- Multiplex lap windings, 43
 - wave windings, 43
- Natural-air-cooled transformers, 403
- Natural-oil-cooled transformers, 407
- Neutral zone, 103, 116, 150
- No-load current, induction motors, 332, 346
 - transformers, 431, 444, 455, 466
 - watt component of, induction motors, 332, 346
 - transformers, 431, 441, 455, 466
- No-load field form, construction of, 23, 180
 - losses in transformers, 431
 - power factor, induction motors, 332, 347
- Non-commutating pole machines, 1
- Number of, armature slots, direct-current machines, 45, 60, 138
 - synchronous machines, 201, 211, 269
- brush sets for wave windings, 39
- coil sides per slot for wave windings, 40
- phases, squirrel-cage windings, 333
- poles, direct-current machines, 21, 29, 136
 - induction motors, 312, 361, 381
- rotor conductors, wound rotor winding, 323

- Number of, slots per pole, direct-current machines, 47
 - turns, high-voltage winding, 414, 439, 451, 463, 472
 - low-voltage winding, 415, 439, 450, 462, 472
- Oil- and water-cooled transformers, 407
- Open-circuit reactance, single-phase induction motors, 372, 373, 388
- Open-circuit saturation curve, direct-current machines, 75, 146
 - synchronous machines, 220, 224, 275
- Operational characteristics, determination of, induction motors, 338, 350, 375, 389
- Output constants, direct-current machines, 18
 - induction motors, 302, 360
 - synchronous machines, 177
- transformers, 411
- Output equation, direct-current machines, 14
 - induction motors, 302, 359
 - synchronous machines, 175
- transformers, 410
- Outside diameter, armature, synchronous machines, 227, 272
 - field yoke, direct-current machines, 79, 145
 - stator core, 304, 312
- Over-commutation, 99
- Per cent impedance, synchronous machines, 245, 276
 - transformers, 430, 443, 466
- Per cent magnetizing current, induction motors, 329, 345
- Per cent pole embrace, direct-current machines, 23, 30, 137
 - synchronous machines, 179, 187, 266
- Per cent reactance, average values of, transformers, 417, 418
 - induction motors, 337
 - synchronous machines, 229, 245, 276
- transformers, 430, 443, 454, 465
- Per cent resistance, average values of, transformers, 417, 418
 - synchronous machines, 245, 276
- transformers, 428, 442, 454, 465
- Per cent slip, induction motors, 338, 350, 375, 389
- Peripheral speed, induction motors, 305
- Phase angle main and auxiliary windings, 374
- Phase difference of commutation, 102, 115, 149
- Polarity of, commutating poles, 1
 - transformers, 418
- Power factor, average values of, slip-ring motors, 301
 - squirrel-cage motors, 299
- Power transformers, 398
- Pull-in torque, synchronous motor, 232, 282, 284
- Radial length of field pole, direct-current machines, 71, 79, 144
 - synchronous machines, 219, 223, 273
- Radiating surface, calculation of, core-type transformer, 444, 456
 - distributed core-type transformer, 467
 - electronic amplifier power supply transformer, 475
 - per watt, transformers, 432
- Rate of change of current, average value of, 104
- Ratio of, air gap and armature tooth ampere-turns to armature ampere-turns, 76, 84, 142
 - armature length to pole pitch, direct-current machines, 20
 - synchronous machines, 178, 186, 266
 - armature outside to inside diameter, synchronous machines, 179
 - core loss to copper loss, distribution transformers, 408, 465
 - power transformers, 408, 442, 454
 - core weight to copper weight of transformers, 409, 441, 453, 464
 - stator length to pole pitch, induction motors, 304
 - stator outside to inside diameters, induction motors, 304
 - window height to width, transformers, 415
- Reactance of short-circuited field winding, synchronous motors, 231

- Reactance voltage, curve, shape of, 108
 - fundamental equation of, 103
 - per coil, 105, 117, 151
- Regulation, average values of, transformers, 417, 418
 - of synchronous generators, 176, 241, 247
 - of transformers, 431, 443, 454, 466
- Resistance of, armature winding, direct-current machines, 59, 63, 141
 - commutating field winding, 91, 119, 153
 - field winding, synchronous machines, 244, 249, 279
 - high-voltage winding, 428, 442, 454, 465, 474
 - low-voltage winding, 428, 442, 454, 465, 474
 - series field winding, 90, 98, 155
 - shunt field winding, 87, 96, 148
 - squirrel-cage winding, induction motors, 333, 339, 349
 - total, transformer windings, 428
- Resistance per phase, armature winding, synchronous machines, 210, 214, 270
 - stator winding, 331, 346
 - wound rotor winding, equivalent value of, 332
- Rotor, current, wound rotor motor, 342
 - diameter, 316, 324, 365, 384
 - end-connection, leakage reactance, synchronous motor, 230
 - frequency, 330
 - laminations, 290
 - reactance, synchronous motor, 230, 280, 283
 - slots, number of, squirrel-cage motors, 318, 357
 - wound rotor motors, 320
 - tooth, density, maximum value of, 324, 325
 - width, minimum value of, 324, 325
 - voltage, wound rotor motors, 323
 - windings, connection of, induction motors, 320
 - yoke density, 324, 326, 367, 386
 - zigzag leakage reactance, synchronous motors, 230
- Sample design, armature winding, direct-current generator, 60
 - synchronous generator, 210
- commutator and commutating pole, 115
 - direct-current motor, 136-161
- diameter and length, direct-current generator, 28
 - synchronous generator, 186
- field winding, synchronous generator, 244
 - losses, efficiency and temperature rise, direct-current generator, 130
 - synchronous generator, 261
- magnetic circuit, direct-current machines, 75, 141
 - synchronous generator, 220
- operating characteristics, squirrel-cage motor, 343
 - rotor, squirrel-cage motor, 324
- shunt and series field winding, direct-current generator, 94
 - stator, squirrel-cage motor, 312
 - synchronous motor, 265-288
 - transformers, 435-475
- Saturation, effect of, on leakage reactance, 324
 - Saturation factor, 367
- Section area of, field yoke, direct-current machines, 72, 79
 - pole, direct-current machines, 71, 78
 - transformer core, 410, 436, 447, 459, 472
- Section-wound coils, transformers, 423
 - Series field, ampere-turns, 85, 97, 154
 - copper loss, 121, 131, 155
 - current, 90, 97, 154
 - winding conductor section, 90, 97, 154
 - design, 89
- Shaft currents, synchronous machines, 162, 255
 - Shape of, bar squirrel-cage winding, 322, 325, 365, 385
 - core section, circular-core-type transformers, 413
 - rectangular-core-type transformers, 412
 - shell-type transformers, 412
- Sheet steel, quality of, transformers, 399
 - thickness of, transformers, 399

- Shell-type transformer, construction of, 403
 - core design, 412
- Short-circuit, characteristic, 235, 247, 275
 - current curves, 100
 - induction motor, 332, 340, 352, 378, 393
 - sustained value of, 430
- ratio, 235, 246, 277
- Shunt field, ampere-turns, 85, 94, 147
 - copper loss, 121, 131, 156
 - current, average values of, 55
 - calculation of, 88, 95, 147
 - rheostat loss, 121
 - winding, conductor section, 87, 95, 147
 - design, 85
 - insulation of, 85
- Silicon sheet steel, properties of, 486-489
- Simplex lap windings, 31
- Simplex wave windings, 35
- Single-phase core-type transformer, core design, 435
 - operating characteristics, 442
 - tank design, 444
 - winding design, 438
- Skew angle, 337, 348, 371
- Skew leakage reactance, induction motors, 337, 349, 371, 372, 388
- Slot leakage reactance, synchronous machines, 226
- Slot size, squirrel-cage winding, 323, 325, 366, 385
- Slots, form of, induction motors, 308, 322
 - partly closed, calculation of area, 310, 315, 364, 383
 - copper space factor, 310, 315, 364, 383
 - per pole per phase, stator winding induction motors, 305, 313
- Sparking at brushes, 101-103
- Spider, construction of, direct-current machines, 3
 - synchronous machines, 172
- Split-phase motor, 360
- Squirrel-cage winding, construction of, induction motors, 295
 - design of, synchronous motor, 280
 - induction motors, 316
- Stabilizing winding, 154
- Star connection, advantages of, synchronous machines, 199
- Starting resistance, direct-current motor, 159
- Starting rheostat, wound rotor motor, 346
- Starting torque, squirrel-cage motor, 341, 355
 - single-phase motor, 376, 379, 394
 - synchronous motor, 231, 285
- Stator, coil, construction of, 305
 - end-connection clearance, 309
 - insulation of, 309
 - copper loss no-load, 332, 346
 - depth, 312
 - design of, 296
 - diameter and length, 303, 313, 361, 386
 - frame, 290
 - laminations, quality of, 289
 - thickness of, 289
 - length, 304, 313, 361, 381
 - slot, size, 306, 315, 361, 384
 - width, 307
 - slots, number of, 306, 313, 361, 384
 - tooth density, maximum value of, 311
 - pitch, minimum value of, 307, 313
 - width, minimum value of, 311
- windings, 305
 - single-phase, 356
 - yoke density, 311, 316, 365, 383
- Straight-line commutation, 99
- Strap copper field coil, insulation of, synchronous machines, 243, 249
 - length, mean-turn of, synchronous machines, 243, 249
 - synchronous machines, 243, 248
- Stray load-losses, A.I.E.E. Standards, direct-current machines, 120
 - synchronous machines, 255, 262, 286
- Stray losses in transformers, 432
- Surface per watt, armature, direct-current machines, 129, 133, 158
 - synchronous machines, 261, 263, 286
- commutator, direct-current machines, 130, 134, 159
- field winding, direct-current machines, 88, 96, 129, 133, 149, 153, 158
 - synchronous machines, 244, 250, 279
- Synchronizing power, 239, 263, 287

- Synchronous machines, classification of, 162
- Synchronous reactance, 234
- Tank surface per watt, corrugated sheet-steel tanks, 433
- plain sheet-steel tanks, 433
- with cooling tubes, 433
- Temperature, in various parts of transformer tank, 432
- of oil at surface, 433
- rise, A.I.E.E. Standards, direct-current machines, 127
- armature, direct-current machines, 129, 133, 158
- commutator, 130, 134, 159
- field winding, direct-current machines, 88, 96, 129, 133, 158
- Thickness of coils, transformer windings, 427
- Thickness of field yoke, direct-current machines, 72, 79, 145
- synchronous machines, 220, 224, 274
- Three-phase, core-type transformer, core design, 447
- operating characteristics of, 453
- tank design, 456
- winding design, 450
- Tooth harmonics, single-phase motors, 357
- Tooth pitch, direct-current machines, 56, 62, 141
- synchronous machines, 202, 211, 269
- Torque, average values of, slip-ring motors, 301
- squirrel-cage motors, 299
- Total ampere-turns per pole, induction motors, 329, 345
- Total bar section, squirrel-cage windings, 320
- Total flux, average values of, transformers, 410
- direct-current machines, 14, 60, 139
- induction motors, 296, 360, 362, 382
- synchronous machines, 174, 213, 269
- transformers, 414, 440, 452, 464
- Total rotor conductor section, slip-ring motors, 321
- squirrel-cage windings, 320, 325, 365, 385
- Transformer, classification of, 398
- construction, types of, 402
- cooling of, 403
- essential parts of, 398
- tank, types of, 407
- temperature rise, A.I.E.E. Standards, 418
- windings, design of, 418
- Transposed conductors, armature coils, synchronous machines, 208, 255
- in transformer windings, 421
- Turns, in series per phase, squirrel-cage winding, 333
- per pole, commutating field winding, 91, 118, 152
- field winding, synchronous machines, 243, 249, 278
- series field winding, 90, 97, 154
- shunt field winding, 88, 95, 147
- Under-commutation, 99
- Ventilated field coil, 87
- Ventilating ducts, in armature, direct-current machines, 5, 75
- synchronous machines, 164, 220, 271
- in rotor core, 290
- in stator core, 290, 313
- Voltage, between commutator bars, 53, 61, 139
- layers, transformer windings, 421
- drop in field winding, synchronous machines, 242, 249, 278
- formula, synchronous machines, 174
- per turn, direct-current armature windings, 50
- transformer windings, 415
- Volume of oil, 454
- Wave windings, multiplex, 43
- progressive, 38
- retrogressive, 38
- Weight, stator, teeth, 345, 373, 388
- yoke, 346, 373, 390
- Width of commutating zone, 101, 115, 149
- Winding constant, induction motors, 296

- | | |
|---|--|
| <p>Winding constant, synchronous machines, 175, 210</p> <p>Winding distribution factor, calculation of, 195, 198, 211</p> <p> definition of, 174</p> <p> induction motors, 296</p> <p> single-phase induction motors, 359</p> <p>Windings for small transformers, 471</p> <p>Window area, single-phase transformers, 415</p> | <p>Window area, three-phase transformers, 416</p> <p>Wire-wound field coil, length, mean-turn of, synchronous machines, 242, 278</p> <p>Zigzag leakage reactance, induction motors, 335, 348, 371</p> <p> synchronous machines, 228</p> |
|---|--|

